

Case Studies of Liquefaction and Lifeline Performance During Past Earthquakes

Volume 2
United States Case Studies

Edited by
T. D. O'Rourke and M. Hamada

Technical Report NCEER-92-0002

February 17, 1992

This research was partially supported by the National Science Foundation under Grant No. BCS 90-25010 and the New York State Science and Technology Foundation under Grant No. NEC-91029.

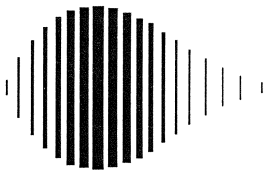

Case Studies of Liquefaction and Lifeline Performance During Past Earthquakes

Volume 2

United States Case Studies

Edited by
T. O'Rourke[1] and M. Hamada[2]

February 17, 1992

Technical Report NCEER-92-0002

NCEER Project Number 90-3008

NSF Master Contract Number BCS 90-25010
and
NYSSTF Grant Number NEC-91029

1 Professor, School of Civil and Environmental Engineering, Cornell University, Ithaca, New York
2 Professor, School of Marine Science and Technology, Tokai University, Shimizu, Shizuoka, Japan

NATIONAL CENTER FOR EARTHQUAKE ENGINEERING RESEARCH
State University of New York at Buffalo
Red Jacket Quadrangle, Buffalo, NY 14261

NOTICE

This report was prepared under the auspices of the National Center for Earthquake Engineering Research (NCEER) through grants from the National Science Foundation, the New York State Science and Technology Foundation, and other sponsors. Neither NCEER, associates of NCEER, its sponsors, nor any person acting on their behalf:

a. makes any warranty, express or implied, with respect to the use of any information, apparatus, method, or process disclosed in this report or that such use may not infringe upon privately owned rights; or

b. assumes any liabilities of whatsoever kind with respect to the use of, or the damage resulting from the use of, any information, apparatus, method, or process disclosed in this report.

Any opinions, findings, and conclusions or recommendations expressed in this publication are those of the author(s) and do not necessarily reflect the views of NCEER, the National Science Foundation, the New York State Science and Technology Foundation, or other sponsors.



Fire following the 1906 San Francisco earthquake as seen by looking northeast from Duboce Park. The fire burned 10.6 km^2, destroying 490 city blocks and causing partial destruction of 32 additional blocks. Fire fighting was severely hampered by ruptured water mains at locations of soil liquefaction. This conflagaration was the largest single fire loss in U.S. history. (photo courtesy of San Francisco Public Library)



Areal view of fire in the Marina following the 1989 Loma Prieta earthquake. Ground deformation from soil liquefaction ruptured water mains of both the Municipal and Auxiliary Water Supply Systems of San Francisco, thereby cutting the buried pipeline supply of water to the Marina. The fire was eventually brought under control by the Portable Water Supply System, composed of special hosing and portable hydrants, which was connected to the city fireboat. Pipelines were ruptured at the same locations of liquefaction and pipeline damage as those during the 1906 earthquake. (photo courtesy of EQE, Inc.)

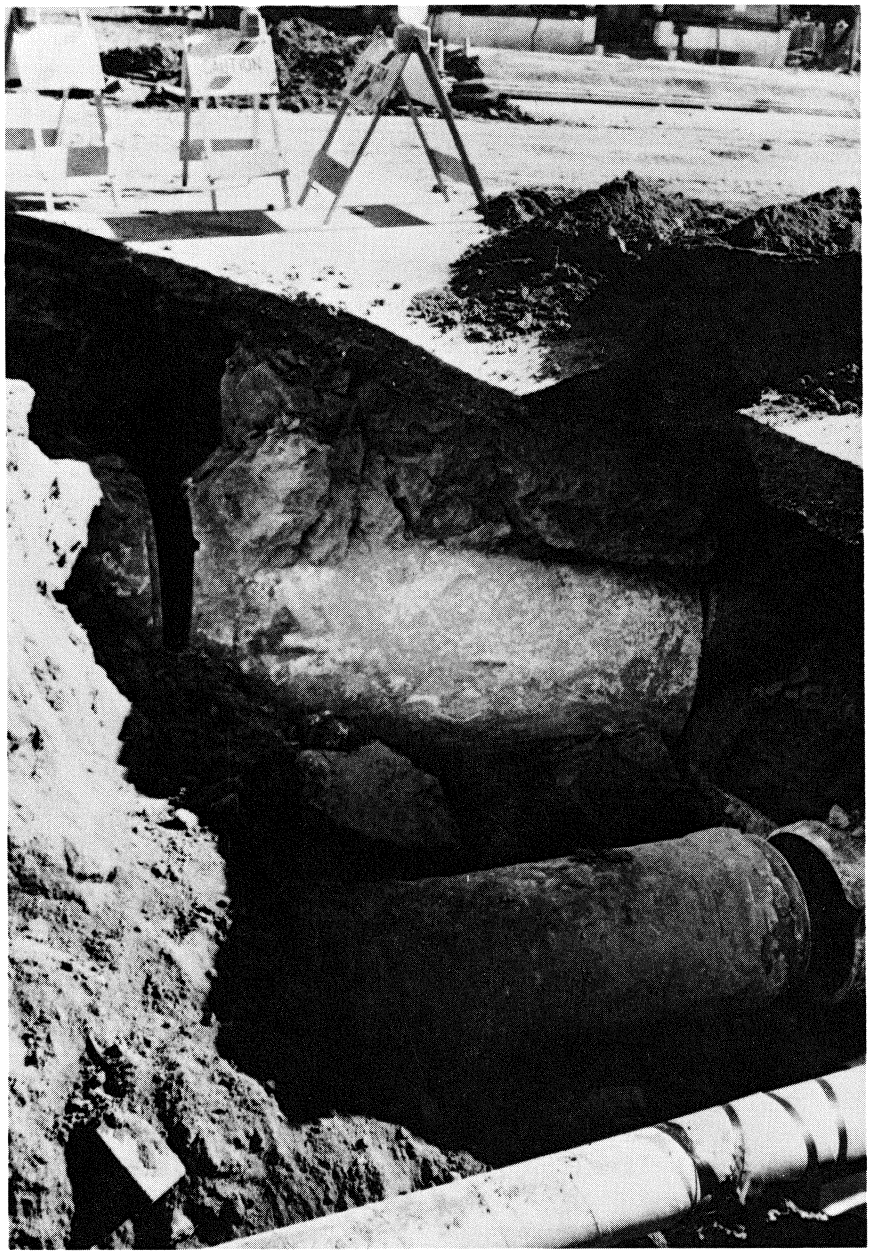

Pipelines damaged by permanent ground movement along the Sylmar segment of the San Fernando fault. This photo shows disengaged segments of water and sewer lines and a buckled gas pipeline. Disruption of lifeline facilities in the 1971 San Fernando earthquake drew worldwide attention to the seismic vulnerability of utility systems and was a major catalyst in the emergence of Lifeline Earthquake Engineering as a distinct and sustainable field of practice.

PREFACE

This volume is one part of a two-volume study of large ground deformations induced by earthquakes and their influence on lifeline facilities. Primary emphasis is placed on soil liquefaction, although ground movements caused by surface faulting, landslides, and consolidation of granular soils are also treated in case histories, where such effects have had serious repercussions on lifelines. Permanent ground deformations, particularly those generated by soil liquefaction, are known to have been the most troublesome source of subsurface structural damage and disruption of critical lifeline facilities in previous earthquakes. There has been substantial interest and research in the United States and Japan focused on these subjects, and this two-volume compilation of case histories represents an important milestone in cooperative Japanese and U.S. efforts to pool research resources, establish a comprehensive data base, and point the way to improved analytical, testing, design, and planning measures to mitigate large ground deformation effects on lifeline systems. Other products of cooperative U.S.-Japan research include the proceedings from joint workshops and bilateral recommendations for improved modeling, siting, design, and construction of buried structures. A brief description of the cooperative research program, supported by the Japanese Association for the Development for Earthquake Prediction and the U.S. National Center for Earthquake Engineering Research, is given in the introductory statement immediately following this preface.

The study of large ground deformation and lifelines can be viewed as a synthesis of two disciplines within the more general field of earthquake engineering. Soil liquefaction has been an area of substantial importance in geotechnical engineering for over 60 years. The study of earthquake-induced liquefaction can be divided historically into three periods of prominent research and practice-oriented activities. In the 1960s, earthquakes in Alaska and Niigata focused attention on soil liquefaction. The resulting field and laboratory investigations helped clarify the factors contributing to soil liquefaction and led to simplified, empirical methodologies for predicting the occurrence of liquefaction. Additional field investigations and laboratory studies in the 1970s and 1980s led to refinements and improvements in procedures to determine the susceptibility of soils to liquefaction. Although some significant advances were realized in the modeling and prediction of ground deformation as a consequence of liquefaction, the emphasis in engineering practice during this period was on understanding and identifying soils on the basis of their **susceptibility** to liquefaction. From about the mid-1980s, the emphasis in research and developments for practice has been shifting to the **consequences** of soil liquefaction. It is recognized that there are several distinct consequences of soil liquefaction, including loss of foundation bearing, buoyancy of underground structures, post-liquefaction consolidation, sand boils, local subsidence, lateral spreads, flow failures, and oscillations leading to fissures and compressive ridges in ground overlying liquefied soil. All or a portion of these consequences can occur at a single site. Accordingly, the mechanisms of large ground deformation are complex, and our understanding of these phenomena requires a comprehensive and accurate data base to provide guidance for analytical and physical modeling, site characterization and planning, and design.

In the 1970s, attention in the earthquake engineering community was directed to the performance of lifelines. Stimulated by the 1971 San Fernando and 1978 Miyagiken-oki earthquakes, an area of research and practice evolved, which focuses on the earthquake engineering performance of lifeline systems. Such systems involve water supply, transportation, gas and liquid fuel, telecommunications, electric power, and wastewater conveyance and treatment. Although primary emphasis was given originally to the response of lifelines to seismic waves, by the 1980s it was recognized that permanent ground deformation also played a critical role and was, in many cases, the most important factor affecting lifeline performance following an earthquake.

The study of lifeline performance and large ground deformation, therefore, should be viewed as a logical extension of research and practice-oriented developments associated with soil liquefaction and with the emergence of lifeline earthquake engineering. We believe that Japan-U.S. cooperative research has helped to promote and consolidate this merger of lifeline and geotechnical interests, and has led to improved engineering practices.

This volume contains five U.S. case histories, including: 1) 1906 San Francisco, 2) 1964 Alaska, 3) 1971 San Fernando, 4) 1979, 1981, and 1987 Imperial Valley, and 5) 1989 Loma Prieta earthquakes. A companion volume contains five Japanese case histories, including: 1) 1923 Kanto, 2) 1948 Fukui, 3) 1964 Niigata, 4) 1983 Nihonkai Chubu, and 5) 1990 Luzon, Philippines earthquakes. Although the Luzon earthquake did not affect mainland Japan, it nonetheless was investigated intensively by Japanese members of the cooperative research team.

Earthquakes were chosen for case history study on the basis of three principal factors. First, there needed to be accurate records of permanent ground deformation, sufficient in detail to evaluate the magnitude, direction, and areal distribution of soil movements. Second, substantial soil explorations were required to provide a reliable view of subsurface conditions and soil properties at the locations of large ground deformation. Third, accurate records were required of ground movement effects on lifeline facilities.

A case history represents the real basis for assessing the effects of an earthquake and for establishing a baseline of performance with which to verify analytical and physical models, develop design procedures, and guide the planning and siting of future facilities. Case histories are also of great value in developing countermeasures against liquefaction, such as site improvement and retrofitting procedures for existing lifelines.

The U.S. and Japanese case histories represent over 84 years of cumulative observations and analyses of earthquake-induced ground deformation and lifeline response. The case histories contained in this volume include the most important earthquakes which have occurred in the United States. As mentioned previously, the 1964 Alaska earthquake, in tandem with the Niigata earthquake of the same year, focused the attention of the engineering community on liquefaction and its devastating effects. These events can be considered as the beginning of the modern era for geotechnical investigations of liquefaction phenomena. The 1971 San Fernando earthquake marks the beginning of concerted research and development pertaining to earthquake effects on lifeline systems, and a major catalyst for the emergence of Lifeline Earthquake Engineering as a distinct and sustainable field of practice. The 1979, 1981, and 1987 earthquakes in the Imperial Valley are a unique combination of seismic events in which recurrent liquefaction

figures prominently. Data from this sequence of earthquakes include in-ground measurements of acceleration, pore pressure response, and permanent ground deformation at a site of soil liquefaction. The 1906 San Francisco earthquake is perhaps the most important seismic event in U.S. history. It is of considerable interest to note that the full significance of this event with regard to liquefaction and lifeline systems was realized only after a re-examination of the historical records following the 1964 Alaska and 1971 San Fernando earthquakes. The relevance of the data contained in the case history in this volume pertaining to liquefaction-induced lateral spreads, the damage they caused to the water delivery system, and their ultimate contribution to fire in San Francisco was substantiated in full by the events of the 1989 Loma Prieta earthquake. Liquefaction at the same locations as those in 1906 and con-sequent damage to the water supply brought the City of San Francisco dangerously close to another major conflagration in 1989.

It is our hope that the information contained in the case history volumes will be applied in the development of improved modeling, better design, and more effective planning. We also hope that it will provide an empirical baseline and guidance for future research in both geotechnical and lifeline earthquake engineering.

T. D. O'Rourke
Professor, Cornell University

M. Hamada
Professor, Tokai University

U.S.-JAPAN COOPERATIVE RESEARCH PROGRAM

The U.S.-Japan Research Program on Earthquake Resistant Design of Lifeline Facilities and Countermeasures for Soil Liquefaction was initiated formally in November, 1988 with the signing of a Memorandum of Understanding between the Japanese and U.S. sides. The document was signed at a ceremony during a workshop in Tokyo, Japan by K. Kubo, Professor Emeritus of Tokyo University, and M. Shinozuka, Sollenberger Professor of Civil Engineering of Princeton University. Professor Kubo signed on behalf of the Association for the Development of Earthquake Prediction (ADEP), the Japanese sponsoring agency. Professor Shinozuka signed on behalf of Robert L. Ketter, the Director of the National Center for Earthquake Engineering Research (NCEER), the U.S. sponsoring agency. A second Memorandum of Understanding was signed in December, 1990 to continue the cooperative program of research. The signatures were K. Kubo, representing ADEP, and M. Shinozuka, the Director of NCEER.

The products of the research include: 1) case history volumes with assessments of the most important geologic features, siting criteria, and structural features which have influenced previous lifeline performance in response to soil displacements, 2) U.S.-Japan workshops and associated publications covering case history data, analytical modeling, and recommendations for improved practices, and 3) a technical summary and recommendations for improved modeling, siting, design, and construction of buried structures.

Major instruments for collaboration and cooperative exchange are program workshops. To date, there have been three workshops. The first was held in Tokyo and Niigata, Japan on November 16-19, 1988. The proceedings of this workshop were published by ADEP, and are available from NCEER. The second workshop was held in Buffalo and Ithaca, NY on September 26-29, 1989. The third workshop was held in San Francisco, CA on December 17-19, 1990. The proceedings of both these workshops are available through NCEER. At the time of publication of this volume, a fourth workshop has been planned for Honolulu, HI on May 27-29, 1992.

Cooperative research between U.S. and Japanese earthquake engineers has resulted in significant new findings about the ways in which large ground deformations are caused by soil liquefaction, their influence on lifelines, and the most effective means of modeling and protecting both soils and structures in the event of a future earthquake. New developments presented and discussed at the workshops include the use of aerial photographs before and after major earthquakes to map ground displacements by photogrammetric techniques, the effects of large ground movements on water supply pipelines and fire following earthquakes, lateral movement effects and damage to pile foundations, and the most suitable modeling methods for large ground deformation and buried lifeline response.

It is hoped that the spirit of cooperation fostered by the research program will contribute to a strong and enduring relationship among Japanese and U.S. engineers. It is believed that the accomplishments of this collaborative activity will encourage additional joint projects and lead to improved understanding and mastery in the field of earthquake engineering.

M. Hamada
Professor, Tokai University

T. D. O'Rourke
Professor, Cornell University

ACKNOWLEDGMENTS

Although acknowledgements are given at the beginning of each case history, as appropriate for those who contributed to data collection and manuscript production, special recognition needs to be extended to several people who have been vitally important for the entire U.S.-Japan case history effort. The editors of this volume thank the National Center for Earthquake Engineering Research (NCEER) and the Association for the Development of Earthquake Prediction (ADEP) for sponsoring this project. In particular, thanks are extended to K. Kubo, Professor Emeritus of Tokyo University, and M. Shinozuka, Director of NCEER, who provided oversight and support for cooperative activity. We also remember the encouragement and enthusiasm of Dr. Robert L. Ketter, the late Director of NCEER.

We thank the National Science Foundation (NSF) for its support. In particular, we thank Drs. W. Anderson, C. Astill, and S.C. Liu of NSF for their interest and encouragement.

We extend our sincere thanks to the members of NCEER who helped facilitate the exchange of information and execution of the program. In particular, we thank Andrea Dargush and Jane Stoyle of NCEER for their dedication and excellent service. Special recognition is extended to Ali Avcisoy, Laurie Mayes, and Kristin Stewart whose help and support were indispensable for a successful project.

T. D. O'Rourke
Professor, Cornell University

M. Hamada
Professor, Tokai University

TABLE OF CONTENTS

Volume 2

Preface v

U.S. - Japan Cooperative Research Program ix

Acknowledgments xi

Table of Contents xiii

Large Ground Deformations and Their Effects on Lifeline Facilities:
1906 San Francisco Earthquake
T.D. O'Rourke, P.A. Beaujon and C.R. Scawthorn 1-i

Case Histories of Lateral Spreads Caused by the 1964 Alaska Earthquake
S.F. Bartlett and T.L. Youd 2-i

Large Ground Deformations and Their Effects on Lifeline Facilities:
1971 San Fernando Earthquake
T.D. O'Rourke, B.L. Roth and M. Hamada 3-i

Liquefaction and Ground Failure in the Imperial Valley, Southern California
During the 1979, 1981 and 1987 Earthquakes
R. Dobry, M.H. Baziar, T.D. O'Rourke, B.L. Roth and T.L. Youd 4-i

Large Ground Deformations and Their Effects on Lifeline Facilities:
1989 Loma Prieta Earthquake
T.D. O'Rourke and J.W. Pease 5-i

Large Ground Deformations and Their Effects on Lifeline Facilities: 1906 San Francisco Earthquake

T.D. O'Rourke, Professor
School of Civil and Environmental Engineering
Cornell University
Ithaca, New York

P.A. Beaujon[1]*, Engineer*
GZA GeoEnvironmental, Inc.
Livonia, Michigan

C.R. Scawthorn, Vice President
EQE, Inc.
San Francisco, California

[1] Formerly P.A. Lane, Graduate Research Assistant, Cornell University, Ithaca, New York.

ACKNOWLEDGMENTS

This case history has benefitted from the assistance of many engineers, utility personnel, and public service employees in San Francisco. The authors wish to thank R. Darragh of Dames & Moore for his encouragement and contributions of maps, subsurface information, and oversight stemming from a long and intensive interest in the geology and foundation conditions in San Francisco. Gratitude also is expressed for help rendered by H. Taylor and S. Vandahni of Harding Lawson Associates, Inc., D. Koutsoftas of Dames & Moore, and J. O'Rourke of Woodward-Clyde Associates. The expertise and assistance of G. Hansen, former archivist with the San Francisco Public Library, is gratefully acknowledged. Members of the San Francisco Fire Department helped to procure information related to this study, including E. Condon, F. Blackburn, and G. Anderson. For their assistance in important data related to utilities, the authors thank J. Cooney and T. Dickerman of the San Francisco Water Department; P. T. Law and S. Yu of the Pure Waters Program; and J. Clark and C. H. Lee of the Pacific Gas & Electric Company. Mr. J. Grech of the Streets and Mapping Division of the San Francisco Bureau of Engineering assisted in the collection of elevation survey data.

Several members of the Cornell staff contributed significantly to the work, including B. Roth, who helped collect and organize field data. J. Tyler of the Cornell Library helped retrieve historic photographs, and D. Meredith provided assistance in procuring high quality reproductions of 1906 aerial photographs of San Francisco. The organization, layout, and drafting of all maps was accomplished by A. Avcisoy, to whom the authors are indebted for his high quality and care. The manuscript was typed by K. Stewart.

The case history incorporates portions of previous publications by the authors prepared for the National Center for Earthquake Engineering Research, notably Technical Report NCEER-89-0007, entitled "Liquefaction Hazards and Their Effects on Buried Pipelines," and Technical Report NCEER-89-0032, entitled "Proceedings of the Second U.S.-Japan Workshop on Liquefaction, Large Ground Deformation, and Their Effects on Lifeline Facilities." These sources are included in the reference list at the end of the case history.

TABLE OF CONTENTS

		Page
Acknowledgments		1-iii
Table of Contents		1-v
List of Tables		1-vii
List of Figures		1-ix

Section		Page
1.0	INTRODUCTION	1-1
2.0	TECTONIC SETTING, INTENSITY, AND FELT EFFECTS	1-2
3.0	HISTORIC EARTHQUAKES PRECEDING 1906	1-4
4.0	ZONES OF LIQUEFACTION-INDUCED GROUND MOVEMENT	1-5
	4.1 Zones of Seismic Intensity	1-7
	4.2 Scope of Work	1-9
5.0	HISTORY AND NATURE OF FILLED AREAS	1-10
6.0	MISSION CREEK AREA	1-13
	6.1 Subsurface Conditions	1-13
	6.2 Ground Displacements	1-16
7.0	SOUTH OF MARKET AREA	1-19
	7.1 Subsurface Conditions	1-19
	7.2 Ground Displacements	1-22
8.0	FOOT OF MARKET AREA	1-27
	8.1 Subsurface Conditions	1-27
	8.2 Ground Displacements	1-28
9.0	MARINA AND NORTH POINT DISTRICTS	1-32
	9.1 Marina District	1-32
	9.2 North Point District	1-34
	9.2.1 Subsurface Conditions	1-34
	9.2.2 Ground Displacements	1-35
10.0	OTHER ZONES OF HIGH INTENSITY	1-35
	10.1 Duboce Park	1-35
	10.2 Steiner and Sutter Streets	1-35

Section		Page
	10.3 Lombard and Octavia Streets	1-36
	10.4 Vallejo Street and Van Ness Avenue	1-36
	10.5 Union and Steiner Streets	1-37
11.0	PERFORMANCE OF SAN FRANCISCO WATER SUPPLY	1-37
12.0	SAN FRANCISCO FIRE	1-44
	12.1 Fire Department in 1906	1-44
	12.2 Earthquake-Generated Fires and Spread	1-46
	12.3 Assessment	1-49
13.0	DAMAGE OF THE GAS SUPPLY SYSTEM	1-51
14.0	PIPELINE BREAKS	1-53
15.0	SUMMARY OF GROUND MOVEMENTS	1-56
16.0	CORRELATION OF LATERAL SPREADS WITH SURFACE AND SUBSURFACE GRADIENTS	1-60
17.0	CONCLUDING REMARKS	1-61
REFERENCES		1-66
APPENDIX A		1-71
APPENDIX B		1-127

LIST OF TABLES

Table		Page
1	Summary of Reservoirs and Water Capacity at Time of Earthquake	1-40
2	Original Ignitions Following 1906 Earthquake	1-47
3	Summary of Lateral Spreads, Surface, and Subsurface Gradients of Locations of Documented Lateral Deformation During the 1906 Earthquake	1-62

LIST OF FIGURES

Figure		Page
1	Map Showing Observed Length of Fault Rupture and MMI for 1906 San Francisco Earthquake	1-4
2	Building Damage in the Foot of Market Area After the 1868 Earthquake	1-6
3a	Distribution of Earthquake Intensity (Modified Mercalli Scale), 1906 Earthquake, San Francisco County	1-8
3b	Zones of MM IX-X Intensity in Study Area, Northeast Section of San Francisco	1-8
4a	Zones of Disturbance Versus Areas of Fill	1-8
4b	Zones of MM IX-X Intensity Versus Fill in Study Area	1-8
5	The Development of the Shoreline in San Francisco Since 1853	1-11
6	Location of Mission Creek Zone	1-14
7	Mission Creek Study Area	1-14
8	Soil Profile Along Mission St. in Mission Creek Area	1-15
9	Earthquake-Induced Ground Movements in Mission Creek Zone	1-17
10	Location of South of Market Zone	1-20
11	South of Market Study Area	1-20
12	Soil Profile Across Head of Old Sullivan Marsh in South of Market Area	1-21
13	Earthquake-Induced Ground Deformations in South of Market Area	1-23
14	Aerial Photograph Showing Liquefaction-Induced Ground Deformation in the South of Market Area	1-25
15	Detailed Map Showing 1906 Ground Deformation in the Area Bounded by Mission, Howard, 7th, and 5th Sts.	1-26
16	Location of the Foot of Market Zone	1-28
17	Soil Profile Near the Embarcadero in the Foot of Market Area	1-29

Figure		Page
18	SPT Values (Blow Counts) Representative of Fills in the Foot of Market Area	1-30
19	Earthquake-Induced Ground Movements in Foot of Market Area	1-31
20	Location of Marina and North Point Areas	1-33
21	1906 Waterfront and Earthquake Damage Relative to Current Marina Street System	1-33
22	1906 San Francisco Water Supply	1-38
23	1906 Water Supply Within San Francisco City Limits	1-40
24	San Francisco Water Supply and Area Burned During the Fire	1-42
25	Reservoir Storage in San Francisco as a Function of Time After the Earthquake	1-44
26	Ignitions in CBD Following the San Francisco Earthquake, at Approximately 6:00 a.m., April 18, 1906	1-48
27	Fires Extinguished and Spread of Initial Ignitions, from Approximately 6:00 to 8:30 a.m., April 18, 1906	1-48
28	Fires and Burnt Sections of San Francisco, at Approximately Midnight, April 18, 1906	1-50
29	Gas Pipeline Feeder System in 1906 San Francisco	1-52
30	Pipeline Breaks and Street Settlements in San Francisco After 1906 Earthquake	1-54
31	Idealized Section Through Lateral Spread	1-58
32	Zones of Potential Large Ground Displacements in San Francisco	1-59
33	Plot of Magnitude of Lateral Movement versus Surface Slope at Locations of 1906 Lateral Spreading	1-62
B.1	Surface Elevation Contours for the South of Market Area	1-128
B.2	Surface Elevation Contours for the Mission Creek Area	1-128

1.0 INTRODUCTION

The 1906 San Francisco earthquake was perhaps the most important seismic event in U.S. history, and among the most significant in the world-wide catalog of destructive earthquakes. The great extent of surface rupturing and widespread area of damaging effects resulted in numerous scientific and engineering studies. As indicated by Ellsworth (1990), the 1906 displacements on the San Andreas fault and associated strain in the adjoining crust prompted Reid (1910) to develop an elastic rebound model for explaining the earthquake source. His theoretical treatment remains today as the principal model of the earthquake cycle.

From an engineering and planning perspective, the 1906 San Francisco earthquake is of considerable interest. The earthquake showed how local geology and soil conditions play a key role in the severity of both shaking and permanent ground deformation. The investigations by Lawson, et al. (1908) show in detail areas of fill and "made" ground in San Francisco where damaging effects of the earthquake were concentrated, thus distinguishing such locations as being vulnerable to seismic excitation. The recognition and characterization of locally vulnerable areas is pursued currently through microzonation and studies of site response and site amplification. Although it was not clearly understood at the time, it is known now that much of the observed permanent deformation was caused by soil liquefaction. A reexamination in recent years of the ground deformations in 1906 (e.g., Youd and Hoose, 1978; O'Rourke and Lane, 1989) has helped in delineating current hazards and in understanding the mechanisms of liquefaction and associated soil movements.

One of the most distinctive features of the earthquake was its influence on lifeline systems and the repercussions of such damage in the urban environment. Fault rupture and violent shaking of timber bridges ruptured the three principal transmission pipelines which conveyed water to San Francisco from reservoirs south of the city. Breaks in the trunk line system for water distribution at locations of liquefaction cut off most of the storage supply inside San Francisco to the burning financial, South of Market, and Mission districts of the city. Approximately 490 blocks were destroyed by fire and an additional 32 were severely damaged (Gilbert, et al., 1907), making the aftermath of the

1906 earthquake the worst single fire loss in U.S. history.

This case history focuses on large ground deformations and related lifeline damage in the City of San Francisco. It is recognized that ground deformations and lifeline disruption occurred at other locations throughout the region affected by the 1906 earthquake. Concentration on San Francisco, however, emphasizes the urban environment. It takes advantage of an extensive body of written accounts, photographic evidence, and subsurface boring records for the city, which could not have been evaluated as comprehensively if the scope of the study had been extended to a broader geographical area. Moreover, San Francisco has been affected by several major earthquakes, with evidence of soil liquefaction recurring in certain parts of the city as many as three times during the years of 1868, 1906, and 1989. Accordingly, the city provides a data base of observed performance and soil conditions which can shed light on the mechanisms of liquefaction, large ground deformation, recurrence and changes in liquefaction, and effects on the buried infrastructure.

Regional seismicity and overall effects of the 1906 earthquake are discussed, followed by a review of soil conditions, land development, and local intensities within the City of San Francisco. Ground deformations and subsurface conditions in the principal areas of 1906 liquefaction are described. The effects of the earthquake on the water transmission and distribution systems are discussed. Earthquake effects on the gas trunk main system also are described. The earthquake fire and its relationship with lifeline damage is analyzed.

2.0 TECTONIC SETTING, INTENSITY, AND FELT EFFECTS

The earthquake occurred on April 18, 1906 at 5:12 a.m. Pacific Standard Time. The main shock had an epicenter near San Francisco (Bolt, 1968). The duration of strong ground shaking was approximately 45 to 60 seconds, the timing of which varied slightly depending on location (Lawson, et al., 1908).

A magnitude of 8.3 commonly is assigned to the earthquake on the basis of Richter's assessment (1958). This magnitude is consistent with an earlier estimate of 8.25 published by Gutenberg and Richter (1954). Thatcher (1975) analyzed

the spectral amplitudes of long period (50 - 100 sec.) surface waves from seismograms published by Lawson, et al. (1908) to obtain an average seismic moment, M_o, of 4.0 x 10^{27} dyne-cm. Using the moment magnitude scale proposed by Hanks and Kanamori (1979), this seismic moment corresponds to a moment magnitude, M_w, of 7.7. As observed by Hanks and Kanamori, the magnitude derived from seismic moment implies that the level of energy released for the 1906 event was below the threshold of a great earthquake. After reviewing the historic and seismological interpretations of the earthquake, Ellsworth (1990) has retained the traditional 8.25 magnitude, except for instances in which quantitative assessments require seismic moment.

The causative fault of the 1906 earthquake is the San Andreas fault, which is the principal rupture complex within a system of faults, predominantly right lateral strike slip in nature, that accommodate most relative movement between the North American and Pacific Plates (Wallace, 1990). The earthquake was generated by rupturing along the northernmost 430 km of the San Andreas fault from just north of San Juan Bautista to Cape Mendocino. The largest relative displacements across the fault were in Marin County, with several locations showing movement of 4.7 m as well as a maximum of 6.4 m on alluvial soil approaching Tomales Bay west of Point Reyes Station (Richter, 1958). The San Andreas fault system has been the subject of numerous studies, most notably a recent collection of papers edited by Wallace (1990), and the reader is referred to these sources for additional details regarding faulting and seismicity.

The shock was felt as far north as Coos Bay, Oregon to as far south as Los Angeles, California, and to the east as far as Winnemucca, Nevada, 480 km inland from the coast (Lawson, et al., 1908). Ground failures were triggered by the earthquake over a 600-km-long segment of the Coast Range (Youd and Hoose, 1978). Lawson, et al. estimated that approximately 454,000 km^2 inland from the coast were affected by perceptible ground shaking. Figure 1 shows a map of the observed fault rupture length and zones of Modified Mercalli Intensities (MMI) associated with the earthquake. The MMI zones were plotted on the basis of interpretations published by Steinbrugge (1982) and Richter (1958). Figure 1 shows an MMI pattern of nearly elliptical and elongated zones, many of which are subparallel to the San Andreas fault and coincident with alluvial valleys. One of the most remarkable features of the earthquake was the clear

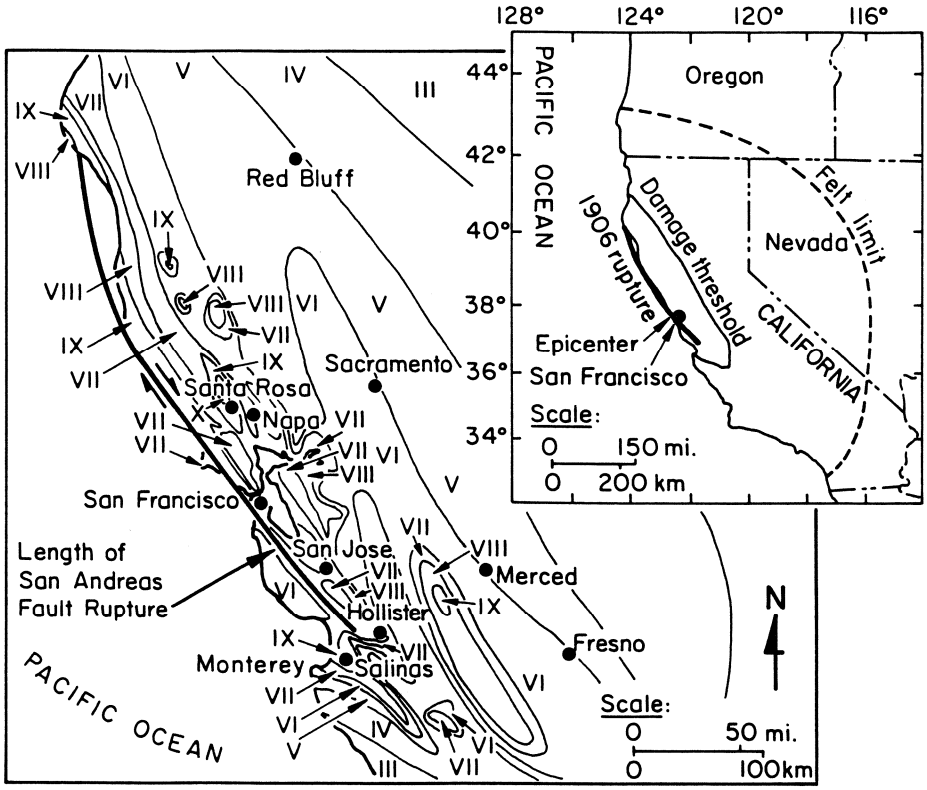

Figure 1. Map Showing Observed Length of Fault Rupture and MMI for 1906 San Francisco Earthquake (after Lawson, et al., 1908; Steinbrugge, 1982)

correlation between seismic intensity and geologic conditions. This is evident on a regional scale, where areas of strongest shaking correspond to sediment filled valleys, and on a local level, as will be illustrated later by a detailed examination of San Francisco.

It frequently is quoted that the earthquake caused 700 deaths, although Richter (1958) has stressed the uncertainty associated with such a body count. Historic data collected and evaluated by Hansen and Condon (1989) suggest that there was considerable political and economic pressure to downplay mortality and property loss statistics related to the earthquake. As a consequence of these types of investigations, it now is believed that the estimated 700 deaths from earthquake and fire are low by a factor of 3 to 4 (Ellsworth, 1990).

3.0 HISTORIC EARTHQUAKES PRECEDING 1906

There were several earthquakes in the 19th century which affected San Francisco

and the San Francisco Bay region. The earthquakes of 1836, 1838, and 1868 are discussed by Richter (1958) and Ellsworth (1990). The probable sources for the 1836 and 1838 earthquakes are the Hayward and San Andreas faults, respectively. The 1868 earthquake on the Hayward fault was preceded by an earthquake on the eastern side of San Francisco Bay in 1865, which caused damage and was recorded by newspaper accounts in San Francisco (e.g., Hansen and Condon, 1989). For the 1865 earthquake, Holden (1898) reports: "On the marshy lands in the vicinity of Howard and Seventh Streets, lampposts, water pipes and gas pipes were broken and thrown out of position. The ground on Howard Street from Seventh to Ninth cracked open, leaving a fissure nearly an inch wide."

The 1868 earthquake had severe effects in San Francisco, and prior to the 1906 event was referred to as "the great San Francisco earthquake" (Ellsworth, 1990). There was substantial damage to structures on "made" ground, especially those near the foot of Market St. where loose sandy fill had been placed in Yerba Buena Cove to reclaim land from the bay. Holden (1898) also noted: "As in 1865, a small crevasse was opened on Howard Street, beyond Sixth." The 1865 and 1868 movements in the South of Market area were precursors of the substantial deformations observed in the same vicinity during the 1906 earthquake.

Figure 2 shows a portion of a map published by Lawson, et al. (1908) that illustrates the most heavily damaged area of San Francisco in 1868. In the figure, the street system and then current waterfront are superimposed on the original shoreline to indicate the area of recent filling. There is a clear concentration of damaged buildings on recent fill, with most of the damage located within a zone, two to three blocks wide, adjacent to and outboard of the old shoreline.

4.0 ZONES OF LIQUEFACTION-INDUCED GROUND MOVEMENT

The aim of this case history is to describe and quantify liquefaction-induced ground movements which occurred in San Francisco. The work draws upon the results of previous studies (e.g., Youd and Hoose, 1978; Hovland and Darragh, 1981; Roth and Kavazanjian, 1984; O'Rourke and Lane, 1989), all of which have focused on the San Francisco area. It expands on the investigations of O'Rourke and Lane (1989) to clarify further the soil and groundwater conditions

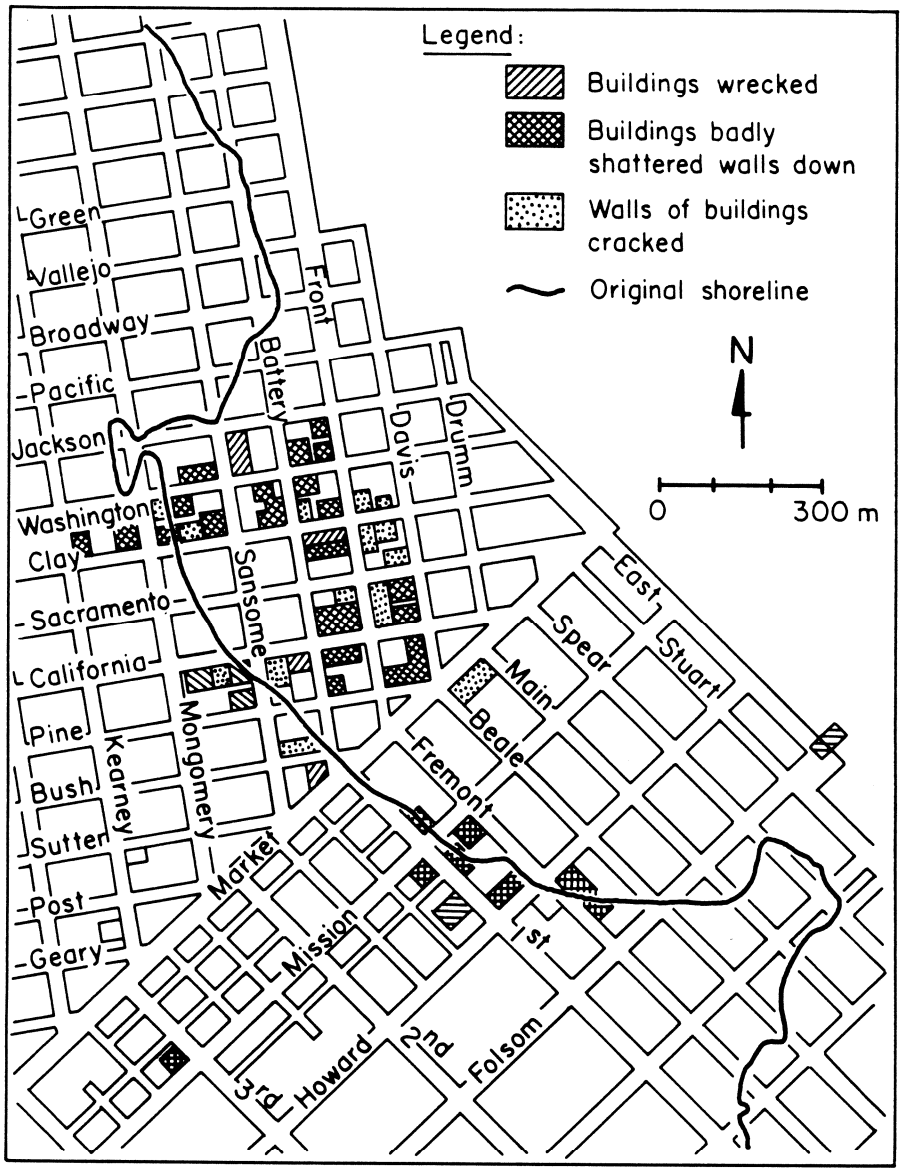

Figure 2. Building Damage in the Foot of Market Area After the 1868 Earthquake (after Lawson, et al., 1908)

at liquefaction sites and to develop maps of ground deformation patterns as they relate to subsurface soils and buried topographical features. The study also evaluates the pattern of damage in the water pipeline system at the time of the earthquake by mapping pipeline breaks in relation to ground movements and subsurface conditions.

4.1 Zones of Seismic Intensity

Figure 3 shows the variation of earthquake intensity in the San Francisco peninsula. The earthquake intensity is expressed in terms of the Modified Mercalli system as proposed by Richter (1958) from an intensity scale originally developed for the San Francisco earthquake, which was reported by Lawson, et al. (1908).

Most of the City of San Francisco was influenced by an intensity of MMI VII to VIII, whereas only about 5% of the built-up area was affected by MMI IX to X. Zones of MM IX to X intensity are useful for delineating locations of earthquake-induced ground failures. An enlarged map of northeast San Francisco is shown in Figure 3b to define more clearly the zones of high intensity in the most heavily developed portion of the city.

It has been pointed out by several researchers (e.g., Lawson, et al., 1908; Youd and Hoose, 1978) that severe movements at the time of the earthquake occurred in areas where fill had been placed along the waterfront, inlets, coves, marshes, and ravines. In Figure 4a, areas of fill (Schlocker, 1974) are mapped in conjunction with zones of large permanent ground deformations delineated by Youd and Hoose (1978) and Hall (1906). Three major zones of ground failures were identified by Youd and Hoose as the Mission Creek, South of Market, and Foot of Market Zones, and each of these are shown in the figure by heavy solid lines. In Figure 4b, areas of fill are mapped in conjunction with zones of MM IX to X intensity. It can be seen from Figures 4a and b that there is a close correspondence between areas of fill, zones of high earthquake intensity, and locations of large permanent ground movements.

Figure 4b provides a convenient reference for identifying locations of potentially large earthquake-induced movements, and serves in this work as a means of organizing the discussion according to three general areas of displacement. The first area of study includes the zones of permanent soil movements mapped by Youd and Hoose (1978) as the Mission Creek, South of Market, and Foot of Market Zones. The second general area includes the Marina and North Point Districts along the northern shoreline. Substantial amounts of fill were placed between 1908 and 1930 in these two areas, with the result that the soil

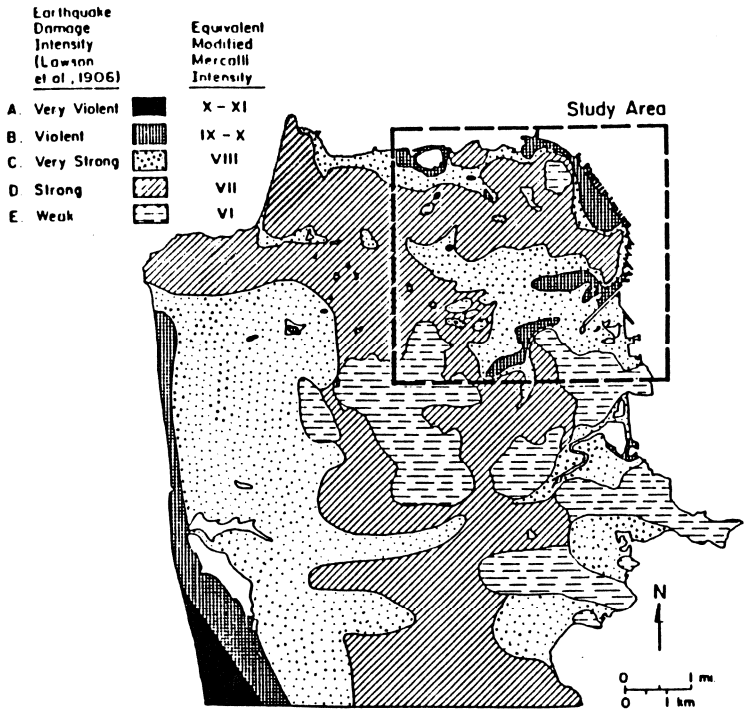

Figure 3a. Distribution of Earthquake Intensity (Modified Mercalli Scale), 1906 Earthquake, San Francisco County (after Youd and Hoose, 1978; Lawson, et al., 1908)

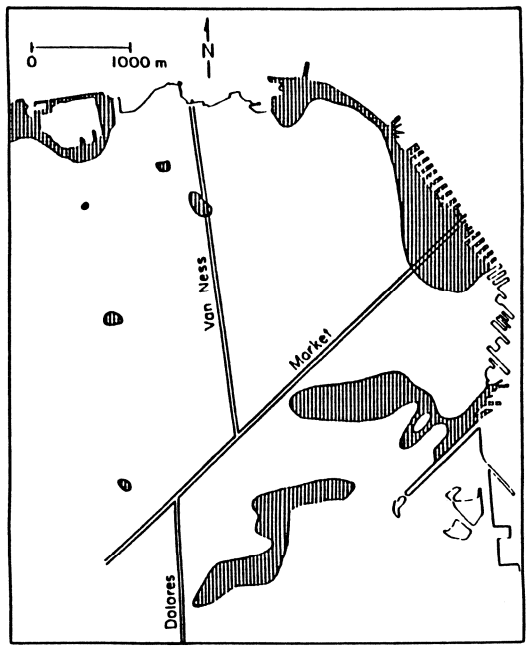

Figure 3b. Zones of MM IX-X Intensity in Study Area, Northeast Section of San Francisco (after Lawson, et al., 1908)

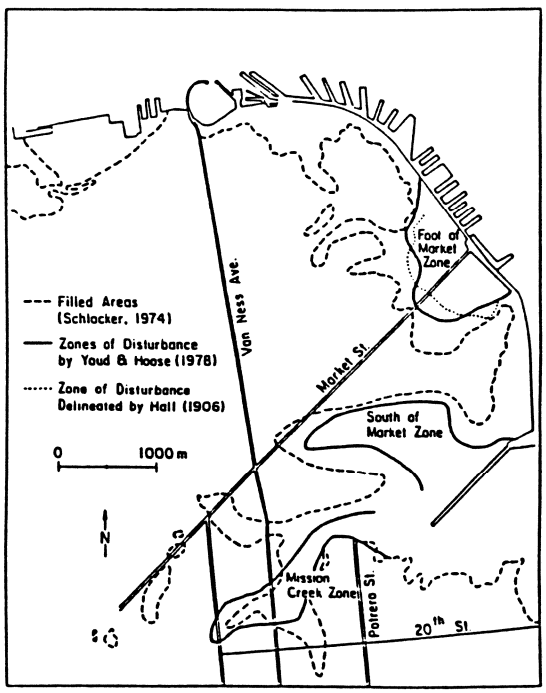

Figure 4a. Zones of Disturbance (after Youd and Hoose, 1978; Hall, 1906) Versus Areas of Fill (after Schlocker, 1974) in Study Area

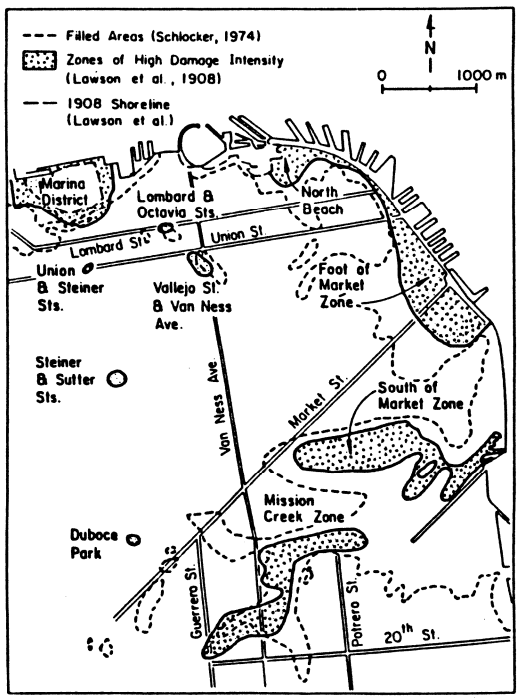

Figure 4b. Zones of MM IX-X Intensity Versus Fill in Study Area

conditions are similar to those in areas which experienced extensive ground deformation during the 1906 earthquake. The third general area includes several small zones which were identified on the basis of high earthquake intensity (equivalent to MM IX) by Lawson, et al. (1908) at the following locations: 1) Duboce Park, 2) Steiner and Sutter Sts., 3) Union and Steiner Sts., 4) Vallejo St. and Van Ness Ave., and 5) Lombard and Octavia Sts.

4.2 Scope of Work

To delineate the boundaries of the filled areas at the time of the earthquake, the original topographical features drawn on the 1853 and 1857 U.S. Coast Surveys of the City of San Francisco and Its Vicinity (U.S. Coast Survey, 1853; 1857) were related to the 1906 street maps, soil surveys (Schlocker, 1974), and current street and topographic maps. Features such as Nob Hill, Potrero Hill, and Russian Hill were used to fix the superposition of the original 1853 survey and later maps showing the street system. Available literature also was reviewed for information on subsurface conditions in each zone (e.g., Youd and Hoose, 1976, 1978; Hall, 1906; Hovland, 1980; Schlocker, 1974), the history and nature of the fills (Dow, 1973; Olmsted, et al., 1977; Roth and Kavazanjian, 1984; Hovland and Darragh, 1981), and the liquefaction potential of subsurface soils (Roth and Kavazanjian, 1984; Youd and Hoose, 1978).

From a review of photographs and historical accounts (e.g., Schussler, 1906; Youd and Hoose, 1976, 1978; Lawson, et al., 1908; Gilbert, et al., 1907; Duryea, et al., 1907; Himmelwright, 1906; Hyde, 1906; Leonard, 1906; Derleth, 1906; Kurtz, 1906; Jordan, 1907; Hall, 1906; Newman, 1906; Hovland, 1980; Reynolds, 1906; Jones, 1906), a catalog of ground displacements was compiled. Several hundred photographs were examined, of which over 100 were selected for detailed study of the ground displacements within the zones of high damage intensity. Cultural objects with standard dimensions, such as curb stones, bricks, and the separations between utility poles, were used to judge the magnitude of movement and distance between points of displacement. Table A.1, given in the Appendix, lists the documented permanent ground deformations from both photographs and literature.

The interpretation of ground movement patterns was aided by reference to a map

of earthquake-induced pipeline breaks prepared by Manson (1908), and a report on the pipeline system performance by Schussler (1906). Fire insurance maps of building stock (e.g., Sanborn Ferris, Inc., 1899; 1905) were studied in conjunction with the photographic record to identify locations and to evaluate the approximate dimensions of ground movements and damage apparent in the photos.

5.0 HISTORY AND NATURE OF FILLED AREAS

The zones of "made" or filled land have been identified as areas of high damage intensity during the 1906 earthquake. In this section, the history and nature of these filled zones are discussed to provide a better understanding of their behavior during the earthquake. A summary of the changes in the shoreline of San Francisco is shown in Figure 5 relative to the streets, thus giving a picture of the progression of filling operations relative to the time span over which they occurred.

Filling of the Yerba Buena Cove was begun in the 1850s. Long wharves were built into the deeper water to accommodate ocean-going ships at Market, California, Washington, Jackson, Pacific, and Broadway Sts. Crosswalks were built perpendicularly to connect the wharves (later, these crosswalks became Sansome, Battery, and Drumm Sts.). A program of cut and fill then was initiated in which the sand dunes to the west were systematically excavated and the material was loose-dumped between the wharves and crosswalks. When a sea wall was constructed, beginning in 1867, the bay mud dredged for its foundations also was used for fill (Roth and Kavazanjian, 1984). Refuse from the city and from several industries also was dumped into the water lot areas (Hall, 1906; Olmsted, et al., 1977; Goldman, 1969). Filling operations in the previous cove were completed by 1900 (Roth and Kavazanjian, 1984).

Before the development of the city, several valleys cut through the high rocky ridges which rimmed the eastern shore of the former Mission Bay. The most prominent of these was Mission Valley, which opened into the bay between Rincon and Potrero Points (Lawson, et al., 1908). One arm of the valley extended northwestward towards 7th and Mission Sts. (South of Market Zone). This formerly was the site of a salt marsh known as Sullivan's Marsh (Hall, 1906). The

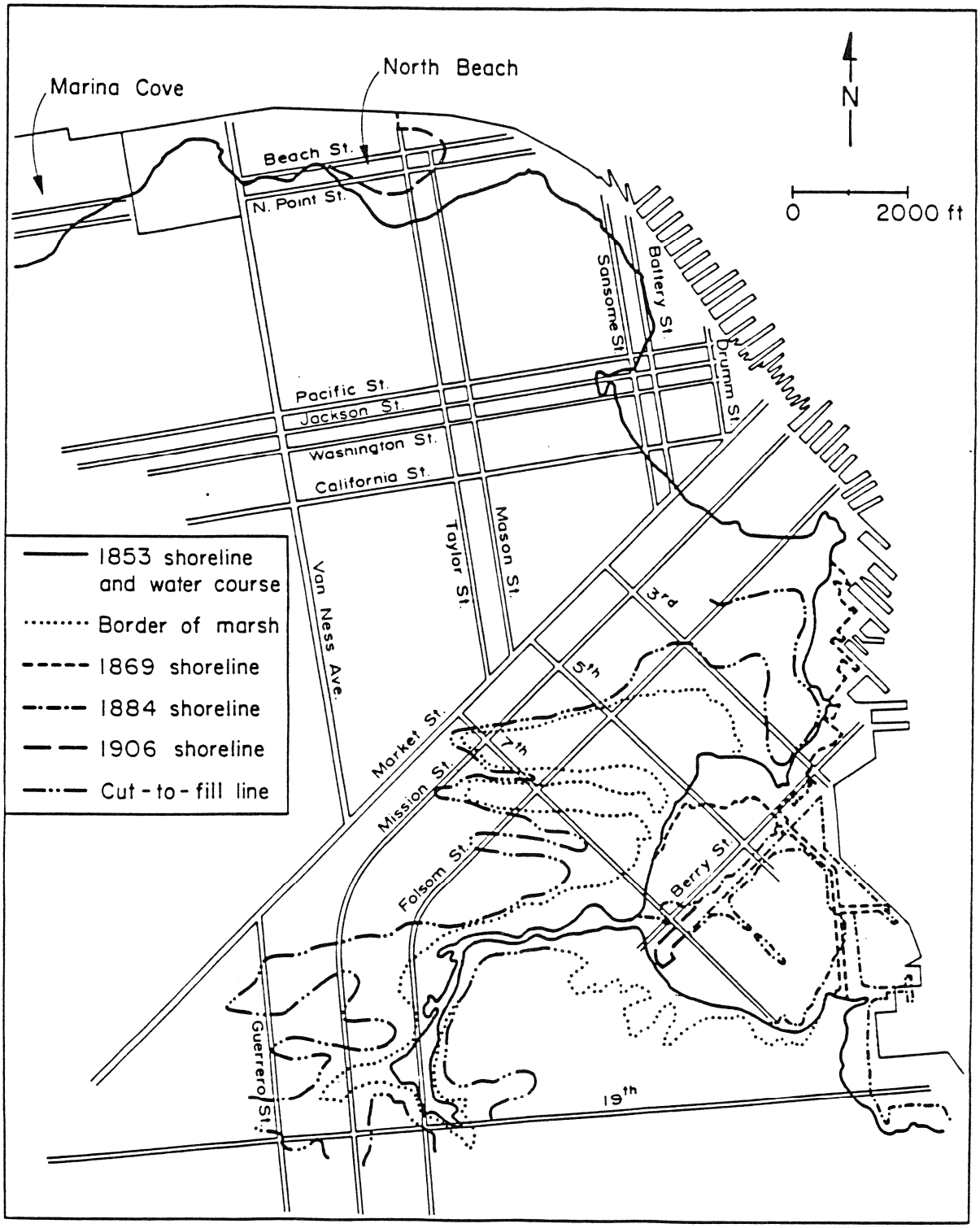

Figure 5. The Development of the Shoreline in San Francisco Since 1853 (after Olmsted, et al., 1977; Roth and Kavazanjian, 1984; Hovland and Darragh, 1981)

marsh has been described as "subterranean lakes, forty to eighty feet deep (12 to 24 m), crusted with a ten-foot (3-m) layer of peat strong enough to bear the weight of a small house..." (Brown, et al., 1932). The former Mission Creek wound around Potrero Hill and then south and westward into a tidal lagoon and contiguous salt marsh (Lawson, et al., 1908) as far south as 19th and Guerrero (Mission Creek Zone). South of the city was another prominent valley, Islais Creek, which emptied into Mission Bay as well.

Difficulties were encountered in filling sections of Folsom St., which crossed Sullivan's Marsh. The marsh was filled mainly with sand, which often settled as much as 2 m overnight, displacing the mud and causing it to heave (Brown, et al., 1932). By 1869, filling had been completed in Sullivan's Marsh as well as a portion of the north shore of Mission Bay, although Mission Creek still was shown on the 1869 U.S. Coast Survey map (Olmsted, et al., 1977). The 1877 Sanborn Index Map (Olmsted, et al., 1977) showed that filling had been completed in the Mission Creek area, with additional fill having been placed along the north shore of Mission Bay as far as Berry St.

The southern portion of Mission Bay below the channel was filled during the period 1884 to 1906 (Hovland, 1980). During this time, the sand dunes already had been removed, and thus the fill probably consisted of rock and refuse debris (Hovland and Darragh, 1981). Lawson, et al. (1908) state that much of the material used in filling the bay was broken rock taken from the grading of neighboring rocky hills.

To protect the water lots at Marina Cove, a sea wall (known as Fair's Seawall) was begun in the early 1890s along the alignment of the current Marina Boulevard. The fill consisted of sand and rock from the San Bruno Mountain quarry and spoil from nearby excavations. Beginning in 1912, fill was placed south of the sea wall to prepare the site for the 1915 Panama-Pacific Exposition. This fill was sand and mud pumped from offshore (Olmsted, et al., 1977). Although the majority of filling was completed by 1915, some minor filling north of Marina Boulevard continued into the 1930s (Olmsted, et al., 1977).

North Beach Cove on the northern shore of San Francisco (see Figure 5) was too shallow to serve as a site for anchoring ships. This area was largely

undeveloped at the time of the earthquake. In the vicinity of North Beach, the majority of the filling was done between 1906 and 1915 (Roth and Kavazanjian, 1984). The fill along North Point St. up to Mason St. dates from the mid-1880s, and at Taylor St. to Beach St. from before 1905.

6.0 MISSION CREEK AREA

The location of the study area for Mission Creek is shown in Figure 6. The Mission Creek area is the site of a former tidal creek and neighboring salt marsh. The locations of the former water course and marsh are shown in Figure 7 as horizontally hatchured and dotted areas, respectively. The elevation contours associated with the former topography and various landform features were taken from the 1853 and 1857 U.S. Coast Surveys.

6.1 Subsurface Conditions

A cross-section traversing the western section of the filled zone is shown in Figure 8, and is located by the line A-A' in Figure 7. The cross-section was prepared from soil borings performed in 1964 for the Bay Area Rapid Transit (BART) system along Mission St. The borings were performed under the supervision of Harding Lawson Associates, Inc., and were made available in this study by courtesy of Parsons, Brinckerhoff, Quade & Douglas, which was part of the engineering group that designed BART, and Harding Lawson. A similar soil profile was prepared by Youd and Hoose (1978) from the same borings. The in-situ penetration data shown in the figure were obtained with a split spoon sampler of 63 mm internal diameter driven by a 1700 kN weight falling 600 mm. Accordingly, the blow counts are not consistent with those obtained by means of the Standard Penetration Test (SPT) (ASTM, 1989) and should not be used in conjunction with liquefaction susceptibility relationships, such as those proposed by Seed, et al. (1983). The borings, however, do provide useful information about the stratigraphy, depth of water table, and relative density of sand deposits on the basis of the relative penetration values.

In general, the cross-section in Figure 8 is consistent with the subsurface topography mapped in Figure 7. The soil borings show loose sandy fill between 17th and 18th Sts., with a maximum depth of approximately 10 m near 18th St.

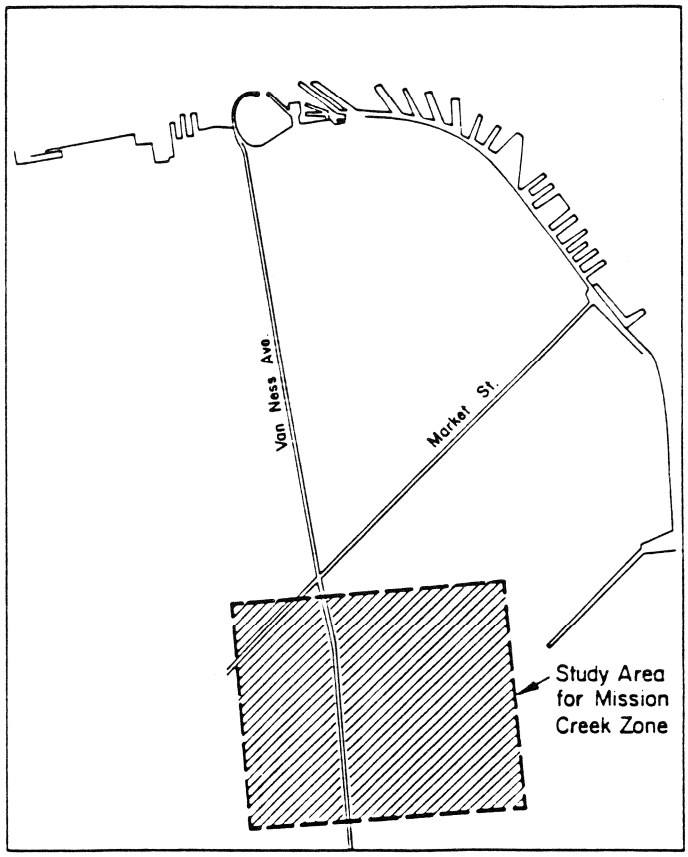

Figure 6. Location of Mission Creek Zone

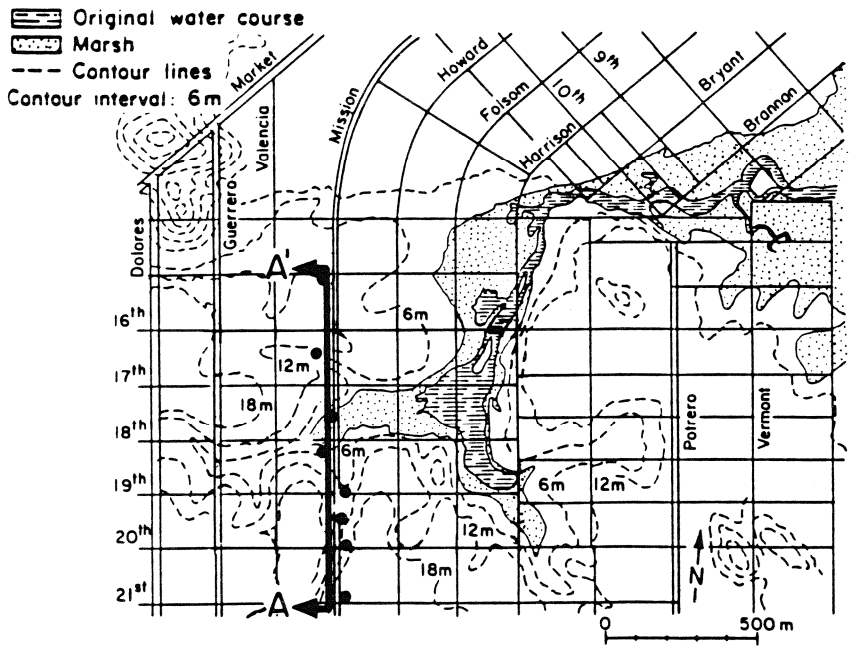

Figure 7. Mission Creek Study Area

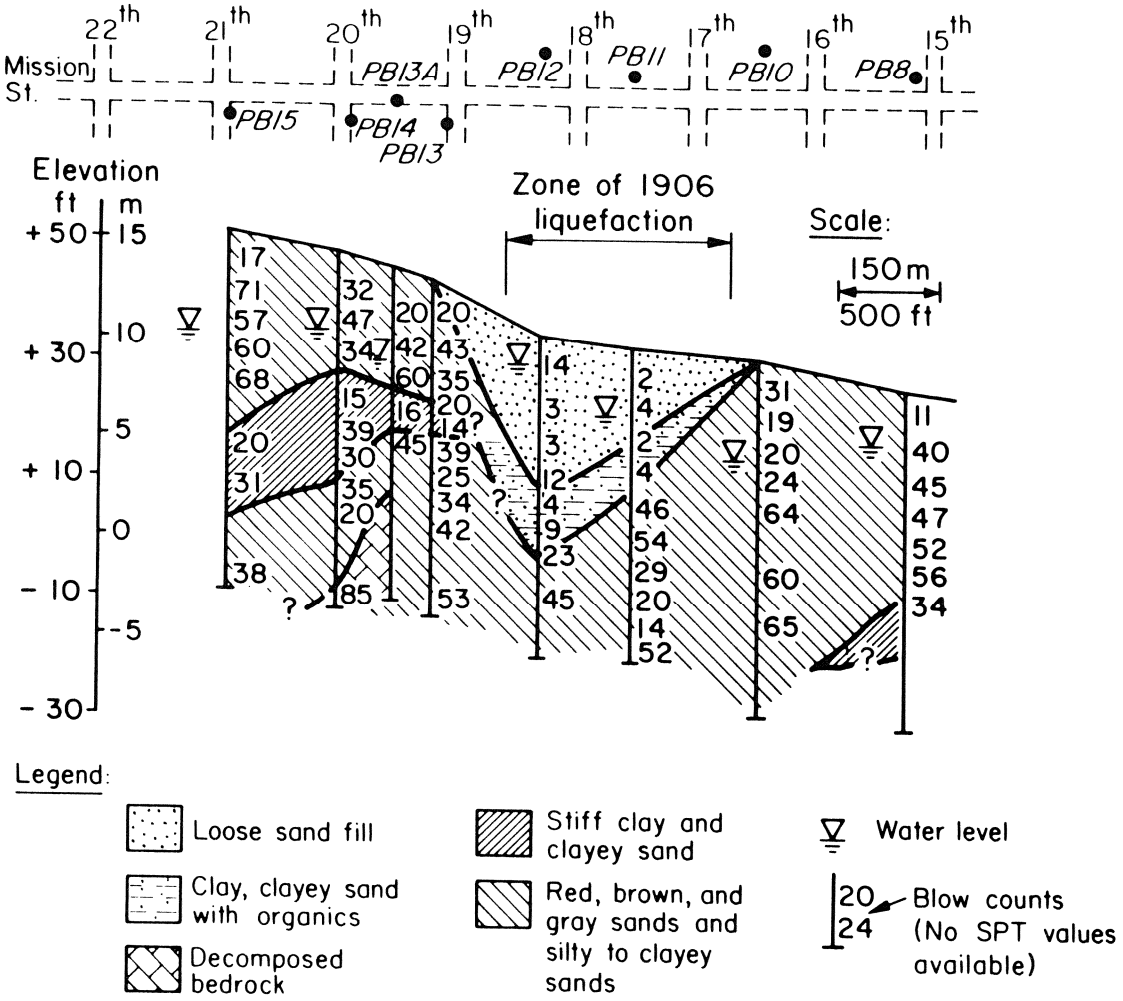

Figure 8. Soil Profile Along Mission St. in Mission Creek Area

The lateral extent of this fill correlates well with the width of the old Mission Creek channel at this location. The fill is underlain by relatively soft organic clay, which again correlates well with the previously mapped marsh conditions at this site.

The cross-section shows the water table at a depth of 1.5 to 5 m between 17th and 18th Sts., where large horizontal and vertical ground movements were reported after the 1906 earthquake (Youd and Hoose, 1978). The average slope for this district is relatively flat; for example, between 19th and Guerrero Sts. and the freeway near 14th St., the slope is on the order of 0.6 percent (0.3 degrees) (Youd and Hoose, 1978). Nevertheless, locally steeper slopes exist.

Between 18th and 19th Sts. in the vicinity of Valencia, for example, the slope is nearly 2 percent (1.1 degrees).

6.2 Ground Displacements

Figure 9 is a map of ground movements which occurred during the 1906 earthquake superimposed on the original topography in the Mission Creek Zone. There are two distinct regions in this zone where large displacements were observed, Zones A and B, as shown in the figure.

There is a close relationship between the original topography and the direction and distribution of soil displacements, as seen in Figure 9c. Even relatively small topographical features, such as the ravine underlying 19th St. between Guerrero and Valencia Sts., influenced ground deformation. At this location, soil movements were canalized by the course of the buried creek. The direction of lateral spreading changed through 90 degrees, from a northerly direction on 19th St. to an easterly direction near Valencia St.

The most severe distortions occurred in areas where the former ravines narrowed, thereby restricting movements to a limited zone. In the region formerly known as "The Willows" (Hall, 1906), along Valencia St. between 18th and 19th Sts., some of the most extreme disturbances occurred. The ground spread eastward down the center of the former channel of the stream, with maximum displacements of 1.8 to 2.4 m over a distance of 45 to 60 m. The displacements were largest directly in front of the former Valencia Hotel, which collapsed in response to the movements. The street sank a maximum of 1.5 m in front of the hotel. The combined horizontal and vertical movements were responsible for the destruction of two water mains, a brick sewer, gas mains, electric and telephone conduits, and cable car tracks.

On Howard St., toward the center of the block, examples of bearing capacity ground failure can be seen in photographs of wood frame houses which were left tilting severely off vertical. The street and the adjacent land in front of the houses settled considerably, up to as much as 1.5 m in areas. Immediately after the earthquake, only about one-third of all the buildings within a four-block area, between 17th and 18th Sts. from Folsom to Valencia Sts., were left

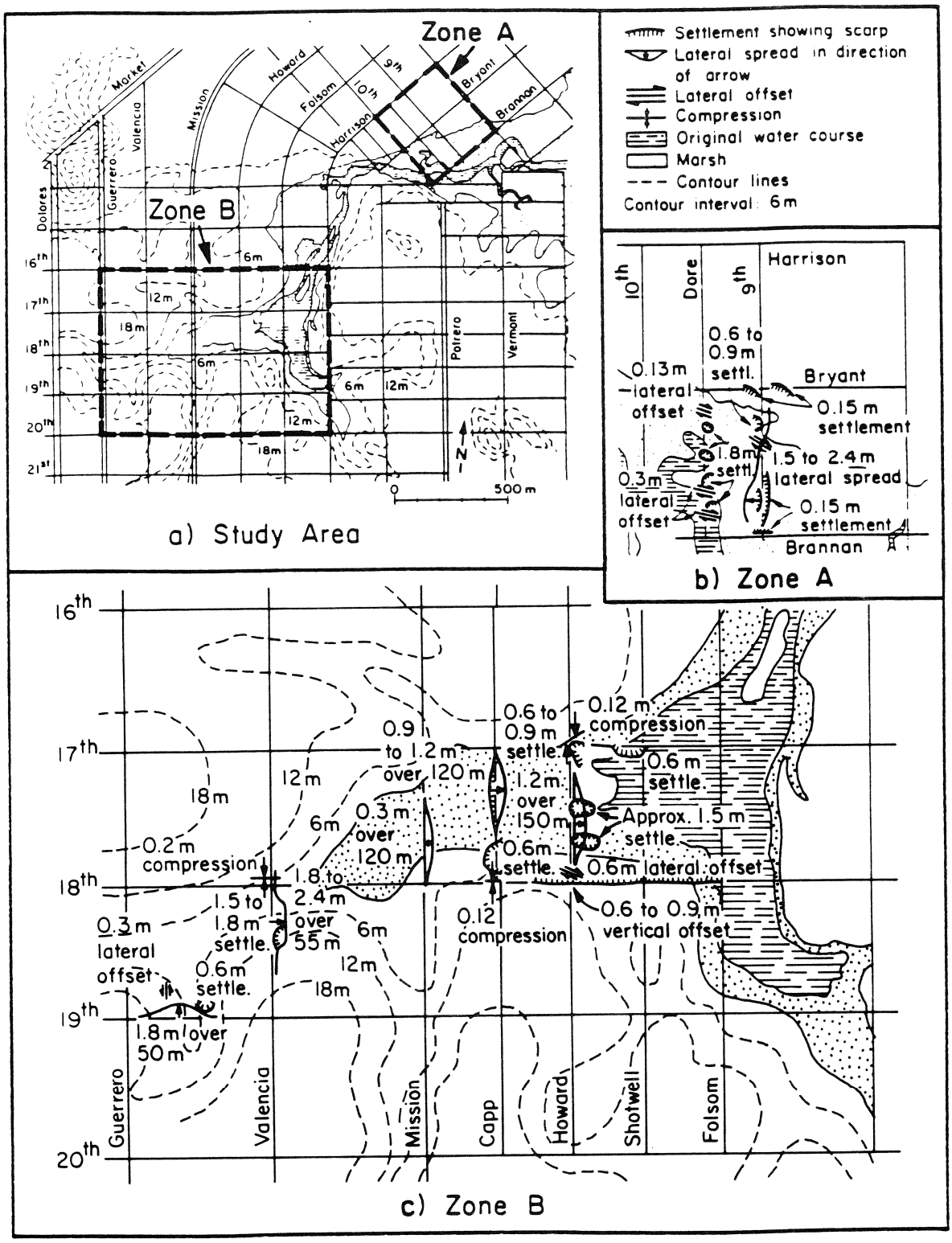

Figure 9. Earthquake-Induced Ground Movements in Mission Creek Zone

in a vertical position (Lawson, et al., 1908).

Compressiive deformations were manifested in the buckling of a granite curb on Capp St. and the arching of cable car tracks on Valencia and Howard Sts. These locations of compression are inconsistent with the general pattern of lateral spreading and subsidence in the area. As soil subsides and spreads laterally, it should result in a net tension at the boundaries of the displacement zone. Tensile fractures can be traced along 18th St., between Folsom and Capp Sts., where slumping of 0.6 to 0.9 m left pavement blocks pulled apart laterally.

One explanation for the strong compressional features is that they are remnants of dynamic compression strains, accentuated because of the liquefied nature of the soil and the abrupt boundary conditions. This type of incoherent motion has been described by Youd (1984) as the result of ground oscillations within zones of soil liquefaction.

The eastern limit of the horizontal ground movements was Folsom St., the edge of the former estuary. Although street settlement was reported along Folsom and Harrison Sts. between 18th and 13th Sts. (Schussler, 1906), no photograph of ground movement in this vicinity could be found.

The other zone of large ground distortions, Zone A in Figure 9b, lies in a two-block area near the mouth of the former Mission Creek, bounded by Brannan, Bryant, 9th, and 10th Sts. In this section, the course of the former creek narrowed as it wound around Potrero Hill immediately to its south, and then widened towards its outlet into Mission Bay. Much of Dore St. towards the northern end of the block overlies a former tributary to Mission Creek, and the southern portion of Dore St. near Brannan St. is directly over a bend in the creek itself. Because of this region's close proximity to the former sand dunes, it is probable that the fill here is mostly dune sand. The liquefaction of this material would explain the large ground movements which occurred in the two-block region.

Large wave-like deformations were reported and photographed along Dore St. Although these deformations had the appearance of wave forms, they were most likely a result of subsidence. A close inspection of several photographs shows that these "waves" can be explained as a succession of local settlement

depressions.

The lateral displacement along Dore St. was eastward, except for a prominent westward offset near Bryant St. This offset was part of the general southwestern slippage toward the former creek channel from Bryant St. Along 9th St., slumping and lateral spreading were westward towards the former channel. A general pattern of slumping can be detected in Figure 9b towards the center of the block bounded by 9th, Dore, Bryant, and Brannan Sts.

7.0 SOUTH OF MARKET AREA

The South of Market Zone is the site of the old Sullivan Marsh, a tidal marsh which once was contiguous with two small tidal streams. Figure 10 locates the South of Market Zone in the downtown area of San Francisco. Figure 11 shows the outline of the former marsh and of the original shoreline of Mission Bay to the south of Brannan St. The ground displacements of the South of Market Zone fall within the boundary of this former salt marsh. This area was filled during the years between 1850 and 1860, predominantly with material excavated from the nearby sand dunes (Roth and Kavazanjian, 1984).

7.1 Subsurface Conditions

A cross-section traversing the northernmost portions of the old Sullivan Marsh is shown in Figure 12, and is located by the line B-B' in Figure 11. The cross-section was prepared from borings performed for foundation explorations and made available by courtesy of Dames and Moore and Harding Lawson Associates, Inc. As was the case for Figure 8, most in-situ penetration values were not obtained according to standard test procedures, and thus should not be used with empirical correlations linking liquefaction susceptibility and SPT measurements. The borings, however, do provide useful information about groundwater levels, stratigraphy, and relative density of sand deposits on the basis of the blow counts which were obtained.

In general, the cross-section in Figure 12 is consistent with the subsurface topography mapped in Figure 11. The soil borings show loose gray sandy fill on Howard St. between 6th and 7th Sts. The borings between Mission and Howard

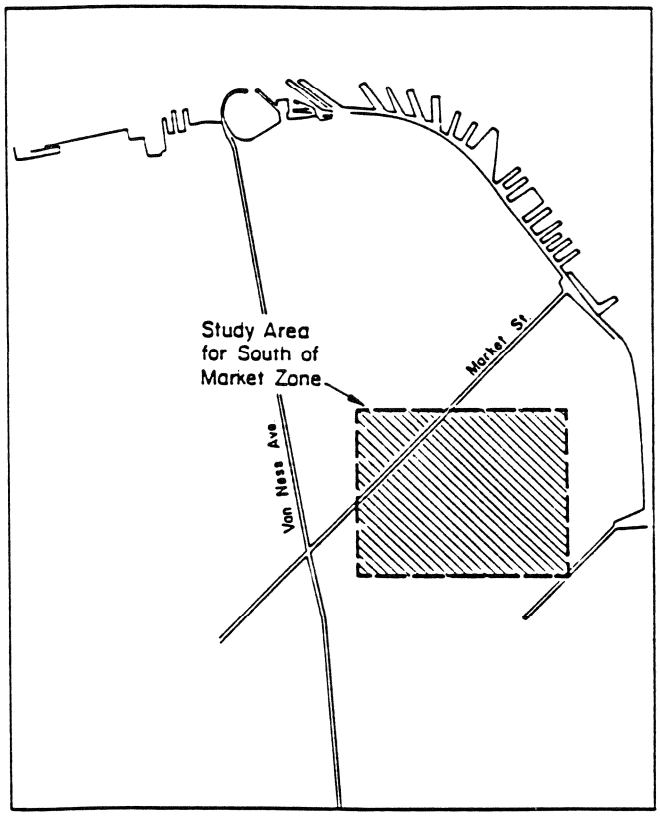

Figure 10. Location of South of Market Zone

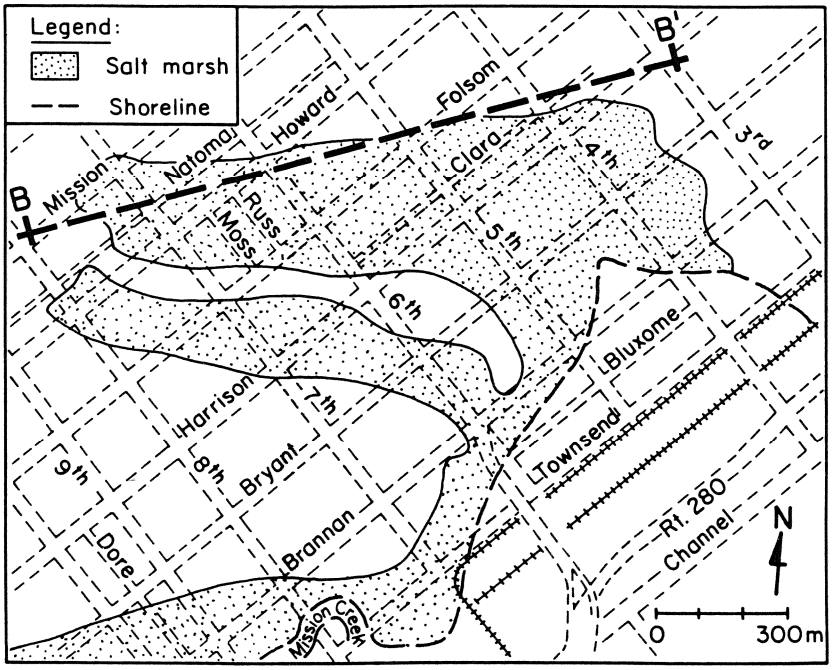

Figure 11. South of Market Study Area

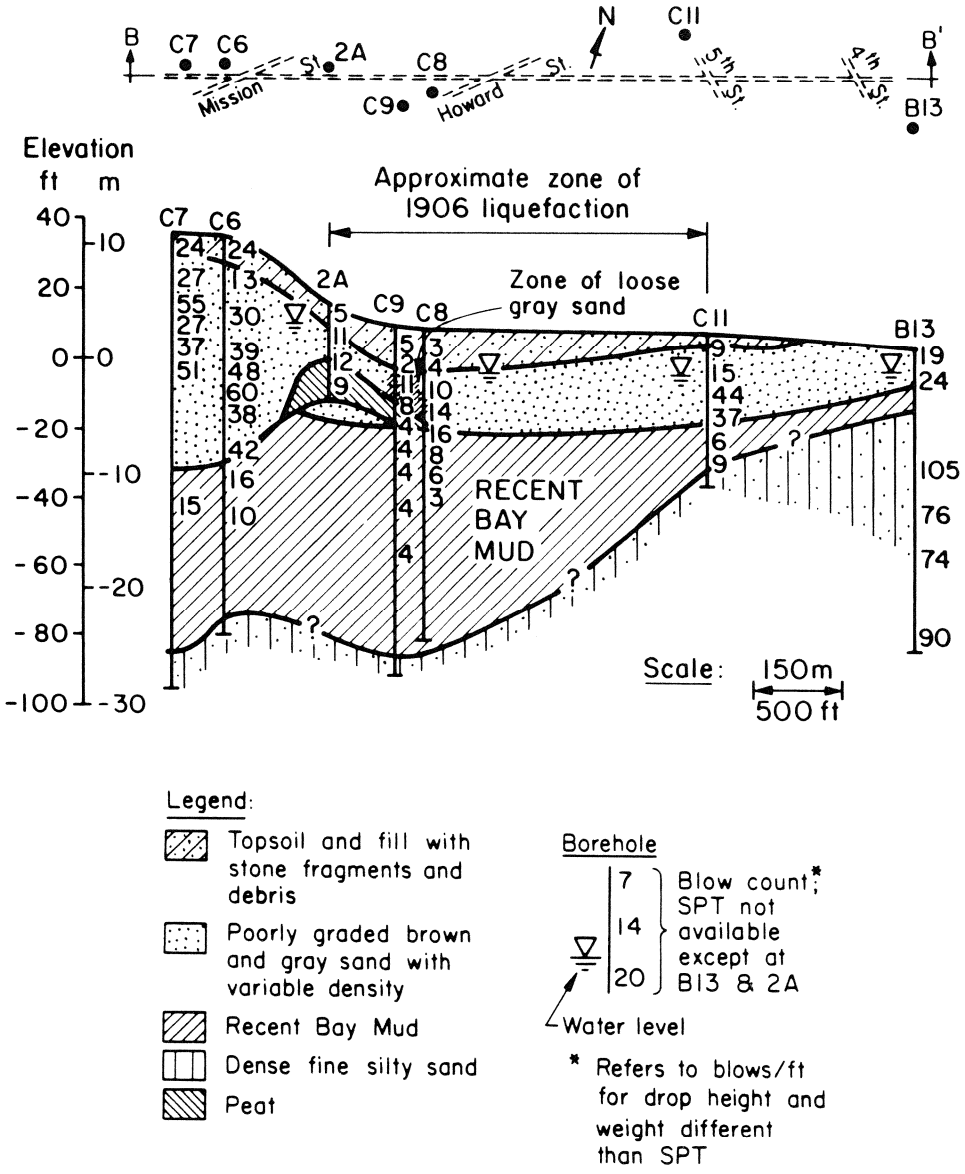

Figure 12. Soil Profile Across Head of Old Sullivan Marsh in South of Market Area

Sts. also show peat, apparently remnant of the former marsh. Denser sands are located outside and at the margins of the old marsh. The sands in the upper elevations of Borings C6 and C7 are dune deposits. The sands and sandy fills are underlain by Recent Bay Mud with a maximum thickness of approximately 20 m. A more detailed study of the subsurface conditions in the South of Market area has been undertaken by Harding Lawson Associates, et al. (1991), and reference to this work should be made for a more comprehensive evaluation of the

underlying soils.

Roth and Kavazanjian (1984) characterized the fills in this zone as being roughly 4.6 to 6.1 m thick. An idealized soil profile of the fill would consist of two layers: a 3.0-m layer of sandy gravel to gravelly sand, underlain by 3.0 to 6.0 m of silty fine sand. Both layers are interspersed with clay seams. The fill appears to contain an increasing amount of gravel and bricks towards the south near China Basin. The rubble sand fill probably was material excavated from the former Steamboat Point Hill (Hovland and Darragh, 1981). The lower layer of fill, that of the dark gray fine sand, probably was derived from excavation of the nearby dune sand. Roth and Kavazanjian (1984) identified as potentially liquefiable layers of silty sand at depths to 3 m, and poorly graded dune sand at depths of 1.5 to 4.6 m.

Although this region had substantial deformations, the average slope is very flat. Along the central axis of the region, from near 8th and Mission Sts. to 4th and Brannan Sts., the average slope is only 0.8 percent (0.5 degrees) (Youd and Hoose, 1978). Locally, especially between Mission and Howard Sts., the slopes down 7th and 6th Sts. can be significantly higher, on the order of 2 to 3 percent (1.1 to 1.7 degrees).

7.2 Ground Displacements

Figure 13 shows the ground movements relative to the shoreline of the former marsh in the South of Market area. The general direction of flow in this zone was northwest to southeast, with maximum horizontal displacements of 0.9 to 1.8 m near the head of the previous marsh. Wave forms, with their crests parallel to the direction of flow, were common. The amplitude and length of the waves were irregular (Lawson, et al., 1908).

The northern limit of ground movements in this zone was Mission St. at 7th St. near the head of the former marsh. The post office, the southern corner of which was founded on filled ground, settled 0.6 m at the building line and 1.5 m at the curb. The ground displaced laterally 1.5 to 2.1 m southwest of the building. A 0.9-m-high monocline near the southwest corner of the building bent cable car tracks and pavement blocks into an arch.

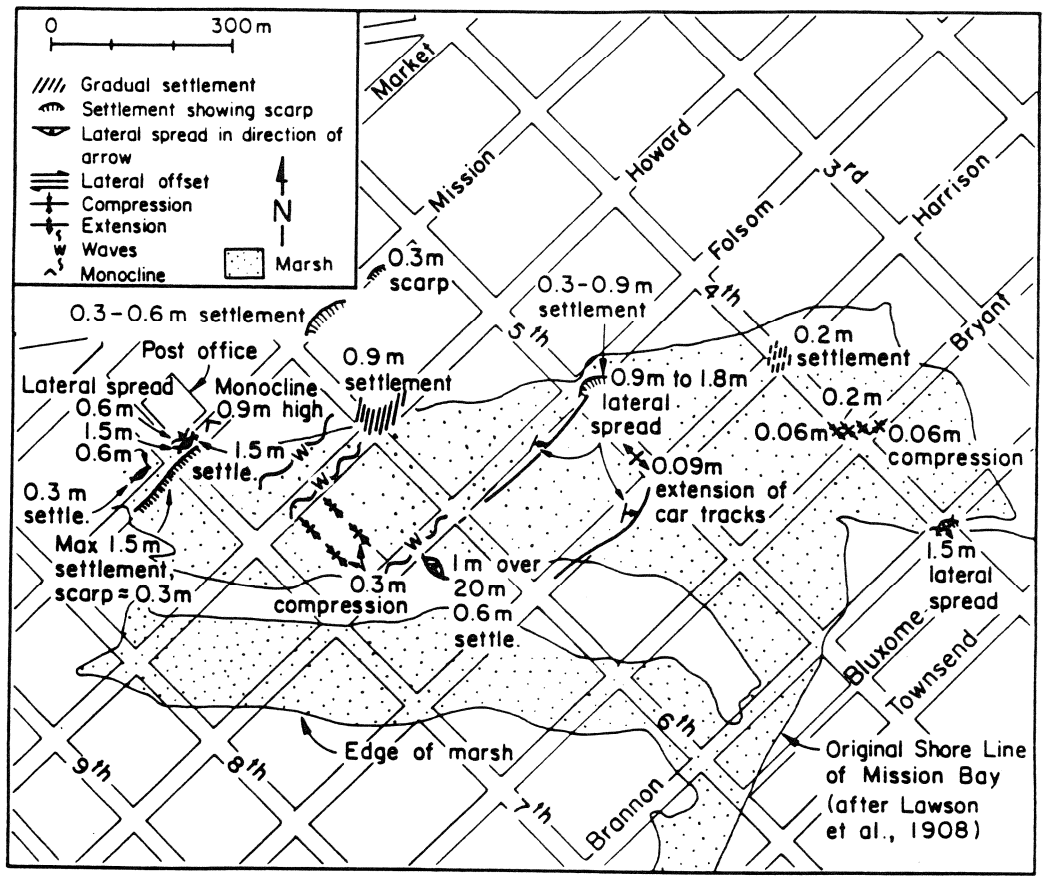

Figure 13. Earthquake-Induced Ground Deformations in South of Market Area

Gradual settlements were seen along the northern boundary of the marsh. At the intersection of 5th and Folsom Sts., the street settled 0.9 m relative to the sidewalk, which was founded on good material. The corner of 4th and Harrison Sts. settled 0.2 m beneath the rails of the cable car tracks.

Near the southeastern limit of the zone, at 4th and Bryant Sts., compressional features were seen. On 4th St., rail tracks were buckled 0.06 m and 0.2 m in the southeast-northwest direction. On Bryant St., rail tracks were buckled 0.2 m in the southwest-northwest direction. At this point, the flow movement was presumed to have been restricted by the sandstone outcrop of Rincon Hill, thus causing the compressive effects, and deflecting the flow to a more southerly direction (Lawson, et al., 1908).

Southeast of Brannan St., in filled areas of the former Mission Bay, the effects of the earthquake were less intense. Lawson, et al. (1908) noted that the material used in filling the bay tended to be a more rubbley material, derived from grading for street construction in the neighboring rocky hills. This material would be less likely to liquefy. It should be recognized that this region was sparsely developed at the time of the earthquake, and so observation of structural damage or ground deformations would have been limited.

Figure 14 presents a remarkable aerial photograph of the area adjacent to 6th St. between Mission and Howard. The photograph was taken by George Laurence (1906) using a patented system of kites and wires to carry a panoramic camera 250 m above the South of Market area (Bronson, 1959). The portion of the photo reproduced in Figure 14 shows clearly the wave-like deformation of sidewalks, vertical scarps caused by settlement, and numerous sand boils. Local ground failure exposing a deformed pipeline also can be seen.

The photograph shows the area bounded approximately by 7th, 5th, Mission, and Natoma Sts. Figure 15 presents a map of the surficial ground deformation, developed for the same area on the basis of published observations and photos as described in Appendix A, as well as the aerial photograph. Wave-like patterns of settlement were observed in the sidewalks along Minna and Natoma Sts. between 6th and 7th Sts. Several prominent scarps occurred on Mission, Minna, and Natoma Sts., which were oriented parallel to the streets. Such an orientation indicates differential settlement, slumping, and lateral movement downslope in an approximate southward direction. The lateral movements parallel to 7th St. were most severe. Maximum southward movement on 7th St. between Mission and Howard was between 1.5 and 2.4 m.

Reynolds, in reporting on the condition of buried electrical conduits, stated: "Along 7th St. from Mission to Howard, the earth was displaced from 5 to 8 ft (1.5 to 2.4 m) in a direction lengthwise to conduit. This caused some of the manholes to crush... The conduit was pulled apart at other places, and cables were wrenched and torn apart from their boxes..."

One block east of the damage on 7th St., there was a multiple collapse of timber frame hotels along the west side of 6th St. from Natoma to Howard St.

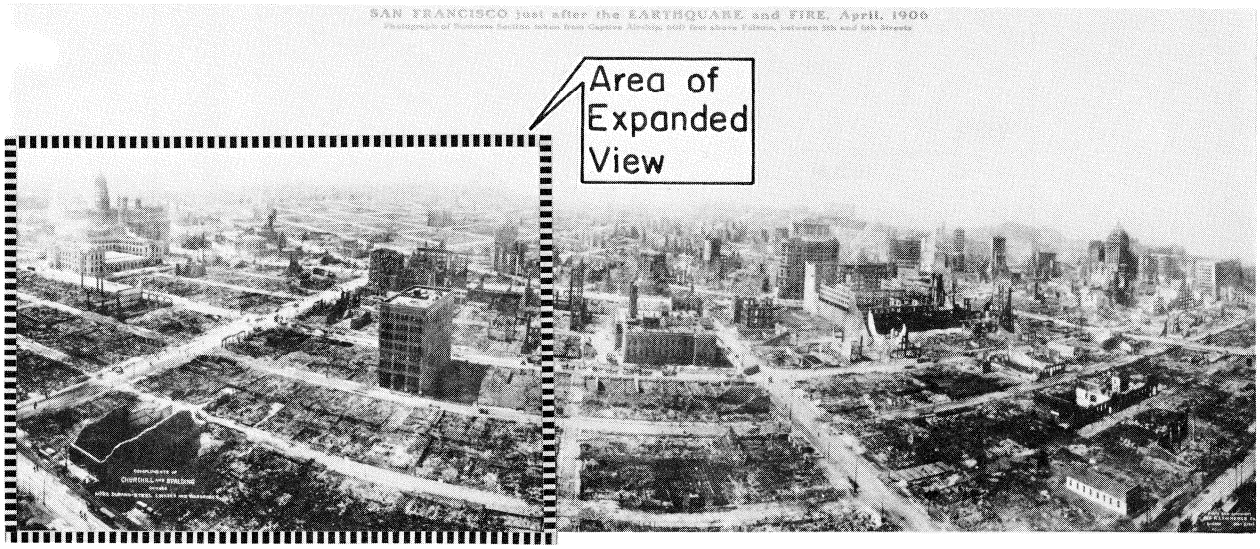

a) Overview

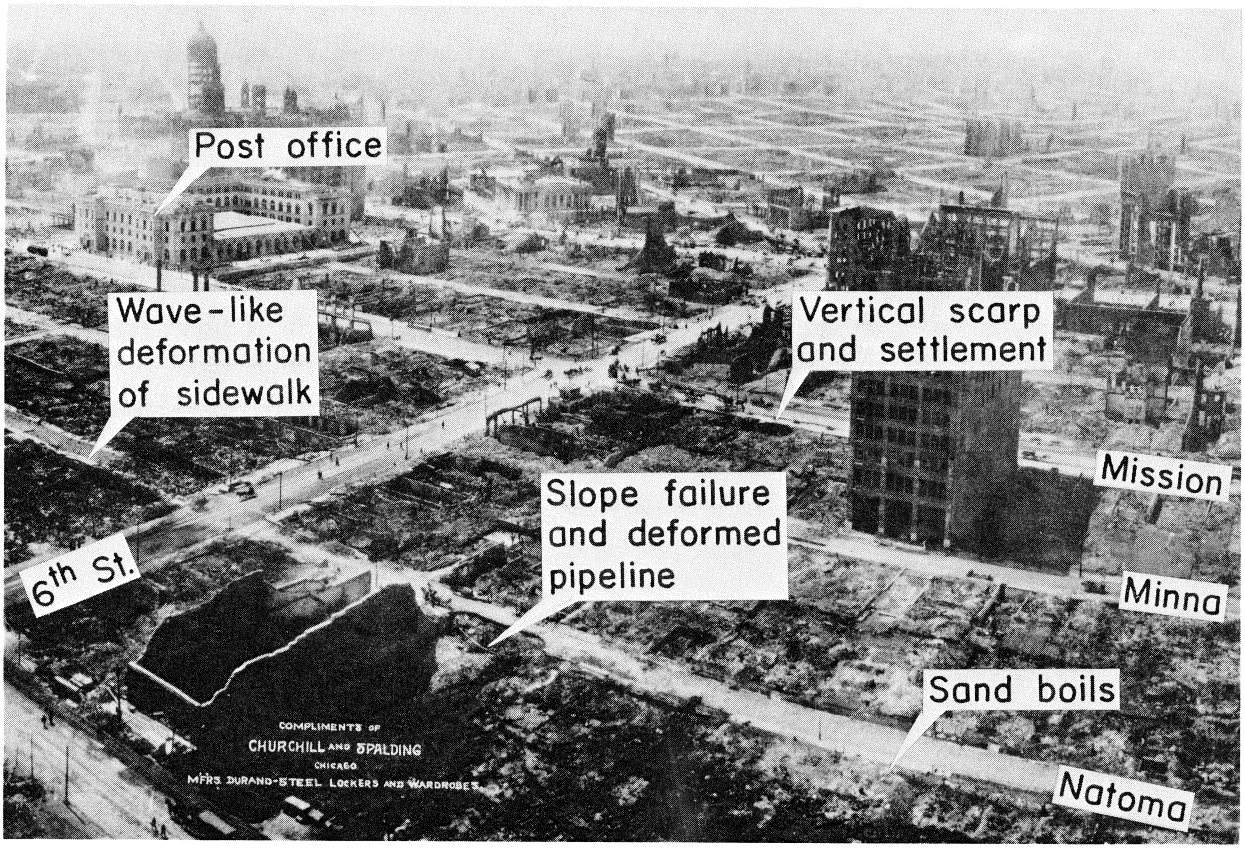

b) Location of Expanded View

Figure 14. Aerial Photograph Showing Liquefaction-Induced Ground Deformation in the South of Market Area (Laurence, 1906)

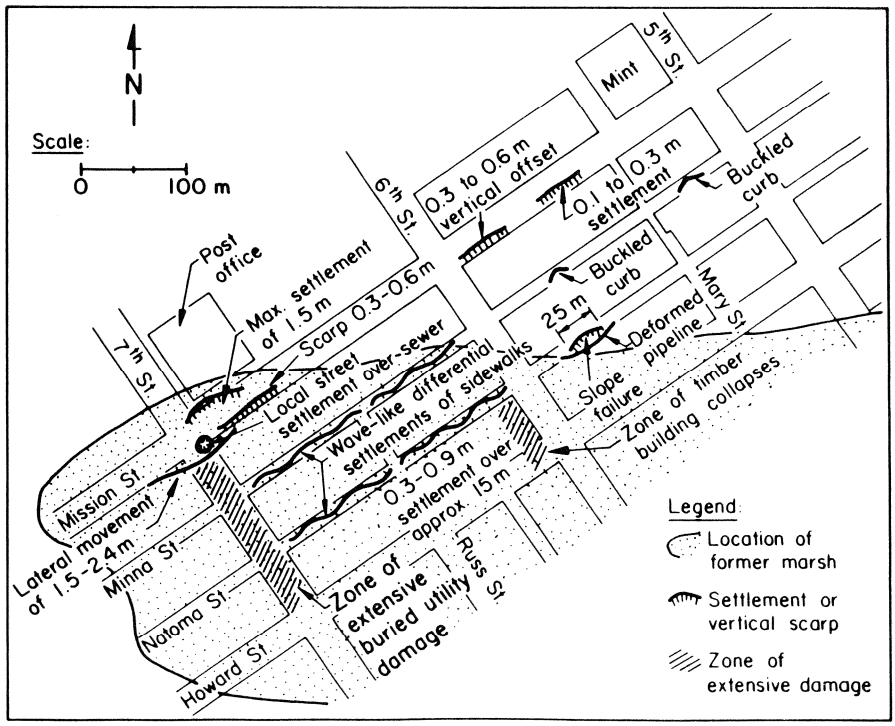

Figure 15. Detailed Map Showing 1906 Ground Deformation in the Area Bounded by Mission, Howard, 7th, and 5th Sts.

Hansen and Condon (1989) maintain that the Nevada, Lormor, Ohio, and Brunswick Houses collapsed in a domino effect, starting with the Nevada House at 6th and Natoma. These hotels allegedly were founded on a filled depression which formed during the 1868 earthquake. It is of interest to note that the building collapses proceeded in a downslope direction, consistent with the direction of liquefaction-induced lateral movements. Water mains were broken in this area, thereby depriving firefighters of water as fire erupted along 6th St. (Hansen and Condon, 1989).

Superimposed on Figure 15 is the area of the previous marsh. It is not clear why significant ground displacements occurred one to two blocks north of the apparent northern boundary of the marsh. Error in locating the marsh from maps which predate the street system represents one possibility. The area north of the marsh bounded by Mission, 5th, and 6th Sts. may be an area where dune sands were excavated and used as fill to develop a more gradual increase in surface elevation north of Howard St. The resulting slope from Mission to Howard would have contributed to southward deformation of soils into areas which liquefied

at the location of the former marsh.

8.0 FOOT OF MARKET AREA

Figure 16, which locates the Foot of Market Zone in the downtown area of San Francisco, also shows the original high-water shoreline of the former Yerba Buena Cove. Development of this area begin in the 1850s and continued until about 1900 (Roth and Kavazanjian, 1984).

8.1 Subsurface Conditions

A cross-section traversing the southeastern portions of the Foot of Market area is shown in Figure·17, and is located by the inset diagram in the same figure. The cross-section was prepared from soil borings performed under the supervision of Dames and Moore (1989) as part of the site exploration for the proposed underground Muni-Metro bus terminal. Along the Embarcadero, soil deposits are nearly 90 m deep. Recent Bay Mud varies in thickness from about 20 to 30 m in the zone delineated by the soil borings. Overlying the Recent Bay Mud is a deposit of loose to medium dense fill, approximately 6 to 9 m deep. The water table varies from approximately 2 to 3 m in depth. As indicated in the profile, a portion of the old sea wall along the waterfront was encountered during the soil exploration. The sea wall was constructed of stone taken from quarries at Telegraph Hill and an offshore area near Richmond (Dames and Moore, 1989), and extends to depths of 10 to 13 m.

The in-situ density of the sandy fill can be inferred from SPT measurements, which were performed in accordance with standard ASTM procedures (1989). A plot of blow count, or SPT values, is shown as a function of depth in Figure 18. The figure also shows the relative frequency of SPT values, based on the total number of recordings in the sample. These plots are similar to those prepared by Dames and Moore (1989), with the exception that additional SPT values (Woodward-Clyde Consultants, 1975) are included. The SPT values indicate that the fill has a highly variable in-situ density, with a tendency for the loosest sand layers to be found at a depth of about 5 to 9 m. This is generally consistent with the findings of Chameau, et al. (1990), who performed CPT soundings in the Foot of Market area along the Embarcadero north of Market

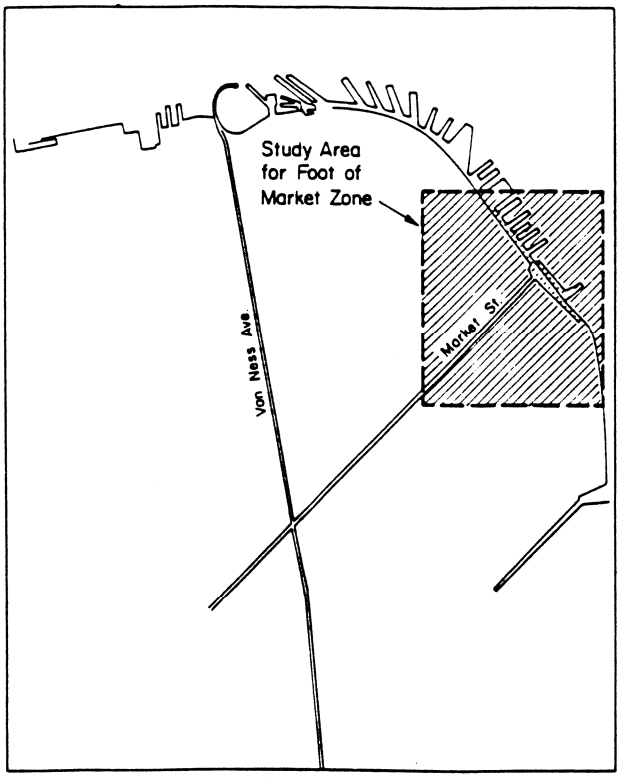

Figure 16. Location of Foot of Market Zone

St. Their investigations showed a zone of low density sand from 6 to 8 m in depth which is prone to liquefaction and a possible source for the large 1906 ground movements observed in this general area.

8.2 Ground Displacements

Figure 19 summarizes the ground displacements in the Foot of Market area in relation to the original high-water shoreline of the former Yerba Buena Cove. The boundary of the disturbance in the Foot of Market Zone delineated by Hall (1906) falls outside the original high-water shoreline. The limit of the fill on Market St. is at the crossing of Sansome St., but the depth of fill coincides with the groundwater table only in the vicinity of First St.

Wave forms again were prevalent on most of the streets eastward of this boundary, with the crest of the waves perpendicular to the general direction of flow. The height of the waves ranged from 0.15 m to 1.5 m. Lower Market St.

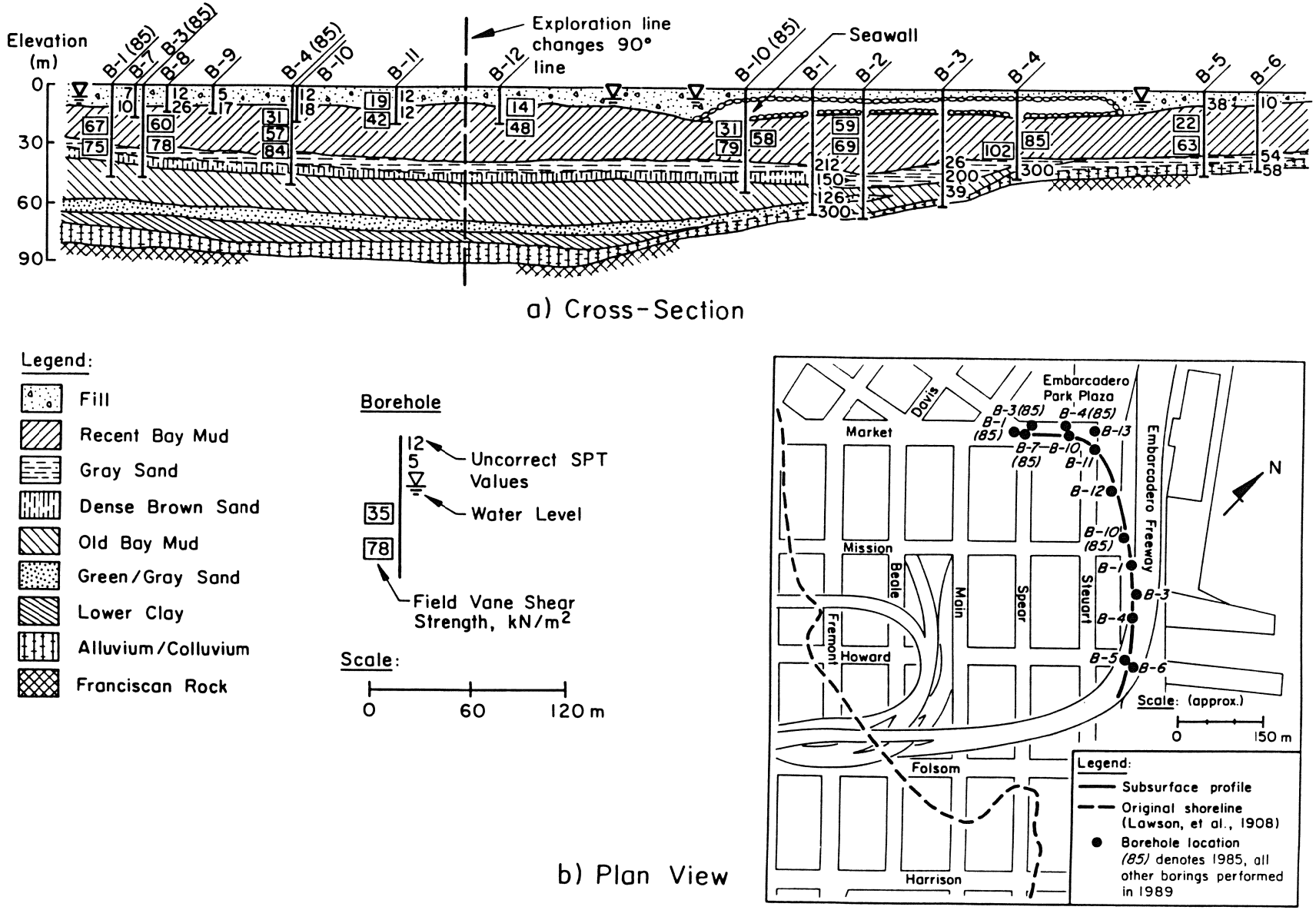

Figure 17. Soil Profile Near the Embarcadero in the Foot of Market Area

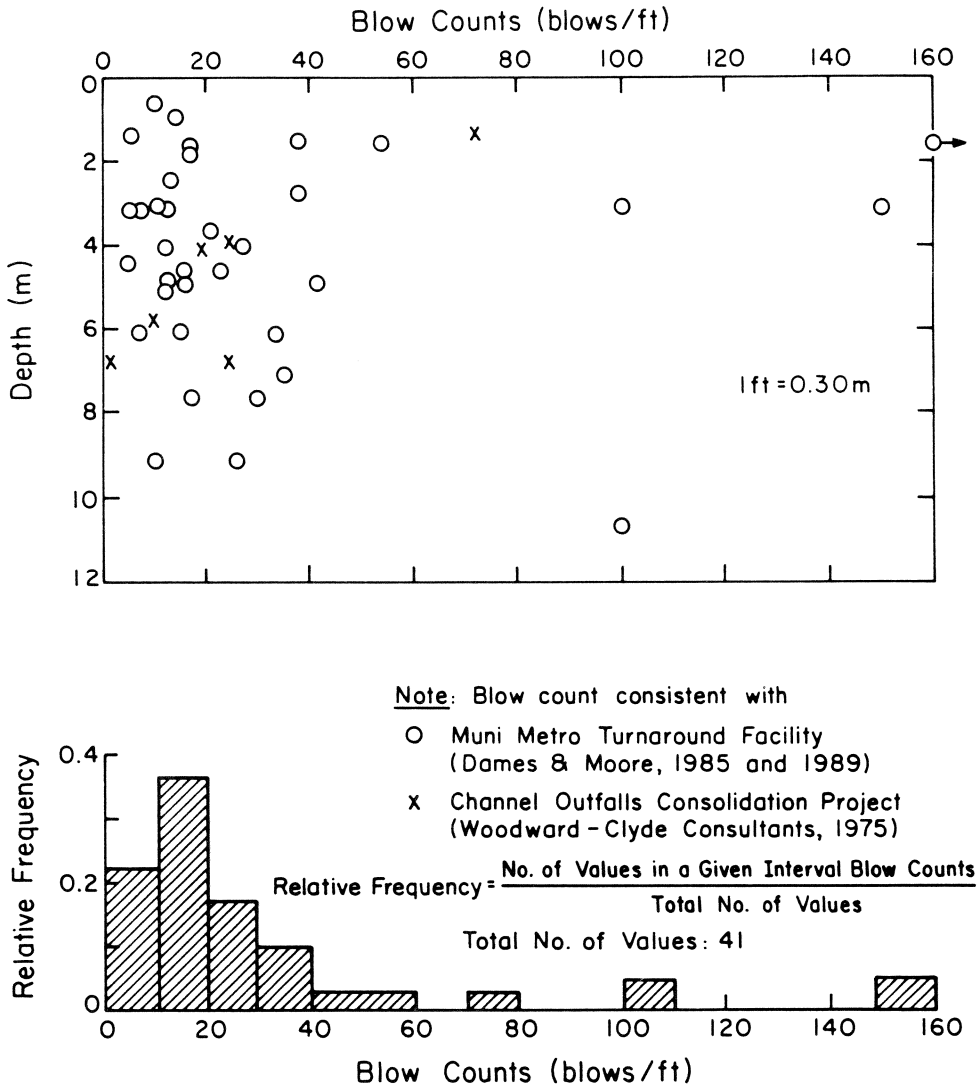

Figure 18. SPT Values (Blow Counts) Representative of Fills in the Foot of Market Area

is a good example of this phenomenon. The wave troughs on Market St. at Spear St. were about 0.3 m and increased in height to about 1.5 m in front of the Union Ferry Building. Waves up to 1.2 m in height also were common along East St. (now the Embarcadero).

Much of the area also experienced settlements. Along Davis St. between Vallejo and California Sts., subsidence of 0.3 to 0.9 m was observed at every street crossing (Hall, 1906). Settlements of 0.6 m also occurred along Spear St. at

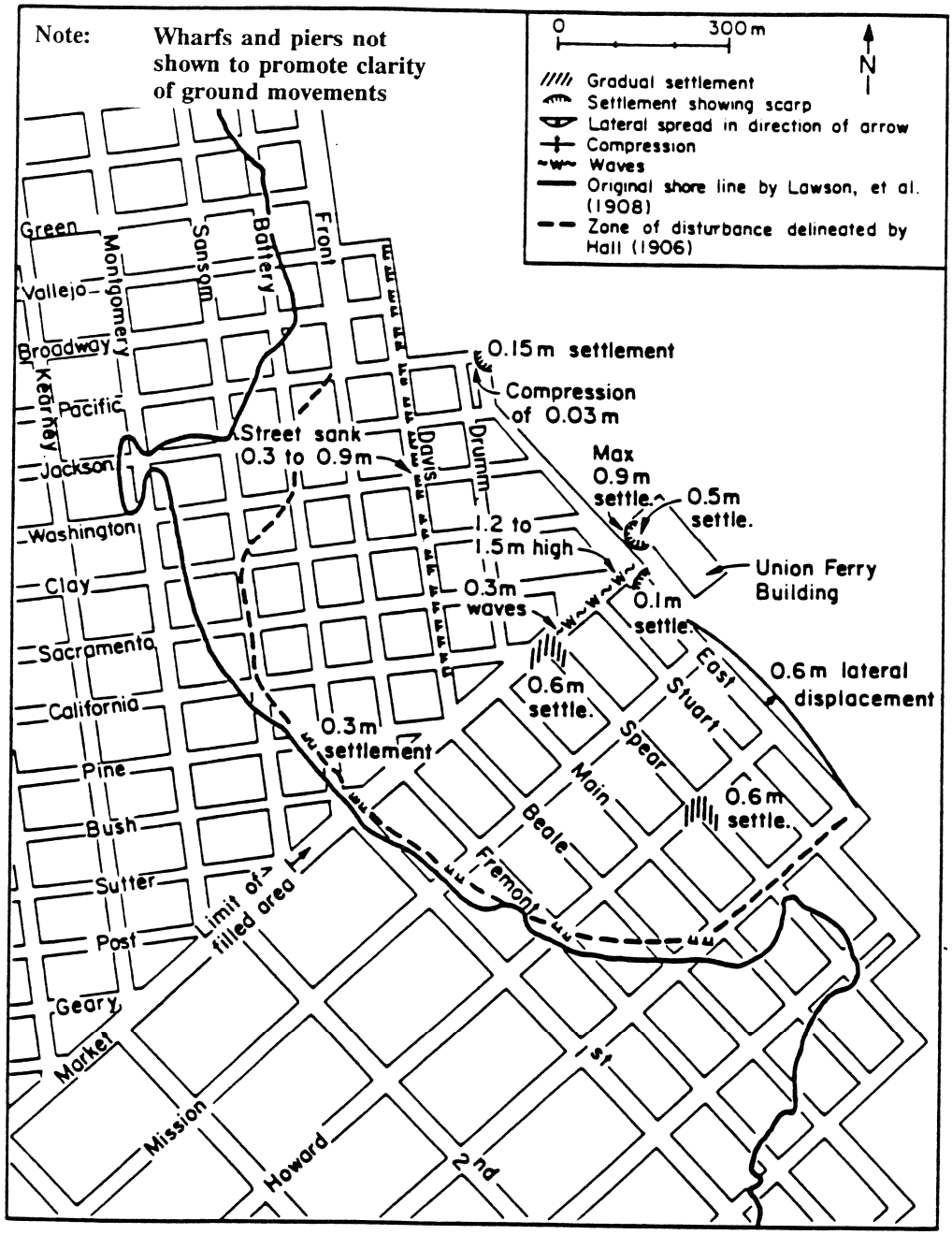

Figure 19. Earthquake-Induced Ground Movements in Foot of Market Area

both Howard and Market Sts. The street settled relative to the sidewalk in front of the northwest corners of both the Aetna Building (Spear and Market Sts.) and the Folger Building (Spear and Howard Sts.). The settlements cited by Hall (1906) on Pine, Market, Mission, Howard, and Folsom Sts. were parallel

to the outline of the original shoreline.

East St., perhaps, had the most extensive damage in this zone. The street, in general, subsided 0.15 to 0.3 m and shifted eastward 0.15 to 0.6 m. The pavement was shoved up against waterfront structures. Twenty-five meters of frontage along the Ferry Building subsided from 0.5 m to a maximum of 0.9 m at the northwest corner.

9.0 MARINA AND NORTH POINT DISTRICTS

As shown by Figure 20, the Marina and North Point areas are located along the northern shore and separated by Black Point. Although some filling had begun in these areas prior to 1906, the majority of the development in these areas took place after the earthquake and subsequent fire. Figure 20 shows the 1908 shoreline, which is approximately the same as that of 1906. Zones of MM IX to X intensity are delineated in the figure by dotted areas. The original coastline, as determined from the 1853 and 1857 coastal surveys, coincides well with the inland boundary of the MM IX to X intensity zones along the northern shore, identifying these areas as fill.

9.1 Marina District

This area formerly was a tidal marsh between the shore and a sandbar, known as Strawberry Island, located near what is now Broderick St. The filled land starts at the mouth of the marsh in the proximity of what is now the intersection of Bay and Scott Sts.

Although the Marina was not extensively developed in 1906, there are nevertheless several historic accounts of damage in this area (Jones, 1906; Gilbert, et al., 1907; Lawson, et al., 1908), some of which are summarized in Figure 21. Lawson, et al. (1908), for example, drew attention to evidence of severe ground shaking in the hatchured zone of Figure 21, extending from North Point St. between Lyons and Broderick to the shore. In this area, timber structures were thrown out of vertical, reminiscent of the shear deformation sustained by four-story timber buildings during the 1989 earthquake. Moreover, the Baker St. sewer was damaged, which implies that permanent ground deformation occurred in

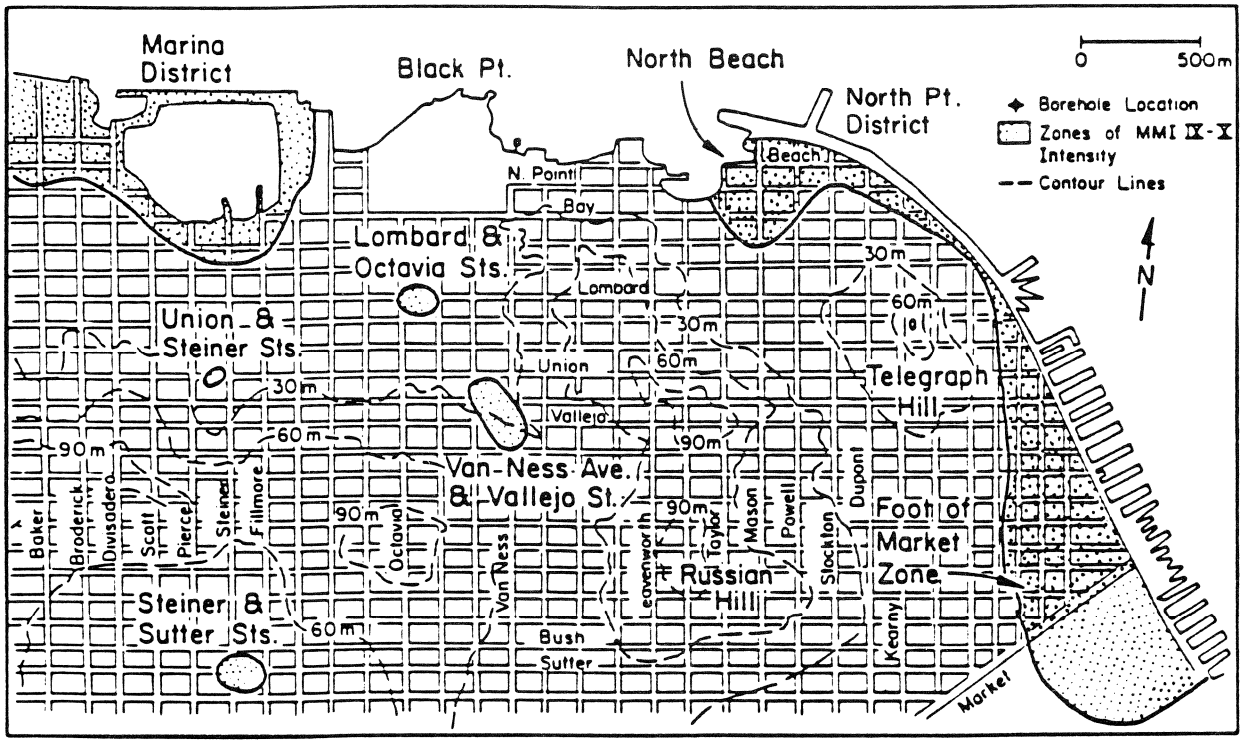

Figure 20. Location of Marina and North Point Areas

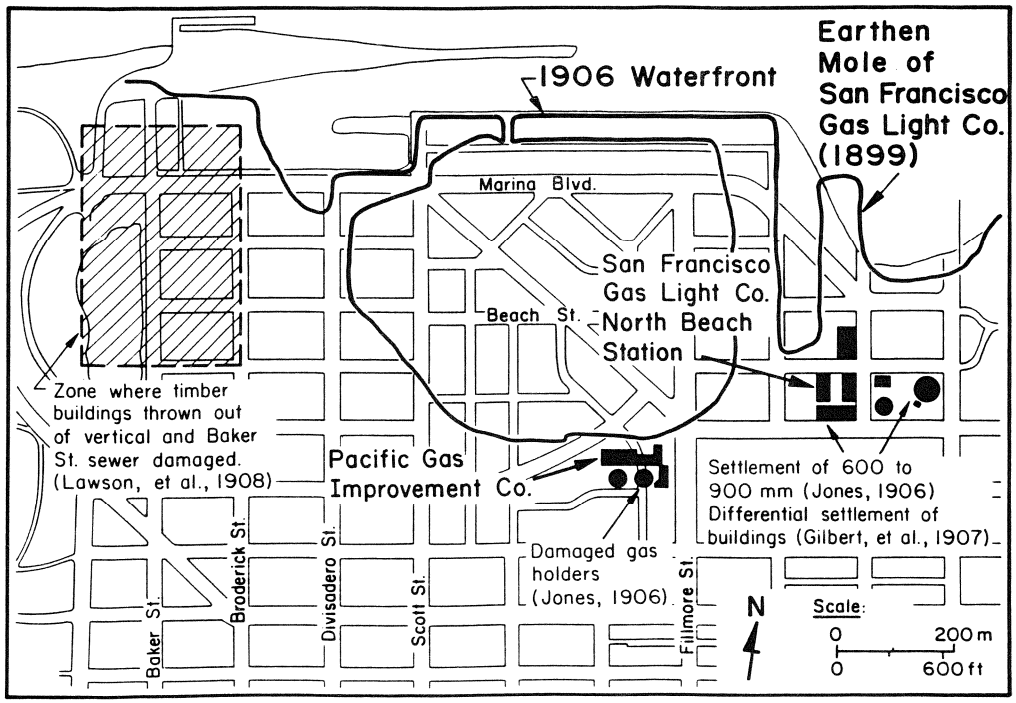

Figure 21. 1906 Waterfront and Earthquake Damage Relative to Current Marina Street System

this area.

The most extensive observations of damage are associated with the coal gasification plants, which were located in the southwestern part of the Marina in 1906. Gilbert, et al. (1907) reported that not a building at the San Francisco Gas and Electric (renamed from the original San Francisco Gas and Light Co.) plant escaped damage, and that the ground settled very considerably at this location. Jones (1906) reported from 600 to 900 mm of settlement adjacent to the principal gas holder at the North Beach Station. The settlement ruptured the 600-mm diameter outlet connections of the holder, causing all the stored gas to escape.

Extensive soil explorations have been performed in the Marina since the 1989 Loma Prieta earthquake. The results of these investigations and the subsurface conditions which they delineate are summarized elsewhere in this volume for the case history of the Loma Prieta earthquake (O'Rourke, et al., 1991).

9.2 North Point District

9.2.1 Subsurface Conditions

Although filling of the district was started in 1865, most fill at North Beach was placed after 1906. The fill is highly variable, including much debris from the earthquake and fire. Roth and Kavazanjian (1984) simplified the fill in this zone as consisting of two layers: 3 m of sandy gravel to gravelly sand, underlain by 3 to 6 m of silty fine sand. Clay seams are interspersed throughout the profile. The fill contains much debris, including brick, wood, and rock fragments. The most likely source for the top layer of fill was located between Jones and Stockton Sts., just south of the North Beach district (see Figure 20) (Roth and Kavazanjian, 1984). This deposit is mapped as an undifferentiated, surficial deposit consisting of the Colma Formation and slope debris. The SPT values estimated by Roth and Kavazanjian are highly variable. The mean corrected SPT value for this layer is 15, with a standard deviation of 15. A dune sand deposit originally located at the base of Russian Hill was the most likely source for the lower silty sand fill layer (Roth and Kavazanjian, 1984). The mean corrected SPT value was estimated as 17, with a standard

deviation of 12. Both fill layers were identified as potentially liquefiable (Roth and Kavazanjian, 1984). The groundwater table is at an average depth of 2.4 m in this area.

9.2.2 Ground Displacements

No photographs showing ground movements resulting from the 1906 earthquake could be found for the North Beach district. However, settlements of several streets were shown on a map presented by Schussler (1906). A three-block region experienced settlements, starting at Bay St. from Taylor to Mason Sts., and then along Mason St. from Bay to North Point Sts., and continuing along North Point St. from Taylor to Powell Sts. Two other streets, Stockton and Dupont (now Grant) Sts., also experienced settlements for less than a block in length just north of North Point St.

10.0 OTHER ZONES OF HIGH INTENSITY

Several additional zones experienced an appreciably high intensity during the 1906 earthquake. These zones are shown in Figures 4b and 20. Damage in these zones can be correlated with the presence of artificial fills resulting from street construction or the filling of small ravines.

10.1 Duboce Park

A small one-block area near the corner of Waller and Portola Sts. showed high intensity. This zone is located on Figure 4b. Unlike the other zones described in this section, this zone was not on "made" land. This block occupies the lower slopes of a small narrow valley and is underlain by a thin strata of sand. Apparently, this sand layer shifted downslope, cracking foundation walls and moving houses eastward. Street pavement also was buckled and broken (Lawson, et al., 1908).

10.2 Steiner and Sutter Streets

In the neighborhood of Steiner and Sutter Sts., located in Figure 20, extensive damage occurred to several structures. A large church on the corner of Bush

and Steiner Sts. collapsed and several small frame buildings nearby were knocked from their underpinnings. Likewise, on Geary St. above Fillmore St., two wooden-framed brick buildings were completely destroyed. No permanent ground movements were documented in this district. This area, located in the Upper Hayes Valley, is underlain by a thick layer of dune sand (Schlocker, 1974).

10.3 Lombard and Octavia Streets

Another small district, less than a block in extent, on Lombard St. between Gough and Octavia Sts., had a high intensity of damage. This is a filled area, formerly the site of a small fresh water lagoon known as Washerwoman's Lagoon (Lawson, et al., 1908). The location of this zone is shown in Figure 20. Although the earthquake damage in this area was of MM IX intensity, no permanent ground movements were recorded (Lawson, et al., 1908). Brown, et al. (1932) also mention this area as suffering severely during the earthquake.

10.4 Vallejo Street and Van Ness Avenue

The corner of Van Ness Ave. and Vallejo St. experienced considerable ground movements. This is the site of a former ravine leading northwestward down to the former Washerwoman's Lagoon. The location of damage can be circumscribed by an ovoid area two blocks long, as shown in Figure 20. The fill is roughly 12 m deep at this point (Lawson, et al., 1908).

This whole area settled, the greatest subsidence being roughly 0.6 m at the intersection of Van Ness Ave. and Vallejo St. Lateral spreading to the north occurred on Van Ness Ave., with a magnitude of approximately 0.9 m at the intersection with Vallejo St., decreasing to about 0.3 m at Green St. (Schussler, 1906). The ground movements caused much damage to the streets, pipelines, and structures. Buildings shifted and were thrown out of vertical, resulting in their foundations being crushed. Sidewalks were thrust over the curbs, and street pavements were fissured and downfaulted (Lawson, et al., 1908). To the east, south, and west of the intersection of Vallejo St. and Van Ness Ave., the sewers were broken for a distance of about 45 m. Water mains also were broken. At one location, a 510-mm-diameter pipe was broken into 0.6-m sections over a

length of about 13 to 17 m (Gilbert, et al., 1907).

10.5 Union and Steiner Streets

Another district of extensive damage, less than a quarter of a block in length, was found on Union St. between Pierce and Steiner Sts. This area is located in Figure 20. This area had been filled as a result of grading the streets. Some of the largest ground movements were found at this location. The north sidewalk moved about 3 m to the north, settling about 3 m below original grade. The south sidewalk settled several centimeters and shifted northward about 1 m.

Although the type of ground displacements seen here resemble those seen in other zones, it is important to note that this slide was not caused by liquefaction. The displacements were a result of unconsolidated fill material shifting downhill into a vacant lot to the north.

11.0 PERFORMANCE OF SAN FRANCISCO WATER SUPPLY

In 1906, water to San Francisco was supplied from two series of reservoirs. South of San Francisco, water was impounded by earth and concrete dams to form the San Andreas, Crystal Springs, and Pilarcitos Reservoirs. Transmission pipelines conveyed water from these reservoirs to a second series of smaller reservoirs within the city limits. Water then was distributed throughout the city by means of trunk and distribution pipelines.

Figure 22 presents a plan view of the 1906 San Francisco water supply adapted from maps prepared by Schussler (1906). At the time of the earthquake, there was a combined volume of 88.7 billion liters in the San Andreas, Crystal Springs, and Pilarcitos Reservoirs. These reservoirs supplied nearly all water for the City of San Francisco in 1906, whereas today they represent approximately one-half of the local storage capacity in the San Francisco Bay area. Transmission pipelines conveying water from the southern reservoirs were built mainly of wrought iron.

Within the city limits, there were approximately 711 km of distribution piping at the time of the earthquake, of which roughly 18.5 and 66.5 km were wrought

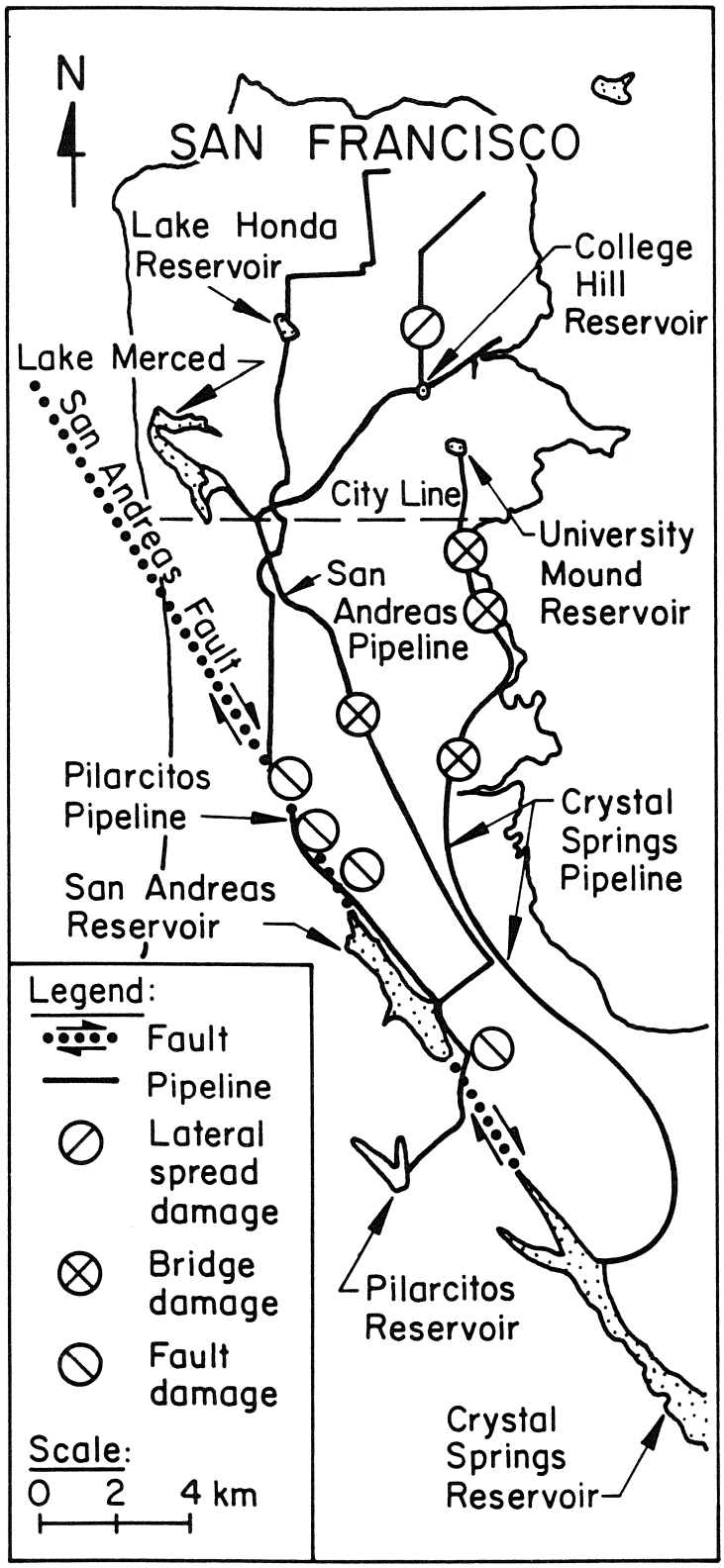

Figure 22. 1906 San Francisco Water Supply (adapted from Schussler, 1906)

and cast iron trunk lines, respectively. These lines were larger than or equal to 400 mm in diameter. The bulk of the system had been constructed during the years of 1870 to 1906.

Superimposed on Figure 22 are the approximate locations of transmission pipeline damage caused by the earthquake. Flow from all transmission pipelines stopped shortly after the earthquake. Because telephone service was out, emergency control information had to be obtained by dispatching personnel into the field where maintenance crews reported on the damage.

Right lateral strike-slip movement along the San Andreas fault ruptured a 750-mm-diameter wrought iron pipeline conveying water from the Pilarcitos to Lake Honda Reservoir. Over 29 breaks were reported north of the San Andreas Reservoir, where the pipeline was constructed parallel to the San Andreas fault. Fault movement near the San Andreas Reservoir was measured as 3.6 to 5.6 m (Lawson, et al., 1908). Pipeline ruptures were caused by tensile and compressive deformation of the line. Over three months were required to reconstruct the pipeline.

Within 16 hours after the earthquake, repairs were made to that part of the Pilarcitos Conduit which was located within the city limits. Water then was pumped from Lake Merced through the Pilarcitos line into Lake Honda at a rate of approximately 25 million liters per day. Dynamic distortion of bridges was responsible for rupturing a 925-mm-diameter wrought iron pipeline conveying water from the San Andreas to College Hill Reservoir, and for rupturing at three swamp crossings an 1100-mm-diameter wrought iron pipeline conveying water from the Crystal Springs to University Mound Reservoir. The wooden trestle bridges all were damaged by strong ground shaking, with no damage or misalignment observed in their timber pile foundations. Approximately three days were required to repair the 925-mm-diameter pipe, and over a month was required to restore the 1100-mm-diameter Crystal Springs Pipeline.

Figure 23 is a map of the 1906 water supply within the San Francisco City limits. Table 1 summarizes the city reservoirs, capacities, and elevations above mean sea level. There were nine reservoirs and storage tanks, for a total capacity of 354 million liters. Approximately 92% of this total, or 325

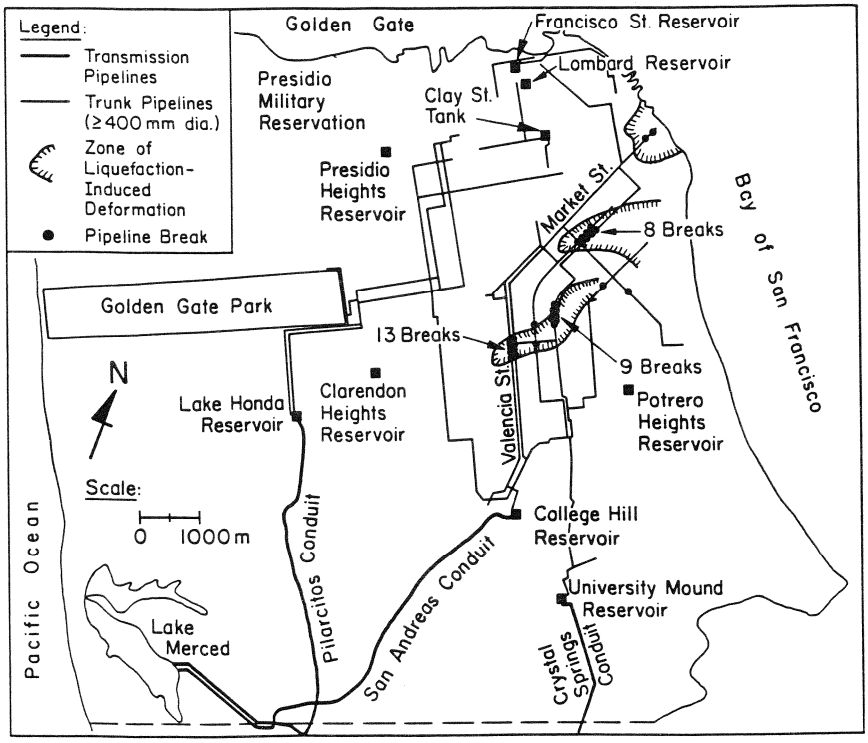

Figure 23. 1906 Water Supply Within San Francisco City Limits

Table 1. Summary of Reservoirs and Water Capacity at Time of Earthquake

Reservoir	Capacity (million liters)	Elevation (m)
University Mound	140.0	50.3
Francisco Street	11.4	41.1
College Hill	53.0	77.7
Lake Honda	124.9	111.3
Lombard Street	9.5	93.0
Potrero Heights	3.0	96.0
Presidio Heights	2.6	122.0
Clay Street Tank	0.9	114.3
Clarendon Heights	1.9	182.9

million liters, were contained in the Lake Honda, College Hill, and University Mound Reservoirs. These reservoirs and the pipelines linking them with various parts of the city were the backbone of fire protection.

All trunk lines, 400 mm or larger in diameter, are plotted in Figure 23. These pipelines were plotted on the basis of a careful review and transcription of the oldest extant (1912) pipeline maps in San Francisco, which were provided by the San Francisco Water Distribution Department, and correlated with reservoir and pressure district maps published by Schussler (1906). Trunk lines are shown connected to the Lake Honda, College Hill, University Mound, Francisco Street, and Clay Street Reservoirs; all other reservoirs were connected to piping 300 mm or less in diameter. As listed in Table 1, the University Mound and Francisco Street Reservoirs are at approximately the same elevation. The Francisco Street Reservoir was filled by water from the University Mound Reservoir, which then was pumped to Presidio Heights. Accordingly, the supply for Presidio Heights and Francisco Street depended on the pipelines from University Mound.

Superimposed on the figure are the zones of lateral spreading caused by soil liquefaction, as delineated by Youd and Hoose (1978). Breaks in the pipeline trunk system crossing these zones are plotted from records provided by Schussler (1906) and Manson (1908). It can be seen that multiple ruptures of the pipeline trunk systems from the College Hill and University Mound Reservoirs occurred in the zones of large ground deformation, thereby cutting off supply of over 56% of the total stored water to the Mission and downtown districts of San Francisco.

Two pipelines, 400 and 500 mm in diameter, were broken by liquefaction-induced lateral spreading and settlement across Valencia St. north of the College Hill Reservoir. These broken pipes emptied the reservoir of 53 million liters, thereby depriving firefighters of water for the burning Mission District of San Francisco. As indicated in previous studies (Scawthorn and O'Rourke, 1988), this local deformation ranks as one of the most devastating events of the 1906 earthquake.

Figure 24 shows a map of the San Francisco water supply and area burned during

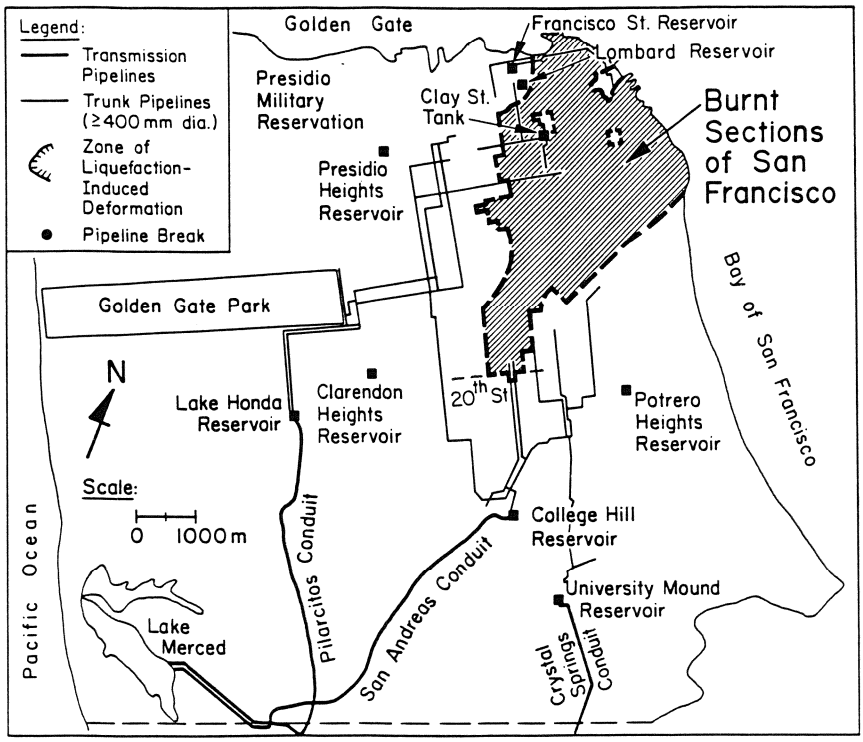

Figure 24. San Francisco Water Supply and Area Burned During the Fire

the fire. All trunk lines of the College Hill and University Mound Reservoirs downstream of the pipeline ruptures are removed from this figure to show the impact and lack of hydraulic conductivity caused by severing these conduits.

With the College Hill and University Mound Reservoirs cut off, only the Clay Street Tank and the Lombard and Francisco Street Reservoirs were within the zone of most intense fire, and therefore capable of providing water directly to fight the blaze. The combined capacity of these reservoirs was only 21 million liters, or 6% of the system capacity. The usefulness of such limited supply was further diminished by breaks in service connections, caused by burning and collapsing buildings. Schussler (1906) identified service line breaks as a major source of lost pressure and water. There were roughly 23,200 breaks in service lines between 15 and 100 mm in diameter. Fallen rubble and collapsed structures often prevented firemen from closing valves on distribution mains to diminish water and pressure losses in areas of broken mains and services.

The southernmost extent of the fire, as shown in Figure 24, was 20th St., where a firebreak had been created by dynamiting houses on the north side of the road. Hansen and Condon (1989) indicate that water was available in this vicinity from abandoned cisterns on Shotwell St. at both 19th and 22nd Sts., local flooding from a broken pipeline at 17th and Howard Sts., and a private water works on 16th St. The broken pipe on Howard St. was one of the main trunk lines of the University Mound Reservoir which crossed the zone of liquefaction-induced ground movement over the old Mission Creek. Water also was conveyed to the firebreak along 20th St. from a portion of the system still operating on 20th and Church St., just one block west of the burnt area.

As is evident in Figure 24, the Lake Honda Reservoir was able to provide a continuous supply of water to the western portion of the city. The fire eventually was stopped along a line roughly parallel to Van Ness Ave., where water still was available from the Lake Honda Reservoir. Moreover, the southern and southeastern extent of the fire is bounded by areas south and southeast of the trunk system ruptures. It is likely that these unburnt areas had water from the University Mound Reservoir.

Figure 25 presents a bar graph showing the reservoir storage in San Francisco as a function of time after the earthquake. The amounts of water corresponding to Day 1 represent the quantities available roughly two hours after the earthquake struck. After four days, less than one-tenth of the initial capacity of the College Hill, University Mound, and Lake Honda Reservoirs still was available. Two factors were critically important in preserving flow. Sixteen hours after the earthquake, water was pumped from Lake Merced into the Pilarcitos Conduit to supply Lake Honda. This action provided an additional 25 million liters/day, thereby maintaining capacity in Lake Honda for distribution to the western parts of the city. After repairs of the San Andreas Conduit over three days, approximately 30 million liters/day were conveyed to the College Hill Reservoir for distribution in the South Mission area of the city. By Day 5, approximately 55 million liters of water were flowing into the city, in addition to the 25 million liters still available in the reservoirs.

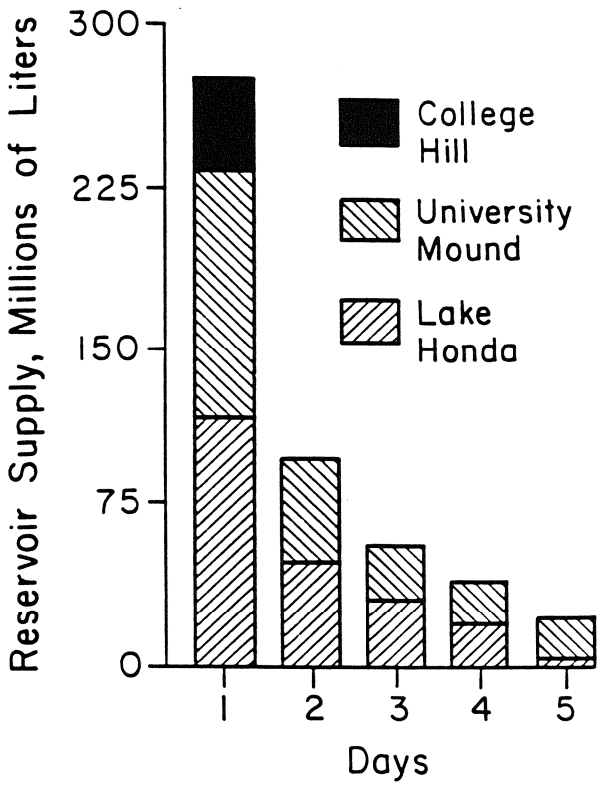

Figure 25. Reservoir Storage in San Francisco as a Function of Time After the Earthquake

12.0 SAN FRANCISCO FIRE

12.1 Fire Department in 1906

The San Francisco Fire Department in 1906 protected approximately 400,000 persons occupying an urbanized area of approximately 55 km^2. The department consisted of a total of 585 full paid fire force personnel (resident within the city and on duty at all times), commanded by Chief Dennis T. Sullivan and deployed in 57 companies (38 engine, 1 hose, 10 ladder, 1 hose tower, and 7 chemical) (Committee of Twenty, 1905). The distribution of these companies was well conceived, being centered about the congested high value district (i.e., the Central Business District or CBD, known in San Francisco as the Financial District), with 24 engine, 8 ladder, 1 water tower, and 7 chemical companies within 3 km of the center of the CBD. All but two of the 38 steam engine companies dated from 1890 or later, and were rated at an average of 680 gpm (2600 l/min.), although the eight engines tested in 1905 averaged only about 70% of

their rated capacity, and the "ability of the men handling the engines was in general below a proper standard." The rated pumping capacity of the 38 first line and 15 relief and reserve engines totaled 35,100 gpm (133,000 l/min.). In summary, the department was rated by the National Board of Fire Underwriters (NBFU) as efficient, well organized, and in general adequate. Nevertheless, the NBFU found serious deficiencies in the city (Committee of Twenty, 1905), and concluded its review of the city and its fire potential with:

> *"...In fact, San Francisco has violated all underwriting traditions and precedent by not burning up. That it has not done so is largely due to the vigilance of the fire department, which cannot be relied upon indefinitely to stave off the inevitable."*

Within moments after the earthquake on April 18, 1906, Chief Dennis T. Sullivan was seriously injured by fallen masonry which hit the fire station where he was sleeping. He died four days afterwards. Ten fire stations sustained major damage (Tobriner, 1988), although no engines were seriously disabled by the earthquake and all went into service (Reed, 1906). Street passage was in general not a problem, and numerous fires were quickly suppressed, although many more could not be responded to.

The NBFU Conflagration Report (Reed, 1906) made the following observation:

> *"the lack of regular means of communication and the absence of water in the burning district made anything like systematic action impossible; but it is quite likely that during the early hours of the fire the result would not have been otherwise, even had none of these abnormal conditions existed."*

That is, the NBFU concluded that even under normal conditions, the multiple simultaneous fires probably would have overwhelmed a much larger department, such as New York's, which had three times the apparatus (Committee of Twenty, 1905). Nevertheless, Bowlen, in his outline of the history of the fire, concluded that by 1:00 p.m. (i.e., about 8 hours after the earthquake):

> *"the fire department, except that it was without its leader, was in fairly good shape, that is the men and horses were in good trim for fighting, the apparatus was in shape and could be worked where there was water. There is not one report of an engine or man going out of commission during the early hours of the fire, and the department was hard at work all the time, even though there was little to show for its effort."*

12.2 Earthquake-Generated Fires and Spread

The number of ignitions following the earthquake has been reported by Reed (1906) and in the Bowlen outline (undated) as approximately 50, but the actual number, locations, and causes never have been summarized in detail. A review of various sources [Bowlen's outline and summary of fire officers' reports (both undated); Argonaut series, 1927] indicates that there were 52 fires and/or explosions, which are listed in Table 2. Ignitions in the CBD are shown in Figure 26.

The conflagration following the 1906 earthquake was a complex fire, actually consisting of several separate major fires which grew together until there was one large burnt area, comprising the northeast quadrant of the city and destroying over 28,000 buildings. The progress of these fires generally has been divided into four periods (Reed, 1906; Bowlen outline), although actual times for these periods differ among sources. Generally, the periods comprise the following times: 1) from the earthquake until mid or late in Day 1, when most of the South of Market area had been destroyed, but the higher value north of Market section still remained largely intact, 2) the night of Day 1 and the early hours of Day 2, when the north of Market section was invaded by the fire, progressing from the west, 3) continued progress of the fire to the north, and a bit to the south, during the remainder of Day 2, and 4) during Day 3, when the fire progressed almost entirely to the north, around Telegraph Hill, and burnt down to the Bay and into the Mission Creek area. The fire mostly was spent or extinguished by the morning of April 21, 1906, approximately four full days after the main shock of the earthquake.

On the basis of the same sources as indicated above for initial ignitions, the progress of the initial ignitions was traced during the first 24 hours following the earthquake. Figure 27 shows the fires that were extinguished and the spread of initial ignitions from approximately 6:00 to 8:30 a.m. on Day 1. The figure concentrates on fires in the South of Market and Foot of Market areas. Loss of water in the South of Market area hampered firemen. For example, Hansen and Condon (1989) report that water in the vicinity of 6th and Folsom St. gave out nearly one hour after the earthquake, with the result that a fire at the Prost Bakery on 6th St. was able to spread unabated in the area.

Table 2. Original Ignitions Following 1906 Earthquake

No.	Location	Responding Company/Comments
1	211 Clay (100' W of Davis)	E12
2	119-123 Clay St	
3	15 Fremont	
4	Drumm and Jackson Sts (401 Drumm?)	
5	Dupont (Grant)@Pacific & Bdwy	T2 extinguished
6	NW crnr William & O'Farrell	E2; exting w/ sand (Capt. Brown)
7	6th & Howard (130-134 6th St)	E6 retreated E fr 6th bet Folsom & Clementina
8	Montgomery bet Bush & Pine	no fire indicated; gas pressurized
9	307-11 Davis nr Clay	E12 extinguished
10	blk bet Calif, Mkt & Davis	very rapid spread, frame bldg; E1
11	Sansome North of Pine	in basement, very rapid spread, frame bldg
12	Calif & Battery, NW corner	
13	219 Front nr Sacramento	E1 respndd, no water
14	Mission & 22nd St	extinguished after 5 hrs; E13,18,24,37,T7,E25
15	GG ave & Buchanan (NW crnr)	extinguished after 5 hrs; E15,23,27,30,34;
16	Fulton & Octavia (NW crnr)	extinguished after 5 hrs; E14,21,34; Chem4;
17	Hayes & Laguna	extinguished after 5 hrs; E14,21,34,Chem4,T6;
18	Ashbury & Waller	E30, extinguished
19	Masonic & Waller	E30, extinguished
20	Ashbury Hgts	E30 (Argonaut reports E30 exting 3 fires Ashbury Hgts)
21	Homestead Dist (FIRES?)	E32; district is S of Mission dist, nr county line
22	Homestead Dist (FIRES?)	E32; district is S of Mission dist, nr county line
23	Pacific @ Leavenworth (NW crnr)	E31; exting w/ sand (NB: not same as E2)
24	17th & Clement	E36; exting by bucket brigade
25	3rd & Clement	E26; exting small fire rear of store
26	Oak nr Stanyon	E22; exting?
27	2625 1/2 Harrison(22nd & 23rd Sts)	E25, T9; exting
28	"Butchertown" (Hunters Pt?)	E11
29	"Butchertown" (Hunters Pt?)	E11
30	Polk bet Bush & Pine (1312 Polk)	E3, T4
31	Bay & Powell	E28; stack collapse on kiln; exting in 2 hrs
32	Bay & Kearny	E20, no water; redirect to foot of Washington St fire
33	Steuart(E)@Mission & Howard	E1,9,38
34	Fremont (E)@Mission & Howard	little water
35	Howard E of 3rd St	spilled coals; E4 (fire stn next dr), little water;
36	282 Natoma (E of 4th St)	
37	Bet 5th & 6th Sts, Mkt to Harrison	No. FIRES & locations unknown; T3 arrives at 0800
38	Bet 5th & 6th Sts, Mkt to Harrison	No. FIRES & locations unknown; T3 arrives at 0800
39	395? Hayes (S) 75' E of Gough	"Ham & Eggs fire"; E14,24,34; see NBFU Fig 14; no water
40	Davis bet Pacific & Bdwy	exting by Chem Co
41	Front bet Vallejo & Bdwy	exting by Chem Co
42	Davis & Vallejo (crnr)	exting by Chem Co
43	East St bet Bdwy & Vallejo	exting by Chem Co
44	Golden Gate Ave nr Divisadero	E30 (poor water, fire confined to 1/4 blk; 12 hses lost)
45	Bush & Kearny	"noticed in neighborhood"
46	Market & Kearny	no water
47	Geary & Stockton (239-241 Geary)	E2, exting, SAR
48	Howard & 12th (NW crnr)	E22, no water, attempted to draft fr sewer unsuccessfully
49	Sutter & Polk (1215 Sutter)	T4, exting
50	Minna & 5th	soon merged with Jessie & 3rd fire
51	Jessie nr 3rd	soon merged with Minna & 5th fire
52	Market & Beale	E1, but "a dozen powerful streams" reqd.

Note: Alphanumerical codes, e.g., E1, T1, Chem 1, denote specific engine, ladder truck, and chemical companies, respectively, of the 1906 San Francisco Fire Department

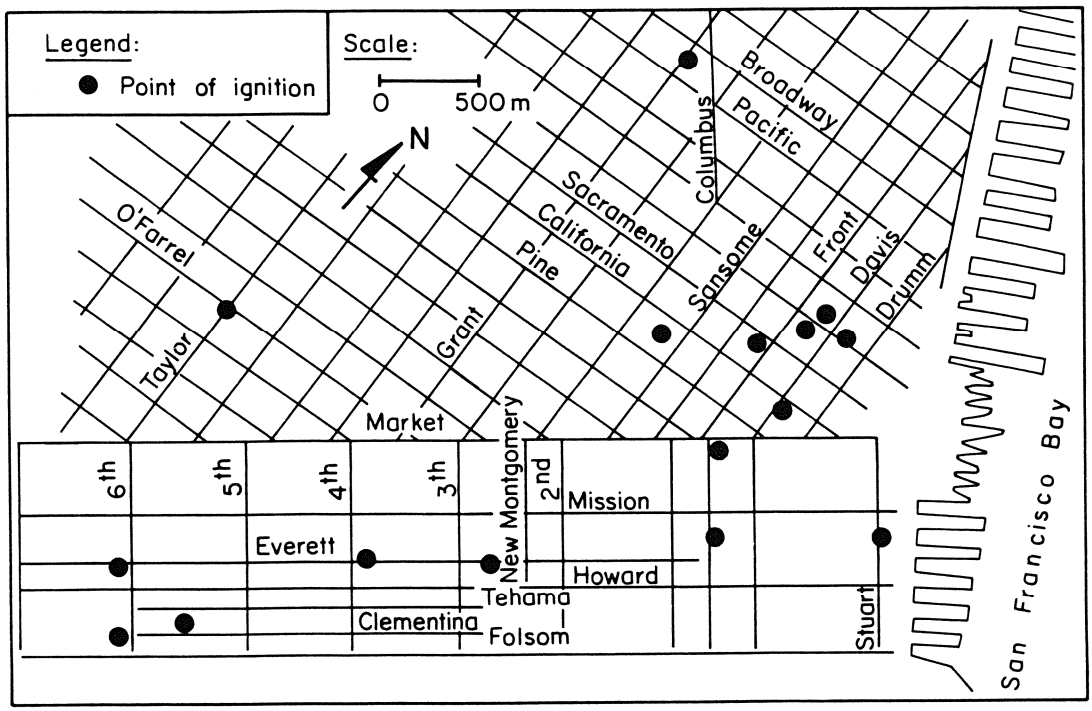

Figure 26. Ignitions in CBD Following the San Francisco Earthquake, at Approximately 6:00 a.m., April 18, 1906

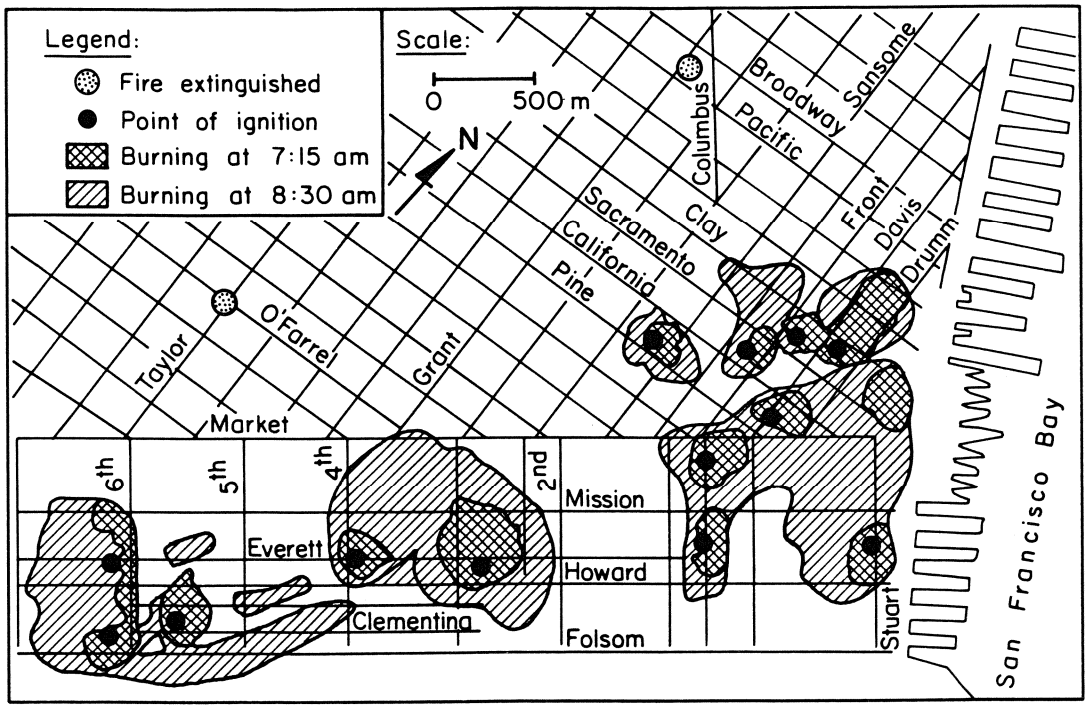

Figure 27. Fires Extinguished and Spread of Initial Ignitions, from Approximately 6:00 to 8:30 a.m., April 18, 1906

Figure 28 shows the burnt and burning areas of the city near the end of Day 1. A substantial portion of the South of Market and Foot of Market areas had been consumed or were burning. Hansen and Condon (1989) report:

> *"There were ten fire stations in the South of Market area before the earthquake...the combination of earthquake damage to firehouses, runaway horses, multiple fires, and necessity to rescue trapped people overwhelmed the resources of the stations. They had lost centralized communications and could not call for assistance, even if it was available."*

Examination of Table 2 indicates 20 of the 52 fires were extinguished, although some not without considerable effort. The Lippmann fire at Mission and 22nd Sts. (No. 14 in Table 2), for example, threatened the major high density residential area known as the Mission District. Four companies fought this fire until late in Day 1, saving the Mission District but being prevented from moving on to other fires. Similarly, fire No. 15, in an area known as the Western Addition, and fires No. 16 and 17 (which quickly merged), nearby 15, required five and four companies, respectively. As Bowlen noted in his outline:

> *"...With eight engines on two fires, how could fifty be cared for?"*

12.3 Assessment

Figure 24 shows a strong correlation between burnt sections of the city and those sections cut off from the College Hill and University Mound Reservoirs by ground failures. Of especial note is the rapid spread of the ignitions south of Market, where water supply was entirely interrupted due to the large ground deformations along Valencia St. and in the immediate South of Market areas. This rapid spread was due to three causes: 1) lack of water for available fire department engines, 2) highly combustible high density wood frame construction, and 3) insufficient fire department engines, which were drawn to concentrate at major fires threatening whole districts, such as at fire Nos. 14 - 17, where water was available, even if in limited quantities.

The spatial relationship between unburnt districts and availability of water implies that pipeline system integrity played a key role in limiting the spread of fire, and that areas suffering from ruptured pipelines fared poorly. This inference must be made with caution, however, since the development of the fire south of Market by mid-afternoon had resulted in a burning perimeter or

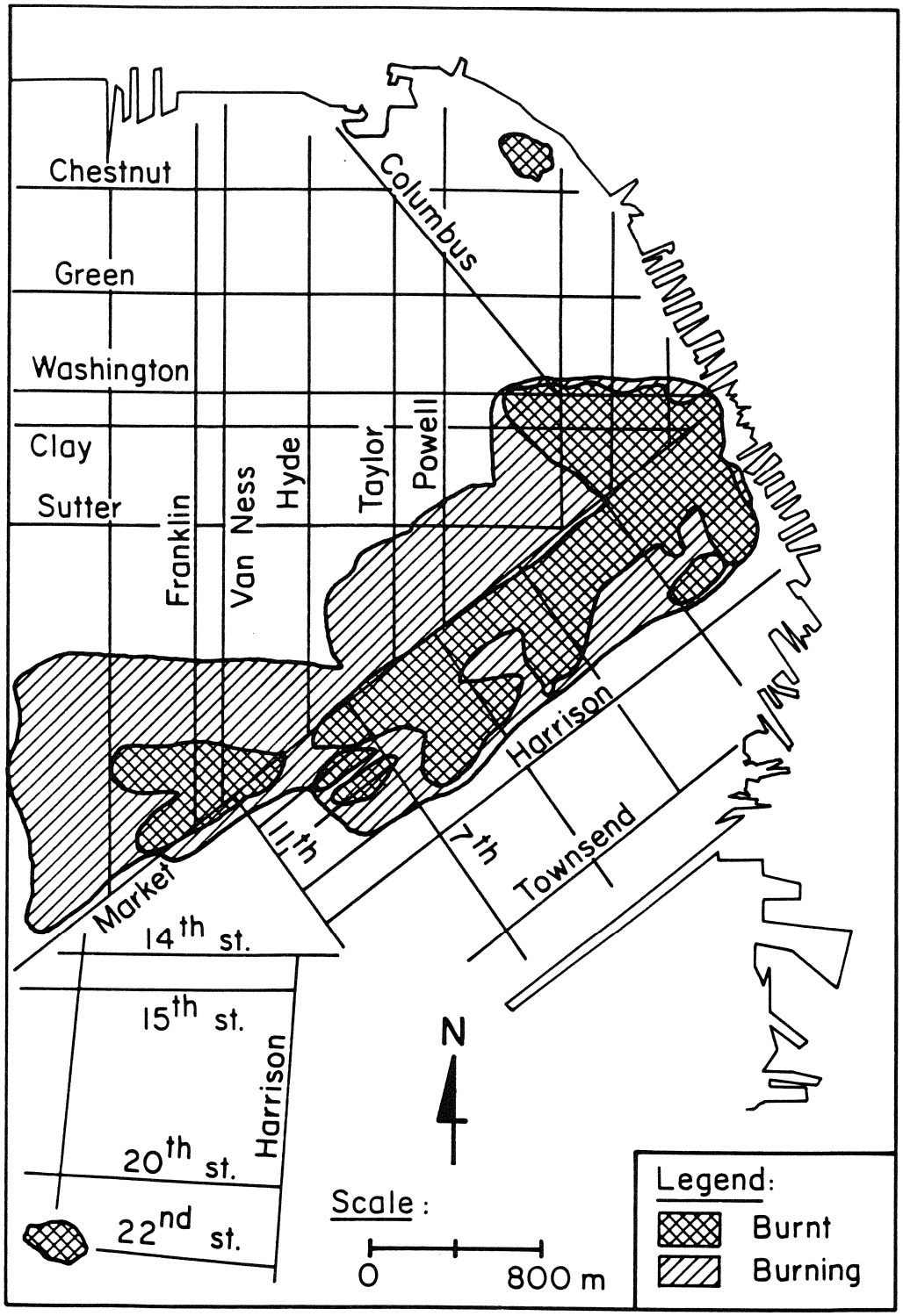

Figure 28. Fires and Burnt Sections of San Francisco, at Approximately Midnight, April 18, 1906

flamefront on the order of 7.5 km. Effective defense along this flamefront would require on the order of one to two hundred handheld lines, or virtually the entire steam engine force of the fire department. Even if effective, this ignores branding (i.e., fire spread by burning debris, flying over defense lines and causing fires behind the fireline) and does not consider whether the water supply system, if intact, could have furnished the required water (95,000 to 190,000 l/min.). Even if this defense had held, the firefighters, fully occupied south of Market, may have been outflanked by fire No. 39 (the "Ham and Eggs" fire), which did indeed sweep down from the west during the second period, outflanking the defending line along Market.

13.0 DAMAGE OF THE GAS SUPPLY SYSTEM

The main source of information about the 1906 gas supply system in San Francisco comes from Jones (1906), excerpts of which also appear in Lawson, et al. (1908). In 1906, the San Francisco Gas and Electric Co. provided gas for the city from four sources: two coal gasification plants at the North Beach Station in the Marina (see Figure 21) and the Potrero Station on Kentucky St. (see Figure 29), and two oil gasification plants at the Martin and Potrero Stations. Damage to the North Beach Station is described in Section 9.1. The earthquake effects at the other stations was described (Jones, 1906) as being *"peculiar, but so lacking in severity that these stations remained in commission."*

A large diameter (600 to 750 mm) cast iron feeder, or trunk, pipeline existed between the North Beach and Potrero Stations, as shown in Figure 29. Jones describes the explosions which occurred in the feeder system:

> *"On the thirty-inch (750-mm) main, running from the Potrero works on Kentucky, Mariposa, Potrero Avenue, Tenth, Market, and Fell to Van Ness Avenue, and thence along Van Ness to Broadway, there were twenty-one explosions. In nearly every case, the explosion took place at a line drip or cross, where the main was weakest, and the earth around the main was thrown up, leaving openings of various sizes up to twelve feet wide and thirty feet long, and on the line of the twenty-four inch (600-mm) feeding main connecting the two stations there were as many as forty breaks due to explosions."*

Settlement and lateral displacement of fill at Vallejo St. and Van Ness Ave. (see Section 10.4) ruptured a 600-mm-diameter gas feeder main where it turned

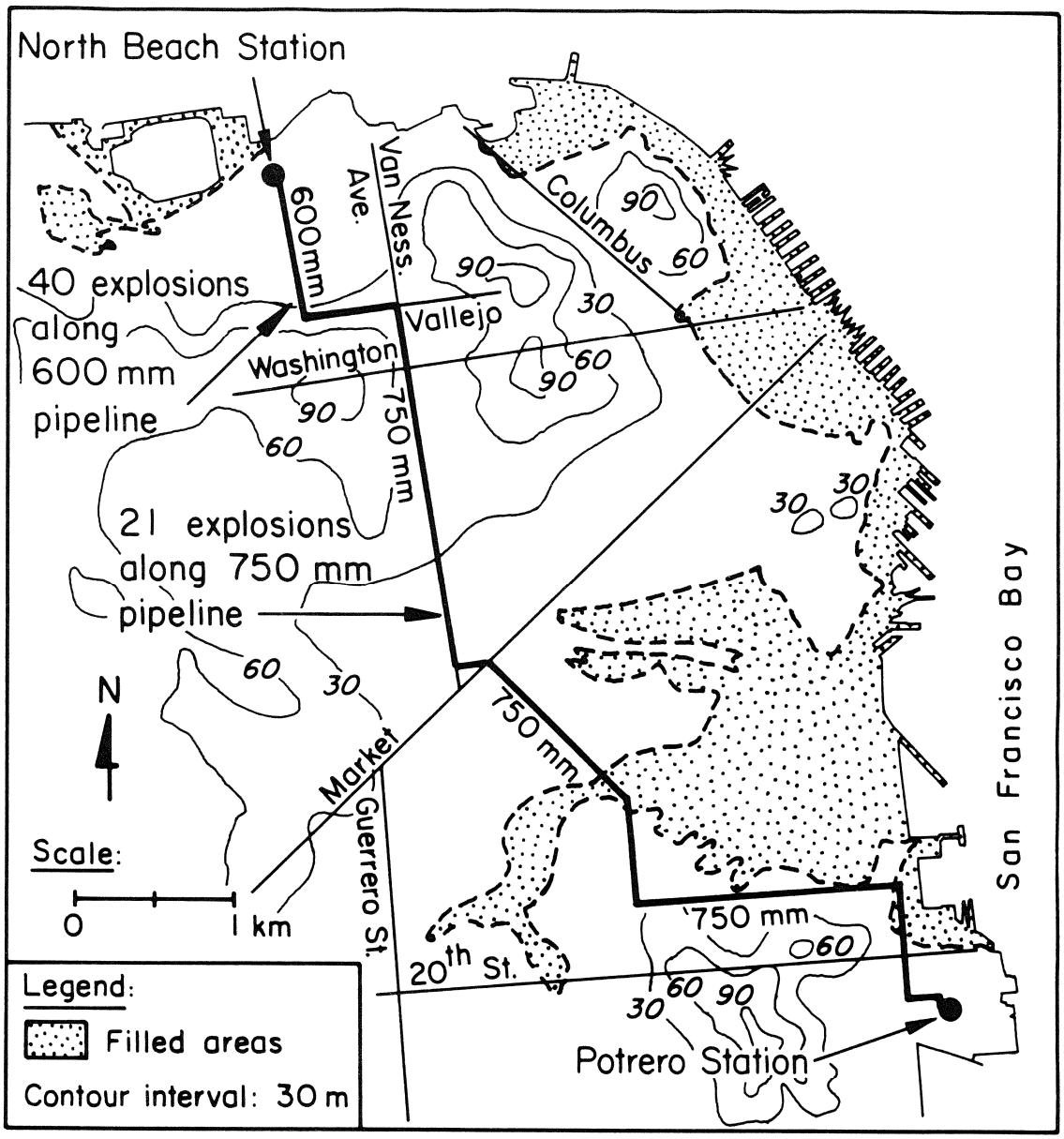

Figure 29. Gas Pipeline Feeder System in 1906 San Francisco

from Van Ness Ave. to Vallejo St. The pipe at this location was pulled apart 550 mm (Jones, 1906). At this location, there were other prominent failures of water and sewer mains, apparently associated with unstable soil used to fill a ravine leading to the former Washerwoman's Lagoon.

Jones (1906) claimed that the explosions occurred after the gas had been shut from the city mains, and inferred that such explosions did little or no damage

to life or property. Hansen and Condon (1989) point out that the large gas mains were along major streets used by refugees to evacuate the city, and that eyewitness accounts indicate that people were injured and killed as a result of the explosions. Reynolds (1906) reported on damage to underground electric cables attributed to gas explosions, and Hyde (1906) asserted that gas main explosions caused serious destruction of city streets and utilities.

14.0 PIPELINE BREAKS

San Francisco's water supply system was severely disrupted by permanent ground movements during the 1906 earthquake. In 1906, the water distribution network was composed principally of cast iron pipes connected by lead caulked bell-and-spigot joints. The trunk system of pipelines, larger than or equal to 400 mm in diameter, was composed of approximately 78% and 22% of cast and wrought iron pipe, respectively. The pipeline network was particularly vulnerable to ground movements because of the brittle nature of the cast iron and the relatively low pullout capacity of the joints. The response of the system to the 1906 earthquake is of significance today, since 85% of the Auxiliary Water Supply System in San Francisco still is composed of cast iron mains.

Figure 30 presents a map of the location of water main breaks resulting from the 1906 earthquake, as reported by Schussler (1906) and Manson (1908). The dotted lines in the figure represent the extent of street subsidence as reported by Schussler (1906). The pipeline breaks and street settlements are overlain on selected former topographical features, such as the original shoreline and border of marshes shown as solid lines, and selected elevation contours represented by the dashed lines. These contour lines and shoreline bound the extent of fill at the time of the earthquake.

There is a remarkable correlation between the locations of pipeline breaks and the subsurface topography. Approximately 50% of all pipeline breaks south of Market St. fall on or within the zero contour lines which mark the boundaries of the in-filled marshes and former bay. Approximately 80% of all pipeline breaks south of Market St. fall on or within the 12 m contour lines. As shown in the figure, all of the street settlements occurred in filled areas.

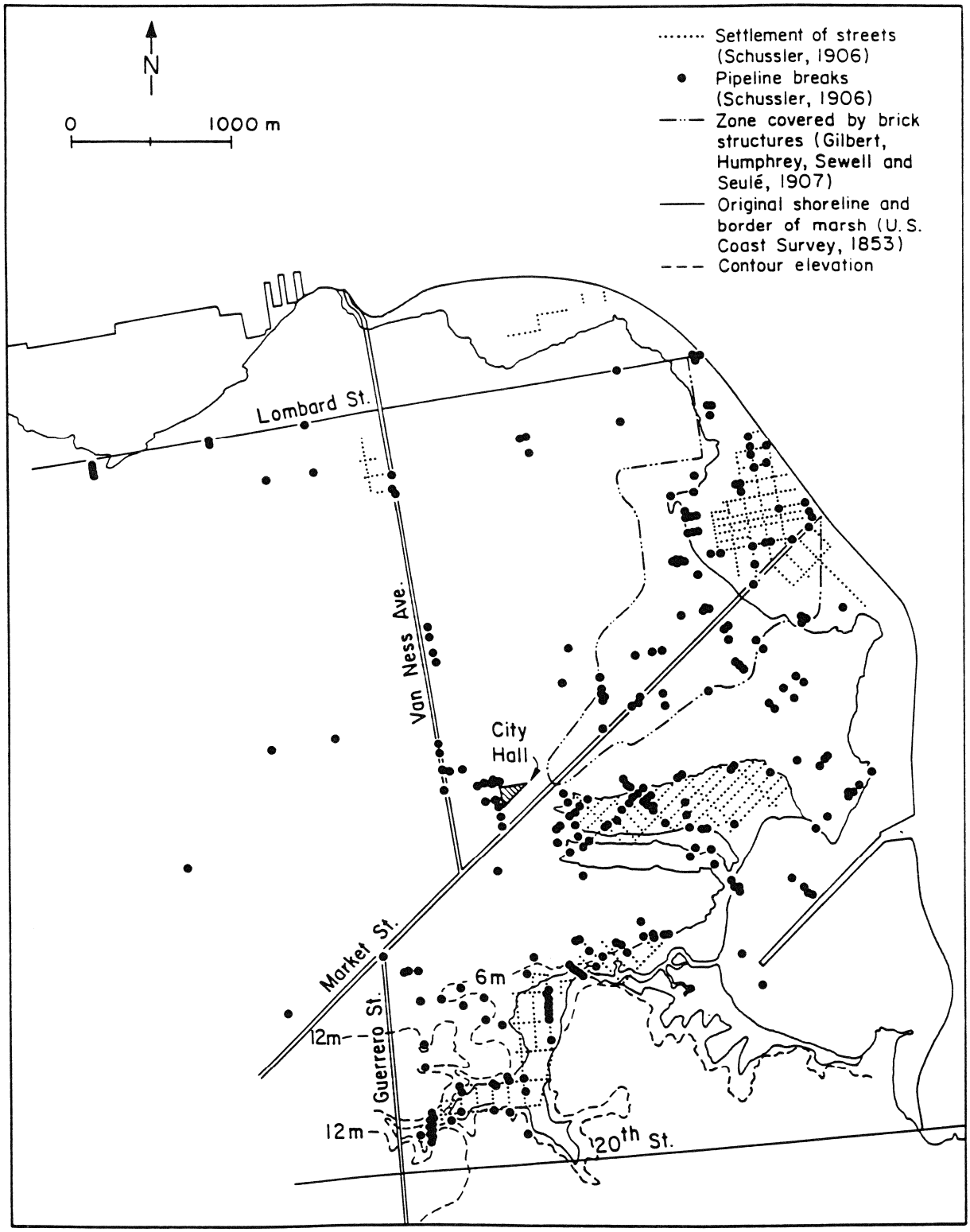

Figure 30. Pipeline Breaks and Street Settlements in San Francisco After 1906 Earthquake (after Schussler, 1906; Manson, 1906)

If a pipeline network is viewed as a system of linear extensometers, the pipeline breaks can be used to identify zones of ground displacements. Data are acquired according to the binary output of damage or lack of damage. The resulting pattern of breaks provides direct evidence of ground displacement. The settlement of the streets, viewed in conjunction with the pipeline breaks, essentially delineates the zones of permanent ground movements.

Several trends are apparent in studying pipeline breaks in the three major zones of ground displacements. In the Mission Creek area, pipeline breaks are concentrated where elevation contours converge or loop outward, signifying buried ravines and narrow stream channels. A large proportion of the breaks lie along the boundary between solid and "made" ground, particularly along the borders of former marshes in the Mission Creek and South of Market areas, and along the shoreline of the former Yerba Buena Cove in the Foot of Market area. The differential movements are most severe along the margins of the in-filled areas, and therefore pipelines are particularly vulnerable in this zone. As Schussler (1906) describes:

> *"...in the large majority of cases, principally confined to and caused by the sudden sinking of the streets over the old swamps, which movement (the same as happened to the city's sewers there) tore the pipe over the swamp away from the pipe on terra firma.*
>
> *In the streets within the main body of the sunken swamp districts, which during the earthquake rapidly moved up and down and sideways, back and forward, like jelly in a shaken bowl, there were also, naturally, a number of breaks in the street pipes, caused by the twisting and rapidly undulating motion of ground in which the pipes had to be laid."*

Outside the three principal zones, several breaks still can be attributed to permanent ground movements. For example, at the intersection of Lombard and Octavia Sts., and at Van Ness Ave. and Vallejo St., pipeline breaks are associated with the smaller zones of MM IX to X intensity.

It should be noted, however, that many of the breaks on solid ground are not associated with permanent ground movement. The damage to pipelines on Market St. between 4th and 5th Sts. was a result of blasting when buildings were leveled in an attempt to contain the spread of the fire (Schussler, 1906). Others are results of the rupture and explosion of gas mains which destroyed sections of streets, along with underground conduits and pipelines (Hyde, 1906). Hyde

(1906) also postulated that another cause of breaks in gas mains may have been the intense heat of the fire which broke out following the earthquake.

Still other breaks on solid ground may have been caused by the collapse of masonry structures. Water main breaks were concentrated near City Hall. The building, a massive brick structure, was completely wrecked by the earthquake. Photographs (Himmelwright, 1906) show entire sections from the upper part of the heavy brick walls which were shaken down, several intact blocks of which weighed as much as several tons. The falling debris most likely was the cause of many of these breaks. The dashed and dotted line shown in Figure 30 outlines the section of downtown San Francisco which contained primarily brick structures. The high number of pipeline breaks in this zone may be associated in part with the collapse of unreinforced masonry buildings.

Several pipeline breaks were described or photographed in the literature and are cataloged in Table A.2 of the Appendix. In addition to the numerous breaks to the water supply system, street subsidence also crushed many of the brick sewers, such as on 14th and Howard, 17th and Howard, and on Valencia St.

15.0 SUMMARY OF GROUND MOVEMENTS

In comparing the original topography with maps of soil movements (see Figures 9, 13, and 19), several observations can be made. The ground movement patterns show a close relationship with the original topography, with the direction and magnitude of lateral spreading controlled in large measure by morphological details. As an example of the influence of underlying topography at 19th and Guerrero Sts., the flow direction changed through 90 degrees as movements were canalized by the course of a buried ravine. The greatest displacements occurred in areas where the contour lines of the original topography converged, indicating a narrowing of the valley or ravine. In these areas, movements were restricted to a relatively narrow zone.

A second important observation involves the close correspondence between locations of lateral spreading and subsidence. Areas of large settlement, some of which resemble sinkholes, developed at the same locations as large lateral displacements. This implies a relatively complex mechanism of deformation, in

which lateral movements follow a downslope course at the same time as volumetric loss in the underlying soil results in caving-type distortion, with prominent surface depressions. This complex relationship between lateral and vertical movement is illustrated in the Mission Creek Zone (see Figure 9), in which volumetric losses in the soil between Dore and 19th Sts. resulted in a large subsidence feature superimposed on a general southeastern trend of lateral spreading.

Compressive deformations were observed in all areas of lateral spreading and subsidence. Several of these compressive features are unusual in that the corresponding mechanism of permanent ground displacement at these locations should have resulted in a net tension. The compressional features are interpreted as evidence of dynamic deformations which occurred as a result of ground oscillations within the zones of soil liquefaction.

The distribution of pipeline breaks along and slightly removed from the margins of the previous marsh areas also is noteworthy and deserves further explanation. Figure 31 shows a cross-sectional view of an area filled with loose granular soil. As liquefaction leads to lateral spreading and consolidation of the underlying sediments, there is a tendency for soil displacements to converge toward the center of the filled area. This lateral extension of the soil promotes subsidence scarps and graben-type features that are consistent with the occurrence of surface depressions. The movement relieves the horizontal restraint against the margins, causing slumping of the fill, even at fill locations above the water table. The slumping is abetted by seismic shaking. This mechanism of marginal slumping effectively extends the zone of influence of soil liquefaction. It leads to a pattern of displacement and associated pipeline damage which is removed from the exact location of the former marsh and bay areas. As a consequence, pipeline breaks occur along elevation contours higher than the original water levels.

By combining the locations of pipeline breaks, patterns of ground displacement, and previous topographical features, it was possible to develop a system for mapping zones of liquefaction hazards in San Francisco. Figure 32 shows the zones of potentially large ground movements, mapped as a result of this study, in relation to the zones of ground failure delineated by Youd and Hoose (1978).

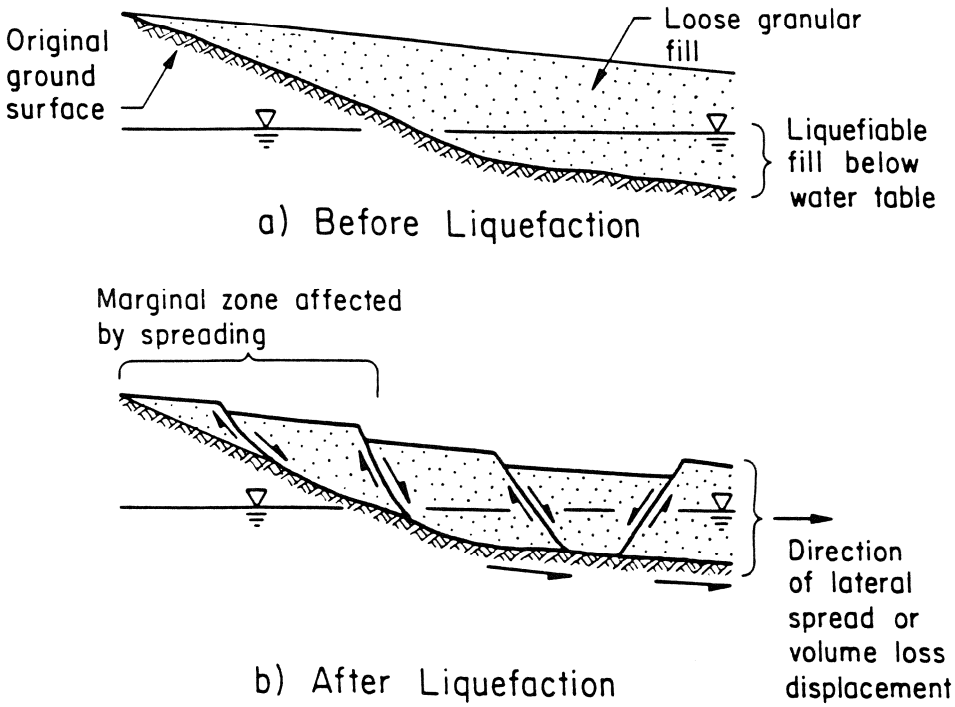

Figure 31. Idealized Section Through Lateral Spread

There is a close agreement between the two studies for the Foot of Market and South of Market Zones. Additional information about the previous topography and locations of pipeline breaks has permitted refinements in the delineation of the Mission Creek Zone. In particular, an additional area looping westward along 14th St. is shown on the basis of the original topography, pipeline breaks located by Schussler (1906) and Manson (1908), and damage to sewers reported by Hyde (1906).

Zones are shown for the Marina and North Beach areas. The Marina includes sandy soils placed by end dumping and hydraulic filling as well as a sand bar, known previously as Strawberry Island. Detailed information about the soils in the Marina is provided elsewhere in this volume by O'Rourke, et al. (1991).

The North Beach area includes soils which were placed by end dumping into the bay both before and after the 1906 earthquake. This area includes Pier 45, where sand boils and lateral spreading were observed after the 1989 Loma Prieta

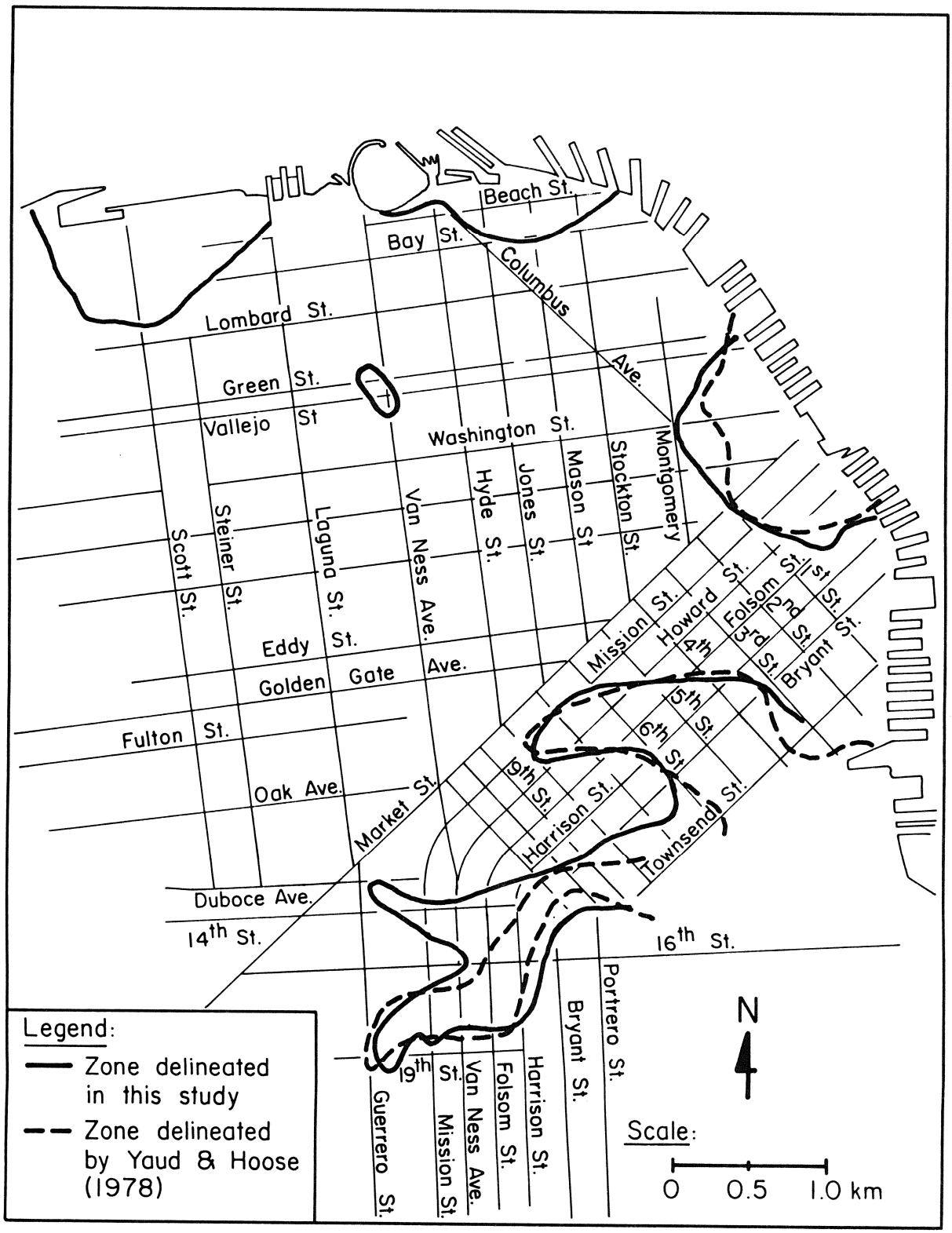

Figure 32. Zones of Potential Large Ground Displacements in San Francisco

earthquake. In Figure 32, only the areas of settlement delineated by Schussler (1906) and fill placed after 1906 were used to identify soils near North Beach which are potentially susceptible to ground deformation. The lack of historic evidence for ground movements at other locations in the North Point area resulted in their exclusion from the map.

The ovoid zone near the intersection of Vallejo St. and Van Ness Ave. involves soil which settled and moved laterally within a ravine leading to the previous Washerwoman's Lagoon. Observations of soil movement and lifeline damage in this area are summarized in Section 10.4.

It should be emphasized that Figure 32 shows areas of potential earthquake-induced soil deformation, developed primarily on the basis of the historic record of deformations observed after the 1906 earthquake. Soil densities, water tables, and continuity of loose fill may have changed at various locations. For example, the Foot of Market area includes many streets within the CBD where deep excavations and installation of pile foundations may have resulted in the densification of adjacent fills. Moreover, the construction of deep basements, sheet and soldier piles left in place around construction perimeters, and the building of subsurface structures (such as BART and reinforced box culverts for storm water storage) will tend to stabilize and reinforce the soils on a district-wide basis against large lateral displacements. Hence, the issues of subsurface infrastructure development and any stabilization resulting therefrom are not addressed in Figure 32. The figure should be biased towards a conservative display of potential deformation, which can serve as a reference for emergency planning, preliminary estimates of disruption, and further geotechnical investigations to clarify subsurface conditions and judge if they are consistent with a permanent ground movement scenario.

16.0 CORRELATION OF LATERAL SPREADS WITH SURFACE AND SUBSURFACE GRADIENTS

Research investigations have shown that the magnitude of lateral spreading was related in some previous earthquakes (e.g., Hamada, et al., 1986) to the gradient, or slope, of the ground surface and of the interface between the base of a liquefiable deposit and underlying non-liquefiable soil. This relationship was investigated for the 1906 earthquake by evaluating surface survey and

subsurface data at locations in the South of Market and Mission Creek areas where lateral movements were observed and documented. Lateral movements observed in the Foot of Market area were not included because the boundary conditions imposed by the seawall were different than those associated with movement in the South of Market and Mission Creek areas. A description of the surface survey data and basis for estimating subsurface gradients is given in Appendix B.

Table 3 lists the observed lateral movement, magnitude of lateral displacement, surface slope parallel to the direction of movement, and slope estimated for the base of the liquefiable deposit at each location. The magnitude of lateral movement was taken as a value halfway between the limits of maximum displacement indicated in Figures 9, 13, and 15 at the locations listed in the table. Where only one value is shown at a particular location, this is the value that was used. In each instance, historic information indicates that the maximum displacement was oriented nearly parallel to the dip direction of the slope.

As shown in Figure 33, the magnitude of lateral displacement follows a trend of increasing ground movement relative to increasing slope gradient. The 1:1 slope in the figure is shown solely as a reference, and does not indicate a statistical fit between this line and the data. In fact, regression analyses do not show a statistically meaningful trend. For example, the best linear fit of the data has an $r^2 = 0.18$, which represents a relatively poor correlation for explaining the variability of the observations.

Regression analysis of lateral displacement relative to basal slope of the liquefied soil did not result in a good fit of the data. Moreover, multiple regression analyses of the displacement relative to both surface and basal slopes resulted in correlations with similar characteristics.

For this relatively sparse data base, a statistically significant relationship cannot be shown between the maximum displacement associated with lateral spreading and the gradient of either the ground surface or the underlying interface between liquefiable and non-liquefiable soil. This lack of correlation is consistent with the findings of Japanese researchers. Using a substantially larger data base taken from case history studies of the 1964 Niigata

Table 3. Summary of Lateral Spreads, Surface, and Subsurface Gradients of Locations of Documented Lateral Deformation During the 1906 Earthquake

Location	Number	Lateral Movement, m	Surface Slope, percent	Slope of Base of Liquefiable Deposit, percent
19th St. and Linda St.	1	1.8	1.60	4.40
Valencia St. between 18th - 19th Sts.	2	2.1	1.80	1.40
Mission St. between 17th - 18th Sts.	3	0.3	1.35	1.35
Capp St. between 17th - 18th Sts.	4	1.0	1.24	0.00
South Van Ness Ave. between 17th - 18th Sts.	5	1.2	1.02	0.00
Mission St. and 7th St.	6	2.0	2.10	2.10
Folsom St. between 5th - 6th Sts.	7	1.4	0.80	0.80
Harrison St. between 5th - 6th Sts.	8	1.4	0.40	0.00

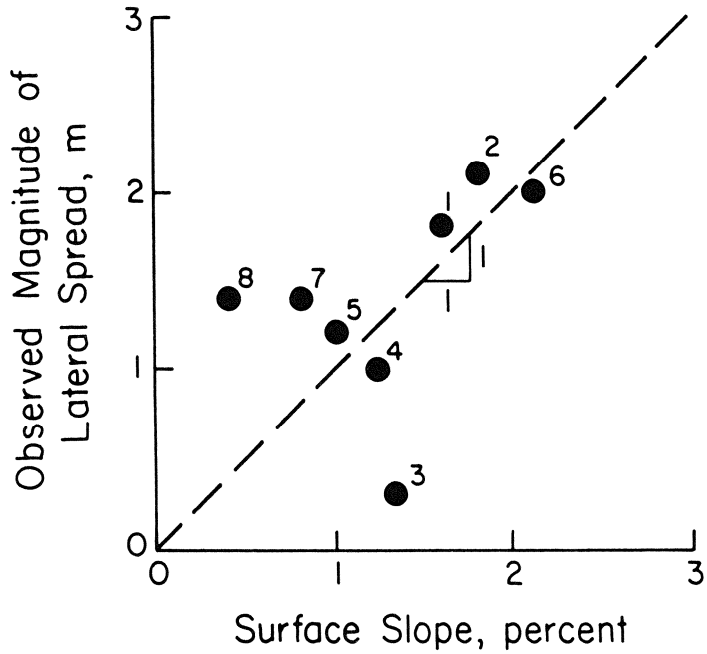

Figure 33. Plot of Magnitude of Lateral Movement versus Surface Slope at Locations of 1906 Lateral Spreading

and 1983 Nihonkai-Chubu earthquakes, Hamada (1992) and Hamada and Isoyama (1992), respectively, have shown a similar lack of statistically significant correlation between gradient and magnitude of lateral movement. These studies point out that, if liquefied soil behaves as a fluid, the displacement magnitude would not necessarily be related to slope. The mechanics of deformation would be more complex, with the ground at higher elevations tending to sink and spread laterally until the fluid achieves a uniform level. Hence, the slope may be important in defining the overall geometry of soil mass subject to flow, but should not necessarily be the controlling parameter in generating local movement at a particular section of the slope.

17.0 CONCLUDING REMARKS

One of the most distinctive features of the 1906 San Francisco earthquake was its influence on lifeline systems and the repercussions of such damage in the urban environment. Fault rupture and violent shaking of timber bridges ruptured the three principal transmission pipelines which conveyed water to San Francisco from reservoirs south of the city. Breaks in the trunk line system for water distribution at locations of liquefaction cut off most of the storage supply inside San Francisco to the burning financial, South of Market, and Mission districts of the city. Approximately 490 blocks were destroyed by fire and an additional 32 were severely damaged (Gilbert, et al., 1907), making the aftermath of the earthquake the worst single fire loss in U.S. history.

The maps of ground displacement and pipeline breaks prepared for this case history show a close relationship with the topographic and geologic characteristics of the surficial deposits. A close relationship is seen between locations of high earthquake damage intensity and areas of fill. All of the ground displacements fall within certain zones where former marshes, gullies, streams, and bays had been filled to prepare for development. Approximately 80% of all pipeline breaks to the south of Market St. occurred within the 12-m elevation contour line of the buried topography, bordering former marsh areas.

The soil displacement pattern was closely related to the buried original topography, with the direction and magnitude of lateral spreading controlled, in large measure, by morphological details. As an example of the influence of

underlying topography, at 19th and Guerrero Sts., the flow direction changed through 90 degrees as movements were canalized by the course of a buried ravine. The largest displacements occurred in areas where the contour lines of the buried topography converged, indicating a narrowing of the valley or ravine. In these areas, movements were restricted to relatively narrow zones. Moreover, the maximum displacement in each instance appears to be oriented nearly parallel with the dip direction of the slope.

There also was a close correspondence between areas of lateral spreading and subsidence. Large areas of settlement, some of which resembled sinkholes, developed at the same locations as large lateral displacements. This implies a complex failure mode, in which lateral movements follow a downslope course at the same time as volumetric loss in the underlying soil results in caving-type distortions, with prominent surface depressions.

The spatial relationship between unburnt districts and availability of water implies that pipeline system integrity played a key role in limiting the spread of fire, and that areas suffering from ruptured pipelines fared poorly. This inference must be made with caution, however, since the development of the fire south of Market by mid-afternoon had resulted in a burning perimeter or flame-front on the order of 7.5 km. Effective defense along this flamefront would require on the order of one to two hundred handheld lines, or virtually the entire steam engine force of the fire department.

System redundancy played a critical role in water delivery after the 1906 earthquake. The ability to disengage the Pilarcitos conduit from the ruptured transmission system south of the city and connect it with Lake Merced was of vital significance. Water to Lake Honda was provided in continuous supply to the western districts of San Francisco where the fire was stopped. The lack of redundancy across zones of large ground deformation in the Mission district meant that pipeline failures resulted in the loss of over 56% of the city supply. Only 6% of the total reservoir capacity was directly accessible at the time of the earthquake to fight the fires in downtown San Francisco.

This case study not only clarifies the state of damage to the 1906 water supply and its relationship with liquefaction-induced ground failure, but also

illustrates where the zones of maximum vulnerability are likely to be in the present system. It also stresses how a functional water supply is not sufficient by itself - a functional fire department of sufficient delivery capability also is required. Accordingly, the study of 1906 San Francisco provides clear and unmistakable lessons with respect to earthquake effects in the urban infrastructure. Permanent ground deformation is shown to be a major source of utility disruption which, in turn, affects emergency response. Planning to reduce seismic risk in urban and suburban environments requires a coordinated geotechnical, lifeline, and emergency services effort.

REFERENCES

American Society for Testing and Materials, "Standard Method for Penetration Test and Split-Barrel Sampling of Soils," Annual Book of Standards (D-1586-84), Vol. 4.08, ASTM, Philadelphia, PA, 1989, pp. 221-225.

Argonaut, "The Great Fire of 1906," weekly newspaper accounts from May 1 to Aug. 20, 1927 published in the Argonaut, San Francisco, CA.

Bolt, B.A., "The Focus of the 1906 California Earthquake," Seismological Society of America Bulletin, Vol. 58, No. 1, pp. 457-471, 1968.

Bowlen, F.J., "Outline of the History of the San Francisco Fire," prepared by F.J. Bowlen, Battalion Chief, S.F.F.D., original manuscript held by California Historical Society Library, San Francisco, CA, undated.

Bowlen, F.J., "Reports of Fire Officers of the San Francisco Fire Department on the Fire of 1906," original manuscript held by Bancroft Library, University of California, Berkeley, CA, undated.

Bronson, W., The Earth Shook, The Sky Burned, Doubleday and Co., Inc., Garden City, NY, 1959.

Brown, A.A., et al., "Subsidence and the Foundation Problem in San Francisco," Report of the Subsoil Committee, ASCE, San Francisco Section, 1932.

Chameau, et al., "Liquefaction of Fill Soils in San Francisco - 1989 Earthquake: A Preliminary Report," Geotechnical Report 90/8, Purdue University, W. Lafayette, IN, July 1990.

Committee of Twenty, "Report of National Board of Fire Underwriters by Its Committee of Twenty on the City of San Francisco, California," H. Evans, Chrmn., July 1905.

Committee on Earthquake Engineering, Liquefaction of Soils During Earthquakes, National Research Council, National Academy Press, Washington, D.C., 1985.

Dames and Moore, "Factual Report Site Investigation for Completion of Preliminary Design - Phase I Muni Metro Turnaround Facility," Vols. I, II, and III, Job No. 185-215-03, San Francisco, CA, Nov. 1989.

Derleth, C. Jr., "Some Effects of the San Francisco Earthquake on Waterworks, Streets, Sewers, Car Tracks, and Buildings," Engineering News, Vol. 55, No. 20, May 1906, pp. 548-554.

Duryea, E. Jr., et al., "The Effects of the San Francisco Earthquake of April 18th, 1906 on Engineering Constructions," Transactions, ASCE, 1907, pp. 208-329.

Ellsworth, W.L., "Earthquake History, 1769 - 1989," The San Andreas Fault System, California, R.E. Wallace, Ed., U.S. Geological Survey Professional Paper 1515, Washington, D.C., 1990, pp. 153-187.

Gilbert, G.K., R.L. Humphrey, J.S. Sewell, and F. Soule, "The San Francisco Earthquake and Fire of April 18, 1906 and Their Effects on Structures and Structural Materials," Bulletin 324, U.S. Geological Survey, U.S. Government Printing Office, Washington, D.C., 1907.

Goldman, H.B., "Geologic and Engineering Aspects of San Francisco Bay Fill," Special Report 97, California Division of Mines and Geology, San Francisco, 1969, pp. 1-29.

Golden Software, Inc., "Surfer," Golden, CO, 1985.

Gutenberg, B. and C.F. Richter, Seismicity of the Earth and Associated Phenomena, 2nd Ed., Princeton University Press, Princeton, NJ, 1954.

Hall, W.H., "Some Lessons of the Earthquake and Fire," San Francisco Chronicle: - I. "Reminiscences of the City's Site as Accounting for Earthquake Effects," May 19, 1906; - II. "A Record of Earthquake Disturbances," May 20, 1906.

Hamada, M., S. Yasuda, R. Isoyama, and K. Emoto, "Study on Liquefaction-Induced Permanent Ground Displacements," Association for the Development of Earthquake Prediction, Tokyo, Japan, Nov. 1986.

Hamada, M., "Large Ground Deformations and Their Effects on Lifelines, 1964 Niigata Earthquake," Technical Report NCEER-92-0001, National Center for Earthquake Engineering Research, Buffalo, NY, Feb. 1992.

Hamada, M. and R. Isoyama, "Large Ground Deformations and Their Effects on Lifelines, 1983 Nihonkai-Chubu Earthquake," Technical Report NCEER-92-0001, National Center for Earthquake Engineering Research, Buffalo, NY, Feb. 1992.

Hanks, T.C. and H. Kanamori, "A Moment Magnitude Scale," Journal of Geophysical Research, Vol. 84, No. B5, pp. 2348-2350, 1979.

Hansen, G. and E. Condon, Denial of Disaster, Cameron and Company, San Francisco, CA, 1989.

Harding Lawson Associates, Dames & Moore, Kennedy/Jenks Chilton, and EQE Engineering, "Draft Report: Marina District and Sullivan Marsh Area Liquefaction Study, San Francisco, California," Report prepared for the City and County of San Francisco Bureau of Engineering, HLA Job No. 17952, 041.04, June, 1991.

Himmelwright, A.L.A., The San Francisco Earthquake and Fire: A Brief History of the Disaster, The Roebling Construction Company, New York, NY, 1906.

Holden, E. S., "A Catalogue of Earthquakes on the Pacific Coast, 1769 to 1897," Smithsonian Miscellaneous Collections, Vol. XXXVII, No. 1087, Smithsonian Institution, Washingon, D.C., 1898.

Hovland, H.J., "Potrero-Embarcadero 230 KV Underground Conduit: Study of the Potential for Earthquake-Induced Ground Movements," Pacific Gas and Electric Company, San Francisco, CA, Sept. 1980.

Hovland, H.J. and R.D. Darragh, "Earthquake-Induced Ground Movements in the Mission Bay Area of San Francisco in 1906," Proceedings, 2nd Specialty Conference of the Technical Council on Lifeline Earthquake Engineering, ASCE, Oakland, CA, Aug. 1981, pp. 293-309.

Hyde, C.G., "The Structural, Municipal, and Sanitary Aspects of the Central Californian Catastrophe - III," The Engineering Record, Vol. 53, No. 24, June 16, 1906, pp. 737-740.

Jones, E.C., "The Story of the Restoration of the Gas Supply in San Francisco After the Fire," Proceedings, 14th Annual Meeting of the Pacific Gas Association, Sept. 1906, pp. 350-364.

Jordan, D.S., Ed., The California Earthquake of 1906: San Francisco, A.M. Robertson, San Francisco, CA, 1907.

Kurtz, C.M., "The Effect of the Earthquake on Street Car Tracks in San Francisco," Engineering News, Vol. 55, No. 20, May 1906, p. 554.

Laurence, G.R., Photograph of San Francisco Just After Earthquake and Fire, April, 1906, G.R. Laurence Co., Chicago, IL, May 1906.

Lawson, A.C., et al., The California Earthquake of April 18, 1906: Report of the California State Earthquake Investigation Commission, Pub. No. 87, Carnegie Institute, Washington, D.C., 1908, 2 Volumes and Atlas, 451 p.

Leonard, J.B., "The Effect of the California Earthquake on Reinforced Concrete," The Engineering Record, Vol. 53, No. 21, May 1906, pp. 643-644.

Manson, M., "Reports on Auxiliary Water Supply System for Fire Protection for San Francisco, California," Report of the Board of Public Works, San Francisco, CA, 1908.

Newman, W.A., "The San Francisco Post Office," The Engineering Record, Vol. 53, No. 22, June 1906, pp. 694-695.

Olmsted, R., N. Olmsted, and A. Pastron, "San Francisco Waterfront: Report on Historical Cultural Resources," San Francisco Wastewater Management Program, City of San Francisco, CA, Dec. 1977, 721 p.

O'Rourke, T.D. and P.A. Lane, "Liquefaction Hazards and Their Effects on Buried Pipelines," Technical Report NCEER-89-0007, National Center for Earthquake Engineering Research, Buffalo, NY, 1989.

O'Rourke, T.D. and J.W. Pease, "Large Ground Deformations and Their Effects on Lifeline Facilities: 1989 Loma Prieta Earthquake," National Center for Earthquake Engineering Research, Buffalo, NY, 1992, this volume.

Reed, S.A., "The San Francisco Conflagration of April, 1906," Special Report to National Board of Fire Underwriters Committee of Twenty, May 1906.

Reid, H.F., "The Mechanics of the Earthquake," Vol. 2 of The California Earthquake of April 18, 1906: Report of the State Earthquake Investigation Committee, Carnegie Institution of Washington Publication 87, 1910.

Reynolds, L.E., "How Electricity Was Served to Consumers and Street Car Lines by the San Francisco Gas and Electric Co. After the Fire," Proceedings, 14th Annual Meeting of the Pacific Coast Gas Association, San Francisco, CA., Sept. 1906, pp. 365-373.

Richter, C.F., Elementary Seismology, W.H. Freeman and Company, San Francisco, CA, 1958, pp. 466-537.

Roth, R.A. and E. Kavazanjian, Jr., "Liquefaction Susceptibility Mapping for San Francisco, California," Bulletin of the Association of Engineering Geologists, Vol. 21, No. 4, Nov. 1984, pp. 459-478.

Sanborn Ferris Map Co., "Insurance Maps, San Francisco, California," Vols. 1-4, New York, NY, 1899 and 1899 updated to 1905.

Scawthorn, C. and T.D. O'Rourke, "Effects of Ground Failure on Water Supply and Fire Following Earthquake: The 1906 San Francisco Earthquake," Technical Report NCEER-89-0032, National Center for Earthquake Engineering Research, Buffalo, NY, Dec. 1989, pp. 16-35.

Schlocker, J., "Geology of the San Francisco North Quadrangle, California," Geologic Survey Professional Paper 782, U.S. Government Printing Office, Washington, D.C., 1974.

Schussler, H., The Water Supply of San Francisco, California, Martin B. Brown Press, New York, NY, July 1906.

Seed, H.B., I.M. Idriss, and I. Arango, "Evaluation of Liquefaction Potential Using Field Performance Data," Journal of Geotechnical Engineering, ASCE, Vol. 109, No. 3, Mar. 1983, pp. 458-482.

Steinbrugge, K.V., Earthquakes, Volcanoes, and Tsunamis: An Anatomy of Hazards, Scandia America Group, New York, NY, 1982.

Thatcher, W., "Strain Accumulation and Release Mechanism of the 1906 San Francisco Earthquake," Journal of Geophysical Research, Vol. 80, No. 35, pp. 4862-4872, 1975.

Tobriner, S., Personal communication regarding data on the 1906 fire and Bowlen outline, University of California, Berkeley, CA, 1988.

U.S. Coast Survey, Topographic Map of "City of San Francisco and Its Vicinity, California," surveyed by R.D. Cutts, 1853.

U.S. Coast Survey, Topographic Map of "City of San Francisco and Its Vicinity, California," surveyed by A.F. Rodgers, 1857.

Wallace, R.E., Ed., "The San Andreas Fault System, California," U.S. Geological Survey Professional Paper 1515, U.S. Government Printing Office, Washington, D.C., 1990.

Woodward-Clyde Consultants, "Geotechnical Investigation for the Proposed Channel Outfalls Consolidation Project, San Francisco, California," D.P.W. 101-966 Controller's Contract No. 50026, report to City and County of San Francisco Department of Public Works, by Woodward-Clyde Consultants, Oakland, CA, 1975.

Youd, T.L. and S.N. Hoose, "Liquefaction During the 1906 San Francisco Earthquake," Journal of the Geotechnical Engineering Division, Vol. 102, No. GT5, May 1976, pp. 425-440.

Youd, T.L. and S.N. Hoose, "Historic Ground Failures in Northern California Triggered by Earthquakes," Geologic Survey Professional Paper 993, U.S. Government Printing Office, Washington, D.C., 1978.

APPENDIX A

Tables A.1 and A.2 are a compilation of the historical accounts of ground movements in San Francisco during the 1906 earthquake, as well as observations from photographs which were used to prepare the maps of ground movements in the main text. References for the two tables are given at the end of Table A.2.

TABLE A.1 DOCUMENTATION OF HISTORICAL ACCOUNTS AND OBSERVATIONS FROM PHOTOGRAPHS ON GROUND MOVEMENTS IN SAN FRANCISCO DURING 1906 EARTHQUAKE.

MISSION CREEK ZONE:

LOCATION	REF*	PHOTO	PAGE	DESCRIPTION
General:	3		238	"As stated briefly above, a similar district of high intensity occurs in an area of made land along the lower portion of the former course of Mission Creek. This district varies in width from 1 to 2 blocks, extending from near the corner of Ninth and Brannan Streets westward for about 3 blocks, then southwestward for about 2 blocks more; and finally, westward some 4 blocks more to a point on Nineteenth Street just east of Dolores Street.
	3		239	...Enough evidence has been cited to demonstrate that high intensity prevailed thruout this district. Here, as in the other tract of made land which occupies the site of the old tidal marsh, the materials used for filling were shaken together, and caused a general depression of the surface over the whole district, accompanied by slumping or flow movements. The surface was deformed into waves, with accompanying fissures and sharp compressional arches. Here too, as in the tract previously described, the materials used for filling constitute a relatively thin rigid layer deposited upon the marshy fringes or in the shallow waters of the creek."
	4		26	"As in districts outside of San Francisco, the greatest damage was done to those structures having insufficient foundations built on soft alluvium or filled ground. The settling of the ground in the mud flats along San Francisco Bay and of the filled ground in old water courses was accompanied with great destruction. It was in such ground that the greatest number of breaks occurred in the cast-iron gas and water mains and the sewers. The breaks in the sewers were not so evident as those in the gas and water mains, for the reason that the latter were under pressure and breaks in them resulted in breaks from the settling of soft or filled ground occurred in Howard and Shotwell streets between Seventeenth and Eighteenth streets, Bryant street between Ninth and Tenth streets, Dore street between Bryant and Brannan streets (Pl. VI, A), and at the corner of Seventh and Mission streets. The settling was greatest in Howard, Dore and Bryant streets, being in Dore street at least 5 feet [1.5 m]."
	8b		739	"...In the Mission district, and in certain other parts of San Francisco, as, for instance, along the courses of former tidal streams, large areas of filled land exist.

* References listed at end of Tables A.1 and A.2.

LOCATION	REF	PHOTO	PAGE	DESCRIPTION
				In such cases, the effect produced by the earthquake was not generally in the form of waves, as already described, for the eastern portion of the city was basin-like, representing local settlement in the streets and adjacent areas, and in some cases, decided misalignment.... The most important local settlements and transverse movements occurred in the vicinity of the Valencia Hotel between 18th and 19th Sts., on Valencia St., on Howard St. between 17th and 18th; on 14th, between Mission and Howard; on Folsom, at the corner of 17th; on Mission, at the corner of 7th, and on Van Ness Ave., between Vallejo and Green Sts. Where the ground was hilly and solid, it was not decidedly affected by the earthquake shock. The distortion of the streets evidently has no relation to the character and nature of the artificial surface. For, of whatever construction this may have been, it is very evident that the street surface would follow the profile and alignment of the ground upon which it rested."
1) 19th near Guerrero	13		32	"Again, at its head between Valencia and Guerrero a side ravine came down from the south. The slip across Nineteenth street of about six and a half feet [2.0 m], as shown by bowing of the line of curbing, outlines the branch of the old depression, which was filled on steep gradient and quite naturally slid easily."
	3	pl. 94A		Photo: 1.8 m lateral spread over a distance of 38 m; 0.6 m sink on north side of 19th St. at western edge of disturbance. Lateral offset of roughly 0.3 m seen at western edge of lateral offset in foreground running across 19th. Photo caption: "View along Nineteenth Street, from Guerrero Street. Both ground and buildings moved north about 6 feet [1.8 m] toward center of old marsh, with component of movement down the channel."
	2	Fig. 50	55	Photo: Same as ref. 3 pl. 94A. Photo caption: "Lateral spread at the Youth's Directory on 19th and Guerrero Streets (loc. 217)."
	1	No. 69	97	Photo caption: "19th St. Looking West. Street & Sidewalk from A to B moved north about 5 feet [1.5m]. Brick building also moved somewhat."
	3		239	"On land made by filling in, "The Willows," a marshy tract formerly extending up the Eighteenth

LOCATION	REF	PHOTO	PAGE	DESCRIPTION
				Street from Mission near the corner of Nineteenth and Guerrero Streets, there was observed a considerable slumping or flow movement of the surface. The photograph (plate 94A) shows the Youth's Directory, a charitable institution for boys, where the street and building were moved northward and slightly eastward, toward the former channel and downstream, fully 6 feet [1.8 m]."
2) Valencia between 18th and 19th	13		32	"Mission creek estuary headed in a salt lagoon between the present lines of Howard, Harrison, Sixteenth and Nineteenth streets, extended northwest nearly to Eleventh and eastward to Mission bay at a point about on the line of King street, between Eighth and Ninth." "VALENCIA-STREET SUBSIDENCE. A number of lesser footmarks of our earthquake are to be seen in the streets between Seventh [17th?] and Eighteenth and east and south of Mission. These all coincide with the irregular limits of our indicated specially soft spots in the former salt marsh area, and we follow them around until we come to another pronounced case of subsidence and slip, which is noticeable in Valencia street between Eighteenth and Nineteenth, in Mission between

LOCATION	REF	PHOTO	PAGE	DESCRIPTION
				Seventeenth and Eighteenth and in Howard from Seventeenth to Eighteenth. Valencia street shows subsidence of one to five and a half feet [0.3 to 1.7 m] and slip of one to six feet [0.3 to 1.8 m] for 450 feet [140 m] in length; Mission shows very slight subsidence and slip of only about one foot [0.3 m] for about 400 feet [120 m] in length, while Howard shows a subsidence of two to three feet [0.6 to 0.9 m] for over 500 feet [150 m] in length and a maximum slip of about four feet [1.2m]. The limits of this movement, platted on the map, exactly outline the ravine in which was formerly located, between Mission and Valencia, "The Willows," San Francisco's place of resort. The whole area was in those days moist land, with a little stream in it for a part of each year, and which has been filled upon between hard hillsides. Being soft beneath and on a down-grade in the line of greatest earthquake vibration, the temblor found in it an easy mark for a pronounced demonstration."
	1		35	"One of the most serious breaks in the main pipe lines was caused by the earthquake shaking and settling down, by from one to five feet [0.3 to 1.5 m], the region between Eighteenth and Nineteenth streets, on Valencia

LOCATION	REF	PHOTO	PAGE	DESCRIPTION
				street. (See Photos 57, 58, 59, 63, 64, and 65.) Here an old swamp had been loosely filled in, many years ago, by any and all kinds of material and rubbish obtainable, the fill being twenty feet or more in depth. Our pipes, which had to be below the pavement of the street, had to cross this region. Being aware of this state of affairs regarding the character of the foundation and fill (I constructed the pipe in 1876), I remembered the location of this swamp, and made our 22-inch pipe of wrought-iron. I put in a number of cast-iron bell joints, with lead joints, which would give or yield somewhat in case of a slight settlement. This pipe is to-day in a perfect condition, except at the points where the swamp dropped down suddenly, during the earthquake, from four to five feet, [1.2 to 1.5 m] which naturally tore off the pipe both at the north and south boundary of the swamp. This serious break was quickly repaired by laying across the swamp and over the top of the pavement and well into terra firma on each side of the sink, a long stretch of 24-inch cast-iron pipe. This gave us a chance to drive a supply of water along Market to Sansome street, to Montgomery avenue, etc., to and into the Francisco Street Reservoir."

LOCATION	REF	PHOTO	PAGE	DESCRIPTION
	1		30	"By 7 o'clock on the evening of April 20, or sixty-two hours after the earthquake, a second stream of water was pouring into its respective city reservoir, the College Hill Reservoir. This reservoir had been emptied of its contents of 11,400,000 gallons [43.1 x 10^6 liters] which it contained at 7 A.M. April 18, by its main arterial pipe, 22-inch diameter, and its companion pipe, 16-inch diameter, both on Valencia street, having both been torn off and destroyed between Eighteenth and Nineteenth streets by the sinking of Valencia street of from one to five feet [0.3 to 1.5 m]."
	1		43	"APPENDIX D. The following are extracts from the report of City Engineer Woodward on the breaks in the San Francisco sewer system caused by the earthquake as published in the "San Francisco Chronicle" of June 17, 1906: '...On Valencia street, between Eighteenth and Nineteenth streets, there was a lateral movement to the east, with a maximum of six feet [1.8 m] and a subsidence with a maximum of five feet [1.5 m]. This occurred in made ground over the old Willows marsh, one of the tributaries of Mission creek."
	1	No. 57	93	Photo caption: "Valencia St. between 18th & 19th

LOCATION	REF	PHOTO	PAGE	DESCRIPTION
				subsided about five feet [1.5 m]; destroying sewers, and besides gas & electric pipes & conduits, tore of one 16" and on 22" water main, which at this point had about 85 lbs pressure."
	1	No. 58	93	Photo: View south (taken from just north of 18th St.); hole in street seen in distance. Shows destruction of area by fire. Photo caption: "View south. Showing 24" [0.6m] and 16" [0.4 m] pipes quickly replaced on Val. St (see 57) on top pavement of Sunken Street."
	1	No. 59	93	Photo: View south; photo taken from south of 18th St. Hole in street in center foreground. Photo caption: "Valencia St. Sunken portion of Str. showing two above emergency pipes on top of pavement; also 5' [1.5 m] sink with car tracks and broken sewer at A."
	1	No. 63	95	Photo: Shows collapse of hotel, (opposite side of street from Valencia hotel?), street sunken, large hole in street. Photo caption: "Valencia Str. near 19th subsided (see No. 59) three Story Hotel collapsed on the left. Few minutes after

LOCATION	REF	PHOTO	PAGE	DESCRIPTION
				picture was taken, the fire swept it clean."
	1	No. 64	95	Photo: View northward. Shows close up of hole in street with the destroyed Valencia Hotel just to the north of hole. Photo taken before fire. Note caption reads that this is same hotel as in No. 63 which is unlikely. Hotel of Photo No. 63 is most likely across the street. Photo caption: "Other view of same [as No. 63], showing large hole in sunken street; also water pipe at x."
	1	No. 65	95	Photo: Shows 18th as the northern edge of disturbance. Shows lateral movement of 2.1 m over at least 9 m (only see half of lateral spread in photo). Photo caption: "View taken on Valencia Str looking north (A-B-C crossing of 18th Str.) showing lateral movement of Str. to East. B-B1 original position of center of west car track. B-B11 being present position since earthquake. Lateral movement fully 7 feet [2.1 m], B1-B11."
	2	Fig. 48A	54	Photo: View northward, most likely between 18th and 19th, near 18th St. (Note discrepancy with photo caption).

LOCATION	REF	PHOTO	PAGE	DESCRIPTION
				Photo caption: "Valencia Street between 17th and 18th Streets (loc. 216). A. View northward shortly after earthquake showing collapsed Valencia Street Hotel in which tens of people were killed. Note lateral displacement of street in front of hotel.
	2	Fig. 48B	54	B. View southward after fire showing lateral and vertical displacements of 6 ft. (1.8 m) and two temporarily repaired arterial water pipelines that were ruptured by the ground movements, cutting off the water supply to a major part of the city." Photo: B. View southward from near 18th at the margin of the zone of deformation. Car tracks clearly show the form of the lateral spreading.
	3		239	"Sewers and water-mains were broken. At Eighteenth and Valencia Streets there was a serious break in the water-pipe. Here, on both sides of the street, the ground sank about 6 feet [1.8 m], causing the roadway to arch in a very noticeable way. Ten-inch [0.25 m] car rails were bowed up into arches from 24 to 30 inches [0.6 to 0.8 m] in height. The Valencia Street Hotel collapsed so that occupants of the fourth story could step out into the street. Casualties in this district can never be known accurately, owing to the immediate onset of the fire, and the complete devastation it produced."
	3	pl. 93B		Photo: View southward. Shows hole in pavement, destruction by fire. Photo caption: "Valencia Street, near Eighteenth. Land in this neighborhood sank about 6 feet [1.8 m], flexing street surface."
	4		8	"Where the same earth flow crossed Valencia street the horizontal movement amounted to 6 feet [1.8 m]."
	5		214	"In the rocky portion of San Francisco the sewers were not affected. In portions where the rock was overlaid with sand, there were no permanent displacements except where the original ground supported a fill; in such areas settlements occurred, and the sewers were destroyed. In filled-in tidal areas, marsh-lands and swamps there was considerable movement in a number of places (the greatest near 16th St. [18th?], and Valencia St., where the settlement was 5 ft. [1.5 m] and the lateral movement 6 ft. [1.8 m]) and in all such disturbed areas the sewers were destroyed."

LOCATION	REF	PHOTO	PAGE	DESCRIPTION
	5	PlXLIX Fig.2		Photo: Similar to that of ref. 1, No. 58. View southward. Intersection of 18th in near foreground (near 2nd rubble pile). Photo caption: "Displacement of Ground at Eighteenth and Valencia Streets, San Francisco."
	5		253	"Plate XLIX, gives some idea of the extent of this movement, both laterally and vertically, at Valencia and 18th Streets, where one of the most serious breaks occurred. It also shows the pipes laid temporarily on the surface to replace those parted underground."
	8b		739	"The most important and interesting case of settlement and throwing out of alignment of streets in San Francisco, due to the vibrations of the temblor, was that of Valencia St., between 18th and 19th Sts., in the Old Mission district. At the point there was formerly a tidal stream, known as Mission Creek, whose existence had long since ceased owing to the fact that its course had been filled in and the land so reclaimed had become thickly built up. The earthquake caused a settlement of from 6 to 8 ft. [1.8 to 2.4 m] for a distance of from 150 to 200 ft. [46 to 61 m] along this street, and at the same time shifted the entire street, with adjacent lands, eastward through a maximum distance of 9 to 10 ft [2.7 to 3.0 m]. This change in alignment and grade could, of course, mean nothing less than the entire destruction of all water and gas mains, electric lighting and telephone conduits, sewers, cable conduits, railroad tracks, etc. The breakage of these important lines, especially to the water mains, was of greatest significance. 'In this case the destruction of the water pipes, of which a 22-in. and a 16-in. were found in this street at this point, meant the cutting off of a large part of the water supply of the portion of the city which was soon to be in flames."
	8b		739	Photo: View similar to that of ref. 1, No. 59 from a little farther south. Hole in street in center distance, behind pedestrians. Clear view of settlement in street. Photo caption: "Temporary Main on Valencia Street... The second picture shows a 24-in. cast-iron pipe line hastily placed in Valencia St. to provide water for the higher districts, whose supply had been cut off by the destruction of the mains in this street between Eighteenth and Nineteenth Sts. A 16-in. pipe to supply the lower downtown districts was also placed here in an incredibly short time."

LOCATION	REF	PHOTO	PAGE	DESCRIPTION
	8b		739	"The most important local settlements and transverse movements occurred in the vicinity of the Valencia Hotel between 18th and 19th Sts., on Valencia St., on Howard St. between 17th and 18th; on 14th, between Mission and Howard; on Folsom, at the corner of 17th; on Mission, at the corner of 7th, and on Van Ness Ave., between Vallejo and Green Sts.."
	8c	---	765	"Destruction of Sewer by Settlement of Street." "In the second picture, taken on Valencia St., between Eighteenth and Nineteenth Sts., the broken sewer is in a deep fill along the former course of Mission Creek."
	8c		767	"Probably at no point were more serious results produced than on Valencia St., between 18th and 19th Sts., already described in connection with street and sewer problems. Two very important distribution mains were located at this point and were, of course, ruptured. One of these pipes, a 22 in. in diameter, supplied the higher districts of the city; the other, a 16 in. pipe, was an important artery of the system furnishing water to the business section."
	9c	---	581	"STREET SUBSIDENCE IN SAN FRANCISCO. VIEW ON VALENCIA ST., NEAR 18TH ST., OPPOSITE SITE OF VALENCIA HOTEL. (It was at this place that street water mains were broken. The street dropped about 4 ft. [1.2 m] and moved eastward about 6 ft. [1.8 m] at the maximum point.."
	9b		551	"The Valencia Hotel, it will be remembered, was situated on Valencia St., near 18th, on filled ground, where once ran the old Mission or Islais Creek [the former Islais Creek was located farther south]. The Valencia Hotel and other cheap brick and frame buildings in that region from Valencia to Howard Sts. very generally collapsed. Many lives were lost in the Valencia Hotel."
3) Four block area between 17th and 18th from Valencia to Folsom	3		239	"Again, along the creek bed from Folsom Street, between Seventeenth and Eighteenth Streets, to the vicinity of Valencia Street at Eighteenth, great destruction was conspicuously prevalent. Less than a third of the

LOCATION	REF	PHOTO	PAGE	DESCRIPTION
				frame dwellings in this tract retained their vertical positions, and a few collapsed completely. Others remained standing only by leaning against each other. The south side of Howard Street, between Seventeenth and Eighteenth Streets, which escaped the fire, furnishes a good illustration of the damage produced here. (See Plate 93A.) As in other places, the streets were deprest, fissured, and thrown into waves. (Plate 90C.) Car rails were arched and bent laterally in a violent fashion. (Plate 92B.)"
(Capp St.)	1	No. 61	95	Photo: Looking south from near 17th toward 18th. Sidewalk on east side subsided 0.6 to 0.9 m and moved laterally eastward, about 0.6 to 1.2 m over 120 m, separating sidewalk slabs. General sink in southern portion of block from just west of the street eastward beyond photo. This depression has a scarp along the southern margin near 18th and another running diagonally about 30 m north of 18th at the northern margin of the sink. Photo caption: "Capp Str & Sidewalk sunken."
	2	Fig. 46	53	Photo: Same as that of ref. 1, No. 61. Photo caption: "Scarps, lateral and vertical displacements in Capp Street between 17th and 18th Streets (loc. 215)."
	2	Fig. 47	53	Photo: View eastward on 18th St. from the intersection of Capp St. Compression ridge running E-W through the intersection of Capp St. at the line of the northern edge of the north sidewalk on 18th St. Curbstone arched at this location (roughly 0.12 strain). Fire destroyed the entire block between Capp and Howard Sts. Howard St. seen in the distance, with houses leaning appreciably. Photo caption: "Buckled curbstone on Capp Street near 18th Street (loc. 215). Buckling was caused by sediments shifting toward old channel of Mission Creek."
(Howard St.)	1	No. 66	97	Photo: View looking southwestward across the intersection, from 17th down Howard. Shows general depression of 0.3 to 0.6 m. Photo caption: "Crossing of 17th & Howard. Street sunken, 12" & 20" pipes ruptured."
	1	No. 70	97	Photo caption: "Crossing 17th & Howard St 16" pipe badly fractured. (not yet repaired)"
	2	Fig. 43	55	Photo: View looking northward on Howard.

LOCATION	REF	PHOTO	PAGE	DESCRIPTION
				Compression ridge runs diagonally from SW-NE. Buckling of car tracks (0.12 m compression). Photo caption: "Buckling of rails by compression on Howard Street (south Van Ness Avenue) near 17th Street (loc. 215). "
	3	Pl. 92B		Photo: Same as ref. 2, Fig. 43. Note view can not be south, as said in caption, because houses on west side of Howard were destroyed by the fire. Photo caption: "Looking south on Howard Street from near Seventeenth Street. Compressional flexure of car rails."
	4	Pl. VIB		Photo: Same as ref. 2, Fig. 43. Photo caption: "BUCKLING CAUSED BY EARTH FLOW, HOWARD STREET, SAN FRANCISCO."
	4		8	"In taking the photograph reproduced in Pl. VI, B, the camera stood on ground made by the filling of Mission Lagoon, an expansion of Mission Creek, and was pointed northward, commanding a portion of Howard street. The made ground here flowed northeastward and the buckling of street-car tracks was caused by its motion."
	8b		740	"On Howard St., at the corner of 17th St., very complete destruction of the brick sewer, as well as most other pipes and conduits in the ground, was caused by the extensive settlements in this region. On Valencia St., near 18th St, similar ruptures were produced."
	1	No. 67	97	Photo: Close up of homes which were most severely tilted. Photo caption: "East Side Howard, between 17th & 18th, showing effects of Earthquake on buildings."
	1	No. 62	95	Photo: View northward down Howard from 18th. Shows lateral offset of 0.3 to 0.6 m running diagonally NW-SE. Block west of Howard destroyed by fire. Houses on east side severely tilted. Car tracks show lateral spread; roughly 1.2 m over 150 m. Photo caption: " Howard St. north of 18th sunken & twisted (see car tracks) One 20" pipe, one 24" and two 6" pipes broken by earthquake"
	2	Fig. 44	51	Photo: View very similar to that of ref. 1, No. 62. Photo caption: "Looking north on Howard Street (South Van Ness Avenue) from near 18th Street toward 17th Street, San Francisco (loc. 215). Rails offset laterally by lateral-spreading ground failure."

LOCATION	REF	PHOTO	PAGE	DESCRIPTION
	4	Pl. LIIIB		Photo: View in the same direction as that of ref. 1, No. 62. Closer view of tilting houses. Shows general depression in front of houses. Photo caption: "GENERAL EARTHQUAKE EFFECT ON FRAME BUILDINGS SITUATED ON ALLUVIAL SOIL. HOWARD STREET, SAN FRANCISCO."
	5	Pl. 36 Fig. 1		Photo: View similar to that of ref. 1, No. 62. Photo caption: "Extreme Case of Earthquake Damage to Frame Buildings in San Francisco. (In Center.)"
	6		18	Photo: Top photo shows close up of tilted houses on east side of Howard St. The lower photo shows general depressions down Howard St. which give an impression of slight waves. Photo caption: "RESIDENCES. Howard Street near Seventeenth Street. The upper view shows two buildings that have been tilted badly out of plumb by the earthquake. The rear portions of the buildings settled about 10 ft [3.0 m]. The telegraph poles are approximately plumb. Note the building on the right, the corner of which has broken into the side of the tilted one. The lower view shows Howard Street, looking west. The front of the two buildings shown in the upper view are approximately in the centre. One building near the left-hand side has tilted away from the street line until it almost disappears."
	8a	---	703	Photo: Close up of tilted houses from directly in front. Depression - at least 0.3 to 0.6 m difference of ground surface in vicinity directly in front of buildings. Photo caption: "Houses on Soft Ground."
	9b	Fig. 11	550	Photo: Similar to that of ref. 8a, p. 703. Photo caption: "THREE WRECKED FRAME HOUSES ON FILLED GROUND, HOWARD ST., BETWEEN 17TH AND 18TH."
	9b		553	"Fig. 11 shows frame houses on Howard St., between 17th and 18th, on filled ground. The house at the extreme left has entirely collapsed."
	1	No. 68	97	Photo: View eastward on 18th from intersection of Howard. Subsidence scarp runs E-W along centerline of 18th. Settlement to the north, extends at least as far east as Shotwell St. Photo caption: "Along 18th from Howard. Street subsided; pipe broken."
	2	Fig. 45	52	Photo: Subsidence and settlement has pulled apart north sidewalk slabs. Southern side of

LOCATION	REF	PHOTO	PAGE	DESCRIPTION
				18th is the boundary of disturbed zone. Photo caption: "Scarps showing vertical movement and northward lateral movement (loc. 215). View eastward on 18th Street. Intersection of Howard Street (South Van Ness Avenue) is in the middle-ground."
	3	Pl. 93A		Photo: View northeast from 18th St. across towards east side of Howard St. Shows destruction by fire of block west of Howard; tilting of houses. Photo caption: "East side of Howard Street, between Seventeenth and Eighteenth Streets."
	3	Pl. 90C		Photo: View eastward along 18th from instersection of Shotwell. Shows subsidence to north along centerline of 18th, down 0.3 to 0.6 m. Length of disturbance appears to be at least 100 m, perhaps all way up to Folsom. Photo caption: "Eighteenth Street, just east of Shotwell. Fissuring and depression of pavement."
4) 14th St. near Howard	4		739	"The most important local settlements and transverse movements occurred ..., on 14th, between Mission and Howard...."
	1	No. 63	95	Photo caption: "14th St east of Valencia, Street torn open See water pipe below."
	1	No. 72	97	Photo caption: "14th St near Valencia. Sewer ruptured. 8" pipe broken. same as No. 63; picture taken from slightly changed point."
	8b	---	737	Photo: View westward on 14th? Appears to have some settlement to the south. Photo caption: "Effect of Broken Sewer on Fourteenth Street. The second picture shows the result of the destruction of a sewer on Fourteenth St., near Howard St. The crown of the sewer was broken in, the surface material washed in, as at A, and the sewer so completely filled with sand as to back up the sewage, as at B, above the elevation of the crown."
5) Block bounded by 9th, 10th, Bryant, and Brannan	3		238	Mission Creek was formerly a sinuous tidal stream, with narrow fringes of salt marsh about its banks. Near its mouth the stream wound around a rocky point where the serpentine hills of the Potrero rose abruptly from its southern bank. Here, along its margin, is found the most sudden transition from high to low intensity that is anywhere encoun-

LOCATION	REF	PHOTO	PAGE	DESCRIPTION
				tered in the city. Along Dore Street, a narrow alley running from Bryant Street to Brannan Street, between Ninth and Tenth Streets, the street pavement was broken into a series of waves. The photographs, plate 89D, looking along Dore Street from Bryant toward Brannan Street; plate 90A, looking from Brannan Street in the reverse direction; and 90B, showing in detail the trough of one of these waves, with the fissuring of the pavement near the farther crest, indicate more clearly that words the great intensity manifested here. Less than 2 blocks south on the hill slopes, more than 50
			239	per cent of the chimneys were left standing, and no serious structural damage was noted. No comment seems needed to establish clearly the fact that the change in the character of the ground, this being the only variable factor, is in some way the cause of the change in the degree of intensity.
				On Ninth Street, east of Dore Street, between Bryant and Brannan Streets, the block pavement was badly damaged by fissuring, slumping, and the formation of surface waves. Frame dwellings were thrown from their underpinning, and a few collapsed. Plate 91A shows a wave trough near Bryant Street, with the resulting disturbance of the pavement. The

LOCATION	REF	PHOTO	PAGE	DESCRIPTION
				dwellings immediately in the trough have dropt from their foundation posts. In plate 91B, looking along Ninth Street from near Brannan Street, is shown the depression and fissuring of the street and its slumping or flow westward toward the former channel of a short branch of Mission Creek, which occupied the present location of Dore Street. Streets, curbing, car tracks, etc., are defected from 6 to 8 feet [1.8 to 2.4 m] from their former positions. The frame dwellings were not destroyed, but a careful examination of the picture will show that most of them are badly injured. Many were left in a dangerous condition by the shock.
				On Tenth Street, between Bryant and Brannan Streets, less violence was noted and the slumping of flow eastward (toward the channel of the little branch of Mission Creek) is scarcely noticeable."
(Dore St.)	2	Fig. 38A	45	Photo: View of whole length of Dore St. In center foreground is a manhole cover which has punched through the pavement. Shows lateral offset, of roughly 0.13 m, near north end of street, marking the northern margin of disturbed zone; four separate depressions, or troughs along length of street; two lateral offsets, of roughly 0.3 m,

LOCATION	REF	PHOTO	PAGE	DESCRIPTION
				in southern section of street; most of the houses are severely tilted. Photo caption: "View along Dore Street from Bryant Street toward Brannan Street, San Francisco (loc. 214). A. Photograph after the 1906 earthquake showing undulations as large as 6 ft (1.8 m) in street. As much as 6 ft (1.8 m) of lateral movement also occurred at this location. B. Dore Street today (September 1974) from approximately the same location as fig. 38A, showing ramps of the James Lick and Central Freeways and other structures constructed since 1906. C. Building at corner of Bryant and Dore Streets damaged by differential vertical and lateral movements."
	3	Pl. 89D		Photo: Similar to that of ref 2, Fig. 38A; taken from a little farther north, nearer Bryant. Northern offset shows more clearly, as well as lateral spread. North of manhole, street shows little deformation. Photo caption: "Looking along Dore Street, from Bryant toward Brannan. Undulating and fractured condition of pavement due to earthquake. Houses thrown off their underpinning and pitched out of the vertical."
	3	Pl. 90A		Photo: View northward up Dore St. The southern 10 m or so of Dore (near Brannan) is not disturbed. Lateral movement is eastward. Photo caption: "Looking along Dore Street from Brannan toward Bryant. Larger undulations near Brannan. Dore Street is on site of an arm of Mission Creek."
	3	Pl. 90B		Photo: View southward on Dore St. Close up view of most southern trough. Shows lateral offset, of roughly 0.3 m, more clearly. Photo caption: "Dore Street, near Brannan. Vertical difference between crest and trough of undulations, 5 feet [1.5 m]."
	4	PL. VIA		Photo: View southward on Dore St. from middle of block. Close up of some of the most severely tilted houses on the east side of the block. Shows more clearly the break up and displacement of the western sidewalk pavement. Photo caption: "SETTLING (5 FEET) [1.5 m] ON DORE STREET, BETWEEN BRYANT AND BRANNAN STREETS, SAN FRANCISCO."
	4		9	" Another example of the effect on the filled-in land in this part of the city is shown in Pl. VI, A, a view of Dore street

LOCATION	REF	PHOTO	PAGE	DESCRIPTION
				between Bryant and Brannan streets. The settling of the soft ground caused the street to drop at least 5 feet [1.5 m] at this place.)"
	4		26	"The most noticeable destruction resulting from the settling of soft or filled ground occurred in Howard and Shotwell streets between Seventeenth and Eighteenth streets, Bryant street between Ninth and Tenth streets, Dore street between Bryant and Brannan streets (Pl. VI, A), and the corner of Seventh and Mission streets. The settling was greatest in Howard, Dore, and Bryant streets, being in Dore street at least 5 feet [1.5 m]."
(Bryant)	2	Fig. 39A	47	Photo: View almost directly east on Bryant. Shows scarp, roughly 0.15 m vertical offset, running diagonally across street in NW-SE direction; subsidence is to the south. Photo caption: "Scarps and right-lateral displacements caused by lateral spreading at two points on Bryant Street near the intersection of Ninth Street (loc. 214). A. Between Ninth and Tenth Streets (?). B. Between Eighth and Ninth Streets."
(Ninth)	2	Fig. 40A	48	Photo: Shows two levels of lateral spread, the greatest movement in the southern part of the street. In the foreground is close up of a depression in 9th St. at the location of the largest lateral spread. Scarp shows roughly 0.15 m settlement. Undulations show isolated depressions of roughly 0.6 to 0.9 m settlement. Photo caption: "Views along Ninth Street between Bryant and brannan Streets (loc. 214). A. View northwestward from near Brannan Street showing lateral displacement of street, rails, curb, walk, and buildings."
	3	Pl. 91B		Photo: Similar to that of ref. 2, Fig. 40A. Taken a little farther SE on Ninth. Photo caption: " Ninth Street, between Bryant and Brannan. Westward lurching of land toward former creek channel where Dore Street now is."
	4	Pl. V		Photo: Same as that of ref. 3, Pl. 91B. Photo caption: "RESULTS OF EARTH FLOW, NINTH STREET, SAN FRANCISCO."
	4		8	"Slips of this character grade into those of wet alluvium or "made ground" resting upon gentle slopes-ground which under ordinary conditions flows or creeps at an almost imperceptible rate, but which by shaking was made

LOCATION	REF	PHOTO	PAGE	DESCRIPTION
				to move several feet or yards in a few seconds. The filled districts of San Francisco afford several examples, and two of these are illustrated by Pls. V and VI, B. The view shown in Pl. V is northwestward on Ninth street, near Brannan. Before the earthquake the car tracks and curb line were straight and approximately level, and this condition was not disturbed on the relatively firm ground shown in the distance. In the nearer part of the view the street crosses a tract of made ground created by filling a valley tributary to a narrow tidal inlet called Mission Creek. The descent of this valley was southwestward, and the made ground flowed in that direction, carrying street and buildings with it."
	4		9	"A permanent disturbance of the ground also resulted in many instances from compacting. Just as sand or grain that has been poured into a measure can be made by shaking to settle down and occupy less space, so various loose formations, and especially artificial fillings, were shaken together by the earthquake and the ground surface lowered. In such compacting the particles making up the aggregate are readjusted so as to fit more closely together and the voids are reduced. In dry formations compacted by the earthquake the reduction of voids was opposed only by the elasticity of the contained air. In wet formations it encountered the effectual resistance of the contained water, and could be accomplished only by the extravasation of some of the water. Ordinarily it was impossible to measure the settling due to compacting, or even to determine its occurrence as a phenomenon independent of ground flow, but it was clearly seen in various localities in San Francisco where those parts of graded streets which retained their simple shapes and straight lines served as reference planes for neighboring parts that were disturbed. (Compare the distance and foreground of Pl. V. [Note: the photograph does show lateral spreading, as mentioned by Gilbert, et al., in the above quotation]. Another example of the effect on the filled-in land in this part of the city is shown in Pl. VI, A, a view of Dore street between Bryant and Brannan streets. The settling of the soft ground caused the street to drop at least 5 feet [1.5 m] at this place.)"
	2	Fig. 40B	48	Photo: General wreckage, can not ascertain ground displacements. Photo caption: "B. View northwestward showing

LOCATION	REF	PHOTO	PAGE	DESCRIPTION
				building damage, some of which is due to southwestward lateral displacement of the ground."
	2	Fig. 40C	49	Photo: View southward on Ninth in mid section of the block. Leaning lamp post locates the photo in relation to Fig. 40A. Close up view of slumping southwestward. House severely tilted. Photo caption: "C. Close-up view of damage in midsection of block."
	2	Fig. 40D	49	Photo: View northward of western side of block towards Bryant. Shows trough, roughly 0.6 to 0.9 m settlement, slumping toward the southwest. Photo caption: "D. Close-up of damage at northwest end of block."
	3	Pl. 91A		Photo: Same as that of ref. 2, Fig. 40D. Photo caption: "Ninth Street, between Bryant and brannan. Undulation and fissuring of pavement and sidewalks. Houses over trough have been dropt from their underpinning."
	2	Fig. 41	50	Photo: Shows scarp across Ninth Street of roughly 0.15 m, slump towards the northwest. Photo caption: "View northeastward on Brannan Street, corner of Ninth Street (loc. 214). The scarp and settlement in the foreground marks the southern boundary of the ground failure on Ninth Street."

SOUTH OF MARKET ZONE:

LOCATION	REF	PHOTO	PAGE	DESCRIPTION
General:	3		236	"High intensity was developed thruout a small elongate district having a width of about two blocks, which extends from near the corner of Eighth and Mission Streets to the vicinity of Fourth and Brannan Streets; from this point the boundaries are irregular and very sinuous, leading to the waterfront at about the crossings of Third Street with Berry and Channel Streets. A glance at the geological map, No. 17, shows that the regularly bounded portion of this district corresponds very closely with the area of a former tidemarsh, drained and flooded by one or two small tidal streams. The former shore line of Mission Bay was just north of Brannan Street, between Fourth and Fifth Streets, so that the irregular seaward portion of the district lies outside the old shore. This is one of two localities in the city, the other being a "made" land tract along the former course of Mission Creek, in which destructive effects of great magnitude were conspicuously developed. Only in very close proximity to the fault was greater violence manifested. For blocks the land surface, paved streets, and building plots alike, were thrown into wave forms, trending east and west about parallel to the length of the

LOCATION	REF	PHOTO	PAGE	DESCRIPTION
				area. The amplitude and wave-length of these earth billows, and the distances to which they extend, are indefinite and irregular. The fissuring and slumping, and the buckling of block and asphalt pavements into little anticlines and synclines (arches and hollows), accompanied by small open cracks in the earth, characterize the land surface. This amount was greatest near the center, or channel, where the street lines were shifted eastward out of their former straight courses, by amounts varying from 3 to 6 feet [0.9 to 1.8 m]. A satisfactory photograph of this phenomenon was not obtainable, owing to the quick convergence of parallel lines in perspective, but to the observer in the field it was a very striking result of the shock. The greater part of the district was occupied by wooden dwellings and shops, with a small percentage of mediocre brick buildings and a few of substantial construction. The fire swept the area clear. Not even heaps of debris remained to cover the ground, most of the destructive effects being obliterated, along with the structures in which they were developed. Enough remained, however. Foundation walls and sidewalk pavements were broken and flexed; sharp little anticlines were produced

LOCATION	REF	PHOTO	PAGE	DESCRIPTION
				in the street by the arching of block paving, as on Russ Street between Folsom and Howard Streets (plate 88C); granite curbing was broken and thrust up into an inverted V, as on Moss Street, between Folsom and Howard Streets (plate 88D): there were fissuring and slumping in the block pavement, as along Columbia Street between Folsom and Harrison Streets (plate 89A), and sharp flexures of the paved streets and car tracks, as on Sixth Street just south of Howard Street. These effects point simply and clearly to the great magnitude of the intensity thruout the greater part of this old swampy district. Attention has already been directed to the slumping or flow movement to the east along the long axis of the area. The heavily ballasted car-tracks on Bryant Street, at the crossing with Fourth Street, were sharply flexed laterally, tho bounded by block paving. (Plate 89.) This was at the eastern end of the district where the marsh formerly bent to the south around the flanks of Rincon Hill, a mass of firm sandstone rising from the floor of Mission Valley. No similar sharp flexures were encountered along east-west streets in the western or central portion of the district, tho lateral displacement

LOCATION	REF	PHOTO	PAGE	DESCRIPTION
				and flat, sinuous curvings of the street lines were common enough; notably on Harrison Street between Fifth and Sixth Streets, and on Folsom Street between Fourth and Seventh Streets. Both these streets cut across the direction of the flow movement at a small angle. These phenomena are easy to understand if, as seems certain, Rincon Hill served as a solid buttress against which the flow to the east was arrested, causing sharp crumpling of the surface near the buttress, with less disturbance farther away. This was combined with a slight tendency to flow southward in the southeastern part of the district. The shaking caused the materials used in filling to settle together and occupy less space so that the surface over the whole district was lowered by amounts varying from a few inches to 3 feet [0.9 m] or more. This is clearly seen in the change of street levels along the margin of the solid ground, where the car rails are bent downward in little monoclines. Occasionally a structure with a relatively good foundation remains at its former level, with the whole neighborhood deprest about it. Such a case is exemplified on Sixth Street, a little south of Howard Street, near the margin of the area. (Plate 89C). The flow movement is

LOCATION	REF	PHOTO	PAGE	DESCRIPTION
				thought to be due simply to the action of gravity, the loose, water-soaked material being compacted into less volume by the shaking. Besides this sinking of the district, and its flow movement, mention has been made of the deformation of its surface into irregular waves, trending approximately east and west parallel with the length of the district. Along the streets running approximately north and south, at right angles to the elongation of the area, car rails were bent abruptly to the side, or raised in arches, and sharp anticlines were formed in the block pavements. Large square concrete slabs, used for sidewalk paving, were thrust one over the other; and in one or two cases a slab entirely covered an adjoining one. These phenomena indicate shortening by compression in the north-south direction. On the other hand, however, a stretching of the surface is shown by fissures in the paving; by places where wedge-like blocks were deprest below the general level; and by the rails of car tracks which were pulled apart in amounts varying from 8 to 12 inches [0.2 to 0.3 m]. Owing to the relatively great and very variable structural strength of paved streets and heavily ballasted car tracks, these phenomena are not developed regularly nor frequently enough to afford a satisfactory test of the hypothesis that they are directly associated with the wave forms into which the surface of this district was thrown. Besides, owing perhaps to the varying rigidity of the materials which make up the surface of the streets and building plots, the wave forms themselves, tho generally prevalent, are not persistent in their extension. The compression and distension effects, however, are believed to be due to the same cause as that which generated the wave forms; for there is no evidence of any true shortening, or lengthening, of the north-south dimension of this district, nor is there any probability of this having occurred. In addition, then to the flow movement and the settling together of the loose materials causing depression, there was some sort of rhythmic movement in this loose earth which produced wave forms in the surface, with places of compression and places of stretching. It is not believed that these surface waves were traveling waves "frozen" as the shock subsided. If they had been of that character, the ground surface should be more broken than it appeared to be; for in relatively rigid materials such waves must develop open fissures along the crests, which would close with crushing in the

LOCATION	REF	PHOTO	PAGE	DESCRIPTION
				troughs. It must be noted, without any attempt at explanation, that the destructive effects of great magnitude which have been described above, are practically confined to the "made" land which occupies the old marsh site. Southeast of Brannan Street, where formerly lay Mission Bay, such effects are of less magnitude, in general; are less regular in their occurrence and are, on the whole, less prevalent. The complete devastation caused by the fire in this neighborhood leaves little to indicate the actual damage to the buildings wrought by the earthquake. Certain hotels or apartment houses are known to have collapsed, and many fatalities must have occurred. Probably a few dwellings were thrown down. A fairly large percentage of the buildings, one must believe, were rendered dangerous for occupation, even tho not completely thrown down. ...The space formerly occupied by Mission Bay has been partly filled to provide building sites, and of course the materials used in filling were deposited in water. The district is occupied in part by structures of great strength, such as railway tracks; in part it is devoid of buildings. Thruout the district, evidence was insufficient and

LOCATION	REF	PHOTO	PAGE	DESCRIPTION
				inconclusive. Except near the former outlet of Mission Creek, and in the area further north formerly occupied by the tidal marsh, the destruction produced does not denote intensity higher than Grade C. Apparently, therefore, land made by filling up spaces of open water is less dangerous, on the whole, than land made by depositing a thin rigid layer of filling upon a tract of marsh land. This, at least, is the lesson in San Francisco. The reasons for it are not very clear. Space forbids a discussion of theories which can not be adequately tested. It may be noted, however, that much of the material used in filling in areas of water has been broken rock derived from the grading down of neighboring rocky hills."
	3		229	"The blocks between the old tide-marsh area, extending east from near the Post-office, and the former course of Mission Creek, give evidence in the form of cracked foundation walls, broken concrete cellar floors, etc., of intensity values high in Grade C. The fire did much to destroy evidence here, as it was a district of wooden dwellings."
	8b		739	"In the Mission district, and in certain other parts of San Francisco, as, for

LOCATION	REF	PHOTO	PAGE	DESCRIPTION
				instance, along the courses of former tidal streams, large areas of filled land exist. In such cases, the effect produced by the earthquake was not generally in the form of waves, as already described, for the eastern portion of the city was basin-like, representing local settlement in the streets and adjacent areas, and in some cases, decided misalignment.... The most important local settlements and transverse movements occurred in the vicinity of...on Mission, at the corner of 7th...."
	13		32	"In the '50s and for some years later the high-water line of Mission bay, a tide-washed mud flat, came to Brannan street, between Fourth and Fifth, swept around to the line of Eighth, then Price, street at Channel and Hooper, then around to the point of high land near the present Central Basin, which point was then known as Point San Quentin. The opposing high-land point on the near side of Mission bay and about at the location of Third and King streets, was known as Steamboat point. ...Adjacent to this mud-flat bay and the tidal estuary were areas of salt marsh land. Little streams of fresh water came to the heads or upper ends of these salt marsh tracts, forming small areas of fresh marsh,

LOCATION	REF	PHOTO	PAGE	DESCRIPTION
				extending back between hills and ridges of the higher lands. A notable area of soft marsh covered most of the space lying west of Brannan and along Fourth and Fifth street to Howard. Another considerable area bordered the bay edge from about the line of Seventh around to Point San Quentin. Another area lay west of the estuary to Folsom street, about on the lines of Fourteenth, Fifteenth and Sixteenth streets, and another area lay around the salt lagoon at the head of the estuary and to the south and west thereof. THE MISSION BAY SOFT SPOT It would be tedious in these articles which the writer is endeavoring to keep within readable limits to catalogue too many dry and hard facts made about hard and soft land, so he does not undertake to trace in detail the outline of the Mission bay and estuary, salt marsh and fresh swamp areas, as these have now again been made evident by the street subsidence and other movements caused by our king shake. The region is a large one. To go slowly step by step around it as we did in the case preceding, on foot, as it were, would take too long; so we move rapidly over most of it as in an auto, and commencing on Townsend street, near the Southern Pacific Railroad yards, we notice a disturbance near Cook street, another in

LOCATION	REF	PHOTO	PAGE	DESCRIPTION
				Brannan, near Ritch; another near Harrison and Fourth; another near Folsom and Fifth, and another near Howard and Sixth. We find that by these we may outline on the map the old salt marsh limit as far as the greater impress of the earthquake's heel, which is found in the neighborhood of the new Postoffice."
1) Post Office, 7th & Mission Sts.	13		32	MISSION AND SEVENTH STREET DISTURBANCE It looks pretty bad on Mission street at and near Seventh, to see the whole street disturbed for about 700 feet in length, to see that this disturbance extended for about 700 feet [210 m] in length, to see that this disturbance extended far down Seventh street, and that an area of the adjacent land had sunk. As an American one cannot but feel glad that the new Postoffice building escaped, though barely, being in this area of depression. As a San Franciscan who knew this spot fifty years age, who saw it a marsh with a little stream running through it, who saw hunters wearing gum boots tramping about shooting jacksnipe in that very area, who later saw it drained for market gardening, and still later saw it filled to a depth often of fifteen feet [3.0 to 4.6 m] with sand dumped off a bank from side dump cars, and then saw it occupied by light wooden houses for a score and a half of years, it seems entirely natural that a real earnest earthquake should make it settle and move just as it has settled and moved. It never had an inducement to get down to a good bearing before. Now it has been shaken to where it will probably stay, and San Francisco will be the better for it. In the block south and west of the Postoffice this old John Sullivan marsh formerly headed. Its course was toward the east, joining an area of salt marsh which bordered Mission bay....The facts now are that under the earthquake influence the filling over this marsh area has settled at a number of places and to depths of from a few inches to three or three and one-half feet [0.9 to 1.1 m]. One of the most pronounced settlements is the one referred to on Mission and Seventh where the subsidence has reached a maximum of about three and one-half feet [1.1 m], as judged by the floor of the Postoffice building and the movement toward the bay, as judged by the street railway track and alignment of the trolley line support poles, has extended for 300 to 600 feet [90 to 180 m] in the length of Mission street,

LOCATION	REF	PHOTO	PAGE	DESCRIPTION
				reached a maximum of about five feet [1.5 m] at a point 175 feet [53 m] south and west of Seventh. Plotting the limits of this disturbance on the map, they are seen to coincide as near as can be measured with the outline of the old Sullivan marsh as shown by the Coast Survey map of 1857, and as the writer distinctly remembers it to have been."
	1	No. 76	99	Photo: Street slumps to the southeast in distant center of photo. Photo caption: "Mission St. near 7th in front of Post Office. Looking S.W. Street at X badly sunken & twisted (See picture No. 77)."
	1	No. 77	99	Photo: Shows monocline (0.6 to 0.9 m high) in street in front of east corner of Post Office. Car rails arched; pavement broken up. Photo caption: "Mission St. in front of Post Office, near 7th; street sunken, raised & twisted. 12" water pipe ruptured."
	1	No. 77A	99	Photo: Looking east on Mission St. in line with the sidewalk in front of the Post Office. Monocline in street in the distance, roughly 1.5 to 2.0 m from the sidewalk. Sidewalk slabs pulled apart. S corner of Post Office sunken, steps down roughly 0.3 to 0.6 m.

LOCATION	REF	PHOTO	PAGE	DESCRIPTION
				Photo caption: "New Post Office. Sidewalk & Street subsided."
	2	Fig. 35A	42	Photo: Front view of S corner of Post Office. Photo Caption: "Damage to San Francisco Post Office, Seventh and Mission Streets, caused by ground failure. A. View of southeast entrance showing differential, vertical movement of lower, nonstructural facing around building."
	2	Fig. 35B	42	Photo: Same as that of ref. 1, No. 77A. Photo caption: "B. View northeastward in front of building showing differential, vertical, and lateral movement of sidewalk."
	2	Fig. 35C	42	Photo: Close up of south corner of Post Office. Shows lateral displacement to the southeast, 0.6 m over 1.5 m. Photo caption: "C. View northeastward in front of Post Office showing settlement around building and lateral displacement of sidewalk to the southeast."
	3	Fig. 94B		Photo: View of the south corner of the building. Shows scarp of roughly 0.2 to 0.3 m across 7th St. in the intersection; subsidence to the southeast.

LOCATION	REF	PHOTO	PAGE	DESCRIPTION
				Photo caption: "San Francisco Post-office, Mission and Seventh Streets. Near corner of building is on edge of old marsh. Ground over marsh sank and lurched."
	3		238	"The new United States Post-office building (plate 94B), at the corner of Seventh and Mission Streets, was just on the margin of the district. It is a steel and granite structure, resting upon a foundation of piling driven to a considerable depth, but not as far as some had considered advisable. At its southwest corner, the streets are deformed into great waves, some with an amplitude of at least 3 feet [0.3 m], causing fissures and sharp compressional arches in the pavement and sidewalks. Some of the granite flanking structures, which did not rest upon the pile foundation of the building, shared this undulatory movement. In consequence, the building appears badly damaged to the casual observer. It is quite true that the structure was terribly shaken and greatly damaged -- such injuries as the destruction of mosaics in the arches of the corridor helped to increase the loss -- but the structure was not in peril of collapse, tho one of the low walls had to be supported by timbers. For the most part, the building survived the ordeal, and is in a safe condition for use."

LOCATION	REF	PHOTO	PAGE	DESCRIPTION
	4		97	"To the south and west of Mission street was an elongated, narrow, curved area in which the earthquake damage was very severe. It was commonly reported that this area, which was not far from the south corner of the post-office building, was a stream bed or ravine that had been filled within the recollection of the older inhabitants of San Francisco...J.W. Roberts, the local representative of the Supervision Architect's Office of the Treasury Department... seemed of the opinion that the material under the building was a natural deposit, and not an artificial fill. But toward
			98	the south it was not of a nature to inspire confidence in its carrying power at the depth shown on the foundation plans. He accordingly obtained authority to lower the footings wherever the material at the depth shown on the plans seemed unreliable, so that the footings of the south half of the building were lowered - some of them, as I remember his statements, to a depth of 20 feet [6 m] or more below the basement floor level. At any rate, he carried them to a point where the material, in his judgement, was sufficiently hard and compact. All this underlying material is very sandy; but at considerable depths, I understand, gravel appears, and the combination is almost as hard as hardpan."

LOCATION	REF	PHOTO	PAGE	DESCRIPTION
	4	Pl. XLIIB		Photo: View northward of an unfinished building directly across from the Post Office on the southwest side of 7th. Foundation settled unevenly roughly 0.3 m; lateral spreading as well. Photo caption: "B. EFFECT OF SETTLING OF GROUND SUBJECTED TO EARTHQUAKE VIBRATIONS, STEEL-FRAME BUILDING UNDER CONSTRUCTION. The concrete basement walls were not reenforced. Post-office in the background."
	4		99	"...there was a partially erected steel frame (Pl. XLII, B) on the southwest side of Seventh street, near the post-office. Before the earthquake all the columns were plumb and in true alignment. As a result of the shock there was a lateral shifting of the column bases--the relative movement being almost 2 feet [0.6 m] in some places--at the cellar floor level. The basement walls of the incomplete building were also shifted horizontally; at the east corner, where the walls had met at a right angle, they had been ruptured by a vertical crack and moved laterally in such a way that the angle between them was reduced to about 75 degrees, as nearly as I could estimate it without taking measurements."
	4	Pl. XLIIIB		Photo: Close up of SE corner of building, and monocline in street, 0.9 m high. Pavement badly broken, car rails arched. Photo caption: "B. EFFECT OF SLIP, MISSION STREET, SAN FRANCISCO. Corner of post-office building at the left."
	4		44	"The ground at the corner of Seventh and Mission streets settled about 5 feet [1.5 m] (Pl. XLIII, B). The floor of the building was slightly cracked at that point, and Mr. Roberts stated that there was a settling of about 1 3/4 inches [0.04 m]."
	4		99	"The south corner of the post-office building is shown in Pl. XLIV, A. Mr. Roberts states that accurate measurements show that the building proper settled a little at this point, but not more than one-eighth inch relative to other parts of the structure. The general appearance of the building bears out this statement. The result is remarkably gratifying when the great extent of the nearby surface disturbance on Mission street is considered. The street went down about 4 or 5 feet [1.2 or 1.5 m] at this point as a result of the earthquake (Pl. XLIII, B)."
	4	Pl. XLIVA		Photo: Similar to that of ref. 1, No. 77A. Photo caption: "A. CRACKS IN MASONRY AND SETTLING OF

LOCATION	REF	PHOTO	PAGE	DESCRIPTION
				OUTER TERRACE, POST-OFFICE BUILDING, SAN FRANCISCO."
	6	---	20	Photo: Same as that of ref. 1, No. 77. Photo caption: "EARTHQUAKE EFFECT. Distortion of the surface of Mission Street near Seventh, showing the southeast corner of the United States Post-Office Building at the left hand side."
	6	---	193	Photo: Photo taken from opposite corner across Mission St. from Post Office. Shows extent of depression in front of southern corner of Post Office. Seventh St. affected to the northwest only half way along building. Photo caption: "UNITED STATES POST OFFICE. Northeast Corner of Seventh and Mission Streets. At the curb in front of the building, on the right-hand side, the ground settled 5 feet [1.5 m] and moved to the east away from the building about 6 feet [1.8 m]. At the building line, the ground settled about 2 feet [0.6 m], causing the displacement of the granite coping, steps, etc., at the sidewalk level, as shown. The sidewalk was originally a straight grade on the right-hand side where the sag is now shown."
	6		192	"UNITED STATES POST OFFICE. N. W. Cor. Seventh and Mission Streets.... At the southwest corner, the ground settled about 2 ft [0.6 m] at the building line and about 5 ft. [1.5 m] at the curb, the entire surface from the building line moving out about 5 ft. [1.5 m] to the south. This distorted the sidewalk and steps of the two entrances, there being cracks in the joints of the cement sidewalk slabs 8" [0.2 m] wide. It was necessary to place two temporary wooden steps of about 8" [0.2 m] rise from the sidewalk in its settled position to that portion of the steps which remain approximately at the original height."
	8a		701	"UNITED STATES POST OFFICE -- ...It is especially noteworthy since it is built upon filled land which everywhere in San Francisco was shown to be very unstable and capable of very great distortion and settlement as a result of the action of the oscillations and vibrations due to the earthquake... The effect of the earthquake throughout this vicinity has been most marked. Streets in this neighborhood have settled very considerably and the sidewalk has also seriously sunk. Mission St., at the corner of 7th, has been thrown bodily southward to the extent of at least two feet [0.6 m]."

LOCATION	REF	PHOTO	PAGE	DESCRIPTION
	8b	---	737	Photo: View eastward on Mission St. from corner of 7th. Southwest corner of the building settled at least 0.1 to 0.2 m. Sidewalk and street displaced laterally, pulling apart sidewalk slabs. Photo caption: "Southwest Corner of U.S. Post Office. The first picture was taken at the corner of Mission and Seventh Sts. The ground is a loose fill and settled considerably, while Mission St. has apparently been thrown to the southeast at this point at least 2 ft. [0.6 m]."
	9c	---	580	Photo: Same as that of ref. 8b, p.737. Photo caption: "SOUTHWEST CORNER POST-OFFICE BUILDING, SAN FRANCISCO. PAVEMENT AND CURBING DISPLACED BY EARTHQUAKE."
	14	---	695	Photo: Two views of the southern corner of the Post Office. The first is a view directly facing the southeast entrance, showing the settlement of the steps and sidewalk relative to the building. The second view is south of Post Office from the intersection looking north. Shows just the edge of the scarp across 7th St.
	14		694	"...The soft upper strata of the surrounding street and sidewalk slipped away from the building [U.S. Post Office] at Seventh and Mission sts., from 1 ft. to 3-1/2 ft. [0.3 to 1.1 m], but the foundations are not defective."

LOCATION	REF	PHOTO	PAGE	DESCRIPTION
2) Howard & 6th	8b		738	Photo: View looking northwest on 6th at intersection of Howard. Gradual settlement, shows no scarp; decreases to the north. Photo caption: "Settlement on Sixth Street. The first picture was taken on Sixth st., just south of Howard St. The amount of drop at the lamp post where the men are standing was fully 2 ft [0.6 m]. The sidewalk north of this point and the street at the junction of Howard appears to have settled but very little."
	9b	Fig. 13	551	Photo: Same as that of ref. 8b, p. 738. Photo caption: "STREET SUNKEN; SIDEWALK IN PLACE BECAUSE ON FOUNDATIONS."
	9b		553	"Fig. 13 shows a drop in Howard St. Where the men are standing a sidewalk on foundations has remained in place."
	3	Pl. 89C		Photo: Shows general settlement of street.
				Photo caption: "C. Sixth Street, near Howard. Once occupied by marsh. Street dropt nearly 3 feet [0.9 m]. Sidewalk held up by piling foundation of a building."
3) Mission & 5th	4	Pl. XXXVIIIA		Photo: View looking north. Shows scarp across Mission street of roughly 0.3 m. Photo caption: "GOOD EARTHQUAKE ENDURANCE OF A BUILDING OF THE MONUMENTAL TYPE: UNITED STATES MIN, SAN FRANCISCO."
4) Near Folsom between 6th and 7th	3		237	"Foundation walls and sidewalk pavements were broken and flexed; sharp little anticlines were produced in the street by the arching of block paving, as on Russ Street between Folsom and Howard Streets (pl. 88C); granite curbing was broken and thrust up in to an inverted V, as on Moss Street, between Folsom and Howard Streets (pl. 88D): there were fissuring and slumping in the block pavement, as along Columbia Street between Folsom and Harrison Streets (pl. 89A), and sharp flexures of the paved streets and car tracks, as on Sixth Street just south of Howard Street. These effects point simply and clearly to the great magnitude of the intensity thruout the greater part of this old swampy district."

LOCATION	REF	PHOTO	PAGE	DESCRIPTION
	3	Pl. 88C		Photo: Compression ridges trending north-south along Russ St. Roughly 0.3 m compression. Photo caption: "C. Russ Street, between Folsom and Howard Streets, San Francisco. Paving blocks forced up into sharp arches and dislodged by compression."
	3	Pl. 88D		Photo: View facing northeast. Compression ridges trending north south (roughly 0.3 m compression in east-west direction). On west side of street is a curb block arched sharply into an inverted V indicating compression in the north-south direction. Photo caption: "D. Moss Street, between Folsom and Howard Streets, San Francisco. Paving blocks archt by compression along sinuous crest, curbing thrown into an inverted V."
	3	Pl. 89A		Photo: View south down Columbia Street. Shows lateral spread; scarp irregular; slumping 0.6 m roughly to east. Photo caption: "Columbia Street, just south of Folsom Street, San Francisco. Slumping, depression, and furrowing of block pavement."
	2	Fig. 33	40	Photo: Same as ref. 3, Pl. 89A.
				Photo caption: "Disruption of block pavement and sidewalk on Columbia Street just south of Folsom Street."
5) Fifth near Harrison	2	Fig. 34	41	Photo: Shows extension of car rails of roughly 9 cm. Pavement blocks pulled apart at this location. Photo caption: "Rails on Fifth Street near Harrison Street, San Francisco, pulled apart by extensional movements associated with lateral spreading of underlying sediments."
	8b		740	"On Fifth St., between Folsom and Harrison Sts., the brick sewer settled with the adjacent land, its crown was destroyed and the channel had become filled with sand which blocked up the sewage to a dangerous extent.
6) (4th, near Bryant)	10	---	554	Photo: Shows compression in car tracks, both by arching and by bending. Photo caption: "STREET CAR TRACK ON 4TH ST., NEAR BRYANT, SAN FRANCISCO, DISTORTED BY EARTHQUAKE."
	10		554	"The view was taken looking north on Fourth street, near Bryant street, shortly after the fire had burned itself out in the vicinity. As this piece of track was observed hours before the fire

LOCATION	REF	PHOTO	PAGE	DESCRIPTION
				devastated both sides of the street of the buildings, it is impossible to attribute the distortion to heat...The common type of track distortion caused by the earthquake waves is also shown in the view on the left hand track. Here both rails are bent upward about 5 ins. in 3 ft [0.13 m in 0.9 m]. The rails bend up in cases of this kind, because of the resistance offered in every other direction by the ties, pavement and track itself."
	3	Pl. 89B		Photo: View looking northeast up Bryant from 4th? Compression of car rails by roughly 0.06 m. Photo caption: "B. Bryant Street, near Fourth Street, San Francisco. Flexure of heavily ballasted car tracks in block pavement; an effect of sharp compression."
	5		265	"...the writer twice passed by a number of brick warehouses on the north side of the Southern Pacific Railroad, between Fourth and Sixth Streets, and took a little time to examine them...They also had the disadvantage of being built on extremely poor foundations, their settlement during the earthquake, with respect to the railroad right of way, just south of them, being about 2 ft [0.6 m]."

FOOT OF MARKET ZONE:

LOCATION	REF	PHOTO	PAGE	DESCRIPTION
General:	3		233	"About the Ferry Building, at the foot of Market Street, is a district of "made" land, shown on map 17, in which high intensity was manifested....In spots the streets sank bodily, certainly as much as 2 feet [0.6 m], probably more. Accompanying this depression, concrete basement floors were broken and arched, as if to compensate for it. The surface of the ground was deformed into waves and small open fissures were formed, especially close to the wharves. Buildings on the water side, along East Street, generally slumped seaward, in some cases as much as 2 feet [0.6 m]. The damage was greatest close to the water's edge, growing less as the solid land was approached, gradually at first, then more rapidly. These phenomena seem to suggest that the materials used in filling were shaken together so as to occupy less space with the accompanying development of waves, fissures, and structural damage. The more recent the filling, the more it would be compacted; hence the greater prevalence and magnitude of destructive effects near the water's edge. As well as could be made out from the inadequate evidence left by the fire, the district which suffered intensity of Grade B

LOCATION	REF	PHOTO	PAGE	DESCRIPTION
				is limited on the landward side by a line drawn from Filbert Street to Market Street, between Battery and Front Streets; thence between First and Fremont Streets to a little south of Folsom Street, where the line turns and runs eastward to the wharves. Flanking this district on the landward side is a narrow, sinuous area limited by a line drawn from Filbert Street to Green Street, just east of Sansome Street; thence between Sansome and Montgomery Streets to Market Street; thence to the corner of Mission and First Streets; thence between First and Fremont Streets to a point south of Folsom Street; thence easterly nearly to the wharves. Between Washington and Sacramento Streets, this boundary is barely east of Montgomery Street. Immediately west of these districts, low intensity prevailed."
	8b		739	"THE STREET PROBLEM.--The effect of earthquake was very marked in San Francisco wherever filled ground existed. The original shore line was far different from that of today and passed around the easterly base of Telegraph Hill to the southerly end of Montgomery Avenue, thence southeasterly to Market Street at Battery Street, thence to Russian Point, thence around the old Mission Bay. All of the lane now lying east of this broken line has been recovered from the sea by filling on the marshes and tidal lands. EARTHQUAKE EFFECTS.--Within this filled district, the vibrations of the earthquake caused a general but irregular settlement. The streets naturally followed the changes in elevation and a wave-like effect was produced. Observations on Market, Mission, East and other streets frequently indicate an amplitude of wave height of two feet [0.6 m], while occasional places are found with greater differences in elevation. ...The most important wave-like distortions were observed on Lower Market and Mission Sts., and on East St. along the present water front."
	9a		503	"The earthquake destruction was most marked on soft and sandy soil and upon made ground. The Ferry building, at the foot of Market St. is decidedly damaged...This building rests upon excellent foundations, but it is supported upon material which seems to have acted like a viscous fluid...All of the made ground between the Market St. water front and the region of Montgomery St. has been decidedly moved and deformed. Wave-like effects are common along

LOCATION	REF	PHOTO	PAGE	DESCRIPTION
				lower Market St. and the water front. Wave-like depressions and crests amounting to four and five feet [1.2 and 1.5 m] are found throughout this region. The same observations can be made in many other localities of the city, where soft ground is met."
	13		32	"THE PRINCIPAL SOFT SPOT. Here are, in general terms, the leading facts of earthquake effect within the area which we may designate as the city's principal soft spot, even though it is not the largest area of marsh and mud flat which has been filled over and built upon. Beginning on the east and west streets at the north limit of the area of disturbance, we find the uppermost evidence on Pacific street at about the corner of Front; then on Jackson street at about the intersection of Battery; next on Washington street at the intersection of Battery; next on the Clay near the intersection Sansome; then on Sacramento, also at the intersection of Sansome; on California it is doubtful whether the disturbance at Sansome is due to general subsidence or only to subsidence toward foundation excavation; on Pine street the upper limit of pronounced street disturbance is about 100 feet [30 m] above Battery; on

LOCATION	REF	PHOTO	PAGE	DESCRIPTION
				Market the line is very distinct at about the foot of Bush street; on Mission a sharp line of subsidence occurs across the street about 100 feet [30 m] below First; on Howard and in the line of Fremont to the east thereof the line is again plainly marked by a crack and subsidence below it; and finally, on the line of Folsom, about seventy feet [21 m] below Beale, a line of subsidence is very distinctly marked diagonally across the street exactly at the location and in the direction of the foot of the old hard ground and edge of the former mud flat. Platting these points on the map it is found that they either lie within or outline very nearly the limit of the former soft spot in the lower portion of the principal business part of the city. Below this bounding line the streets are nearly all waved, there being depressions of from six inches [0.15 m] to as much as four feet [1.2 m] in one or two places and two or three feet [0.6 or 0.9 m] at quite a number of points. While it cannot be said that the whole street area within this zone has sunk, a considerable portion of it has, and near the water front most of it has sunk from six to twelve inches [0.15 to 0.3 m], with several areas of greater depression.

LOCATION	REF	PHOTO	PAGE	DESCRIPTION
				Davis street, from Vallejo to California street, presents perhaps the extreme case, there being distinct depressions of from one to three feet [0.3 to 0.9 m] at every street crossing or within every block; but it is apparent that some of this is due to slip of the street filling into building foundation areas, consequent upon failure of retaining walls and poor foundation os the buildings themselves. The area of about eighty feet [24 m] frontage which has sunk to a maximum of about eighteen inches [0.46 m] in front of the Market-street Ferry building, and the depression of somewhat greater area and to a maximum depth of about three feet [0.9 m], at the northwest corner of the same building, are the extreme cases of subsidence along the main waterfront. Contrasted with the very heavy masonry Ferry building, founded on piles and concrete, which has not sunk at all, these subsidences will illustrate the point that it is only the soft mud and loose filling thereon which has been disturbed by the earthquake. There are places on the north and south streets where the whole street appears to have been thrown a few inches toward the bay and at East street, which is the waterfront street, there is much evidence of similar movement to about six to eighteen inches

LOCATION	REF	PHOTO	PAGE	DESCRIPTION
				[0.15 to 0.46 m] where the pavement has been shoved against wharves, piers and other water-front structures and caused to buckle up. Street and water-front railway rails are in a number of places buckled up six inches to two feet [0.15 to 0.6 m] or are thrown as much as six inches [0.15 m] out of line. Throughout the filled area above street-corner silt basins have been tripped out of plumb and bulged into sidewalk area, and sewer manholes in street intersections are in several places canted up, showing sewer disturbance beneath; while granite curbs for 100 feet [30 m] or more in length were tripped up by unequal movement of street pavements and the underlying ground and thrown out bodily on their sides upon the pavement or sidewalk. The Market-street Railway track, carried on a prism of concrete founded on piles for its length within this area, did not sink with the street on each side of it and is yet nearly on its original grade except at one point, where it has sunk apparently about four inches [0.1 m] for several hundred feet. It is noticeable that streets have sunk least or not at all in front of the newer deep-piled foundations for adjacent build

LOCATION	REF	PHOTO	PAGE	DESCRIPTION
				ings -- Market street in front of the Hotel Terminus and in front of the Buckley building, for instance -- and this indicates that a part of the street movements is due to settlements into cellar and foundation excavations on failure of their retaining walls. A curious revelation is noticed on the west side of Davis street, between the Broadway and Pacific street. Here in 1857 was the water-front wharf. When the street was filled in it is evident that all the piles were not removed. The street pavement, which is basalt blocks, has sunk six inches [0.15 m] or more for the full length of the frontage, and the position of the pile heads for about half the length is marked by their punching the pavement up in little pyramids, and for the other half length the position of the pile bents with caps on is shown by the pavement sinking on either side of the caps, leaving ridges of paving blocks over them. Evidences of old structures beneath the surface and filling are brought out in a similar way at a number of points."

LOCATION	REF	PHOTO	PAGE	DESCRIPTION
1) East St.	8b	---	739	Photo: View on East St. looking west up Pacific St. Scarp running NW-SE across East St., slight subsidence to north. Car rails bent into arch-compression of roughly 0.1 m. Photo caption: "Tracks at East and Pacific Streets. The first picture shows the distortion of car tracks and the line of the local fault in East St. at its junction with Pacific St., along the water front. This territory is within the area of made land on the marshes of the old harbor front."
	9b	Fig. 14	552	Photo: Same as that of ref. 8b, p. 739. Photo caption: "DEFORMATION STREET RAILWAY TRACKS, EAST AND PACIFIC

LOCATION	REF	PHOTO	PAGE	DESCRIPTION
				STS., NEAR FERRY BUILDING."
			553	"Fig. 14 shows the destruction of car rails and street surface, corner East and Pacific Sts., near the Ferry Building."
	11	Fig. 12	125	Photo: Same as that of ref. 8b, p. 739. Photo caption: "Rupture of Car Tracks and Pavement on East Street, Corner of Pacific Street."
	9b	Fig. 15	552	Photo: View looking west on Market. Shows roughly 0.1 m scarp and crack running across width of East St. Crack crosses tracks which are not disturbed. Street slumps to the south. Photo caption: "CRACK IN PAVEMENT IN FRONT OF FERRY BUILDING."
			553	"Fig. 15 is a similar view in front of that building [Ferry Building]."
	11	Fig. 11	123	Photo: Similar to that of ref. 9b, Fig. 15. Photo caption: "Street Surface in Front of the Ferry Tower, Showing Undulations and Cracks in the Asphalt Pavement."
	1	No. 71	97	Photo: View northward [?] on East St. near Ferry building. No exact location given. Shows cracks in pavement resembling a graben formed by lateral spread eastward as much as 1.0 m.
				Photo caption: "Street on Waterfront badly broken up."
	2	Fig. 31	37	Photo: Similar to that of ref. 1, No. 71. Photo caption: "Cracks and separations in roadway pavement near the San Francisco waterfront caused by lateral spreading in the foot of Market zone."
	6	---	19	Photo: Similar to that of ref. 1, No. 71. Photo caption: "EARTHQUAKE EFFECT. A fissure on East Street near the water front. Note the settlement of the street surface as shown by the exposed curb at the right had side. In this locality the ground was "made," or artificially filled in."
2) Lower Market St.	3		236	"..The cable-car system on lower Market Street...were constructed upon piling to secure permanence of grade. On both sides of them the street sank in places as much as 2 feet [0.6 m], and the pavement was broken, fissured, and thrown into waves."
	11		98	"Within the confines of the city of San Francisco one finds evidence of great variation in shock closely related to and to be explained by the nature of the surface topography. It is a general observa-

LOCATION	REF	PHOTO	PAGE	DESCRIPTION
				tion that the earthquake waves transmitted by the softer and less coherent materials and formations appeared to be much more destructive than waves which traversed the hard and more elastic rocks and other sound deposits. The billow-like effects that appeared in the streets of San Francisco near the Ferry house are most excellent examples of deformations in soft, incoherent materials. The sliding and rolling effects observed on some of the sand dunes and especially along the hillside at the northern end of Van Ness Avenue may be cited as allied phenomena."
	1	No. 63	95	Photo: View eastward toward Ferry building from foot of Market. Shows pavement broken up; street thrown into waves. Photo caption: "Market St. near Ferry. Street subsided. 16" water pipe ruptured."
	4	Pl XLVIA		Photo: View of Ferry building. Shows undulations in street just in front, the crest trending N-S. Shows subsidence along NW corner of building. Photo caption: "A. BRICKWORK THROWN DOWN BY EARTHQUAKE VIBRATION, TOWER OF UNION FERRY BUILDING, SAN FRANCISCO."
	4		135	"The Union Ferry Building (Pl. XLVI,A), with the exception of its high tower, was little injured, and the level of its floors was no perceptibly changed. At the same time, the streets at its front, which rested simply on the made soil, were rolled into waves 3 or 4 feet [0.9 to 1.2 m] in height."
	5		319	"On Market Street, near the Ferry House, the cable tracks resting upon piles moved very little in comparison with the collapse of the street surface on both sides of the car tracks."
	5	Pl. XXXV Fig.2		Photo: View east on Market St. towards Ferry building. Shows settlement of street relative to sidewalk roughly 0.9 m. Photo caption: "Destruction of Buildings of Type 2 Construction at Foot of Market Street, San Francisco."
	6		226	"UNION FERRY BUILDING.... The street surface at the N.W. corner settled 2' [0.6 m], cracking the asphalt pavement and carrying down a large section of the sidewalk."
	1	No. 60	95	Photo: View looking west up Market St. Aetna building on left in distance. Shows settlement around car rails and waves.

LOCATION	REF	PHOTO	PAGE	DESCRIPTION
				Photo caption: "Market St. west of Steward sunken & 16" pipe broken."
3) Spear St.	5		288	"The Folger Building, on Howard Street...but otherwise the building was not damaged; and yet, at this very site, the street in front of the building had settled about 2 ft [0.6 m]."
	6		28	"FOLGER BUILDING. S.W. Cor. Howard and Spear Streets....The street level settled about 2 ft. [0.6 m] at the northeast corner of the building, but there are no earthquake cracks visible in the walls at this point.
	1	No. 78	99	Photo: View southwest up Market St. from Spear St. Aetna (or Young) building in left foreground of photo. Shows subsidence of roughly 0.6 m of street relative to sidewalk. Photo caption: " Market St. Cor. of Spear St. Street sunken several feet. 16" water pipe ruptured."
	4	Pl. XXVA		Photo: View looking SE down Spear St. from Market St. Shows subsidence of street of roughly 0.6 m relative to sidewalk. Photo caption: "A. SUBSIDENCE OF STREET IN FRONT OF AETNA BUILDING, SAN FRANCISCO."
	4		76	"The steel-frame structure at the corner of Spear and Market streets...Pl. XXV, A, shows the corner of the building and the subsidence of the street at this point. The inlet at the corner indicates the original level of the street. There was a vault under the Market street sidewalk, immediately behind the wall at the curb line. The basement floor in this vault was of concrete and had a total thickness of 7 or 8 inches [0.2 m]. The earthquake caused the earth to bulge up in the portion of the basement under the sidewalk, rupturing the concrete floor and turning it up on its edge, so that where there had previously been a clear headroom of 7-1/2 feet [2.3 m] the highest point of the bulge was within 3-1/2 feet [1.1 m] of the beams carrying the sidewalk."
			32	"The basement floor, which was of concrete 7 or 8 inches [0.2 m] thick, was pushed up under the sidewalk, reducing the headroom at this point from 8 feet to 3-1/2 feet [2.4 to 1.1 m], approximately. This bulging was probably

LOCATION	REF	PHOTO	PAGE	DESCRIPTION
				caused by settling (Pl. XXV, A), as the foundation piling did not extend under the sidewalk."
	6		80	Photo: Shows subsidence of 0.6 m of street relative to sidewalk. Photo caption: "YOUNG (OR SELLER) BUILDING...The foundations on the east side has settled, and the east and west walls are out of plumb about 5"..."
	6	---	81 84	"YOUNG OR SELLER BUILDING. S.W. Cor. Spear and Market Streets...Levels on the water table show that the N.E. and S.W. corners are 3" and 6" lower respectively than the N.W. corner. These facts would indicate that the foundations had moved sufficiently to tilt the entire building to the east. From marks on the curb of the sidewalk, it is also apparent that the surface of the ground settled considerably around the N.E. corner."
	7	---	643	Photo: Young Building and sidewalk on good foundations; street in front subsided 0.6 to 0.9 m. View shows corner of Spear and Market Sts., looking southeast. Settlement less up Spear St. to the southeast. Note other references place this building at Spear not Stewart. Photo caption: "The Young Building."

LOCATION	REF	PHOTO	PAGE	DESCRIPTION
	7		643	"The Young Building is at the corner of Stewart and Market Sts. This building was within one block of the water-front...The building is on pile foundation, as it is situated in the portion of the city that is constructed on filled ground. The portion of the street on the corner, it will be seen, has settled on this account about 2 ft [0.6 m]."

OTHER LOCALITIES:

LOCATION	REF	PHOTO	PAGE	DESCRIPTION
1) Duboce Park	3	Pl. 90D		Photo caption: "Southwest corner Portola and Waller Streets. Buildings have shifted down hill slightly, upper parts more than lower." Photo: Difficult to ascertain ground movements.
	3		240	"Near the corner of Waller and Portola Streets, not far north of the head of Market Street, is a locality, less than a block in extent, where houses were shifted slightly on their foundations; their upper stories were moved farther eastward (downhill) than the foundations, as a result of shearing in the framework of the basement or of the first story of the buildings. (Plate 90D.) There also occurred minor bucklings and breaking of the thin asphalt pavement. The intensity, which belongs low in the range of Grade B, diminishes rapidly in all directions, and the district is surrounded by a band where the intensity is Grade C. Here a thin layer of sand reposes upon the slopes of a little upland valley between the low serpentine hills to the east and the high chert hills to the west. The effects are such as would be produced by a shaking downhill of this thin sand layer, with the structures which rest upon it."
2) Steiner and Sutter Sts.	3	Pl. 87B		Photo caption: "Geary and Street, between Filmore and Steiner Streets, San Francisco. Buildings of mediocre construction on sand and alluvium of no great depth." Photo: Ground movements difficult to ascertain.
	3	Pl. 92A		Photo caption: "St. Dominic's Church, Bush and Steiner Streets. Brick and masonry structure upon sand and alluvium of no great depth." Photo: Ground movements difficult to ascertain.
	3		231	"In the neighborhood of the crossing of Steiner and Sutter Streets, there is an irregularly bounded district a little larger than a city block in which several buildings not conspicuously weak were totally destroyed. St. Dominic's Church, at the corner of Steiner and Bush streets, was a complete ruin, as the illustration (plate 92A) shows. Its steeple towers were ruined, its roof fell in, and all its walls were so badly cracked that it became a menace to the neighborhood....Near by small frame dwellings were pitched from their underpinning. On Geary Street, just above Fillmore Street, two wooden-framed brick buildings standing side by side -- the Albert Pike Memorial Temple (Masonic)

LOCATION	REF	PHOTO	PAGE	DESCRIPTION
				and a Jewish Synagogue--were utterly wrecked, as the illustration shows. (Plate 87B.) The Girls' High School near by on O'Farrell Street, at Scott Street, poorly and flimsily built, was badly damaged. Its walls were much cracked and portions of the gable walls were thrown down. This district of Grade B intensity is on the floor of Upper Hayes Valley and is surrounded by a relatively broad area in which Grade C effects prevail. It lies near the base of the hills which hem in the valley on the east. The surface strata are sand and alluvium extending to no great depth, unless the slopes of the bedrock hills change suddenly where they pass under the mantle of loose materials. No explanation can be offered for the occurrence of this limited area of high intensity (Grade B) unless it be that the district has been converted into "made" ground by extensive grading in the preparation of the surface for building sites and streets."
3) Vallejo St. and Van Ness Ave.	1	No. 73	99	Photo caption: "Van Ness Avenue between Vallejo St. & Broadway." Photo: Shows abrupt subsidence of street, with 0.1 to 0.2 m scarp across street.
	1	No. 74	99	Photo caption: "van Ness Ave. near Vallejo. 8" [0.2 m] water pipe ruptured." Photo: Shows 0.1 to 0.2 m scarp across street, lateral spreading.
	1	No. 75	99	Photo caption: "vaNess Ave. between Vallejo & Broadway." Photo: Shows subsidence of street of 0.1 to 0.3 m, and lateral spreading of roughly 0.3 m.
	1		43	"The vicinity of Van Ness avenue and Vallejo street is one of the prominent points of interest. It was found that Van Ness avenue had been more or less affected from a point 150 feet [46 m] south of Vallejo street, the greatest subsidence being two feet [0.6 m] at the crossing of Vallejo street. There was also subsidence of Vallejo street from 150 feet [46 m] on each side of Van Ness avenue. There was a lateral movement to the north on Van Ness avenue of about three feet [0.9 m] on Vallejo street, decreasing to about one foot [0.3 m] on Green street, the ground and buildings upon it having been moved bodily so that now the buildings encroach upon the neighboring lots or upon the street. As a result of the subsidence and lateral movement the sewers extending east, south and west of the crossing of Van Ness avenue and Vallejo street

LOCATION	REF	PHOTO	PAGE	DESCRIPTION
				were broken for about 150 feet [46 m]. The scene of the disturbance was an old fill of about forty feet [12 m] which had been made years ago in the ravine leading to the northwest to the lagoon formerly called Washerwoman's bay."
	2	Fig. 52	58	Photo caption: "Disruption of Van Ness Avenue over a filled in ravine. Lateral movements as great as 3 ft (0.9 m) and vertical movements as great as 2 ft (0.6 m) occurred at this location." Photo: Shows jagged scarp across street.
	3		231	"At the corner of Vallejo Street and Van Ness Avenue, fissures were formed in the asphalt paving, sidewalk pavements were thrust over the curbing, and water-mains and sewers were broken. Buildings were thrown out of the vertical, and foundations and lower story walls were shifted and crusht. The walls about the foundation of one brick building were actually deformed into undulations with much consequent cracking. This building was so badly damaged that it had to be taken down. Surrounding this corner is a small ovoid district, about 2 blocks in extent, in which the intensity was clearly of Grade B. This was once a sharp ravine and had
				been filled to a depth of 40 feet [12 m] in order to provide a suitable grade for streets and buildings. The filling was shaken together and moved slightly downhill."
	4		118	"At one point on Van Ness avenue (see B, Pl. LVI) [shows location on map], where I happened to see the mains uncovered, a heavy water pipe, apparently about 20 inches [0.51 m] in diameter, had been broken into pieces not more than 2 feet [0.6 m] long. The total length of the break, however, was not more than 40 or 50 feet [12 to 15 m], so far as I could judge from what I saw uncovered."
4) Lombard and Octavia Sts.	3		232	"On Lombard, between Gough and Octavia Streets, is a little area, less than a

LOCATION	REF	PHOTO	PAGE	DESCRIPTION
				block in extent, in which the destructive effects were of Grade B. No particularly notable effects were produced. It is a district of made land, formerly the site of a little lagoon in the sands, known as Washerwoman's Lagoon."
5) Union and Steiner Sts.	3	Pl. 88B		Photo caption: "Slip of a fill on Union Street, just west of Steiner Street, San Francisco." Photo: Shows lateral movement and subsidence of street and sidewalk. Resembles lateral spreading.
	3		232	"A portion of Union Street, between Pierce and Steiner Streets, not more than a quarter of a block in length, where a filling had been made to equalize the street grade, was shaken down into the adjacent building lot on the north. The north sidewalk was shifted about 10 feet [0.3 m] to the north, and deprest about 10 feet [0.3 m] below its original level. The south sidewalk was deprest a few inches and shifted to the north from 2 to 3 feet [0.6 to 0.9 m]. The paving and the cable conduit suffered more severe damage than at any other point in the city. The photograph (plate 88B) conveys a graphic conception of the very great violence which occurred here. The phenomena have no general significance, however, despite their striking character, being merely a sliding of unconsolidated material not supported on the sides. But that such places are dangerous building sites, especially in regions subject to seismic disturbances, is unequivocally demonstrated."
	2	Fig. 53	58	Photo caption: "Slump in Union Street between Pierce and Steiner Streets." Photo: Same as that of ref. 3, Pl. 88B.
	1	No. 79	99	Photo caption: "Union St. between Steiner & Pierce St. Street, cable road, sidewalks, water & other pipes & sewer moved laterally several feet [0.3 to 0.6 m]. Note: A-A_1-B shows former position of center slot of North Track. (looking west.)" Photo: Shows lateral movement and subsidence to the north.
	1	No. 80	99	Photo caption: "Same as No. 79, only taken from different point. Note destruction of formerly straight sidewalk." Photo: View similar to that of ref. 3, Pl. 88B. View west.
	1	No. 81	99	Photo caption: "Union St. with Cable Road. Same as No. 79, only taken in opposite direction, looking from west to east."

LOCATION	REF	PHOTO	PAGE	DESCRIPTION
6) Marina District	3		232	"Along the north shore water-front, between Fillmore and Steiner Streets, from bay Street to the water's edge, was a plot of made ground occupied by a gas-producing plant. Here brick walls were cracked and partly thrown down; part of the wooden framework was wrenched out of position, and the chimney stack was broken. One of the large gas-containers was badly wrecked, but whether its destruction was caused directly or in some secondary way, as by rapid leakage, is not known. The intensity was clearly Grade B."
	4		27	"The group of building comprising the plant of San Francisco Gas and Electric Light Company, built on the soft ground along San Francisco Bay just west of Fort Mason, was badly shaken, and none of the buildings escaped damage...The ground settled very considerably under the vibrations of the earthquake, and further destruction was caused by the unequal settling of the building ...The end wall of the retort house was pushed out 1 foot [0.3 m] at the center, but was saved from collapse by the tie-rods which held it to the roof truss."
	3		232	"Along Lyon, Baker, and Broderick Streets, north of North Point Street, is a small locality 2 blocks wide and 4 blocks long, where the Baker Street sewer was broken and frail frame buildings were thrown out of the vertical. This district was partly made land, but the greater part was on the point of a sand-pit. Unquestionably extensive grading had been done to prepare the ground for building."

TABLE A.2 DOCUMENTATION OF PIPELINE BREAKS RESULTING FROM GROUND MOVEMENTS IN SAN FRANCISCO DURING 1906 EARTHQUAKE.

PIPELINES BREAKS:

LOCATION	REF	PHOTO	PAGE	DESCRIPTION
	1		43	"APPENDIX D. The following are extracts from the report of City Engineer Woodward on the breaks in the San Francisco sewer system caused by the earthquake as published in the "San Francisco Chronical" of June 17th, 1906: ...He further summarizes the following breaks in the sewers: 'On Fourteenth street, between Valencia and Harrison streets; on Harrison street, between Twelfth and Thirteenth streets; on Eleventh street, between Harrison and Bryant streets; on Ninth street, between Bryant and Brannan streets; on Dore street, between Bryant and Brannan streets; on Laguna street, between Greenwich and Lombard streets; on Seventeenth street, between Folsom and Harrison streets; on Howard street, between Seventeenth and Eighteenth streets."
	4		19	"The failure to control the fire by reason of the crippling of the water supply was not due to the failure of the system outside of the city, but to the breaks in the distributing mains within the city, which rendered unavailable about 80,000,000 gallons of water store within the city limits. The breaks occurred (see the map, PL. LVI) wherever the pipes passed through soft or made ground. No breaks occurred where the cast-iron pipe was laid in solid ground or rock."
	4		26	"The settling of the ground in the mud flats along San Francisco Bay and of the filled ground in old water courses was accompanied with great destruction. It was in such ground that the greatest number of breaks occurred in the cast-iron gas and water mains and the sewers. The breaks in the sewers were not so evident as those in the gas and water mains, for the reason that the latter were under pressure and breaks in them resulted in breaks in the streets themselves. The most noticeable destruction resulting from the settling of soft or filled ground occurred in Howard and Shotwell streets between Seventeenth and Eighteenth streets, Bryant street between Ninth and Tenth streets, Dore street between Bryant and brannan streets (Pl. VI, A), and at the corner of Seventh and Mission streets."
	5		253	"In San Francisco, all serious fractures of water mains, as a result of the earthquake, were due to lateral displacements, or subsidences of filled or soft ground across which, unfortunately, the main

LOCATION	REF	PHOTO	PAGE	DESCRIPTION
				supply pipes from the lower and middle service distributing reservoirs passed. The map, Plate XLVIII, shows these areas bordered with a heavy line where clearly defined and with a broken line where not so distinctly and connectedly traceable. The displacement laterally amounted in places to as much as 6 or 7 ft. [1.8 or 2.1 m]; vertically, it amounted to several feet."
	8b		740	"Attention might well be called to the destruction of gas mains during the fire, owing to the fact that these were badly shattered by the earthquake in certain places, probably for the most part where they passed from soft to firm ground and vice versa. It is possible to believe that some explosions of gas occurred due to the heat of the fire itself. Many of the explosions produced serious destruction of the streets in their vicinity, and probably wrecked large water pipes, sewers, etc., which would otherwise have been uninjured."
	8b		740	"THE SEWAGE PROBLEM.--The construction and maintenance of sewers in certain parts of San Francisco where filled land exists has always presented a difficult problem. As an example, it may be said that in 1903, when the Sixth St. sewer, between Howard and Folsom Sts. was reconstructed, it was found that the former sewer had settled from 6 to 9 ft. [1.8 to 2.7 m] during the twenty years of its existence. The distortion was ultimately such as to cause failure of the crown in certain places. As the result of the earthquake, however, many of the effects which had been produced very slowly before, were caused at once with very serious consequences. Brick sewers, the usual type for the larger conduits, were in many places distorted, their crowns were broken and their earth covering was carried into them, causing almost complete stoppage in some cases.
MISSION CREEK ZONE:				
1) Valencia St. between 17th and 18th	1	No. 57	93	Photo: Shows destruction of sewer; does not show water mains. Photo caption: "Valencia Str. between 18th & 19th subsided about five feet [1.5 m]; destroying sewer, and besides gas & electric pipes & conduits, tore of one 16" [0.41 m] and one 22" [0.56 m] water main, which at this point had about 85 lbs pressure."
	1	No. 59	93	Photo: Another view of photo, ref 1, No. 58. Does not show sewer, but does show street subsidence and lateral spread.

LOCATION	REF	PHOTO	PAGE	DESCRIPTION
				Photo caption: "Valencia Str. Sunken portion of Str. showing two above emergency pipes on top of pavement; also 5' [1.5 m] sink with car tracks & broken sewer at A."
	1	No. 64	95	Photo: Shows street subsidence; does not show pipe. Photo caption: "Other view of same [ref. 1, No. 63 showing Valencia Hotel], showing large hole in sunken street; also water pipe at x."
	3		239	"Sewers and water-mains were broken. At Eighteenth and Valencia Streets there was a serious break in the water-pipe. Here, on both sides of the street, the ground sank about 6 feet [0.2 m], causing the roadway to arch in a very noticeable way. (Plate 93B.)"
	8b	---	738	Photo: On Valencia. Shows general destruction by fire, but ground displacements are unclear. Shows explosion crater in middle of street. Photo caption: "Disruption of Valencia Street... The disruption of the street in the second picture was caused by the explosion of a large gas main."
	8b	---	739	Photo caption: "Temporary Main on Valencia Street... The second picture shows a 24-in. [0.6 m] cast-iron pipe line hastily placed in Valencia St. to provide water for the higher districts, whose supply had been cut off by the destruction of the mains in this street between Eighteenth and Nineteenth Sts. A 16-in. [0.4 m] pipe to supply the lower downtown districts was also placed here in an incredibly short time."
	8b		739	"The earthquake caused a settlement of from 6 to 8 ft. [2 to 2.4 m] for a distance of from 150 to 200 ft. [46 to 61 m] along this street, and at the same time shifted the entire street, with adjacent lands, eastward through a maximum distance of 9 to 10 ft. [2.7 to 3.0 m]. This change in alignment and grade could, of course, meant nothing less than the entire destruction of all water and gas mains, electric lighting and telephone conduits, sewers, cable conduits, railroad tracks, etc. The breakage of these important lines, especially to the water mains, was of greatest significance. In this case the destruction of the water pipes, of which a 22-in. and a 16-in. [0.61 and 0.41 m] were found in this street at this point, meant the cutting off of a large part of the water supply of the portion of the city which was soon to be in flames."

LOCATION	REF	PHOTO	PAGE	DESCRIPTION
	8c	---	765	Photo caption: "Destruction of Sewer by Settlement of Street....In the second picture, taken on Valencia St., between Eighteenth and Nineteenth Sts., the broken sewer is in a deep fill along the former course of Mission Creek."
	8c		767	"PIPES DESTROYED BY UNEQUAL SETTLEMENT.--Wherever filled ground existed, settlement in greater or less degree took place as the result of the tremblor. Pipes passing from comparatively firm and incompressible earth into such softer materials or vice versa, suffered considerably. This effect was particularly noticeable in San Francisco on account of the large number of places where such conditions were to be found. Probably at no point were more serious results produced than on Valencia St., between 18th and 19th Sts., already described in connection with street and sewer problems. Two very important distribution mains were located at this point and were, or course, ruptured. One of these pipes, 22 in. [0.56 m] in diameter, supplied the higher districts of the city; the other, a 16-in. [0.41 m] pipe, was an important artery of the system furnishing water to the business section."
	9b	Fig. 10	550	Photo: Similar to that of ref. 8b, p. 738, but closer view. Photo caption: "Exploded Gas Main, on Valencia St., near Market."
	9c	---	581	Photo: Shows street subsidence and lateral spread; does not show broken pipes. Photo caption: "STREET SUBSIDENCE IN SAN FRANCISCO. VIEW ON VALENCIA ST., NEAR 18TH ST., OPPOSITE SITE OF VALENCIA HOTEL. (It was at this place that street water mains were broken. The street dropped about 4 ft. and moved eastward about 6 ft. at the maximum point. The 24-in. [0.6 m] main on the left was laid after the fire. All buildings in this vicinity were burned."
2) Howard and 17th	8b		740	"On Howard St., at the corner of 17th St., very complete destruction of the brick sewer, as well as most other pipes and conduits in the ground, was caused by the extensive settlements in the region. On Valencia St., near 18th St., similar ruptures were produced."
	9	Fig. 20	554	Photo caption: "GENERAL WRECKAGE OF CAR TRACKS, SEWER, WATER AND GAS PIPES, HOWARD AND 17TH STS., SAN FRANCISCO."

LOCATION	REF	PHOTO	PAGE	DESCRIPTION
				Photo: Shows car track pulled apart, destruction of pipes. Two pipes [0.3 and 0.51 m ?] pulled out at the joints.
	9		554	"Fig. 20 shows a street view, taken April 25, at the corner of Howard and Seventeenth Sts., where the ground was much distorted. The car tracks are twisted out of shape, the brick sewer is broken and the water and gas pipes are wrenched and snapped. A redwood plug has been driven into the broken water main, but the pipe is badly leaking. Views of this kind were common in the first week after the fire."
	1	No. 66	97	Photo: Shows subsidence of street. Does not show pipes. Photo caption: "Crossing of 17th & Howard. Street sunken, 12" & 20" [0.3 & 0.51 m] pipes ruptured."
3) Howard St. 18th	1	No. 62	95	Photo: Shows lateral and spread and street subsidence; does not show pipes. Photo caption: "Howard St. north of 18th sunken & twisted (see car tracks). One 20" [0.51 m] pipe, one 24" [0.6 m] and two 6" [0.15 m] pipes broken by earthquake."
	1	No. 68	97	Photo: Shows street subsidence and lateral spread; does not show pipe. Photo caption: "Along 18th from Howard. Street subsided, pipe broken."
4) 14th near Howard	8b	---	737	Photo: Shows street subsidence near sewer. Complete destruction by fire to left of photo. Photo caption: "Effect of Broken Sewer on Fourteenth Street....The second picture shows the result of the destruction of a sewer on Fourteenth St., near Howard St. The crown of the sewer was broken in, the surface material washed in, as at A, and the sewer so completely filled with sand as to back up the sewage, as at B, above the elevation of the crown."
	8b		740	"On 14th St., between Mission and Howard Sts., practically the same effects were produced. The crown was broken in many places and sand from the street filled the channel to such an extent that sewage was backed up above the original crown line. These breaks were indicated on the surface by great holes where all the covering, including the stone block paving, had settled down into the sewer."
5) 14th and Valencia Sts.	1	No. 63	95	Photo caption: "14th St. east of Valencia. Street torn open. See water pipe below."

LOCATION	REF	PHOTO	PAGE	DESCRIPTION
SOUTH OF MARKET:				
1) Howard and 7th	1	No. 70	97	Photo: Shows broken pipe; pipe sheared abruptly near the joints from soil displacements. Photo caption: "Crossing 7th & Howard St. 16" pipe badly fractured (not yet repaired)."
2) 5th St.	8b		740	The more important breaks in main sewers observed by the writer may be described as follows: On Fifth St., between Folsom and Harrison Sts., the brick sewer settled with the adjacent land, its crown was destroyed and the channel had become filled with sand which blocked up the sewage to a dangerous extent.
	1		43	"APPENDIX D....The Fourth and Sixth street sewers were also greatly damaged, some of them showing a vertical and horizontal movement of as much as five or six feet."
FOOT OF MARKET ZONE:				
	13		32	"Throughout the filled area above street-corner silt basins have been tripped out of plumb and bulged into sidewalk areas, and sewer manholes in street intersections are in several places canted up, showing sewer disturbance beneath..."

LOCATION	REF	PHOTO	PAGE	DESCRIPTION
OTHER LOCATIONS:				
1) Vallejo St. Van Ness Ave.	1	No. 74	99	Photo: Shows street and subsidence and lateral movement; does not show pipe. Photo caption: "Van Ness Ave. near Vallejo. 8" [0.2 m] water pipe ruptured."
	4		118	"At one point on Van Ness Avenue (see B, Pl. LVI) [shows location on map], where I happened to see the mains uncovered, a heavy water pipe, apparently about 20 inches [0.51 m] in diameter, had been broken into pieces not more than 2 feet [0.6 m] long. The total length of the break, however, was not more than 40 or 50 feet [12 to 15 m], so far as I could judge from what I saw uncovered."
	1		43	"The vicinity of Van Ness Avenue and Vallejo Street is one of the prominent points of interest. It was found that Van Ness Avenue had been more or less affected from a point 150 feet [46 m] south of Vallejo Street, the greatest subsidence being two feet [0.6 m] at the crossing of Vallejo Street. There was also subsidence of Vallejo Street from 150 feet [46 m] on each side of Van Ness Avenue. There was a lateral movement to the north on Van Ness Avenue of about three feet [0.9 m] on Vallejo Street, decreasing to about one

LOCATION	REF	PHOTO	PAGE	DESCRIPTION
				foot [0.3 m] on Green Street, the ground and buildings upon it having been moved bodily so that now the buildings encroach upon the neighboring lots or upon the street. As a result of the subsidence and lateral movement the sewers extending east, south and west of the crossing of Van Ness Avenue and Vallejo Street were broken for about 150 feet [46 m]."
2) Union and Steiner Sts.	1	No. 79	99	Photo caption: "Union St. between Steiner & Pierce St. Street, cable road, sidewalks, water & other pipes & sewer moved laterally several feet [0.3 to 0.6 m]. Note: A-A_1-B shows former position of center slot of North Track. (looking west.)"
South of Market	15		369	The four underground cables from Station A (23rd St. and Georgia Ave.) to Sub-station No. 4 (8th St. between Mission and Howard Sts.) were so badly wrecked by the earthquake and gas explosion that they were out of commission for some ten or twelve days.
			369	Along Seventh Street, from Mission to Howard, the earth was displaced from five to eight feet (1.5 to 2.1 m) in a direction lengthwise to conduit. This caused some of the manholes to crush like egg shells, although they were twelve-in. (300-mm) concrete walls. The conduit was pulled apart at other places, and cables were wrenched and torn from their boxes and in some cases pulled apart between manholes, so that these breaks were not discovered until after we had tested with full voltage.
General	16		353	Beginning at seven o'clock Wednesday morning, there were successive explosions in the feeding mains connecting the Potrero and North Beach stations. On the thirty-inch main, running from the Potrero works on Kentucky, Mariposa, Potrero Avenue, Tenth, Market and Fell to Van Ness Avenue, and thence along Van Ness to Broadway, there were twenty-one explosions. In nearly every case, the explosion took place at a line drip or cross where the main was weakest, and the earth around the main was thrown up, leaving openings of various sizes up to twelve feet wide and thirty feet long, and on the line of the twenty-four inch feeding main connecting the two stations there were as many as forty breaks due to explosions.
			362	Gas mains in streets running east and west were broken and drawn apart, while the street mains in streets running north and south were crushed together and telescoped, or else

LOCATION	REF	PHOTO	PAGE	DESCRIPTION
				raised out of the ground in inverted Vs. This rule applied generally with but few exceptions.
			355	Among the obstacles to be overcome in repairing the feeding mains, and some of the larger distributing mains, was the removal of water from the pipes where the mains of the Spring Valley Water Company had broken in proximity to a break in the gas main, thus filling large districts with water and sand. In some places the mains were so filled with water that it backed up to the meters, filling them also.
Marina	16		351	At the North Beach station the gas was shut off at the inlet of the meter, and the valves were closed at the inlet of the 2,000,000-foot (57,000-m^3) storage holder. The writer arrived on the ground at this time and found that the 24-in. (600-mm) outlet connections of this holder were broken off between the holder and the outlet valves, so that all attempts to seal the drip pots of the holder by syphoning water from the holder tank did not succeed in saving any of the gas in the holder, which grounded on the wooden framework.
Van Ness and Vallejo	16		352	On this same Wednesday, the street-main gang commenced repairs on the 24-inch (600-mm) trunkline main at the junction of Van Ness Avenue and Vallejo Street, where the street had settled 24 inches (600 mm), breaking the main, and the pipe was pulled apart 18 inches (450 mm).
Foot of Market	16		362	Someone has suggested that if pipes, either water or gas, were laid on solid pile foundation in filled ground, that they would be immune from earthquake damage. On Jackson Street between Drumm and Davis Streets, which is made land, the street main was laid on a line of piles which went to hard pan. The piles were not purposely driven to sustain the pipe, but happened to be in the line of the main when it was laid. This pipe broke over the center of each pile, nine in number, and was not broken in the made ground, where it was unsupported.
South of Market	12		20	Captain Cullen did find some water in sewer lines, the source of which came from a broken water main at Seventh and Howard Streets. For a time, this helped keep the blaze from crossing from the bakery on the west side of Sixth Street to the east side. However, by 6:15 a.m., about one hour after the earthquake, the bakery fire began to

LOCATION	REF	PHOTO	PAGE	DESCRIPTION
				rapidly spread..."Our water supply gone out," wrote Cullen, "and the fire was then raging around our engine."
Mission Creek			89	Thursday at 11 a.m., wrote Captain Cullen, "The fire being beyond danger at this point we again picked up the remaining hose in our possession and proceeded to 17th and Howard Sts., there being considerable water in a large hole in the middle of the street owing to a broken main, with stones and sand we dammed the water that was running to waste and put our Engine to work..."

REFERENCES - TABLES A.1 and A.2

1. Schussler, H., The Water Supply of San Francisco, California, Martin B. Brown Press, New York, NY, July 1906, 103 p.

2. Youd, T.L. and S.N. Hoose, "Historic Ground Failures in Northern California Triggered by Earthquakes," Geologic Survey Professional Paper 993, U.S. Government Printing Office, Washington, D.C., 1978, 177 p.

3. Lawson, A.C., et al., The California Earthquake of April 18, 1906: Report of the California State Earthquake Investigation Commission, Pub. No. 87, Carnegie Institute, Washington, D.C., 1907, 2 Volumes and Atlas, 451 p.

4. Gilbert, G.K., R.L. Humphrey, J.S. Sewell, and F. Soule, "The San Francisco Earthquake and Fire of April 18, 1906 and Their Effects on Structures and Structural Materials," Bulletin 324, U.S. Geological Survey, U.S. Government Printing Office, Washington, D.C., 1907, 170 p.

5. Duryea, E. Jr., et al., "The Effects of the San Francisco Earthquake of April 18th, 1906 on Engineering Constructions," Transactions, ASCE, 1907, pp. 208-329.

6. Himmelwright, A.L.A., The San Francisco Earthquake and Fire: A Brief History of the Disaster, The Roebling Construction Company, New York, NY, 1906, 270 p.

7. Leonard, J.B., "The Effect of the California Earthquake on Reinforced Concrete," The Engineering Record, Vol. 53, No. 21, May 1906, pp. 643-644.

8a. Hyde, C.G., "The Structural, Municipal, and Sanitary Aspects of the Central Californian Catastrophe - II," The Engineering Record, Vol. 53, No. 23, June 1906, pp. 700-705.

8b. Hyde, C.G., "The Structural, Municipal, and Sanitary Aspects of the Central Californian Catastrophe - III," The Engineering Record, Vol. 53, No. 24, June 16, 1906, pp. 737-740.

8c. Hyde, C.G., "The Structural, Municipal, and Sanitary Aspects of the Central Californian Catastrophe - IV," The Engineering Record, Vol. 53, No. 25, June 1906, pp. 765-769.

9a. Derleth, C. Jr., "Report by Prof. C. Derleth," Engineering News, Vol. 55, No. 18, May, 1906, pp. 503-504.

9b. Derleth, C. Jr., "Some Effects of the San Francisco Earthquake on Waterworks, Streets, Sewers, Car Tracks, and Buildings," Engineering News, Vol. 55, No. 20, May 1906, pp. 548-554.

9c. Derleth, C. Jr., "Additional Examples of Street Subsidence in San Francisco," Engineering News, Vol. 55, No. 21, May 1906, pp. 580-581.

10. Kurtz, C.M., "The Effect of the Earthquake on Street Car Tracks in San Francisco," Engineering News, Vol. 55, No. 20, May 1906, p. 554.

11. Jordon, D.S., Ed., The California Earthquake of 1906: San Francisco, A.M. Robertson, San Francisco, CA, 1907, 360 p.

12. Hansen, G. and E. Condon, Denial of Disaster, Cameron and Company, San Francisco, CA, 1989, 160 p.

13. Hall, W.H., "Some Lessons of the Earthquake and Fire," San Francisco Chronicle: - I. "Reminiscences of the City's Site as Accounting for Earthquake Effects," May 19, 1906; - II. "A Record of Earthquake Disturbances," May 20, 1906.

14. Newman, W.A., "The San Francisco Post Office," The Engineering Record, Vol. 53, No. 22, June 1906, pp. 694-695.

15. Reynolds, L.E., "How Electricity Was Served to Consumers and Street Car Lines by the San Francisco Gas and Electric Co. After the Fire," Proceedings, 14th Annual Meeting of the Pacific Coast Gas Association, San Francisco, CA., Sept. 1906, pp. 365-373.

16. Jones, E.C., "The Story of the Restoration of the Gas Supply in San Francisco After the Fire," Proceedings, 14th Annual Meeting of the Pacific Gas Association, Sept. 1906, pp. 350-364.

APPENDIX B

DETERMINATION OF SURFACE AND SUBSURFACE GRADIENTS

B.1 SURFACE ELEVATIONS

Surface elevations and contours for the South of Market and Mission Creek areas of San Francisco were evaluated on the basis of survey data provided by the Streets and Mapping Division of the Bureau of Public Works of the City of San Francisco. Measurements provided by the City were obtained by optical leveling at major street intersections. At each intersection, typically several points are established as cuts on curbs, manhole rims, and fire hydrants. In general, the leveling accuracy for this type of survey is roughly $\pm$ 5 mm.

Surface contours were determined from city survey measurements in 1985 and 1990 for the South of Market area, and from measurements in the 1970s and 1991 for the Mission Creek area. In addition, each intersection in the areas of interest was inspected by research personnel, and an approximate field assessment was made of surface gradient to check generally and confirm the city survey data.

Figures B.1 and B.2 present surface contour maps of the South of Market and Mission Creek areas determined from recent city survey data. Contour lines were drawn from elevation measurements at street intersections using a statistical extrapolation procedure known as kriging, which is contained in the computer program Surfer (Golden Software, Inc., 1985). The current contours, shown as dark solid lines, are referenced to the City Datum, which is located at 2.5 m above mean sea level. The original contours, shown as dashed lines, are referenced to sea level (presumed mean sea level).

The surface contour lines are shown relative to both the street system and zones of fill, as delineated in Figures 9 and 13. By comparing the lateral movements plotted in Figures 9, 13, and 15 with the elevation contours of Figures B.1 and B.2, it can be seen that the directions of maximum lateral deformation tend to be nearly parallel to the dip directions of the slopes at the locations of observed displacement.

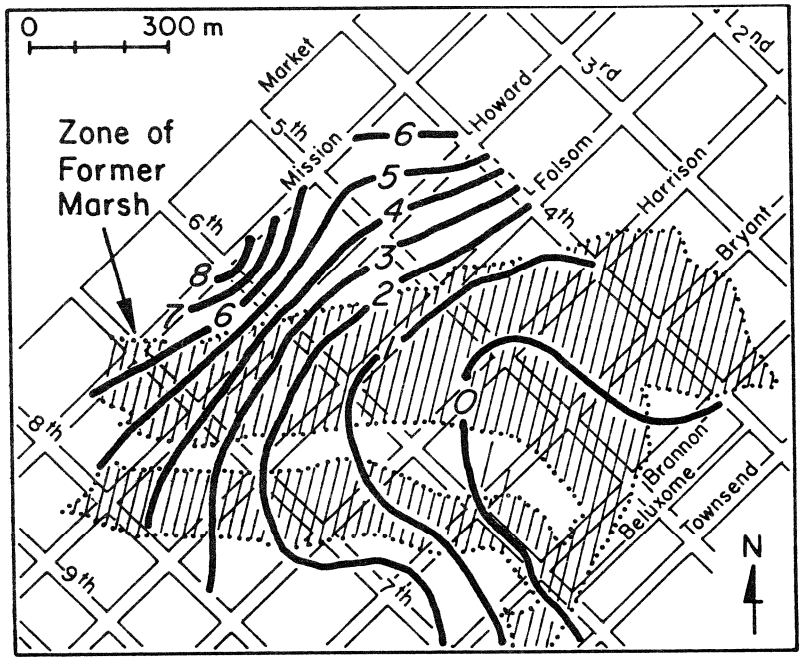

Figure B.1. Surface Elevation Contours for the South of Market Area

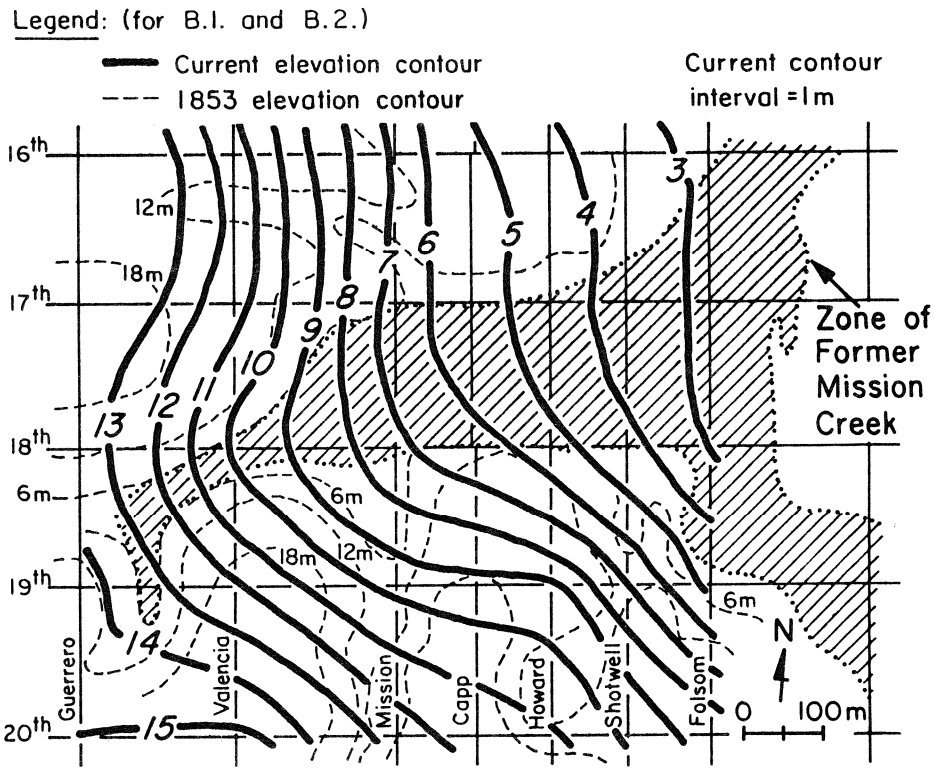

Figure B.2. Surface Elevation Contours for the Mission Creek Area

B.2 SUBSURFACE GRADIENTS

The gradients along the bases of liquefiable deposits in the Mission Creek area were estimated from elevation contours mapped by the 1853 and 1857 U.S. Coast Surveys, as shown in Figure 9. In using the 1853 and 1857 survey data, it was assumed that the original topography and elevations at Mission Creek form the base of the fill placed in Mission Creek during development of this area in the nineteenth century. Bottom elevations of the fill were checked where possible with existing borehole data. The agreement between depths inferred from the original contour plots and borehole investigations are in very good agreement. Similar gradients in the South of Market area were estimated from the same survey sources, as well as borehole data summarized by Harding Lawson Associates, et al. (1991). Because the original maps of the South of Market area show very little surface relief, estimates were made primarily on the basis of the borehole data summarized by Harding Lawson Associates, et al. (1991).

B.3 EVALUATION OF SURFACE CONTOURS

Using current surface elevations to evaluate gradients for correlation with 1906 ground deformation requires that the current elevations in areas of interest be similar to those of 1906, or at least be such that the current surface slopes are similar to those of 1906. Topographic maps prepared near the time of the 1906 earthquake were checked with current topographic maps, and no clear differences in elevations were found at the locations of 1906 lateral spreads in the South of Market and Mission Creek areas. Because minimum contour intervals of existing maps generally are 3 m or larger, this check only permitted an evaluation of gross changes in topography. Historical photographs also were examined to judge whether significant changes in elevation were brought about because of reconstruction after the 1906 earthquake. It does not appear from the photographic record pertaining to the South of Market or Mission Creek areas that elevation changes because of filling, releveling, and street and sidewalk resurfacing would have amounted to more than 0.3 to 0.5 m of local change. Alterations of this sort are not likely to have changed the general surface gradient to an appreciable extent.

The Streets and Mapping Division of the Bureau of Public Works helped by

tracing their records of surface elevation back 50 to 70 years in various zones of the South of Market and Mission Creek areas. Elevations determined in the 1910s, 1920s, and 1930s generally were within 200 to 300 mm agreement with the current elevations of similar survey points at selected street intersections. Given the assessments based on topographic maps, historical photographs, and settlement surveys, it seems that elevations in the South of Market and Mission Creek areas have not changed by more than about 300 to 500 mm relative to the time of the 1906 earthquake. Any change apparently has been confined to a relatively small area. It is likely, therefore, that the general surface gradients determined by current surveys are representative of those in 1906.

Case Histories of Lateral Spreads Caused by the 1964 Alaska Earthquake

Steven F. Bartlett, Research Assistant
Department of Civil Engineering
Brigham Young University
Provo, Utah

T. Leslie Youd, Professor
Department of Civil Engineering
Brigham Young University
Provo, Utah

ACKNOWLEDGEMENTS

We wish to express our appreciation to those who contributed information to this report. We are grateful to Rodney A. Combellick of the Department of Natural Resources, Division of Geological and Geophysical Surveys, State of Alaska, for furnishing borehole data (Boreholes TA-B-4, TA-C-4 and TA-C-6) located along the Turnagain Arm near Portage, Alaska. We also thank Fred R. Brown of Shannon & Wilson, Inc., for the borehole log at Ship Creek in Anchorage, Alaska.

We thank Tom Brooks of the Alaska Railroad for allowing us to review railroad bridge plans and files. Also, we acknowledge the assistance of Gordon Keith, Ken Lowney and Don Holland of the Alaska Department of Transportation in locating and reviewing highway bridge construction reports and foundation investigations.

We extend a special thanks to Scott R. McMullin who assisted us in our topographical surveys near the damaged bridges. Also, we are grateful to Sheryl Bartlett for inserting the many figures and photos into this report.

TABLE OF CONTENTS

	Page
Acknowledgments	2-iii
Table of Contents	2-v
List of Tables	2-vii
List of Figures	2-ix

Section		Page
1.0	INTRODUCTION	2-1
2.0	TECTONIC SETTING, FAULT RUPTURE, AND PHYSIOGRAPHIC EFFECTS	2-3
	2.1 Tectonic Setting	2-3
	2.2 Fault Rupture	2-4
	2.3 Physiographic Effects	2-7
3.0	LIQUEFACTION-INDUCED GROUND FAILURE	2-10
	3.1 Introduction	2-10
	3.2 Liquefaction and Types of Liquefaction-Induced Ground Failure	2-10
	3.3 Lateral Spread	2-11
	3.4 Seismic, Geological, Topographical, and Soil Controls of Lateral Spread Damage	2-13
	3.5 Empirical Technique for Determining Thickness, Continuity, and Depth of Liquefied Zone	2-18
4.0	CASE HISTORIES OF LATERAL SPREADS FROM THE 1964 ALASKA EARTHQUAKE	2-23
	4.1 Introduction	2-23
	4.2 Selection of Case Histories	2-24
	4.3 Seismic Factors at Case History Bridges in South-Central Alaska	2-30
	4.4 Bridges at the Head of the Knik Arm	2-37
	4.5 Railroad Bridge at Milepost 114.3, Ship Creek in Anchorage	2-72
	4.6 Bridges Along Southern End of Turnagain Arm	2-76
	4.7 Damaged Highway Bridges at Snow River	2-105
	4.8 Damaged Railroad Bridges at the Resurrection River	2-113
5.0	SUMMARY AND CONCLUSIONS	2-122
REFERENCES		2-125

LIST OF TABLES

Table		Page
1	Factors Influencing Liquefaction and Horizontal Ground Displacement	2-14
2	Case Histories of Lateral Spread Damage to Select Railroad and Highway Bridges Resulting from the 1964 Alaska Earthquake	2-24
3	Damage to Select Bridges in South-Central Alaska	2-26
4	Estimated Strong Ground Motion Duration: Liquefaction Sites in South-Central Alaska	2-34
5	Estimated Maximum Accelerations at Selected Liquefied Sites in Southern Alaska	2-36

LIST OF FIGURES

Figure		Page
1	Index Map of South-Central Alaska	2-3
2	Map of Alaska Showing Location of Aleutian Trench and Previous Major Earthquakes	2-5
3	Distribution and Depth of Aftershocks from March 27 to December 31, 1964	2-6
4	Areas of Tectonic Uplift and Subsidence in South-Central Alaska	2-8
5	Horizontal Displacement that Accompanied the Earthquake	2-9
6	Chart for Evaluation of Liquefaction Potential of Sands for Earthquakes of Different Magnitudes	2-21
7	Relationships Between CSRL and $(N_1)_{60}$ Values for Silty Sands for Magnitude 7.5 Earthquakes	2-22
8	Example of Standard Penetration Data and Liquefaction Analysis for a Bore Hole on the Knik River	2-23
9	Amplification-Attenuation Relationship for Modifying Bedrock Acceleration at Soft Soil Sites	2-36
10	Topography of Knik and Matanuska Rivers, Alaska	2-38
11	Profile of and Displacements at Bridge Milepost 146.4	2-40
12	Contour Map of Knik River	2-42
13	SPT Profile and Analysis, Bore Holes K5A and K8	2-44
14	Grain-Size Distribution Charts, Bore Hole K5A	2-45
15	Grain-Size Distribution Charts, Bore Hole K8	2-46
16	Broken and Displaced Piers at Bridge Milepost 147.1	2-47
17	Contour Map of Secondary Channels of Matanuska River	2-49
18	Profile of and Displacements at Bridge Milepost 147.1	2-50
19	SPT Profile and Analysis, Bore Holes M-3 and M-4	2-52
20	Grain-Size Distribution Charts, Bore Holes M-3 and M-4	2-53

Figure		Page
21	Grain-Size Distribution Charts, Bore Hole M-4	2-54
22	Pre- and Post-Earthquake Base Plate Positions, Bridge Milepost 147.4	2-55
23	SPT Profile and Grain-Size Data, Bore Hole M-10	2-57
24	Grain-Size Distribution Charts, Bore Hole M-10	2-58
25	Pre- and Post-Earthquake Base Plate Positions, Bridge Milepost 147.5	2-59
26	SPT Profile and Grain-Size Data, Bore Hole M-12	2-61
27	Broken Trestle at Southern End of Bridge Milepost 148.3	2-63
28	Estimation of Ground Displacement at Damaged Trestle from Inclination of Broken Telephone Pole, Bridge Milepost 148.3	2-64
29	Profile of Matanuska River	2-65
30	Contour Map of Matanuska River	2-66
31	SPT Profile and Analysis, Bore Holes M-17 and M-20	2-69
32	Grain-Size Distribution Charts, Bore Hole M-17	2-70
33	Grain-Size Distribution Charts, Bore Hole M-20	2-71
34	Combined SPT Log for the Knik and Matanuska Rivers	2-72
35	Map and Profile of Ship Creek, Anchorage, Alaska	2-73
36	Construction of and Damage to Ship Creek Bridge at Milepost 114.3	2-74
37	SPT Profile and Analysis, Bore Hole B-16, Ship Creek	2-75
38	Location of Bore Holes Along the Railroad and Highway Near Portage, Alaska	2-77
39	Damaged Railroad and Highway Bridges Across the Twenty-Mile River	2-78
40	Construction of and Damage to Twenty-Mile River Bridge	2-80
41	Contour Map of the Twenty-Mile River	2-82
42	SPT Profile and Analysis, Bore Holes 8 and 10	2-83

Figure		Page
43	SPT Profile and Analysis, Bore Holes 11 and 14	2-84
44	Grain-Size Distribution Charts, Bore Holes 10, 11, 14	2-85
45	Ground Cracks at Portage Creek Near Railroad Bridges at Mileposts 63.5 and 63.6	2-86
46	Damage to Railroad Bridge at Milepost 63.5	2-87
47	Contour Map and Pile Displacements at Milepost 63.5	2-89
48	SPT Profile and Analysis, Bore Holes 4 and 6	2-90
49	SPT Profile and Analysis, Bore Holes 7 and TA-B-4	2-91
50	SPT Profile and Grain-Size Data, Bore Holes TA-C-4, 6, 7	2-92
51	Grain-Size Distribution Charts, Bore Hole TA-B-4	2-93
52	Damage to Bridge at Milepost 63.0	2-95
53	Topography and Displacements at Bridge Milepost 63.0	2-96
54	SPT Profile and Grain-Size Data, Bore Hole 2	2-97
55	Contour Map of Placer River at Highway Bridge 629	2-100
56	SPT Profile and Analysis, Bore Holes 1 and TA-C-6	2-101
57	SPT Profile and Analysis, Bore Holes 3 and 4	2-102
58	Grain-Size Distribution Charts, Bore Holes 1, 3, 4	2-103
59	Combined SPT Log for Portage Area	2-104
60	Bridge Locations at Snow River	2-106
61	Photograph of Displaced Highway Pier	2-108
62	Construction and Displacement of Concrete Pier, Bridge 605A	2-109
63	Grain-Size Distribution Charts, Bore Hole 1A, Snow River	2-109
64	Contour Map of Snow River	2-110
65	SPT Profile and Analysis, Bore Holes 1A and 5L	2-111
66	Combined SPT Log for 4 Bore Holes at Snow River	2-112

Figure		Page
67	Ground Fissures, Bridge, and Bore Hole Locations, Resurrection River and Mineral Creek	2-113
68	Displacements at Bridge Milepost 3.0	2-114
69	Displacements at Railroad Bridge Milepost 3.2	2-115
70	Displacements at Railroad Bridge Milepost 3.3	2-116
71	Contour Map of Resurrection River and Mineral Creek	2-117
72	Penetration Logs for Bore Holes 3, 6, 8	2-118
73	Grain-Size Distribution Range for Soils Sampled at Mineral Creek	2-119
74	Penetration Profile and Analysis, Bore Holes 3 and 6	2-120
75	Penetration Profile and Analysis, Bore Holes 8 and 9	2-121
76	Plot of LSI Values for Damaged Bridges	2-124

CASE HISTORIES OF LATERAL SPREADS CAUSED BY THE 1964 ALASKA EARTHQUAKE

1.0 INTRODUCTION

The March 27, 1964 Alaska earthquake was one of the most powerful earthquakes of this century. The U.S. Coast and Geodetic Survey reported the main shock magnitude as 8.3 to 8.4 on the M_L scale and 9.2 on the M_w scale (Hansen et al., 1966, Kanamori, 1978). The epicenter was located in the Chugach Mountains near the northern end of Prince William Sound about 130 km east-southeast of Anchorage (McCulloch and Bonilla, 1970). Fortuitously, most of the stricken region was sparsely populated, lessening the loss of life and property. Nonetheless, the earthquake's social and economic impact to the residents of Alaska was substantial. One hundred and fourteen people died. Public and private property losses were estimated at $311 million (1964 value) by the Federal Reconstruction and Development Planning Commission (Hansen et al., 1966).

The Alaska earthquake generated widespread crustal warping, propagated long-lasting intense ground shaking and triggered numerous ground failures and landslides in south-central Alaska. Tectonic subsidence, as much as 2 to 2.5 meters in some places, subjected coastlines along the Kenai Peninsula and Kodiak Island to tidal inundation. Three to four minutes of moderate to severe ground shaking affected 130,000 to 195,000 square km surrounding the epicenter (Hansen, et al., 1966, Housner and Jennings, 1973). In downtown Anchorage, landslides demolished many buildings. Additionally, in south Anchorage, 75 homes were destroyed or damaged by the massive Turnagain Heights landslide. Other towns such as Cordova, Homer, Kodiak, Seward, Valdez and Whittier also suffered substantial damage to their ports and coastline facilities from flooding, tsunamis, liquefaction of shoreline deposits and submarine landslides.

Lateral spreads (a type of liquefaction-induced ground failure) were also particularly destructive to highway and railroad bridges within a 130 km radius of the zone of energy release. Ninety-two highway bridges were severely damaged

or destroyed. Another 49 highway bridges received moderate to light damage. Total damage to the highway system was $46 million (1964 value), $25 million was incurred by highway bridges and $21 million by roadways (Kachadoorian, 1968). Approximately 75 railroad bridges were moderately to severely damaged. Estimated cost to repair damaged railroad facilities approached $35 million (1964 value); 25 percent of that total for reconstruction of embankment and tracks and 7 percent to repair railroad bridges and culverts (McCulloch and Bonilla, 1970).

This report focuses on lateral spread damage to railroad and highway bridges on the Knik River, Matanuska River, Ship Creek, Twenty-Mile River, Portage Creek, Placer River, Snow River and Resurrection River (Figure 1). In order to understand and analyze the seismic, geological, topographical and soil conditions contributing to ground displacement and damage we: 1) estimate the duration and amplitude of strong motion at the damaged bridges, 2) describe the type of damage and estimate the amount of horizontal ground displacement occurring at the bridges, 3) discuss the local surficial geological conditions, 4) present topographical maps and channel cross-sections from surveys completed at the damaged bridges and 5) evaluate the liquefaction susceptibility of the foundation soil by analyzing standard penetration and grain-size distribution data.

The collection and interpretation of these data are vital to understanding the relationship between liquefaction-induced ground failure and bridge damage. Also, measurements of horizontal ground displacement combined with measurements of seismic, geological, topographic and soil factors are needed to develop empirical relationships for predicting liquefaction-induced horizontal ground displacement (Bartlett and Youd, 1990). Finally, this report provides insight into the hazards associated with construction and maintenance of man-made structures and facilities on liquefaction-prone soils.

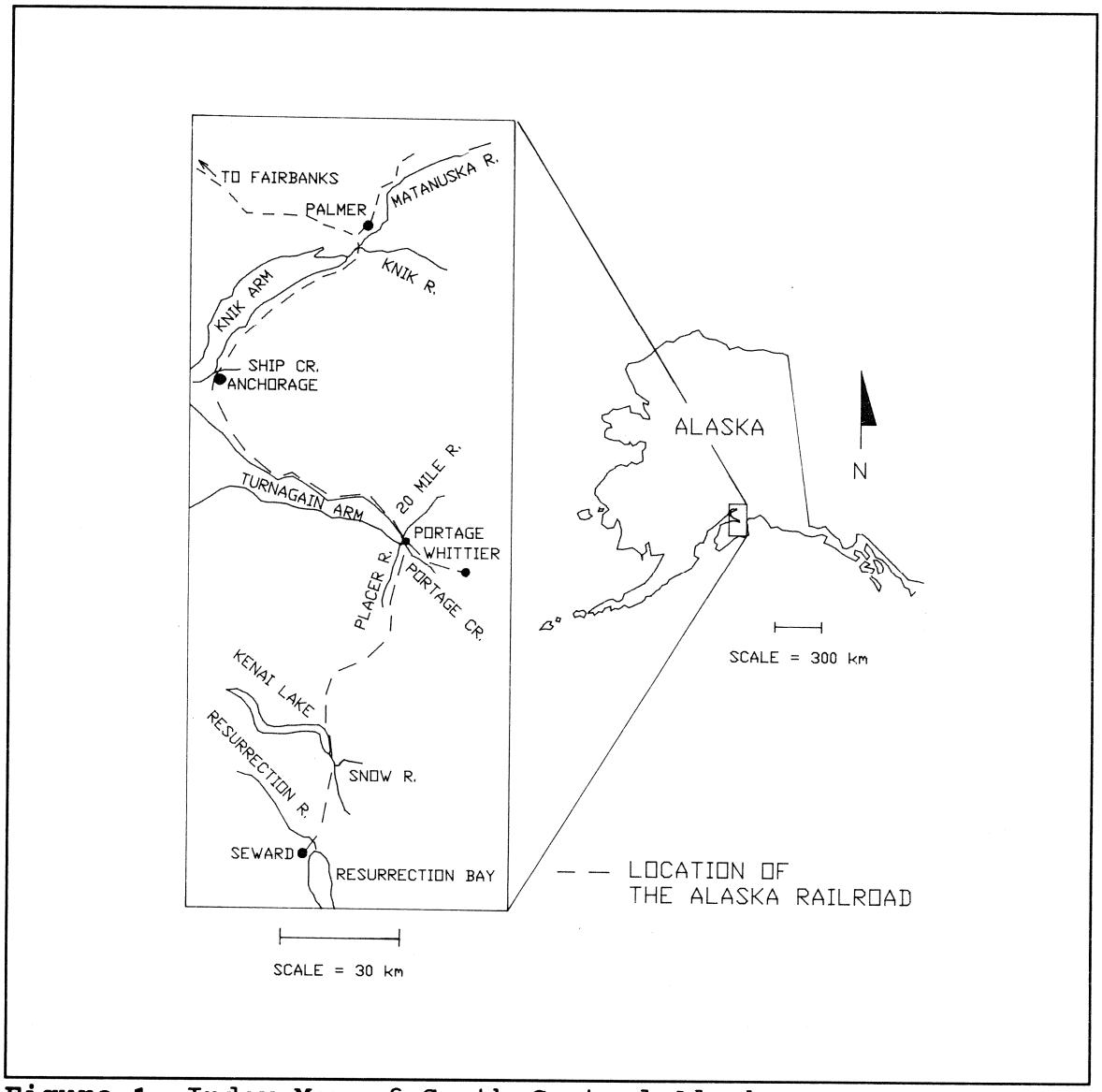

Figure 1 Index Map of South-Central Alaska.

2.0 TECTONIC SETTING, FAULT RUPTURE AND PHYSIOGRAPHIC EFFECTS

As an introduction and background to subsequent sections of this report, the tectonic setting, nature of fault rupture and physiographic effects of the 1964 Alaska earthquake are summarized.

2.1 TECTONIC SETTING

The height and ruggedness of the Alaska's mountains attest to the substantial tectonic activity ongoing along the state's southern margin. Subduction of the

Pacific plate under the North American plate creates the spectacular Alaskan, Chugach, Wrangell and Aleutian Mountain Ranges and produces the long narrow band of volcanic islands comprising the Aleutian Volcanic Arc-Trench system. Movement along faults associated with the subduction zone generates a band of seismicity roughly paralleling the southern coastline and the Aleutian Trench (Figure 2). Approximately 6 percent of the world's large shallow earthquakes are located in this seismic zone. Since 1912, three earthquakes of magnitude 7 or larger have occurred within 100 km of the 1964 epicenter (Hudson and Cloud, 1973). The most recent episode of crustal deformation along the Pacific and North American boundary in Alaska began in late Pliocene time and continues to the present. Comparison of pre- and post-earthquake triangulation surveys indicates that strain was probably developing beneath the Aleutian Arc prior to the 1964 earthquake. Plafker noted that pre-earthquake strain occurred coincidental with a low-angle megathrust fault which dips northwestward beneath the North American Plate near the Aleutian Trench. Rupture of the megathrust fault and of secondary, higher-angle thrust faults located within the overthrust plate generated the earthquake (Plafker, 1965, 1971).

The spatial distribution of aftershocks supports subduction-zone tectonics as the chief mechanism for the earthquake. Most of the numerous aftershocks occurred in a broad band lying northwest of the Aleutian Trench and parallel with the topographical trend of the Chugach and Kenai Mountains, Kodiak Island and the Aleutian Islands (Figure 3).

2.2 FAULT RUPTURE

The moment magnitude, (M_w), of 9.2 assigned to the Alaska earthquake (Kanamori, 1978), qualifies it as the second largest earthquake of this century. For great earthquakes, such as the 1964 Alaska earthquake, M_w, which is defined in terms of energy, is a better measure of earthquake magnitude. Other estimates of the earthquake magnitude, such as surface wave magnitude, (M_s), range from 8.0 to 8.7 M_s with 8.4 M_s being the generally accepted value (Hudson and Cloud, 1973).

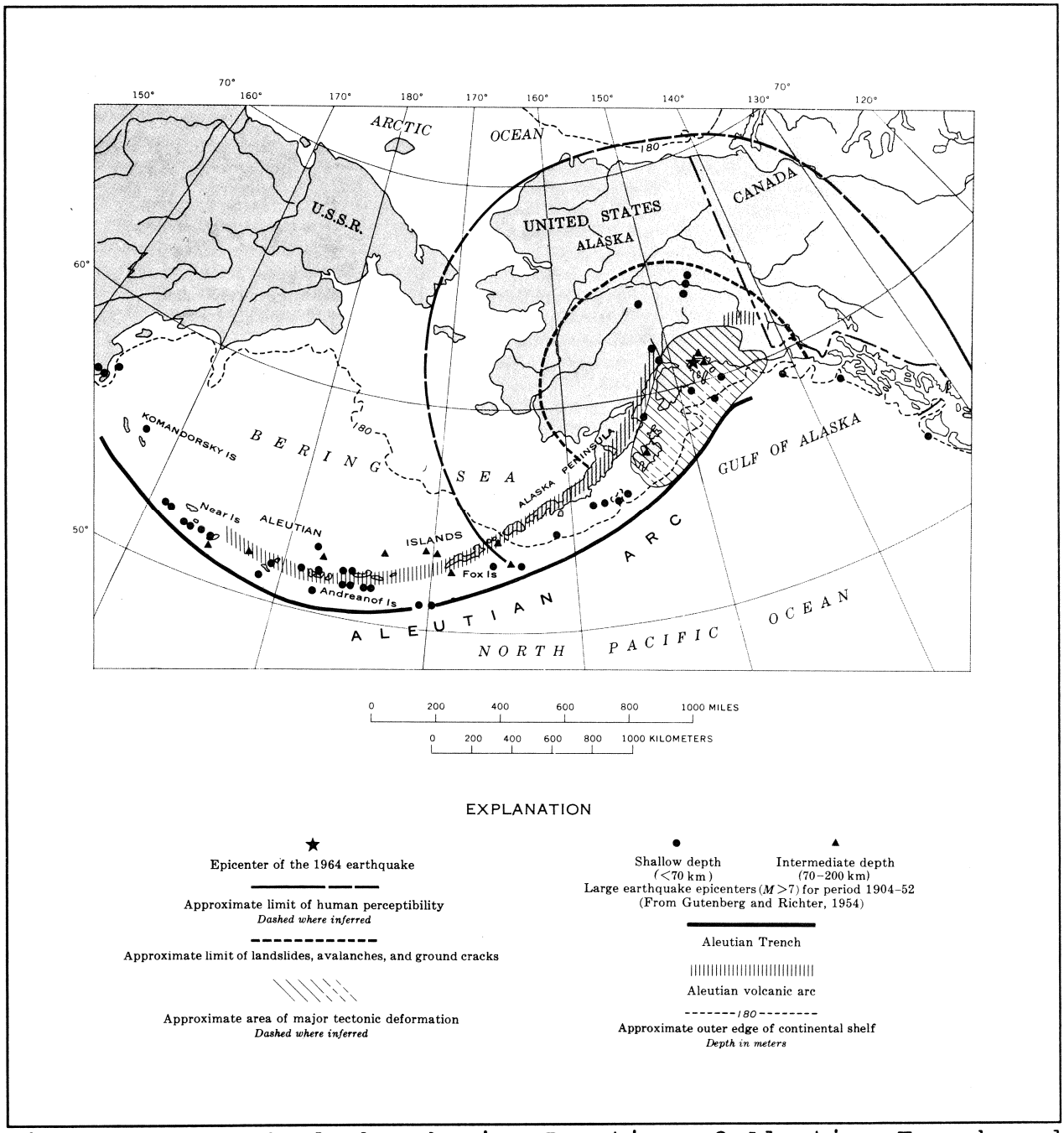

Figure 2 Map of Alaska Showing Location of Aleutian Trench and Previous Major Earthquakes (after Plafker, 1971).

Fault rupture during the earthquake generated a complex series of shocks in the Gulf of Alaska. The epicenter for the initial shock was located in the Chugach Mountains along the Unakwik Inlet to Prince William Sound (61.1 degrees N., 147.7 degrees W., Hansen et al., 1966, McCulloch and Bonilla, 1970, see Figure 3). The

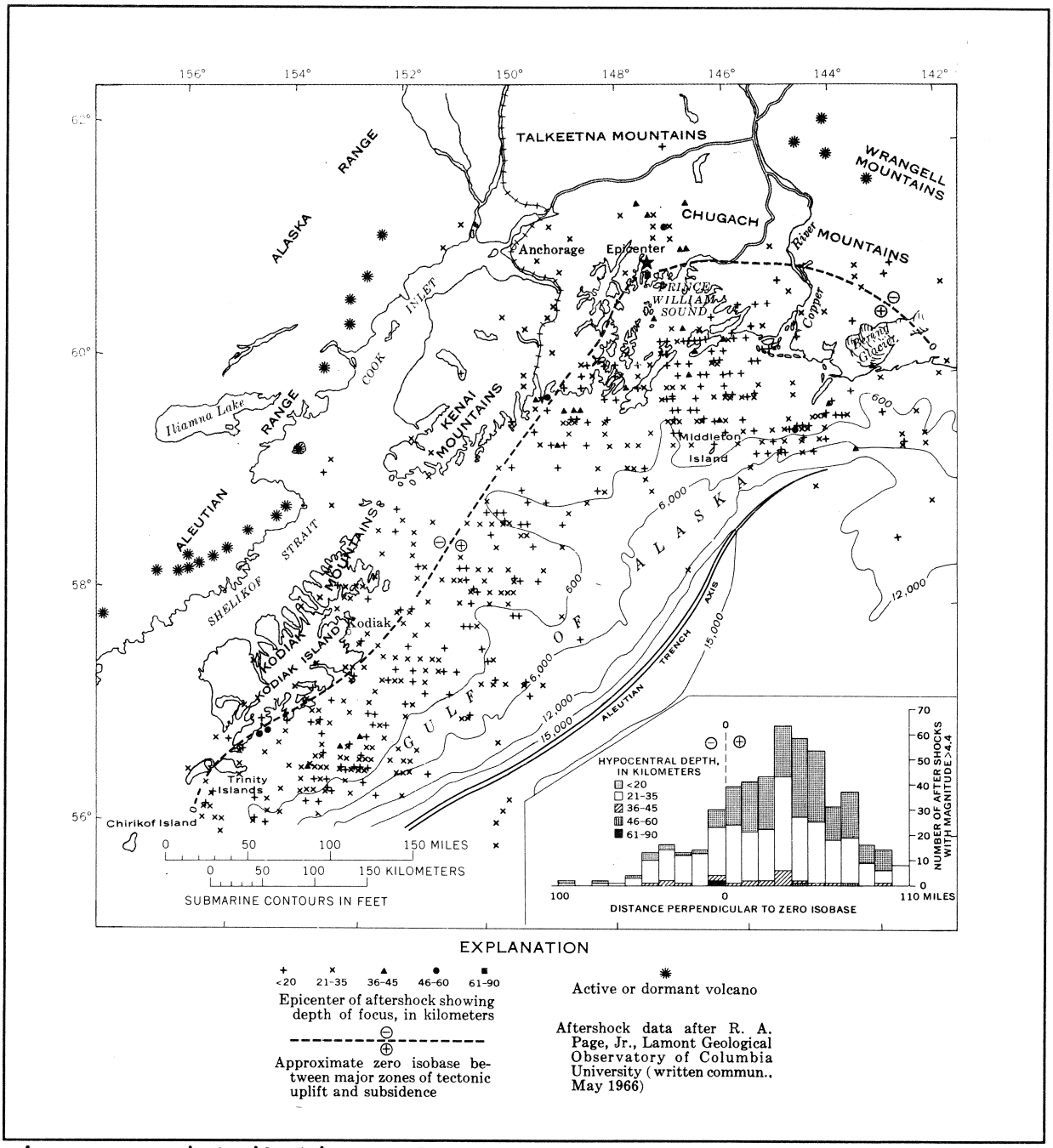

Figure 3 Distribution and Depth of Aftershocks from Mar. 27, to Dec. 31, 1964 (after Plafker, 1971).

depth to the hypocenter is not well defined, but has been estimated to be between 20 and 50 km (Hansen et al., 1966). Wyss and Brune (1967) using P-phases analysis, report three distinct shocks during the main event followed by an additional three or four subsequent shocks shortly after the main event. The

series of main event and subsequent shocks occurred at 9, 19, 28, 29, 44, and 72 seconds after the initial rupture and were located at increasing distances southwest of the epicenter.

Seismologists agree that fault rupture propagated in a southwesterly direction from the epicenter at a rate of approximately 3 km per second for a distance of 600 to 800 km (Toksoz et al., 1965; Furumoto, 1967, Wyss and Brune, 1967). A southwestwardly direction of propagation is also supported by the pattern of power loss in south-central Alaska. Severe ground shaking in Anchorage triggered an overload at the Bernice Lake Power Plant, located about 100 km southwest of Anchorage, approximately 15 to 20 seconds before the plant superintendent felt the first tremors at Bernice Lake (Plafker, 1971).

Observed surface faulting was limited to two faults, both located on the southwestern end of Montague Island (largest island at mouth of Prince William Sound - see Figure 3). The Patton Bay fault (a system of echelon reverse faults, strike N 37 deg. E, dip 50 to 85 deg. NW) had a maximum dip-slip displacement of 8 m (Pflaker, 1971). The fault extended along the ocean floor southwest of Montague Island for at least another 27 km (Malloy, 1964). The shorter Hanning Bay fault (a continuous reverse fault, striking N 47 E and dipping 52 to 75 deg NW) had a maximum of 6 m dip-slip displacement (Pflaker, 1971). Both faults are believed to be subsidiary faults and not the generative fault for the earthquake. No additional displacements were verified along other land faults; however, land faults are suspected at localities where surficial deposits were marked by linear zones of fissures and landslides. Presumably, unobserved submarine faulting of the ocean floor was extensive in the Gulf of Alaska (Pflaker, 1971).

2.3 PHYSIOGRAPHIC EFFECTS

The earthquake produced an impressive amount of warping in the continental crust and oceanic floor. Tectonic deformation paralleled the arc-trench system and was caused by thrusting along the subduction zone. As much as 286,000 square

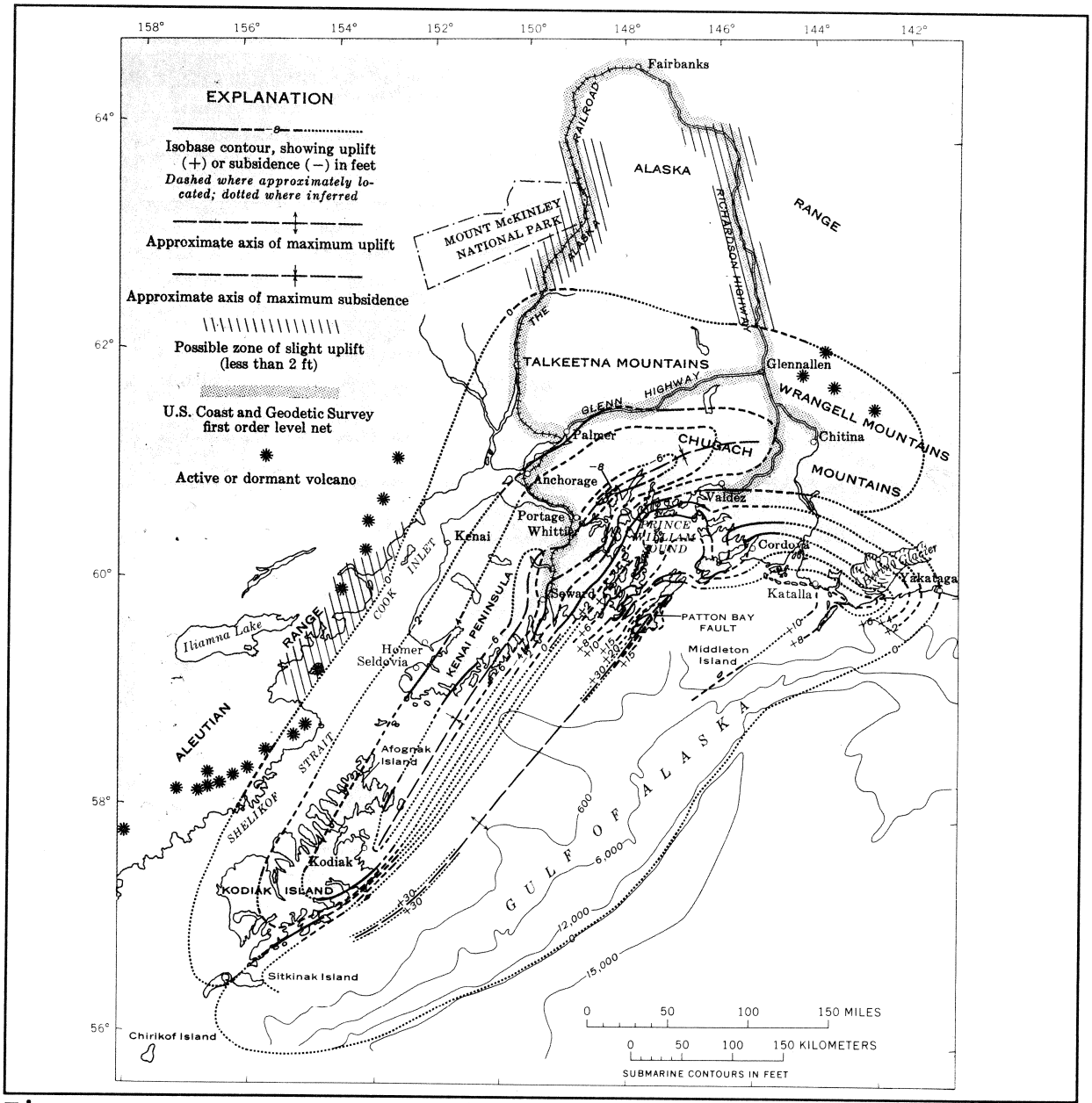

Figure 4 Areas of Tectonic Uplift and Subsidence in South-Central Alaska (after Plafker, 1968).

kilometers of tectonic elevation change occurred along the southern coastal region and in the Gulf of Alaska. The zone of regional uplift was separated from the zone of regional subsidence by a hinge-line of zero crustal elevation change which trends southwestward and eastward from the epicenter (Figure 4). Tectonic uplift south and southeast of the hinge-line was locally as great as 11.5 m at Montague Island. Tectonic subsidence north and northwest of the hinge-line was

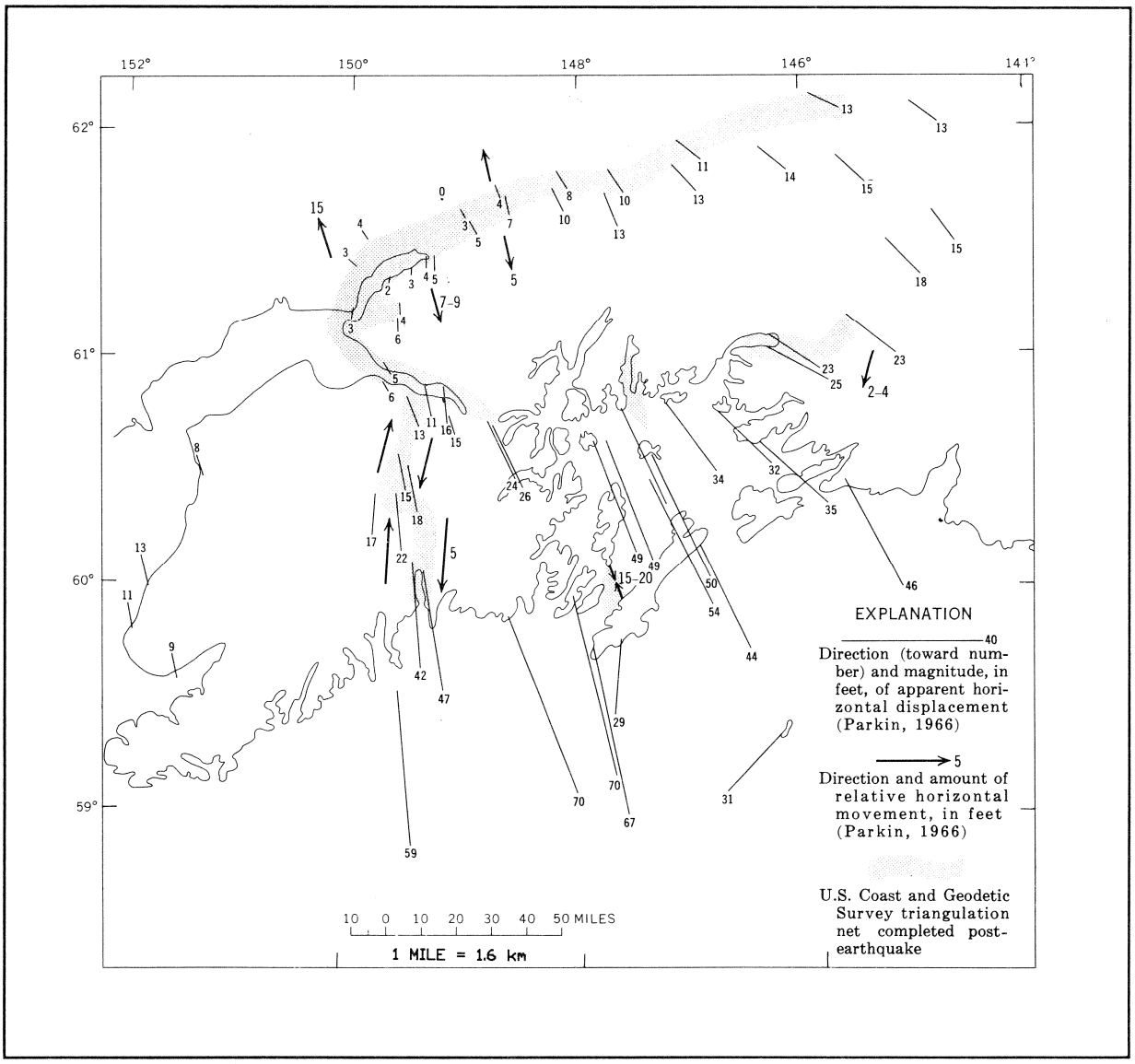

Figure 5 Horizontal Displacement that Accompanied the Earthquake (after McCulloch and Bonilla, 1970).

as great as 2.5 m. Much of the Kenai Peninsula, Turnagain Arm of the Cook Inlet and Kodiak Island subsided from 0.5 to 2 m.

Tectonic subsidence exposed many coastline and port facilities to tidal inundation and erosion from wave action. At some localities, dynamic compaction of loose saturated cohesionless soils added approximately 1 to 2 m to the total subsidence. For example, the town of Portage located at the southern terminus of Turnagain Arm subsided about 2.7 m. Regional tectonic subsidence accounted

for approximately 1.5 m of the total subsidence and soil compaction and settlement contributed the additional 1.2 m (McCulloch and Bonilla, 1970). Long stretches of railroad and highway embankment along the eastern and southern shores of Turnagain Arm were flooded and subsequently badly eroded. Tidal encroachment forced the abandonment of Portage.

Horizontal shifting of the crust was also substantial. The pattern of horizontal displacement is complex and is a combination of fault displacements superimposed upon regional crustal warping. Regionally, much of the Kenai Peninsula and Prince William Sound shifted 2 to 21 m to the south-southeast (Figure 5).

3.0 LIQUEFACTION-INDUCED GROUND FAILURE

3.1 INTRODUCTION

This section describes liquefaction-induced ground failure, lateral spread and the nature of lateral spread damage to several Alaskan railroad and highway bridges. The seismic, geological, topographical and soil factors, which appear to influence horizontal ground displacement and lateral spread damage, are listed and summarized.

3.2 LIQUEFACTION AND TYPES OF LIQUEFACTION-INDUCED GROUND FAILURE

During strong ground shaking, cyclic shear stresses near the surface cause soil particles to shift and fall into voids within the soil fabric as the particles attempt to obtain a denser packing. Below the watertable, any collapse of the soil fabric requires the porewater to bear more of the soil weight. If cyclic loading occurs rapidly, excess pore pressures (i.e., pore pressure above hydrostatic) do not have time to dissipate. If strong shaking is sustained, excess pore pressure continues to rise. As induced pore pressures approach the overburden pressure, the soil looses strength and behaves as a liquid. A liquefied soil has lost much of its ability to resist shear deformation or support weight and in a liquefied condition it behaves similarly to quicksand.

Loose saturated cohesionless soils (e.g., sand, gravel and silt) commonly liquefy when subject to strong shaking. Dense cohesionless soils do not usually liquefy because they dilate during shear and resist further densification and shear displacement. Also, because of their plastic nature, the liquefaction potential of a soil with a clay content equal to or greater than 15 percent is generally reduced (Seed et al., 1983, 1985).

Liquefaction occurring at depth may be manifest at the surface in a variety of ways. **Ground fissures** are common. Liquefied sand is frequently ejected at the surface to form **sand boils.** Discharged groundwater may pool on the surface. **Ground settlement** is also common as the soil reconsolidates. Liquefied soil may exhibit a **loss of bearing strength** causing structures founded at the surface to settle or tip. Buried objects within the liquefied soil may **rise buoyantly** to the surface. If the terrain is flat, the liquefied soil and the overlying non-liquefied surficial soil may oscillate back and forth in response to earthquake waves. **Ground oscillations** may not produce a net permanent horizontal displacement, but they can damage rigid structures that lie on or within the oscillation zone. If the terrain is steep, liquefied soil may flow until arrested by a decrease in ground slope or some other impediment. Ground displacement resulting from this type of failure (i.e., **flow failure**) is catastrophic and very destructive to structures.

3.3 LATERAL SPREAD

Although all varieties of liquefaction-induced ground failure are important, we have limited our research of the 1964 Alaska earthquake to a type of liquefaction-induced ground failure called lateral spread. Lateral spread damage was extensive at several railroad and highway bridges along the Alaska Railroad and the Seward-Anchorage Highway. Lateral spread is probably the most common and pervasive type of liquefaction-induced ground failure. During lateral spread, blocks of intact surficial soil displace along a shearing zone located below the water-table where the soil's shear strength has been reduced to permit downslope

movement by gravitational and inertial forces. Displacement commonly occurs towards a topographical depression such as a stream or river channel. Past studies of lateral spreads have documented permanent ground displacement on slopes as small as 0.3 percent. Lateral spreads are common on slopes up to 5 percent and occasionally have been documented on steeper slopes. Lateral spreads exhibit many morphological features common to other types of mass movement. Extensional cracks and small scarps or grabens often form at the head. Shear zones along the flanks frequently offset objects traversing the lateral spread. Radial cracks and compressional features, such as folds and pressure ridges, commonly form at the toe.

Permanent ground deformation resulting from lateral spread is not as catastrophic as flow failure, but may still be large enough to damage many structures. Typically, horizontal displacements range from a few centimeters to several meters. Rigid structures on or within the extensional zone are typically cracked and torn apart. Structures located near the margins of the lateral spread are sheared and offset by differential movement. Structures at the toe are commonly compressed and buckled.

Lateral spreads during the 1964 Alaska earthquake caused narrowing of many stream and river channels as liquefied soil beneath the channel and a considerable portion of the adjacent floodplain displaced toward the channel. At some sites, extensional fissures parallelling the channel were found as far as 200 to 300 m from the river banks (McCulloch and Bonilla, 1970). The majority of horizontal ground displacement took place in the line of the bridges perpendicular to the channel. Movement of the floodplain and banks toward the channel decreased channel widths by as much as 2 m. At some bridge crossings, piles in the middle of the channel rose relative to those near the bank, indicating that channelward movement was accompanied by a welling up of liquefied material within the channel (McCulloch and Bonilla, 1970).

Compressive forces from channel closure arched, buckled or jack-knifed many railroad bridge decks, leaving the rail bent and unusable. Many simply-supported concrete highway bridge decks collapsed due to differential displacement of support piers. Most bridge abutments were tipped as the base of the abutment was shifted channelward and the top remained fixed to the bridge superstructure. Streamward displacement of railroad bridge abutments and bulkheads commonly crushed wooden deck stringers leaving those members splintered and broken. In some instances, the stringers were driven up and over the bulkheads in response to compressive deformation (McCulloch and Bonilla, 1970).

In addition to channel narrowing, post-earthquake resurveys of displaced bridge abutments and piers revealed that some abutments and piers had a component of downstream displacement. In some instances, displaced piles near the channel center were displaced farther downstream relative than piles near the banks (McCulloch and Bonilla, 1970).

3.4 SEISMIC, GEOLOGICAL, TOPOGRAPHICAL AND SOIL CONTROLS OF LATERAL SPREAD DAMAGE

Youd and Perkins (1978, 1987), Hamada, et al. (1986) and Bartlett and Youd (1990) have discussed several seismic, geological, topographic and soil factors which influence the amount of horizontal ground displacement resulting from lateral spread (Table 1). These factors are introduced in this section. The following section, Section 4, documents many of these factors for 12 damaged bridges in south-central Alaska.

TABLE 1
FACTORS INFLUENCING LIQUEFACTION AND HORIZONTAL GROUND DISPLACEMENT

Seismic Factors

- Earthquake magnitude
- Distance to nearest fault rupture or seismic source
- Maximum horizontal ground acceleration
- Duration of ground motion

Geological and Topographical Factors

- Mode of deposition
- Total thickness of unconsolidated sediment
- Depth to groundwater
- Ground Slope
- Proximity to and height of free face

Soil Factors

- Age of sediment, degree of consolidation and cementation
- Grain size distribution of particles
- Mean grain size of particles (D_{50})
- Silt content (particles < 0.075 mm)
- Clay content (particles < 0.005 mm)

- Density state of granular layers and residual shear strength of liquefied soil
- Thickness, continuity and depth of liquefied zone

3.4.1 SEISMIC FACTORS

Earthquake magnitude is a measure of the amount of seismic energy released by the earthquake. Large magnitude earthquakes produce widespread and large permanent ground displacement, whereas permanent ground displacement is smaller and more limited for moderate sized earthquakes.

For major earthquakes, destructive ground failure occurs near the seismic energy source and diminishes with increasing distance from the fault rupture. In their report of the 1964 Alaska earthquake, McCulloch and Bonilla found that ground fissures and lateral spread damage increased near the zone of maximum strain-energy release. Other investigators have used the nearest distance to fault rupture or the nearest distance to the surface projection of fault rupture to

predict horizontal ground displacement and damage (Youd and Perkins, 1987; Bartlett and Youd, 1990).

Ground motion must have sufficient duration and amplitude to generate excess pore pressure and initiate liquefaction. Increased duration of ground motion results in a greater extent of soil liquefaction and prolongs the time that liquefied soil is subjected to mobilization down slope by gravitational and inertial forces. Duration of strong ground motion increases with earthquake magnitude. Also duration increases slightly with distance from the zone of seismic energy release.

The maximum or peak horizontal ground acceleration, a_{max}, is often used to describe the intensity of ground shaking for many analyses such as the simplified procedure (Seed and Idriss, 1971, Seed et al., 1983, 1985). The value of a_{max} decreases with distance from the zone of energy release. Once the soil has liquefied, the amount of horizontal ground displacement and damage increases with increasing a_{max}.

3.4.2 GEOLOGICAL AND TOPOGRAPHICAL FACTORS

3.4.2.1 MODE OF DEPOSITION AND DEPTH TO GROUNDWATER

McCulloch and Bonilla (1970) noted that surficial geology and depth to the water-table strongly influenced the type and extent of bridge damage during the 1964 Alaska earthquake. In areas where bridges and embankments crossed active floodplain deposits, liquefaction damage to highway and railroad bridges was extensive. They summarized the significant role liquefaction-induced ground failure played in producing damage to bridges and embankments underlain by saturated, uncompacted, cohesionless sediment:

> "... of greatest importance in terms of potential damage in seismically active areas, is a general loss of strength experienced by wet -laid unconsolidated granular sediments (silt to coarse gravel) that allowed embankments to settle and enable sediments to undergo flow like displacements toward topographic depressions, even in flat-lying areas."

Depositional environment controls particle size, sorting, and compaction of sediment. These factors in turn influence soil susceptibility to liquefaction and ground displacement. In Alaska, structures located on bedrock or glacial till overlying bedrock received little to no damage from lateral spread. Lateral spread of alluvial fans and fan deltas was limited to the distal fringes where the water-table was near the surface. Lateral spread damage to structures founded on glacial outwash terraces was negligible in areas where the water-table was deep and severe where the water-table was near the surface. Ground displacement and damage on inactive floodplains was generally slight (McCulloch and Bonilla, 1970).

3.4.2.2 TOTAL THICKNESS OF UNCONSOLIDATED SEDIMENT

Lateral spread damage in Alaska appears to be related to the total thickness of underlying unconsolidated sediment. Damage to railroad and highway bridges was generally slight at sites underlain by less than 15 m of unconsolidated sediment, moderate where sediment thickness was 15 to 30 m and severe at sites underlain by more than 30 m of unconsolidated sediment (McCulloch and Bonilla, 1970).

3.4.2.3 GROUND SLOPE

Once a layer has liquefied, the component of gravity acting parallel to the shear zone becomes a driving force for movement downslope. From studies of the 1964 Niigata and 1983 Nihonkai Chubu earthquakes, Hamada, et al. (1986) found that horizontal ground displacement is a function of ground slope.

3.4.2.4 PROXIMITY TO AND HEIGHT OF FREE FACE

Because of the lack of restraining forces, horizontal ground displacements are generally larger near a free face (e.g., escarpment, bluff, incised stream or river channel). Horizontal ground displacement and damage generated by the 1964 Alaska earthquake increased near river channels and topographical depressions (McCulloch and Bonilla, 1970).

3.4.3 SOIL FACTORS

3.4.3.1 AGE OF SEDIMENT, DEGREE OF CONSOLIDATION AND CEMENTATION

With time, soil consolidates and the soil particles are bonded together by minerals carried in the groundwater. Consolidation and cementation increase the soil's shear strength and its resistance to liquefaction and deformation. McCulloch and Bonilla (1970) observed that ground cracks and damage were less abundant in older inactive floodplain deposits than in active floodplain deposits.

3.4.3.2 GRAIN-SIZE DISTRIBUTION AND MEAN GRAIN-SIZE OF SOIL PARTICLES

Particle size also influences liquefaction susceptibility and displacement. Permeable soils dissipate excess pore pressures more rapidly, thus, preventing or reducing the time soil is liquefied and subject to mobilization. For example, liquefied sandy gravel and fine gravel does not appear to displace as much as clean sand (Bartlett and Youd, 1990).

The presence of a less permeable layer above a liquefied layer also retards the dissipation of pore pressure. If confinement of the susceptible layer is appreciable, pore pressure build up is expedited and liquefaction occurs sooner. Confinement may also lengthen the time that the soil remains liquefied and subjected to displacement.

3.4.3.3 SILT AND CLAY CONTENT

Preliminary regression analyzes of U.S. and Japanese data suggest that silty soils may not displace as much as clean sands (Bartlett and Youd, 1990). Clayey soils, because of their higher plasticity, have more resistance to liquefaction than clean sands (Seed et al., 1983, 1985).

3.4.3.4 DENSITY STATE OF GRANULAR LAYERS AND RESIDUAL SHEAR STRENGTH OF LIQUEFIED SOIL

The amount of ground displacement is a function of the liquefied soil shear strength. A liquefied soil retains some of its resistance to shear deformation.

This strength is termed the steady-state or residual shear strength (Poulos, 1981; Seed et al., 1988, Marcuson et al., 1990). Shear deformation will continue as long as the combined gravitational and inertial driving force exceeds the residual shear strength of the soil.

The Standard Penetration Test, SPT (ASTM D1586-84, 1990), is widely used to approximately estimate the in-situ shear strength, residual shear strength, relative density and other engineering properties of cohesionless soils. Seed (1987) developed empirical correlations for estimating residual strength from the SPT blow count, N. For this report, we include profiles of SPT N values versus depth from soil logs near the damaged bridges, but N is not converted to values of residual shear strength.

3.4.3.5 THICKNESS, CONTINUITY AND DEPTH OF LIQUEFIED ZONE

The nature, degree and distribution of shear strength loss within a liquefied soil profile is not well understood. Conceptually, layers, lenses and other discontinuities in the soil influence the distribution of liquefaction and affect the soil's gross resistance to mobilization. This influence suggests that large horizontal displacements can be expected where thick continuous zones of liquefiable sediments exist. Japanese researchers have found thickness of the liquefied zone to be a significant predictor of horizontal ground displacement (Hamada et al., 1986). Likewise, our preliminary regression analyzes of U.S. and Japanese case histories of lateral spread ground failure demonstrate that thickness of the liquefied zone and depth to the top of the liquefied zone are significant predictors of horizontal ground displacement (Bartlett and Youd, 1990).

3.5 EMPIRICAL TECHNIQUE FOR DETERMINING THICKNESS, CONTINUITY AND DEPTH OF LIQUEFIED ZONE

In post-earthquake investigations of liquefaction sites, the thickness, continuity and depth of the liquefied zone cannot be determined by direct observation. Thus, the simplified procedure for liquefaction analysis is widely

used to analyze which zones in the subsurface profile are susceptible to liquefaction (Seed and Idriss, 1971; Seed et al., 1983, 1985). Zones which are shown to be susceptible to liquefaction by analysis are often assumed to be the same zones that liquefied during an earthquake.

In this report, we use the simplified procedure to identify layers susceptible to liquefaction and infer that these layers may have liquefied during the 1964 Alaska earthquake. By performing the analysis throughout the profile, the simplified procedure allows us to estimate the thickness, continuity and depth of zones which were susceptible to liquefaction. We have written a program in dBase III to perform the liquefaction analysis. The following briefly outlines the simplified procedure and how the computer program uses it to estimate the thickness, continuity, and depth of the zone(s) susceptible to liquefaction.

For a particular SPT value, N, the simplified procedure compares the cyclic stress ratio generated by the earthquake (CSRE) to the cyclic stress ratio required to generate liquefaction in the soil (CSRL). If CSRE exceeds CSRL, the soil is assumed to have liquefied. CSRE is a function of earthquake magnitude, maximum ground acceleration and vertical total and effective in-situ stresses. From laboratory cyclic shear tests, Seed and Idriss (1982, 1983, 1985) defined the average cyclic shear stress developed on a horizontal plane during cyclic loading as τ_h. They showed that the average shear stress induced in the soil by an earthquake is approximated by:

$$\tau_h = 0.65 \ (a_{max} \ / \ g) \ * \ \sigma_o \ * \ r_d \qquad (1)$$

where a_{max} is the maximum ground acceleration, g is the acceleration of gravity and σ_o is the in-situ vertical stress. The stress reduction factor, r_d, is used to decrease τ_h with depth. The earthquake induced shear stress is divided by the

in-situ effective vertical stress, σ_o' to define the cyclic stress ratio induced by the earthquake, CSRE:

$$CSRE = \tau_h / \sigma_o' = 0.65 \ (a_{max} / g) * (\sigma_o / \sigma_o') * r_d \qquad (2)$$

The stress reduction factor, r_d , is a function of depth, z, in m and differs according to the soil type. An average value for r_d is given by (Liao, 1986):

$$r_d = 1 - 0.00765 \ z \quad (\text{for } z \leq 10 \text{ m}) \qquad (3)$$

$$r_d = 1.174 - 0.0276 \ z \ (\text{for } z > 10 \text{ m}). \qquad (4)$$

CSRL is calculated from SPT N and is adjusted for σ_o', the amount of energy delivered by the driving hammer and the fines content of the soil (<0.075 mm). The standard penetration blow count, N, is normalized to an effective stress of 100 kPa using the equation:

$$N_1 = C_N * N \qquad (5)$$

where N_1 is the normalized blow count and C_N is an overburden correction factor. C_N is estimated by:

$$C_N = (\sigma_o')^{1/2}/10 \qquad (6)$$

where σ_o' is in kPa (NRC, 1985). The value of N_1 is then corrected for the measured hammer energy ratio, ER_m, delivered to the drill stem (a hammer energy ratio of 60 percent is the standard):

$$(N_1)_{60} = N/60 * ER_m. \qquad (7)$$

The value of $(N_1)_{60}$ is the final corrected blow count used to calculate CSRL. Finally, CSRL for a given magnitude of earthquake, is determined from $(N_1)_{60}$ using curves developed by Seed et al. (1983, 1985) (Figure 6). There curves are only used for clean sands and must be adjusted for the percentage of fines in the soil (particle size < 0.075 mm). Figure 7 shows how CSRL varies with the fines content of the soil for a magnitude 7.5 earthquake. The liquefaction program

corrects CSRL for the percentage of fines in the soil. Values of CSRL for soils with fines contents between 5 and 35 percent are interpolated from the 5, 15 and 35 percent fines curves shown in Figure 7. Currently, no guidelines exist on how to correct CSRL for soils with fines contents greater than 35 percent. CSRL for soil with a fines content greater than 35 percent is not extrapolated beyond the 35 percent fines CSRL curve (i.e., CSRL for soils with fines content > 35 percent is set equal to CSRL for soils with fines content = 35 percent).

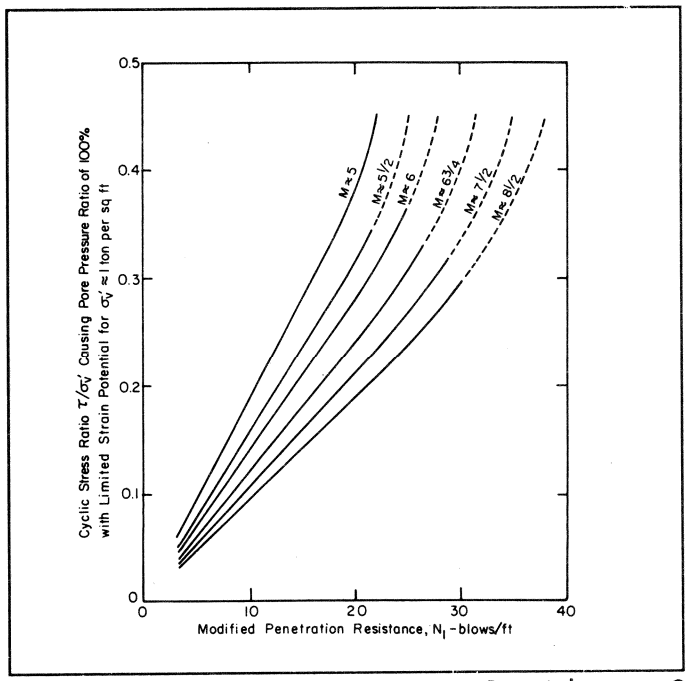

Figure 6 Chart for Evaluation of Liquefaction Potential of Sands for Earthquakes of Different Magnitudes (after Seed and Idriss, 1982).

The liquefaction analysis program interpolates SPT blow count values, N, within the soil profile at 0.1 m increments for liquefaction susceptibility. (SPT values are linearly interpolated between reported values of N). A factor of safety against liquefaction, FS, is calculated for each 0.1 m increment by:

$$FS = CSRL/CSRE. \quad (8)$$

Increments were FS < 1 are marked as liquefiable. The program also converts cone penetration test (CPT) data to SPT N values using a relationship developed by Seed and DeAlba (1986) and extended to larger grain sizes by Andrus and Youd (1989). Once the cone penetration tip resistance has been converted to $(N_1)_{60}$, CSRL is calculated.

Figure 8 is an example of liquefaction analysis for Boreholes K-5A and K-8 located on the Knik River. The left side of the diagram shows the standard penetration blow count, N, versus depth and the soil layers. The right side of the diagram is a plot of CSRE and CSRL versus depth. The solid line is the cyclic stress ratio induced by the earthquake, CSRE, and the dashed line is the cyclic stress ratio required to generate liquefaction, CSRL. Layers susceptible to liquefaction are indicated by a CSRL that is less than CSRE (i.e., when the dashed line falls on the left side of the solid line). The data and analyses represented in these plots provide a means to estimate the thickness, continuity and depth of the liquefied zone for liquefaction sites.

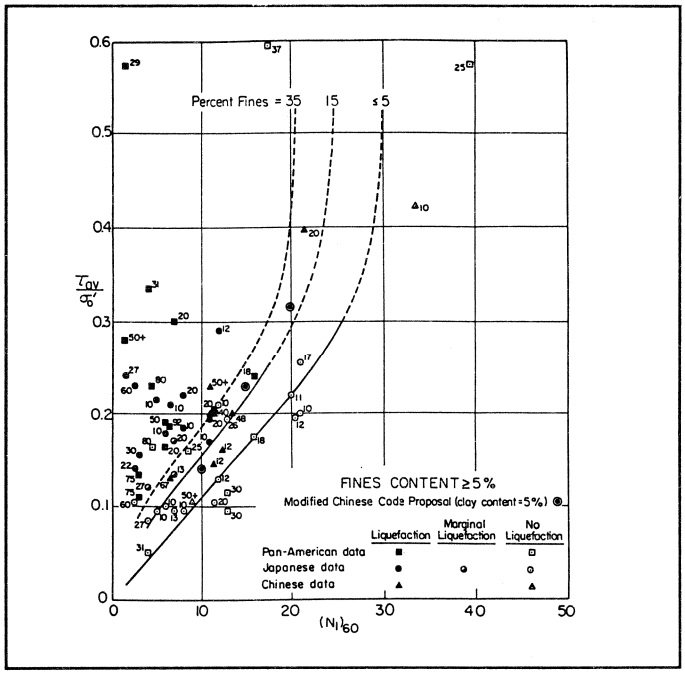

Figure 7 Relationships between CSRL and $(N_1)_{60}$ Values for Silty Sands for Magnitude 7.5 Earthquakes (after Seed et al., 1985).

As seismic input for our analyses of the 1964 Alaska earthquake, we used M_w = 9.2 and the estimated maximum site accelerations given in Table 4. The hammer energy ratio for the Alaska Department of Transportation SPT logs was not measured. For our analysis, we assumed the hammer energy ratio to be 45 percent. (A hammer energy ratio of 45 percent is typical for most donut hammers being used in the 1960s, (Seed et al., 1985)). The hammer energy ratio for the Alaska Division of Geology and Geophysics standard penetration log (Borehole # TA-B-4, Portage Creek) is reported to be 60 to 65 percent.

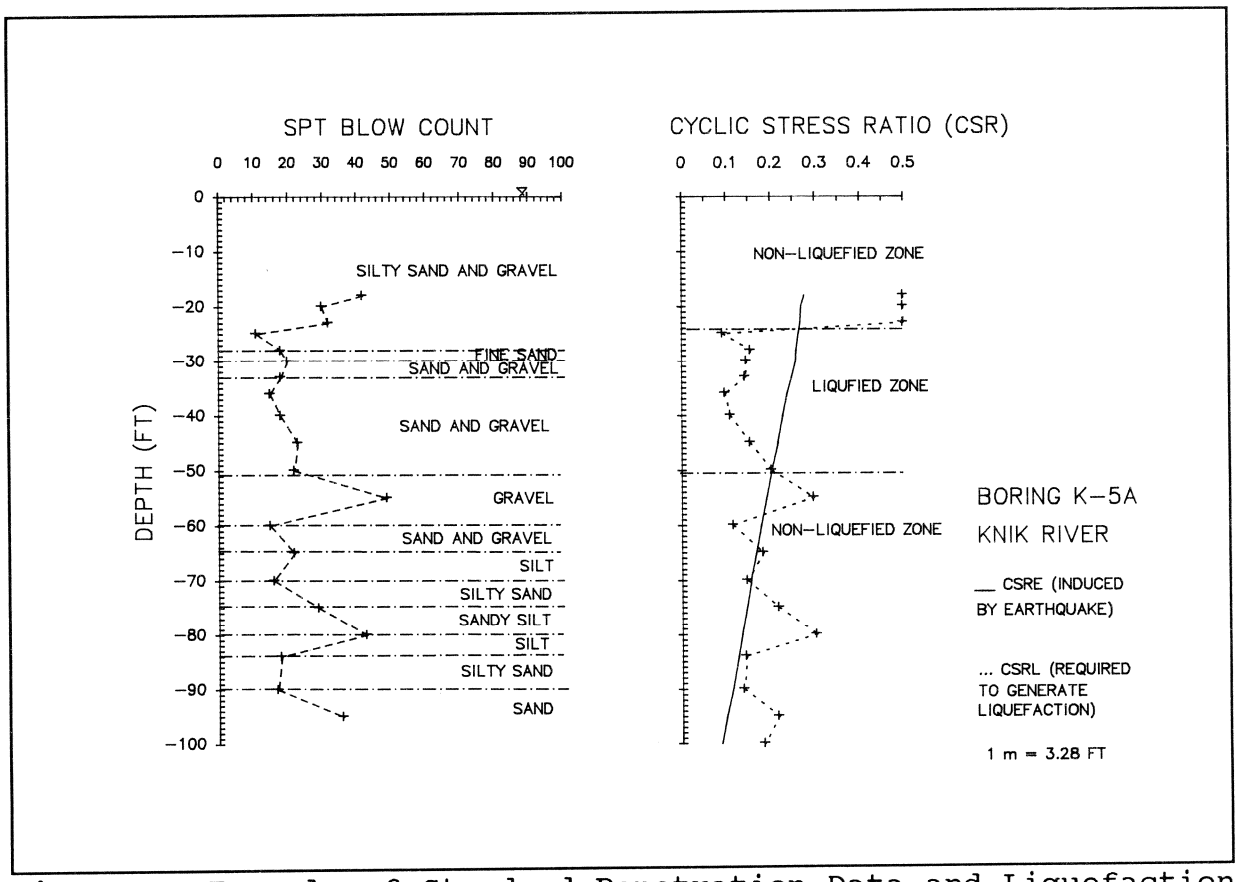

Figure 8 Example of Standard Penetration Data and Liquefaction Analysis for a Bore Hole on the Knik River.

4.0 CASES HISTORIES OF LATERAL SPREADS FROM THE 1964 ALASKA EARTHQUAKE

4.1 INTRODUCTION

Now that we have summarized many of the seismic, geological, topographical and soil factors which appear to influence horizontal ground displacement and damage, we turn to the collection and documentation of these factors for liquefaction sites during the 1964 Alaska earthquake. This section discusses lateral spread damage to several railroad and highway bridges resulting from the 1964 Alaska earthquake. It outlines the criteria to select the damaged bridges included in this study. Seismic factors (i.e., distance to fault rupture, strong ground motion duration and maximum horizontal acceleration) are estimated at the damaged bridges. Geological, topographical and soil conditions are presented and discussed. Soil profiles showing estimated thicknesses of liquefiable layers at the damaged bridges are presented.

4.2 SELECTION OF CASE HISTORIES

Railroad and highway bridges spanning the Knik River, Matanuska River, Ship Creek, Twenty-Mile River, Portage Creek, Placer River, Snow River and the Resurrection River were selected as important case histories of lateral spreads generated by the 1964 Alaska earthquake (Figure 1). Table 2 lists the bridges and their location. Table 3 summarizes the bridge length, type, vertical and horizontal distortion of the bridge caused by ground movement, the net compression of the streambed sediments determined by relative horizontal movement of bents and the maximum horizontal displacement reported for a single pile or pier. For ease of presentation, these bridges have been combined into five groups according to physiographic location: 1) damaged bridges at the **head of the Knik Arm** (i.e., Knik and Matanuska Rivers), 2) damaged bridge at **Ship Creek** in Anchorage, 3) damaged bridges along the **southern end of Turnagain Arm** (i.e., Twenty-Mile River, Portage Creek and Placer River), 4) damaged bridges at **Snow River** and 5) damaged bridges at the **Resurrection River.**

TABLE 2
CASE HISTORIES OF LATERAL SPREAD DAMAGE
TO SELECT RAILROAD AND HIGHWAY BRIDGES
RESULTING FROM THE 1964 ALASKA EARTHQUAKE

Bridge Name	Location
Railroad Bridge Milepost 146.4	Knik River
Highway Bridge Number 1121	Knik River
Railroad Bridge Milepost 147.1	Matanuska River
Railroad Bridge Milepost 147.4	Matanuska River
Railroad Bridge Milepost 147.5	Matanuska River
Railroad Bridge Milepost 148.3	Matanuska River
Railroad Bridge Milepost 114.3	Ship Creek, Anchorage
Railroad Bridge Milepost 64.7	Twenty-Mile River
Railroad Bridge Milepost 63.5	Portage Creek, Portage
Railroad Bridge Milepost 63.0	Portage Creek, Portage
Highway Bridge Number 629	Placer River
Highway Bridge Number 605A	Snow River
Railroad Bridge Milepost 3.0	Resurrection River
Railroad Bridge Milepost 3.2	Resurrection River
Railroad Bridge Milepost 3.3	Resurrection River

These bridges were selected as case histories on the basis of: 1) liquefaction was reported at the bridge, 2) documentation of bridge damage is adequate to estimate horizontal ground displacement, and 3) availability of subsurface soil investigations and topographical surveys.

4.2.1 REPORTING OF LIQUEFACTION AND LATERAL SPREAD

Several investigators were careful to note evidences of liquefaction near the damaged bridges. For example, reports of sand boils, sand ejecta, and fissures were common. For all case history bridges, there is little doubt that liquefaction was responsible for most bridge and embankment damage.

4.2.2 HORIZONTAL GROUND DISPLACEMENT

The measurement and documentation of horizontal ground displacement in conjunction with a good description of bridge damage are vital to understanding and analyzing the relationship between horizontal displacement and structural damage. In their report on damage to the Alaska Railroad, McCulloch and Bonilla measured and recorded the amount of channel narrowing, bridge deck compression and pile and pier displacement for many damaged railroad bridges. Their excellent observations and measurements are the basis for many of our estimates of horizontal ground displacement at the railroad bridges. Unfortunately, in most cases, investigators of damage to the highway failed to measure and document the horizontal ground displacement incurred by damaged highway bridges. Because horizontal ground displacements were not documented for the majority of damaged highway bridges, our discussion is focused primarily on damaged railroad bridges.

An important question arises about the accuracy of using displacements of bridge substructural components to estimate horizontal ground displacements. How well do measurements of displaced abutments, piles and piers represent the actual ground displacements occurring at that locality? Does soil-structure interaction significantly impede movement of the ground or substructural components as liquefied soils are mobilized beneath a bridge?

Table 3 Damage to Select Bridges in South Central Alaska (after McCulloch and Bonilla, 1970).

Bridge Milepost or Number	Length (m)	Distance from fault (km)	Type of Construction	Vertical Distoration
MP 146.4	261	100	Ten 24.4-m steel through griders and four 4.3-m open wood trestle spans on north approach	None reported
No. 1121	Not Completed	100	Highway bridge under construction at time of earthquake; 4 concrete piers in place.	None reported
MP 147.1	128	100	Three 37.5-m steel through trusses with one 7.8-m steel beam span on each approach	None reported
MP 147.4	53	100	One 37.5-m steel through truss with one 7.8-m steel beam span on each approach.	None reported
MP 147.5	203	100	Steel griders supported by concrete piers.	None reported
MP 148.3	122	100	Steel griders with five 24.4-m spans supported by concrete piers.	None reported
MP 114.3	59	119	One 37.5-m through steel truss with one 10.7-m steel beam span on each approach.	None reported
MP 64.7	128	60	Seven span 128-m long steel-truss structure supported by concrete piers.	Northern abutment settled 0.27 m relative to U.S.G.S. bench mark.
MP 63.5	46	60	Open wood trestle; ten 4.6-m spans.	North half of bridge arched up 0.3 m at bent 7; south half of bridge ached down 0.3 m at bent 3.
MP 63.0	59	60	Open wood trestle with planked walkway outside rails; thirteen 4.6-m spans.	0.5 m.
No. 629	137	60	137-m reinforced concrete bridge supported by timber piles.	West approach subsided 0.2 m; East approach subsided 0.6 m.

Table 3 (cont.) Damage to Select Bridges in South Central Alaska (after McCulloch and Bonilla, 1970).

Bridge Milepost or Number	Length (m)	Distance from fault (km)	Type of Construction	Vertical Distoration
MP 3.0	57	31	Two 24.4-m through steel grider spans with one 4.1-m open wood trestle on each end.	None reported.
MP 3.2	41	31	Open wood trestle; nine 4.6-m spans.	0.08 m arch.
MP 3.3	41.5	31	One 24.4-m through steel grider span with two 4.3-m open wood trestle on each end.	None reported.

Table 3 (cont.) Damage to Select Bridges in South Central Alaska (after McCulloch and Bonilla, 1970).

Bridge Milepost or Number	Horizontal Distortion	Net Compression of Streambed Sediments Determined by Relative Horizontal Movement of Bents	Maximum Displacement of a Single Pile, Pier or Bent
MP 146.4	Net compression of 219 mm measured from abutment to abutment.	Not reported.	Pier # 10 on north end of bridge moved 232 mm toward the channel.
No. 1121	Bridge not completed at the time of the earthquake.	Not reported.	4 piers in-place moved a maximum of 0.6 meters toward channel.
MP 147.1	Not reported.	Not reported.	Third pier displaced about a foot toward channel center.
MP 147.4	Not reported.	Not reported.	North pier shifted approximately 254 mm toward channel.
MP 147.5	Not reported.	Not reported.	Southern-most pier shifted 219 mm toward channel.
MP 148.3	Seventy foot span sheared anchor bolts and jammed.	Not reported.	Northern-most pier shifted 0.24 m toward the channel.
MP 114.3	330 mm of compression measured from abutment to abutment.	Distance between end piers decreased 381 mm.	Both end piers moved approximately 191 mm toward channel.
MP 64.7	1.57 m of compression measured from abutment to abutment.	Not reported.	2nd Pier from north displaced 0.46 m toward channel.
MP 63.5	North approach offset 3 m west relative to south approach.	Not reported.	2nd pile from north end of bridge moved 1.85 m toward channel.
MP 63.0	Sharp bend of 2.4 m maximum displacement in 13.7 m. North approach approximately 0.36 m west of south approach.	2.1 m.	3rd pile from south moved 1.9 m toward the channel.
No. 629	Collapsed.	Approximately 0.9 m of convergence.	Not reported.

Table 3 (cont.) Damage to Select Bridges in South Central Alaska (after McCulloch and Bonilla, 1970).

Bridge Milpost or Number	Horizontal Distortion	Net compression of Streambed Sediments Determined by Relative Horizontal Movements of Bents	Maximum Displacement of Single Pile, Pier or Bent
MP 3.0	Central pier 203 mm west and outer piers 51 mm west of approaches.	0.34 m measured at deck level.	Both approaches moved 0.3 m downstream.
MP 3.2	Middle of bridge 250 mm west of approaches.	241 mm.	Both abutments moved 254 mm downstream.
MP 3.3	Middle span 0.76 m west of south bulkhead and 0.15 m west of north bulkhead.	Not reported.	Approach shifted 0.76 m downstream.

Because pile, pier and abutment connections to the bridge superstructure appeared to have been easily broken at most bridges, McCulloch and Bonilla concluded that the displacement of the piles, piers and abutments closely reflected the movement of the foundation material. Also, they noted that most displaced piles and piers showed little rotation and appear to have been carried passively by the mobilized soil.

4.2.3 SUBSURFACE SOIL INVESTIGATIONS AND TOPOGRAPHICAL SURVEYS

To investigate subsurface soil conditions at the damaged bridges, we acquired soil logs from the Alaska Department of Transportation containing SPT N values, grain-size data and soil classifications. We also include standard penetration and cone penetration logs collected by the Alaska Division of Geology and Geophysics from liquefiable sites near Portage.

Most existing topographical surveys in Alaska were not at an adequate scale to define ground slope, channel depth and downstream gradient near most damaged bridges. During the summer of 1989, we visited the bridge sites and cross-sectioned the channels and surveyed the surrounding topography. To supplement our survey data, we obtained bridge construction cross-sections from the Alaska Railroad and the Alaska Department of Transportation.

4.3 SEISMIC FACTORS AT CASE HISTORY BRIDGES IN SOUTH-CENTRAL ALASKA

4.3.1 DISTANCE TO NEAREST FAULT RUPTURE OR SEISMIC SOURCE

The distance to nearest fault rupture or distance to the zone of major energy release is commonly used as an independent variable in empirical equations that predict strong ground motion. In Section 4.3.3, we estimate the maximum horizontal ground acceleration at the damage bridge sites. However, before doing so, we must first estimate the distance from the damaged bridges to the nearest fault rupture.

Because minimal surface faulting was noted following the 1964 Alaska earthquake, it is difficult to precisely define the distance from the damaged bridges to the nearest fault rupture. In Figure 4, crustal subsidence is separated from crustal uplift by a line of zero crustal change (zero contour line, Figure 4). This hinge line approximately divides upthrown and downthrown crustal blocks activated by the earthquake and most likely demarcates the limit of thrust faulting that occurred at depth. We have used the contour of zero elevation change in Figure 4 to represent our best estimate of the surface projection of zone of seismic energy release.

4.3.2 DURATION OF GROUND MOTION

The 1964 Alaska earthquake produced a long duration of ground shaking throughout south-central Alaska. Unfortunately, there were no strong motion recording devices in Alaska at the time of the earthquake. We use personal observations and timings of vibrations from mechanical automatic recording devices to estimate the duration of perceptible ground motion. We also use empirical relationships based on earthquake magnitude and epicentral distance to estimate the duration of strong ground motion.

Many observers report that the earthquake began with a rolling motion which lasted for about a half a minute to a minute. The motion then became notably stronger for another 3 to 4 minutes (Plafker, 1971). Housner and Jennings, 1973, produced a pseudo-accelerogram for the ground motion at Anchorage using a tape recorded description of the shaking. By listening to an observer's tape-recorded description of the shaking and background noise from moving furniture and other items, Housner and Jennings estimate that Anchorage experienced about 1 minute of strong ground motion (>0.05g), followed by another 3 minutes of lesser, but perceptible motion. They further note that the strongest shaking increased to a maximum at 20 seconds elapsed time and then decreased. Starting at 36 seconds, a second phase of strong shaking reached a maximum at 53 seconds and then decreased. A third phase of shaking, less intense than the previous 2 began at

66 seconds and reached a maximum at 75 seconds and continued to 120 seconds. After 120 seconds, shaking was still perceptible and continued to 220 seconds. McCulloch and Bonilla (1970) give the following description of ground motions felt by a worker at the Eklutna Hydroelectric Power Plant (located on bedrock, a few kilometers east of the confluence of the Knik and Matanuska Rivers, see Figure 1). The worker reported the earthquake started with 10 to 15 seconds of rolling motion, then the motion lessened in intensity, followed by violent motions which continued approximately 2 minutes. At Whittier, (Figure 1), trace vibrations from an outside air temperature recording device founded on bedrock showed oscillating motions for nearly four minutes. At the southern end of Turnagain Arm at Portage, observers felt perceptible ground motion for as long as 15 minutes (Kachadoorian, 1966). Portage is underlain by several hundred meters of fine grained sediment (McCulloch and Bonilla, 1970). At Kenai Lake, which is underlain by at least 60 m of unconsolidated sediment, witnesses reported that large trees swayed back and forth as if blown by a strong wind for approximately 8 minutes. Observers at Seward timed the perceptible ground motion for 3 to 4 minutes (McCulloch and Bonilla, 1970). Other observers on bedrock sites on the Kenai Peninsula and Kodiak Island timed the shaking for 2 1/2 to 5 minutes (Plafker, 1971).

From these reports, we surmise that perceptible ground motion in south-central Alaska lasted a minimum of 2 1/2 minutes. At localities underlain by thick deposits of unconsolidated sediment, perceptible ground motion was considerably longer than 2 1/2 minutes. At these localities, perceptible ground motion lasted from 3 to 15 minutes.

Estimates of duration of perceptible ground motion are not as useful for engineering purposes as measurements of duration of strong ground motion. Perceptible ground motion may continue for a considerable time after strong ground motion has ceased. In general terms, strong ground motion is shaking of sufficient severity to damage structures. At Anchorage, strong ground motion

appears to have lasted a minimum of 1 minute and a maximum of 2 minutes. At the Eklutna Power Plant near the Knik River "violent" ground motion lasted a maximum of 2 minutes. Thus, based on these reports, strong ground motion in south-central Alaska appears to have lasted between 1 to 2 minutes.

Empirical relationships based on earthquake magnitude and epicentral distance or distance to the fault rupture can be used to estimate the duration of strong ground motion for non-instrumented sites. Krinitzsky and Chang (1988) present an equation for estimating strong ground motion duration, D, for subduction zone earthquakes with a focal depth equal to or greater than 20 km:

$$\log D(\text{sec}) = -2.36 + 0.43M + 0.30\log(r/10) \qquad (9)$$

where M is the earthquake magnitude and r is the epicentral distance in kilometers. Krinitzsky and Chang combined data from both hard and soft soil sites to develop Equation 9. (Note: In general, duration of strong ground is longer on soft soil sites than on hard soil sites due to amplification by soft sediments (Idriss, 1990).

Table 4 lists the duration of strong motion estimated by Equation 9 for damaged bridge sites in south-central Alaska. For this analysis, we used M_w equal to 9.2 and an epicentral distance scaled from Figure 3.

TABLE 4
ESTIMATED STRONG GROUND MOTION DURATION
LIQUEFACTION SITES IN SOUTH-CENTRAL ALASKA

Bridge Location	Epicentral Distance (miles, km)		Duration (s)
Knik & Matanuska Rivers	59	95	77
Ship Creek in Anchorage	84	135	86
Twenty-Mile River near Portage	52	84	75
Portage Creek near Portage	52	84	75
Placer River near Portage	52	84	75
Snow River near Kenai Lake	86	138	87
Resurrection River near Seward	91	147	88

The estimates of strong ground motion from Equation 9 meet the constraints of felt observations (i.e., all values are between 1 and 2 minutes). Thus, the values predicted by Equation 9 appear to be reasonable estimates of strong ground motion duration at the liquefaction sites.

4.3.3 MAXIMUM HORIZONTAL GROUND ACCELERATION

The maximum horizontal ground acceleration at the damaged bridges must also be estimated. For the 1964 Alaska earthquake, equations that use distance from the nearest fault rupture are preferable to methods that use epicentral distance because of the extreme length of fault rupture. Joyner and Boore (1988) give the following relationship for peak horizontal ground acceleration on rock or stiff soil sites:

$$\log y = a+b(M-6)+c(M-6)^2+d(\log r)+kr+s \qquad (10)$$

where y = is the larger of the two horizontal components of peak horizontal acceleration expressed as a fraction of gravity and M is the moment magnitude. The remaining parameters are empirically determined coefficients: a = 0.49, b = 0.23, c = 0.0, h = 8.0, d = -1.0, k = -0.0027 and s = 0.0 and $r = (r_0^2 + h^2)^{1/2}$,

where r_o is the shortest horizontal distance in kilometers from the recording site to the vertical projection of the earthquake fault rupture.

Equation 10 predicts ground acceleration on both rock and soil sites, but does not account for amplification of ground motion by soft sediment. We believe that strong ground motion amplification was likely at all of the bridge sites because of the presence of thick uncompacted fluvial, deltaic and estuarine deposits under the bridges. For example, damaged bridge sites at the Knik and Matanuska Rivers, Twenty-Mile River, Portage Creek, Placer River and Snow River are underlain by a considerable thickness of dense silty estuarine or tidal deposits capped by 6 to 30 meters of less dense fluvial deposits.

Idriss (1990) used ground motion data from soft soil sites in Mexico City (1985 earthquake) and the 1989 Loma Prieta earthquake as well as dynamic analyses to develop the empirical curve plotted in Figure 9. Figure 9 indicates that bedrock accelerations beneath soft soil sites are amplified by the soft sediment below 0.4 g and attenuated above 0.4 g. We have used this curve to estimate the amplification or attenuation of ground motion (relative to bedrock peak acceleration) at soft soil sites.

We used the curve in Figure 9 to adjust maximum accelerations calculated from Equation 10 for amplification or attenuation due to soft sediment conditions. Table 5 shows the maximum horizontal acceleration on rock or stiff soil calculated from Equation 10 and the maximum ground acceleration adjusted for soft soil amplification or attenuation.

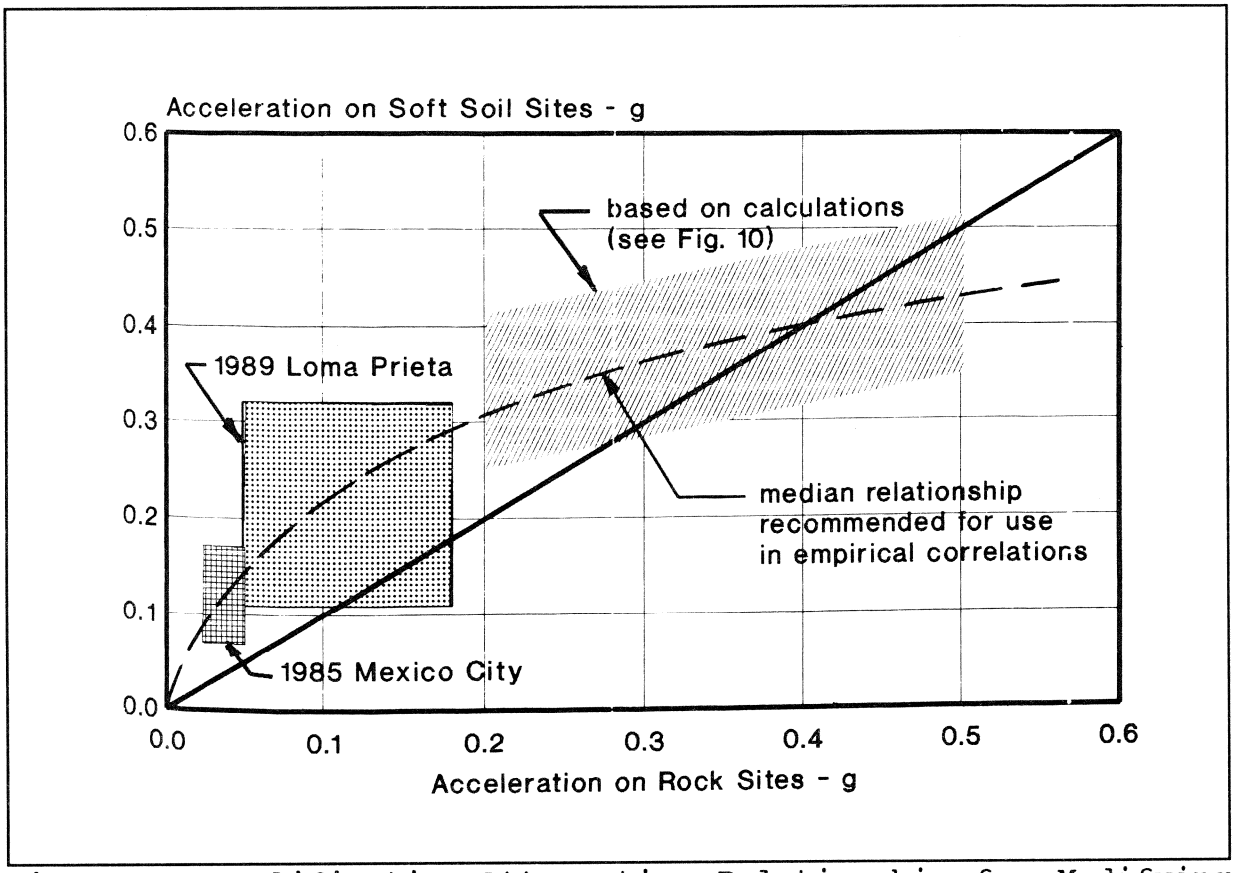

Figure 9 Amplification-Attenuation Relationship for Modifying Bedrock Acceleration at Soft Soil Sites (after Idriss, 1990).

TABLE 5
ESTIMATED MAXIMUM ACCELERATIONS AT SELECTED LIQUEFIED SITES IN SOUTHERN ALASKA

Bridge location	Distance to fault rupture r_0(km)	a_{max}* rock	a_{max}* soft soil
Matanuska and Knik Rivers	100	0.09	0.21
Ship Creek and Anchorage	119	0.07	0.18
Twenty-Mile River, Portage Creek and Placer River	60	0.19	0.31
Kenai Lake and Snow River	35	0.37	0.39
Resurrection River and Seward	31	0.44	0.41

* expressed as fraction of g.

4.4 BRIDGES AT THE HEAD OF THE KNIK ARM

4.4.1 INTRODUCTION

Approximately 48 km northeast of Anchorage and a few km east of the northern end of the Knik Arm, the Alaska Railroad and Glenn Highway bend northward across the Knik and Matanuska Rivers (Figure 1). The westward flowing Knik River leaves the Chugach Mountains and joins the southwesterly flowing Matanuska River to form a broad floodplain in the lower Matanuska Valley. At the railroad and highway crossing, the two rivers are separated by a kilometer of lowland with little topographical relief (Figure 10). Utermohle reports that the Matanuska Valley has been heavily glaciated and its lower reaches are predominately underlain by glacial drift. Fluvial and tidal processes continue to rework the drift to form a thick sequence of fluvial, deltaic and estuarine deposits (Utermohle, 1963). These rivers meander back and forth across the lowland dissecting glacial outwash deposits to form braided channels separated by flat-top glacial outwash deposits which are 2.5 to 3.6 m above the water-level in the channel (McCulloch and Bonilla, 1970).

Soil logs from foundation investigations for the adjacent Glenn Highway, show that the glacial outwash is 15 to 25 m thick and consists of gray sand and gravel with some thin beds of sand and silt (McCulloch and Bonilla, 1970, Utermohle, 1963). Recent fluvial sediment, predominately sand and gravel, is interbedded with the outwash gravel. Trainer (1953) reports that the fluvial gravel is generally finer than the outwash gravel. Sediments below the outwash deposits are 0.3 to 1 m beds of fine sand and silt.

Lateral spreads and ground fissures along the banks of the Knik and Matanuska Rivers caused slight to moderate damage to 5 railroad bridges (Figure 10). These bridges are located approximately 100 km from the zone of energy release and mark the northern extent of significant damage to the Alaska Railroad. Fissures from channelward movement were widespread and especially large in point bar, channel bar and channel deposits on the active flood plain. McCulloch and

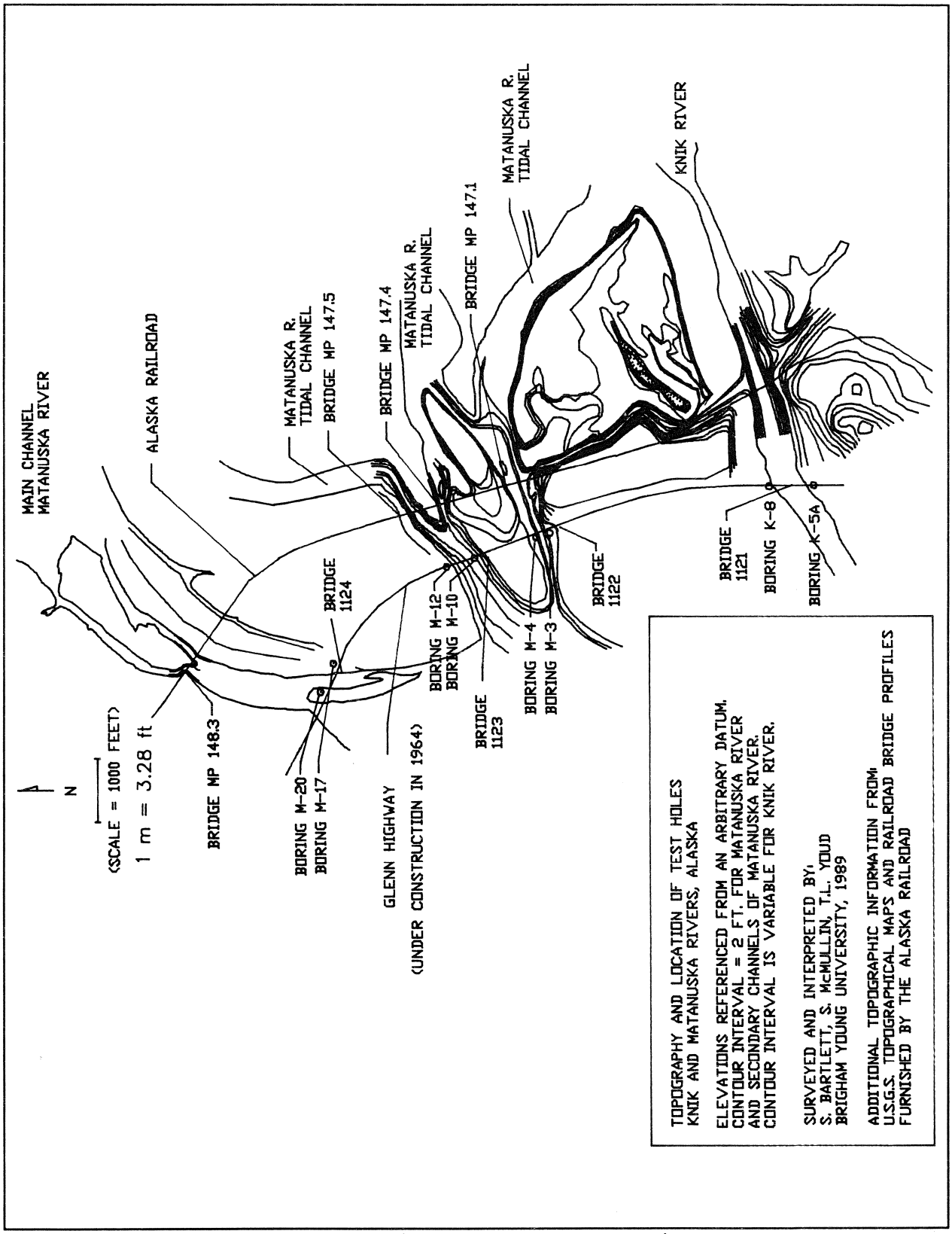

Figure 10 Topography of Knik and Matanuska River, Alaska.

Bonilla (1970) report that ground fissures were smaller and less abundant in glacial outwash deposits between the river channels. The decrease of fissures in outwash sediments may have been controlled in part by a deeper watertable. Also, the decrease of fissures in these deposits may have been partly due to their greater age and better compaction and cementation.

4.4.2 RAILROAD BRIDGE AT MP 146.4 AND GLENN HIGHWAY BRIDGE NO. 1121, KNIK RIVER

4.4.2.1 GROUND FAILURE DISPLACEMENT AND DAMAGE

The railroad bridge, at Milepost 146.4, crosses the main channel of the Knik River approximately 500 m east of Glenn Highway Bridge No. 1121 (Figure 10). This bridge is 261 m long and consists ten steel girder spans supported on 10 concrete piers (Figure 11). Damage to the bridge was primarily due to channelward movement of liquefied soils on the north side of the river. Measurement of relative pier displacements indicate that pier #10 on the north end of the bridge moved 0.23 m toward the channel (McCulloch and Bonilla, 1970, see displacement arrows drawn on Figure 11). Net compression of the bridge deck, measured from abutment to abutment, was 0.22 m. No relative displacement was measured between the southern most pier and the southern abutment founded on bedrock (McCulloch and Bonilla, 1970).

Ground fissures in the vicinity of the bridge were restricted to channel deposits along the north bank and approach fill. Approximately 100 m of embankment just north of the bridge was scarred by fissures and shifted an unknown amount toward a north-south trending secondary channel which parallels the embankment (McCulloch and Bonilla, 1970).

Four highway bridges on the adjacent Glenn Highway were in the preliminary stages of construction during 1964 (Figure 10). A temporary access bridge spanned the Knik River and a pilot road for the new highway alignment had been bulldozed between the Knik and Matanuska Rivers. An airphoto and ground crack map of the Knik River floodplain shows fissures on both sides of the Knik River at the

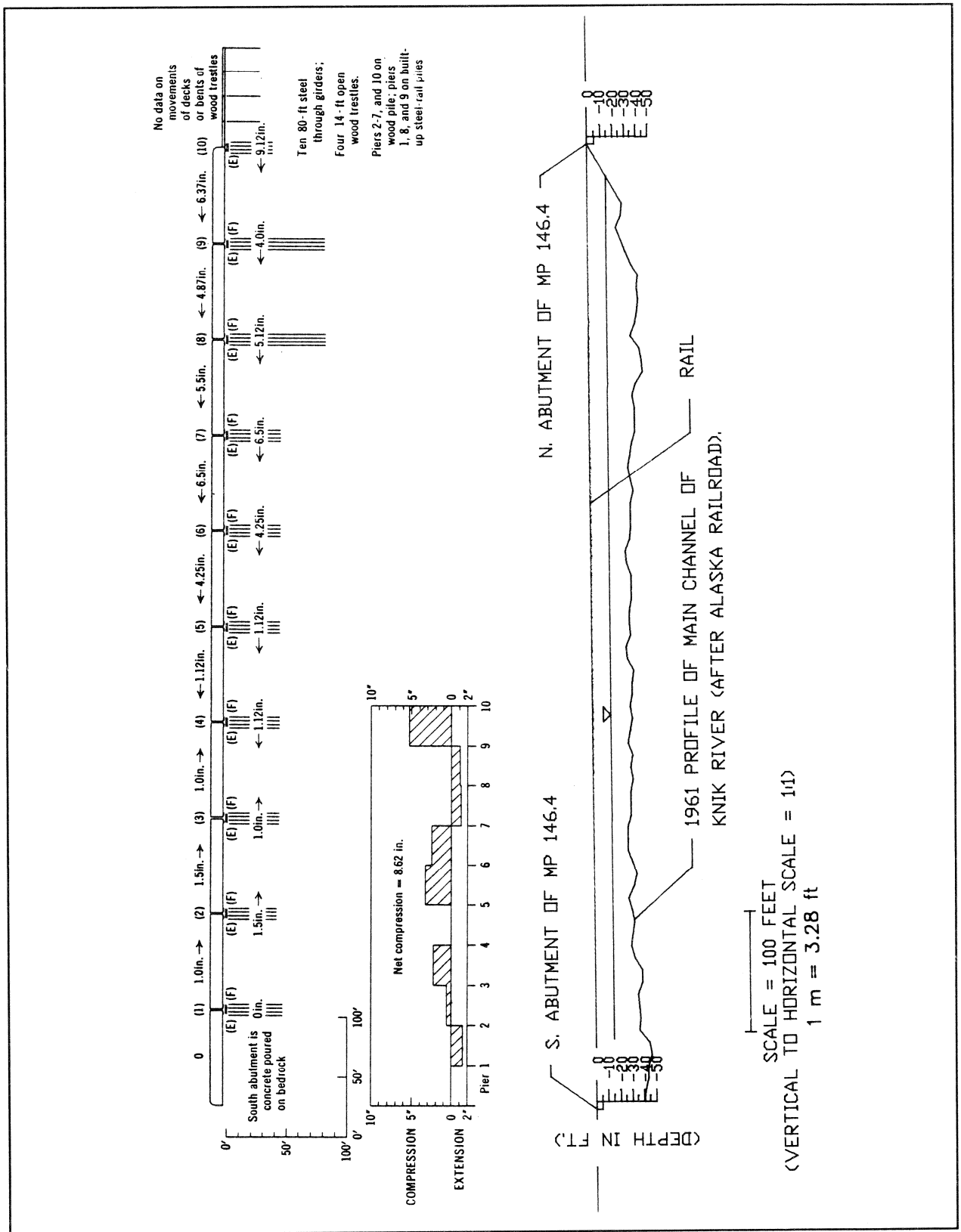

Figure 11 Profile of and Displacements at Bridge Milepost 146.4

highway crossing (see Plate #1, McCulloch and Bonilla, 1970). Fissures in a point bar deposit on the south side of the river at the construction site of Highway Bridge No. 1121 are scores of meters long and a few meters wide. Four newly completed concrete piers founded in this point bar deposit displaced a maximum of 0.6 m toward the Knik River (Ross et al., 1973).

4.4.2.2 TOPOGRAPHY

We conducted a survey of the Knik and Matanuska crossings to map the topography and measure ground slopes and channel depths. Because of brush and difficult access, we were unable to complete a survey line along the railroad and measure the ground slope perpendicular to the channel at the bridges. However, we were able to complete a survey line on natural ground just west of and parallel to the Glenn Highway. From this line we were able to take several side-shots westward along the river banks and to the railroad bridges. This survey line traversed all channels of the Knik and Matanuska Rivers and is used to estimate the ground slope perpendicular to the channels at the railroad bridges. Because of the flat broad floodplain at this locality, we feel that ground slope perpendicular to the channel does not change dramatically between the highway and railroad alignments.

The floodplain on the north and south side of the Knik River at the Glenn Highway slopes approximately 0.5 of a percent toward the water's edge on both sides of the Knik River (Figure 12). We were unable to profile the downstream gradient of the Knik River between the railroad and the highway. However, the westwardly flowing Knik River probably flows along a gradient similar to the gradients of the adjacent Matanuska River and its secondary channels. Downstream gradients for the Matanuska River range from 0.04 to 0.10 percent.

At the railroad crossing, the Knik River is approximately 260 m wide and 6 m deep. We did not sound the channel bottom in 1989, but a 1961 sounding by the Alaska Railroad indicates that the bottom of the Knik River was approximately 11 m below finished rail grade and averaged 6 m below the water elevation

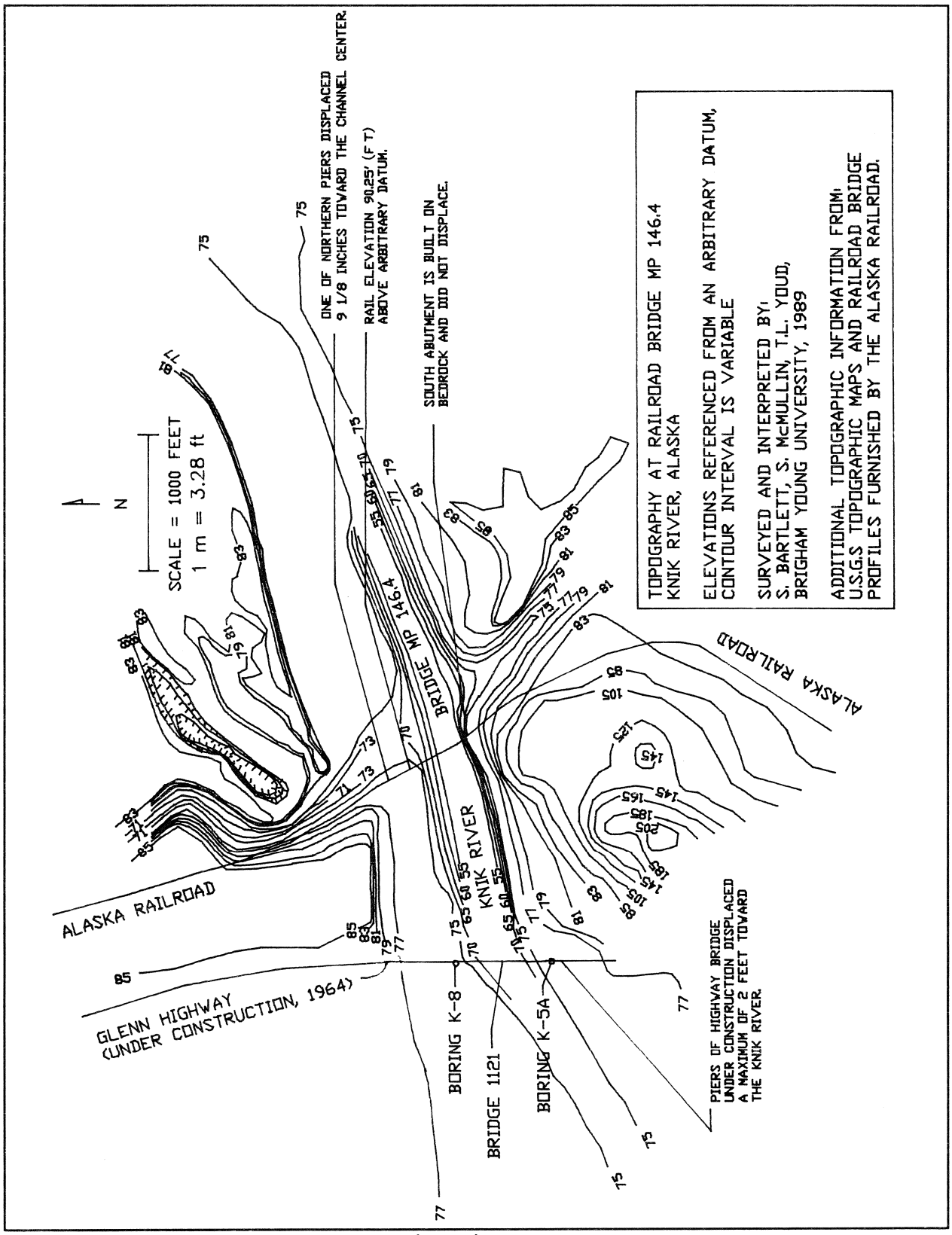

Figure 12 Contour Map of Knik River.

in river (Figure 11). On the south side of the Knik river and west of the tracks, outcropping bedrock produces a prominent knoll (Figure 12). Near the north abutment of Bridge 146.4, a small tidal channel drains into the Knik River. Glacial outwash deposits north and east of the bridge form flat-top knolls which stand approximately 2.5 to 3 m above the water level in the river.

4.4.2.3 SUBSURFACE SOIL CONDITIONS

Soil data from two boreholes, K-5A and K-8, (see Figure 12 for location), show that subsurface sediments at the highway crossing generally consist of 18 to 20 m of sand, silty sand and sandy gravel (Figure 13). Below 20 m, the sediments are finer and more dense and consist of 0.3 to 1 m thick alternating layers of fine sand and silt.

Figures 14 and 15 are examples of a grain size distribution charts for soil samples taken at different depth intervals within the boreholes. Each line type (i.e., solid, dashed, dot, and dashed-dot represents a soil sampled at the corresponding interval shown in the legend. For classification purposes, the boundary lines dividing the gravel (>4.75 mm), sand (4.75 mm to 0.075 mm), silt (0.075 mm to 0.005 mm) and clay (<0.005 mm) size particles have been included.

Liquefaction analysis using the simplified procedure (see Section 3.5) for Borehole K5A indicates that the majority of the liquefiable sediment is in a zone 8 to 15 m below the surface (Figure 13). The SPT values for this zone average 17 and range from 11 to 23. Liquefaction analysis for Borehole K-8 shows liquefiable sediment to a depth of approximately 17 m below the surface (Figure 13). The SPT values for this zone average 17 and range from 6 to 35. Below 17 m the soil is not liquefiable as indicated by considerably higher penetrations resistances.

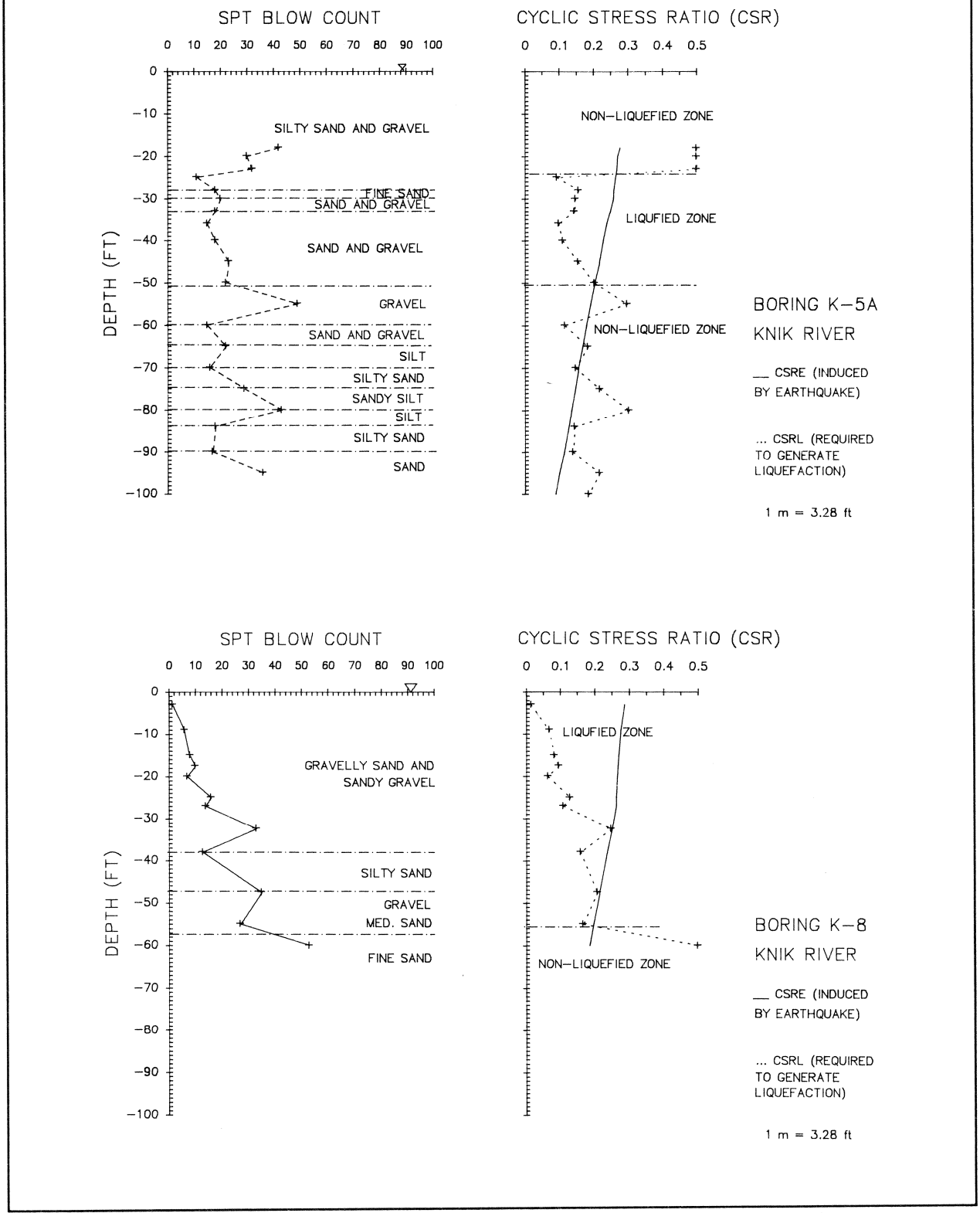

Figure 13 SPT Profile and Analysis, Bore Holes K5A and K8.

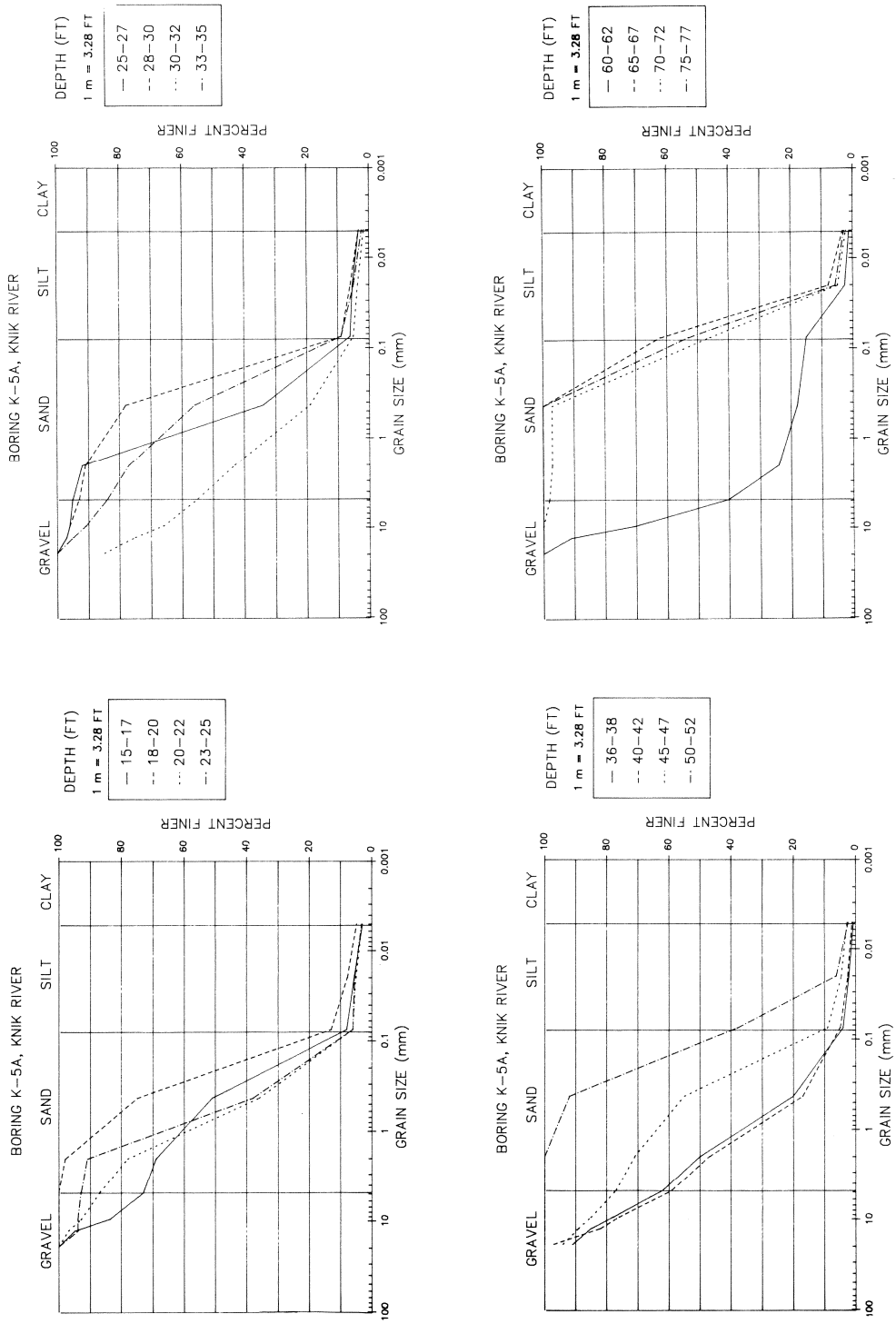

Figure 14 Grain-Size Distribution Charts, Bore Hole K5A.

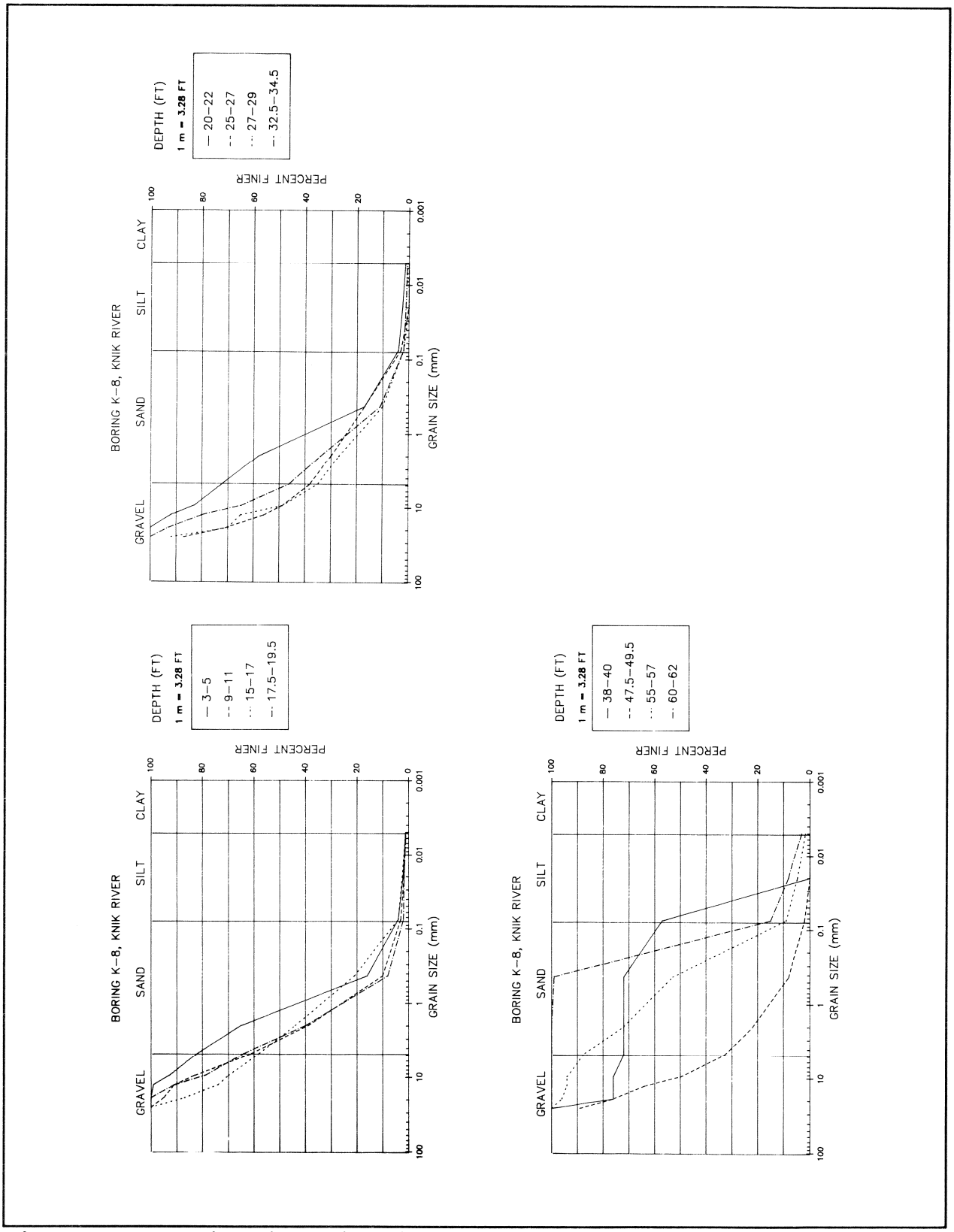

Figure 15 Grain-Size Distribution Charts, Bore Hole K8.

4.4.3 RAILROAD BRIDGE AT MILEPOST 147.1, SECONDARY CHANNEL OF MATANUSKA RIVER

4.4.3.1 GROUND FAILURE DISPLACEMENT AND DAMAGE

Approximately 1 km north of Bridge Milepost 146.4, the railroad crosses a secondary channel of the Matanuska River at Milepost 147.1 (Figure 10). Railroad Bridge 147.1 is 128 m steel truss structure. Three 38 m central spans are supported on concrete piers. Two 7.6 m steel-beams end spans connect the abutment with the pier at each end of the bridge.

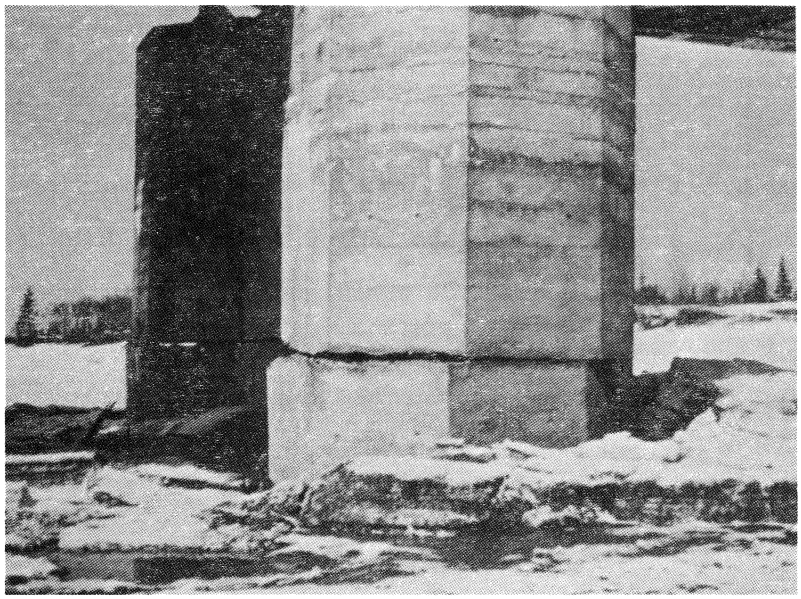

Figure 16 Broken and Displaced Piers at Bridge Milepost 147.1.

Liquefaction of channel deposits caused ground fissures on both sides of the river. Lateral spread of the channel deposits displaced piers about 1 foot toward the channel center. McCulloch and Bonilla report displacements and damage at this bridge as follows:

"The anchor bolts in the short end spans tore free and spalled away the concrete, and the steel was jammed against the adjacent large steel spans. The third pier which, like the others, was reinforced with one-half-inch vertical bars 18 inches on centers was sheared off near its base along a fracture that followed a pour joint most of the way across the pier. The buried base of the pier was displaced about a foot south toward the river. The displacement tilted the upper part of the pier about 8 inches and produced an offset of about 4 inches at the break [Figure 16] (McCulloch and Bonilla, 1970)."

4.4.3.2 TOPOGRAPHY

At railroad Milepost 147.1, flat-top glacial outwash knolls stand approximately 3 m above the channel bottom on both sides of the river. At the southern end of Railroad Bridge 147.1, a small tidal channel parallels the embankment for a considerable distance and joins the Knik River to the south (Figure 10 and Plate #1, McCulloch and Bonilla, 1970).

During our traverse near the Glenn Highway, we measured a floodplain that slopes approximately 0.6 percent toward the channel south of Highway Bridge No. 1122 (Figure 17). The floodplain north of the highway bridge slopes approximately 0.1 percent toward the channel. Our survey shows the downstream gradient of the Matanuska River between the highway alignment and Railroad Bridge 147.1 is approximately 0.1 percent.

We sounded the channel bottom beneath Railroad Bridge 147.1 in July of 1989. At this time, the channel had incised 2.4 to 3.0 m below the floodplain and the channel bottom averaged 6 m below rail elevation (Figure 18). However, comparison of our 1989 channel sounding with a 1958 sounding by the Alaska Railroad (Figure 18) revealed that between 0.6 to 3.6 m of deposition has occurred in the channel between 1958 and 1989. Thus, the 1958 channel cross-section probably more closely represents the channel configuration at the time of the earthquake.

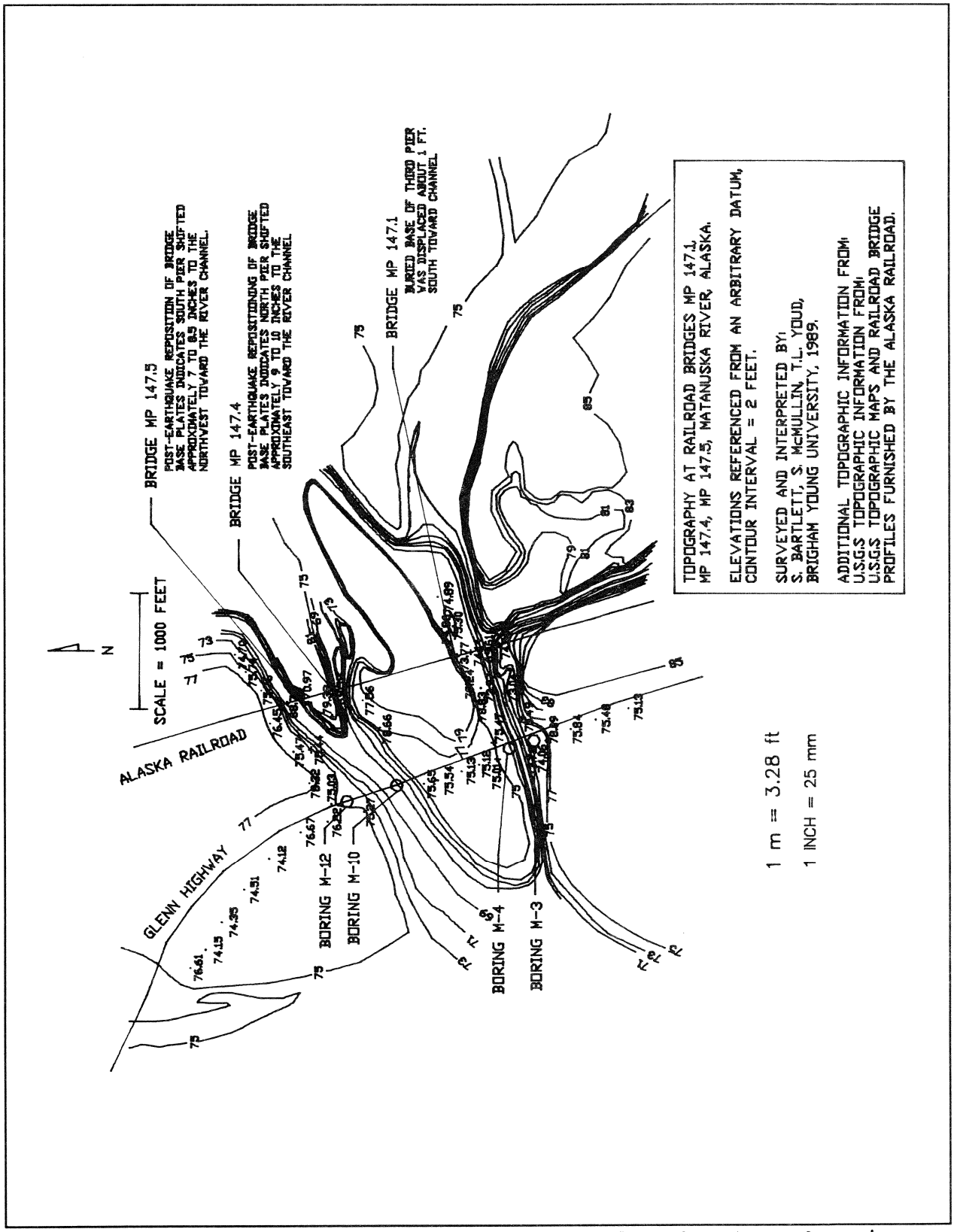

Figure 17 Contour Map of Secondary Channels of Matanuska River.

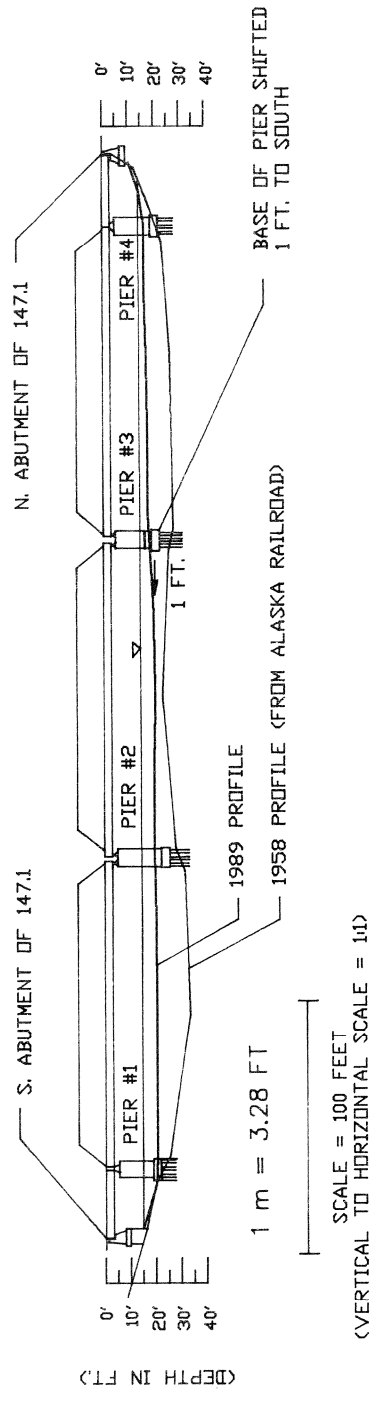

Figure 18 Profile of and Displacements at Bridge Milepost 147.1

4.4.3.3 SUBSURFACE SOIL CONDITIONS

The subsurface soil profile at Boreholes M-3 and M-4 (Utermohle, 1963), located approximately 260 m west of the railroad on the Glenn Highway, (Figure 17) consists of 12 m of layered sandy gravel, fine gravel and sand underlain by a considerable thickness of 0.3 to 1 m layers of alternating silty sand and silt (see profiles and grain-size data shown in Figures 19 - 21).

Liquefaction analysis for Borehole M-3 indicates that a sandy gravel is liquefiable in a zone from the surface to a depth of 12 m (Figure 19). The SPT values average 15 and range from 9 to 24 in this zone. At Borehole M-4, the majority of the liquefiable sediments are restricted to the upper 12 m of the profile. Analysis indicates liquefaction susceptibility in gravel and fine sandy gravel to a depth of 12 m (Figure 19). The SPT values in this zone average 16 and range from 11 to 24. Marginal susceptibility to liquefaction is also indicated in several thin zones of silty sand and sandy silt beginning at a depth of 12 m to a depth of 24 m. The SPT N value of 4 at a depth of 26 m appears to be anomalously low. The sediment at that depth probably did not liquefy or liquefaction was too deep to have affected the bridge.

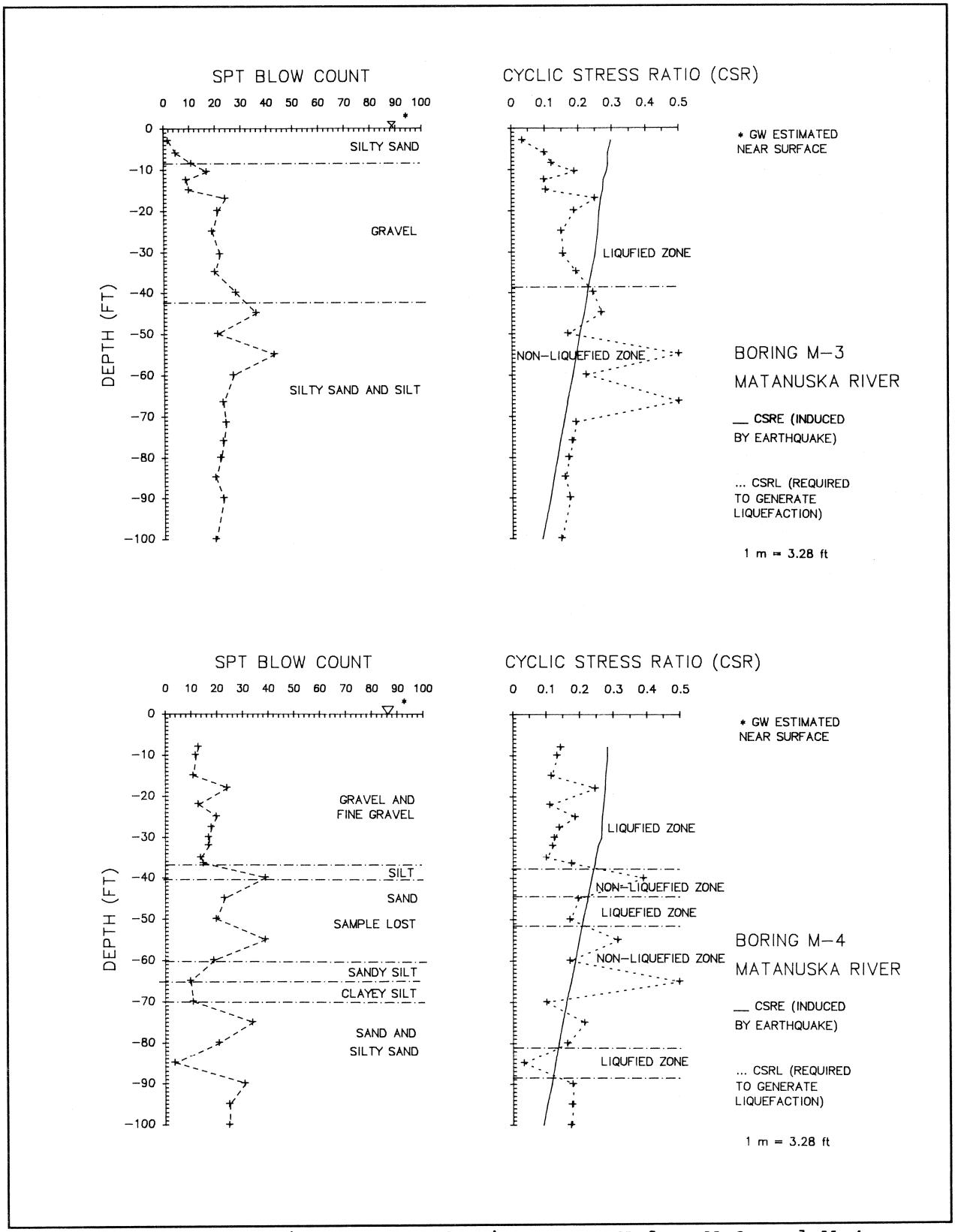

Figure 19 SPT Profile and Analysis, Bore Holes M-3 and M-4.

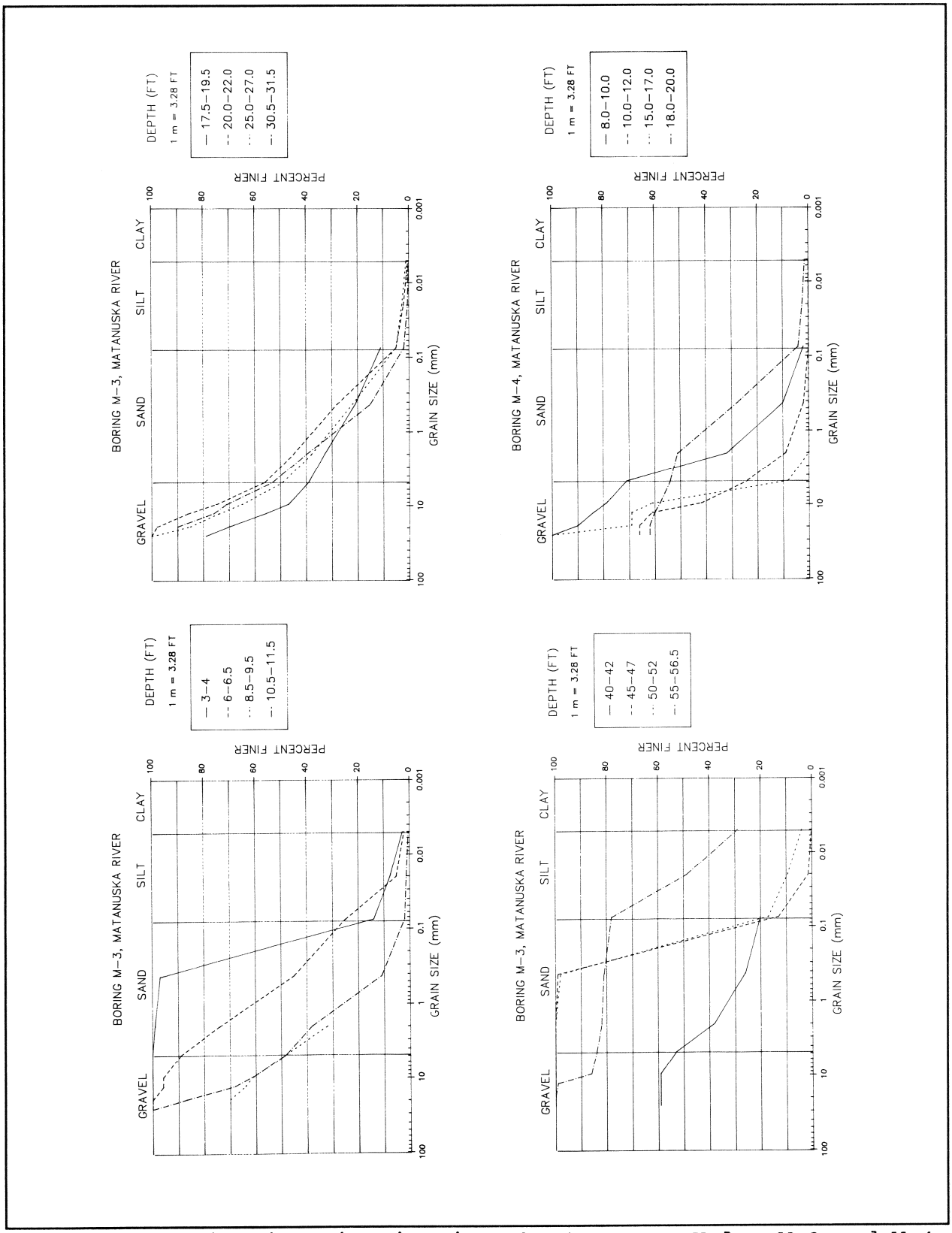

Figure 20 Grain-Size Distribution Charts, Bore Holes M-3 and M-4.

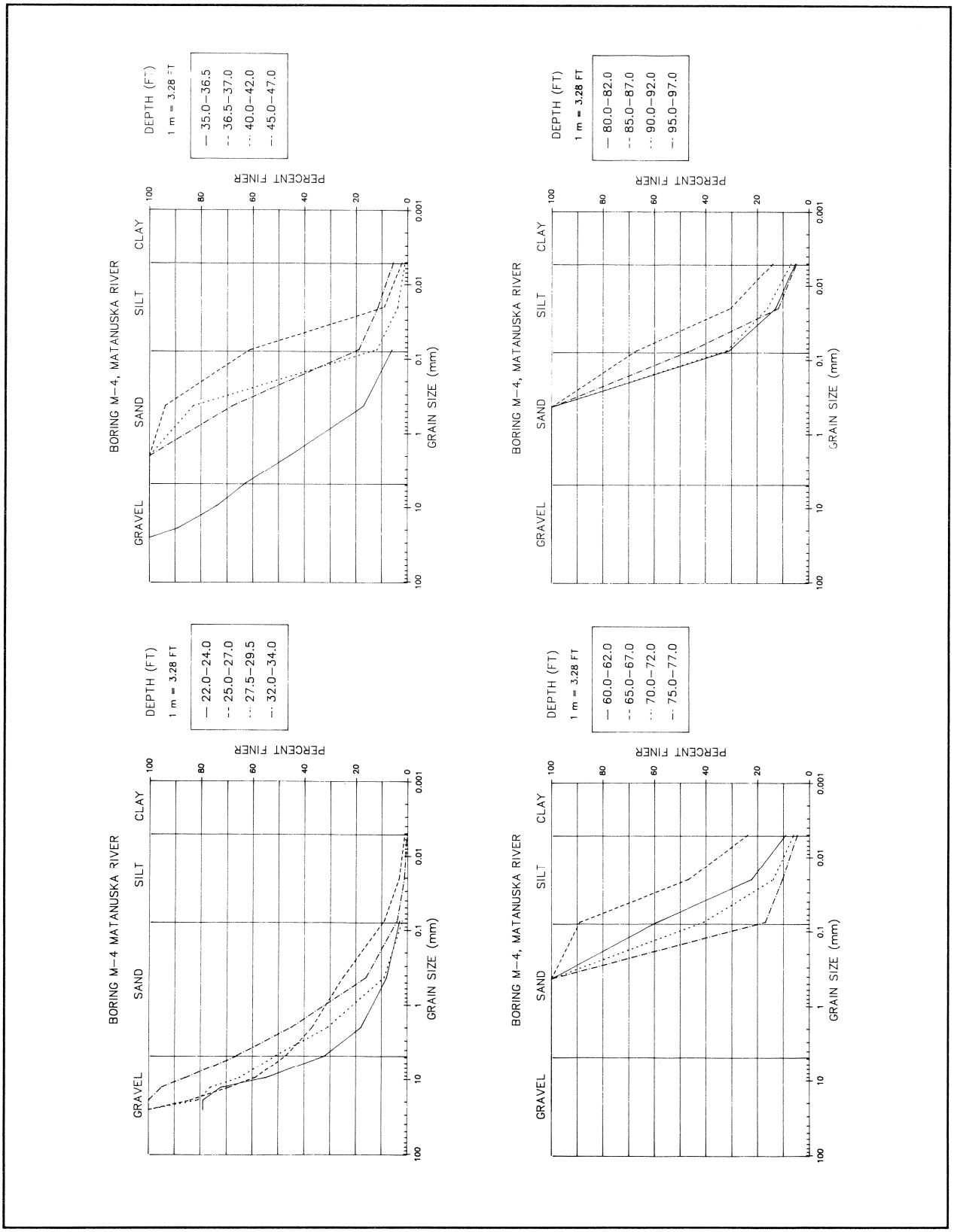

Figure 21 Grain Size Distribution Charts, Bore Hole M-4.

4.4.4 RAILROAD BRIDGE AT MILEPOST 147.4, SECONDARY CHANNEL OF MATANUSKA RIVER

4.4.4.1 GROUND FAILURE DISPLACEMENT AND DAMAGE

Railroad Bridge Milepost 147.4 is a 37.5 m steel truss structure with 7.6 m steel-beam spans on each end. Both ends of the truss are supported by concrete piers. McCulloch and Bonilla did not mention ground displacement or damage at this bridge. However, channelward displacement must have occurred at the bridge. Ground fissures roughly paralleling the banks, were present on both sides of the bridge and were particularly wide in a old meander scar on the north bank (see Plate #1, McCulloch and Bonilla, 1970).

From our observations of the bridge footings and concrete pier caps, channelward movement of the north pier during the earthquake apparently sheared the anchor bolts which tied the footing to the pier. Detachment of the pier from the truss enabled the pier to move channelward without significantly damaging the bridge. Following the earthquake, the bridge truss was reused and realigned by resetting the span footings on the pier. In so doing, footings on the north pier were repositioned from 190 to 200 mm to the north and from 110 to 170 mm to the west and rebolted to the pier (Figure 22). The footings on the south pier were not repositioned. By comparing the present base plate set with the pre-earthquake base plate set, we calculate that the north pier had shifted approximately 230 to 250 mm southeastward toward the channel. This displacement

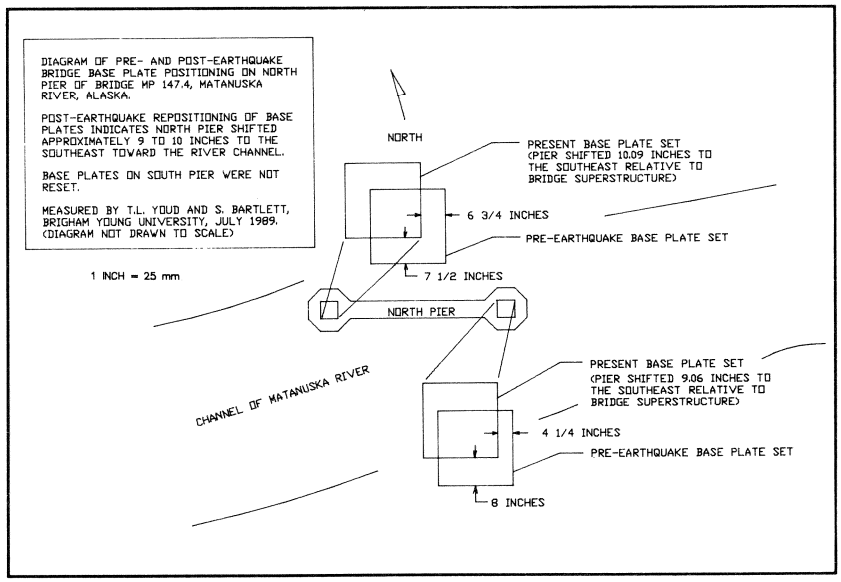

Figure 22 Pre- and Post-Earthquake Base Plate Positions, Bridge Mile Post 147.4.

is consistent with pier displacements of 0 to 0.6 m reported at other nearby bridges.

4.4.4.2 TOPOGRAPHY

A bifurcated channel of the Matanuska River passes under the railroad bridges at Mileposts 147.4 and 147.5 and joins a few hundred meters west of the railroad (Figure 17). Our survey along the Glenn Highway showed that south of Highway Bridge No. 1123, the ground slopes approximately 0.1 percent to the south. North of the bridge, natural ground slopes approximately 0.3 percent to the south (Figure 17). Our survey of the channel at Bridge 147.4 measured an average channel depth of 3 m. Glacial outwash deposits on both banks stand 2.5 to 3 m above the channel bottom (Figure 17). The downstream gradient of the Matanuska River between the railroad and the Glenn Highway is approximately 0.1 percent.

4.4.4.3 SUBSURFACE SOIL CONDITIONS

Borehole M-10, (Utermohle, 1963), located approximately 300 m west on the Glenn Highway (Figure 17) reveals that the upper 9 m of the profile is composed of layers of coarse sand, gravel and fine gravel (see profiles and grain-size data shown in Figures 23 - 24). From 9 to 17 m, the profile consists of a clean medium grained sand. Below 17 m, the sediment becomes finer and consist of alternating layers of fine sand and silty sand.

A liquefaction analysis for Borehole M-10 indicates that the upper 17 m of the profile may have liquefied during the 1964 earthquake (Figure 23). The SPT values for this zone average 13 and range from 4 to 30. Some marginal liquefaction is also indicated in sand and silty sand starting at 19 m and extending to a depth of 23.5 m. A SPT value of 14 was measured in this layer.

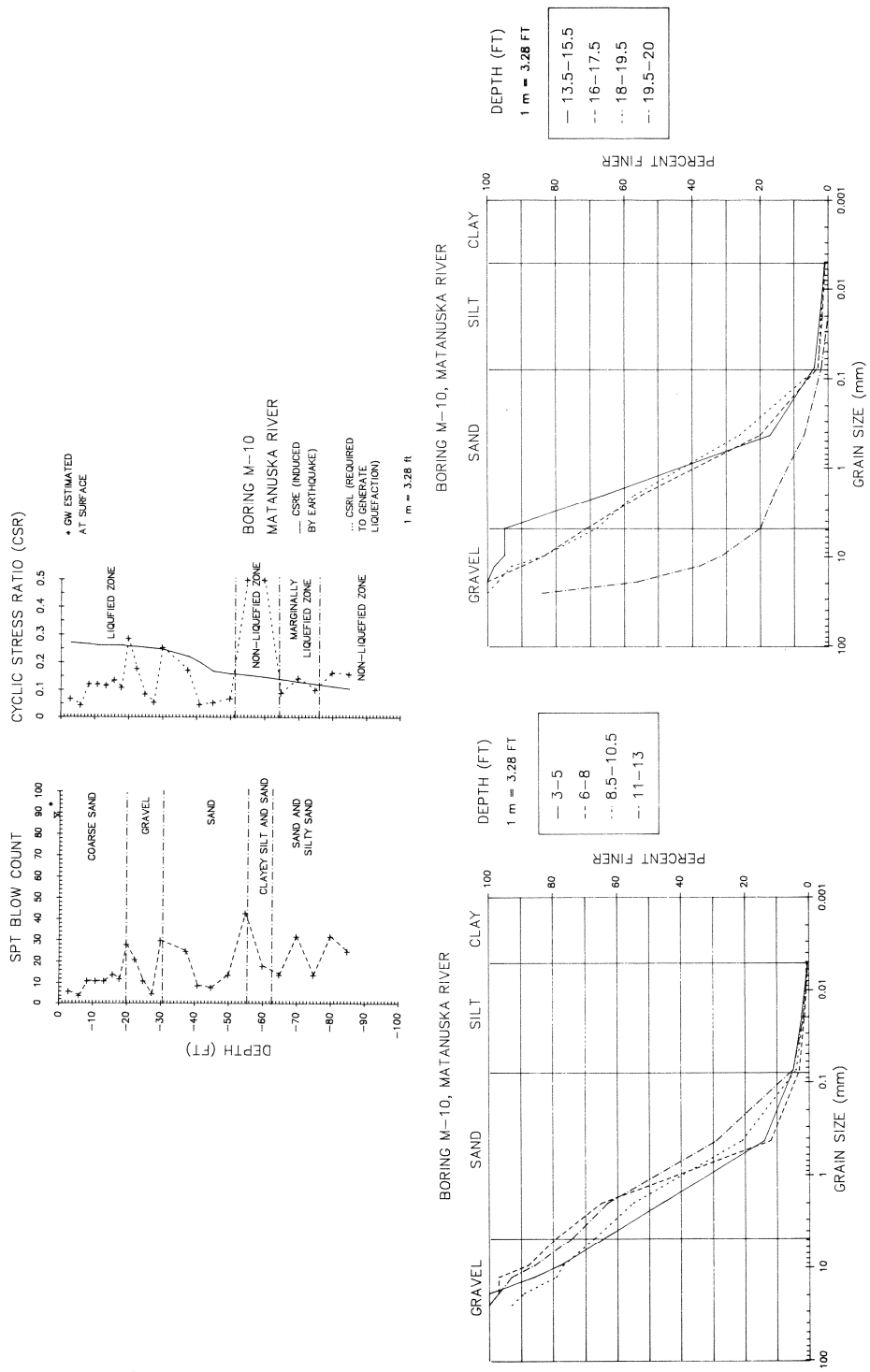

Figure 23 SPT Profile and Grain-Size Data, Bore Hole M-10.

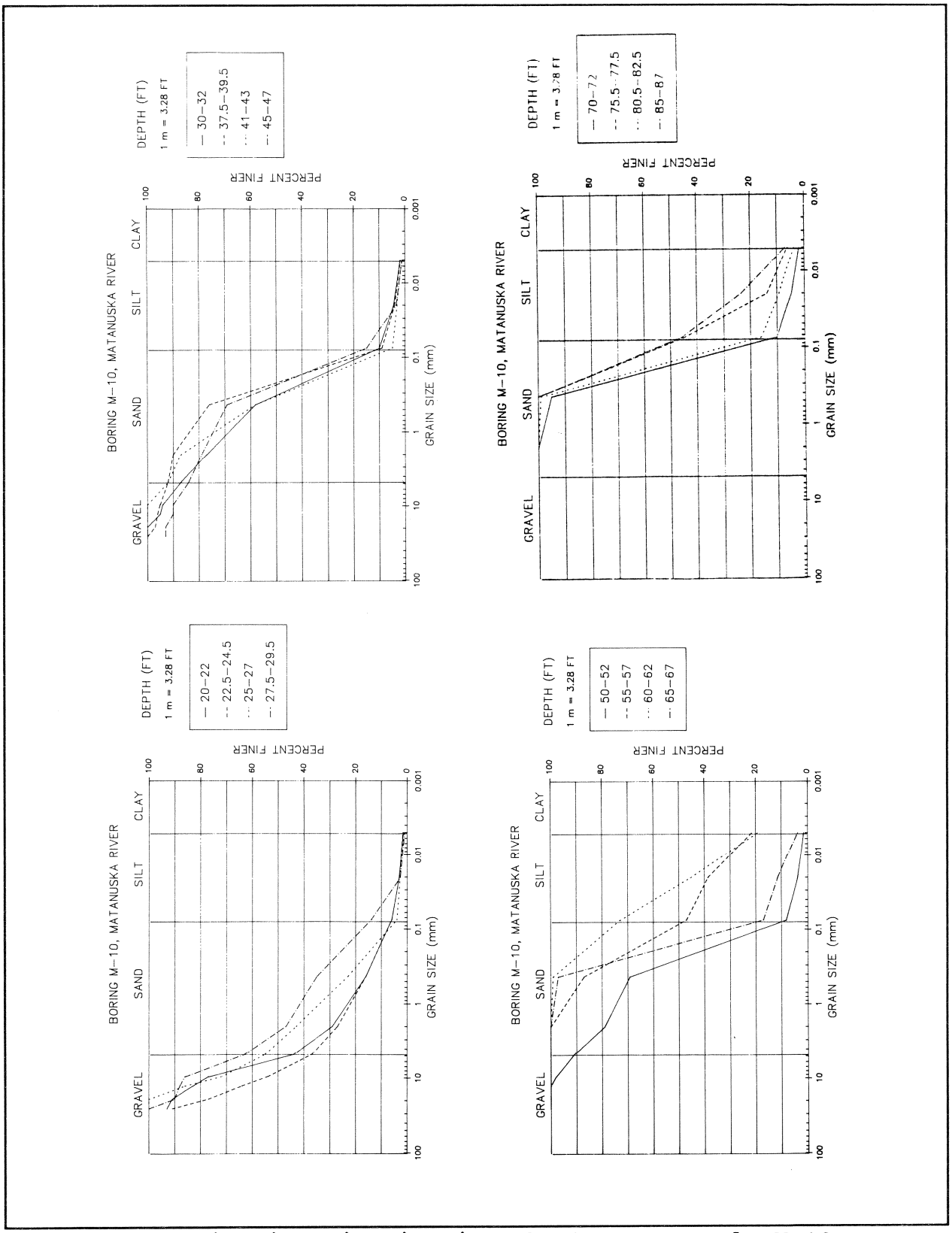

Figure 24 Grain-Size Distribution Charts, Bore Hole M-10.

4.4.5 RAILROAD BRIDGE AT MILEPOST 147.5, SECONDARY CHANNEL OF MATANUSKA RIVER

4.4.5.1 GROUND FAILURE DISPLACEMENT AND DAMAGE

The Railroad Bridge at Milepost 147.5 crosses a secondary channel of the Matanuska River. The bridge is 203 m long and consists of steel girders supported by concrete piers (McCulloch and Bonilla, 1970). Like the other bridges in the area, lateral spread of channel deposits displaced abutments and piers about a foot toward the river channel. McCulloch and Bonilla report the following displacements at Bridge 147.5:

> ". . . [the] piers and abutments were jammed streamward against the central spans. Piers and abutments were also displaced horizontally; the north abutment and pier shifted about 1 foot west [downstream] and the third pier [from the north] moved about 1 foot south, toward the channel."

McCulloch and Bonilla did not report any displacement at the south abutment or piers. Our inspection of the top of the southern-most pier showed that the footings had been reset after the earthquake. As we did for Bridge Milepost 147.4, we compared the pre- and post-earthquake base plate sets (Figure 25). From this comparison, we noted that the southern-most pier displaced approximately 75 to 125 mm northward toward the channel and about 150 to 175 mm westward downstream. Thus, amount of streamward displacement measured at the southern-most pier is very similar to the streamward displacement reported at the north end of the bridge.

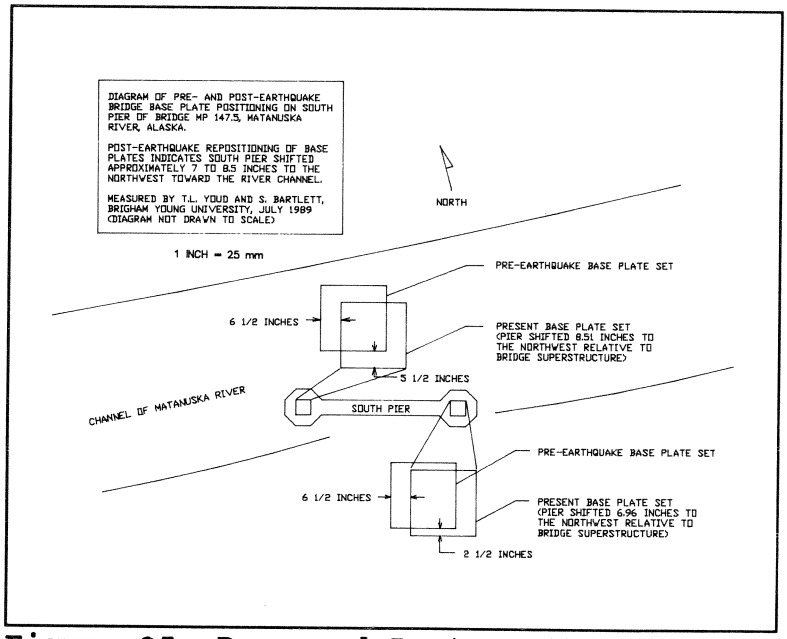

Figure 25 Pre- and Post-Earthquake Base Plate Positions, Bridge Mile Post 147.5.

4.4.5.2 TOPOGRAPHY

Downstream displacement of the north abutment and the northern-most and southern-most piers of the railroad bridge occurred along a very gentle downstream gradient. Our profile of the channel under Bridge No. 147.5 shows the river flowing westward along a 0.04 to 0.06 percent gradient. The average depth of the channel bottom at the bridge is approximately 2.5 to 3 m below the glacial outwash deposits on both banks (Figure 17). The floodplain south of the bridge measured at the Glenn Highway slopes approximately 0.1 percent to the south. North of the bridge the floodplain slopes 0.3 percent to the south (see discussion of topography for Railroad Bridge Milepost 147.4).

4.4.5.3 SUBSURFACE SOIL CONDITIONS

Borehole M-12 is located approximately 300 m west of the railroad alignment on the adjacent Glenn Highway Bridge (Utermohle, 1963). Like other soil profiles in the area, the upper 20 m is comprised of layered sand and gravel and below 20 m the sediment is chiefly alternating layers of silty sand and silt (see profile and grain-size data shown in Figure 26).

Liquefaction analysis reveals that most of the profile is liquefiable to a depth of 11 m, except in a thin zone at 6 m where an unusually high N of 51 was reported in a fine gravel (Figure 26). The SPT values in the liquefiable zones range from 2 to 18, with an average of 11. Below 11 m, N increases sufficiently to make most of the remainder of the profile nonliquefiable.

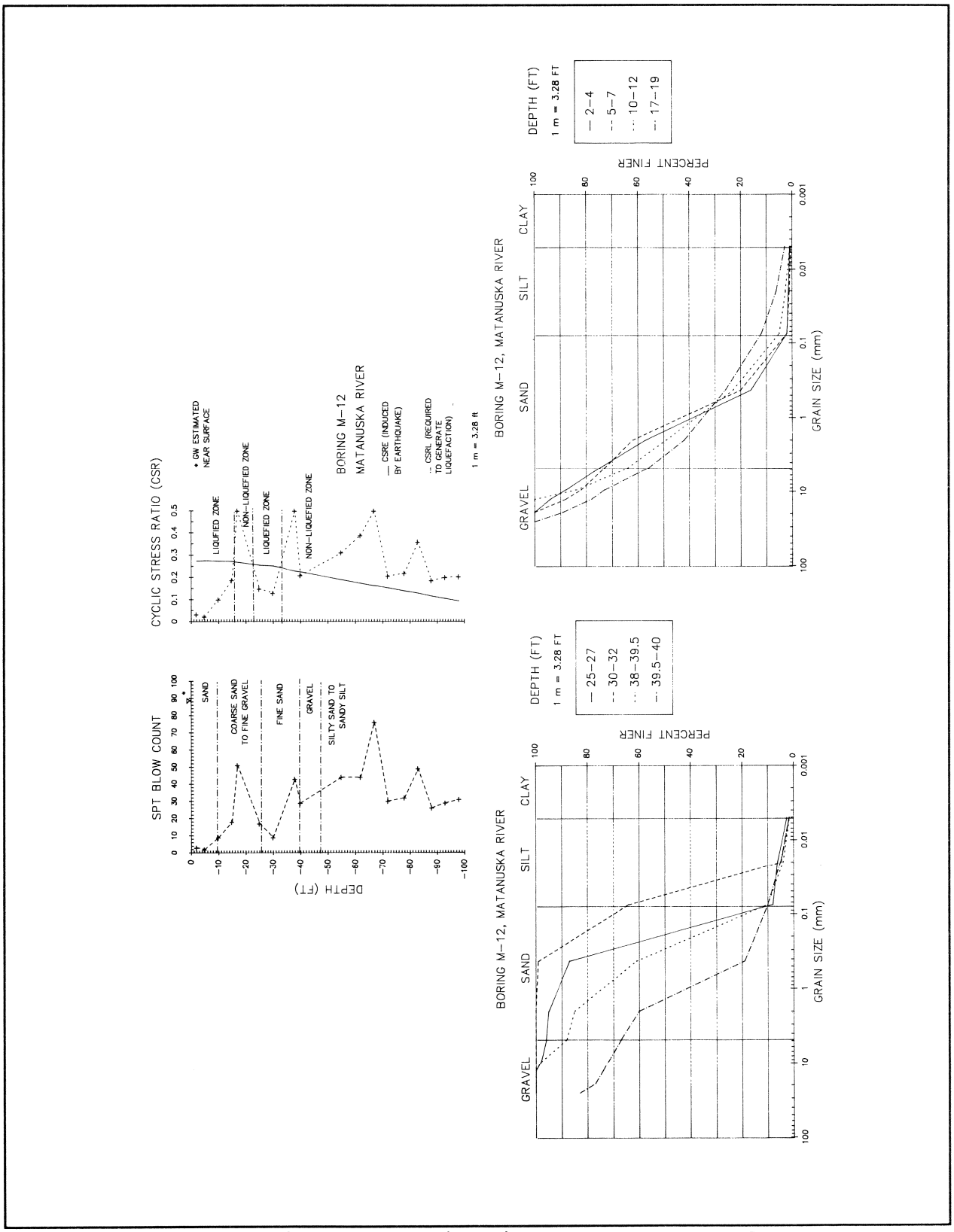

Figure 26 SPT Profile and Grain-Size Data, Bore Hole M-12.

4.4.6 RAILROAD BRIDGE AT MILEPOST 148.3, MAIN CHANNEL OF MATANUSKA RIVER

4.4.6.1 GROUND FAILURE DISPLACEMENT AND DAMAGE

The Railroad Bridge at Milepost 148.3 spans the main channel of the Matanuska River. The bridge is a 122 m long steel-girder structure with five 24 m spans supported by concrete piers. McCulloch and Bonilla (1970) were unable to visit this bridge before repair was completed, but they recorded the following terse damage report given by a railroad worker, B.E. Cannon:

> "[The] Seventy-foot [sic] span sheared anchor bolts and jammed. Lurch [ground] crack humped bridge but did not break [the] piles. Pile bents 48 to 59 demolished."

Our inspection of the northern-most pier of the bridge revealed that the footing was 0.24 m off-center of the timber pile cap. This offset suggests that the northern pier moved approximately 0.24 m toward the channel relative to the bridge deck.

South of the bridge, the tracks are supported by 180 m of wooden trestle over a large point bar deposit. Lateral spread of the point bar toward the channel caused large ground fissures to develop under the trestle. Approximately 30 m of trestle near the bridge's southern end was irreparably damaged (Figure 27). McCulloch and Bonilla describe the fissures and damage:

> ". . . [the southern] 575 feet of the approach embankment to the bridge over the main channel of the Matanuska River (148.3) was heavily damaged by ground cracks. . . . large cracks are reported to have crossed the tracks diagonally, and the embankment was lowered at least 4 feet. Severe cracking also occurred in the wide bank of channel deposits at the south end of the bridge. According to Bruce Cannon, the cracking "demolished" the 48th through the 59th wood-pile bents. This is the only railroad bridge in which the wood-piles were broken by ground cracks. Figure 139 [Figure 27, this report], taken after channel deposits had been bulldozed to replace the destroyed bridge, shows that some of the cracks were several feet wide (McCulloch and Bonilla, 1970)."

The damage to the trestle on the south end of the bridge is noteworthy because displacement at this location appears to be greater than at any other location on the Knik and Matanuska Rivers. (The largest documented displacement reported to date is a 0.6 m displacement of newly placed concrete piers at Highway Bridge No. 1121 (see Section 4.4.2.1). From the damage description by McCulloch and Bonilla, it is not clear whether the reported 1.2 m of embankment lowering

consisted mostly of ground and embankment settlement or was partly comprised of horizontal ground displacement. Ground fissures on the oblique appear to a few meters wide (Figure 27). Lateral spread displacement of the same order likely occurred beneath and caused the damage to the trestle.

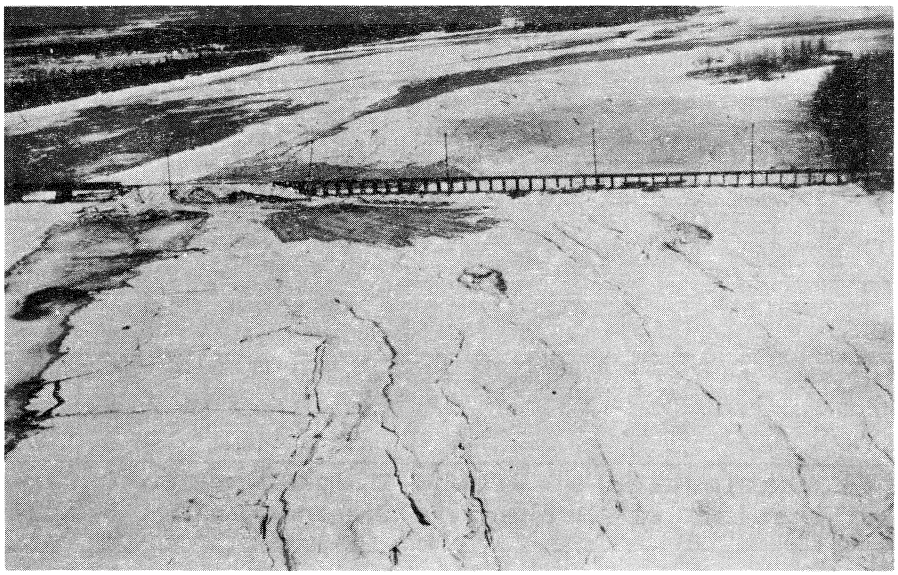

Figure 27 Broken Trestle at Southern End of Bridge Milepost 148.3.

The broken and tilted telephone pole (second telephone pole from left end of bridge - see Figure 27) offers an opportunity to estimate the horizontal ground displacement at the damaged trestle. The base of the telephone pole appears to have moved toward the river, breaking the pole approximately 3 m above its base. Tension in the telephone wires seem to have restrained the top of the pole from moving appreciably. Thus, assuming that the top of the pole remained stationary and using the pole's height and its angle of inclination, we calculate that base of the telephone pole shifted approximately 1.3 m toward the channel. Thus, several pieces of evidence indicate that ground displacement in the vicinity of the broken trestle was approximately 1.3 m (Figure 28).

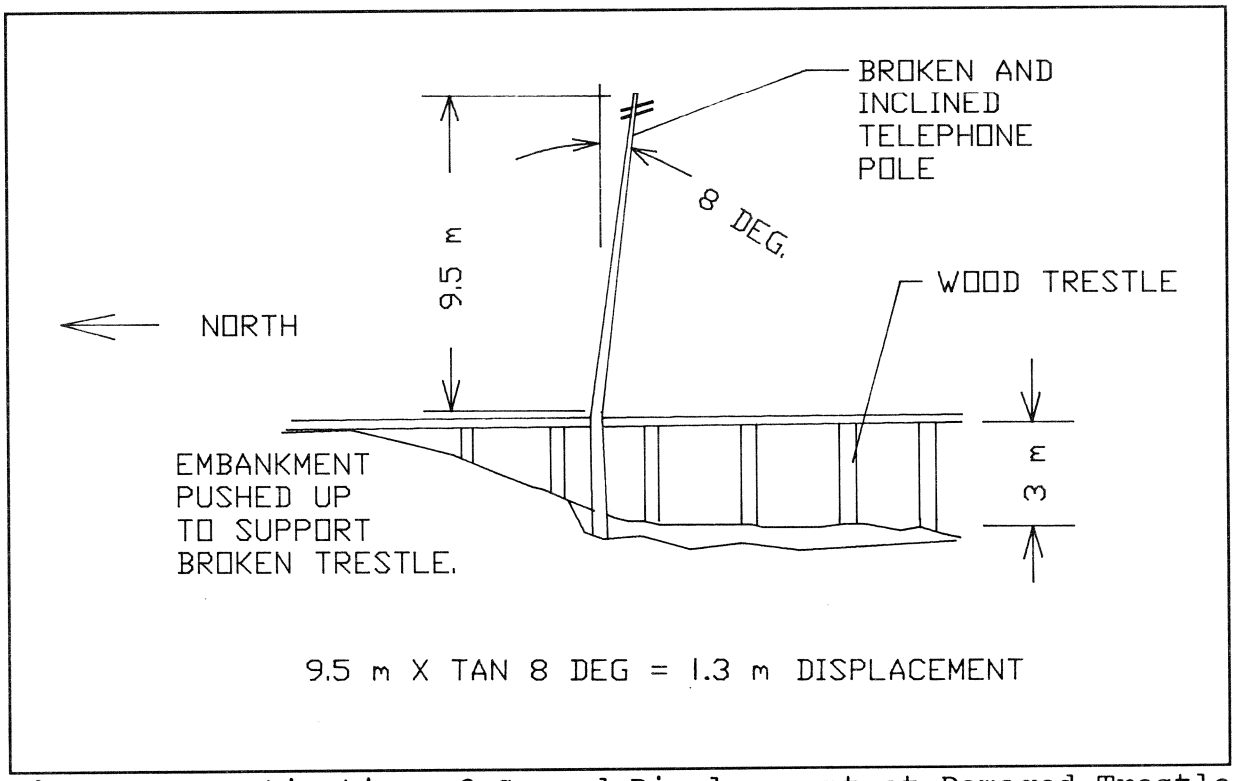

Figure 28 Estimation of Ground Displacement at Damaged Trestle from Inclination of Broken Telephone Pole, Bridge Mile Post 148.3.

4.4.6.2 TOPOGRAPHY

Because of the depth and current in the river, we were unable to sound the main channel of the Matanuska River. However, a 1937 cross-section of the Matanuska River channel by the Alaska Railroad shows the average channel depth was 7.5 to 9 m below rail elevation and 4.5 to 6 m below the banks (Figure 29). We assume these depths generally represent the 1964 channel configuration. The fissured point bar deposit on the south side of the bridge slopes approximately 0.7 percent toward the channel (Figure 30). On the north side of the river at the Glenn Highway, a levy slopes approximately 0.8 percent away from the channel. The downstream gradient on the main channel of the Matanuska River is approximately 0.05 percent between the railroad and the highway bridges.

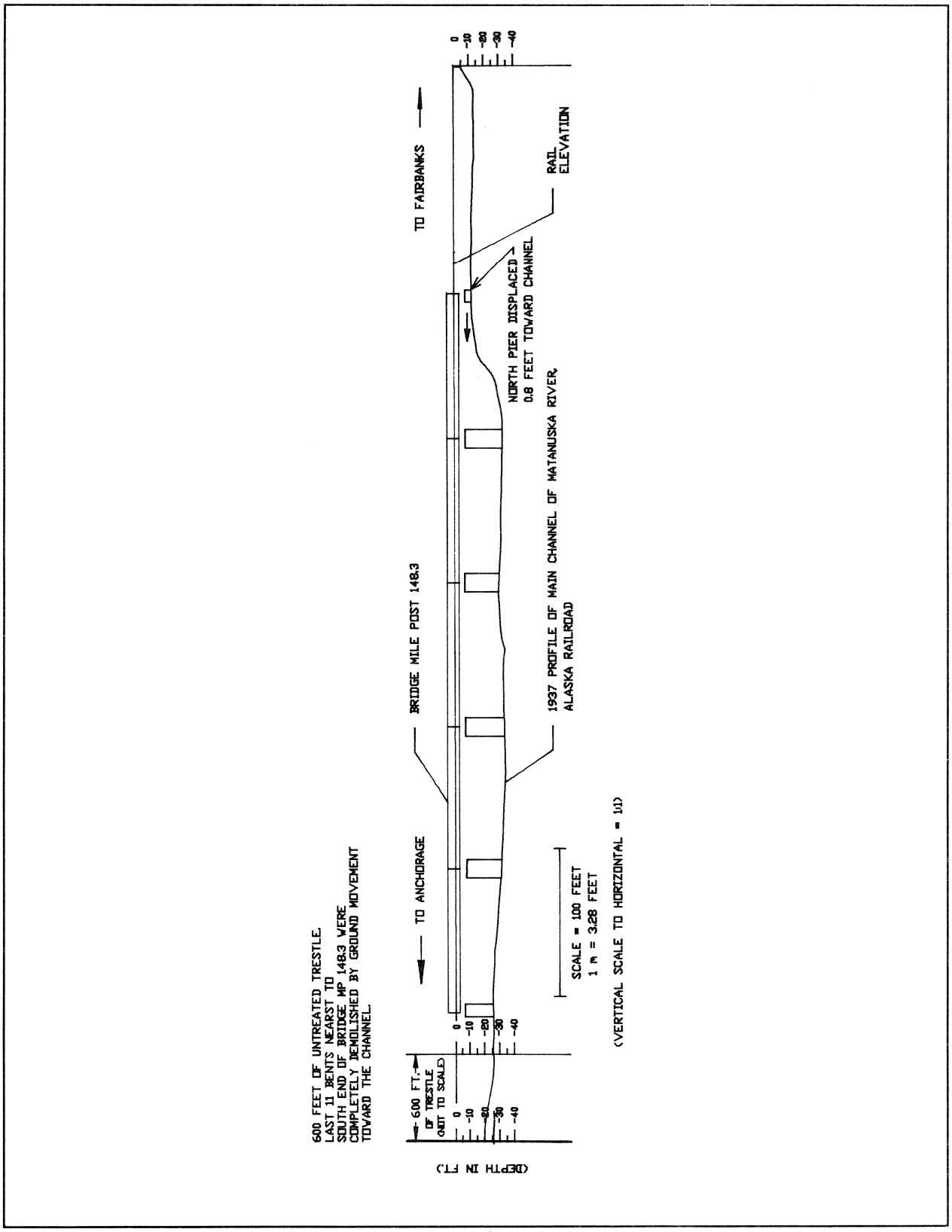

Figure 29 Profile of Matanuska River.

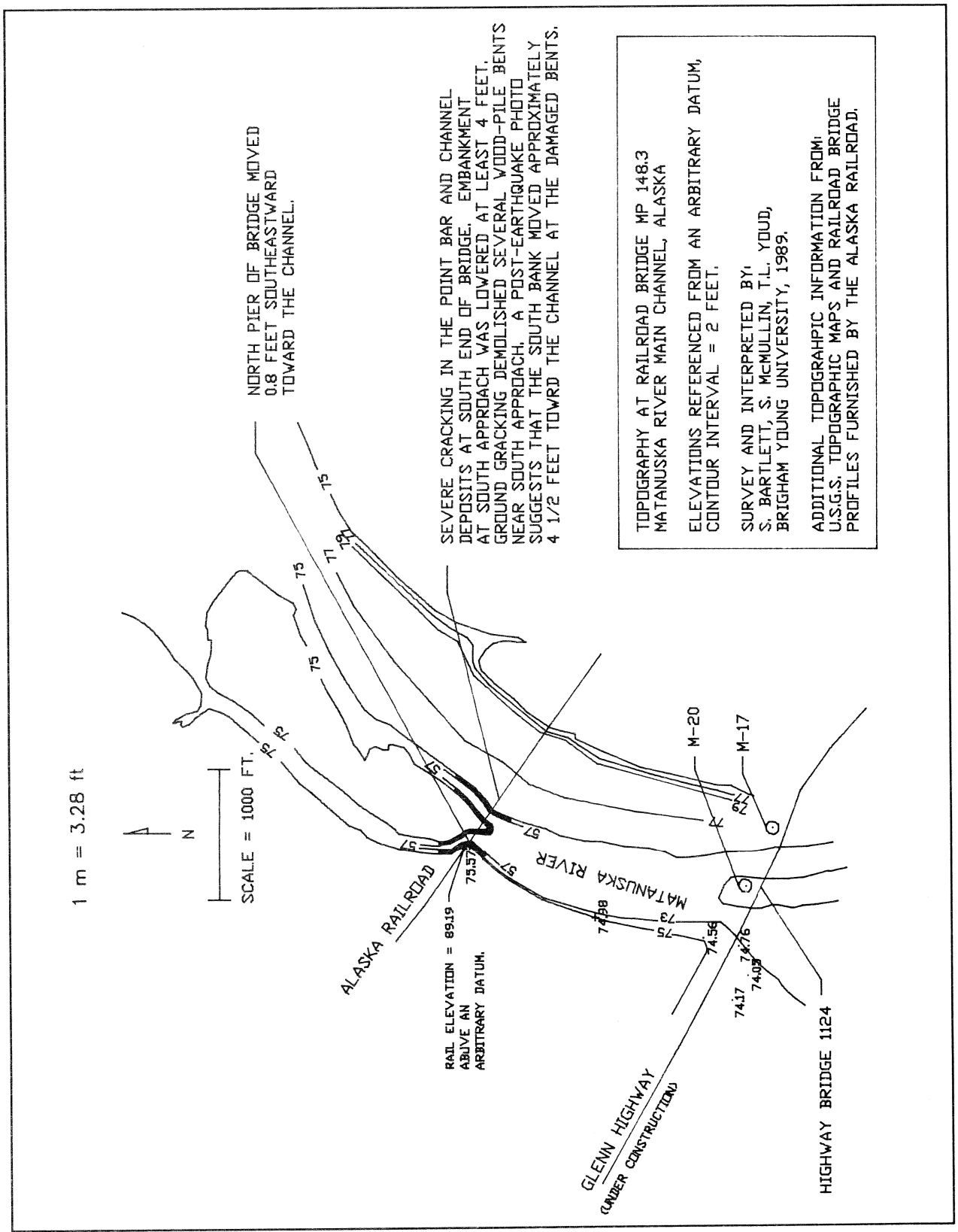

Figure 30 Contour Map of Matanuska River.

4.4.6.3 SUBSURFACE SOIL CONDITIONS

Two highway boreholes (Utermohle, 1963), M-17 and M-20, located approximately 650 m south of Railroad Bridge Milepost 148.3, were drilled in point bar and channel bar deposits, respectively (Figure 30). Sediment from Borehole M-17 is mainly layers of sand and gravel to a depth of 24 m except for a 4.5 m thick silt and clayey silt beginning at a depth of 9 m (see profile and grain-size data shown in Figures 31 - 33). At Borehole M-20, the subsurface soil consists of sand and silty sand with some fine gravel to a depth of 20 m. Below 20 m, a silt layer extends to depth of 25 m.

The substantial ground displacement and fissures at the south end of the railroad bridge are partly due to the high liquefaction susceptibility of the point bar sediments. Relatively low N values in Borehole M-17 indicate that most of the profile is liquefiable to a depth of 20 m, except for the silt and clayey silt layer encountered at 9 to 14 m (Figure 31). The SPT values in the liquefiable zone(s) average 14 and range from 6 to 22. Liquefaction analysis of the channel bar deposit (i.e., Borehole M-20) indicates liquefiable sediment in predominately sand from the surface to a depth of 8.5 m (Figure 31). Liquefaction susceptibility is also indicated in a sand to silty sand beginning at 15 m and extending to a depth of 20 m. The SPT values in the liquefiable zones average 19 and range from 9 to 32.

4.4.7 SUMMARY OF GROUND FAILURE AT THE KNIK AND MATANUSKA RIVERS

In general, railroad bridge abutments at the Knik and Matanuska River moved an average of 0.3 m toward the river channels and 0.3 m downstream. Piers also shifted as much as 0.6 m toward the channel and 0.3 m downstream. Lateral spread of point bar deposits toward the Matanuska River sheared the base of several wooden trestles at the south end of the railroad bridge. Ground displacement at this locality was approximately 1.3 m.

Liquefaction analysis for a composite log of the 8 boreholes at the Knik and Matanuska Rivers reveals that much of the upper 20 m of the profile is potentially liquefiable (Figure 34). These liquefiable sediments are mostly sand and gravels with SPT values less than 20. Silty sands and silts below the liquefiable sands and gravels are predominantly nonliquefiable. (As input for this analysis, we used a maximum site acceleration of 0.21 g, M_w of 9.2, a dry and moist unit weight for the soil of 15.7 and 18.9 kN/m^3, respectively. Also, we adjusted the cyclic stress ratio required for liquefaction, CSRL, for an average fines content of 14 percent).

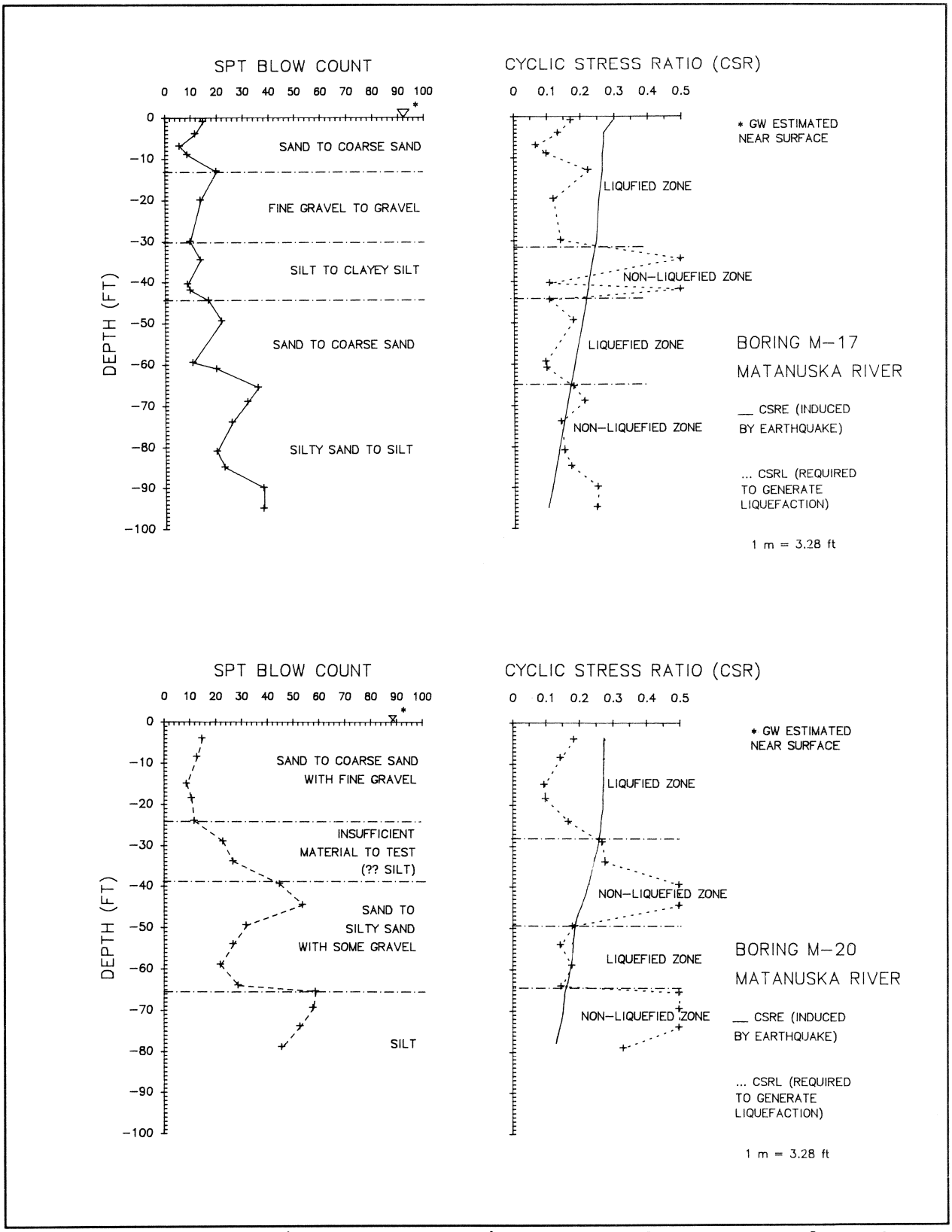

Figure 31 SPT Profile and Analysis, Bore Holes M-17 and M-20.

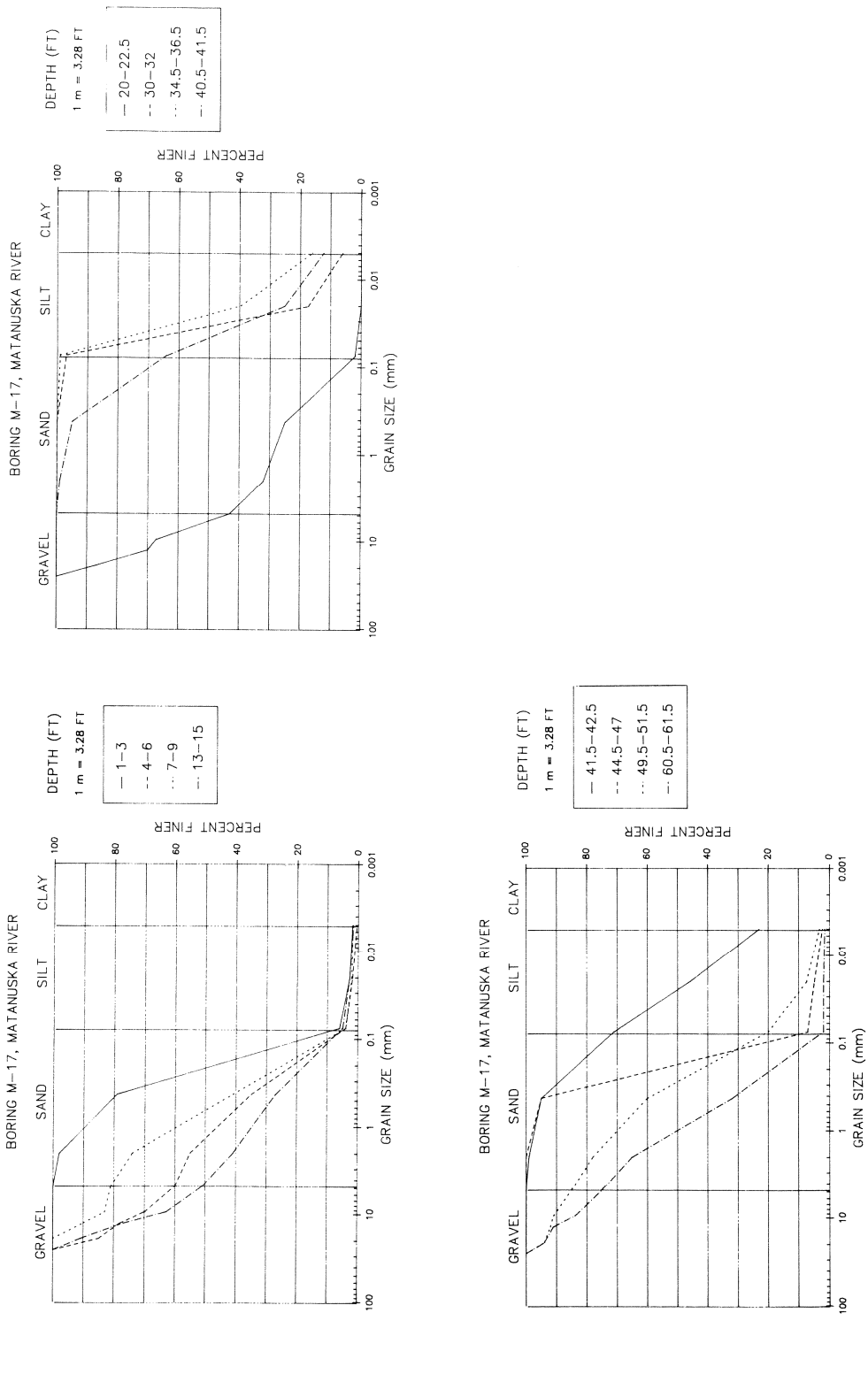

Figure 32 Grain-Size Distribution Charts, Bore Hole M-17.

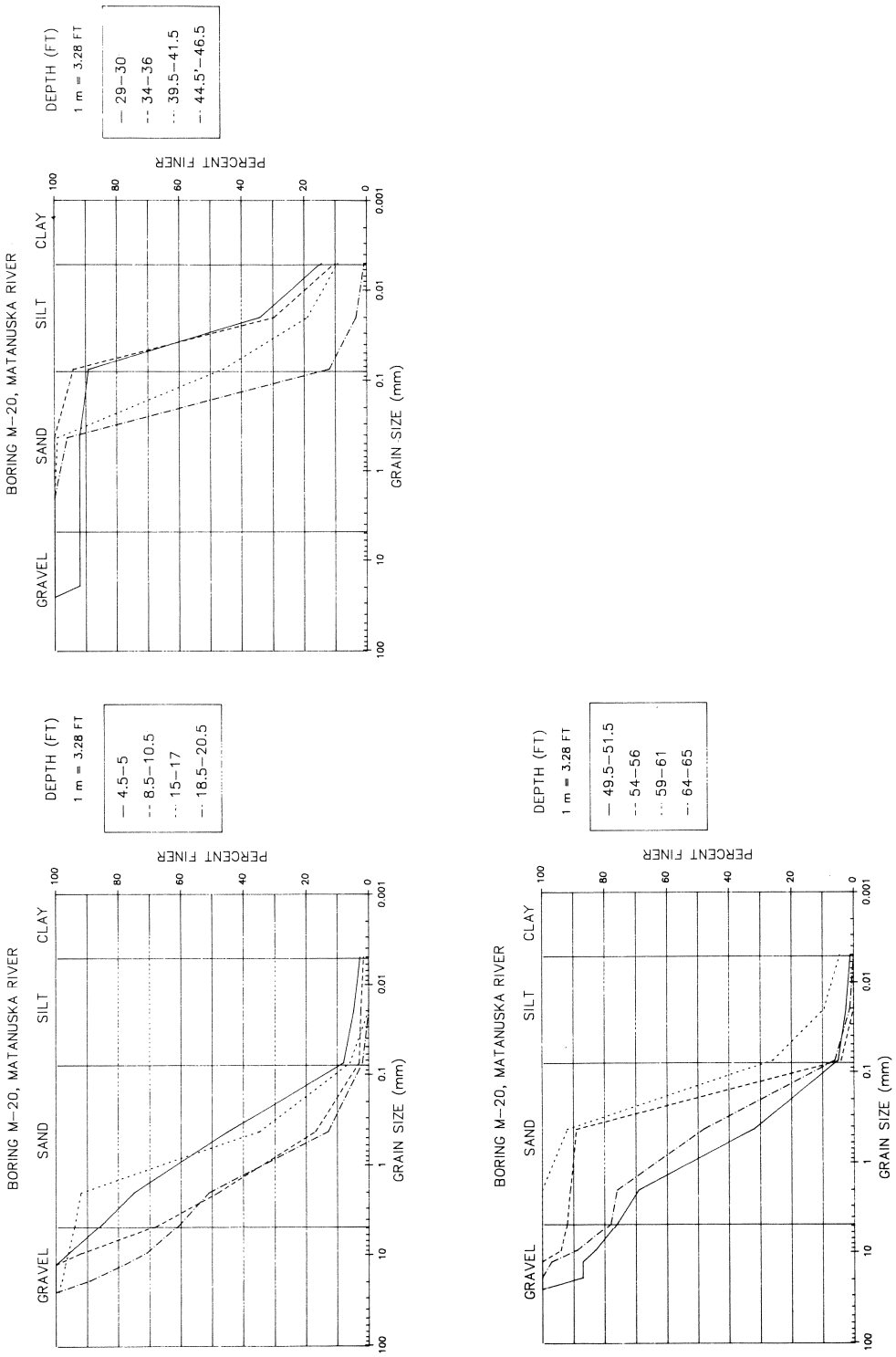

Figure 33 Grain-Size Distribution Charts, Bore Hole M-20.

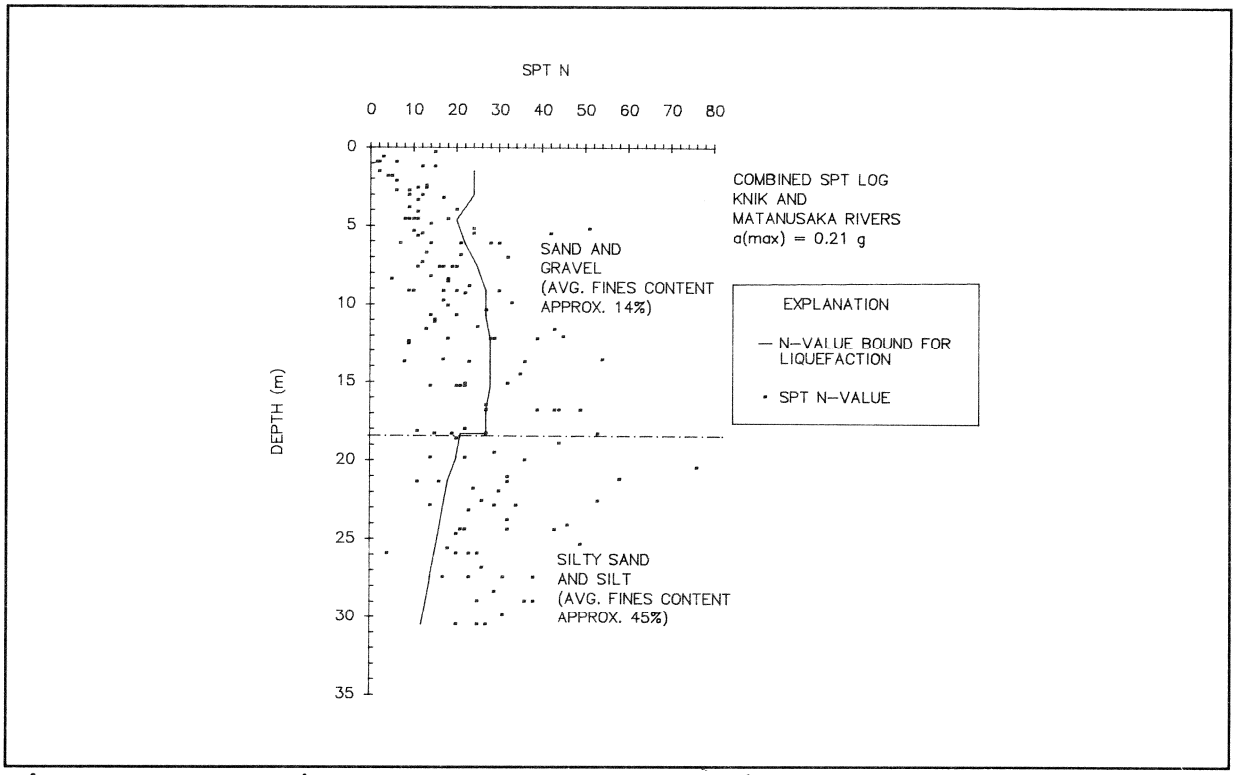

Figure 34 Combined SPT Log for the Knik and Matanuska Rivers.

4.5 RAILROAD BRIDGE AT MILEPOST 114.3, SHIP CREEK IN ANCHORAGE

4.5.1 INTRODUCTION

Ship Creek originates in the Chugach Range east of Anchorage and flows westward across the Anchorage lowland before draining into Knik Arm (Figure 1). Just east of its confluence with the Arm, Ship Creek has formed a 1 km wide valley separating downtown Anchorage to the south from Government Hill and Elmendorf Air Force Base to the north (Figure 35). Approximately 250 m north of First Avenue, the Alaska Railroad crosses Ship Creek at Milepost 114.3. Beyond that point, the rail continues eastward along Ship Creek Valley for another 5 km before turning northeastward.

4.5.2 GROUND FAILURE DISPLACEMENT AND DAMAGE

Railroad Bridge at Milepost 114.3 is a 37.5 m steel truss structure supported by concrete piers with a 10.6 m steel beam at each end (Figure 36). The concrete

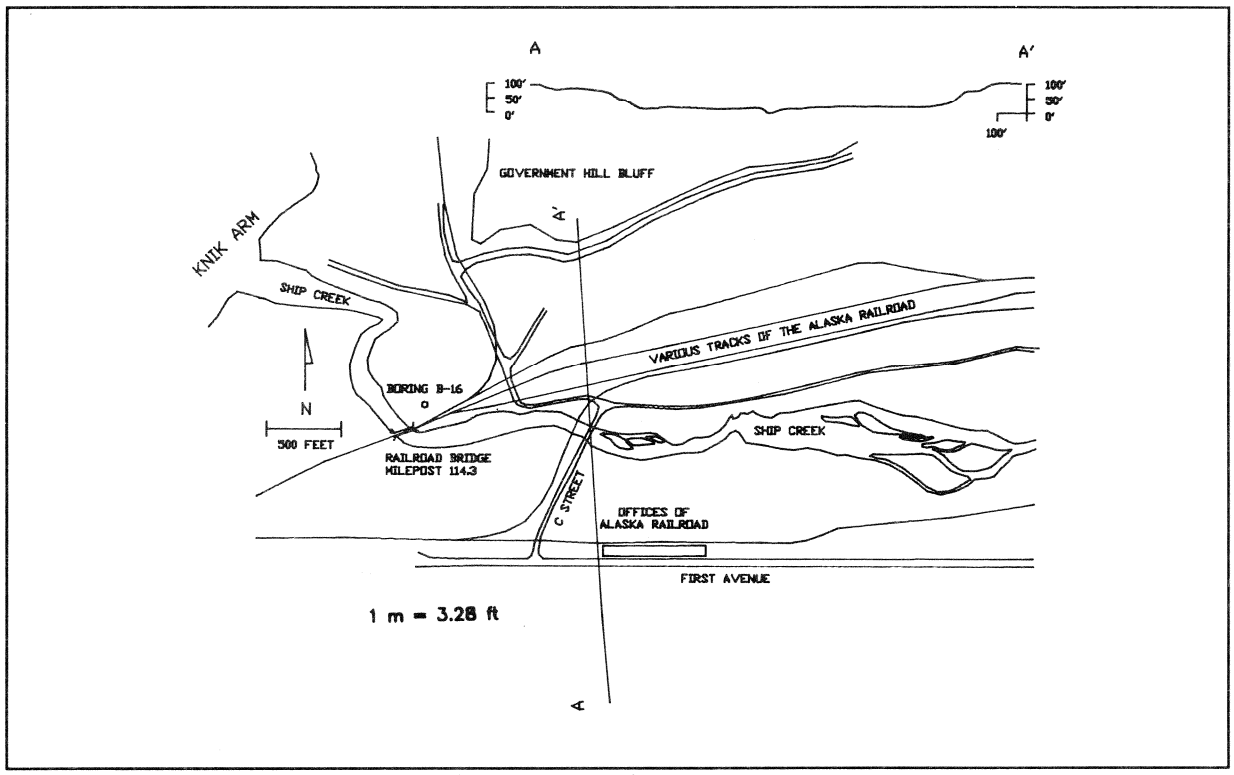

Figure 35 Map and Profile of Ship Creek, Anchorage, Alaska.

piers are founded on 45 wooden piles driven to a depth of 9 to 10.5 m. The abutments are supported by three railroad rails welded at the crown. These piles are driven to a depth of 20 to 38 m and the outside rows battered at a 13 degree angle (McCulloch and Bonilla, 1970). McCulloch and Bonilla report:

> "Abutments and piers shifted streamward, the deck was put in compression, and each end span jammed against the central span and into the abutment backwalls. Total compression at the deck was about 13 inches. Movement of the piers was so great that the expansion bearings were reset 9 1/2 inches from their former positions and the fixed bearings were displaced 5 1/2 inches (McCulloch and Bonilla, 1970, see Figure 36).

Lateral spread of stream banks toward the channel center caused approximately 325 to 375 mm of stream closure. (The distance measured from abutment to abutment decreased 325 mm, whereas, the distance between end piers decreased 375 mm - see Figure 36).

4.5.3 TOPOGRAPHY

A cross-section of Ship Creek Valley from the Alaska Department of Highways shows that Ship Creek is approximately 5 m deep and 40 m wide (Figure 35). The

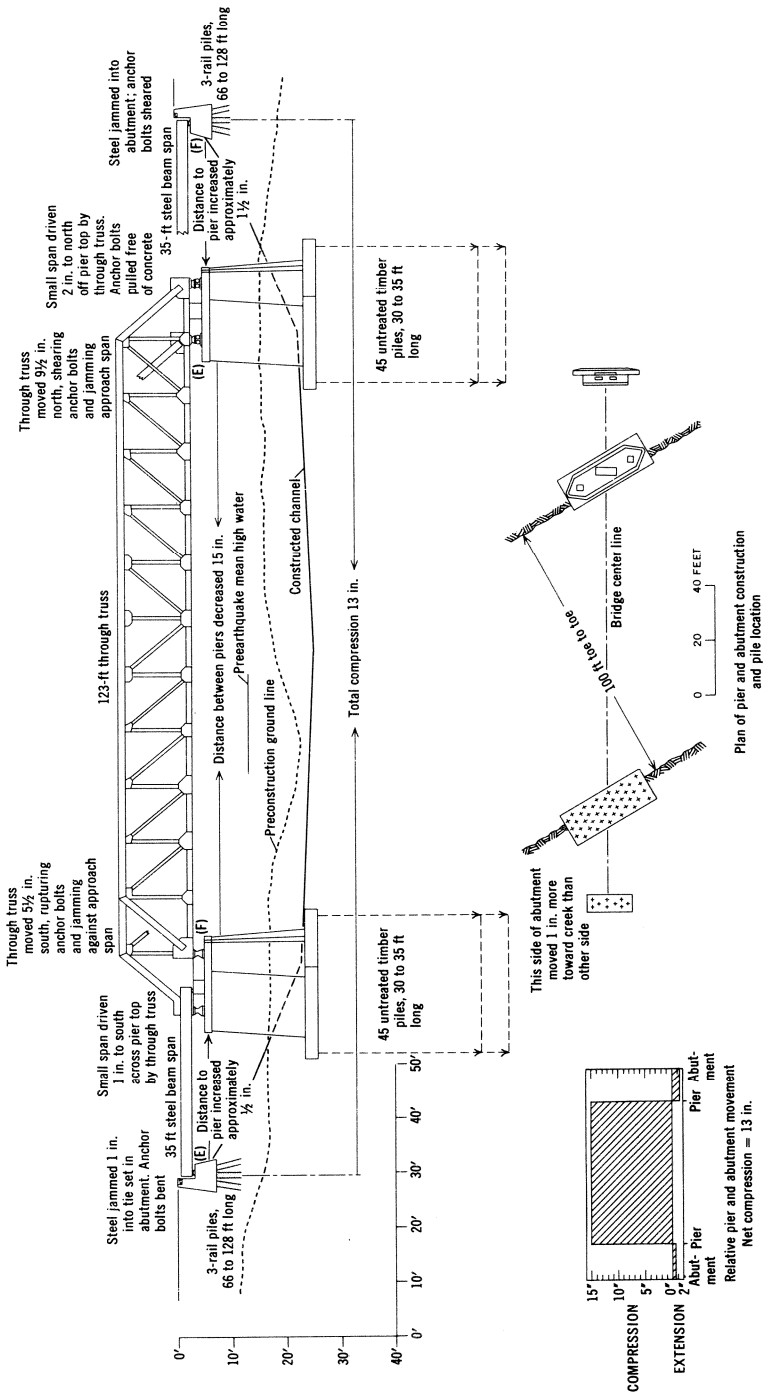

Figure 36 Construction of and Damage to Ship Creek Bridge at Milepost 114.3 (after McCulloch and Bonilla, 1970).

floodplain slopes approximately 3 percent into the channel on both sides of the creek.

4.5.3 SUBSURFACE SOIL CONDITIONS

At the bridge crossing, Ship Creek has deposited a veneer of fluvial gravel, sand, and silt upon estuarine-marine silt and clay. Borehole B-16 (Shannon and Wilson, 1987), located approximately 60 m north of the north bridge abutment is shown in Figure 35. Subsurface soils at this location consist of silt (from 0 to 6 m), underlain by a coarse sand with some gravel (from 6 to 9.5 m - see Figure 37).

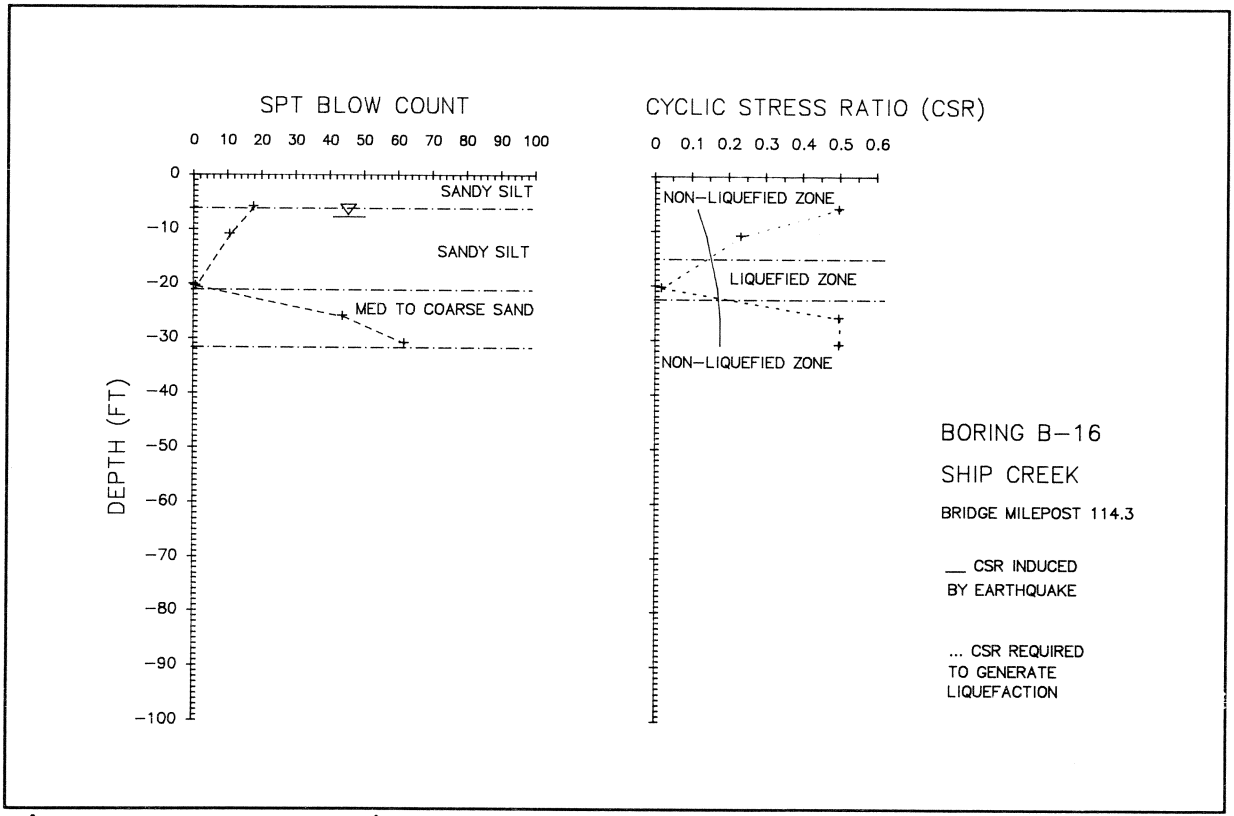

Figure 37 SPT Profile and Analysis, Bore Hole B-16, Ship Creek.

Liquefaction analysis of Borehole B-16 indicates that a zone from 4.5 to 6.5 m deep is liquefiable (Figure 37). The SPT values in this 1.5 m thick zone average 4 and range from 1 to 7. The SPT values in the underlying sand beginning at 6.5 m are too high to make the sand liquefiable.

4.6 BRIDGES ALONG SOUTHERN END OF TURNAGAIN ARM

4.6.1 INTRODUCTION

Southeast of Anchorage, the Alaska Railroad and Seward-Anchorage Highway parallel the northeast shore of Turnagain Arm (Figure 1). For much of the distance between Anchorage and Portage, the railroad and highway are confined to a narrow corridor between the Chugach Mountains and the shore of Turnagain Arm. A few kilometers north of Portage, the railroad and highway leave the steep coastline and cross the floodplain of Twenty-Mile River (Figure 38). From Portage, the Alaska Railroad and Seward-Anchorage Highway continue southeastward and cross two channels of Portage Creek. A few kilometers south of Portage, the railroad and highway routes separate. The railroad continues in a southerly direction along the eastern edge of Placer River. The Seward-Anchorage Highway bends westward around the southern end of Turnagain Arm and crosses the floodplain of Placer River about 1.2 km from the highway junction.

Like the Matanuska Valley, Turnagain Arm is a glacially carved trough where braided rivers meet the ocean. The tidal range in the Arm fluctuates approximately 12 m (Ross et al., 1973), forming a broad tidal flat at its southern terminus. The steepness of the valley walls bordering the Arm suggests that bedrock lies at a considerable depth below the unconsolidated sediment that fills the valley. Two water wells drilled at Portage penetrated sediment to a depth of 200 m without encountering bedrock. Most of the sediment found in these deep wells consists of silt and clayey silt apparently of estuarine origin. Coarser active and inactive fluvial deposits comprise the upper 12 m of the profile (McCulloch and Bonilla, 1970). Near the coastline, fluvial deposits from these rivers are inter-fingered with estuarine sediment. The water-table is very close to the surface throughout most of the area. Kachadoorian reports that groundwater was within 0.6 m of the surface near Portage at the time of the 1964 earthquake (Kachadoorian, 1968).

The floodplains of the Twenty-Mile River, Portage Creek and the Placer River coalesce at the southeastern edge of Turnagain Arm to form a broad flat flood plain dissected by sloughs and secondary channels. The floodplain is relatively flat with low topographical relief; the highest part standing only 6 m above high tide (McCulloch and Bonilla, 1970). Annual tidal fluctuation in the Arm is as much as 12 m (Utermohle, 1965). During high tide, flow in the Twenty-Mile River, Portage Creek and Placer River is reversed.

Approximately 1.5 m of regional tectonic subsidence resulting from the earthquake left many parts of the highway and railroad embankment within the tidal range and subject to flooding. Approximately 1 m of silt has been deposited on the floodplain around Twenty-Mile River since the earthquake. Subsidence and the subsequent deposition have slightly altered the channel configurations and downstream gradients in the area, but we assume that the rivers and creeks have returned to equilibrium since 1964 and channel geometries are similar to pre-earthquake conditions.

Lateral spread damage to railroad and highway bridges along the southern end of Turnagain Arm was extensive. McCulloch and Bonilla report 15 of the 17 railroad bridges in the area were

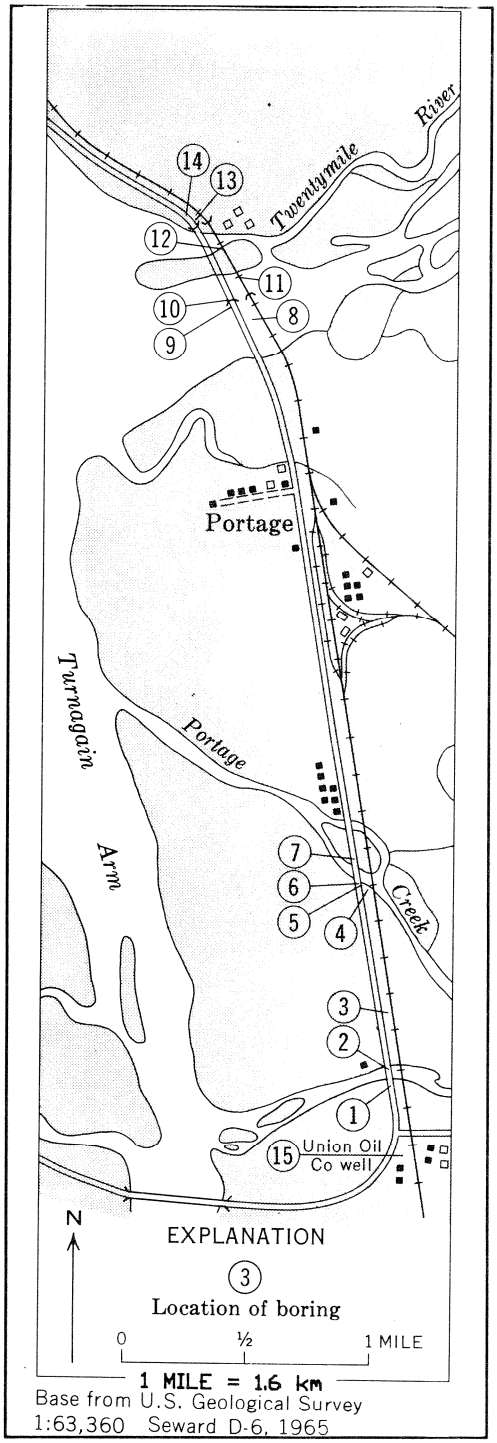

Figure 38 Location of Bore Holes along the Railroad and Highway near Portage, Alaska (after McCulloch and Bonilla, 1970).

open wood trestles on wooden piles. Of the 15 wood trestle bridges, four were damaged beyond repair; two of these were replaced with new bridges and two were replaced with culverts. Highway bridge damage along the southern end of Turnagain Arm was some of the most severe in south-central Alaska. All of the 15 highway bridges in the area were severely damaged or destroyed (Kachadoorian, 1968). Many highway bridges partially or completely collapsed.

4.6.2 RAILROAD BRIDGE AT MILEPOST 64.7, TWENTY-MILE RIVER

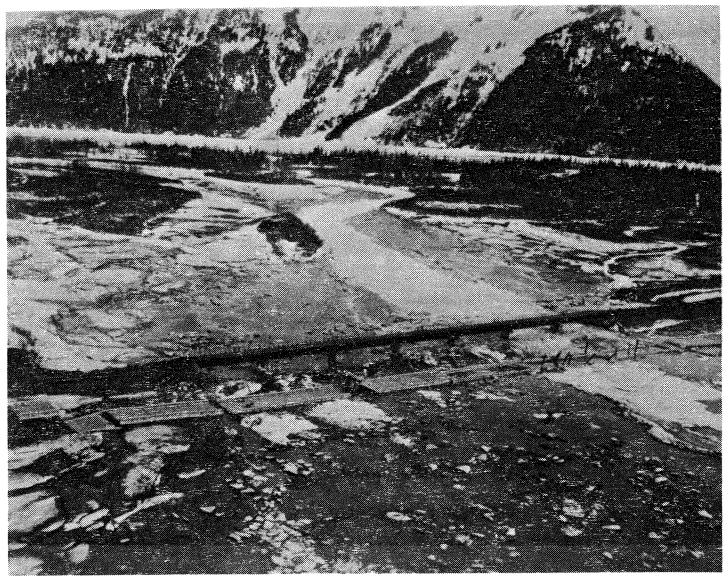

Figure 39 Damaged Railroad and Highway Bridges across the Twenty-Mile River.

The Railroad Bridge crossing the Twenty-Mile River is a 7 span 127.7 m long steel-truss structure supported by concrete piers (Figure 39). The piers and abutments are each founded on 11 to 14 steel piles composed of three railroad rails welded together at the crown (McCulloch and Bonilla, 1970).

4.6.2.1 GROUND FAILURE DISPLACEMENT AND DAMAGE

Evidence of liquefaction was abundant on the both sides of Twenty-Mile River. McCulloch and Bonilla report damage to the embankment (starting from the south side of the Twenty-Mile River and continuing to the north side).

> "Settlement occurred along the main-line embankment as it approached the Twenty-Mile River Bridge. In the last 200 feet south of the bridge, settlement increased abruptly to 5 feet, where the embankment was severely fractured by cracks that ran approximately parallel to the track in the upper edge of the slope of the fill. These cracks were joined to others in the adjacent flood-plain sediments by cracks running approximately normal to the embankment. Similar cracking, but with more pronounced tension cracks, some of which also had small lateral displacements, occurred in the north bridge approach."

Earthquake damage to Railroad Bridge Milepost 64.7 was substantial, but the bridge remained passable (McCulloch and Bonilla, 1970). McCulloch and Bonilla visited the bridge after repairs had been made. Hence, they did not have an opportunity to measure differential movements between all the spans and piers. They report however that the bridge was compressed approximately 1.6 m by lateral spread of the river banks toward the channel:

> "Displacements shown on the Figure [40] are only larger movements of two piers relative to the bearings of the overlying spans. Movement of the piers must have been more general, because compression at the deck level jammed all the trusses together, and drove the end trusses into the abutments and broke away the backwalls. Anchor bolts were sheared on three piers and the abutments. The positions of the rebuilt abutment backwalls and the base of the pre-earthquake abutments indicate that total compression was about 5 feet 2 inches (McCulloch and Bonilla, 1970)."

A post-earthquake study by the Alaska Railroad revealed that the northern abutment had settled 0.27 m relative to a U.S.G.S. bench mark located on bedrock 3 km to the north. Because no differential settlement was observed in the bridge substructure, it appeared that all piers must have settled somewhat uniformly from compaction of the underlying sediment (McCulloch and Bonilla, 1970).

All spans of the adjacent highway bridge (Bridge #634) collapsed (Figure 39). The south and north approach to the highway bridge subsided 0.5 and 0.1 m respectively. The north bridge abutment was broken by fissures and all piles were broken (Kachadoorian, 1968).

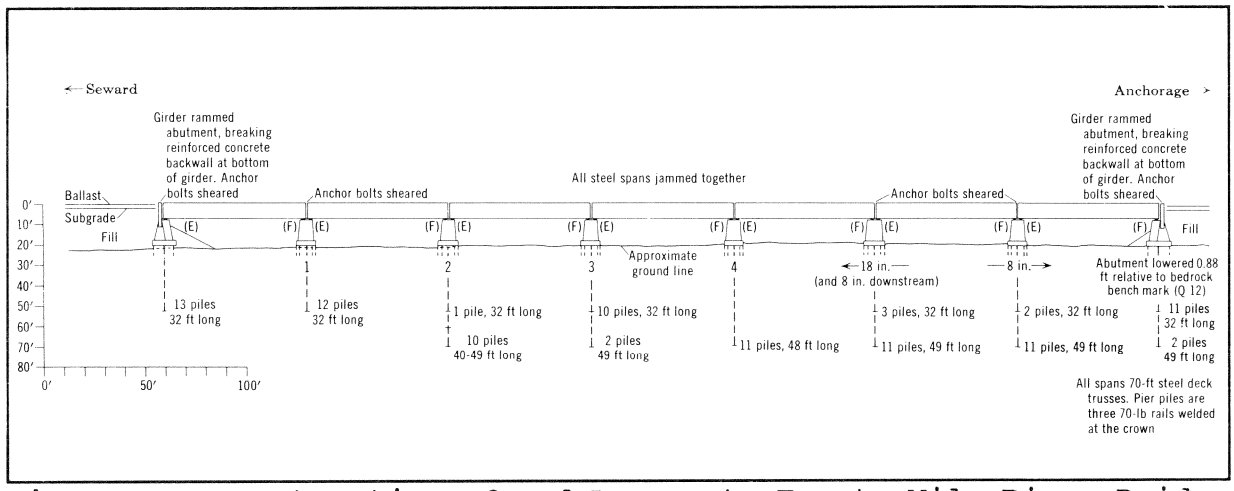

Figure 40 Construction of and Damage to Twenty Mile River Bridge (after McCulloch and Bonilla, 1970).

4.6.2.2 TOPOGRAPHY

Topographical relief on the north and south side of the Twenty-Mile river is small (Figure 41). In 1989, we measured a levy that slopes approximately 0.2 percent away from the channel on the north side of the river. The floodplain on the south side of the river slopes approximately 0.1 percent toward the channel. Presently, the river bottom is 5 m below the floodplain near the bridge. The downstream gradient of the river is 0.06 percent to the west. A 1950 cross-section by the Alaska Railroad at the bridge shows the channel bottom at 5.7 to 6.9 m below rail elevation and approximately 3.6 m lower than top of bank. Our 1989 survey of the channel, revealed a channel bottom approximately 9 m below rail elevation and approximately 4.8 m lower than top of bank (Figure 41). However, vertical elevation changes at the bridge resulting from tectonic subsidence and subsequent deposition and the raising of the bridge piers approximately 1.5 m during bridge repair, make it difficult to establish how the channel cross-section has changed since 1950.

4.6.2.3 SUBSURFACE SOIL CONDITIONS

Utermohle reports that subsurface conditions near the Twenty-Mile River are quite similar to those observed at the Knik and Matanuska Rivers except that gravel is

more limited and smaller at the Twenty-Mile River. The sediment at the Knik and Matanuska River was commonly 20 percent medium and coarse grained gravel, whereas, at Twenty-Mile River it was only about 5 percent medium and coarse grained gravel (Utermohle, 1965). The location of four boreholes (#14, #11, #10, #8) drilled for the reconstruction of Highway Bridge No. 634 (Utermohle, 1965) are shown on Figure 41. The soil logs show layers of gravel, silty gravel and sand in the upper 6 to 9 m (Figures 42 - 44). In general, sediments below 9 m become finer and less gravelly with depth. Liquefaction analyses for Boreholes #14, #11, #10, #8 indicates that N averages 20.7 in the liquefiable zone(s) and ranges from 10 to 33 (Figures 42 - 43). The liquefiable sediments begin at an average depth of 5.0 m and average 9.3 m thick for these four boreholes.

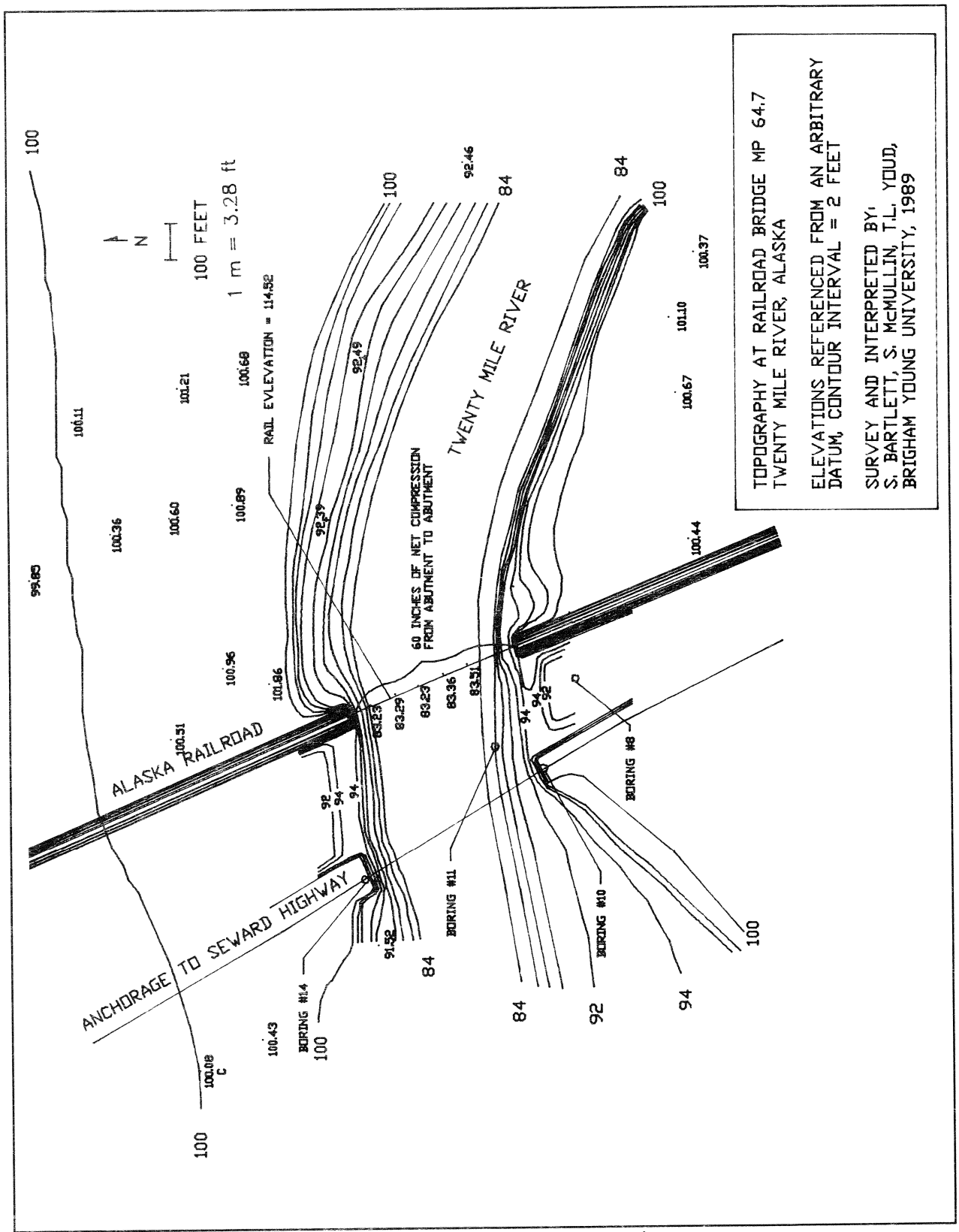

Figure 41 Contour Map of the Twenty-Mile River.

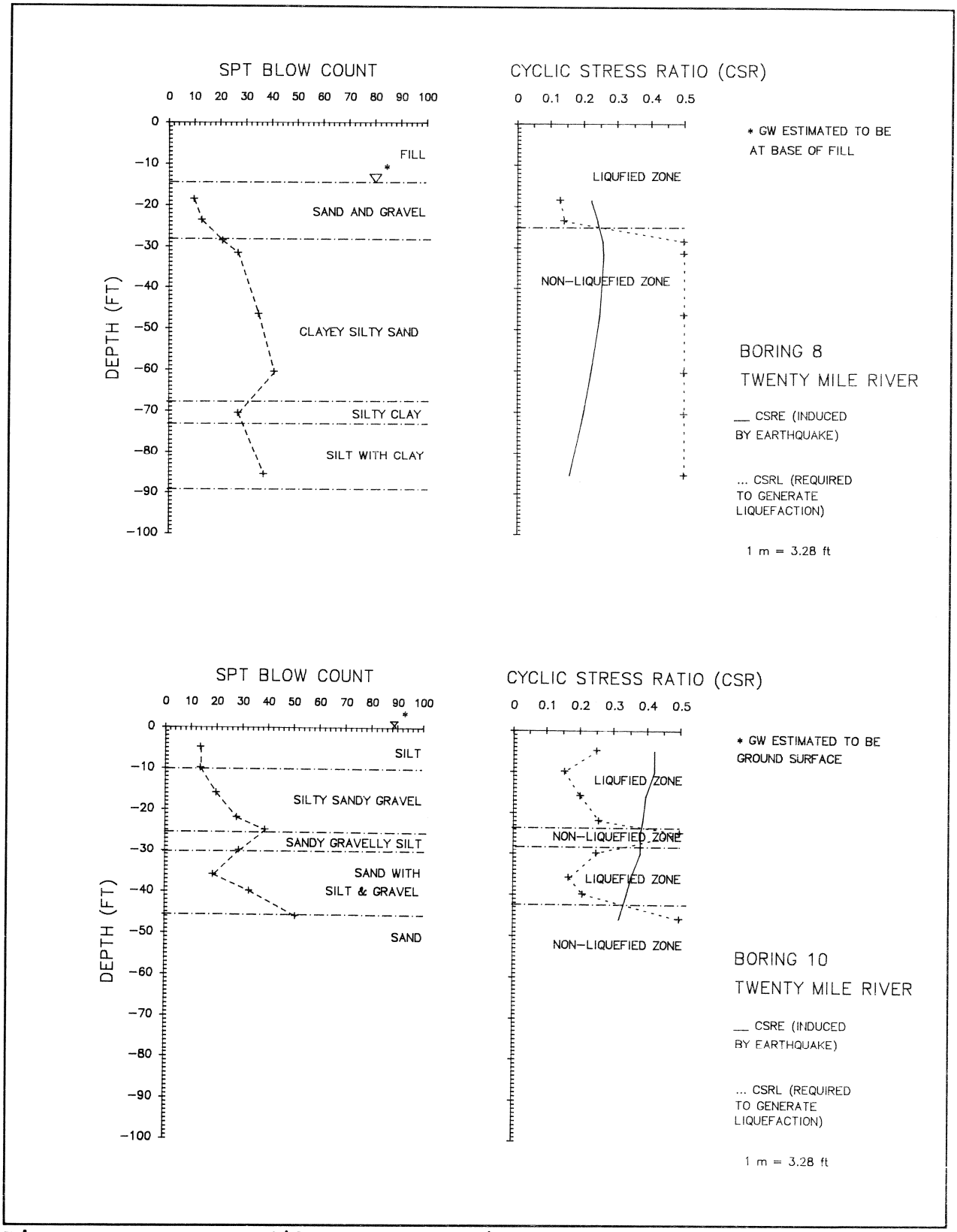

Figure 42 SPT Profile and Analysis, Bore Holes 8 and 10.

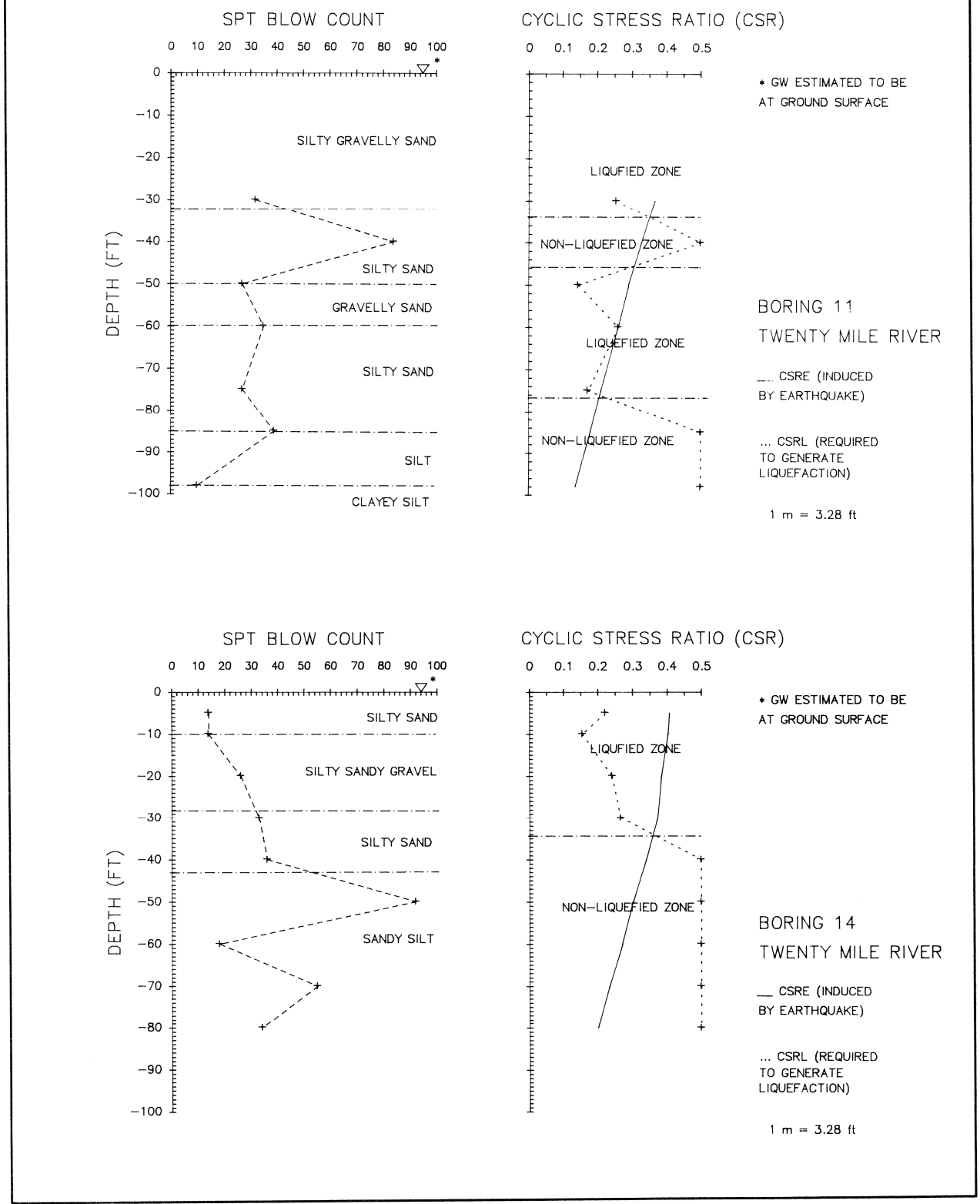

Figure 43 SPT Profile and Analysis, Bore Holes 11 and 14.

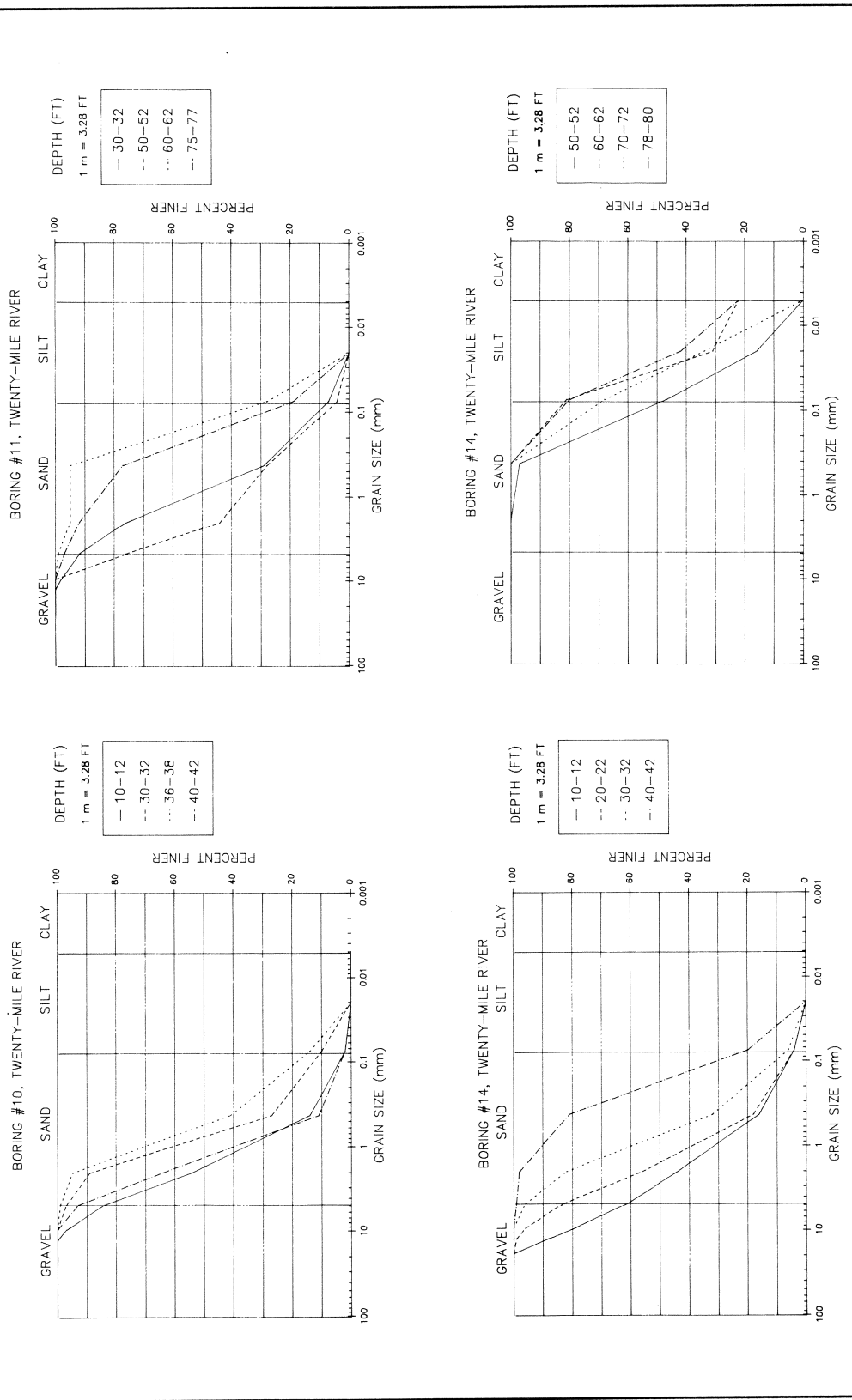

Figure 44 Grain-Size Distribution Charts, Bore Holes 10, 11, 14.

4.6.3 RAILROAD BRIDGE AT MILEPOST 63.5, PORTAGE CREEK

South of Portage the Alaska Railroad crosses two channels of Portage Creek (Figure 38). In 1964, a small island separated two railroad bridges at Mileposts 63.6 and 63.5. Both bridges were irreparably damaged. The northern bridge was replaced with a culvert and the southern bridge was replaced with a new bridge following the earthquake.

4.6.3.1 GROUND FAILURE DISPLACEMENT AND DAMAGE

Ground fissures were prevalent on both sides of the southern bridge (Figure 45). One hundred and twenty meters south of the bridge, the rail was pulled apart 0.3 m by a crack which crossed the railroad and highway embankment. On the small island which separates the railroad bridges, an orthogonal pattern of fissures offset sections of the adjacent highway 0.6 m. The railroad embankment on the island settled as much as 1.6 m (McCulloch and Bonilla, 1970). McCulloch and Bonilla summarize the ground displacement and damage near Bridge Milepost 63.5 as follows:

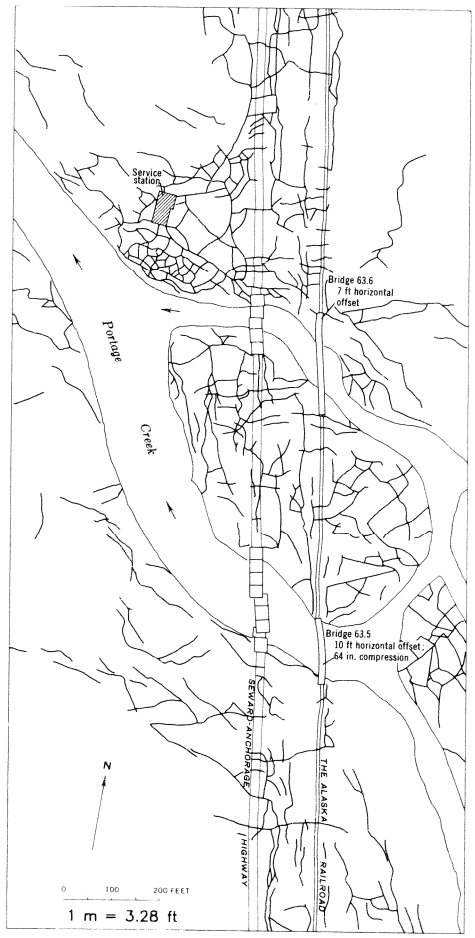

Figure 45 Ground Cracks at Portage Creek near Railroad Bridges at Mile Posts 63.5 and 63.6 (after McCulloch and Bonilla, 1970).

> "Compression at Bridge 63.5, a 149.6-foot 11-bent open wood trestle, was so great that the deck was driven through, and 64 inches beyond, the south bulkhead; the deck rode upward and over the top of the embankment fill. This overthrusting produced a sag at the south end of the bridge deck, because the fill had not been locally lowered at the bulkhead. Beneath the deck the tops of the piles were progressively higher toward the center of the stream, and where the deck was supported by the piles it was arched

upward about 1 foot [Figure 46]. At the south end, compression also tore about 56 feet of rails from the ties that were frozen in the ballast and bowed the rails 10 1/2 feet to the west. At the north bulkhead the stringers rammed 2 inches into the fillers. Compression was accompanied by a considerable amount of streamward shifting of the piling, and the bridge was skewed horizontally about 10 feet, its south end moving east relative to its north end (McCulloch and Bonilla, 1970)."

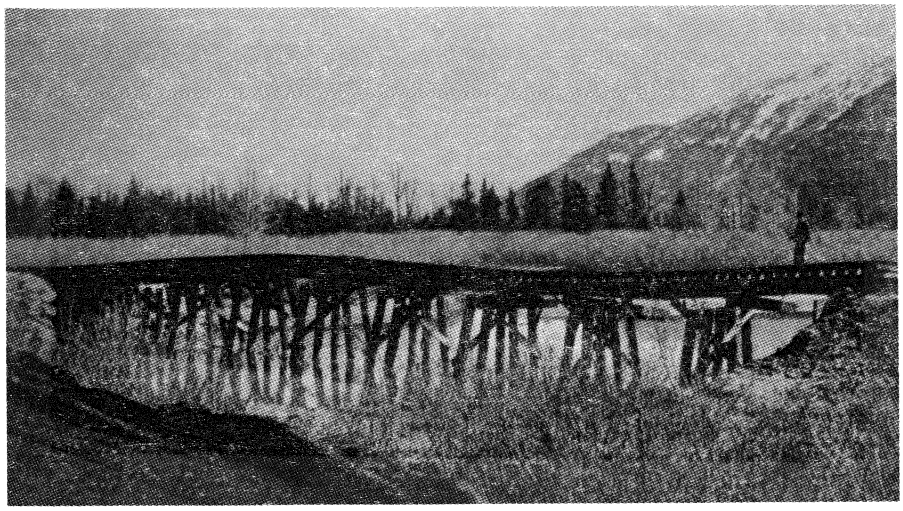

Figure 46 Damage to Railroad Bridge at Mile Post 63.5 (south abutment is on right-hand side, from McCulloch and Bonilla, 1970).

The inset on Figure 47 shows the depth of pile penetration and channelward pile displacements for Bridge 63.5. It appears that the south end of the bridge (left end of inset) displaced streamward considerably more than the north end. The second pier on the south end of the bridge displaced 1.85 m toward the channel. The end pier on the north side of the bridge did not displace. Because the alignment of the bridge was oblique to the channel, lateral spread toward the channel skewed the railroad bridge deck approximately 3 m (inset on Figure 47).

The adjacent highway bridge (Bridge No. 631) collapsed. Kachadoorian reports the following in a summary table of earthquake highway damage:

"[The] south approach subsided 18 inches; [the] north approach subsided 24 inches. Both abutments [were] destroyed; all piling destroyed, spans [were] twisted and [had] collapsed, some [were] under water (Kachadoorian, 1968)."

4.6.3.2 TOPOGRAPHY

Since 1964, siltation has filled the steam channel which flowed to the north and under the northern bridge. The floodplain north and south of Bridge 63.5 slopes approximately 0.2 percent toward the channel. Presently, the channel beneath the bridge is approximately 6.7 m below rail elevation and 3.7 m below the stream banks (Figure 47, 1989 survey). This channel of Portage Creek flows westward along a 0.11 percent gradient into Turnagain Arm.

4.6.3.3 SUBSURFACE SOIL CONDITIONS

The subsurface soil conditions at Portage Creek are very similar to those at Twenty-Mile River. Boreholes from the adjacent highway (Utermohle, 1965) reveal that the upper 12 to 15 m of the profile is comprised of coarser grained soil (e.g., sand, gravelly sand and sandy gravel) with some inter-bedded silty sand and sand silt (see profiles and grain-size data shown in Figures 48 - 51). Below 12 to 15 m the sediment is finer and consists predominately of silty sand, sandy silt and silt.

A liquefaction analysis of 4 highway bridge boreholes (#4, #6, #7, #TA-B-4) indicates that N averages 17 in the liquefiable zone(s) and ranges from 5 to 28 (Boreholes #4, #6, #7 are from Utermohle, 1965, Borehole #TA-B-4 is SPT log provided by the Alaska Division of Geology and Geophysics). Liquefiable sediments begin at an average depth of 3 m and are on average 7.5 m thick for the four boreholes. Borehole #TA-C-4 (Figure 50), a cone penetration log provided by the Alaska Division of Geology and Geophysics, has been converted to an equivalent SPT log (see Section 3.5). Analysis of the CPT data indicates liquefiable sediment at 5.5 to 7 m in sand to silty sand and from 8.8 to 9.8 m in sand to sandy silt. The calculated thickness of liquefiable sediment is notably less for the CPT log. Thus, the continuous CPT log discovered more non-liquefiable soil layers than were sampled by standard penetration testing.

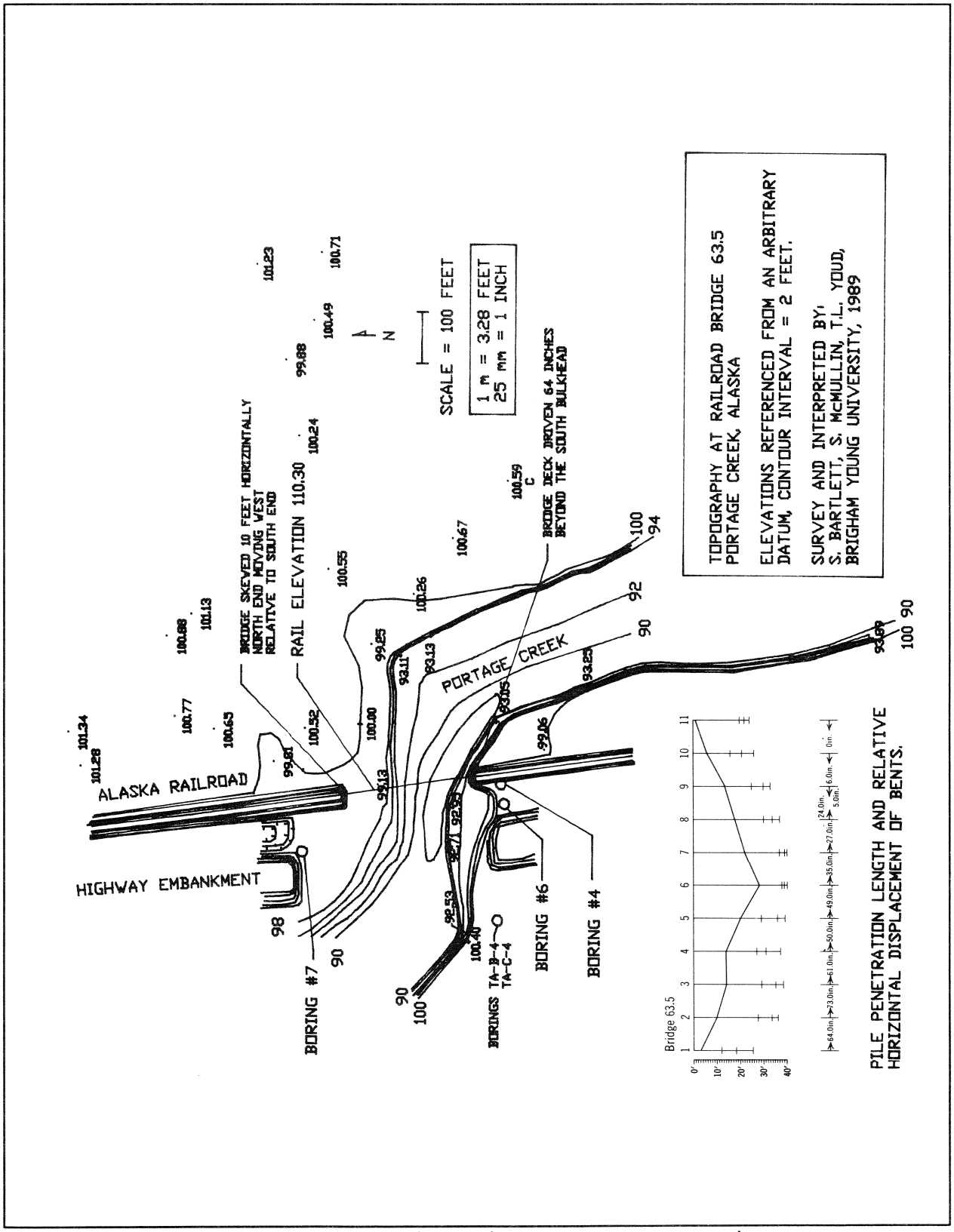

Figure 47 Contour Map and Pile Displacements at Milepost 63.5.

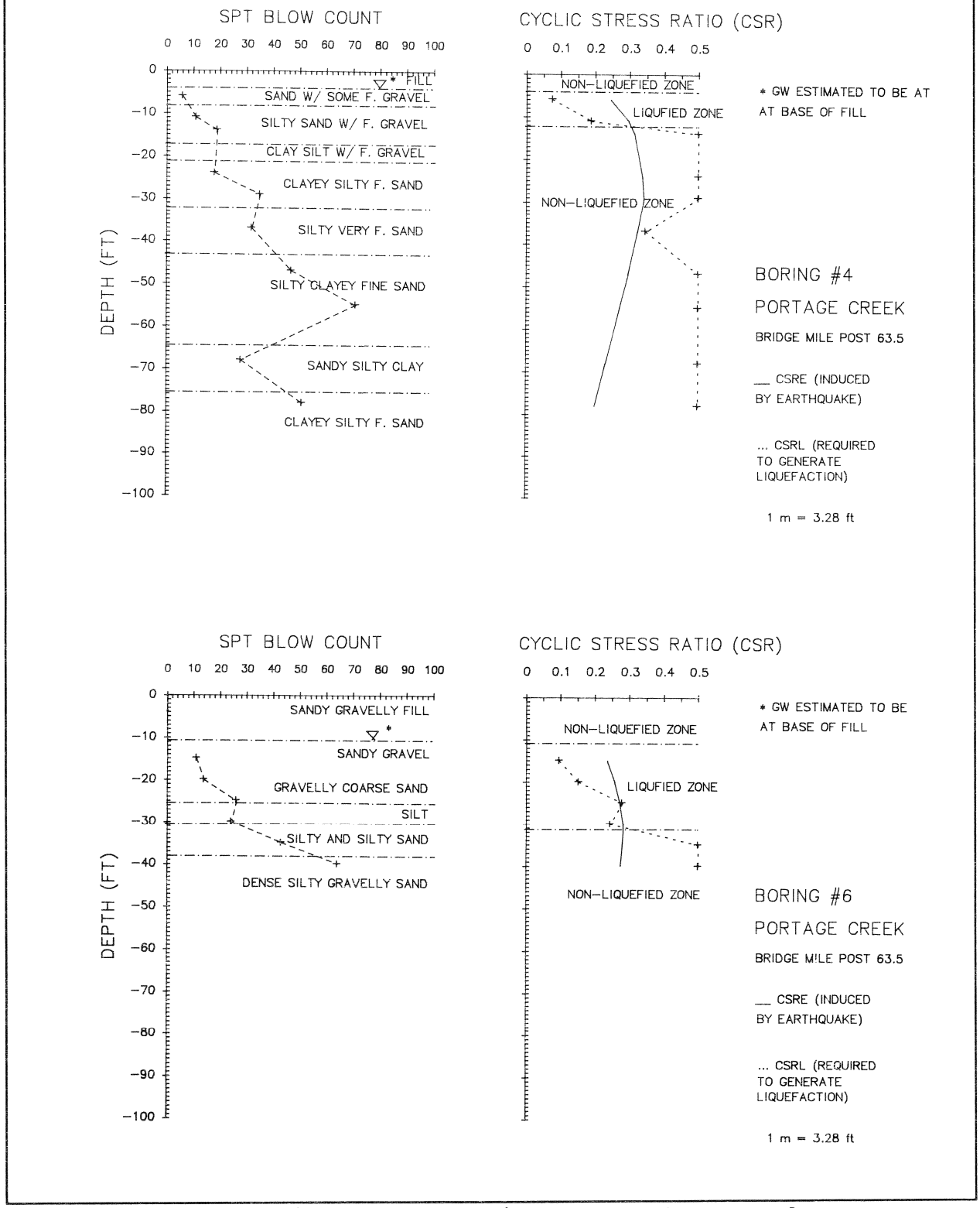

Figure 48 SPT Profile and Analysis, Bore Holes 4 and 6.

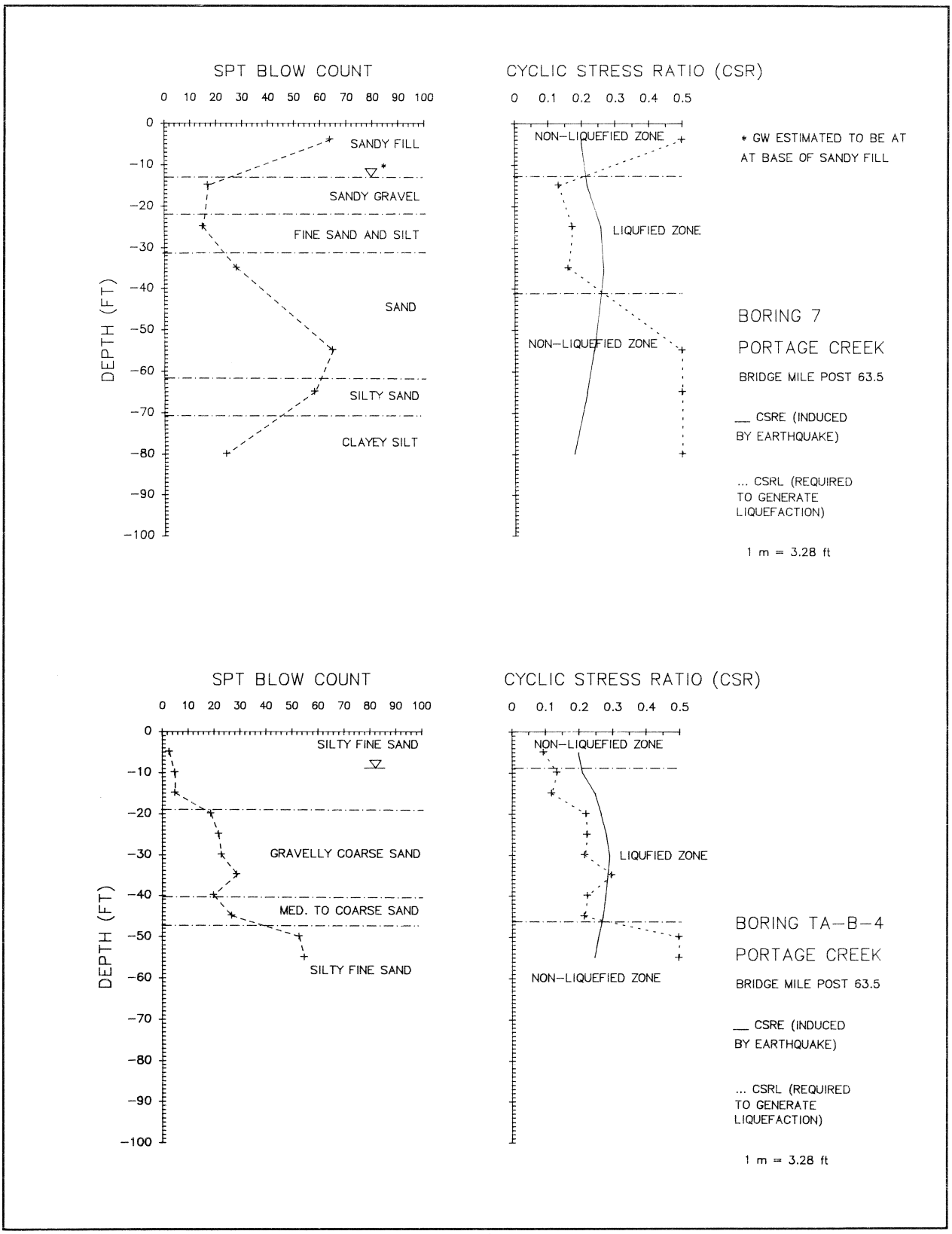

Figure 49 SPT Profile and Analysis, Bore Holes 7 and TA-B-4.

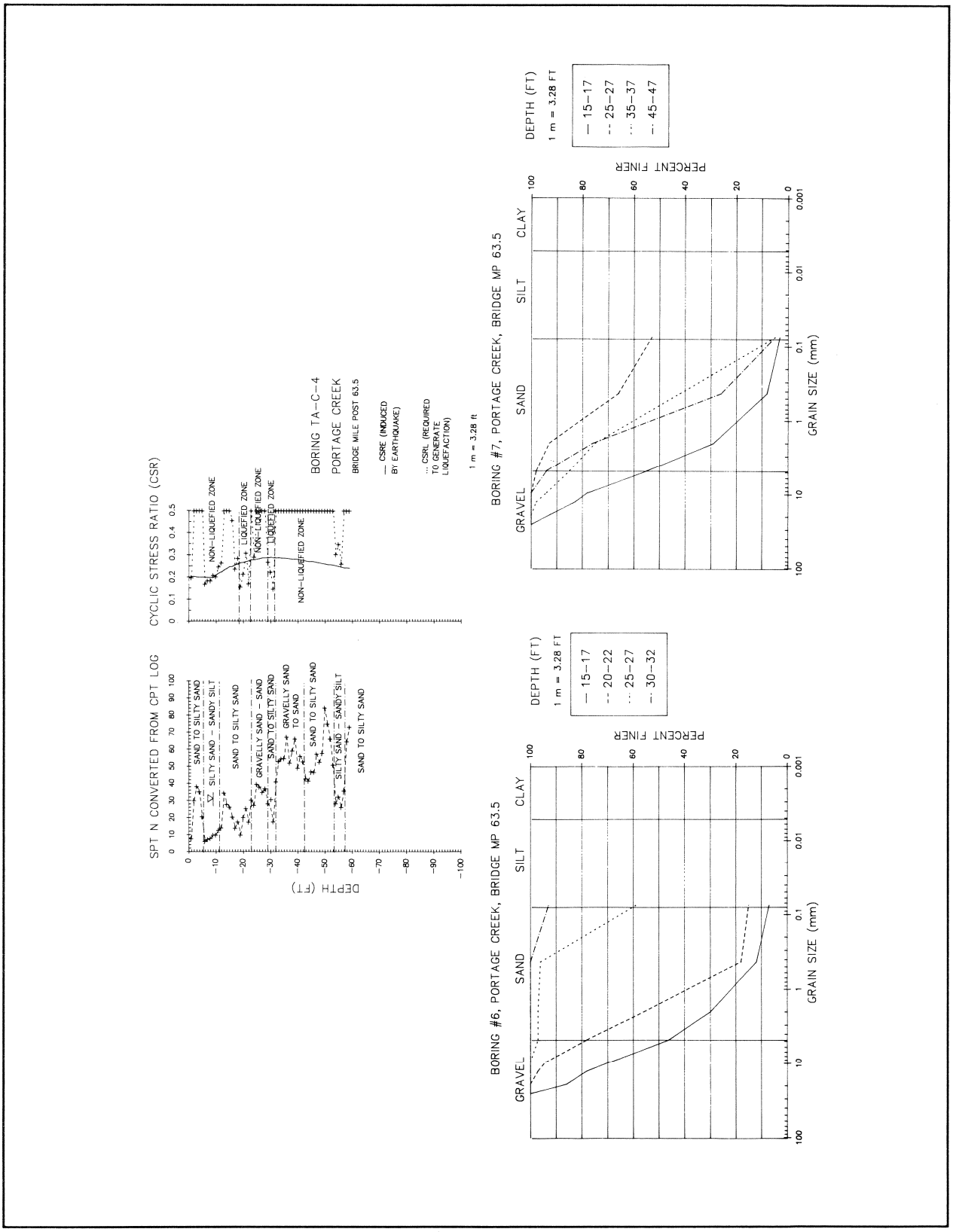

Figure 50 SPT Profile and Grain-Size Data, Bore Holes TA-C-4,6,7.

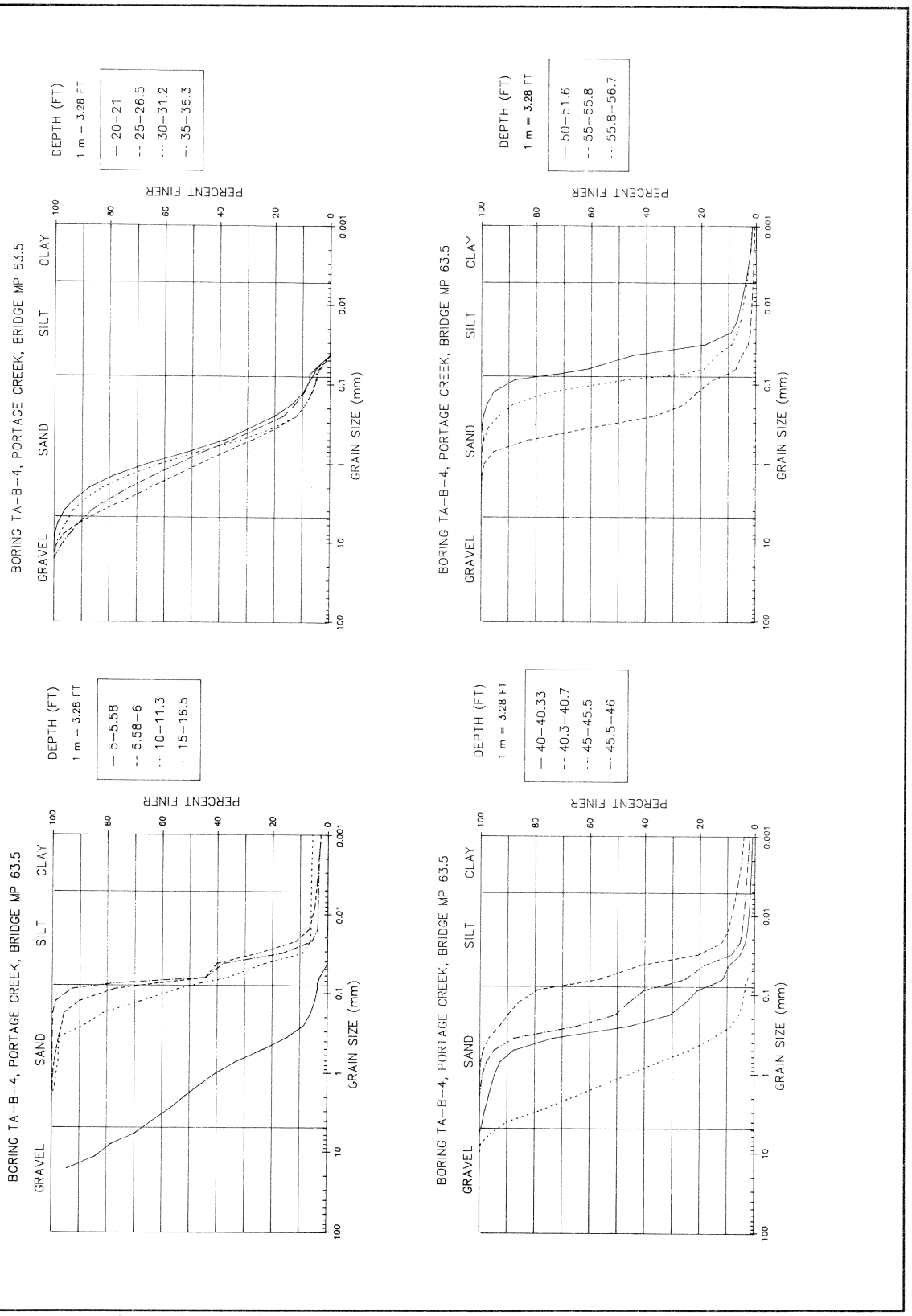

Figure 51 Grain-Size Distribution Charts, Bore Hole TA-B-4.

4.6.4 RAILROAD BRIDGE AT MILEPOST 63.0, PORTAGE CREEK

One kilometer south of the Bridge at Milepost 63.5, the Alaska Railroad and Seward-Anchorage Highway cross another channel of Portage Creek near Railroad Milepost 63.0 (Figure 38, channel just north of Union Oil Company Well). This bridge is a 59.4 m 14-bent open wood trestle (McCulloch and Bonilla, 1970).

4.6.4.1 GROUND FAILURE DISPLACEMENT AND DAMAGE

McCulloch and Bonilla describe ground fissures on the north side of the creek:

> "Six tension fractures lying within, and produced by, the 200-foot-wide zone of stream-margin cracking crossed the embankment north of Bridge 63.0. One fracture in the zone, about 35 feet north of the bridge was about 3.5 feet wide, and the embankment south of the fracture shifted 1 foot to the west [Figure 52 - foreground].

McCulloch and Bonilla report damage to the bridge deck as follows:

> ". . .[The deck] was compressed approximately 7 feet. The compression produced a sharp lateral kink in the deck with a deflection of about 8 feet and the stringers were broken at the apex of the kink. . . .[the] bents not torn free of the bridge were dragged laterally through the sediments by the deflecting deck, and most bents shifted streamward."

Embankment settlement on both sides of the bridge also occurred:

> "The embankment on both sides of the bridge was lowered, 8 inches at the south bulkhead and about 2 feet at the north bulkhead beyond the few feet of embankment bulldozed up by the deck. The entire embankment north of the bridge was lowered, about 3 feet near the bridge. . . (McCulloch and Bonilla, 1970)."

An inspection of the channelward pile displacements recorded by McCulloch and Bonilla suggests that the most of the displacement occurred on the north side of the bridge (see inset on Figure 53 also see Plate #3, McCulloch and Bonilla, 1970). In addition to 2.1 m of deck compression, McCulloch and Bonilla show that the north abutment displaced 0.36 m downstream (inset on Figure 53).

All spans of the adjacent highway bridge (No. 630) collapsed from differential ground movement. The north and south approaches subsided 1.1 and 0.7 m respectively (Kachadoorian, 1968).

4.6.4.2 TOPOGRAPHY

Figure 53 is a topographical map of the bridge site surveyed in 1989. The floodplain north of the bridge slopes 0.2 percent away from the channel at the

bridge. South of the bridge, the floodplain slopes less than 0.05 percent toward the channel. The channel is incised approximately 5 m below rail elevation and 2 m below the top of bank. This channel of Portage Creek flows on a 0.25 percent gradient into Turnagain Arm.

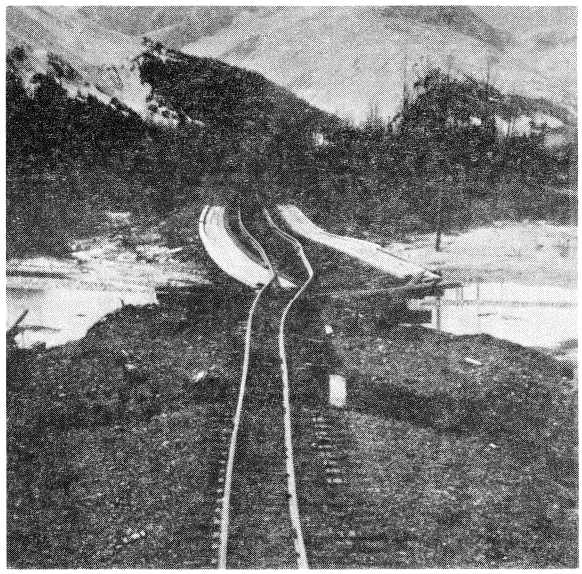

Figure 52 Damage to Bridge at Milepost 63.0 (looking south - from McCulloch and Bonilla, 1970).

4.6.4.3 SUBSURFACE CONDITIONS

A subsurface investigation for the reconstruction of the adjacent highway bridge (Utermohle, 1965) shows the upper 2.5 m of the profile is composed of a silty sandy gravelly fill (Figure 54). From 2.5 to 8 m, the soil is mainly a sandy silt. Below 8 m, dense silty sand and sandy gravel extend to 21 m. Liquefaction analysis of Borehole #2 indicates that a layer of sandy silt and silty sand is liquefiable from 4.5 to 11.7 m. The SPT values average 24 in this zone and range from 18 to 36 (Figure 54).

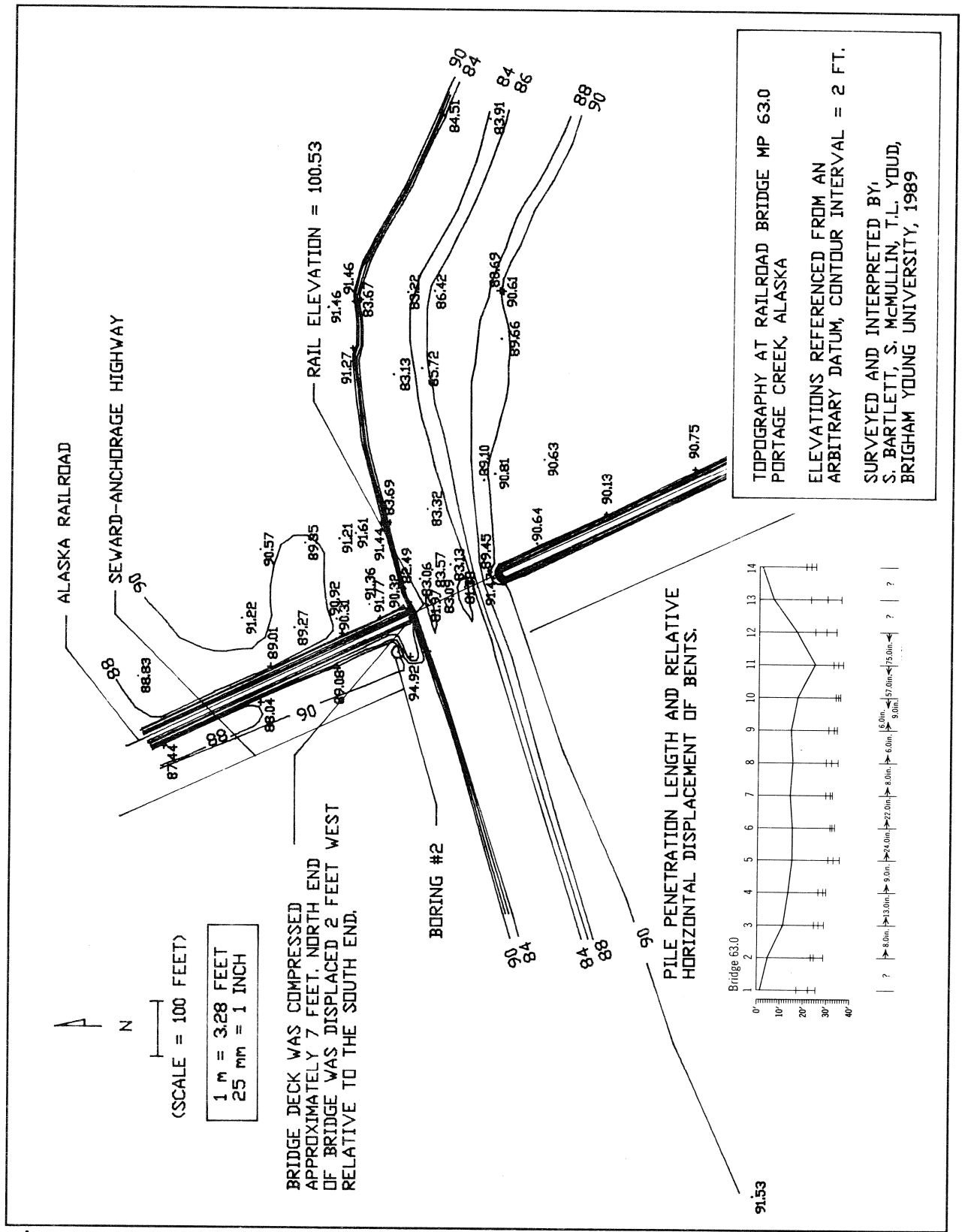

Figure 53 Topography and Displacements at Bridge Mile Post 63.0.

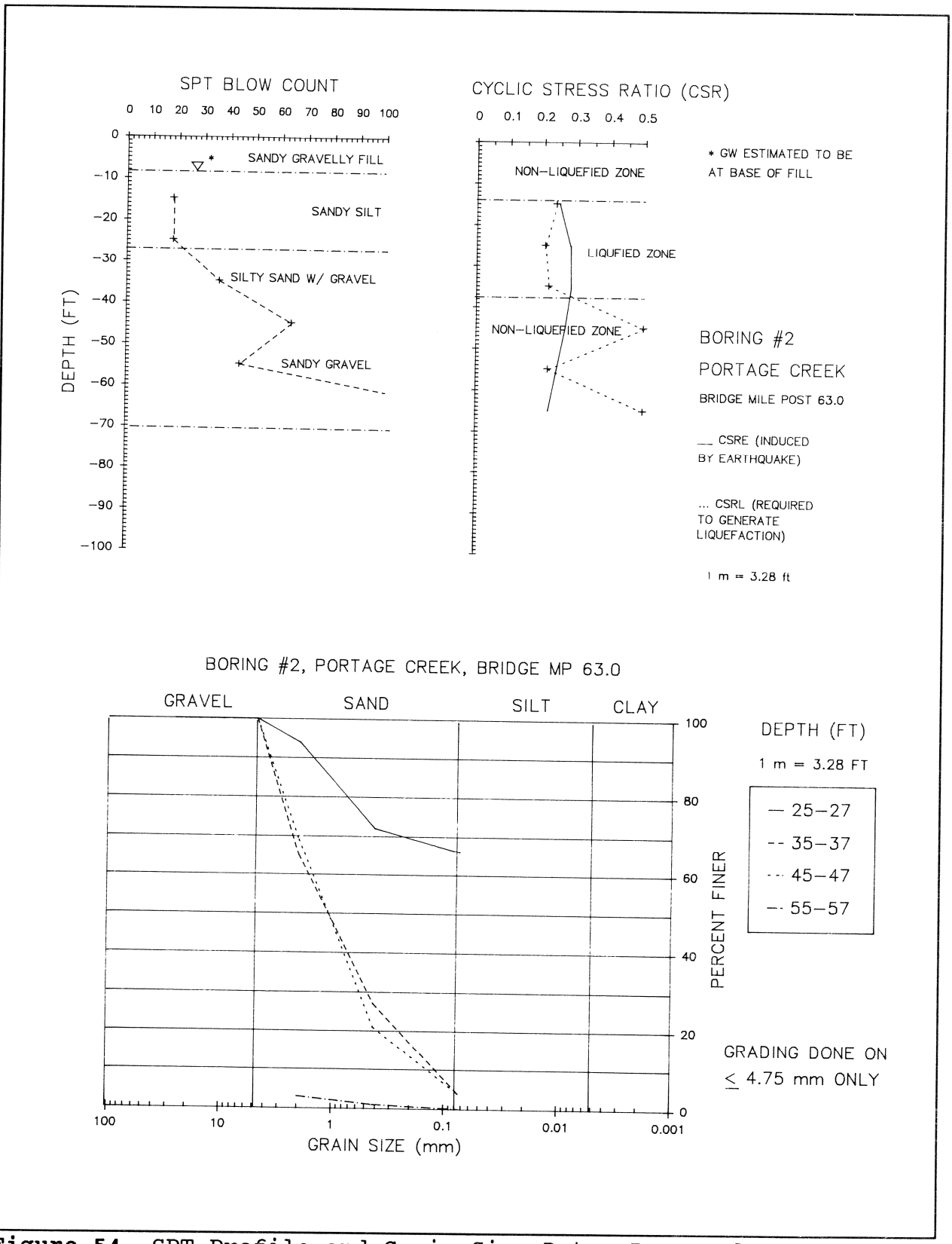

Figure 54 SPT Profile and Grain-Size Data, Bore Hole 2.

4.6.5 HIGHWAY BRIDGE NUMBER 629, MAIN CROSSING PLACER RIVER

4.6.5.1 GROUND FAILURE DISPLACEMENT AND DAMAGE

Approximately two-tenths of a kilometer south of Railroad Milepost 63.0, the Seward-Anchorage Highway leaves the Alaska Railroad. The highway makes a large bend around the southern tip of Turnagain Arm and crosses the floodplain of the Placer River via Bridge No. 629 (Figure 38). Before the earthquake, this bridge was a 137 m reinforced concrete bridge supported by timber piles. The bridge collapsed from channelward movement of liquefied sediments. Kachadoorian gives a terse description of the damage:

> "Both abutments [were] destroyed; all pilings destroyed; many [piles] punched through concrete roadway; all spans collapsed. West approach subsided 7 inches; east approach subsided 22 inches (Kachadoorian, 1968)."

Unfortunately, no estimates of horizontal ground displacement or horizontal shifting of the highway bridge were given. However, McCulloch and Bonilla report that approximately 1 km north of the bridge (where the railroad embankment parallels the Placer River) the east bank of the Placer River moved approximately 1 m westward toward the channel.

> "This entire section embankment [north of Railroad Bridge 62.1] throughout the fracture area was displaced about 3 feet westward toward the major channel of the Placer River, which suggests that the cracking was related to streamward movement of the material beneath the entire low flood-plain surface (McCulloch and Bonilla, 1970).

Thus, we estimate that ground displacement on the east bank of the Placer River was approximately 1 m toward the channel.

4.6.5.2 TOPOGRAPHY

At the bridge, a broad flat floodplain is incised by a 3 to 4 m deep channel (Figure 55, 1989 survey). Our survey line perpendicular to the channel reveals less than 150 mm elevation change for at least 120 m on both sides of the river. A levy slopes approximately 0.1 percent away from the channel on each bank. Our downstream profile indicates that the river flows northward into Turnagain Arm on a 0.10 to 0.15 percent gradient.

4.6.5.3 SUBSURFACE SOIL CONDITIONS

Three boreholes logs (#1, #3, #4) from an ADOT foundation investigation for the reconstruction of the bridge (Utermohle, 1965) and one cone penetration log, TA-C-6, provided by the Alaska Division of Geology and Geophysics are reproduced in Figures 56 - 57. The subsurface sediments at the bridge are layers of coarse sand and sandy gravel in the upper 12 m of the profile. Sediments below 12 to 15 m are finer and consist of layers of fine sand, silty sand, silt and clayey silt (see profiles and grain-size data shown in Figures 56 - 58).

Liquefaction analyses of the SPT and CPT data reveals that the majority of the liquefaction probably occurred in coarse sand and sandy gravel in the upper 10 m of the profile. A liquefaction analysis of Borehole #1, located near the west abutment of Bridge #629, indicates liquefiable sandy gravel from 2.4 to 5.2 m and liquefiable coarse gravel from 5.2 to 7.9 m (Figure 56). The SPT values in these zones average 26 and range from 17 to 35. A liquefaction analysis of Borehole #3 (located in the center of the channel) indicates that most of the profile is non-liquefiable except for a marginally liquefiable silty fine sand at 17 m (Figure 57). An analysis of Borehole #4, located near the east abutment, indicates a liquefiable layer of coarse sand extending from a depth of 3.6 m to a depth of 10.4 m. The SPT values for this zone averages 33 and ranges from 26 to 42 (Figure 57). A liquefaction analysis of the cone penetration log, TA-C-6, located the west bank of the Placer River, indicates a liquefiable layer of silty sand to sandy silt extending from the surface to a depth of 2 m. However, this surface layer was probably deposited following the earthquake (Borehole TA-C-6 was drilled in 1984). Also, a minor amount of liquefiable sediment is indicated in a thin 0.6 m thick sand to silty sand layer at a depth of 10 m (Figure 56).

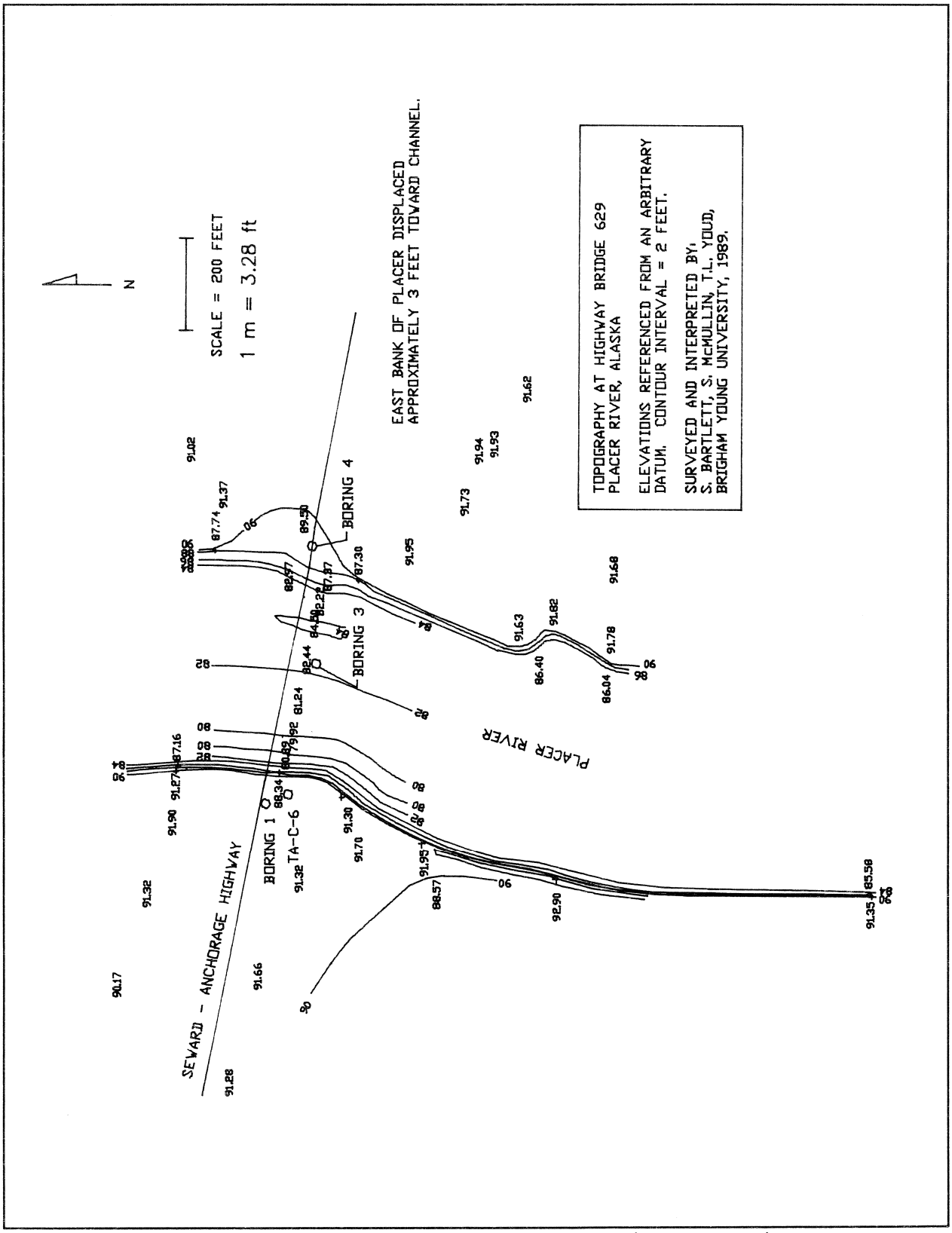

Figure 55 Contour Map of Placer River at Highway Bridge 629.

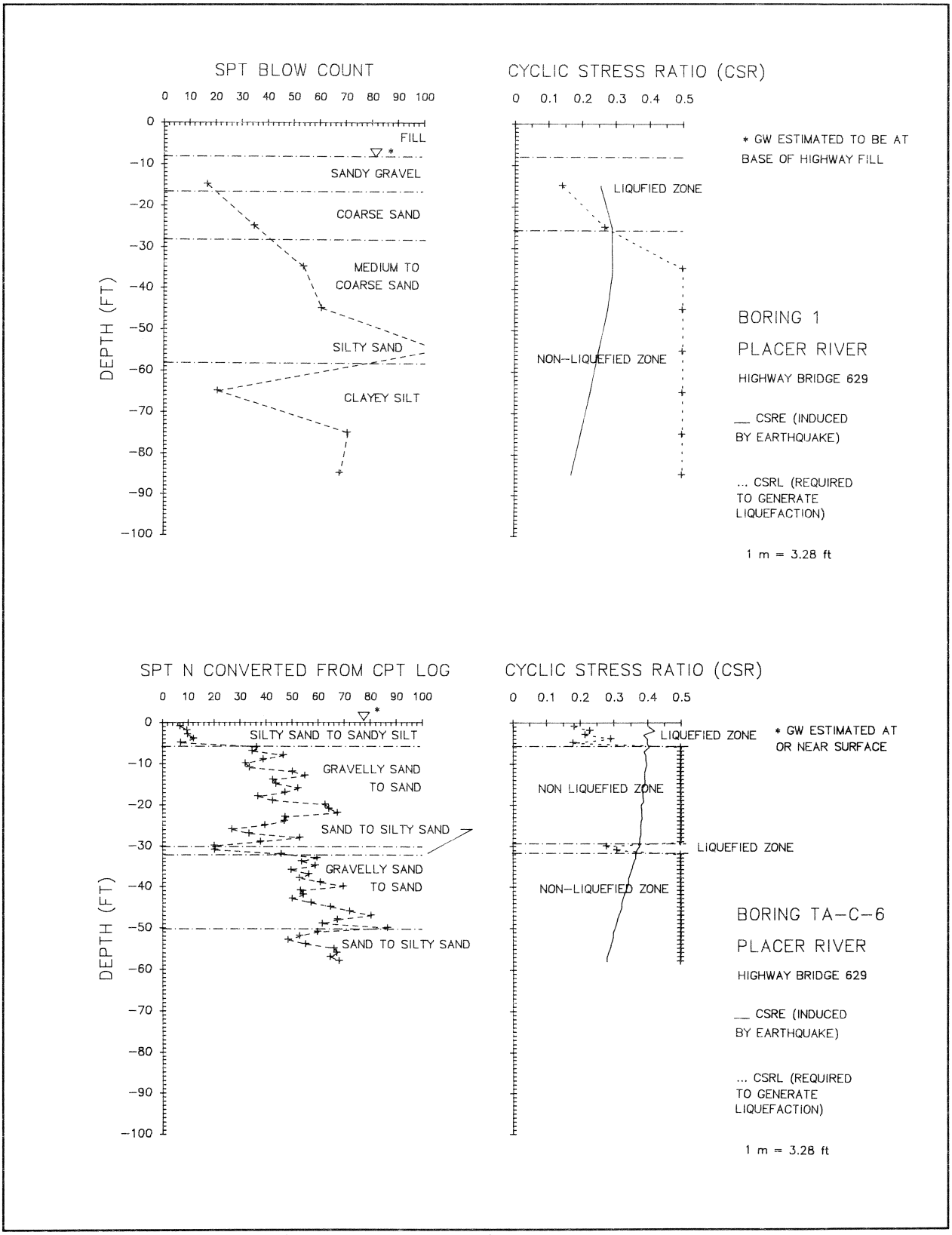

Figure 56 SPT Profile and Analysis, Bore Holes 1 and TA-C-6.

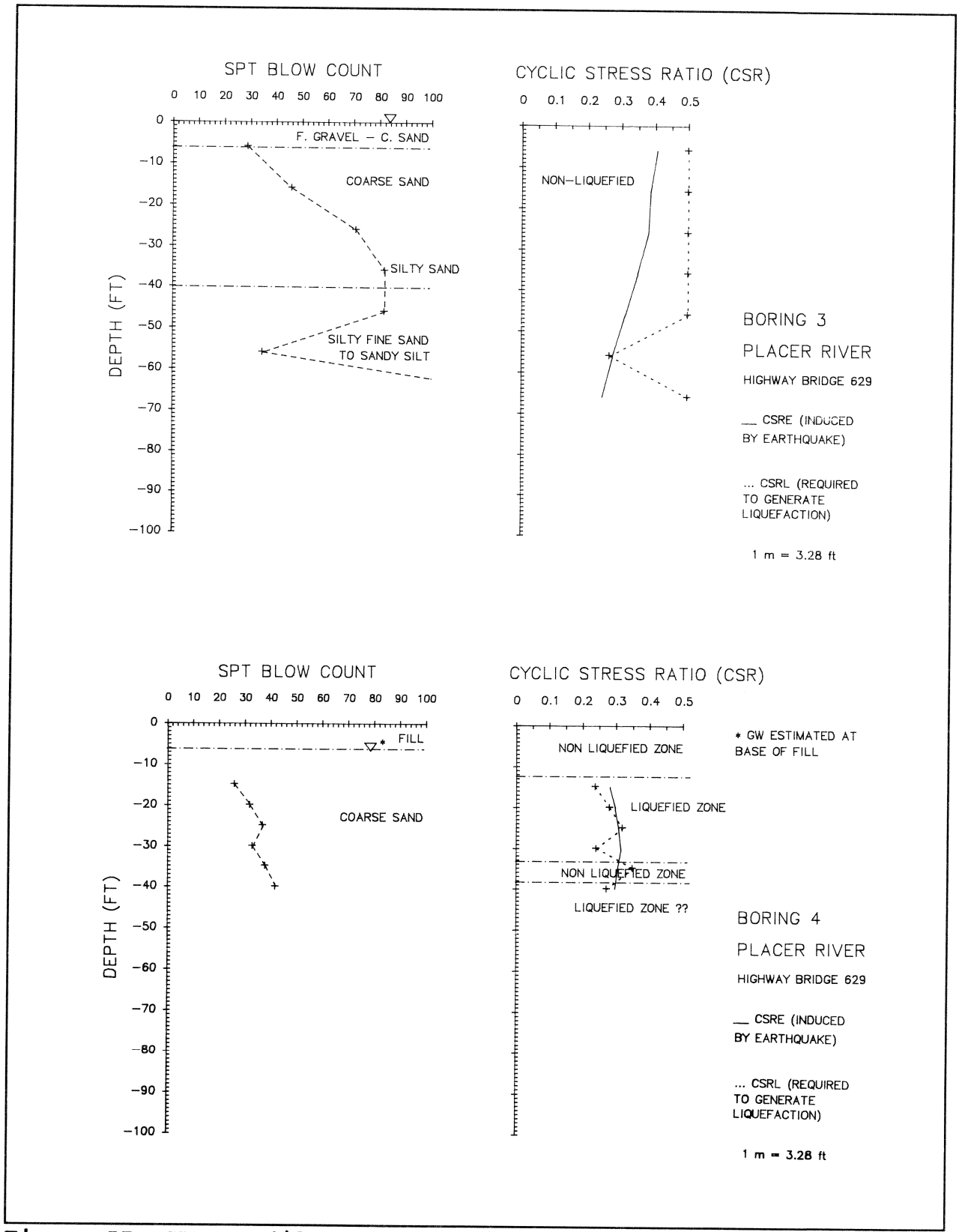

Figure 57 SPT Profile and Analysis, Bore Holes 3 and 4.

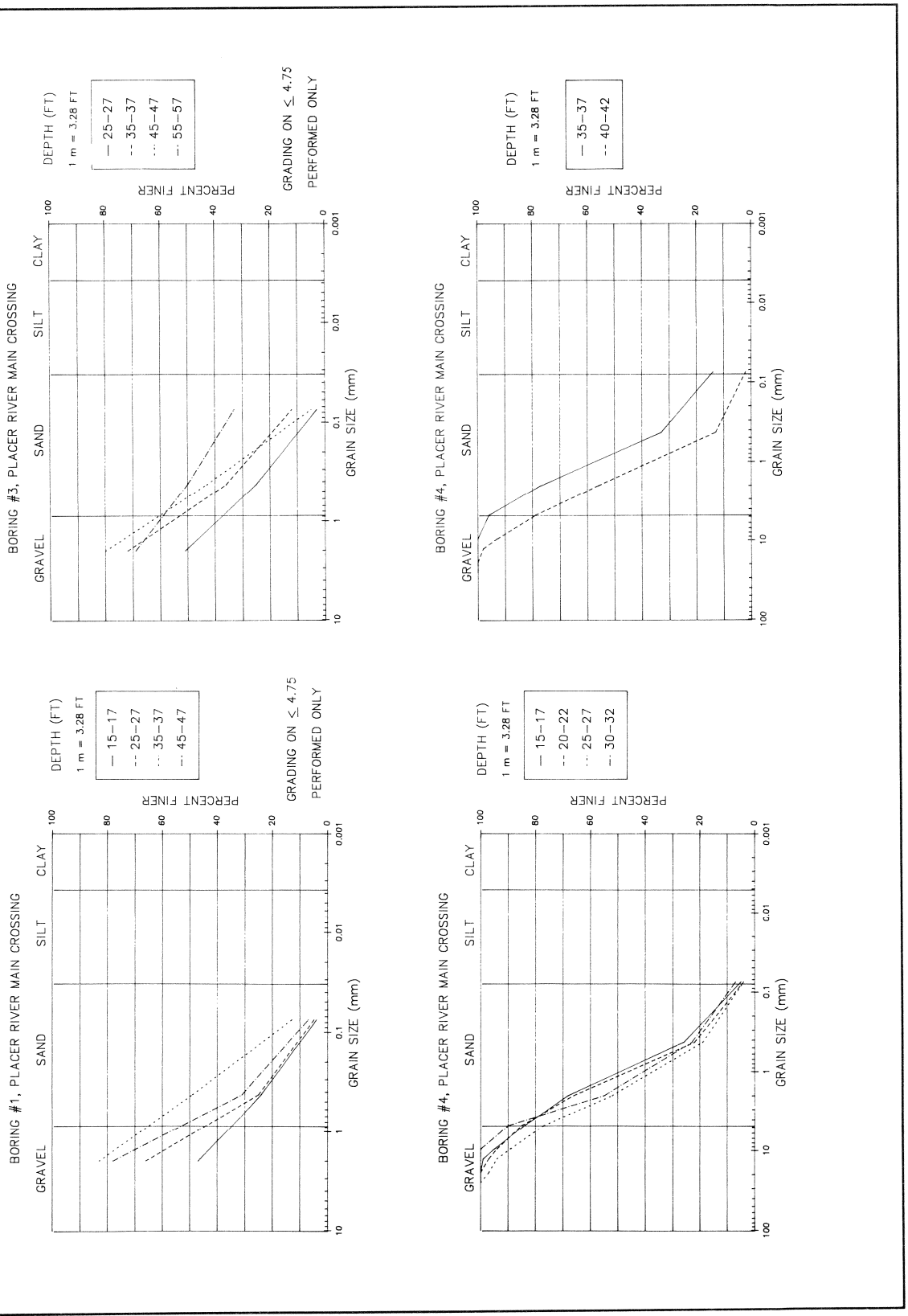

Figure 58 Grain-Size Distribution Charts, Bore Holes 1, 3, 4.

4.6.6 SUMMARY OF GROUND FAILURE AT SOUTHERN END OF TURNAGAIN ARM

Lateral spread displacements along the southern end of Turnagain Arm were as large as 3 m (Kachadoorian, 1966). One to two meters of channel closure was common at many bridges. Downstream displacements of abutments and piers were approximately one foot.

Liquefaction analysis for a composite log of the 14 boreholes at Twenty-Mile River, Portage Creek and Placer River reveals that the upper 11 m of the profile is potentially liquefiable (Figure 59). (As input for this analysis, we used a maximum site acceleration of 0.31 g, M_w of 9.2, a dry and moist unit weight for the soil of 15.7 and 18.9 kN/m^3 respectively. Also, we adjusted the cyclic stress ratio required for liquefaction, CSRL, for an average fines content of 23 percent).

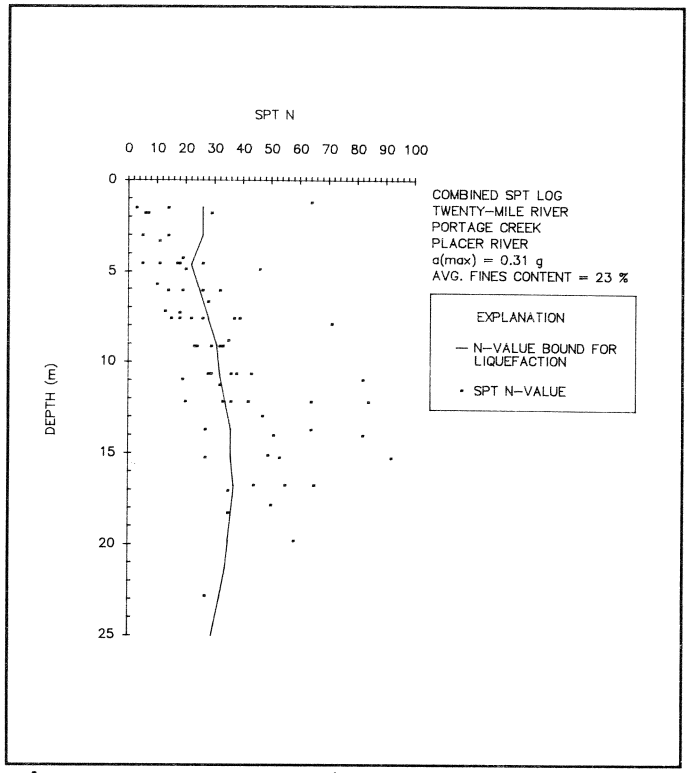

Figure 59 Combined SPT Log for Portage Area.

Lateral displacements near Portage were greater than ground displacements at the Knik and Matanuska Rivers despite the fact that sediments at Portage are denser (i.e., N values are higher on average, compare Figures 34 and 59). Our analyses show that N in liquefiable sediments at Portage averages 20 compared to an average N of 14 for liquefiable sediments at the Knik and Matanuska Rivers. Furthermore, at Portage, the average thickness of sediments with $N \leq 20$ is 4.2 m compared to 17.1 m at the Knik and Matanuska Rivers. Undoubtedly, the larger ground acceleration experienced at the southern end of Turnagain Arm was partly responsible for the larger ground

displacement and damage. We estimate that strong ground motion at Portage reached a maximum horizontal acceleration of 0.31 g and lasted about 75 seconds (see Sections 4.3.2 and 4.3.3).

4.7 DAMAGED HIGHWAY BRIDGES AT SNOW RIVER

4.7.1 INTRODUCTION

Approximately 22 km north of Seward, the Alaska Railroad and Seward-Anchorage Highway separate in the lower Snow River Valley. The Alaska Railroad bends abruptly to the east and crosses the Snow River at the railroad bridge near Milepost 14.5. From this bridge, the tracks continue northward along the eastern side of the valley to the southern end of Kenai Lake (Figure 60). The Seward-Anchorage Highway continues northward along the western side of the valley and turns eastward across the Snow River delta at the southern end of Kenai Lake.

The north-south trending glacially carved Snow River Valley is filled with unconsolidated fluvial and deltaic deposits. McCulloch and Bonilla suggest that Kenai Lake was once higher and extended farther south into Snow River Valley. Rapid filling of Kenai Lake by the sediment laden Snow River caused the shoreline to regress northward to its presents position. This scenario suggests that recent fluvial deposits in the northern Snow River Valley are underlain by finer lacustrine and deltaic sediments (McCulloch and Bonilla, 1970). Boreholes drilled just south of Kenai Lake along the present highway alignment indicate that the sediment below 7.6 m deep is finer than surficial gravelly fluvial deposits. The deepest borehole revealed that fine sand and silt extends to at least 53 m below the surface (Utermohle, 1962).

In 1964, the Alaska Department of Highways was beginning a construction project to replace 4 highway bridges (#603, #604, #605, #606) which cross the floodplain of Snow River (Figure 60). The old bridges had asphalted timber plank decks with

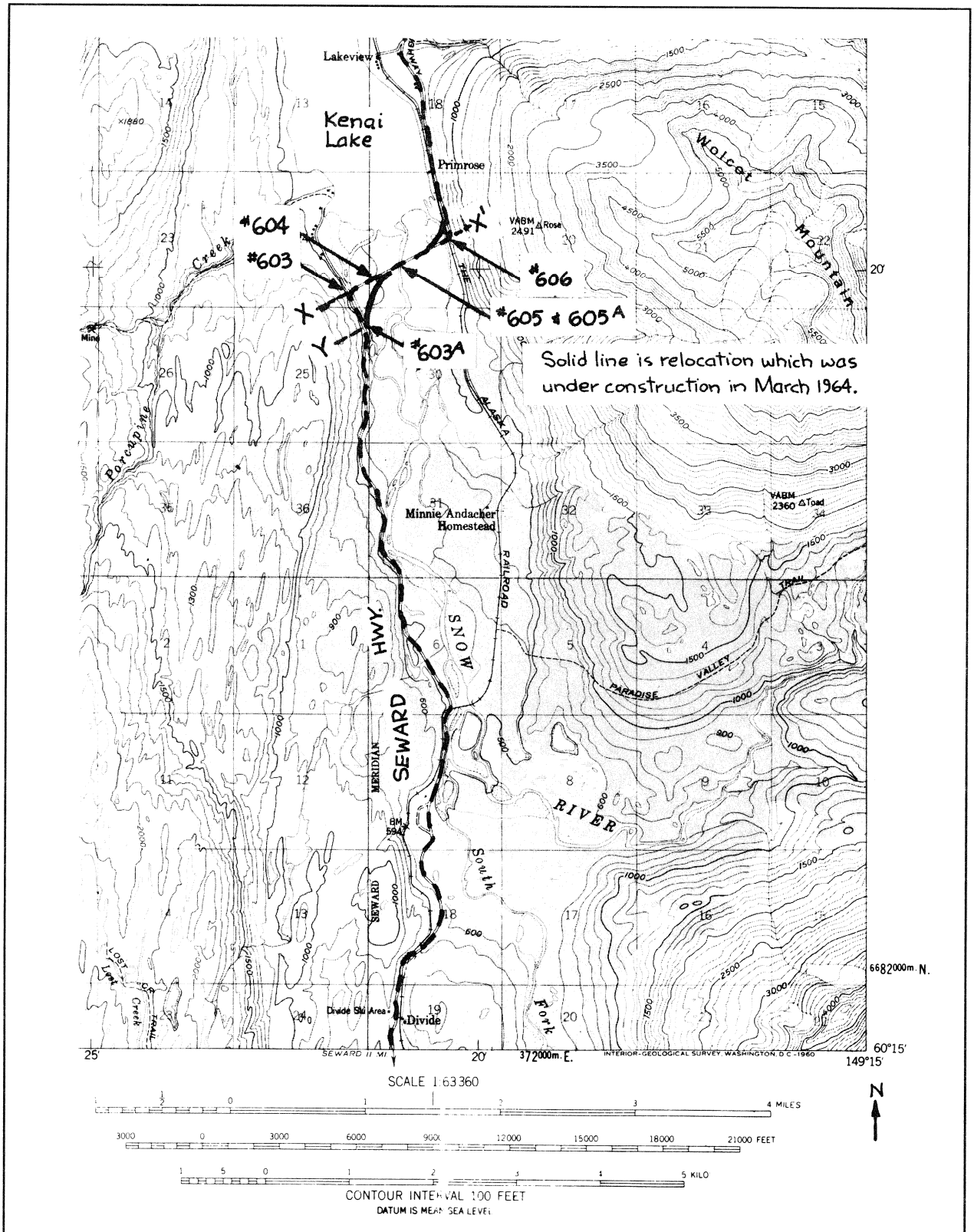

Figure 60 Bridge Locations at Snow River (after Ross et al., 1973)

timber stringers supported by concrete abutments and timber piles. The new Bridges, #603A and #605A, are steel girder structures with reinforced concrete decks. Four out of six concrete piers were in place at Bridge 605A during the earthquake.

The old highway bridges at Snow River suffered severe damage from horizontal ground displacement and differential settlement. Kachadoorian reports damage to southwestern most bridge (No. 603) as "severe". The bridge deck was compressed and had a wavy appearance. In many places, the pile caps had separated from the buckled deck. The approach fills on both side of Bridge 603 subsided from 1.2 to 1.8 m. Similar damage was incurred by Bridge 604.

> "Roadway bowed up in middle; bridge in compression, deck wavy; deck in places is off cap. Approaches subsided about 6 feet. Surrounding sediment settled as much as 12 feet (Kachadoorian, 1968)."

Highway Bridge 605 at the main channel crossing was damaged beyond repair.

> "Third bent from north end did not settle. All others [bents] settled as much as 12 ft; 3 spans nearest south end slightly twisted and rolled. Approach subsided about 6 feet. Surrounding sediments settled about 12 feet (Kachadoorian, 1968)."

Highway Bridge 606, an overpass structure which spanned the Alaska Railroad on the south-eastern edge of Kenai Lake, collapsed onto the railroad tracks.

> "South end of bridge pulled 6 inches away from abutment; bridge slightly canted and wavy. Piles on west side settled 6 inches to 2 feet lower than east side in the first 1,120 [from south end]. For next 100 feet, timber bents all canted south and offset. Last 225-250 feet [north end] completely destroyed; it fell or twisted to ground about 75 feet below, destroying roadway and bents (Kachadoorian, 1968)."

4.7.2 HIGHWAY BRIDGE 605A, SNOW RIVER MAIN CROSSING

The new Highway Bridge 605A across the main channel of Snow River paralleled the existing wooden structure (Bridge No. 605). At the time of the earthquake, 4 of 6 concrete piers were completed to top of shaft.

4.7.2.1 GROUND FAILURE DISPLACEMENT AND DAMAGE

Liquefaction-induced ground failure displaced one of the four free standing piers 2.4 m downstream toward Kenai Lake. The other 3 piers also displaced an

unspecified amount downstream. Ross, et al. (1973) describe the liquefaction and ground displacement observed in the vicinity of the piers as follows:

> "Four of the heavy concrete piers had been completed to top of shaft [Figure 61]. These piers (each supported on 21 concrete-filled steel-tube piles, extending an average of about 90 feet below adjacent streambed level) underwent tilting and lateral displacement during the earthquake. Damage surveys revealed a maximum of 8 ft. lateral displacement of the shaft tops downstream and up to 15 deg. tilt upstream. . . Longitudinal movements were less [Figure 62].
>
> From comments of first hand observers and from the behavior of bridge foundations, it is clear that liquefaction of cohesionless soils did occur in this region. Reports mention that "mud" oozed up in cracks and that the 10 foot high road embankment was reduced to the level of the flood plain. The preferred downstream movement of the footings and upstream tilt of the pier shafts indicates liquefaction at depth below footing level, possibly accompanied by a lakeward flow along a zone that was well below the ground surface (Ross et al., 1973)."

4.7.2.2 TOPOGRAPHY

The pier displacements at the Snow River were primarily downstream along the regional gradient toward Kenai Lake. Our survey revealed that the river flows northward along a 0.1 percent gradient in the vicinity of the bridge. Figure 63 is a reproduction of a 1962 construction contour map for Bridge 605A. In 1962, the main channel of the Snow River was about 50 m wide and 1.8 to 2.5 m deep.

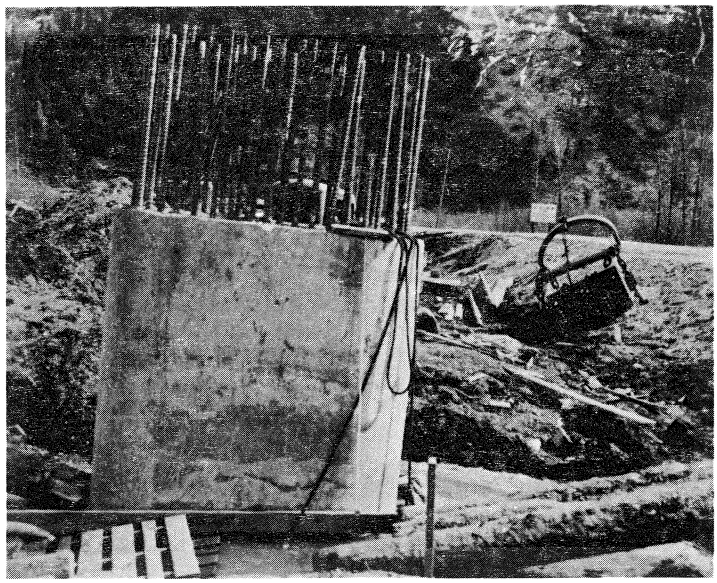

Figure 61 Photograph of Displaced Highway Pier (looking east, from McCulloch and Bonilla, 1970).

4.7.2.3 SUBSURFACE SOIL CONDITIONS

The subsurface sediment near the displaced piers consists of fine grained silty sand (Figure 64) extending from the surface to approximately 30 m. Below 30 m, the soil is alternating layers of silty sand and sandy silt. Borehole 5L (Ross et al., 1973) is located approximately 6 m east of the displaced pier shown in Figure 63 and Borehole #1A (Utermohle, 1962) is located 40 m east of the same pier.

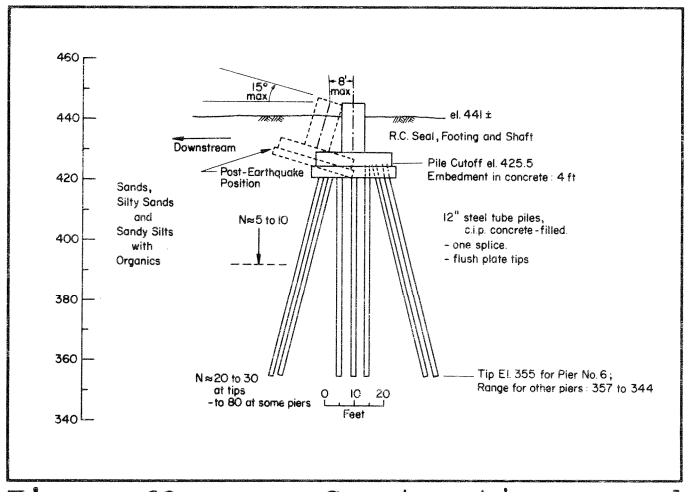

Figure 62 Construction and Displacement of Concrete Pier, Bridge 605A (after Ross et al., 1973).

The sediment at Snow River is liquefiable for a considerable depth below the ground surface. Our analysis shows that deposits in Borehole 5L are liquefiable to a depth of 30 m below the surface (Figure 65). The SPT values for Borehole 5L average 11 and range from 3 to 25. Deposits in Borehole #1A are liquefiable to at least 30 m (i.e., to the bottom of the borehole). The SPT values for Borehole #1A also average 11 and range from 6 to 19 (Figure 65).

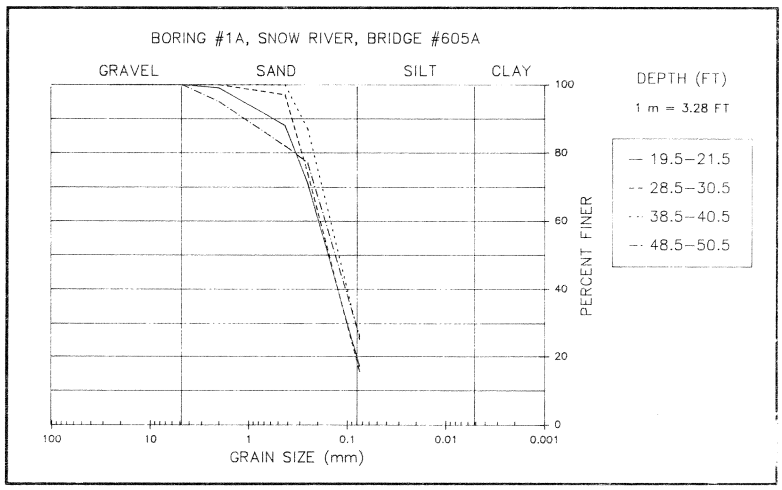

Figure 63 Grain-Size Distribution Charts, Bore Hole 1A, Snow River.

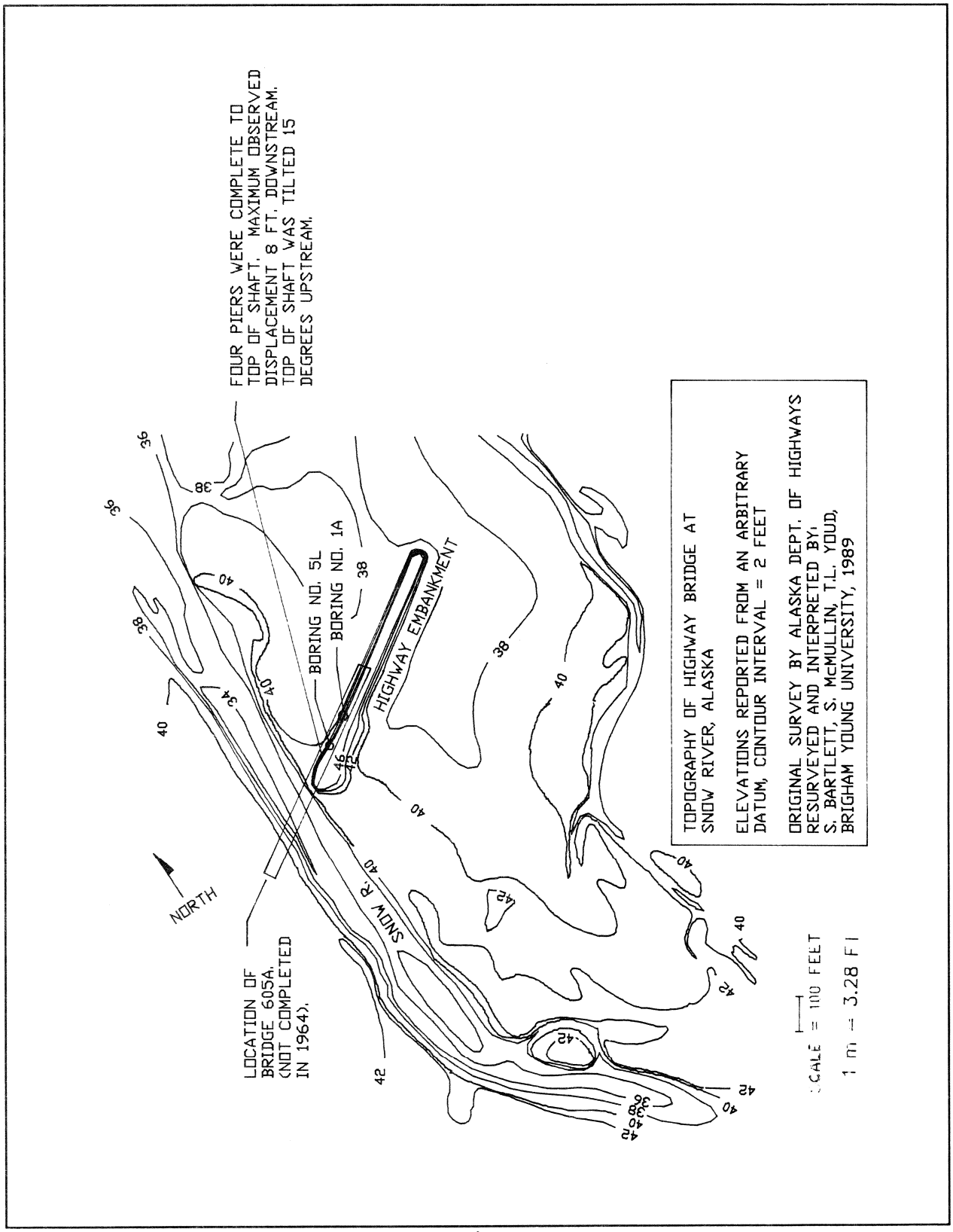

Figure 64 Contour Map of Snow River.

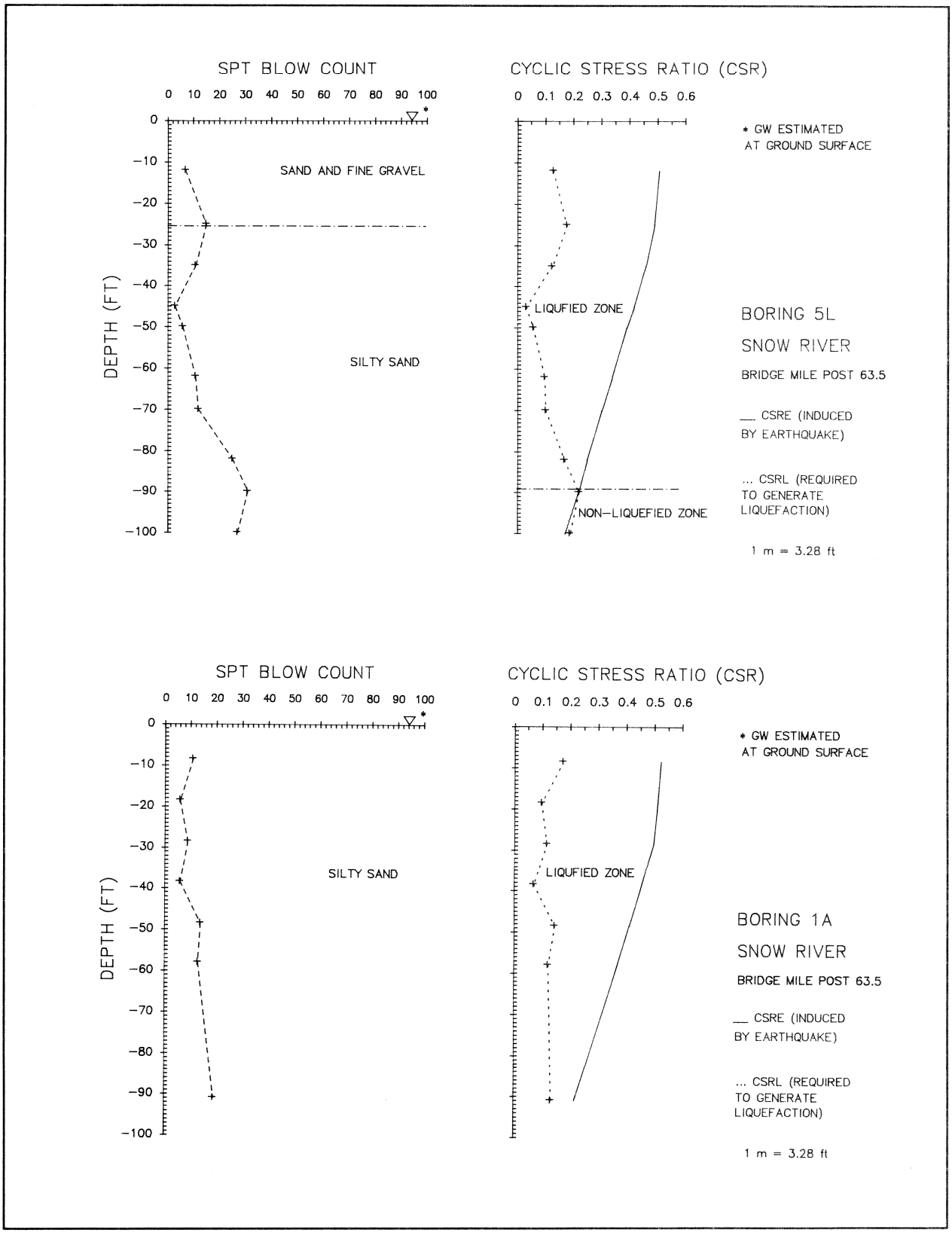

Figure 65 SPT Profile and Analysis, Boreholes 1A and 5L.

4.7.3 SUMMARY OF GROUND FAILURE AT SNOW RIVER

Horizontal ground displacement and liquefaction damage was large at Snow River for two primary reasons: 1) the relatively close proximity of Snow River to the zone of seismic energy release, and 2) the presence of thick deposits of saturated relatively uncompacted cohesionless soil. The Snow River is approximately 35 km from the fault rupture and strong ground motion may have lasted as long as 90 seconds and reached a maximum amplitude of about 0.4 g (see Sections 4.3.2 and 4.3.3). Ground motion of this intensity and duration probably contributed greatly to the damage seen at Snow River.

Liquefaction analysis of combined SPT data from 4 boreholes at Snow River indicates that the silty sand, sand and fine gravel are the most "liquefiable" of any of the case histories reviewed in this report (Figure 66). On average, the SPT values are less than or equal to 10 in the upper 10 m of the profile. This analysis also suggests that the profile is potentially liquefiable to a depth of 30 m. (As input for this analysis, we used a maximum site acceleration of 0.39 g, M_w of 9.2, a dry and moist unit weight for the soil of 15.7 and 18.9 kN/m^3 respectively. Also, we adjusted the cyclic stress ratio required for liquefaction, CSRL, for an average fines content of 20 percent).

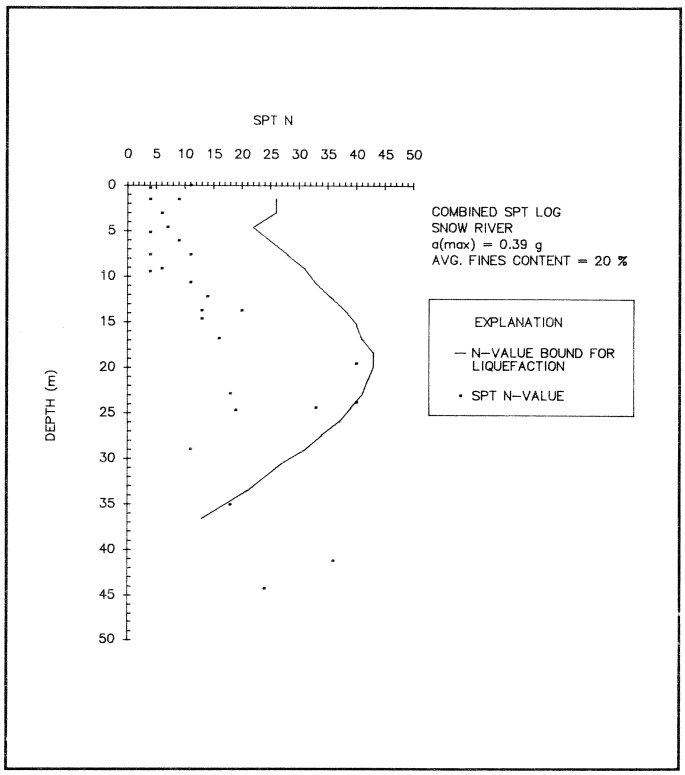

Figure 66 Combined SPT Log for 4 Bore Holes at Snow River.

4.8 DAMAGED RAILROAD BRIDGES AT THE RESURRECTION RIVER

4.8.1 INTRODUCTION

A few kilometers north of Seward, the Alaska Railroad and Seward-Anchorage Highway cross the floodplains of Resurrection River and Mineral Creek (Figure 1). Ground fissures and displacements were abundant on the Resurrection River floodplain after the earthquake (Figure 67). McCulloch and Bonilla describe the nature of liquefaction ground failure as follows:

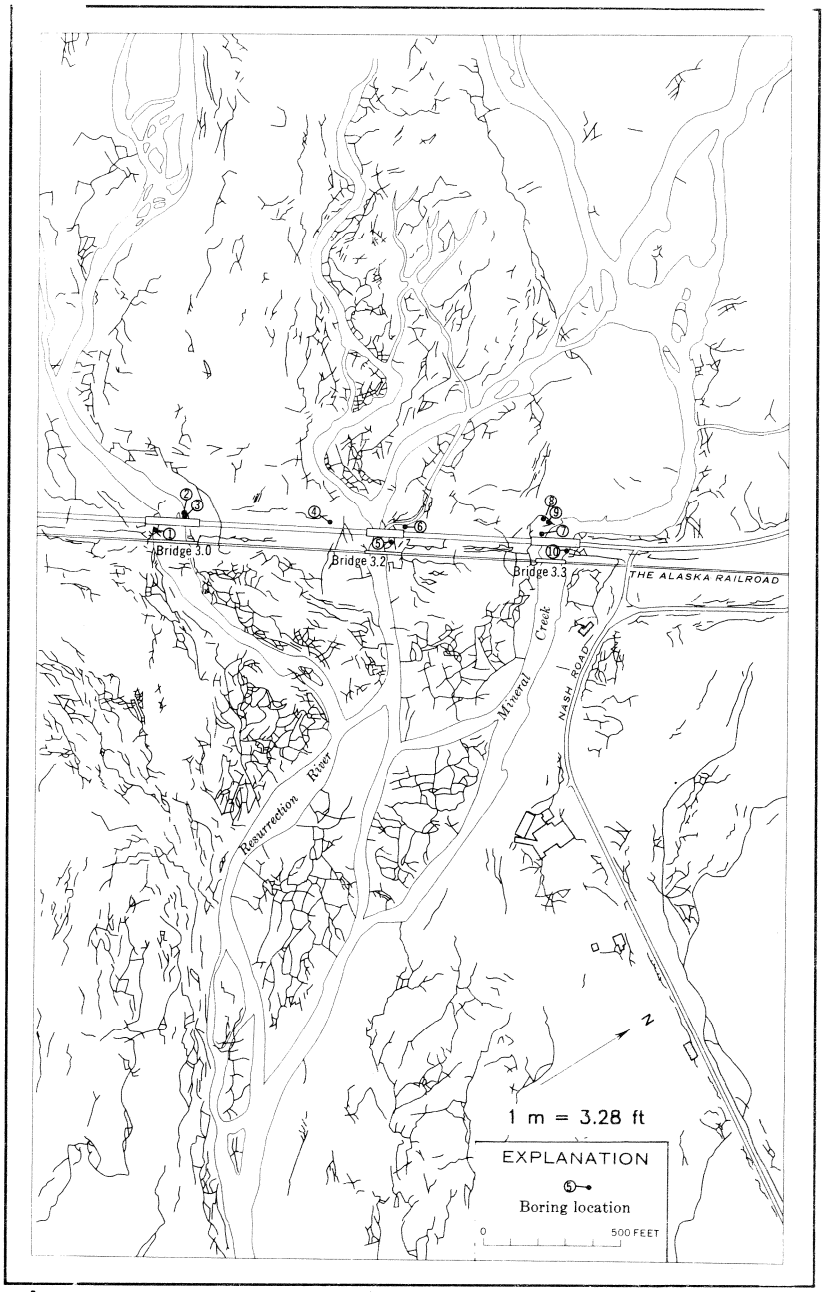

Figure 67 Ground Fissures, Bridge and Bore Hole Locations, Resurrection River and Mineral Creek (after McCulloch and Bonilla, 1970).

"Where the parallel highway and railroad fills passed from Jap Creek fan onto Resurrection River floodplain, cracking between the fills was more pronounced and water was discharged along the fractures. These fractures did not seriously affect the fills. However, were the fills lay on the extensively and severely fractured active and inactive floodplain sediments along the rivers, damage increased. Minor failures occurred within the fills, but most of the damage resulted from lateral displacement and cracking of the underlying sediments. As indicated by damage to the bridges, all of which were so severely damaged that they had to be replaced with entirely new structures, the flood-lain sediments were mobilized

to depths in excess of 30 feet. The movement of the underlying sediments carried the railroad fill as much as 30 inches to the southeast, and the grade was broken by tension fractures (McCulloch and Bonilla, 1970)."

In the following section, we discuss ground failure displacement and damage for Railroad Bridges at Mileposts 3.0 and 3.2 crossing Resurrection River and for a Railroad Bridge at Milepost 3.3 crossing Mineral Creek (Figure 67).

4.8.2 RAILROAD BRIDGES AT MILEPOST 3.0, 3.2, AND 3.3, RESURRECTION RIVER AND MINERAL CREEK

4.8.2.1 GROUND FAILURE DISPLACEMENT AND DAMAGE

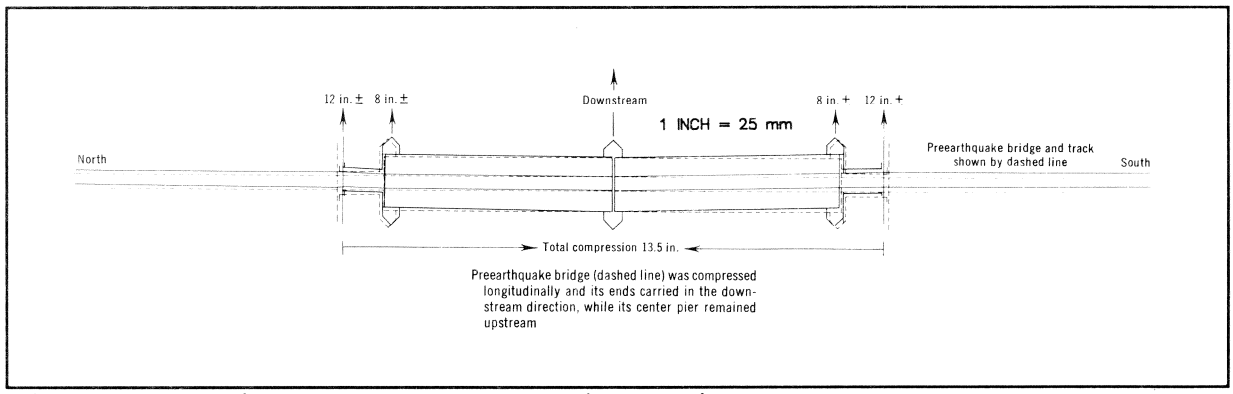

Figure 68 Displacements at Bridge Milepost 3.0 (after McCulloch and Bonilla, 1970).

Prior to the earthquake, the railroad bridge across the southern branch of Resurrection River at Milepost 3.0 was a 57 m long steel girder structure. Two 24.4 m girders were supported by 3 pile-supported piers. Four rows of nine piles were driven beneath the central pier and three rows of nine piles were placed under the end piers. At both ends, 4.1 m of open wood-trestle supported the end spans between the bulkheads and the end piers. McCulloch and Bonilla describe the damage to this bridge:

> "Compression at deck level totaled 13 1/2 inches. The steel deck beams were driven 4 and 5 1/2 inches into the ends of the wood stringers, and the wood stringers were driven 1.5 and 2.5 inches into the bulkheads. . . . Piles at the bulkheads and piers were shifted streamward. All moved with no detected vertical rotation. The horizontal displacement ranged from 1 1/2 to 11 inches. . . In addition to moving streamward, the outer piers shifted 8 inches downstream of the central pier, and the bulkheads and approach fills were carried 4 to 5 inches more; the central pier was thus left 12 to 13 inches upstream of the approaches [Figure 68] (McCulloch and Bonilla, 1970)."

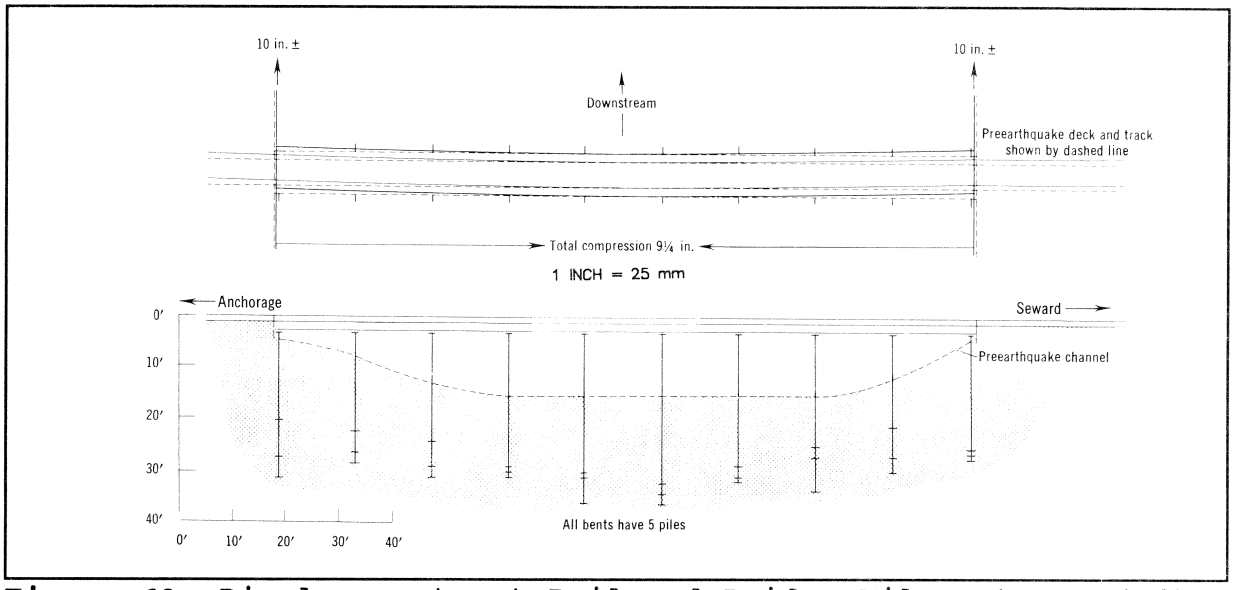

Figure 69 Displacements at Railroad Bridge Milepost 3.2 (after McCulloch and Bonilla, 1970).

The railroad bridge across the northern branch of the Resurrection River at Milepost 3.2 was a 41 m, nine-span, open-wood trestle. McCulloch and Bonilla report the damage to this bridge:

"Deck level compression drove the stringers 1 1/4 inches into the north bulkhead, crushed the fillers, and drove the top of the bulkhead back into the fill. At the south bulkhead the stringers were driven 8 inches pas the piles into the bulkhead, and here, too, the top of the bulkhead was shoved back into the fill. There was no appreciable settlement of the south approach fill, but the north fill settled about 5 inches relative to the bulkhead, and the bulkhead was pulled down about 3 inches below the deck by the fill. Settlement of about this same amount continue to the next bridge [Bridge at Milepost 3.3]. As shown in Figure [69], the downstream shifting of the bents increased away from the center of the stream, the ends of the bridge and the approach fills being carried about 10 inches downstream from the center of the bridge. There was also some crowding of the piles toward the stream, but the displacements were not measured (McCulloch and Bonilla, 1970)."

The railroad bridge crossing Mineral Creek at Milepost 3.3 was a 41.5 m steel girder bridge (one 24.4 m central span with 4.3 m pile-supported open trestle at each end). McCulloch and Bonilla note that damage to this bridge was very similar to the damage incurred to the Bridge at Milepost 3.0. They describe the displacement and damage as follows:

"Compression, totaling about 19 inches developed at the deck level, driving stringers into bulkheads and into the central steel spans. At the north bulkhead the stringers were shoved at least an inch pas the piles, forcing the bulkhead bents into the fill. ... At the south bulkhead the stringers drove about a foot pass the piles. ... Piles in the bents and piers shifted streamward ranging from

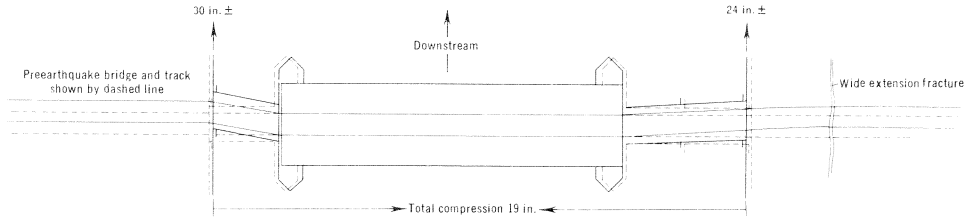

Figure 70 Displacements at Railroad Bridge Milepost 3.3 (after McCulloch and Bonilla, 1970).

1 to 20 inches. ... As at the adjacent bridges, the grade was shifted to the southeast, parallel to the stream which skewed the approach spans and left the central span about 30 inches upstream (McCulloch and Bonilla, 1970, see Figure 70)."

4.8.2.2 TOPOGRAPHY

In 1989, the southern branch of the Resurrection River had incised a 1.8 m deep channel under the Bridge at Milepost 3.0 (Figure 71). The natural ground south of the river slopes less than 0.05 percent toward the channel (measured parallel to the airport access road. The ground north of the river slopes approximately 0.1 percent toward the channel. At the bridge crossing, this branch of the Resurrection River flows on a 0.1 percent gradient to the southeast toward Resurrection Bay.

Because of swift current, we were unable to sound the channel depth at the northern branch of Resurrection River and at Mineral Creek. However, bridge construction profiles for these two channels indicate that they are approximately the same depth as the southern branch. On the south side of the northern branch of Resurrection River, the ground slopes less than 0.01 percent away from the channel. North of the same channel, the ground slopes approximately 0.7 percent into the channel. The ground on both sides of Mineral Creek slopes approximately 0.9 percent into the channel. Both the northern branch of Resurrection River and Mineral Creek flow on a 0.3 percent gradient.

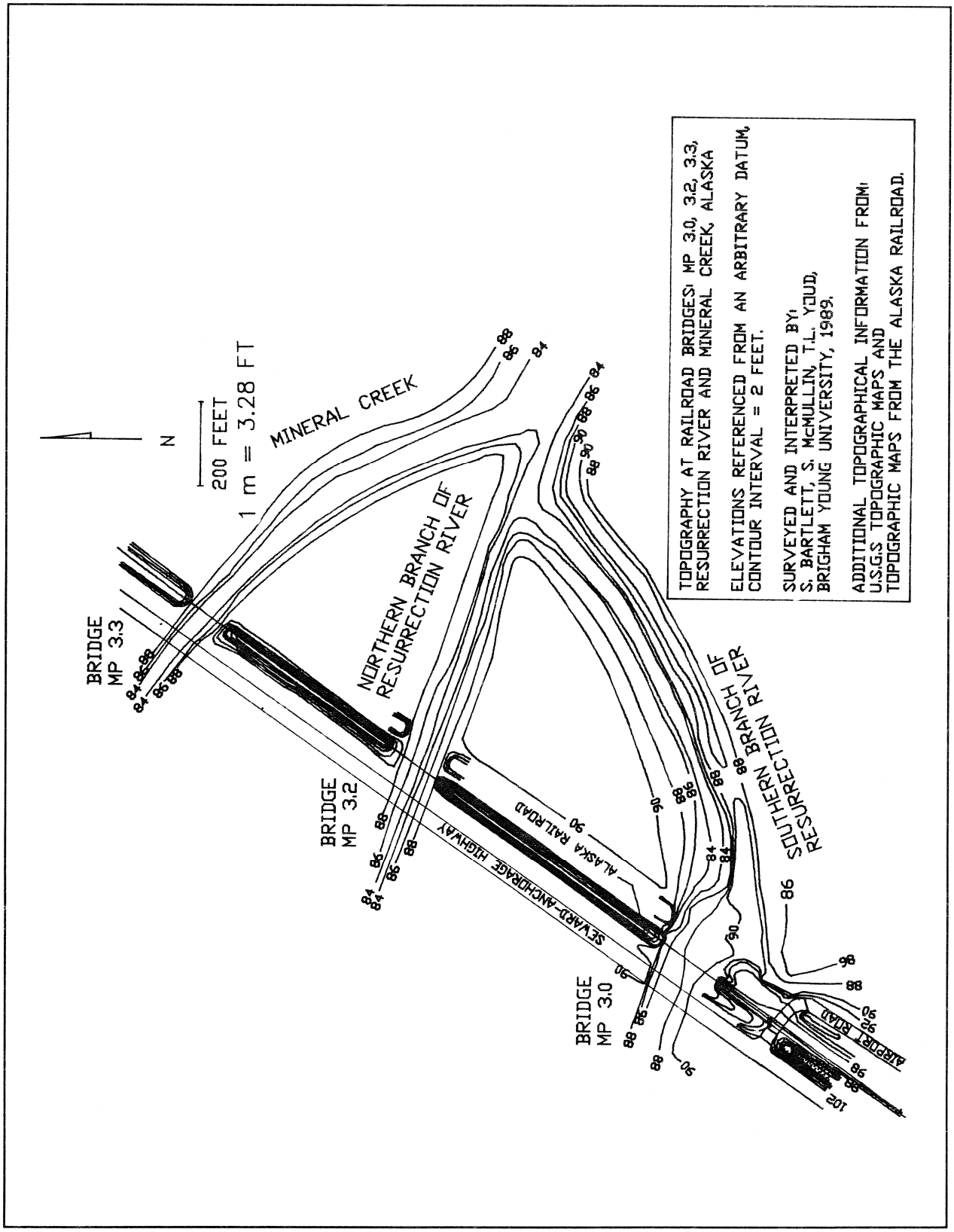

Figure 71 Contour Map of Resurrection River and Mineral Creek.

4.8.2.3 SUBSURFACE SOIL CONDITIONS

The thickness of fluvial and glaciofluvial sediments in the Resurrection River Valley is not well known. At the highway and railroad crossing, a borehole drilled to a depth of 29 m did not encounter the base of the alluvium (McCulloch and Bonilla, 1970). Tidal silts and clay probably underlay the alluvium (Ross et al., 1973).

McCulloch and Bonilla describe the subsurface conditions from boreholes taken at the adjacent highway bridges (see Figure 67 for borehole locations).

> "All the sediments are noncohesive; field identifications range from sandy and silty gravel to fine gravel to gravel. With the exception of hole 2, at Bridge 3.0, in which cobbles were found below 20 feet, the gravel averaged less than three-fourths of an inch in diameter, with a maximum of about 3 inches. All the sediments were saturated, the ground-water table lying at, or within 2 feet of, the surface. Penetration resistance generally increased downward, although there were some inversions. Within the depth of the sediments penetrated by the piling, the materials were compact to dense. Penetration resistance on a standard penetrometer (140-lb, 30-in drop, 2-in sample spoon) was 30 to 40 blows per foot, a second penetrometer (342-lb hammer, 30-in. drop 2 1/2 in. penetrometer) encountered resistance of 20 to 25 blows per foot (McCulloch and Bonilla, 1970).

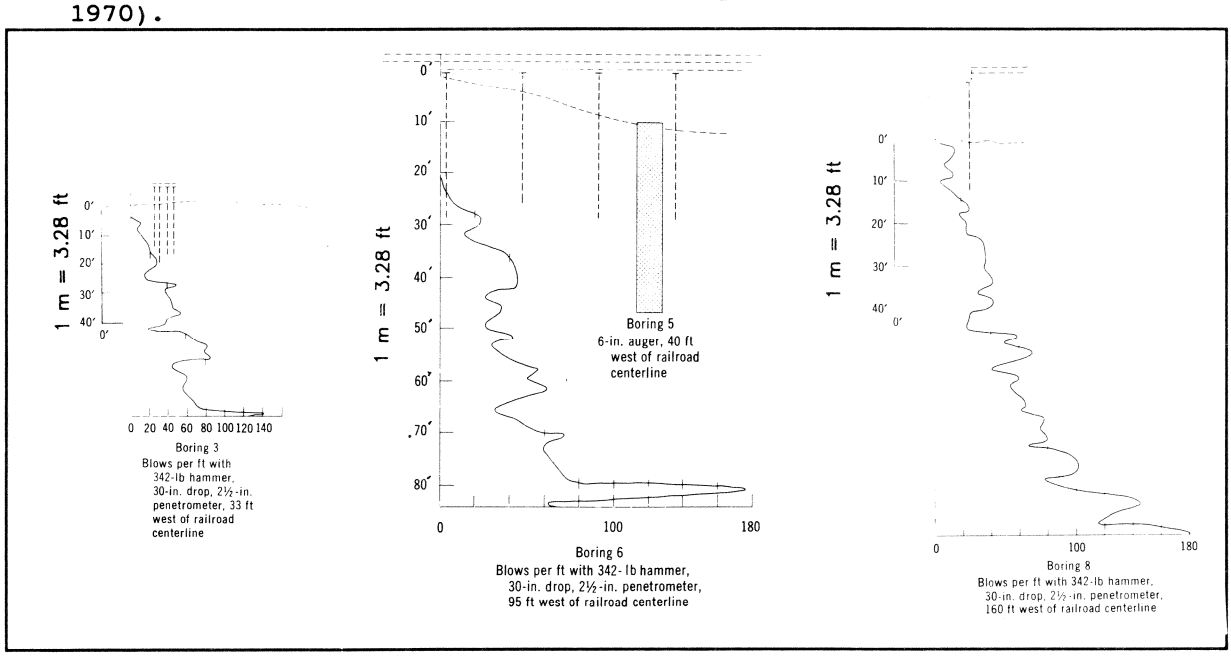

Figure 72 Penetration Logs for Bore Holes 3, 6, 8 (342 lb. hammer - after McCulloch and Bonilla, 1970).

We have converted the penetration resistances of the 155 kg hammer (Figure 72) to standard penetration resistances and performed liquefaction analyses for these logs (Figures 73 - 74). (For these analyses, we corrected N for the difference in the weight of the driving hammer. We did not correct N for the difference in sampler diameter because the inside diameter of the 63.5 mm non-standard sampler was not documented. However, N uncorrected for the sampler diameter is probably with ± 20 percent of N corrected).

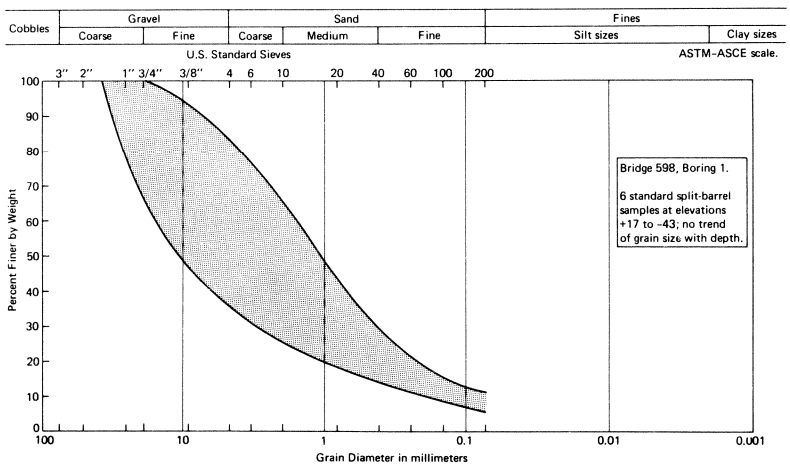

Figure 73 Grain-Size Distribution Range for Soils Sampled at Mineral Creek (after Ross et al., 1973).

Also, we have included a chart showing the range of grain-size distribution for SPT samples taken near the Highway Bridge at Mineral Creek (Figure 73). Also included is a SPT log at the same locality (Borehole 9, Figure 75). Our liquefaction analyses of these four boreholes indicate that some layers of gravel and fine gravel are liquefiable in the upper 20 m of the profile (Figures 74 - 75).

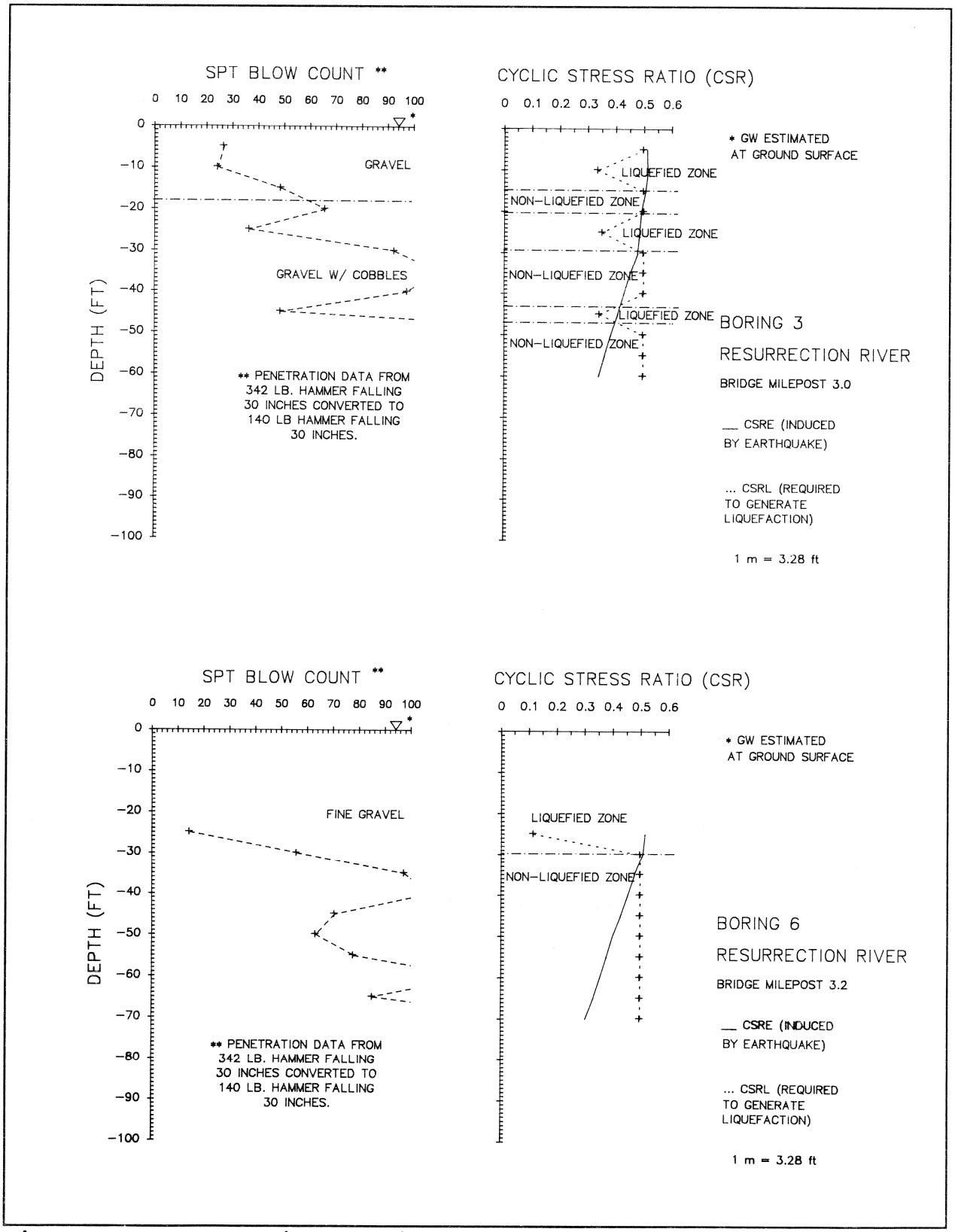

Figure 74 Penetration Profile and Analysis, Bore Holes 3 and 6.

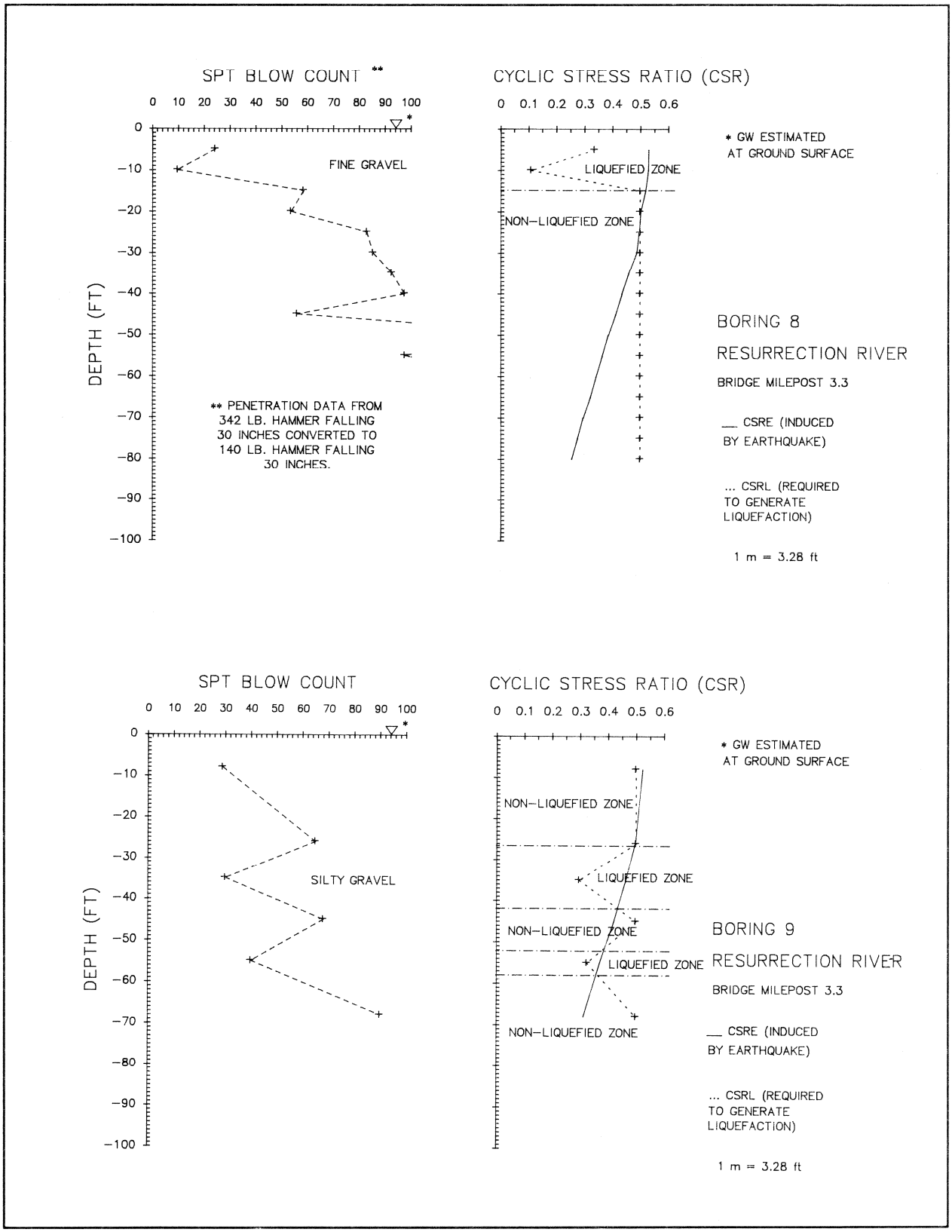

Figure 75 Penetration Profile and Analysis, Bore Holes 8 and 9.

5.0 SUMMARY AND CONCLUSIONS

The 1964 Alaska earthquake generated liquefaction over a widespread area in south-central Alaska. Damaged railroad and highway bridges along the Alaska Railroad and Highway are important case histories of liquefaction-induced ground displacement and consequent damage.

Reports from observers and empirical relationships suggest that strong ground motion lasted from 1 to 2 minutes in the region of significant liquefaction and bridge damage. Empirical magnitude-distance relationships predict that the maximum horizontal ground acceleration was approximately 0.2 g at the Knik and Matanuska Rivers and Ship Creek, 0.3 g at the southern end of Turnagain Arm and 0.4 g at the Snow and Resurrection Rivers.

Liquefaction at these sites primarily occurred in recent fluvial silt, sand and gravel. Lateral spread of the floodplain and river banks toward channel centers narrowed channel widths and severely compressed numerous railroad and highway bridges. Bridge abutments and piers moved as much as 3 m toward river channels and 2.5 to 3 m downstream at Portage and the Snow River.

Downstream displacements of bridge piers were as great as 0.6 m in the Matanuska Valley on a slope of about 0.05 to 0.10 percent and 2.4 m or more down a slope of about 0.10 percent. These slopes are much smaller than the 0.3 percent minimum noted from prior investigations (NRC, 1985). Thus, during large magnitude earthquakes, lateral spreads on highly susceptible materials may undergo considerable displacement on slopes as gentle as 0.05 percent.

Evaluation of past distributions of liquefaction effects has shown that both the severity and abundance of effects rapidly diminish with distance from the seismic energy source. To quantify and analyze the attenuation of severity of liquefaction effects, Youd and Perkins (1987) introduced the concept of "liquefaction severity index (LSI)." LSI is defined as the general maximum

ground displacement of lateral spreads on liquefiable, gently-sloping, late-Holocene fluvial and deltaic deposits. LSI is calculated by dividing the maximum horizontal ground displacement of lateral spreads, measured in millimeters, by 25. Figure 76 plots the LSI values at the damaged bridge sites reviewed in this study versus the horizontal distance from the surface projection of energy source in kilometers. Also, the LSI line for the 1964 Alaska earthquake predicted from the Youd-Perkins LSI equation is plotted as the dot-dashed line on Figure 76.

We draw three important conclusion about the severity of liquefaction-induced ground failure from the examination of Figure 76. (1) No horizontal displacement, measured at the damaged bridges, exceeded the LSI line predicted for the 1964 Alaska earthquake. Thus, the LSI appears to be a conservative upper bound for most of the ground displacements incurred by the 1964 Alaska earthquake. (2) Distance from the seismic energy source is a major factor controlling displacement. For example, horizontal ground displacement was larger near Portage (up to 3 m) than at the Matanuska River (up to 1.4 m). The bridges located near Portage were much closer to the zone of seismic energy release than those in the Matanuska Valley (60 and 100 km respectively). (3) The amount of horizontal ground displacement is also influenced by the density, texture and uniformity of the subsurface soil. For example, the maximum displacement of 0.75 m at the Resurrection River is smaller than might be expected for a locality so near the zone of seismic energy release. (Peak accelerations and duration of strong ground motion at the Resurrection River were estimated to be about 0.4 g and 90 s respectively). The apparent reasons for these smaller displacements at the Resurrection River compared to other sites were the thinner liquefiable layer (3 to 5 m) and the gravelly texture of the liquefied material. Thus, for comparable distances from the zone of seismic energy release, relatively thick uniform sandy sediments with low SPT values experienced larger ground displacements than thinner more heterogeneous gravelly sediments with higher SPT values.

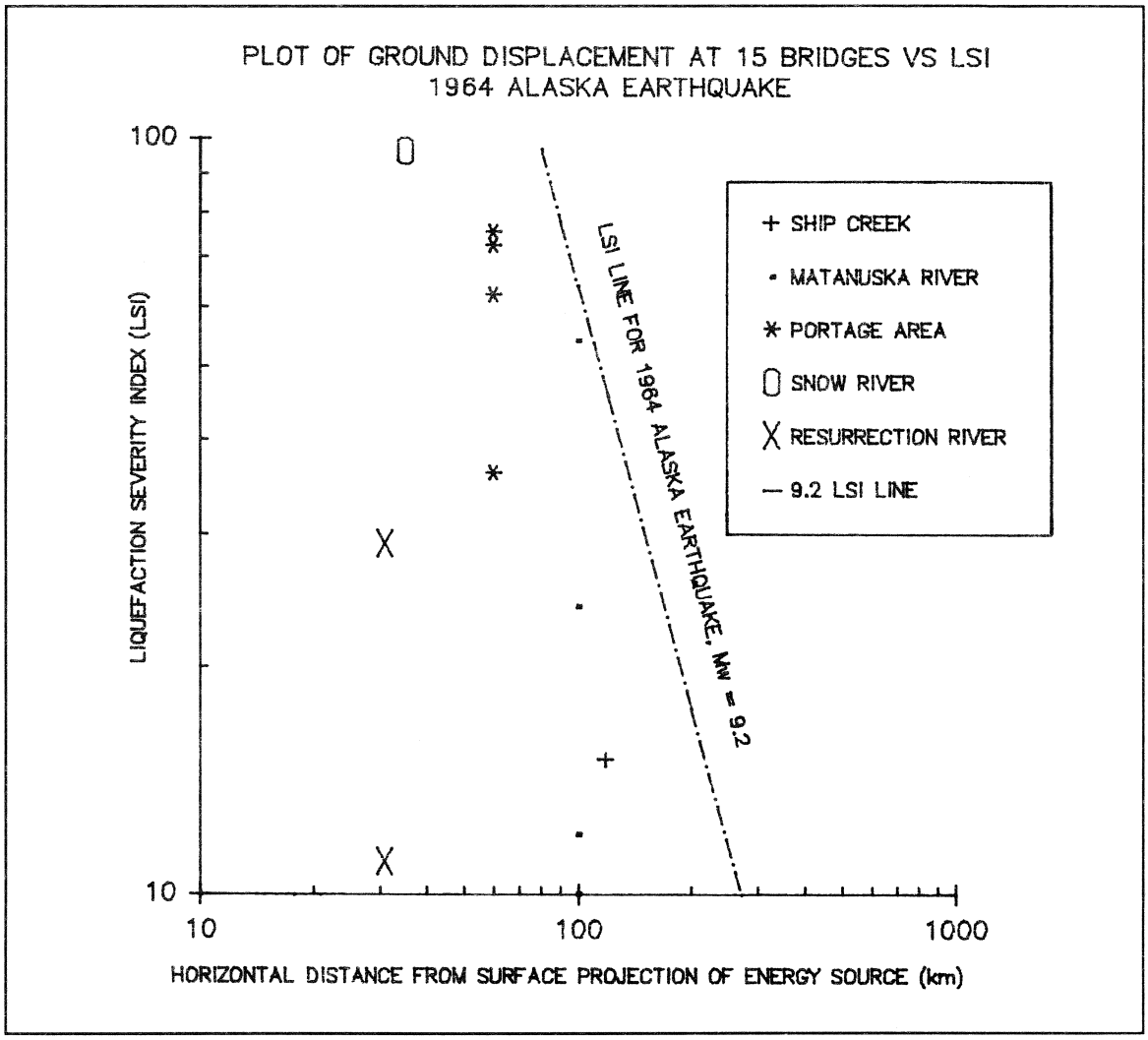

Figure 76 LSI Values for Damaged Bridge Sites.

Finally, liquefaction-induced ground failure and bridge damage spawned by the 1964 Alaska earthquake demonstrates a potential hazard to bridges built on liquefiable soils in earthquake prone regions. The 1964 Alaska earthquake is a poignant reminder of our challenge to improve our methods of estimating ground failure displacement and its consequences.

REFERENCES

Andrus, R. D., Youd, T. L., 1989, "Penetration Tests in Liquefiable Gravels," Proceedings of the 12th International Conference on Soil Mechanics and Foundation Engineering, A. A. Balkema Publishers, Vol. 1, pp. 679-682.

Bartlett, S. F., Youd, T. L., 1990, "Evaluation of Ground Failure Displacement Associated with Soil Liquefaction: Compilation of Case Histories," Miscellaneous Paper S-73-1, Prepared for Department of the Army, U.S. Army Corps of Engineers, Washington, D.C., 84.

Earthquake Spectra, May 1990, "Loma Prieta Earthquake Reconnaissance Report,Supplement to Volume 6, Published by Earthquake Engineering Research Institue, El Cerrito, CA, 448 p.

Furumoto, A. S., 1967, "Analysis of Rayleigh Waves, Part 2 of "Source Mechanism of the Alaska Earthquuake and Tsunami of 27 March 1964," Pacific Science, Vol., 21, No. 3, pp. 311-316.

Hamada, M., Yasuda, S., Isoyama, R., Emoto, K., 1986, "Study of Permanent Ground Displacement Induced by Seismic Liquefaction," Published by the Association for the Development of Earthquake Prediction in Japan, Tokyo, Japan, 87 p.

Hansen, W. R., Eckel, E. B., Schaem, R. E., Lyle, W. G., Chance, G., 1966, "The Alaska earthquake, March 27, 1964: Field investigations and reconstruction effort," U.S.G.S. Professional Paper 541, Government Printing Office, Washington, D.C., 111 p.

Housner G. W., Jennings, P. C., 1973, "Reconstituted Earthquake Ground Motion at Anchorage," The Great Alaska Earthquake, Engineering Volume, National Academy of Sciences, Washington, D.C., 1973, pp. 43-72.

Hudson, D. E., Cloud, W. K., 1973, "Seismological Background for Engineering Studies of the Earthquake," The Great Alaska Earthquake, Engineering Volume, National Academy of Sciences, Washington, D.C., 1973, pp. 18-42.

Idriss, I. M., 1990, "Response of Soft Soil Sites during Earthquakes," H. Bolton Seed Memorial Symposium Proceedings, Vol. 2, BiTech Publishers LTD, Vancouver, B.C., Canada, pp. 273-289.

Joyner, W. B., Boore, D. M., 1988, "Measurement, Characterization, and Prediction of Strong Ground Motion," Earthquake Engineering and Soil Dynamic II, ASCE Geotechnical Special Publication No. 20, ASCE, New York, New York, pp. 43-102.

Joyner, W. B., Boore, D. M., 1981, "Peak Horizontal Acceleration and Velocity from Strong-Motion Records From the 1979 Imperial Valley, California, Earthquake, Seismological Society of America Bulletin, 71(6), pp. 2011-2038.

Kachadoorian, R., 1968, "Effects of the Earthquake of March 27, 1964, on the Alaska Highway System," U.S.G.S. Professional Paper 545-C, Government Printing Office, Washington, D.C., 66 p.

Kachadoorian, R., 1966, "Effects of the Earthquake of March 27, 1964 at Whittier Alaska," U.S.G.S. Professional Paper 542-B, Government Printing Office, Washington, D.C., 21 p.

Kanamori, H., 1978, "Quantification of Earthquakes," Nature, Vol. 271, pp. 411-414.

Krinitzsky, E. L., Chang, F. K., 1988, "Magnitude-Related Earthquake Ground Motions, "Bulletin of the Association of Engineering Geologists, Vol. XXV, No. 4, pp. 399 - 423.

Liao, S. S. C., 1986, "Statistical Modeling of Earthquake-Induced Liquefaction", Ph.D. Dissertation, Department of Civil Engineering, Massachusetts Institute of Technology, 470 p.

Malloy, R. J., 1964, "Crustal Uplift Southwest of Montague Island, Alaska," Science, Vol. 146, No. 3647, pp. 1048-1049.

Marcuson, W. F., Hynes, M. E., Franklin, A. G., 1990, "Evaluation and Use of Residual Strength in Seismic Safety Analysis of Embankments," Earthquake Spectra, Vol. 6, No. 3, pp. 529-572.

McCulloch, D. S., Bonilla, M. G., 1970, "Effects of the Earthquake of March 27, 1964, on the Alaska Railroad, U.S.G.S. Professional Paper 545-D, Government Printing Office, Washingtion, D.C., 161 p.

National Research Council, 1985, Liquefaction of Soils During Earthquakes, National Academy Press, Washington D.C., 240 p.

Parkin, E. J., 1966, "Horizontal Displacement, Part 2 of Alaskan Surveys to Determine Crustal Movement," U.S. Coast and Geodetic Survey, 11 p.

Plafker, G., 1971, "Tectonics," The Great Alaska Earthquake, Geology Volume, National Academy of Sciences, Washington, D.C., pp. 47-122.

Plafker, G., 1968, "Tectonics of the 1964 Alaska Earthquke," U.S.G.S. Professional Paper 543 I, Government Printing Office, Washington, D.C.

Plafker, G., 1965, "Tectonic Deformation Associated with the 1964 Alaskan Earthquake," Science, Vol. 148, No. 3678, pp. 1675-1687.

Poulos, S. J., 1981, "The Steady State of Deformation," Journal of the Geotechnical Engineering Division, ASCE 107(GT5), pp. 553-562.

Ross, G. A., Seed, H. B., Migliaccio, R. R., 1973, "Performance of Highway Bridge Foundations," The Great Alaska Earthquake of 1964, Engineering Volume, National Academy of Sciences, Washington D.C., pp. 190-242.

Schnabel, P. B., Lysmer, J., Seed H. B., 1972, "SHAKE: A computer program for Earthquake Response Analysis of Horizontally Layered Sites," Report No. UCB/EERC-72/12, Earthquake Engineering Research Center, University of California, Berkeley, 18 p.

Seed, H. B., and Idriss, I. M., 1971, "Simplified Procedure for Evaluation of Soil Liquefaction Potential," Journal of Soil Mechanics and Foundations Division, ASCE, Vol. 97, No. SM9, pp. 1249 - 1273.

Seed, H. B., Idriss, I. M., 1982, Ground Motions and Soil Liquefaction During Earthquakes, Earthquake Engineering Research Institute Monograph, El Cerrito, CA, 134 p.

Seed, H. B., Idriss, I. M., Arrango, I., 1983, "Evaluation of Liquefaction Potential Using Field Performance Data," Journal of Geotechnical Engineering, ASCE, Vol. 109(3), pp. 458 - 482.

Seed, H. B., Tokimatsu, K., Harder, L. F., Chung, R. M., 1985, "Influence of SPT Procdures in Soil Liquefaction Resistance Evaluations," Journal of Geotechnical Engineering, ASCE Publication, Volume 111, No. 12, Dec. 1985, pp. 1425-1445.

Seed, H. B., De Alba, P., 1986, "Use of SPT and CPT Tests for Evaluating the Liquefaction Resistance of Sands," Use of In-Situ Test in Geotechnical Engineering, Geotechnical Special Publication No. 6, ASCE, New York, New York, pp. 281-302.

Seed, H. B., 1987, "Design Problems in Soil Liquefaction," Journal of Geotechnical Engineering, ASCE Publication, Vol. 113, No. GT8, August 1987, pp. 827-845.

Seed, H. B, Seed, R. B., Harder, L. F., Jr., Jong, H. L., 1988, "Re-Evaluation of the Slide in the Lower San Fernando Dam in the Earthquake of February 9, 1971," Report No. UCB/EERC-88/04, University of California, Berkeley, CA.

Shannon and Wilson, 1987, "Geotechnical Report, MLP Transmission Line Relocation, Ship Creek to Port, Anchorage Alaska," Shannon and Wilson INC., Geotechnical Consultants, Anchorage, Alaska.

Toksoz, M. N., Ben-Menahem, A., Harkrider, D. G., 1965, "Source Mechanism of Alaska Earthquake from Long-Period Seismic Susrface Waves," Am. Geophys. Union Trans., Vol. 46, No. 1, p. 154.

Trainer, F. W., 1953, Preliminary report on the geology and groundwater resources of the Matanuska Valley agricultural area, Alaska: U.S.G.S. Water-Supply Paper 1494, 116 p.

Utermohle, G. E., 1962, "Amended Copy, Foundation Study Report, Snow River Bridge #605, Project Number F 031-1(6), Anchorage District, Alaska Department of Transportation, Anchorage, Alaska, 28 p.

Utermohle, G. E., 1963, "Foundation Study Report, Knik and Matanuska River Bridges, Bridge Numbers 1121, 1122, 1123, 1124, Project Number F 042-1(7), Anchorage District," Alaska Department of Transportation, Anchorage, Alaska, 37 p.

Utermohle, G. E., 1965, "Foundation Investigation, Twenty Mile River, Bridge No. 634, Project No. ERFO-36(1), Anchorage District," Alaska Department of Transportation, Anchorage, Alaska, 5 p.

Utermohle, G. E., 1965, "Foundation Investigation, Portage River No. 1 (#630) and Portage River No. 2 (#631), Project No. ERFO-20(1), Anchorage District," Alaska Department of Trasportation, Anchorage, Alaska, 8 p.

Utermohle, G. E., 1965, "Foundation Investigation, Placer River #1 and Placer River Main Crossing, Bridges #627 and 629, Project No. ERFO-20(1), Anchorage District," Alaska Department of Transportation, Anchorage, Alaska, 9 p.

Wyss, M., Brune, J. N., 1967, "The Alaska Earthquake of 27 March 1964 - A Complex Multiple Rupture," Seismol. Soc. America Bull., Vol. 57, No. 5, pp. 1017-1023.

Youd, T. L., Perkins, D. M., 1978, "Mapping Liquefaction-Induced Ground Failure Potential," Journal of the Geotechnical Engineering Division, ASCE, Vol. 104, No. GT4, April, 1978, pp. 433-446.

Youd, T. L., Perkins, D. M., 1987, "Mapping of Liquefaction Severity Index," Journal of Geotechnical Engineering, ASCE, Vol. 113, No. 11, November, 1987, pp. 1374-1392.

Large Ground Deformations and Their Effects on Lifeline Facilities: 1971 San Fernando Earthquake

T.D. O'Rourke, Professor
School of Civil and Environmental Engineering
Cornell University
Ithaca, New York

B.L. Roth[1]*, Senior Engineer*
GAI Consultants
Pittsburgh, Pennsylvania

M. Hamada, Professor
School of Marine Science and Technology
Tokai University
Shimizu, Shizuoka, Japan

[1] Former Graduate Research Assistant, School of Civil and Environmental Engineering, Cornell University, Ithaca, New York

ACKNOWLEDGMENTS

The authors wish to express their gratitude to those who have provided valuable assistance in the preparation of this report. Special thanks are extended to Charles F. "Ted" Voyles, William P. Lundy, Louis Cetina, and others at the Metropolitan Water District of Southern California, who generously shared their knowledge and information concerning the 1971 San Fernando earthquake. Gratitude is extended to Robert Bryant of the Los Angeles Department of Water and Power for providing information on pipeline and subsurface conditions, and to Charles Minges of the Los Angeles Bureau of Engineering for providing control point information and maps. We also thank Geoff Martin of the Earth Technology Corporation for his help in obtaining site exploration information. The assistance of Rusty Brown at the University of California at Santa Barbara, and Gary Brusse of Pacific Western Aerial Survey, who helped obtain the photographs for the photogrammetric analyses, is deeply appreciated. In addition, the following individuals generously contributed valuable information: Michael J. Bennett, James Lienkaemper, Michael Moore, and Malcolm Clark of the U.S.G.S. in Menlo Park, CA; Robert Pride and Mark Schluter of Converse Consultants; Phillip Mulvey of the U.S. Army Corps of Engineers, Los Angeles; Cuong Nguyen of the California Department of Transportation; Carolyn S. Marks of Whittier College; and Allan G. Barrows of the California Division of Mines and Geology. We are grateful to Charles F. "Ted" Voyles and William P. Lindy of the Metropolitan Water District of Southern California, and Walter W. Hoye of the Department of Water and Power, City of Los Angeles, for reviewing the draft of this report.

Special thanks are extended to Ali Avcisoy, who did an excellent job of preparing the figures. The assistance of Amy Peters, for her thoughtful and cheerful participation, Laurie Mayes for her help in preparing numerous transmittals, and Kristin J. Stewart for her preparation of the manuscript, is deeply appreciated.

Ground deformation measurements using pre- and post-earthquake air photos were conducted by the Japanese members of the Japan-U.S. Cooperative Research on Liquefaction, Large Ground Deformation, and Their Effects on Lifeline Facilities. We would like to thank Professor K. Kubo of Tokai University for his assistance in heading the Japanese team. We also express our sincere appreciation to Mr. I. Yasuda of Hasshu Co., Ltd. for performing the measurements.

TABLE OF CONTENTS

		Page
Acknowledgments		3-iii
Table of Contents		3-v
List of Tables		3-vii
List of Figures		3-ix

Section		Page
1.0	INTRODUCTION	3-1
2.0	TECTONIC SETTING, INTENSITY, AND FELT EFFECTS	3-2
3.0	STRONG MOTION DATA	3-3
4.0	COLLECTION AND EVALUATION OF DATA	3-6
5.0	LOCATIONS OF LARGE GROUND DEFORMATION	3-8
6.0	GROUND DEFORMATION WEST OF THE UPPER VAN NORMAN RESERVOIR	3-11
	6.1 Joseph Jensen Filtration Plant Facilities	3-11
	Finished Water Reservoir	3-13
	Filters, Settling, and Mixing Basins	3-14
	Main Control Building	3-14
	East-West Conduits	3-14
	6.2 San Fernando Powerplant	3-15
	6.3 Surficial Ground Movements	3-15
	6.4 Cumulative Lateral and Vertical Movements	3-15
	6.5 Air Photo and Optical Survey Measurements	3-17
	6.6 Subsurface Conditions	3-19
7.0	GROUND DEFORMATION EAST OF THE UPPER VAN NORMAN RESERVOIR	3-27
	7.1 Buildings East of the Upper Van Norman Reservoir	3-27
	San Fernando Valley Juvenile Hall	3-27
	Sylmar Converter Station	3-30
	7.2 Highway Facilities	3-31
	7.3 Surficial Ground Movements	3-31
	7.4 Air Photo and Optical Survey Measurements	3-32
	7.5 Subsurface Conditions	3-34

Section		Page
8.0	OVERVIEW OF LARGE GROUND DEFORMATION	3-39
9.0	PIPELINE DAMAGE AT UPPER VAN NORMAN RESERVOIR	3-45
10.0	GROUND DEFORMATION ALONG THE SAN FERNANDO FAULT	3-52
11.0	PIPELINE PERFORMANCE ALONG SAN FERNANDO FAULT	3-53
	11.1 Gas Distribution Pipelines	3-54
	11.2 Water Distribution Pipelines	3-55
12.0	PIPELINE REPAIRS RELATIVE TO THE FAULT ZONE	3-58
13.0	PERFORMANCE OF GAS TRANSMISSION PIPELINES	3-60
14.0	OVERVIEW OF PIPELINE PERFORMANCE	3-62
REFERENCES		3-65

Appendix		Page
A	LIST OF GEOTECHNICAL INVESTIGATIONS	3-72
B	PHOTOGRAMMETRIC ANALYSIS	3-76

LIST OF TABLES

Table		Page
1	Information Summary for Pipelines Affected by Ground Movements	3-47
2	Summary of Information for Gas Transmission Pipelines	3-61
B.1	Accuracy of Permanent Ground Displacement Measurements	3-80
B.2	Comparison of Vectors of Displacement Determined by Two Measurement Techniques	3-83

LIST OF FIGURES

Figure		Page
1	Tectonic Setting of San Fernando Earthquake	3-4
2	Map of Modified Mercalli Intensities Associated with the Earthquake	3-4
3	Strong Motion Accelerograms	3-5
4	Region of Most Severe Earthquake Damage	3-10
5	Areas of Large Ground Deformation	3-10
6	Plan View of Joseph Jensen Filtration Plant	3-12
7	Map of Surficial Ground Cracks, Sand Boils, and Pressure Ridges Near Joseph Jensen Filtration Plant	3-16
8	Aerial View of Joseph Jensen Filtration Plant	3-16
9	Cumulative Displacements Across the Joseph Jensen Filtration Plant	3-18
10	Displacements Determined from Air Photo Analyses and Optical Surveys, Joseph Jensen Filtration Plant	3-18
11	Locations of Soil Borings and Soundings at the Joseph Jensen Filtration Plant	3-20
12	Soil Profile at Cross-Section A-A', Joseph Jensen Filtration Plant	3-20
13	Soil Profile at Cross-Section B-B', Joseph Jensen Filtration Plant	3-21
14	Soil Profile at Cross-Section C-C', Joseph Jensen Filtration Plant	3-21
15	Soil Profile at Cross-Section D-D', Joseph Jensen Filtration Plant	3-22
16	Soil Profile at Cross-Section E-E', Joseph Jensen Filtration Plant	3-22
17	Soil Profile Along North-South Axis of Joseph Jensen Filtration Plant	3-23

Figure		Page
18	Typical Grain Size Distribution Curves for Alluvial Soils at Joseph Jensen Filtration Plant	3-25
19	Contours of Equal Elevation for the Base of Loose Saturated Alluvium at the Joseph Jensen Filtration Plant	3-25
20	Contours of Equal Thickness of Loose Saturated Alluvium at the Joseph Jensen Filtration Plant	3-26
21	Plan View of East Side of Upper Van Norman Reservoir	3-28
22	Map of Surficial Ground Cracks, Sand Boils, and Pressure Ridges East of Upper Van Norman Reservoir	3-29
23	Displacements Determined from Air Photo Analyses and Optical Surveys, East of Upper Van Norman Reservoir	3-33
24	Locations of Soil Borings and Soundings East of Upper Van Norman Reservoir	3-35
25	Soil Profile at Cross-Section A-A', East of Upper Van Norman Reservoir	3-36
26	Soil Profile at Cross-Section B-B', Juvenile Hall	3-37
27	Soil Profile at Cross-Section C-C', Juvenile Hall	3-37
28	Soil Profile at Cross-Section D-D', Sylmar Converter Station	3-38
29	Typical Grain Size Distribution for Alluvial Soils East of Upper Van Norman Reservoir	3-38
30	Contours of Equal Elevation for the Base of Loose Saturated Alluvium East of Upper Van Norman Reservoir	3-39
31	Plan Views of Upper Van Norman Reservoir Area Showing Geologic Structure, Geomorphology, and Groundwater	3-40
32	Cross-Sectional Views of Joseph Jensen Filtration Plant Showing Large Ground Deformation and Cumulative Joint Openings of Overflow Conduit Along Sections B-B' and C-C'	3-42
33	Plan View of Juvenile Hall Landslide, East Side of Upper Van Norman Reservoir	3-46
34	Pipelines Affected by Permanent Ground Movements Near Upper Van Norman Reservoir	3-47

Figure		Page
35	Locations of Pipeline Repair, West Side of Upper Van Norman Reservoir	3-49
36	Locations of Pipeline Repair, East Side of Upper Van Norman Reservoir	3-51
37	Plan View of Surface Faulting and Replaced Gas Distribution Pipelines	3-54
38	Plan View of Repairs of Gas Distribution Pipelines	3-56
39	Plan View of Replaced and Repaired Water Distribution Pipelines	3-57
40	Gas Pipeline Repairs as a Function of Distance from the Fault Zone	3-59
41	Water Pipeline Repairs as a Function of Distance from the Fault Zone	3-60
42	Plan View of Breaks and Explosion Craters for Gas Transmission Pipelines	3-61
B.1	Map Showing Outline of Mapped Area, Flight Lines, and Control Points Near the Van Norman Reservoir	3-77
B.2	Map of West Side of Upper Van Norman Reservoir Illustrating the Photogrammetric Technique	3-77
B.3	Regional Tectonic Movements Represented by Horizontal Displacements of Control Points and Contours of Elevation Change	3-81
B.4	Vectors of Displacement Along San Fernando Road Determined by Two Measurement Techniques	3-83
B.5	Method of Adjusting Vectors of Displacement Determined by Photogrammetric Technique	3-84
B.6	Vectors of Displacement Determined from Air Photo Analysis Along the Crest and West of the Upper Van Norman Reservoir	3-85

LARGE GROUND DEFORMATIONS AND THEIR EFFECTS ON LIFELINE FACILITIES: 1971 SAN FERNANDO EARTHQUAKE

1.0 INTRODUCTION

The 1971 San Fernando earthquake was an event of considerable engineering and seismological significance for at least three reasons. To start, the earthquake generated an unprecedented amount of data on strong ground and building motion. More strong motion records of engineering interest were acquired during this one earthquake than during the previous 39-year history of the U.S. cooperative network recording program (Cloud and Hudson, 1975). From a geotechnical perspective, liquefaction-induced ground movements and slope failures caused substantial structural damage and left the lower San Fernando Dam precariously close to catastrophic failure (Cortright, 1975). Studies of the sliding mechanisms and dynamic instabilities affecting the San Fernando Dams have improved our understanding of soil liquefaction (e.g., Seed, et al., 1973 and 1975; GEI Consultants, Inc., 1988) and have contributed to the national program for assessing dam safety (Committee on Safety Criteria for Dams, 1985). From a lifelines perspective, damage and disruption of public utilities focused worldwide attention on service networks and stimulated interest in lifeline earthquake engineering as a viable, continuing area of research and practice.

Perhaps the most distinctive feature of the earthquake was its influence on lifeline systems. Nearly 900,000 customers in the combined jurisdictions of the Los Angeles Department of Water and Power and Southern California Edison Company were affected by electrical power outages (Wong, 1973; Southern California Edison Company, 1973). Telephone equipment in the General Telephone Company Sylmar central office was destroyed, disrupting the use of nearly 10,000 phones (Steinbrugge, et al., 1971). The damage was especially severe for buried conduits, including water supply, gas, liquid fuel, and wastewater pipelines.

Most permanent ground deformation was concentrated in two areas: the Van Norman Reservoir complex and along the San Fernando fault. The Van Norman

Reservoir complex is the terminus of two aqueducts which supplied 80% of the water for the City of Los Angeles. Liquefaction-induced soil movements affected bypass pipelines, channels, pump stations, and filtration facilities within and adjacent to the complex. There were 22 breaks in two major trunk lines (Steinbrugge, et al., 1971; Subcommittee on Water and Sewerage, 1973), primarily caused by liquefaction-induced soil movements. Major damage was sustained by the Joseph Jensen Filtration Plant, Juvenile Hall, and Sylmar Converter Station as a result of ground deformation caused by liquefaction. Over 1400 individual repairs were made in the Los Angeles water distribution system, with nearly 900 repairs in the vicinity of the Sylmar segment of the San Fernando fault (Steinbrugge, et al., 1971). Approximately 6 km of distribution mains in the City of San Fernando were damaged beyond repair by surface faulting and had to be replaced (McCaffrey and O'Rourke, 1983). Damage from large ground deformation resulted in the loss of gas supply to 17,000 customers, with as many as 380 gas main and service breaks. Over 38 km of mainline sewers were reconstructed as a result of earthquake damage (Subcommittee on Water and Sewerage Systems, 1973).

This case history focuses on large ground deformations and related lifeline damage near the Upper Van Norman Reservoir and the Sylmar and Mission Wells segments of the San Fernando fault. Ground motion intensity, regional seismicity, and strong motion records are discussed, followed by an in-depth description of site conditions, subsurface soils and groundwater, and ground deformations. Information is presented on damaged pipelines, conduits, and foundations, and relationships are examined between large ground deformations and pipeline and foundation response.

2.0 TECTONIC SETTING, INTENSITY, AND FELT EFFECTS

The earthquake occurred on February 9, 1971 at 6:01 a.m. Pacific Standard Time. It registered a magnitude 6.4 on the Richter scale and affected an area of 220,000 km^2 including southern California, western Arizona, and southwestern Nevada (Coffman, et al., 1982). The epicenter was located about 13 km north-northeast of San Fernando in the western San Gabriel Mountains at geographical coordinates 34°24'N, 118°23.7'W. The focal depth of the earthquake was 8.4 $\pm$ 4 km (Bolt and Gopalakrishnan, 1975). Surface faulting occurred

close to the south front of the San Gabriel Mountains within the San Fernando and Sylmar communities.

The San Fernando Valley is located within the middle of the Transverse Range Structural Province, which consists of a series of east-west trending mountain ranges and structural features that cut across the northwest trend of the Peninsular and Coast Mountain Ranges to the south and north, respectively. As seen in Figure 1, the San Andreas fault makes a wide west-northwest bend as it crosses the Transverse Ranges. This bend produces north-south compressional forces that are relieved by east-west trending reverse faults such as those in the Sierra Madre fault zone (Rogers, 1979). Evidence of continuous movement along the Sierra Madre fault zone is seen in the scarps on alluvial fans in the Cucamonga Canyon (Morton and Baird, 1975), in the steepness of the canyon sides of Big Tujunga and Pacoima (Oakeshott, 1975), and in the sharp topographic break between the San Fernando Basin and the San Gabriel and Santa Susana Mountain fronts (Wentworth and Yerkes, 1971).

The felt effects of the earthquake were evaluated by the U.S. National Oceanographic and Atmospheric Administration (N. H. Scott, 1973). The Modified Mercalli Intensity scale (MMI) of 1931 (Wood and Neumann, 1931) was used to assign a numerical value to the effects of the earthquake. Five intensity zones were delineated, as shown on the isoseismal map in Figure 2. The maximum intensity zone was 530 km^2, with effects rated from MMI VIII to XI. An MMI rating of X was ascribed to zones of large permanent ground deformation associated with surface faulting within the Sylmar segment of the San Fernando fault and liquefaction-induced landslides in the Lower and Upper San Fernando Dams. An MMI intensity of XI was assigned to the damage at the Olive View Hospital. Here, an earthquake resistant structure nearly was destroyed by intense ground shaking, and two persons were killed (N. H. Scott, 1973).

3.0 STRONG MOTION DATA

Two hundred and forty-one accelerograph recording stations were affected, of which 175 were installed on highrise buildings in downtown Los Angeles (Cloud and Hudson, 1975). Figure 3 provides a sample of strong motion accelerograms recorded during the earthquake. Figure 3 shows the time record of

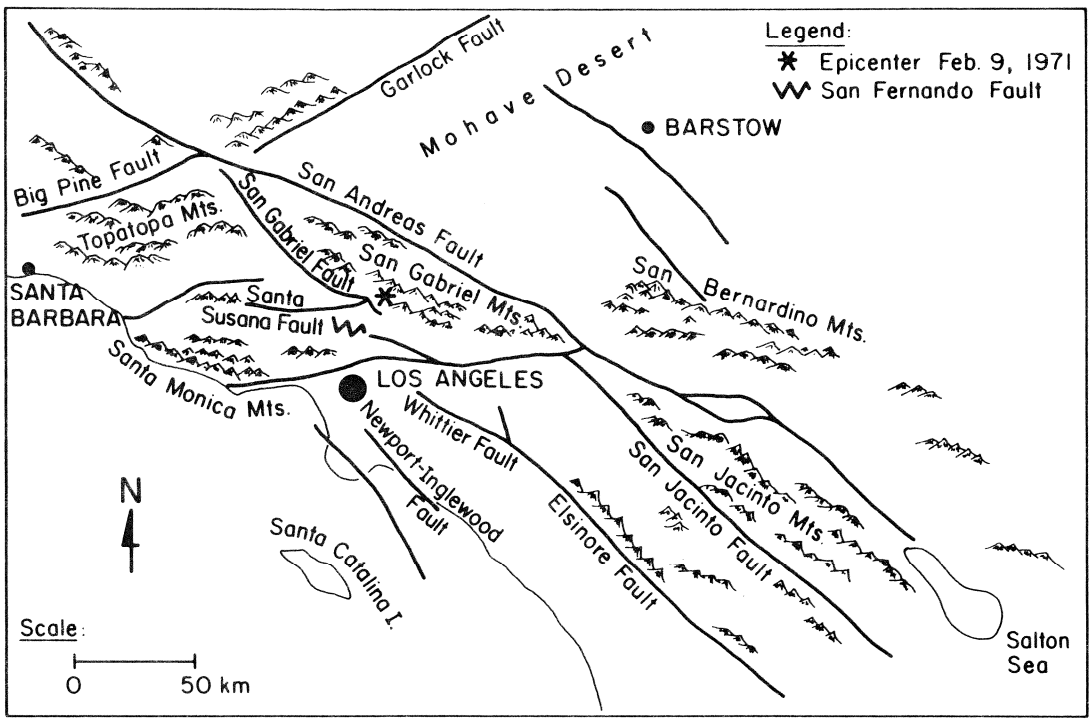

Figure 1. Tectonic Setting of San Fernando Earthquake

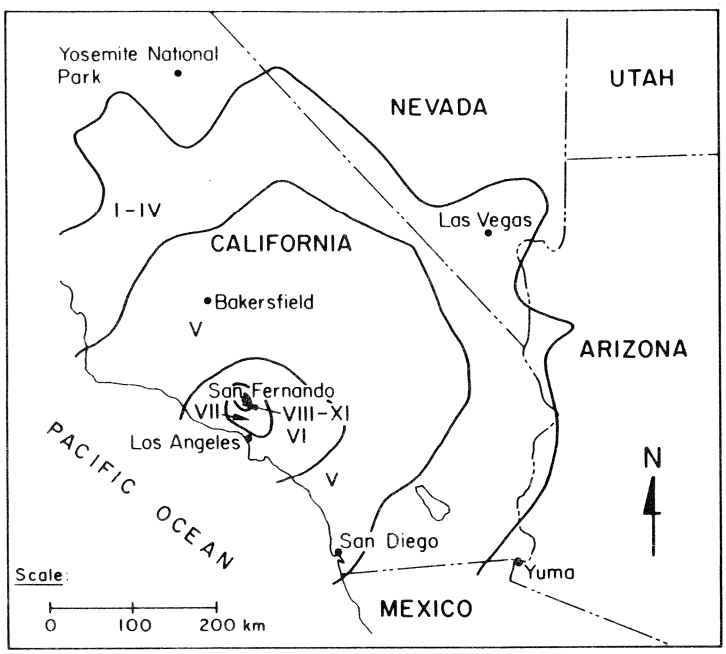

Figure 2. Map of Modified Mercalli Intensities Associated with the Earthquake (after N. H. Scott, 1973)

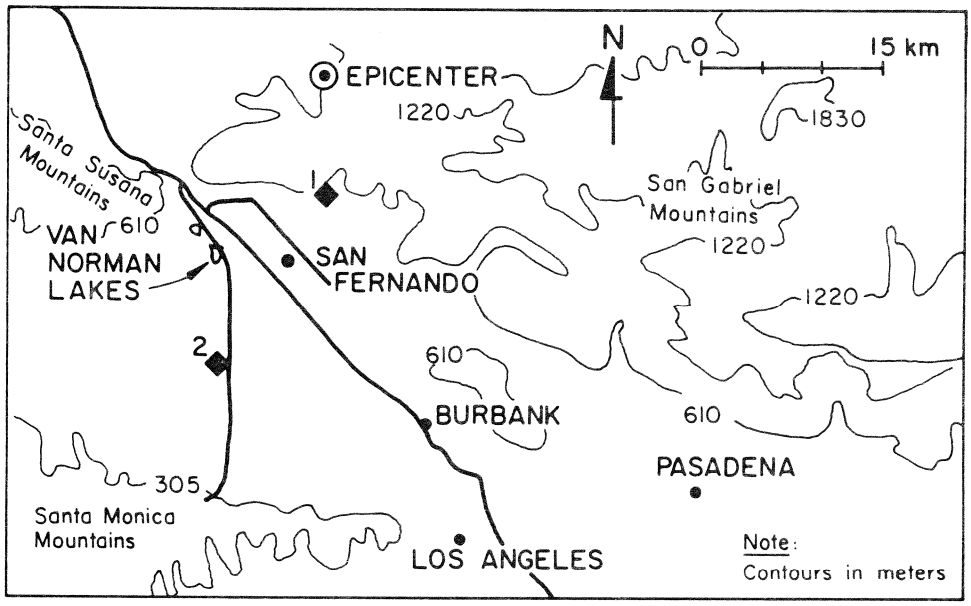

a) Location of Strong Motion Instruments

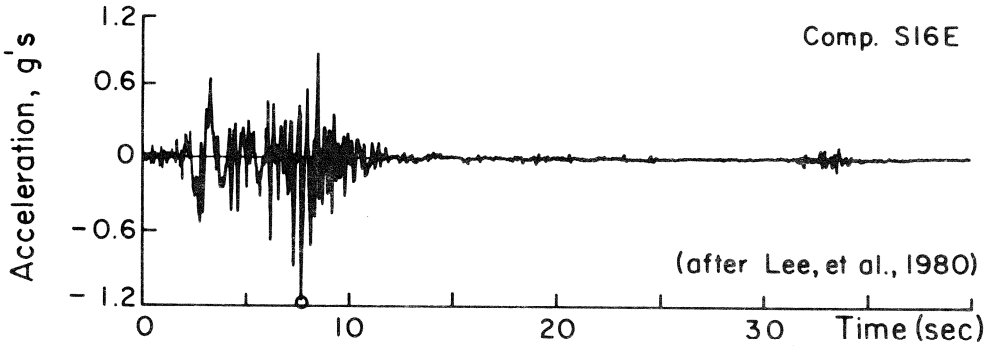

b) Accelerogram Pacoima Dam (Location 1)

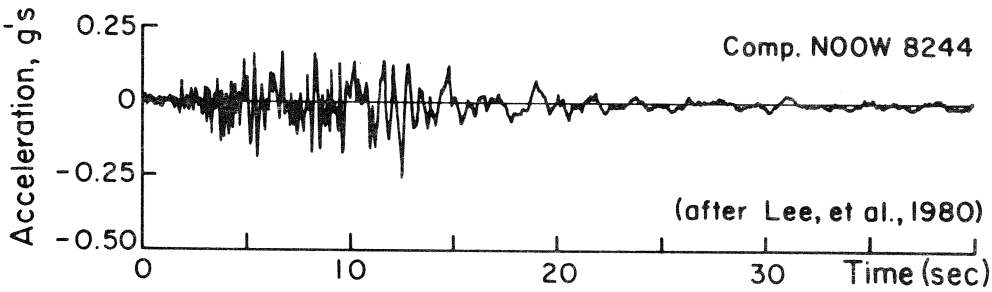

c) Accelerogram 8244 Orion Blvd. (Location 2)

Figure 3. Strong Motion Accelerograms

acceleration of the horizontal component with the peak acceleration at a given site. The locations of selected strong motion instruments relative to the earthquake epicenter are shown in the upper map of the figure.

The strong motion record closest to the epicenter was acquired at Pacoima Dam, 8 km south of the epicenter and 4 km north of the surface faulting. Acceleration histories of the horizontal components of motion are shown in Figure 3b. The accelerograph at Pacoima Dam was positioned near the south abutment on a granitic ridge. During the main shock, the accelerograph was jolted in such a way that it was slightly tilted. This tilt extended operation of the accelerograph, and resulted in a continuous record of aftershocks for about six minutes. The record from the main shock showed vertical accelerations of 0.72 g and horizontal accelerations of 1.25 g, the highest ever recorded for an earthquake (Cloud and Hudson, 1975).

An accelerogram from 8244 Orion Boulevard, Los Angeles, CA, also is shown in Figure 3. The strong motion instrument was located about 28 km south of the epicenter. The recording, which was obtained on the first floor of a seven-story reinforced concrete building situated on alluvial soils, indicates a maximum horizontal component of 0.27 g.

Another important source of strong motion data was the seismoscope, located about 17 km south of the epicenter on the east abutment of the Lower San Fernando Dam. The seismoscope recording, its interpretation, and conversion to acceleration history are described by R. F. Scott (1973) and Seed, et al. (1975). Allowing for the uncertainties involved in the seismoscope record interpretation, Scott suggested that peak accelerations of 0.55 to 0.6 g could be inferred from the record.

4.0 COLLECTION AND EVALUATION OF DATA

Information about large ground deformations was collected from a variety of sources, starting with a detailed review of the published literature and professional engineering reports commissioned by the Metropolitan Water District of Southern California (MWD), Los Angeles Department of Water and Power (LADWP), State of California Department of Transportation (CDOT), and the

County of Los Angeles (CLA). Stereo pair and oblique aerial photographs of the site before and after the earthquake were collected and examined, including a review of stereo pair photographs from 1929, 1945, and 1954 to gain insight about landforms, soils, and cultural changes surrounding the Van Norman Reservoirs.

Site visits were made, and discussions conducted with key personnel of water, power, state, and gas utility agencies, who were either present at the time of the earthquake or were involved in post-earthquake damage assessment and reconstruction. The discussions included interviews with surveyors, who performed post-earthquake measurements, and welders, who repaired damaged high pressure pipelines. Information was collected on the construction, operating conditions, and repairs of buried pipelines from the Southern California Gas Company, City of San Fernando, Getty Oil Company, Mobil Oil Company, MWD, and LADWP.

A detailed study was performed of the landforms and topography visible in 1900, 1928, and recent topographic maps. Several hundred photographs of ground movements and facility damage were examined, and used to locate characteristics of interest, and integrated into the study as a supplement and check on other sources of information.

Over 200 soil borings and 72 cone penetration soundings were collected from MWD, LADWP, the U.S. Geological Survey (USGS), and California Department of Transportation. Standard penetration test (SPT) data were corrected for overburden pressure and energy efficiency according to the recommendations of Seed, et al. (1983) and Seed and De Alba (1986). Nonstandard penetration test data from earlier geotechnical reports were evaluated in context of the SPT results. Statistical correlations were developed between nonstandard and SPT test data where possible, and used to refine and expand the data acquired in earlier studies. Cone penetration test (CPT) data were used in conjunction with SPT values and groundwater observations to delineate soils vulnerable to liquefaction. A summary of the geotechnical reports, borehole records, and test data reviewed as part of this study is provided in Appendix A.

Panchromatic stereo pair photographs before (Mar., 1968) and after (Feb. and

Mar., 1971) the earthquake were obtained from the air photo library of the University of California at Santa Barbara, and evaluated in conjunction with vertical aerial photographs from the USGS and U.S. Army Corps of Engineers. Photogrammetric analyses of the stereo pair air photos were performed by Japanese researchers (ADEP, 1990). Survey control point data for the photogrammetric analyses were provided by the Los Angeles Bureau of Engineering. Optical surveys at ground level along the San Fernando Road and Upper Van Norman Dam were used to check vertical and horizontal surface movements determined by the analysis of pre- and post-earthquake aerial photos. Moreover, the accuracy of the photogrammetric measurements was checked by comparing selected measurements with cumulative displacements estimated from post-earthquake observations of buried facilities at the Joseph Jensen Filtration Plant, confirming that stable points on the Saugus Formation did not show movement exceeding measurement error, and comparing post-earthquake utility locations with pre-earthquake as-built alignments. A summary of the photogrammetric analytical techniques, with an assessment of quality and measurement accuracy, is presented in Appendix B.

5.0 LOCATIONS OF LARGE GROUND DEFORMATION

Large ground deformations were associated with all sources of permanent earthquake ground movements classified by O'Rourke and McCaffrey (1984), including surface faulting, liquefaction, landslides, consolidation of cohesionless soil, and tectonic uplift. The most severe effects on lifeline facilities were generated by liquefaction-induced soil movements and surface faulting, which are the primary sources of deformation examined in this case history.

There were thousands of landslides in the hilly and mountainous terrain above San Fernando Valley (Morton, 1975), but for the most part, they occurred in relatively remote areas where there was little impact on lifeline facilities. A few landslides were significant and deserve some comment. Soil slumps occurred near the First Los Angeles Aqueduct, and a large landslide caused extensive damage to a 1900-mm-diameter welded steel pipeline conveying water as part of the Second Los Angeles Aqueduct (Subcommittee on Water and Sewerage Systems, 1973). The above-ground pipe pulled apart at mechanical couplings above the slide and suffered compression failure near the toe.

A regional view of the areas affected by permanent ground deformations in relationship to the earthquake epicenter is shown in Figure 4. Although most surface effects were within the area of the figure, there were some instances of landsliding and ground movements located north and east of the epicenter. Tectonic movements along the San Fernando fault are shown in Figure 4. The greatest length of surface fault breakage occurred at the base of the San Gabriel Mountains, east of the City of San Fernando. However, the most significant effects to public works were experienced in the City of San Fernando and in the Sylmar District of the City of Los Angeles.

Figure 5 shows two areas of large ground deformation which are the principal zones of interest in this case history. The locations are the area surrounding the Upper Van Norman Reservoir and the area along the Mission Wells and Sylmar segments of the San Fernando fault.

Considerable ground deformation caused by liquefaction was observed near the Upper Van Norman Reservoir. On the west side of the reservoir, cracks extended from the Van Gough School to the west edge of the reservoir. The most extensive ground cracks occurred at the Joseph Jensen Filtration Plant. Ground cracks on the northeast side of the reservoir extended from the Juvenile Hall, through the Converter Station, to the east shore of the reservoir. Ground cracks caused by soil liquefaction also were seen around the tail race pond and near the San Fernando Powerhouse. Permanent ground movements resulting from soil liquefaction also were noted northeast and east of the Lower Van Norman Reservoir at Blucher Avenue (Lew, et al., 1971).

The Mission Wells and Sylmar segments of the San Fernando fault trend easterly through a populated area. The Sylmar segment was traced for a length of about 2.5 km, beginning from the east near the intersection of Glen Oaks and Hubbard Streets, to west of the intersection of Maclay and Gladstone Avenues. The fault damaged parking lots, streets, buried utilities, houses, industrial tracts, and stores in a zone about 360 m wide (Barrows, et al., 1973).

Although not specifically treated in this case history, the Santa Susana fault is the closest known occurrence of tectonic movement to the facilities at the Upper Van Norman Reservoir. Numerous occurrences of shattered ridge tops,

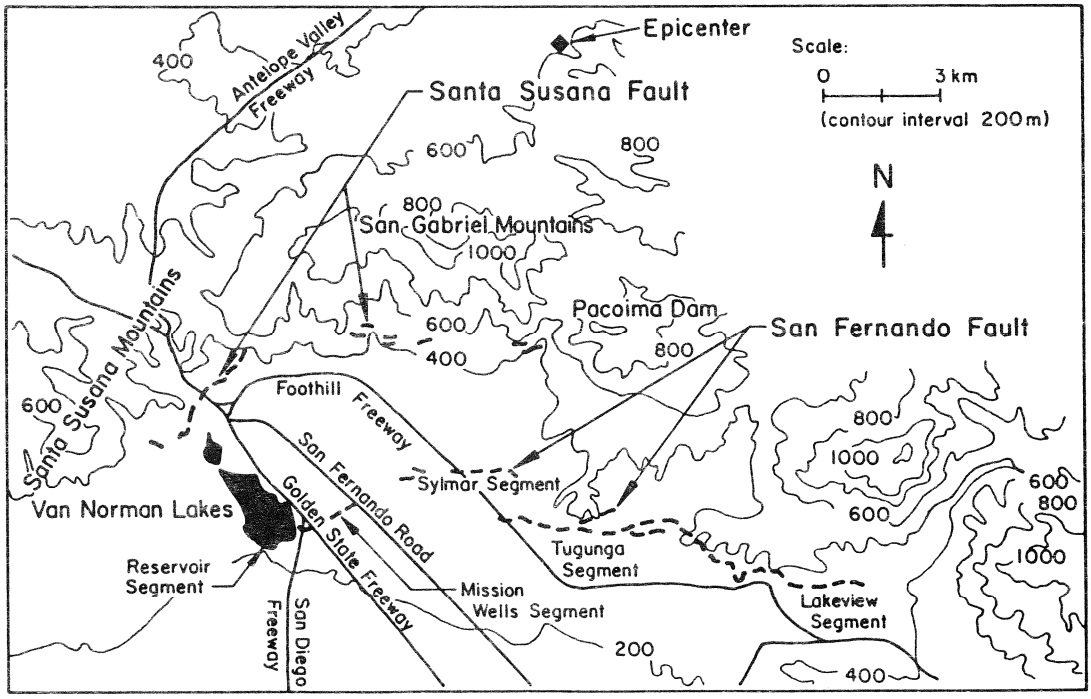

Figure 4. Region of Most Severe Earthquake Damage

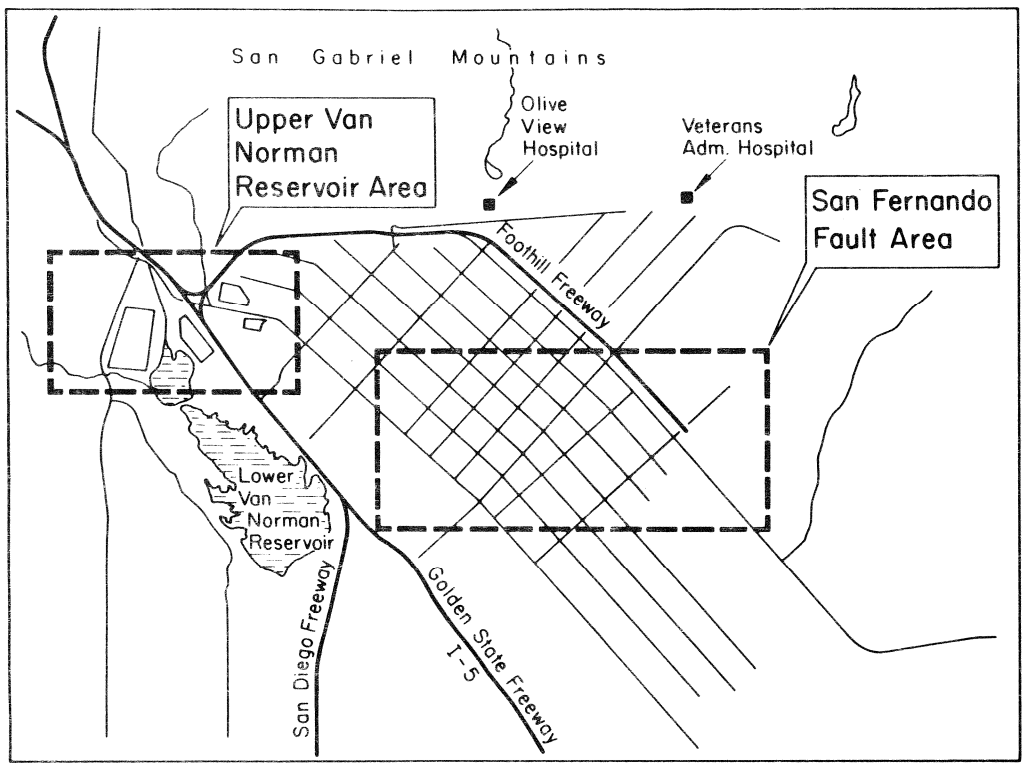

Figure 5. Areas of Large Ground Deformation

which are indicative of high vertical accelerations, occurred near the fault (Weber, 1975). Shattered ridge tops also were observed in the hills above the Olive View Hospital (Nason, 1971). The Santa Susana fault intersects the Golden State Freeway at the San Fernando Pass and damaged several power lines and towers (Barrows, et al., 1973).

6.0 GROUND DEFORMATION WEST OF THE UPPER VAN NORMAN RESERVOIR

The area immediately west of the Upper Van Norman Reservoir is the location of the Joseph Jensen Filtration Plant, which is owned and operated by The Metropolitan Water District of Southern California (MWD). At the time of the earthquake, the plant was under construction, with approximately 85% of the facilities complete (Subcommittee on Water and Sewerage Systems, 1973). As a result of the earthquake and associated ground deformations, substantial damage was sustained by the plant. Post-earthquake investigations were performed to assess the characteristics and causes of damage (e.g., Converse Davis and Associates, 1971; Woodward-Lundgren and Associates, 1971; Dixon, 1973; Marachi, 1973; Wyllie, et al., 1973; Smith, 1974), and subsequent investigations were undertaken for site improvement and to construct new facilities as part of a program for expanding the plant facilities (Scott, 1987; Woodward-Clyde Consultants, 1989). The preconstruction exploration, post-earthquake investigations, and subsequent site improvement and new facilities studies represent a formidable body of technical papers and professional reports, making the Joseph Jensen Filtration Plant site one of the most intensely investigated and documented sites of earthquake-induced large ground deformation.

6.1 Joseph Jensen Filtration Plant Facilities

Figure 6 shows a plan view of the Joseph Jensen Filtration Plant and areas immediately surrounding it. The plant occupies an area approximately 1200 by 460 m at an elevation ranging from 15 to 25 m above the base of the Upper Van Norman Reservoir. Water for treatment enters the north side of the plant through the Balboa Inlet Tunnel and Influent Conduit, after which it passes through the Mixing and Settling Basins and Filters. The Effluent Channel carries water to the Finished Water Reservoir or through a bypass conduit to

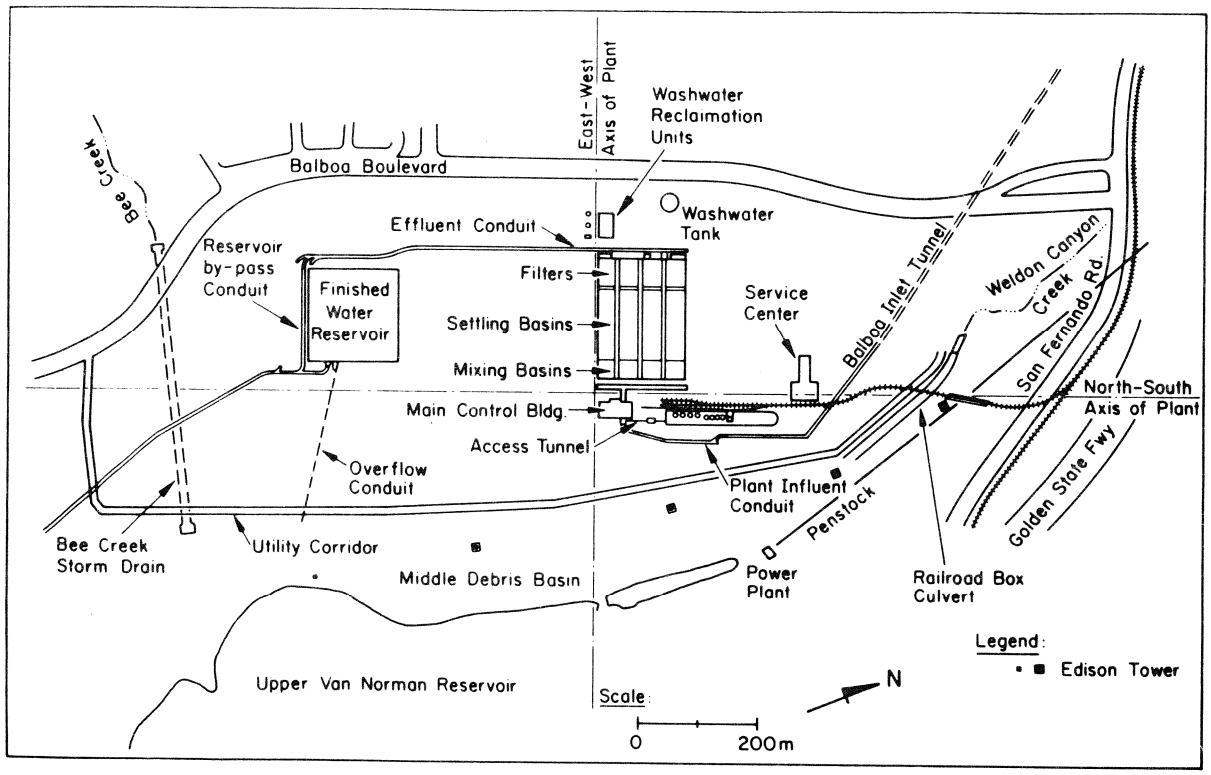

Figure 6. Plan View of Joseph Jensen Filtration Plant

the south. Earthquake damage to the plant has been described in various published accounts (Subcommittee on Water and Sewerage, 1973; Wyllie, et al., 1973; Smith, 1974) and professional engineering reports (Woodward-Lundgren and Associates, 1971; MWD, 1971; Johns, 1973). Only a brief summary of damage to the facilities is presented in this work.

Structural damage at the plant can be divided into two broad categories: damage resulting from transient ground deformation and inertial forces on structures, and damage caused in large measure by permanent differential ground displacements. Structures damaged as a result of high inertial forces and dynamic displacements in adjacent soil include the Finished Water Reservoir (FWR), Effluent Conduit, and Railroad Box Culvert. Each of these structures was buried or partially buried at the time of the earthquake. Permanent differential vertical and lateral soil movements were apparent in most facilities, but are especially relevant to the overall pattern of large ground deformations in the Filters, Settling and Mixing Basins, Main Control Building

(MCB), and buried conduits oriented approximately in an east-west direction.

The Effluent Conduit is a reinforced double box culvert, with each barrel 2.6 m wide and 2.3 m high, buried at a depth of roughly 6 m. The Railroad Box Culvert is a four-barrel reinforced concrete box, with each barrel 2.6 m deep and 3.7 m wide, buried in an embankment 4.9 m to the top of the structure. Both conduits were oriented approximately perpendicular to the east-west component of strong ground shaking. Field observations (Wyllie, et al., 1973) indicate that differential lateral displacements were generated by seismic shaking over the heights of the buried structures, causing lateral racking and wall failure. The most severely damaged structure at the plant was the FWR, which likewise was affected by racking and wall failure.

Finished Water Reservoir. The FWR is an underground reinforced concrete structure with inside plan dimensions of 159 by 150 m. The reservoir roof was a 360-mm thick flat slab, which was supported by 600 spirally reinforced, 600-mm diameter concrete columns on 6-m spacings. The roof was designed to carry 2.4 m of fill, of which approximately 1.8 m had been placed on the northern half of the structure at the time of the earthquake.

Inertial forces were induced by ground shaking in the roof slab and overlying fill, causing high in-plane forces in the roof diaphragm, which in turn were transmitted as shears to the perimeter walls (Wyllie, et al., 1973). Numerous joint failures were evident in the roof. The west wall failed at its base for over 120 m, causing the wall to displace eastward and drop 0.6 m. The east wall also failed at its base and moved into the reservoir as much as 50 mm. Settlements[1] of the floor slab were relatively uniform at 50 to 100 mm, and settlement of the eastern wall varied from 190 to 230 mm. Lateral movements of the structure were 75 to 150 mm to the east and 50 mm northward.

As discussed in forthcoming sections, permanent ground movements increased in an eastward direction from behind the Filters and Effluent Channel toward the Utility Corridor. Structures oriented in an east-west direction would

[1]Settlements, unless otherwise noted, are relative to plant datum near the western side of the Filters

therefore be expected to show signs of increasing displacement as a function of their proximity to the Utility Corridor. Structures which reflect this pattern of increasing ground deformation in an easterly direction include three main groups: Filters, Settling and Mixing Basins; MCB; and East-West Conduits.

Filters, Settling, and Mixing Basins. Maximum settlement beneath the Filters was 13 mm, with lateral displacement at the eastern side of roughly 90 mm. Settlement in the Settling Basins generally was 40 mm or less. Settlements along the eastern edge of the Mixing Basins were from 40 to 125 mm. The principal damage in these structures was differential movement at expansion joints, broken subdrains from differential settlement, and fractured walls.

Main Control Building. This building is a two-story steel frame structure with reinforced concrete shear walls, a 3.7-m deep basement, and a 60 by 28-m, two-way slab and grade beam mat foundation. There was very minor structural damage to the building, with the main deformation at expansion joints of the Influent Conduit where it passes beneath the structure. Horizontal and vertical displacements at the expansion joints of the Influent Conduit immediately east and west of the MCB were 150 and 100 mm, respectively. Survey measurements indicate that the MCB moved approximately 170 mm east, 125 mm south, and settled near its southeast corner about 50 mm.

East-West Conduits. These structures include the Bee Canyon Storm Drain, Overflow Conduit, and Balboa Inlet Tunnel. The Bee Canyon Storm Drain is a 450-m long, triple-barrel reinforced concrete box culvert, with each barrel being 2.1 by 3.0 m in cross-section. Damage to this structure was typical of that in other conduits. There were numerous keyed joint failures, with lateral separations of 3 to 60 mm and vertical offsets of 3 to 40 mm. Most longitudinal reinforcing through the joints failed in tension and shear.

Joint separations and offsets at the Overflow Conduit, Influent Conduit, and Balboa Inlet Tunnel provide records of cumulative displacements along the longitudinal axes of these structures. The cumulative joint movements are discussed in conjunction with ground deformations in a forthcoming section.

6.2 San Fernando Powerplant

The Los Angeles Department of Water and Power's San Fernando Powerplant No. 3 was a reinforced concrete building, housing two 3000-kw hydroelectric generating units. Damage to the building was caused by permanent differential settlement and seismic shaking, and is described by Lew, et al. (1971), the Committee on Water and Sewerage (1973), and Wong (1973). Differential settlement of 0.2 to 0.3 m at the building ruptured the 2430-mm-diameter steel penstock of the First Los Angeles Aqueduct and broke its bypass gate. The facility, which was built in 1921, had not been designed with an articulation joint where the penstock entered the powerhouse. The resulting inability to accommodate differential movement at this critical connection contributed to the severity of damage.

6.3 Surficial Ground Movements

Figure 7 shows ground cracks and fissures, sand boils, and locations of soil heave along pressure ridges, as mapped and reported by Converse Davis and Associates (1971), Woodward-Lundgren (1971), and Youd (1973). Stereo pair air photo interpretation, in combination with a careful study of oblique aerial and ground level photographs, was used to supplement the information summarized on existing maps. Most of the large ground deformations and cracks were east of the north-south plant axis, except those around the FWR. Cracks to 240 mm wide were mapped, with a maximum vertical displacement of 490 mm. A pressure ridge about 330 m long, 1.5 m wide, and 0.3 to 0.6 m high developed at the base of the slope (Dixon, 1973; Youd, 1973). Several sand boils were seen at the base of the fill slope and in the southeast part of the site.

Figure 8 is a composite view of two vertical aerial photographs, taken after the earthquake, of the Joseph Jensen Filtration Plant and surrounding areas. This figure provides a photographic reference of the site to be viewed in conjunction with Figures 6 and 7. Selected facilities and ground deformations are labeled in the figure.

6.4 Cumulative Lateral and Vertical Movements

There are three groups of structures at the Joseph Jensen Filtration Plant

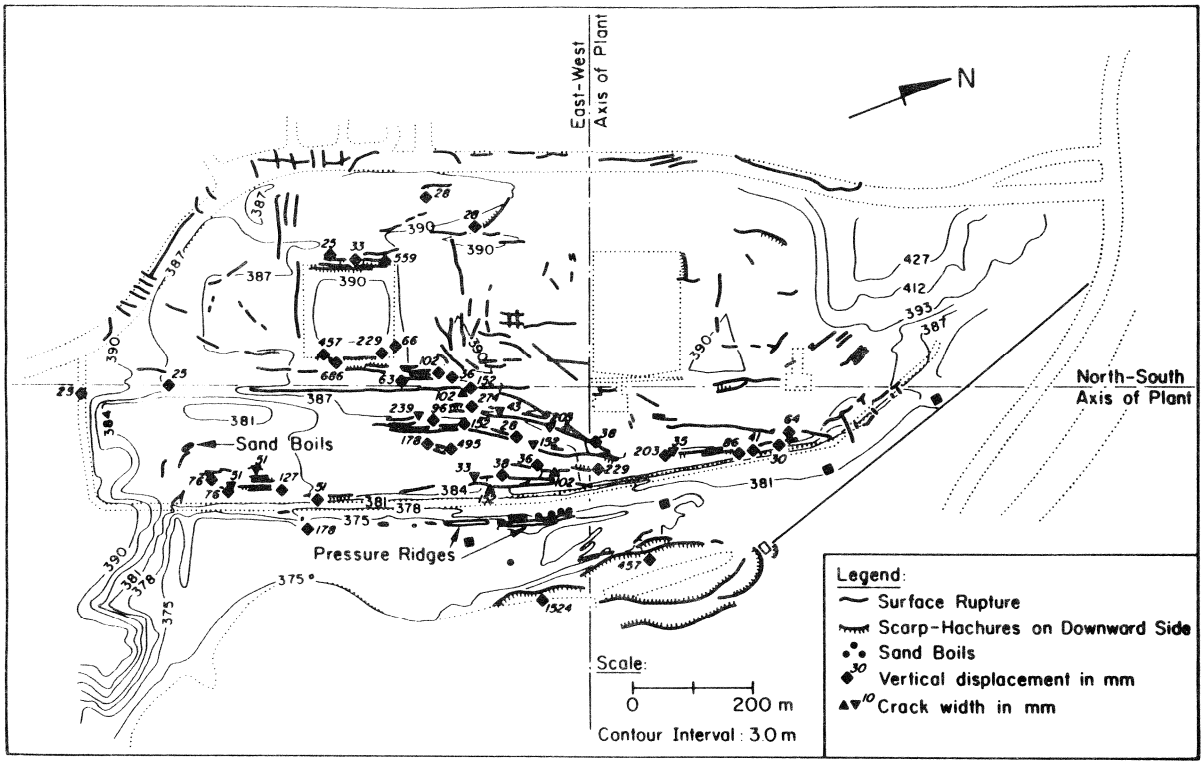

Figure 7. Map of Surficial Ground Cracks, Sand Boils, and Pressure Ridges Near Joseph Jensen Filtration Plant

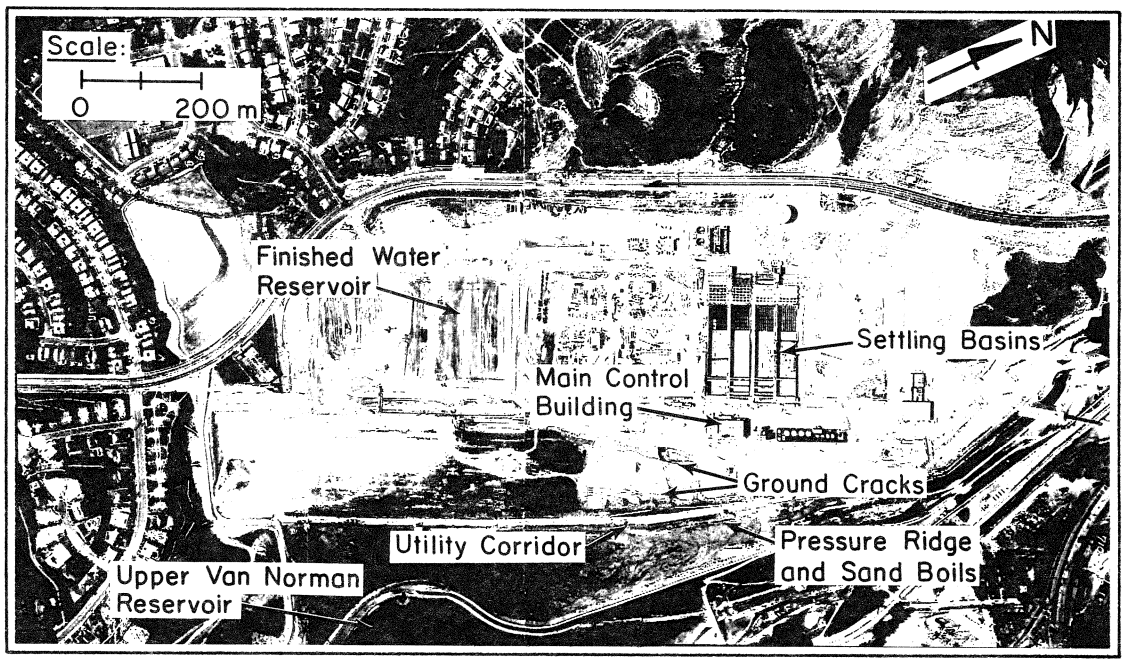

Figure 8. Aerial View of Joseph Jensen Filtration Plant

which provide records of cumulative lateral and vertical movement in the east-west direction. They include the 1) FWR and Overflow Conduit, 2) Filters, Settling and Mixing Basins, MCB, and Influent Conduit, and 3) the Balboa Inlet Tunnel. As part of this study, site survey information, photos, field notes, and post-earthquake measurements of these structures were used to develop cumulative displacement plots, as shown in Figure 9.

Settlements and horizontal movements are plotted as dashed and solid lines, respectively. Much of the cumulative displacement was evaluated from measured joint separations and offsets along the Overflow Conduit, the portion of the Influent Conduit oriented east-west beneath the MCB, and the Balboa Inlet Tunnel. Lateral and vertical ground movements were transmitted directly to these buried structures, which responded much like linear extensometers by showing relative displacements at joints. The resulting cumulative displacement plots in Figure 9 indicate how movements were distributed across the facilities and provide indirect evidence for the distribution of permanent ground deformation.

6.5 Air Photo and Optical Survey Measurements

As mentioned previously, photogrammetric analyses were performed by Japanese researchers on air photos taken before and after the earthquake (see Appendix B). The results of these analyses are shown in Figure 10 as vectors of horizontal movement and measurements of settlement and heave. Optical survey measurements performed by MWD also are shown at various locations. For example, lateral offsets surveyed along the north-south plant axis and settlements at several key structures are included in the figure.

The air photo analyses show lateral movements along the Utility Corridor, typically 2 to 3 m, in an easterly direction toward the reservoir. At the eastern terminus of the Overflow Conduit, air photo measurements show lateral movements of 1.3 to 2.2 m, which agrees reasonably well with the total cumulative movement shown at this location in Figure 9.

As an additional check on accuracy, measurements of the alignment along the eastern edge of the Utility Corridor were made from high quality vertical air

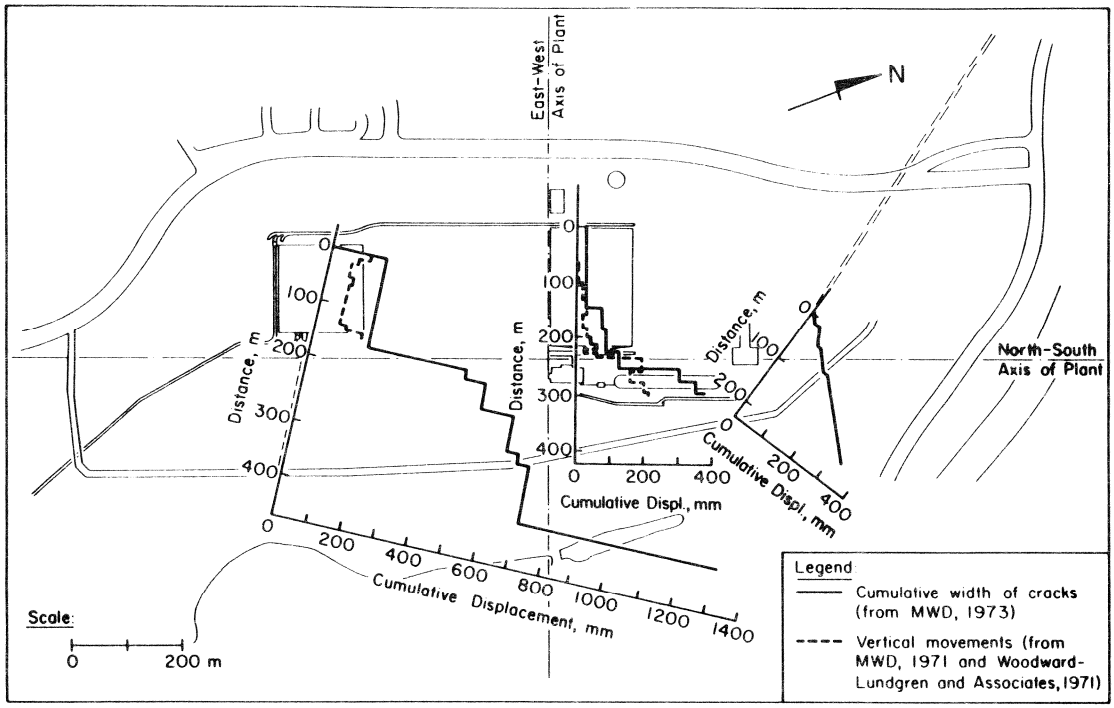

Figure 9. Cumulative Displacements Across the Joseph Jensen Filtration Plant

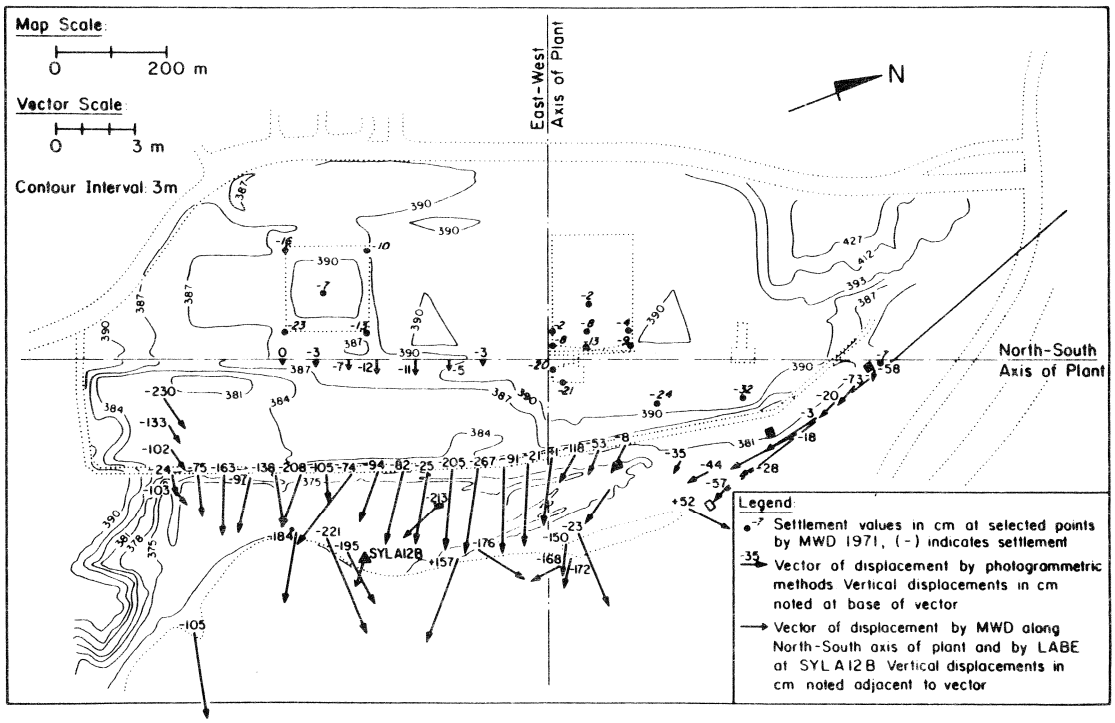

Figure 10. Displacements Determined from Air Photo Analyses and Optical Surveys, Joseph Jensen Filtration Plant

photos and compared with LADWP records of the as-built alignment. The comparison showed an eastward displacement of the alignment of approximately 2 m $\pm$ 1 m.

The ground displacements represented by vectors and magnitudes of settlement or heave in Figure 10 predominantly result from liquefaction, soil slumping, and landsliding. To a lesser degree, however, there is a ground displacement component resulting from regional tectonic movements. As explained in detail in Appendix B and as shown in Figure B.3, the magnitude and direction of regional tectonic movements at the Joseph Jensen Filtration Plant are estimated to be 0.45 m westward and 0.15 m vertically up.

6.6 Subsurface Conditions

Published accounts of the soils and groundwater conditions at the Joseph Jensen Filtration Plant (e.g., Dixon and Burke, 1973; Marachi, 1973; Smith, 1974) disclose three types of deposits: artificial fill, alluvium, and weathered to intact sandstone of the Saugus Formation. The eastern portion of the site was filled with materials described as mixtures of silty sands, sandy silts, and sands with gravel and occasional zones of silt and clayey silt (Dixon and Burke, 1973). The thickness of the fill varies from zero on the west side of the site to 17 m on the east.

As part of this study, 130 boring logs and 62 CPT soundings were reviewed, representing over 2500 m of probing performed for site preparation, post-earthquake investigations, and site expansion evaluations.

Figure 11 shows a plan view of selected borehole and CPT soundings used to delineate subsurface conditions. The borings and soundings are identified in the legend according to the various engineering studies for which they were performed. Figures 12 through 17 show soil profiles along transverse and longitudinal cross-sections as interpreted from the borehole and cone penetration data. The SPT and CPT values registered in Figures 12 through 17 were acquired from tests performed according to ASTM D1586 and D3441 (ASTM, 1989), respectively.

Transverse cross-sections are shown from south to north across the site in

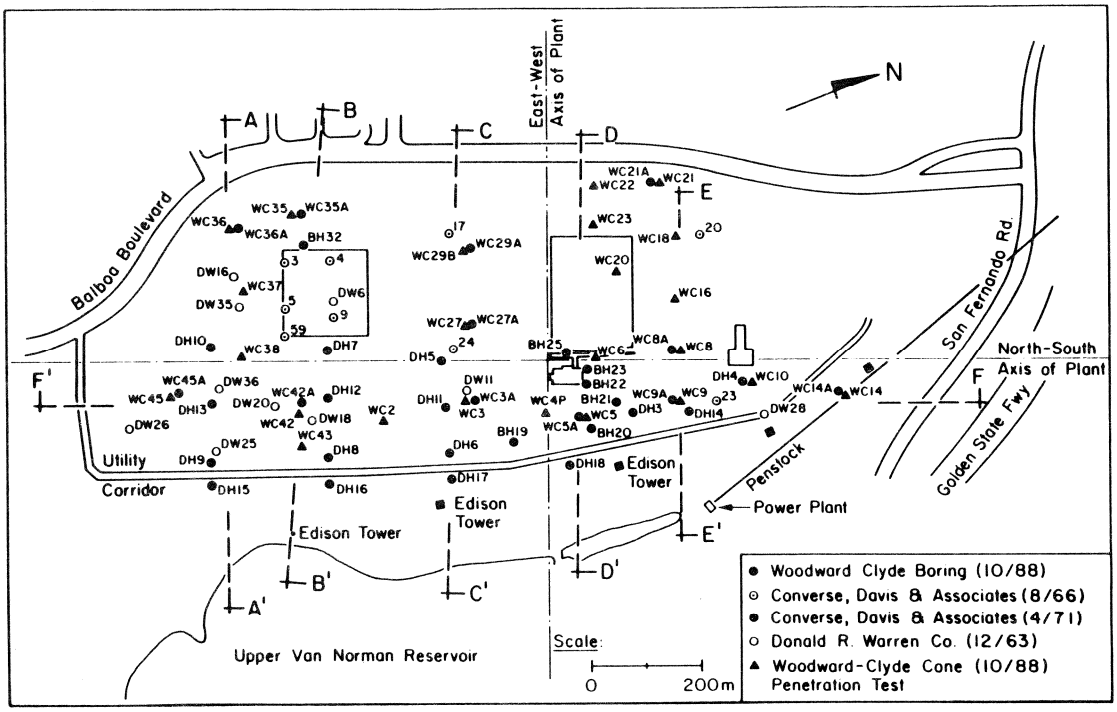

Figure 11. Locations of Soil Borings and Soundings at the Joseph Jensen Filtration Plant

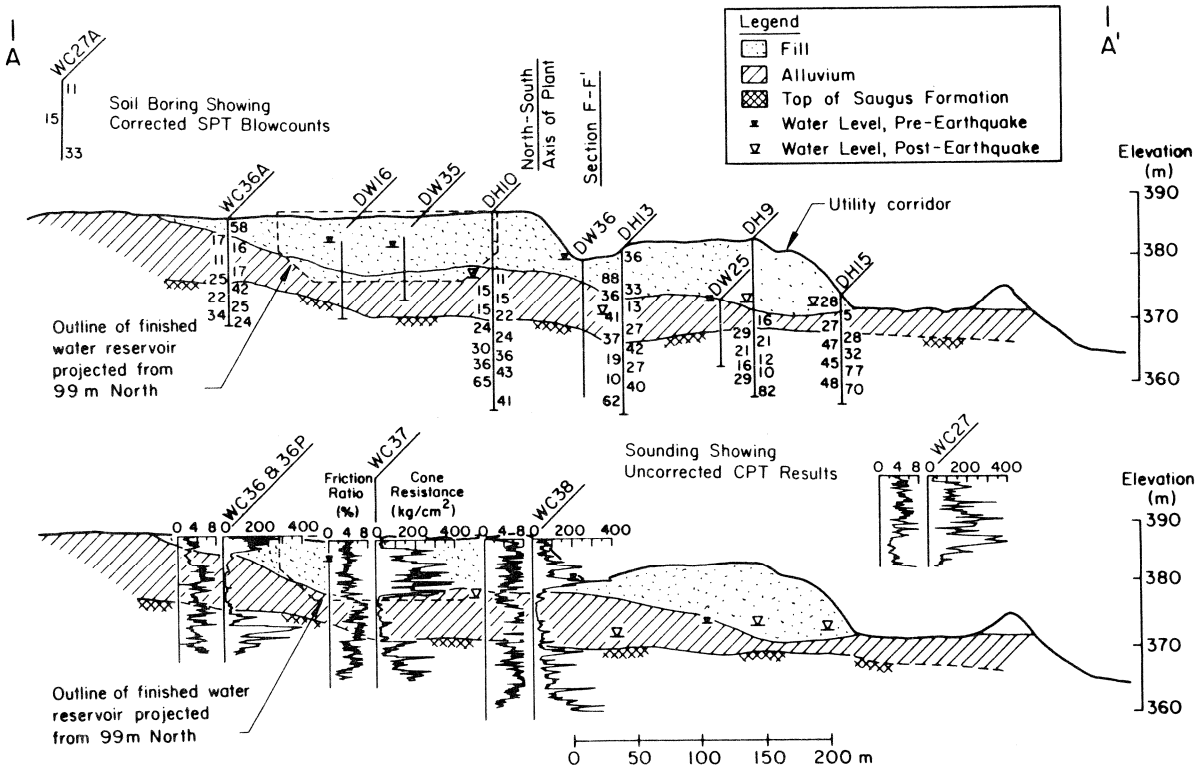

Figure 12. Soil Profile at Cross-Section A-A', Joseph Jensen Filtration Plant

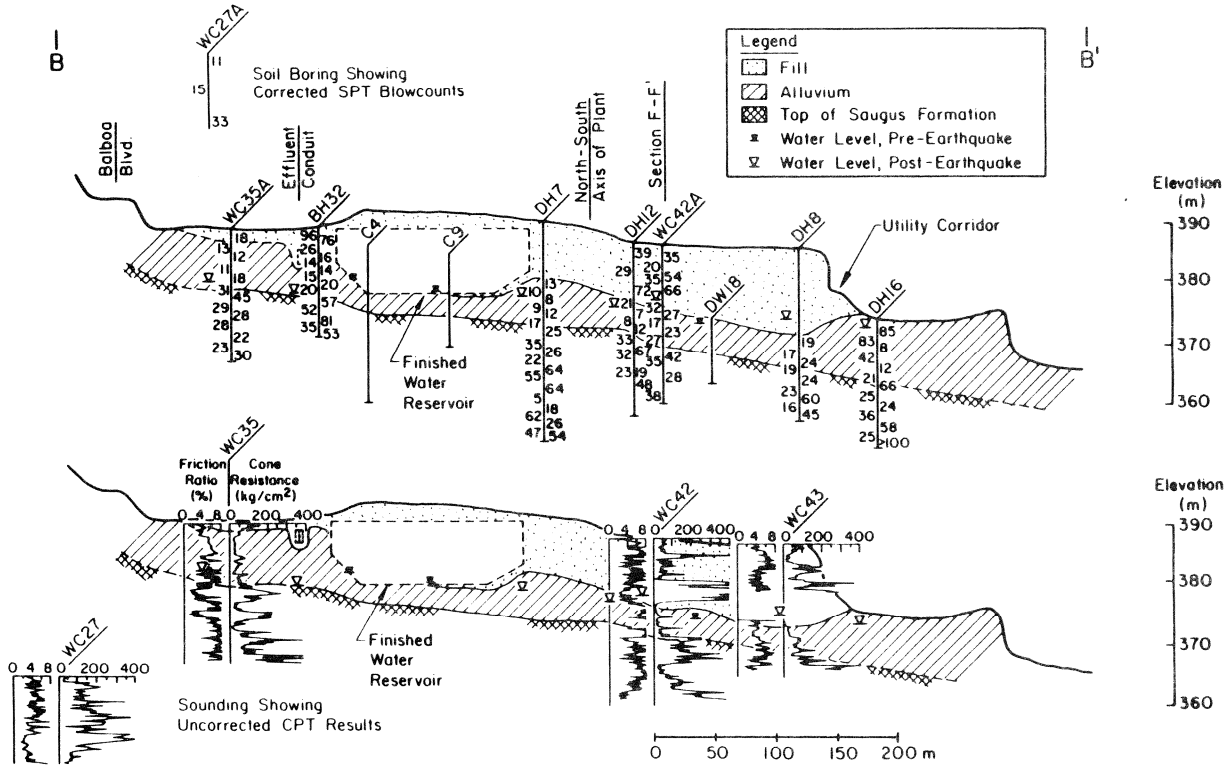

Figure 13. Soil Profile at Cross-Section B-B', Joseph Jensen Filtration Plant

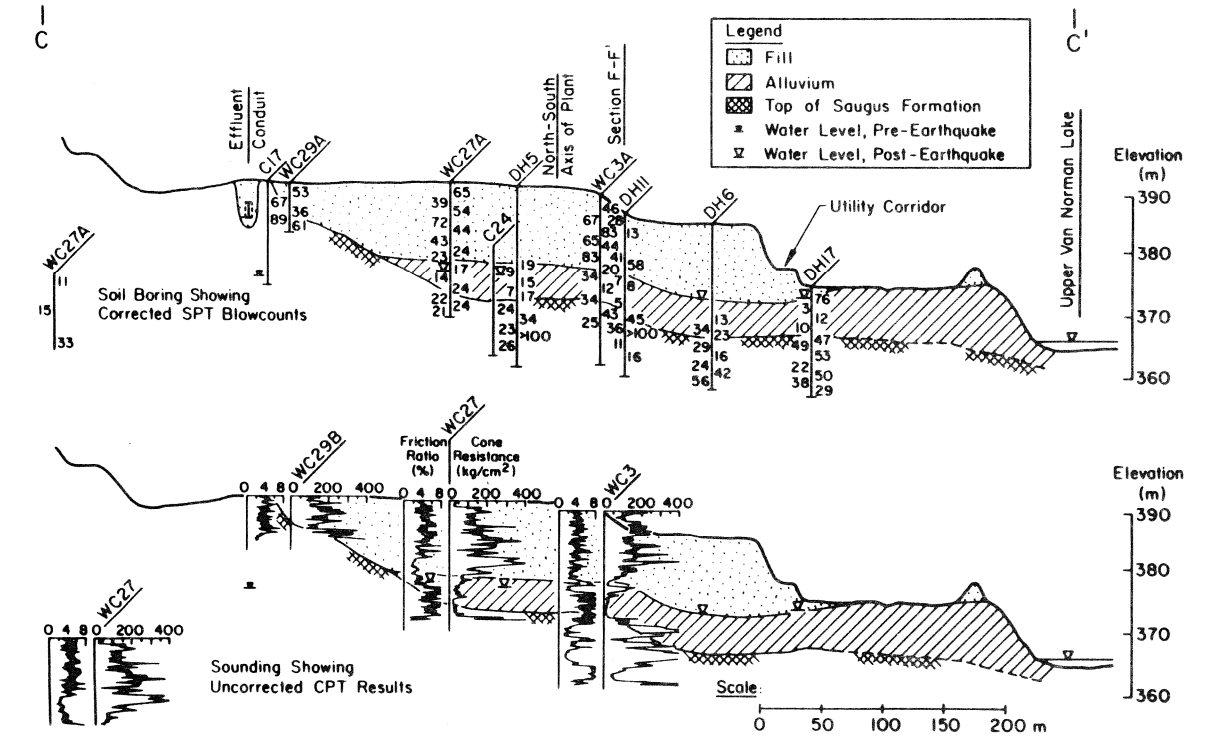

Figure 14. Soil Profile at Cross-Section C-C', Joseph Jensen Filtration Plant

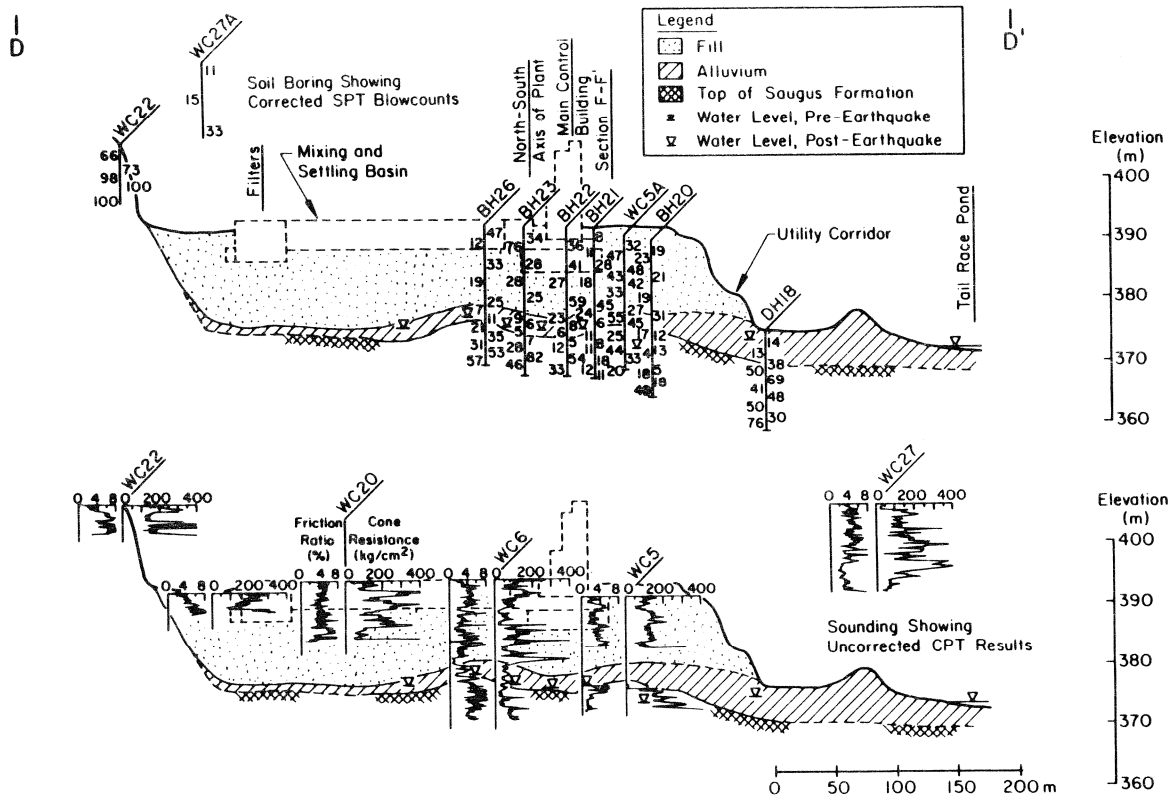

Figure 15. Soil Profile at Cross-Section D-D', Joseph Jensen Filtration Plant

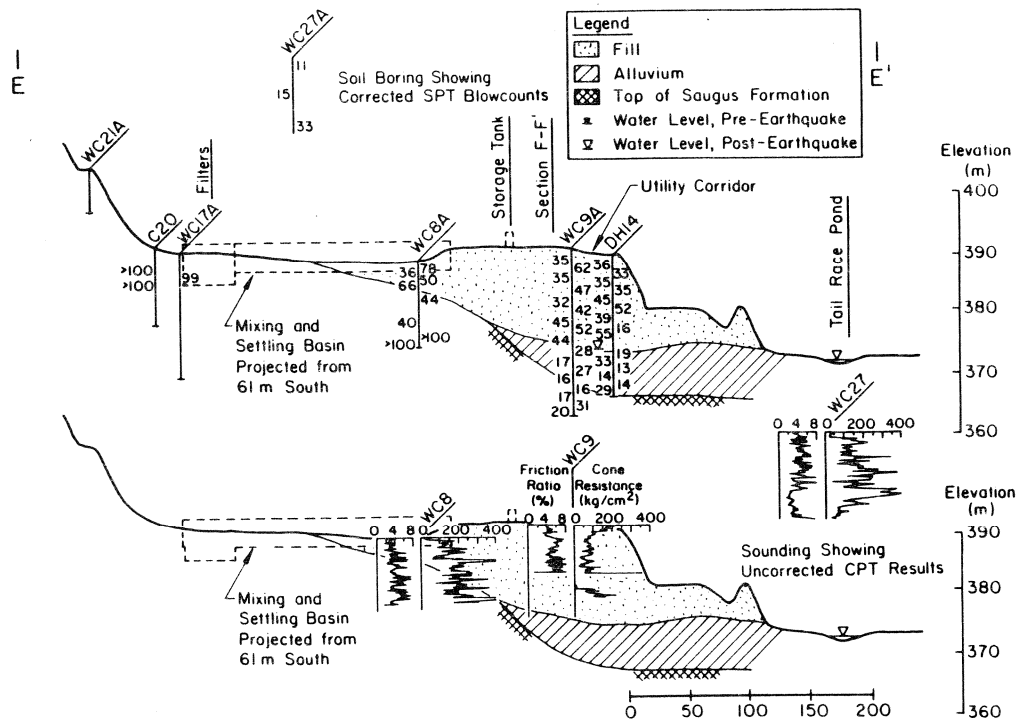

Figure 16. Soil Profile at Cross-Section E-E', Joseph Jensen Filtration Plant

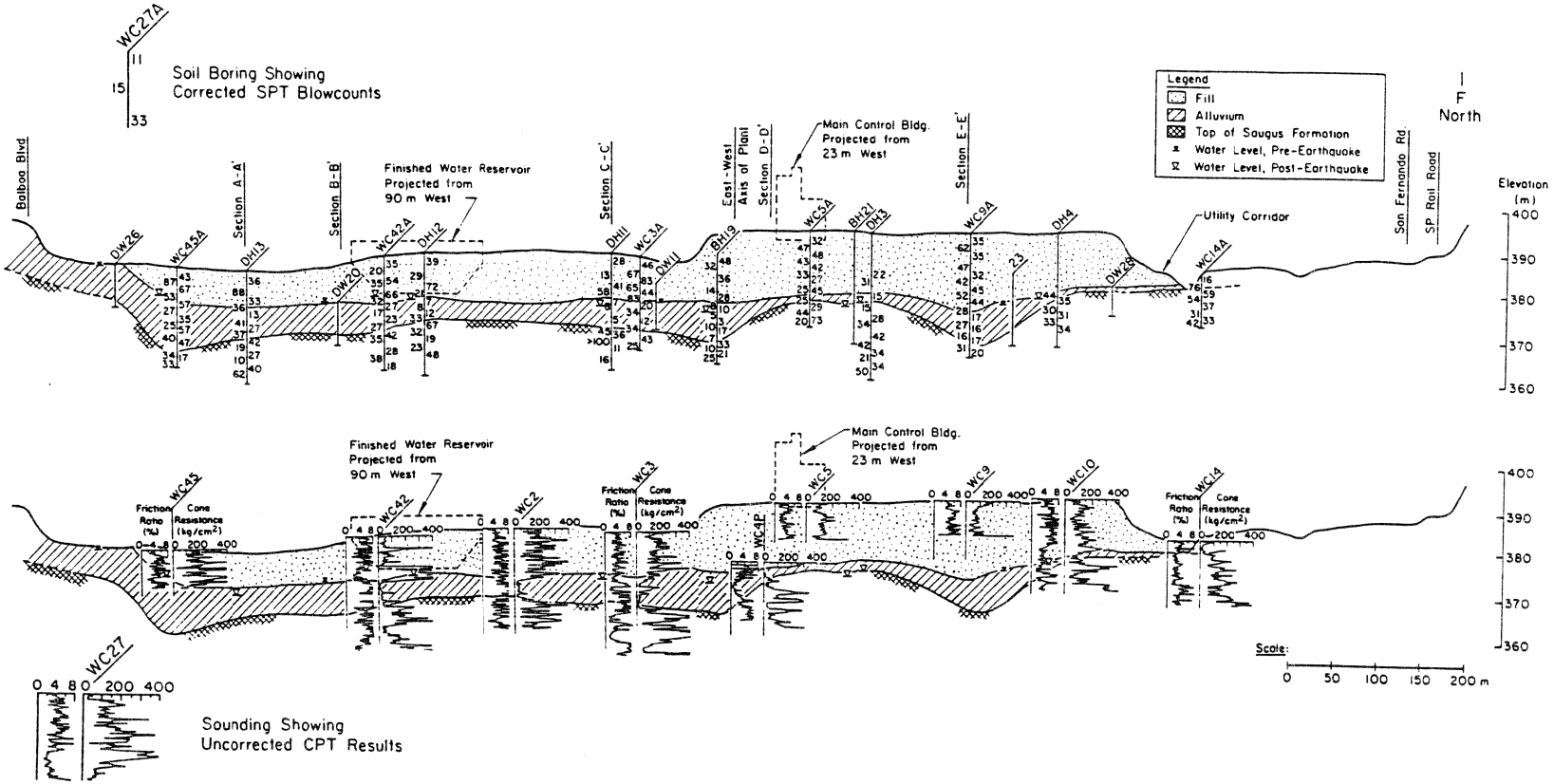

Figure 17. Soil Profile Along North-South Axis of Joseph Jensen Filtration Plant

Figures 12 through 17, and a longitudinal view along the north-south plant axis is presented in Figure 17. The alluvium is shown in each profile as a hatchured zone. It was drawn on the basis of field descriptions presented in the geotechnical reports, correlated with locations of locally low SPT and CPT readings.

Water tables are shown on the soil profiles for two different times. Groundwater levels measured during post-earthquake investigations are shown as open triangles. In general, they varied from approximately El 370 to 375. Preconstruction water tables are shown in the soil profiles as solid triangles, and are indicative of a slightly higher level. Dewatering is the most likely reason for the relatively low levels during construction (Smith, 1974). A recent examination of water well measurements (R. F. Scott, 1987) indicates that the groundwater has risen after 1978 to a level 1 to 2 m higher than at the time of the earthquake. In general, it appears that the water table at the time of the earthquake was approximately at the contact between the fill and alluvium under those portions of the site east of the north-south plant axis.

The alluvium, as indicated by the low SPT and CPT measurements, was in a relatively loose saturated state, and therefore subject to liquefaction. Soil liquefaction has been proposed by several investigators (Dixon and Burke, 1973; Youd, 1973) as the principal cause of large ground deformations at the Joseph Jensen Filtration Plant. The alluvium contains a substantial amount of fine grained material, generally consisting of 30 to 60% by weight of fines (Dixon and Burke, 1973). Typical grain size distribution plots are shown in Figure 18. The alluvium increases in thickness north to south across the site, which correlates closely with the trends of increasing ground deformation. As shown in Figures 14 and 17, the alluvium is locally thick near the central part of the plant, about 100 m south of the MCB. This was the location of the largest and most severe ground deformation, as evidenced by the ground cracks and measured displacements shown in Figures 7 and 10, respectively.

A three-dimensional perspective of the zone of loose alluvium at the Joseph Jensen Filtration Plant can be gained by examining Figures 19 and 20.

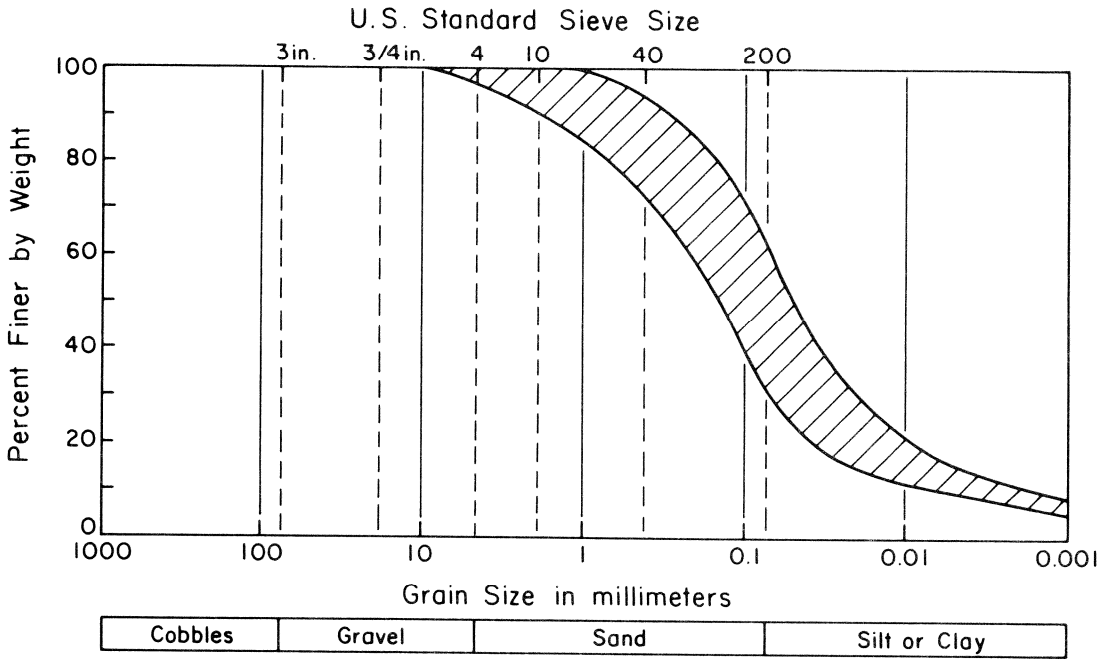

Figure 18. Typical Grain Size Distribution Curves for Alluvial Soils at Joseph Jensen Filtration Plant

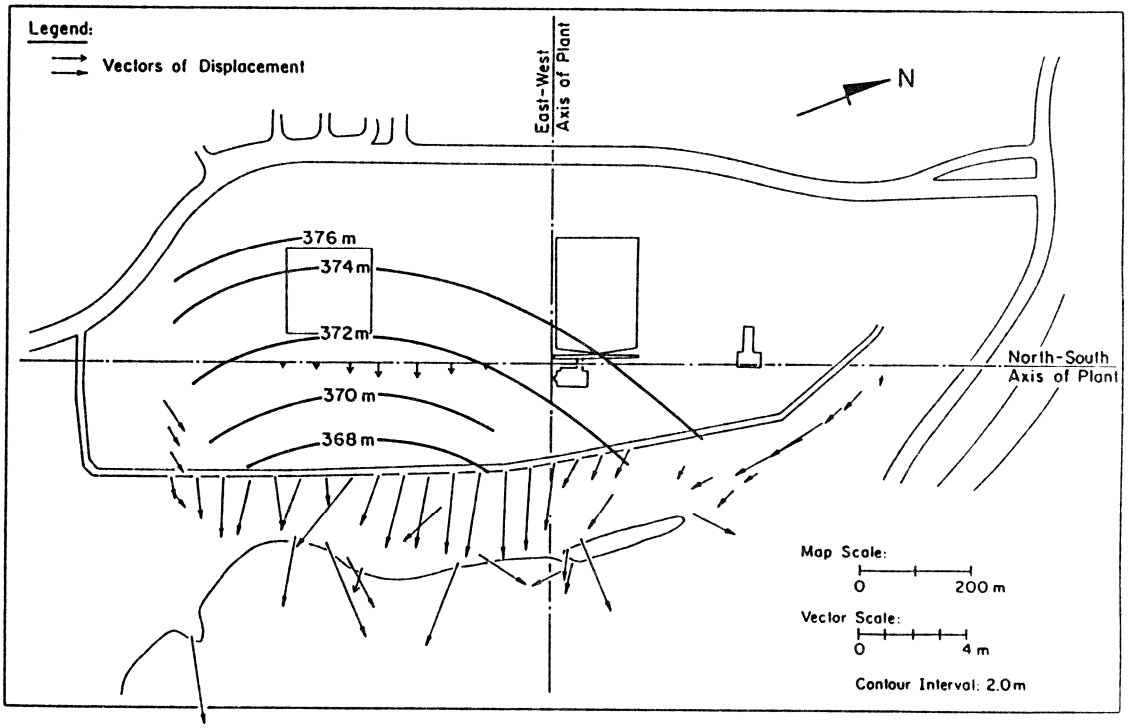

Figure 19. Contours of Equal Elevation for the Base of Loose Saturated Alluvium at the Joseph Jensen Filtration Plant

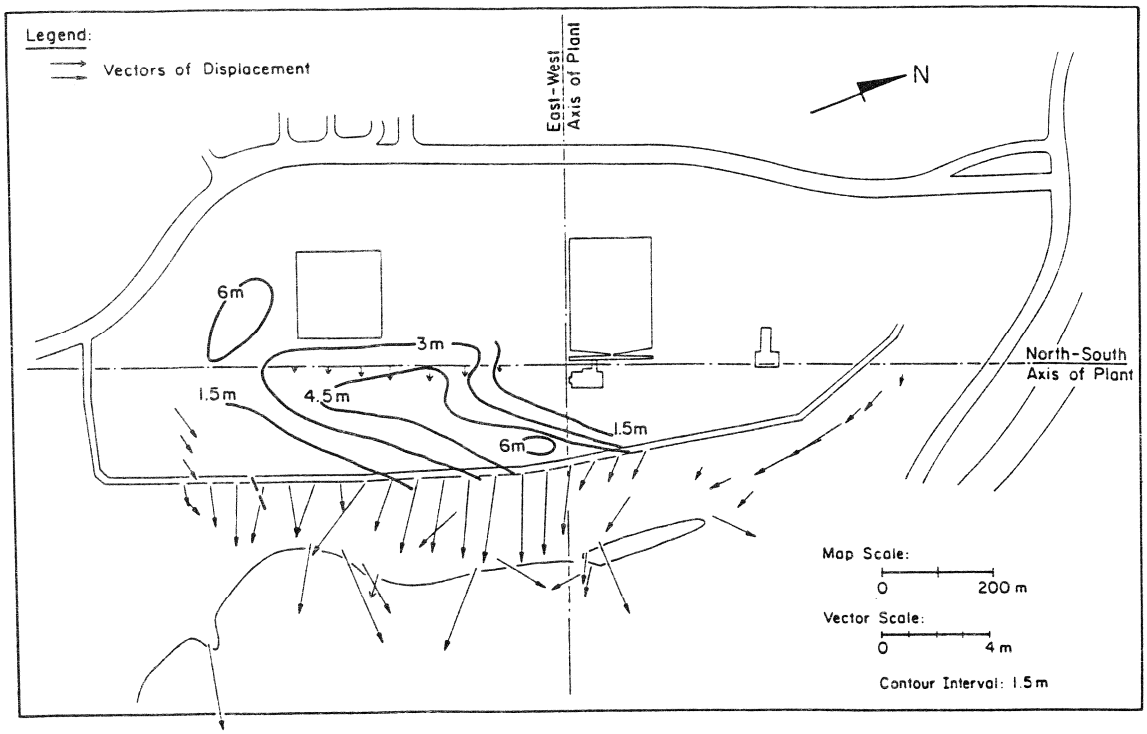

Figure 20. Contours of Equal Thickness of Loose Saturated Alluvium at the Joseph Jensen Filtration Plant

Figures 19 and 20 show the depth to the bottom and thickness of the loose, saturated alluvium, respectively. Vectors of displacement, mapped by photogrammetric techniques, also are shown in the figures.

The bottom of the loose alluvium was established on the basis of the boring log descriptions, SPT, and CPT data. The base of the loose alluvial soils usually coincided with the top of the Saugus Formation. However, in some cases, a meter or so of the upper surface of the Saugus Formation was highly weathered and thus was considered to behave as loose soil. The highly weathered Saugus Formation was most prevalent near the intersection of the north-south and east-west plant axes. The corrected SPT values are as low as 7 within the upper 1 m of the Saugus Formation at this location. The contours in Figure 19 show the elevation above sea level of the base of the loose alluvium. It is apparent that this basal surface slopes downward toward the Upper Van Norman Reservoir at an angle of about 1.0 to 2.0°. Moreover, the contours show a concave pattern with greatest depth and slope near the central part of

the site, where the most severe ground deformations were mapped.

Figure 20 shows contours of constant thickness for the zone of loose, saturated alluvium. The thickness of this zone was determined from borehole records, SPT and CPT data, and water level measurements, and corresponds roughly with the thickness of alluvium below the water table illustrated in Figures 12 through 17. The greatest thickness of loose, liquefiable alluvium is located under the zone of largest permanent ground deformation.

7.0 GROUND DEFORMATION EAST OF THE UPPER VAN NORMAN RESERVOIR

Figure 21 presents a plan view of the area east of the Upper Van Norman Reservoir in which major transportation arteries, the San Fernando Valley Juvenile Hall, and Sylmar Converter Station are shown. This area was subjected to large ground deformations as a result of the earthquake. Lateral spreading caused by soil liquefaction has been identified as the primary source of ground movement. The large ground deformations have been described in various published papers (e.g., Youd, 1971 and 1973; Fallgren and Smith, 1973; Weber, 1975; Fallgren and Smith, 1975; O'Rourke and Tawfik, 1983; ADEP, 1990), and several geotechnical reports have been prepared which evaluate the soil conditions and describe the pattern and causes of soil displacements (Fallgren and Smith, 1971; J. D. Scott, 1973; Fugro, 1975; Bennett, 1989).

7.1 Buildings East of the Upper Van Norman Reservoir

Both the Juvenile Hall and Sylmar Converter Station sustained significant damage as a consequence of the permanent ground deformation. The damage to these structures has been discussed as part of a general review of earthquake-induced ground failure effects on buildings by Youd (1989), and in detail in post-earthquake reconnaissance reports by Lew, et al. (1971), Thompson (1973), and Schoustra and Yann (1973). Only a brief summary of the building damage is given in this report.

San Fernando Valley Juvenile Hall. The Juvenile Hall occupies an area 320 by 420 m northeast of San Fernando Road. There were 12 separate one to two-story buildings on site during the earthquake, each constructed of reinforced

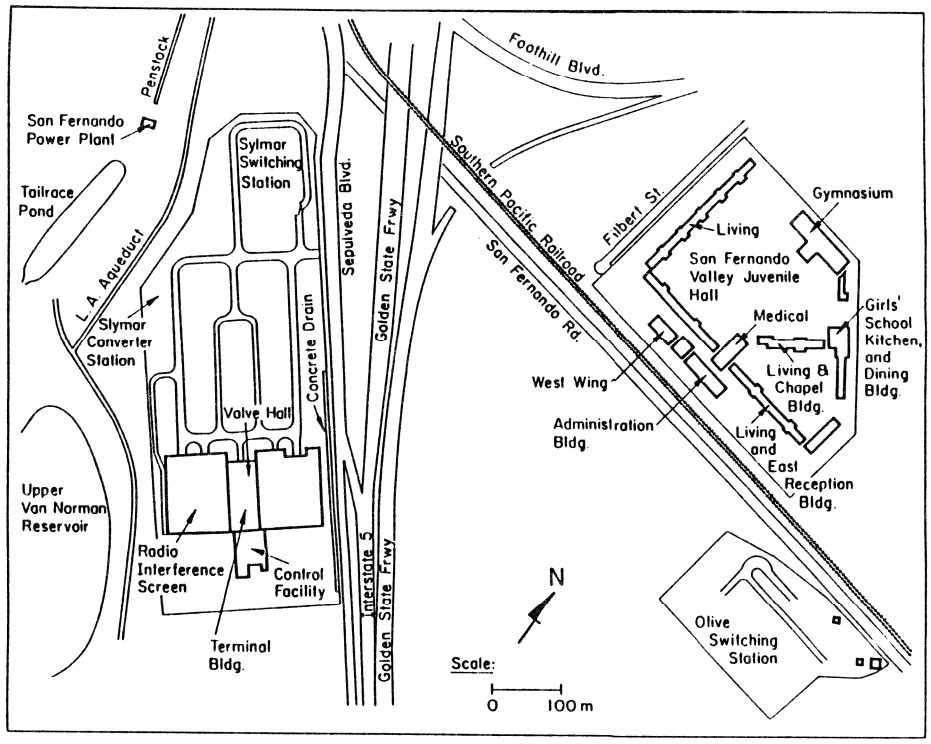

Figure 21. Plan View of East Side of Upper Van Norman Reservoir

concrete hollow block walls with concrete floor slabs on grade and concrete roofs. Thompson (1973) reports that the floors and roofs are supported by pan-joist or one-way slab systems, framing to the walls or concrete beams and columns. Concrete bearing walls and columns are supported by spread footing foundations.

Damage to the buildings was caused by a combination of strong ground acceleration and permanent differential ground movement. The head scarp of a lateral spread was located beneath the southeastern portion of the site, with the northwestern boundary of the spread cutting diagonally from the western wing of the Administration Building through the Living Units and Chapel Building to the junction between the one-story and two-story portions of the Girls' School and Kitchen, Dining, and Gymnasium Building. (See Figure 22 for surficial ground cracks and general deformation pattern.) Ground movements along the western boundary of the lateral spread involved right lateral offset and vertical downfaulting to the southeast.

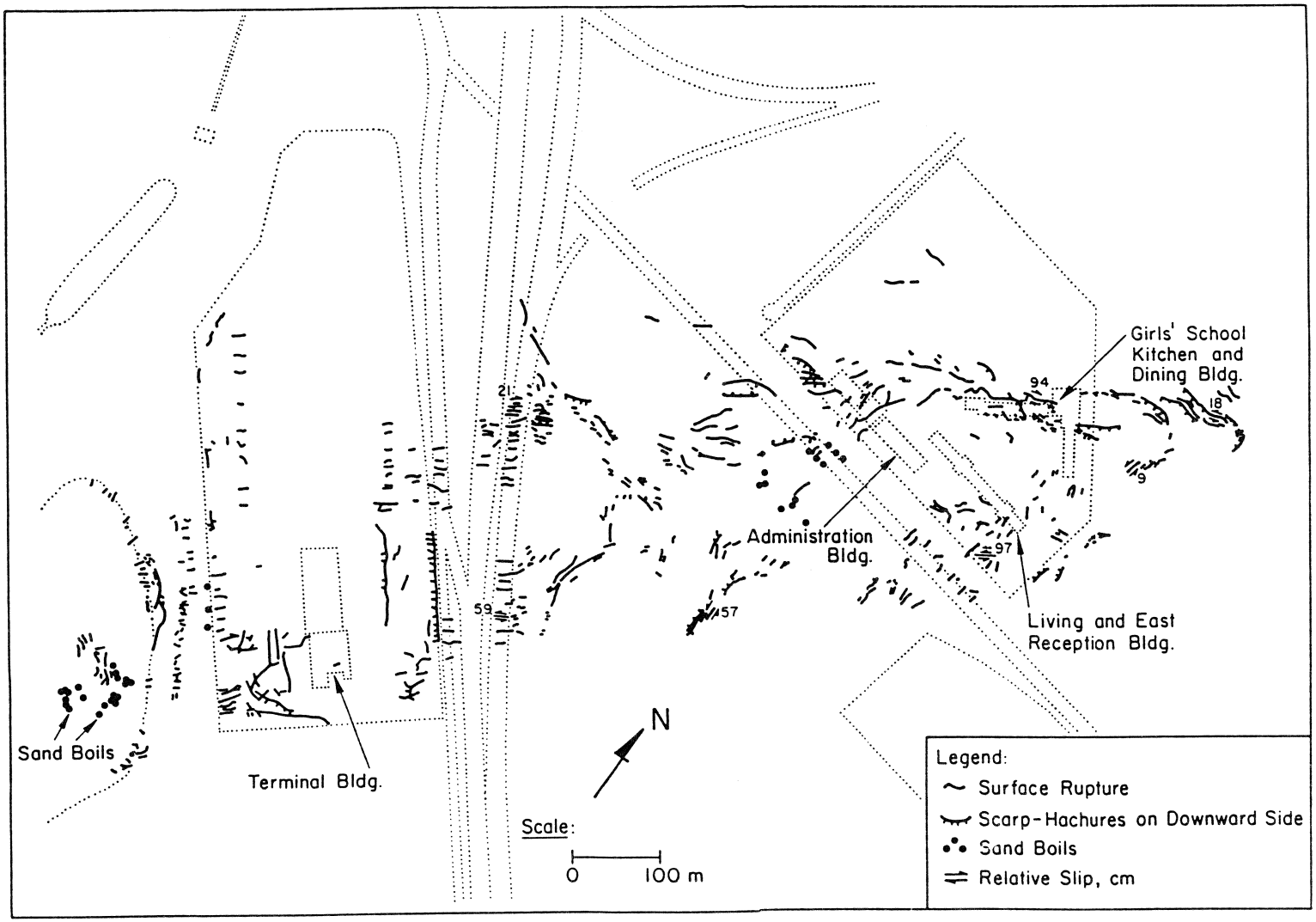

Figure 22. Map of Surficial Ground Cracks, Sand Boils, and Pressure Ridges East of Upper Van Norman Reservoir

Youd (1989) reports that lateral shear deformation of 0.76 m across a 9-m-wide zone fractured and rotated the spread footings and slab-on-grade floor of the western wing of the Administration Building. Approximately 75% of the roof structure of this building collapsed, with severe distortion and collapse of concrete block bearing and shear walls (Thompson, 1973). In addition, ground cracks with 300 and 600-mm vertical and horizontal offsets, respectively, developed in the central portion of the Living Units and Chapel Building.

The classroom wing of the Girls' School separated about 300 to 450 mm from the remainder of the building where the northern boundary of lateral spreading passed beneath the structure. There was no separation or expansion joint at this location, and ground distortion resulted in locally severe damage to the walls, roof structure, and floor slabs (Thompson, 1973).

Shear deformation of 0.5 m over a 6-m-wide zone under the east end of the east wing of the Living and East Reception Building was reported by Youd (1989). This deformation occurred near the northeastern margin of lateral spreading and was associated with local areas of heavy damage to floors, walls, and roof.

Sylmar Converter Station. Damage to electrical equipment at this facility was caused principally by strong ground shaking (Wong, 1973), although there were several instances of damage from permanent soil displacements. Differential settlements of 100 to 225 mm were measured at transformer pads which were 4.6 by 8.8 m in plan dimensions (Schoustra and Yann, 1973). Westward lateral movements of approximately 0.6 m stretched radio interference cages, rupturing the cross-bracing of the vertical panels. Permanent ground deformation also damaged manholes and electrical conduits.

Youd (1989) and Schoustra and Yann (1973) describe damage of the Converter Station Terminal Building. This structure was intersected by approximately 0.3 m of left lateral offset near the eastern margin of lateral spreading. Shear deformation imposed by the spread damaged the building at the junction between the control facility and valve hall. The two portions of the building are founded on reinforced bearing walls and spread footings. They are physically separated above grade, and connect below grade only at one location,

where the two portions share a common basement wall. Damage between the two portions occurred as buckling of the lighter floor slab of the control facility. The concrete pedestal, which marked the below-grade structural connection between both parts of the building, was spalled and ruptured. There were no difficulties with the steel framework above, and local damage at the connection was repaired relatively easily.

7.2 Highway Facilities

The highway interchange for Interstates 5 and 210, shown in the northern portion of Figure 21, suffered the most severe damage of the entire earthquake-damaged transportation system (Prysock and Egan, 1981). Settlement was caused by soil densification of the fill underlying Routes 5 and 210 in the vicinity of the interchange. Differential settlements at bridge approaches was as high as 0.3 to 0.6 m (California Division of Highways, 1973). One area of damage directly attributable to lateral spreading occurred along Route 5 immediately north of the eastern half of the Sylmar Converter Station, where an eastward lateral offset of 1.5 m was visible in the northbound highway lane (Prysock and Egan, 1981). Along the eastern margin of lateral spreading at this location, there was prominent compressive buckling of the pavement (see Figure 22).

7.3 Surficial Ground Movements

The locations of ground cracks, lateral offsets, compressional features, and sand boils, which were mapped and presented by Fallgren and Smith (1971a,b) and Youd (1973), are shown in Figure 22. Stereo pair aerial photographs and ground level photos were used as additional sources of information to develop the map of surficial ground movements. The zone of ground cracks extended downslope from the Juvenile Hall to the Upper Van Norman Reservoir over a distance of 1220 m. The average width of the zone was 300 m.

Horizontal strike slip displacements mapped on the east and west margins of lateral spreading are shown in the figure. The largest of these offsets measured 0.58 m. Backhoe trenches, which were excavated perpendicular to northeast-southwest trending cracks, through the yard of the Juvenile Hall, exposed

cracks displaying curvature at depth towards the interior portions of the lateral spread (Fallgren and Smith, 1975). Numerous sand boils were found near the margins of, as well as within, the lateral spread. Sand boils were found at the base of the Sylmar Converter Station fill, in the field south of San Fernando Road, and at the base of the railroad embankment (Youd, 1973).

7.4 Air Photo and Optical Survey Measurements

The results of photogrammetric analyses performed by Japanese researchers (ADEP, 1990) are shown in Figure 23. Vectors representing the before and after positions of various cultural features and the magnitude of vertical movements are plotted. Optical survey measurements along Route 5 and the east property line of the Sylmar Converter Station are shown by vectors with open arrow heads (Fallgren and Smith, 1971a,b; Youd, 1973; O'Rourke and Tawfik, 1983). The vectors of movement determined by photogrammetric analyses are in close agreement with offset measurements along San Fernando Road reported by Youd (1973). A maximum downslope displacement of 2.3 m was measured along San Fernando Road by the photogrammetric analyses.

The displacement vectors and ground ruptures show a well-defined zone of movement in which the general orientation of displacement changed from a direction almost due south near the Juvenile Hall to a southwest direction at Route 5. In addition, an abrupt change in the magnitude of horizontal displacement occurred across an approximately 2.4-m-deep flood control channel immediately to the east of the Sylmar Converter Station. Downslope of the drainage channel, the magnitude of the horizontal displacements increased. The average inclination of the ground surface throughout the area of lateral spreading was 1.5°, with a maximum slope through the Juvenile Hall of about 3°.

The magnitude and direction of the vectors of ground movement predominantly result from liquefaction, soil slumping, and landsliding. A lesser component of the ground deformation vectors is the result of regional tectonic movements. As explained in detail in Appendix B and as shown in Figure B.3, the magnitude and direction of regional tectonic movements northeast of the Upper Van Norman Reservoir are estimated to be 0.69 m westward and 0.3 m up (Yerkes, et al., 1974).

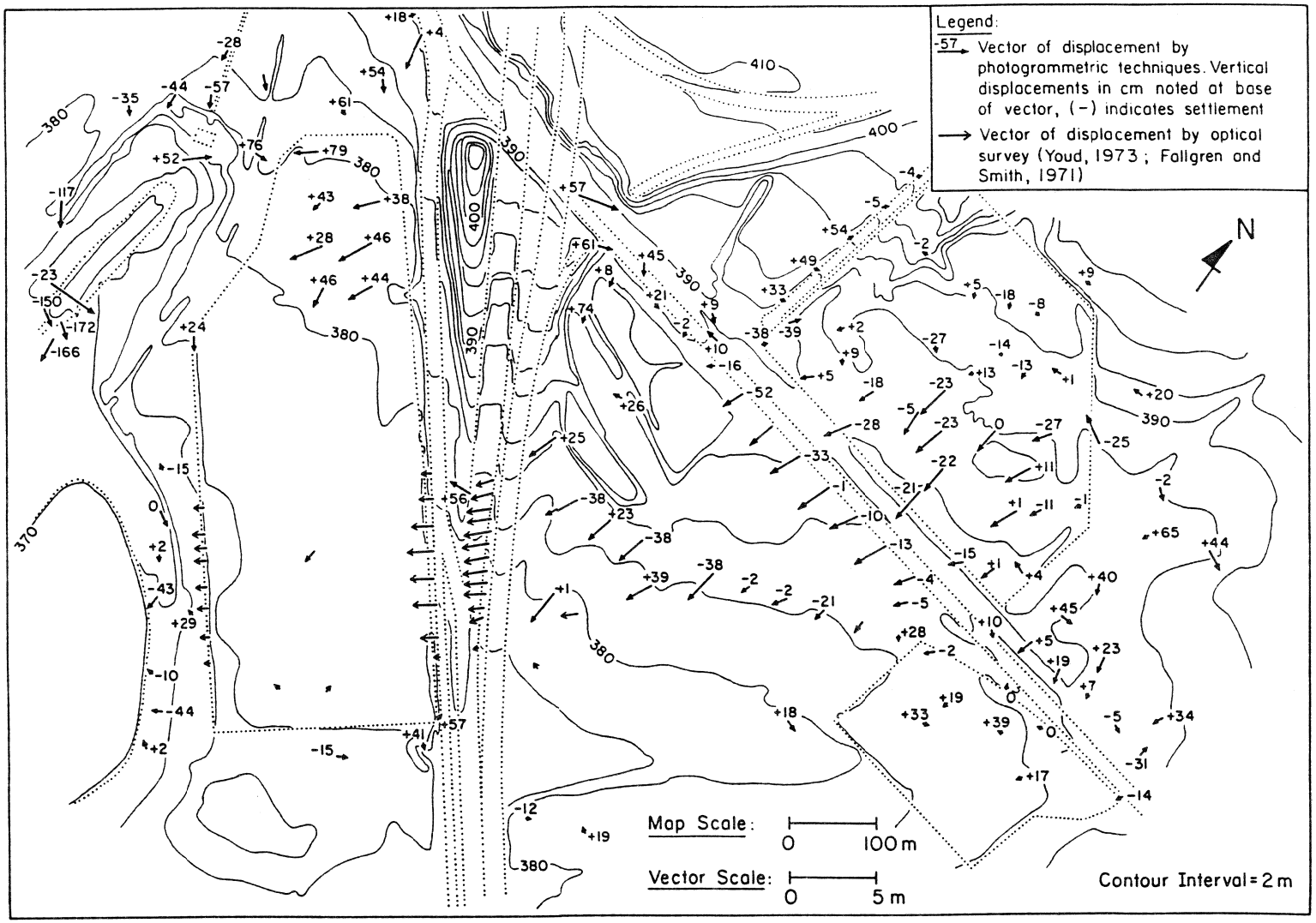

Figure 23. Displacements Determined from Air Photo Analyses and Optical Surveys, East of Upper Van Norman Reservoir

7.5 Subsurface Conditions

Subsurface soil and groundwater conditions in the zone of lateral spreading have been described in published reports by Youd (1973), Fallgren and Smith (1975), Brown (1975), and Bennett (1989), as well as in the geotechnical engineering reports listed in Appendix A. Three basic soil types were encountered: artificial fill, loose to moderately dense alluvium, and dense alluvium. In addition, the Saugus Formation was encountered in a 12-m-deep trench at the northwest corner of the Juvenile Hall (Fugro, 1975) and in borings south of the lateral spread. The fill material consists of clayey silt, sand, silty sand, and dense clayey sand. The alluvium consists of loose to moderately dense sandy silt and silty sand with some layers of clayey material. The thickness of the loose alluvium is greatest, up to 15 m, in the central areas of lateral spreading.

As part of this study, 76 boring logs, 10 CPT soundings, and nine backhoe trench reports were reviewed. The boring locations, as well as a legend indicating the firm or agency responsible for the borings, is shown in Figure 24. Figures 25 through 28 show soil profiles transverse and parallel to the longitudinal axis of the lateral spread. Standard penetration test measurements were performed by the USGS essentially in accordance with ASTM 1586 (ASTM, 1989). These data were corrected for overburden stress and energy efficiency, and plotted in the soil profiles. No other standardized in-situ tests were performed.

Water table elevations are shown in the soil profiles as open triangles. The water table elevations are from borings that were taken between 1966 and 1981. The elevation of the groundwater table does not appear to have varied substantially from the time of construction of the Upper Van Norman Reservoir (Bennett, 1989). The depth to the groundwater table at the Sylmar Converter Station varies between 3 and 6 m below the ground surface. The depth to the groundwater varies from about 6 to 12 m across the Juvenile Hall facility, with the most shallow water at the southern edge of the property. A contour plot of the depth to the water table at the northeast side of the Upper Van Norman Reservoir has been presented by Brown (1975).

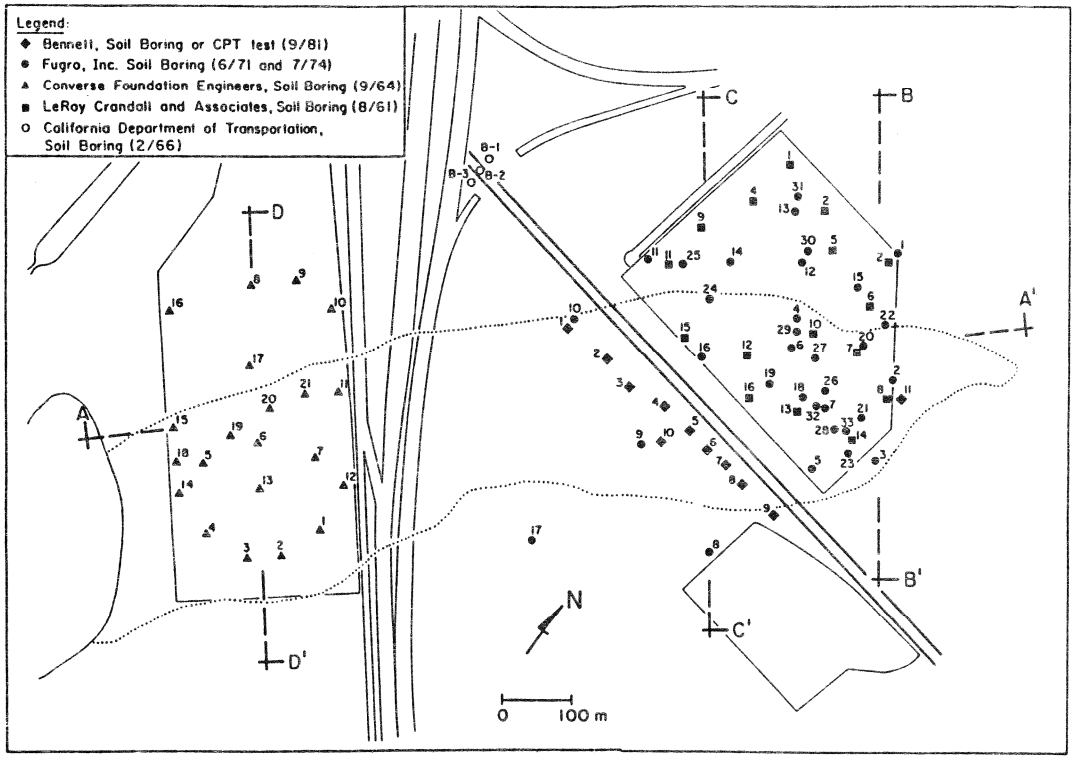

Figure 24. Locations of Soil Borings and Soundings East of Upper Van Norman Reservoir

The loose alluvium below the water table has been considered by many investigators to have liquefied during the 1971 earthquake (Youd, 1971 and 1973; MWD, 1973; Fallgren and Smith, 1975; Bennett, 1989). This zone is represented by the hatchured pattern below the groundwater table in Figures 25 through 28. The loose alluvium contains between 10 and 80% fines and up to 20% by weight of clay. A representative grain size distribution curve for the alluvium is shown in Figure 29.

The borings, CPT soundings, and grain size analyses presented by Bennett (1989) enabled a refined liquefiable zone to be defined for the soils along San Fernando Road. This zone was identified as a loose sandy silt and silty sand with average fine fraction of 70%. Because of the lack of in-situ and laboratory tests in other areas of the landslide, it was not possible to follow this subunit throughout the soil profiles.

The bottom depth of the loose alluvium is shown by contours of equal elevation in Figure 30. The basal surface of the liquefiable material was determined

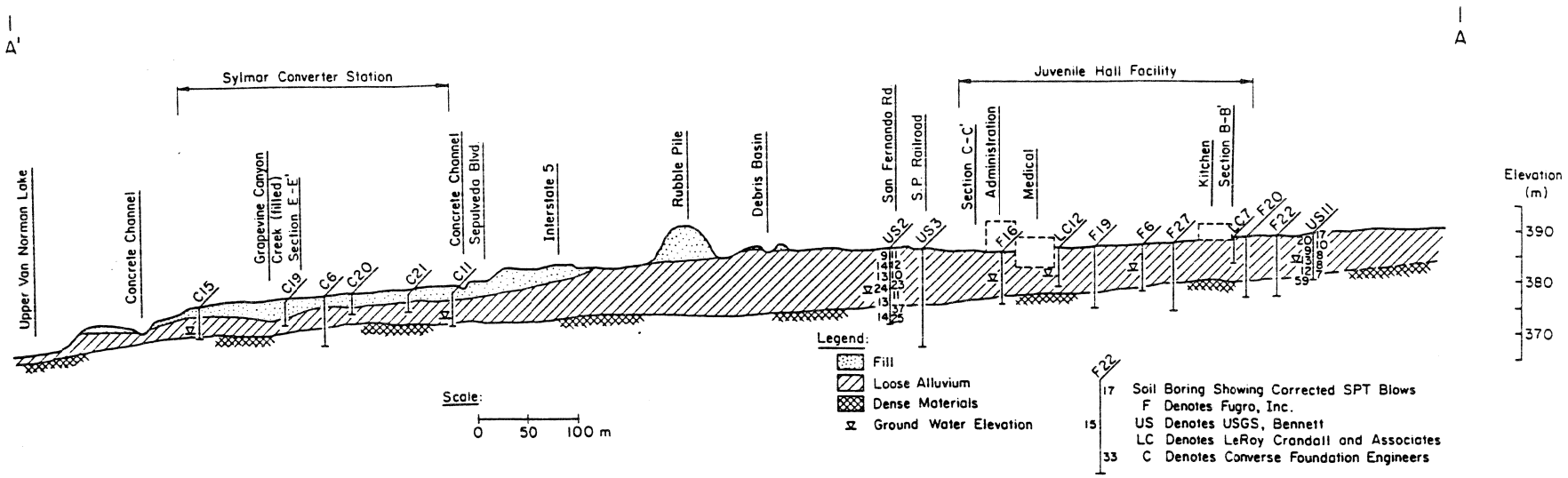

Figure 25. Soil Profile at Cross-Section A-A', East of Upper Van Norman Reservoir

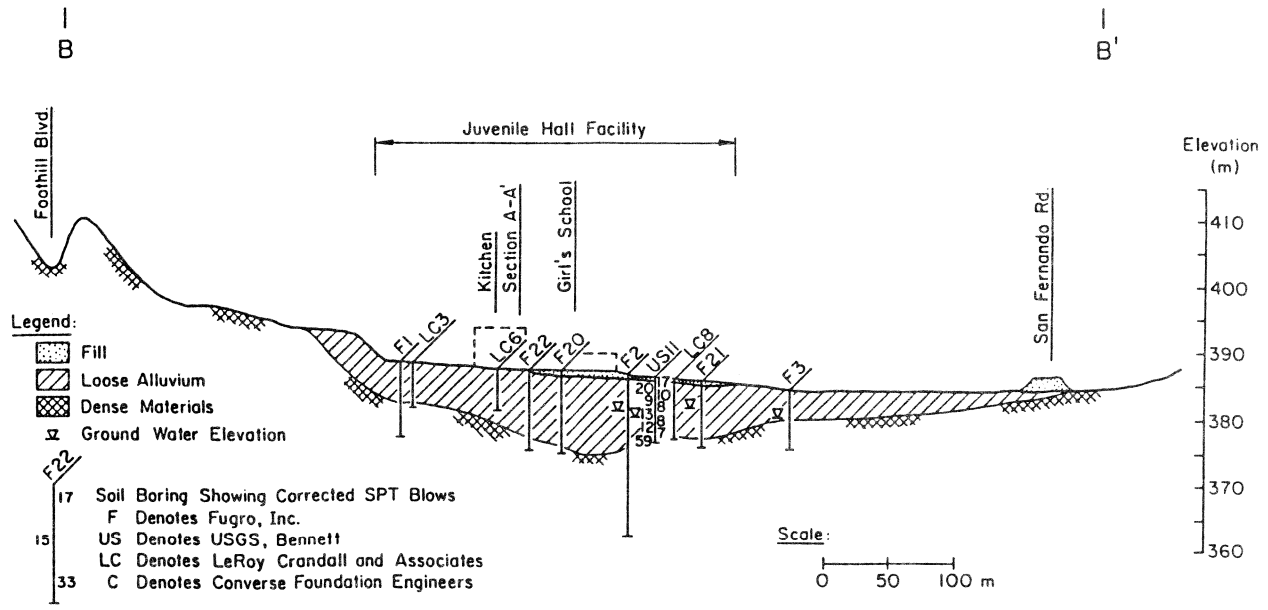

Figure 26. Soil Profile at Cross-Section B-B', Juvenile Hall

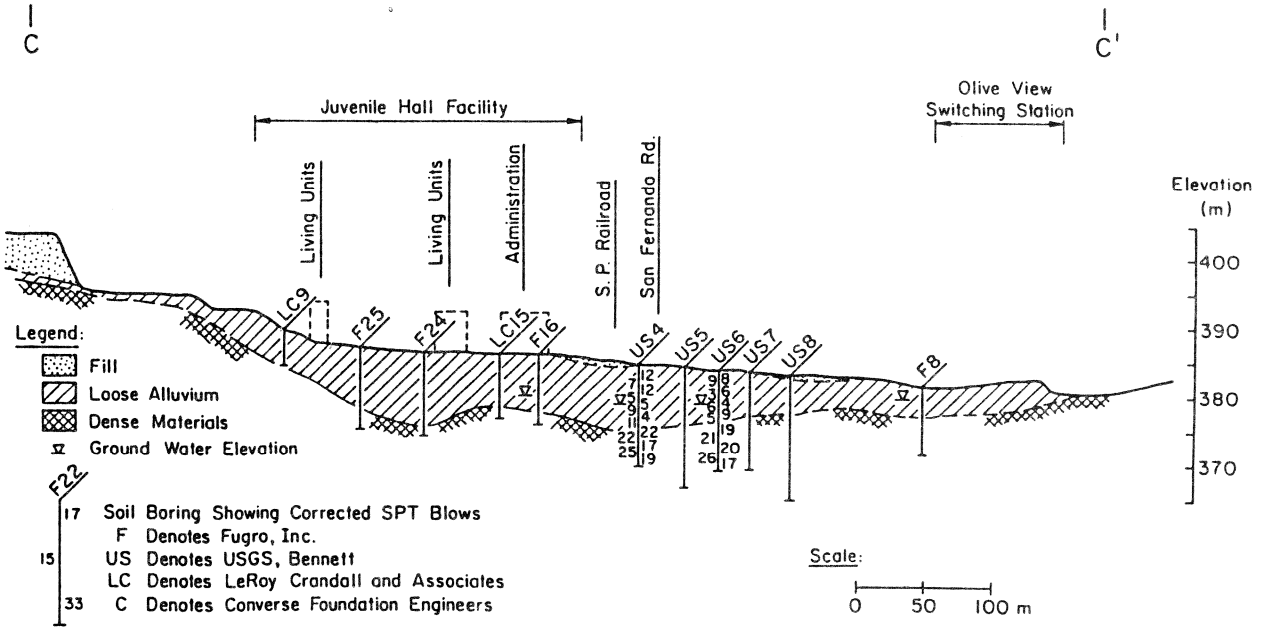

Figure 27. Soil Profile at Cross-Section C-C', Juvenile Hall

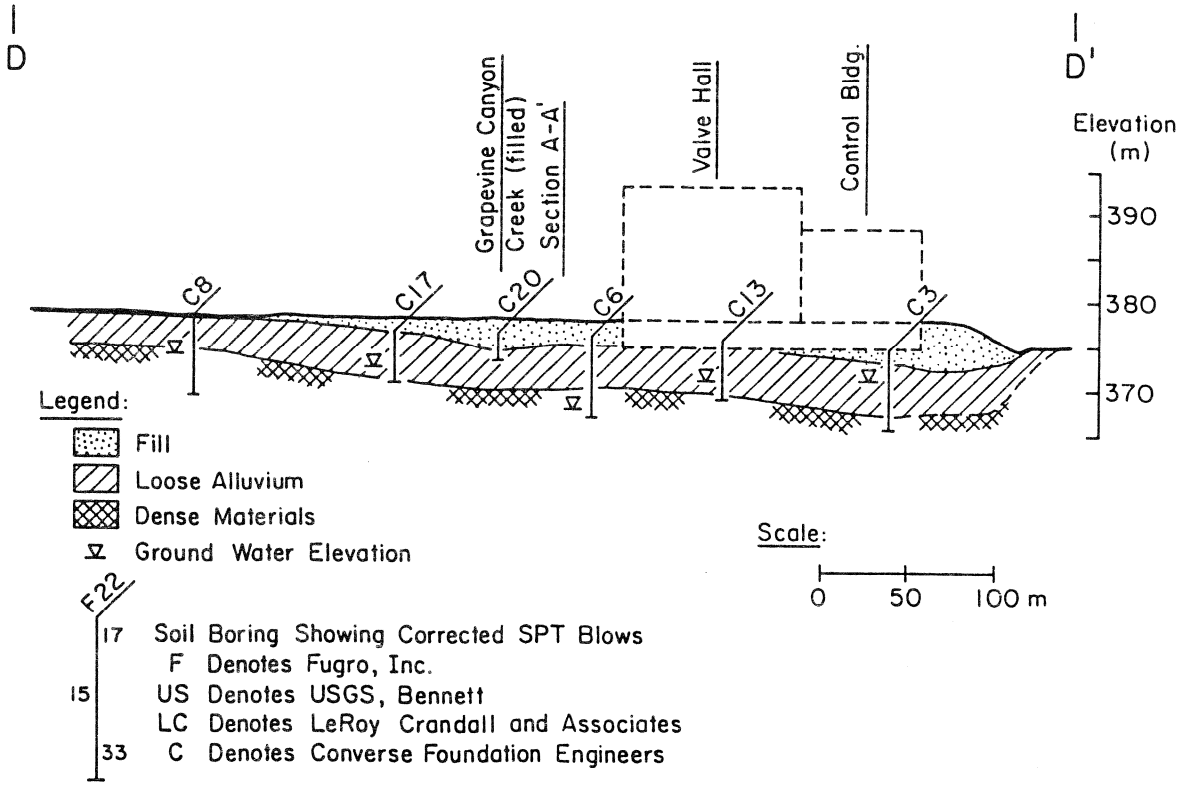

Figure 28. Soil Profile at Cross-Section D-D', Sylmar Converter Station

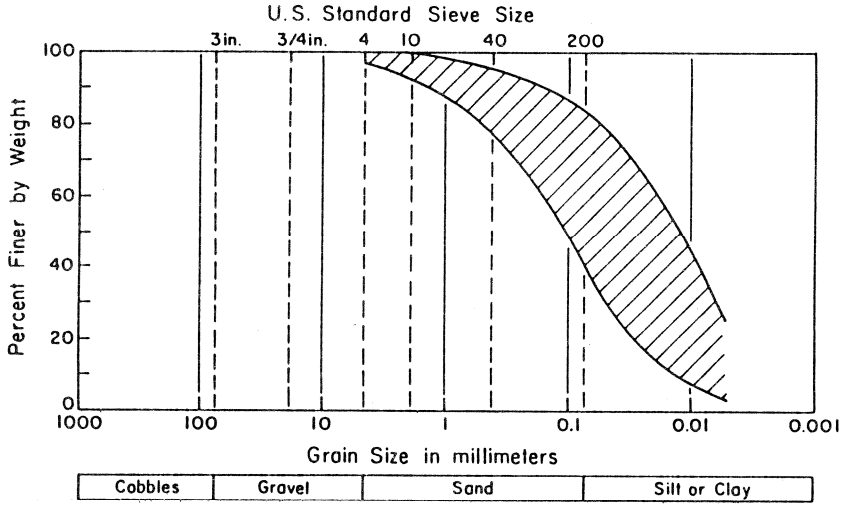

Figure 29. Typical Grain Size Distribution for Alluvial Soils East of Upper Van Norman Reservoir

from the boring logs and CPT soundings reviewed for this study. Bennett (1989) distinguishes the dense sandy subsoils as an old geomorphic surface at

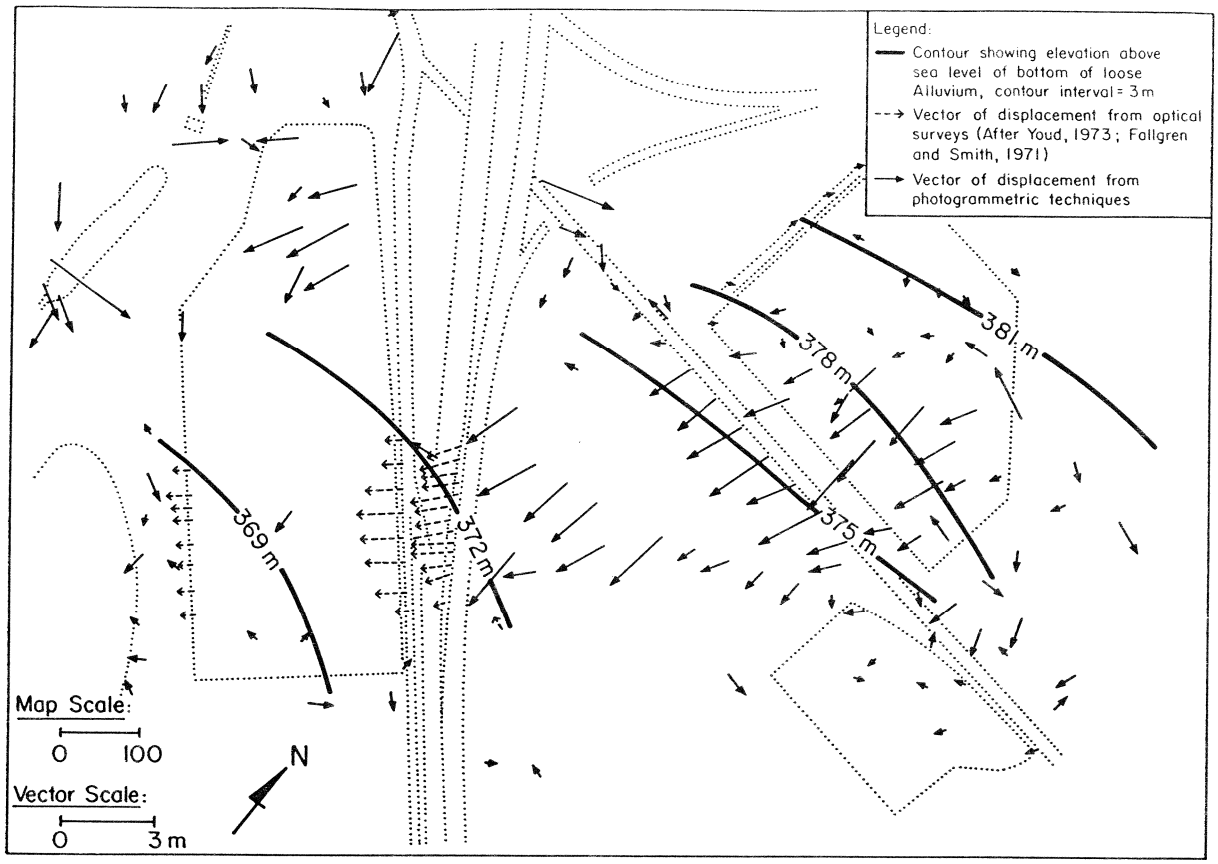

Figure 30. Contours of Equal Elevation for the Base of Loose Saturated Alluvium East of Upper Van Norman Reservoir

least 35,000 years old (1989). Elsewhere, in a 12-m-deep trench excavated through the Juvenile Hall yard, the dense underlying materials were described as the Saugus Formation (Fugro, 1975). The gradient of the bottom alluvium surface is shown in Figure 30 to dip towards the west through the Converter Station and to the southwest through the Juvenile Hall at an angle of about 1°.

8.0 OVERVIEW OF LARGE GROUND DEFORMATION

Figure 31 presents a sequence of three maps which illustrates the structural geology, geomorphology, and groundwater regime surrounding the Upper Van Norman Reservoir. Superimposed on all maps, for common reference, are the zones of large ground deformation as delineated by the surficial cracking and offsets plotted in Figures 7 and 22.

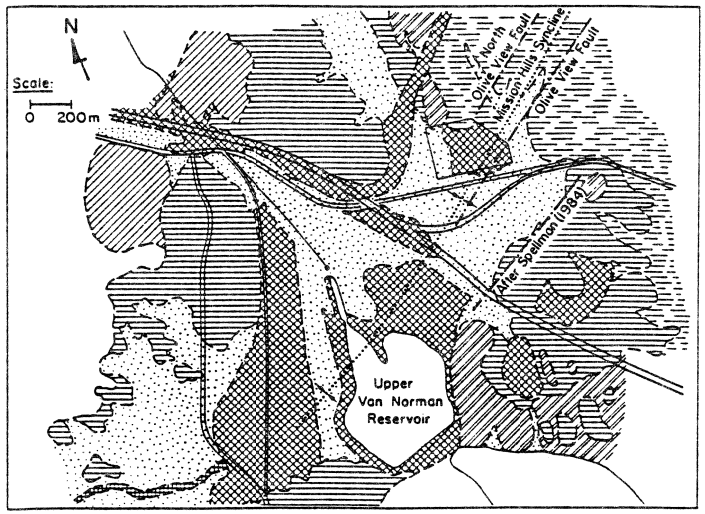

a) Geologic Structure

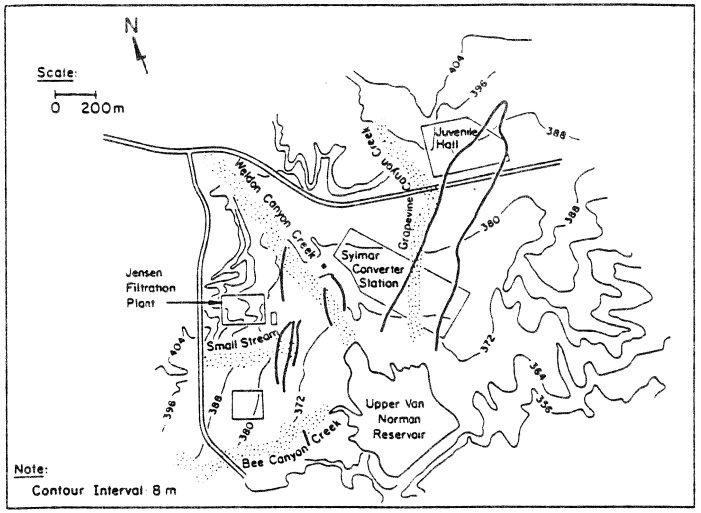

b) Geomorphology

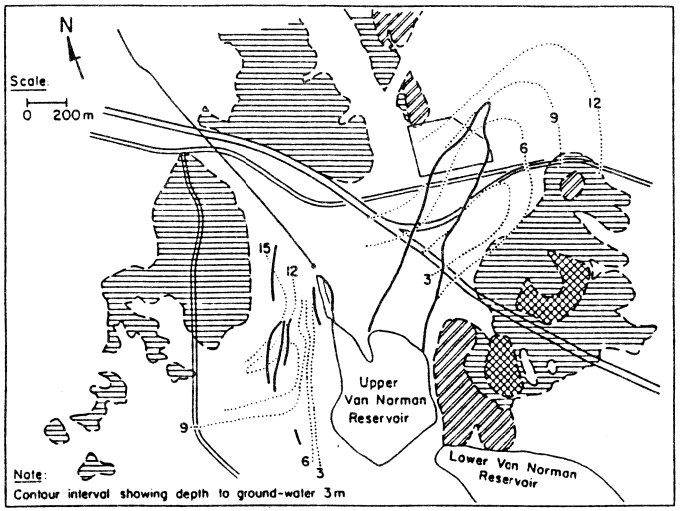

c) Groundwater

Legend:

- Artificial Fill
- Present Stream Channel Deposit
- Present Flood Plain Deposits
- Younger Alluvium and Colluvium
- Older Alluvium and Colluvium
- Saugus Formation
- Pico Formation
- ..... Synclinal Axis, Concealed
- —·— Inferred Fault
- — — Contact between Rock Units
- ~~~ Ground Cracks, Hachures on Downthrown Block

Figure 31. Plan Views of Upper Van Norman Reservoir Area Showing Geologic Structure, Geomorphology, and Groundwater

The boundaries of the alluvial fans and active stream channels, where soils most susceptible to liquefaction are deposited (Youd and Perkins, 1978; O'Rourke and Lane, 1989), are controlled by the geologic structures and outcrop locations shown in Figure 31a. At the northeast side of the Upper Van Norman Reservoir, the structural features that formed the southwest trending alluvial filled trough are the Mission Wells Syncline, the Olive View fault, and the North Olive View fault. A topographic lineament identified as an inferred fault by Spellman (1984) and Bennett (1989) behaves as a southern boundary for the deposition of recent alluvium into the trough. South of this boundary is either Saugus Formation (Barrows, et al., 1975) or an old geomorphic surface (Spellman, 1984; Bennett, 1989). Both the direction of the lateral spread, as seen in Figure 22, and the trend of Grapevine Creek Canyon, is deflected from due south to southwest, approximately paralleling the inferred fault and trend of the Mission Wells Syncline.

The synclinal structure extends into the western side of the Upper Van Norman Reservoir, where it provides a natural trough for deposition by the stream and debris flows from Weldon and Bee Canyons. Both these streams can be seen in Figure 31b together with a third source of alluvium and debris, identified as a small stream in the figure. This feature is shown clearly in 1929 air photos of the site. Air photos taken in 1945 and 1954 show a debris basin extending for about 150 m beneath the present eastern edge of the fill slope.

In Figure 31c, depth to groundwater contours are plotted, as inferred from the borehole records reviewed in this study and the depth to water table mapped by Brown (1975). The groundwater table along the western side of the Upper Van Norman Reservoir intersected loose alluvial deposits beneath the eastern half of the Joseph Jensen Filtration Plant. On the eastern side of the reservoir, the water table increases in depth to the north and west. In contrast to the southern flank of the lateral spread, which abuts against firm materials, the northern boundary of the Juvenile Hall slide appears to be controlled by the groundwater level.

Figures 32a and b show detailed views of the deformational features of the lateral spread at the Joseph Jensen Filtration Plant, and are cross-sections at C-C′ and B-B′, respectively (see Figure 14). The open-headed vectors in

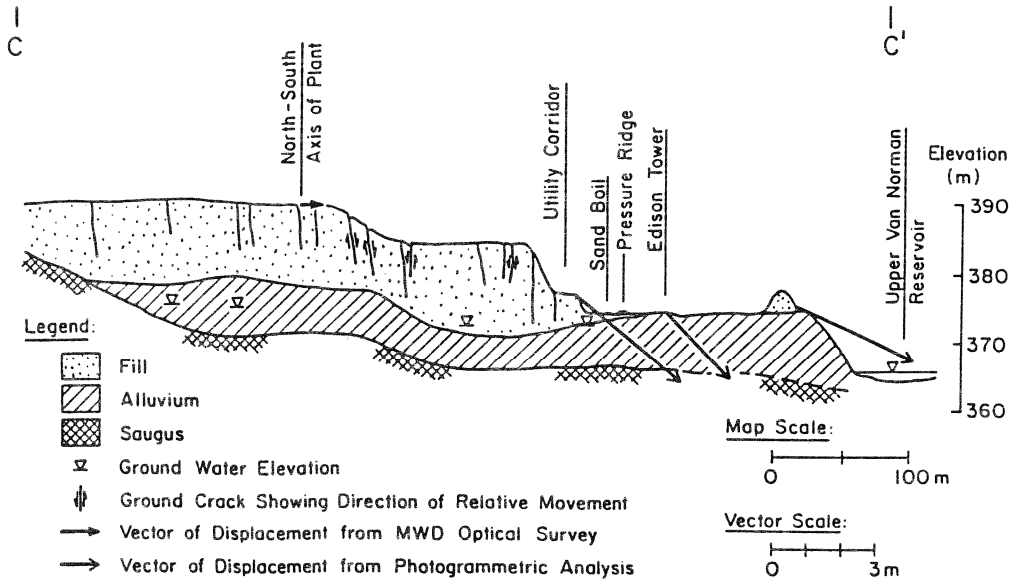

a) Section C-C'

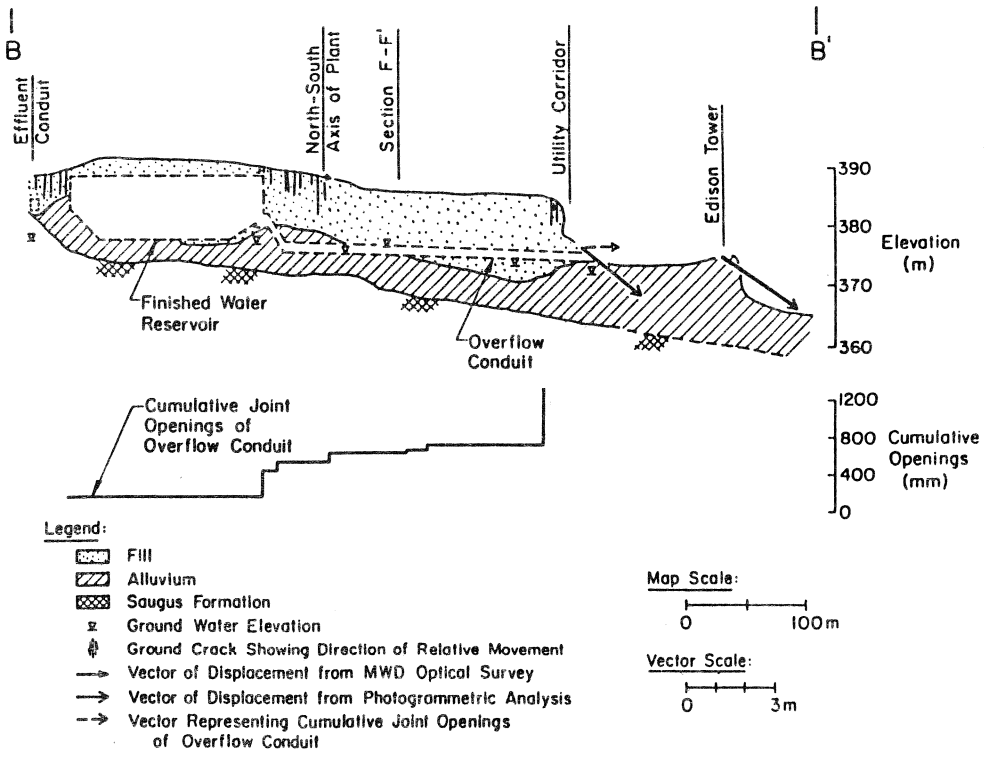

b) Section B-B'

Figure 32. Cross-Sectional Views of Joseph Jensen Filtration Plant Showing Large Ground Deformation and Cumulative Joint Openings of Overflow Conduit Along Sections B-B' and C-C'

the figures represent horizontal and vertical components of displacement as determined by photogrammetric analyses. The solid-headed vectors represent the horizontal and vertical components of displacement as determined by optical surveys conducted by MWD (Youd, 1973). Figures 32a and b also show the ground cracks projected below ground surface, and an exaggerated scale profile of the sand boils and pressure ridge.

Figure 32b shows a sectional view of the finished Water Reservoir and the Overflow Conduit. Openings of the joints of the 2.4 m diameter conduit are shown, and a plot of the cumulative horizontal displacement across the water reservoir and along the conduit is provided. The cumulative displacement plot in this figure is identical, except in scale, to the one presented in Figure 9. The maximum lateral displacement inferred from the joint openings is illustrated by the dashed horizontal vector at the utility corridor. It can be seen that the magnitude of movement represented by this vector agrees well with the horizontal component of displacement, as determined by air photo measurements, at both the utility corridor and the Edison Tower in the Middle Debris Basin.

The landslide at the Joseph Jensen Filtration Plant has been described by Converse, Davis, and Associates (1971) as liquefaction of the loose alluvium, followed by eastward movement of the east face of the fill slope and subsequent graben formation in the areas west of the fill slope. The vectors of movement east of the utility corridor are approximately the same magnitude, implying that this section moved as a discrete unit. The thickest deposits of loose saturated alluvium are located beneath this block, as shown by the contours presented in Figure 20. Moreover, this location of thick alluvium corresponds with the debris deposits shown in historic photographs, as well as former stream channels, as indicated in Figure 31b.

As the eastern part of the soil deposits moved toward the reservoir, tensile stresses developed in the fill which were relieved by cracks, joint openings in conduits, and grabens. Further west, in the zone where the Influent Conduit, MCB, and the west edge of the FWR are located, shaking and loss of lateral support led to settlement and eastward lateral movement. The zone of ground deformation was, thereby, effectively extended into other areas of the

fill by the relief of horizontal restraint at the margins of the lateral spread. This mechanism, where loss of lateral support and continued slumping occur beyond the zone of permanent lateral spreading, has been described as marginal slumping by O'Rourke and Lane (1989).

As illustrated in Figure 31, the lateral spread on the eastern side of the Upper Van Norman Reservoir was influenced by the geologic structure, geomorphology, and groundwater regime. The resulting pattern of ground movements involves at least two distinct zones of deformation corresponding to a lower zone southwest of Route 5 and an upper zone northeast of this location. Figure 33 shows a dissected view of the Juvenile Hall slide in which the upper and lower zones are illustrated. In the upper zone, vectors of lateral displacement, as determined from photogrammetric analyses, are drawn at selected locations to show continuous profiles of horizontal movement. In the eastern portion of the slide, the cross-sectional areas of lateral displacement are approximately equal, implying that the volume of movement was approximately constant at various locations downslope from the Juvenile Hall.

In the central portion of the slide, there is a prominent change in both the direction and cross-sectional area of movement. The change in movement direction most likely is governed by the underlying Saugus Formation, which borders the south margin of the slide. Compressional features were observed in this area, most notably in the heave and buckling of the pavement of the northbound lane of Route 5 (Prysock and Egan, 1981).

The lower zone of the slide is presented as a separate projection in the left side of the figure. Photogrammetric measurements were not possible in this zone, and lateral offsets previously plotted by Youd (1973) are shown. There was an abrupt discontinuity in the displacement across a 2.4-m-deep flood control channel, parallel to and just west of the converter station property line. Youd (1973) reports that the maximum lateral movement absorbed by the channel was 1.2 m. The displacements immediately east of the channel are plotted near the base of the upper zone, and the horizontal offsets immediately west of the channel are plotted at the right-hand margin of the lower zone projection.

Cross-section A-A' in Figure 33 shows the soil profile beneath the flood control channel, as interpreted from boring logs presented by Converse Foundation Engineers (1966). The water table, represented by an open triangle, is located at 3.3 m below the ground surface and 1.0 m below the bottom of the concrete channel. The bottom of the loose alluvium is shown to be 5.8 m below the ground surface.

As mentioned previously, approximately 1.2 m of lateral displacement were absorbed across the channel. This loss of movement implies that there was some combination of volume change in the soil, as well as lateral and vertical deformation of the channel, sufficient to reduce lateral spreading by 80% over a relatively short distance of 10 m. After the earthquake, about 0.6 m of heave was observed at the invert of the channel and the lining was offset and buckled (Youd, 1973). It is difficult to account for the large loss in lateral movement purely on the basis of observed channel deformation, or to explain the large reductions as a function of the notch-like geometry and decreased depth to water table. Because there are substantial practical implications for hazard mitigation associated the effects of the channel, the mechanisms giving rise to the decreased deformation should be explored in greater detail.

9.0 PIPELINE DAMAGE AT UPPER VAN NORMAN RESERVOIR

Figure 34 shows a plan view of the Upper Van Norman Reservoir area, on which are superimposed major transmission and trunk pipelines affected by permanent ground movements during the earthquake. In total, 11 transmission and trunk pipelines crossed areas of lateral spreading and liquefaction-induced large ground deformations. Table 1 summarizes information about the pipelines that includes dimensions, installation date, composition, joint type, coating, depth of soil cover, and nominal operating pressure at the time of the earthquake. The outside diameter (O.D.) and wall thickness for each pipe are listed. Each pipeline is numbered for purposes of referencing the pipeline as shown in the figure with information summarized in the table. In general, the pipelines were buried in medium to dense sand and silty sand above the water table. Transmission pipelines for natural gas, liquid fuel, and water were involved, representing different dimensions, joint design, operating

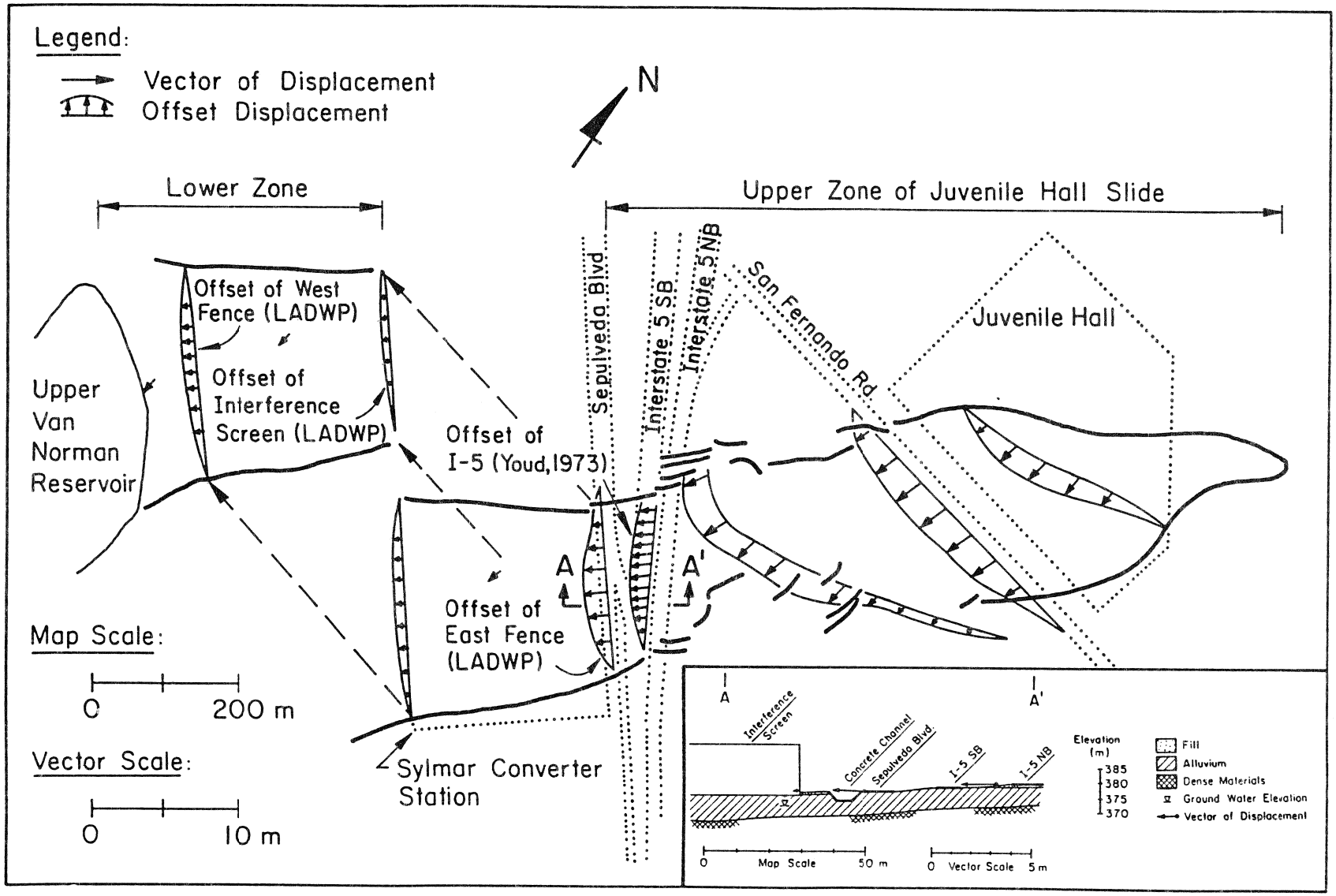

Figure 33. Plan View of Juvenile Hall Landslide, East Side of Upper Van Norman Reservoir

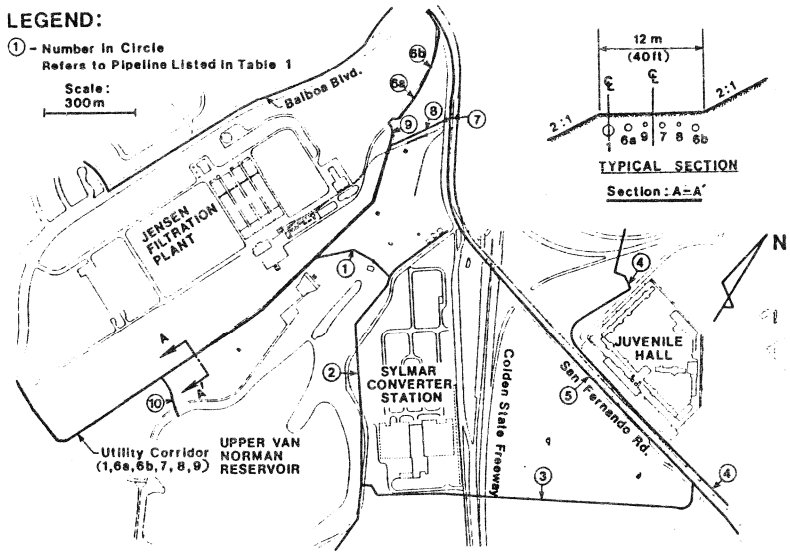

Figure 34. Pipelines Affected by Permanent Ground Movements Near Upper Van Norman Reservoir (after O'Rourke and Tawfik, 1983)

Table 1. Information Summary for Pipelines Affected by Ground Movements

Number	Pipeline	Dimensions	Installation Date	Composition	Joints	Coating	Depth of Cover	Operating Pressure
1	DWP Granada Trunk Line	1260mm O.D.; 6.4mm wall thickness	1967	Steel, ASTM A-283 Grade C	Arc welded slip joints on 9m centers	Cement, 25.4mm thick	1.0m	0.7-1.4MPa
2	DWP Upper Van Norman By-Pass	1370mm O.D.; 7.9mm wall thickness	1968	Steel, ASTM A-283 Grade C	Arc welded slip joints on 9m centers	Cement, 25.4mm thick	1.0-1.2m	0.7-1.4MPa
3	DWP Olden St. Diversion Line	760mm O.D.; 6.4mm wall thickness	1958	Steel, ASTM A-283 Grade C	Arc welded slip joints on 9m centers	Cement, 25.4mm thick	1.0-1.2m	0.7-1.4MPa
4	SCG Line 85	660mm O.D.; 6.4mm wall thickness	circa 1930	Steel, presumed yield stress of 230MPa	Initially flame welded but later arc welded with chill rings on 9m centers	Not reported	1.2-1.8m	1.4MPa
5	SCG Line 1001	324mm O.D.; 5.6mm wall thickness	1926	Steel, presumed yield stress of 174MPa	Flame welded joints on 12m centers	Not reported	1.0-1.2m	1.0MPa
6a, 6b	SCG Lines 3000 & 3003	760mm O.D.; 9.5mm wall thickness	1966	Steel, X-52 Grade	Arc welded girth joints on 12m centers	Asphalt, fiberglass, asbestos felt	1.0-1.2m	1.4-3.2MPa
7	SCG Line 120	560mm O.D.; 7.2mm wall thickness	1966	Steel, X-52 Grade	Arc welded girth joints on 12m centers	Asphalt, fiberglas and asbestos felt	1.0-1.2m	1.4MPa
8	Getty Oil Company Line	170mm O.D.; 7.2 mm wall thickness	1966	Steel, API Grade B	Arc welded girth joints on 12m centers	Coal tar enamel & fiberglas	1.0-1.2m	0.7-1.0MPa
9	Mobil Oil Corporation Line	400mm O.D.; 7.9mm wall thickness	1966 1969	Steel, X-52 Grade	Arc welded girth joints on 12m centers	Coal tar enamel & fiberglas	1.0-1.2m	No internal pressure at time of earthquake
10	DWP Plant Connection	1524mm O.D.; 9.5mm wall thickness	1970	Steel, ASTM A-283 Grade C	Arc welded slip joints on 9m centers	0.6m thick reinforced concrete encasement	2.0m	No internal pressure at time of earthquake

pressures, welding practices, and age. Pipelines operated by the Los Angeles Department of Water and Power and the Southern California Gas Company are prefaced by DWP and SCG, respectively.

The pipelines had welded joints. In the table, reference to arc and flame welding means welding by electric arc and oxyacetylene techniques, respectively. Two types of joints were prevalent. Lines 1, 2, 3, and 10 had welded slip joints, at which the end of one pipe is flared to create a bell into which the straight end of the adjoining pipe is fitted. A fillet weld usually is placed around the outside diameter to connect structurally the two pipe segments. The resulting joint transmits axial load with a slight eccentricity, which limits its axial load carrying capacity, as analyzed and discussed by O'Rourke and Tawfik (1983) and Tawfik and O'Rourke (1986). Lines 6a, 6b, 7, 8, and 9 had welded girth joints, where the beveled ends of adjoining pipes were welded to form straight, continuous connections. These welds, which are standard in modern high pressure gas and petroleum pipelines, result in minimal axial eccentricity.

Pipeline 4 along the San Fernando Road originally was constructed with oxyacetylene welds, but later was repaired and rewelded using electric arc techniques. The line was composed of 9-m-long pipe segments connected by means of a narrow pipe section, or chill ring, that fits into the belled ends of the pipe segments. The circumferential interface between each belled end and the chill ring was welded, forming a structurally continuous joint.

On the west side of the reservoir, most of the pipelines were buried along a utility corridor. A typical cross-section of the corridor is shown as an inset in Figure 34. Lines 6a and 6b in the corridor were identical with respect to dimensions, construction, and operating pressures.

Figure 35 shows a plan view developed by O'Rourke and Tawfik (1983) of the area west of the Upper Van Norman Reservoir on which are superimposed ground ruptures associated with liquefaction-induced slope failures in this locality. The locations of pipeline damage were determined from repair records provided through the courtesy of the LADWP and the Getty Oil Company. The information in the repair records was supplemented by discussion with utility personnel.

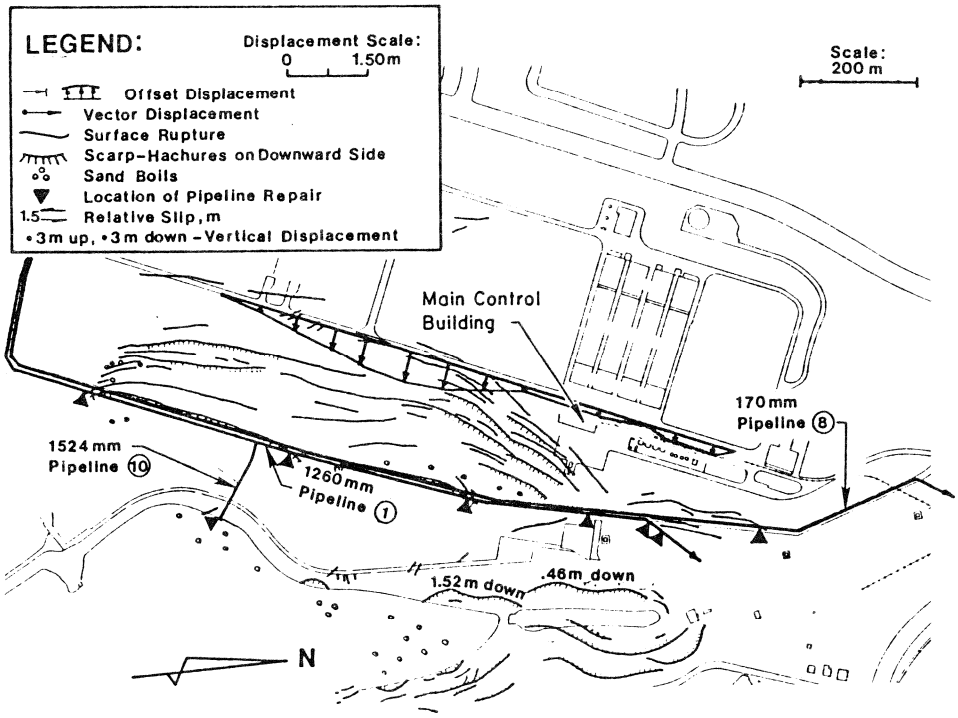

Figure 35. Locations of Pipeline Repair, West Side of Upper Van Norman Reservoir

The ground ruptures and surface displacements plotted on the drawing are taken from Figures 7 and 10.

Most of the pipelines in the utility corridor were not damaged, including the three lines operated by the Southern California Gas Company and one operated by the Mobil Oil Corporation (see Figure 34 and Table 1). Some gas pipelines were cut and rewelded after the earthquake, principally to relieve residual stresses and make adjustments for deformations caused by the ground movements. Pipeline 8, operated by the Getty Oil Company, failed in tension across a weld at the northern boundary of the landslide area.

The most prominent damage was sustained by Pipeline 1. Damage to this pipeline, known as the Granada Trunk Line, occurred in three principal ways, including deformations at a bend, welded slip joints, and mechanical couplings. The most severe damage occurred where the pipeline branches to the northeast and leaves the utility corridor. The combined bend at this location involves a change in both horizontal direction and vertical elevation as the pipeline angles down the 1V:2H slope of the utility corridor embankment.

Severe bending deformation occurred near this location, with approximately 0.5 m of transverse displacement over an axial distance of 3 to 4 m. Immediately to the northeast, a mechanical coupling had been installed with a special harness to allow up to 50 mm of axial displacement. The coupling was severely battered and compressed. Its harness was deformed substantially. Damage to another mechanical coupling was observed at the southernmost boundary of the landslide area. South of the combined bend, there were several locations of severe compressive wrinkling at welded slip joints. The Subcommittee on Water and Sewerage (1983) reports that there were eight slip joints damaged. Only three locations of repair between the combined bend and the damaged mechanical joint at the southern boundary of movement could be confirmed by reference to repair records, and these are shown in the figure. Discussions with utility engineers indicates that most of the damaged slip joints were located within 300 m south of the combined bend.

Pipeline 10 was damaged at its eastern end. This pipeline transports water from the overflow conduit of the Joseph Jensen Filtration Plant to the Upper Van Norman Reservoir. The overflow conduit was affected by ground movements in two areas, including a 0.6-m opening about 150 m west of its connection with Line 10 and a 0.3-m opening near its western connection with the FRW. Pipeline 10 was damaged at two mechanical couplings that joined the pipeline to a discharge structure at the west side of the reservoir. The couplings were severely battered and compressed.

Figure 36 shows a plan view developed by O'Rourke and Tawfik (1983) of the area east of the Upper Van Norman Reservoir, on which are superimposed transmission pipelines and ground ruptures associated with the lateral spreading in this locality. The approximate locations of pipeline damage, as well as the locations of explosion craters, are indicated. The explosion craters were 3 to 4 m in diameter and were formed by the sudden release of high pressure gas.

The locations of pipeline damage were determined from repair records provided by SCG and LADWP. Two locations of pipeline repair coincide with the locations of explosion craters. The craters were fixed independently of the repair records by means of oblique air photographs. The information in the

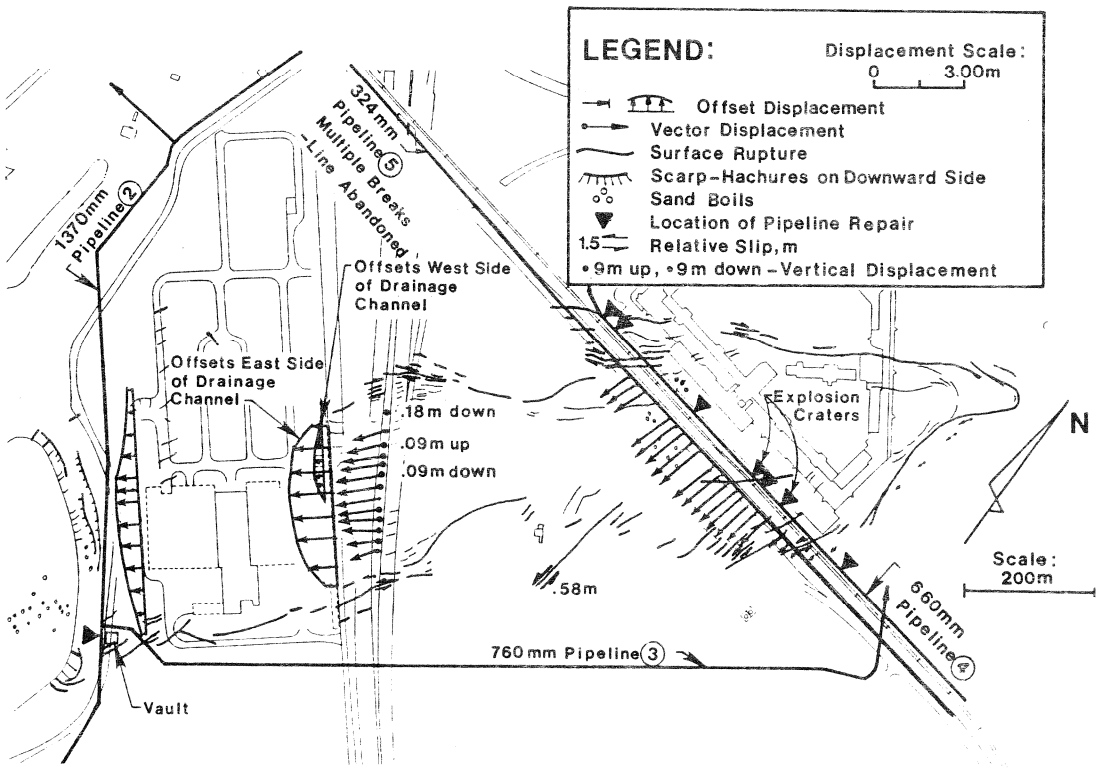

Figure 36. Locations of Pipeline Repair, East Side of Upper Van Norman Reservoir

repair records was supplemented by discussion with utility personnel.

Two gas transmission pipelines along the San Fernando Road were damaged. Pipeline 5 had multiple breaks and was abandoned. This pipeline also was damaged at locations southeast of the Juvenile Hall in the vicinity of the San Fernando fault zone, as discussed in a forthcoming section. Pipeline 4 was repaired at 7 locations within the lateral spread. This pipeline was not damaged at any other location within the San Fernando area, although it did cross the Mission Wells segment of the San Fernando fault. The vector displacements along San Fernando Road provide a good estimate of the net ground deformation imposed on the pipelines. It should be remembered, however, that the locations of most severe differential movement may have changed during the earthquake as the zone of lateral spreading developed. It is most likely that the first ruptures in Pipeline 5 occurred at the locations of the explosion craters. These ruptures were near the southeastern margin of the lateral

spread, where the pipeline was subjected to substantial tension from left lateral soil movement across the pipe. The records indicate that tensile failures were repaired at the three locations near the southern boundary of soil movement.

The maximum displacement within the lateral spread was approximately 2.0 m. Near the southeastern margin of the spread, most of this displacement developed over a distance of 70 m. The maximum lateral offset measured across a single ground rupture was 0.58 m, and is shown in the figure.

Two water transmission pipelines were located within and near the zone of lateral spreading. Damage was observed at only one location, where Pipeline 2 was connected to a ball valve and mechanical joint at a reinforced concrete vault. The mechanical joint was severely deformed and showed signs of repeated impact, or battering. This battered joint was compressed.

The offset displacements along the western boundary of the converter station provide a good estimate of the net ground deformation imposed on Pipeline 2. Although the pipeline was subjected to a maximum lateral displacement of approximately 0.7 m, there was no damage. It should be emphasized that the differential displacement per distance along Pipeline 2 was significantly less than that of the gas transmission pipelines along San Fernando Road.

10.0 GROUND DEFORMATION ALONG THE SAN FERNANDO FAULT

Five principal zones, or segments, of surface displacement have been identified along the San Fernando fault (Weber, 1975), extending from the Lower Van Norman Reservoir to Big Tujunga Wash (see Figure 4). Offset measurements and descriptions of surface displacements have been reported by numerous investigators (e.g., U.S. Geological Survey Staff, 1971; Barrows, et al., 1973; Sharp, 1975; Weber, 1975). The actual rupture surface was relatively complex. There was a marked thrust, or compressive, component of movement along the Tujunga segment, whereas the Mission Wells and Sylmar segments were characterized by smaller thrusts with larger vertical components of movement (Sharp, 1975). All segments displayed prominent left lateral components of slip.

Figure 37 shows a plan view of the Mission Wells and Sylmar segments of the San Fernando fault, as well as a zone of prominent ground ruptures and street cracks, referred to by Eguchi, et al. (1981) as the Harding School fault area. Each zone of prominent ground movement is bounded in the figure by a solid line.

The Mission Wells segment trends east-northeast and shows both left lateral and reverse displacement. Where it crosses Osceola Street, in the middle of the segment, the fault dips 60° north with the northern block uplifted 250 mm, thrusted 200 mm to the south, and left laterally displaced 30 mm (U.S. Geological Survey Staff, 1971; Weber, 1975). The segment had a length of nearly 1 km.

The 3-km-long Sylmar segment trends east-west across a densely populated area. The width of the zone of surface ruptures varied from 30 to 200 m. In the central part of the segment, displacements across the entire fault zone were composed of 1.9 m of left lateral slip, 1.4 m of vertical offset, and 0.6 m of thrust (U.S. Geological Survey Staff, 1971). The largest individual ground ruptures showed displacements approximately one-half of the maximum displacements across the entire width of the zone. Most of the left lateral slip and thrust was concentrated along the southern 25 to 80-m-wide section of the fault zone. North of this section, vertical offsets and extension fractures were the predominant forms of ground rupture (U.S. Geological Survey Staff, 1971).

The Harding School fault area is located between 0.2 and 1.0 km north of the eastern part of the Sylmar segment. This zone contained surface breaks that were offset vertically and downward to the north with right lateral displacements. The maximum displacements were relatively small, varying from 10 to 50 mm. Weber (1975) suggests that these displacements reflect a tension release across bedding planes in the underlying bedrock.

11.0 PIPELINE PERFORMANCE ALONG SAN FERNANDO FAULT

The study area for pipeline damage is shown as an inset in Figure 37 and is bounded by a dashed line in the main part of the figure. Within the study

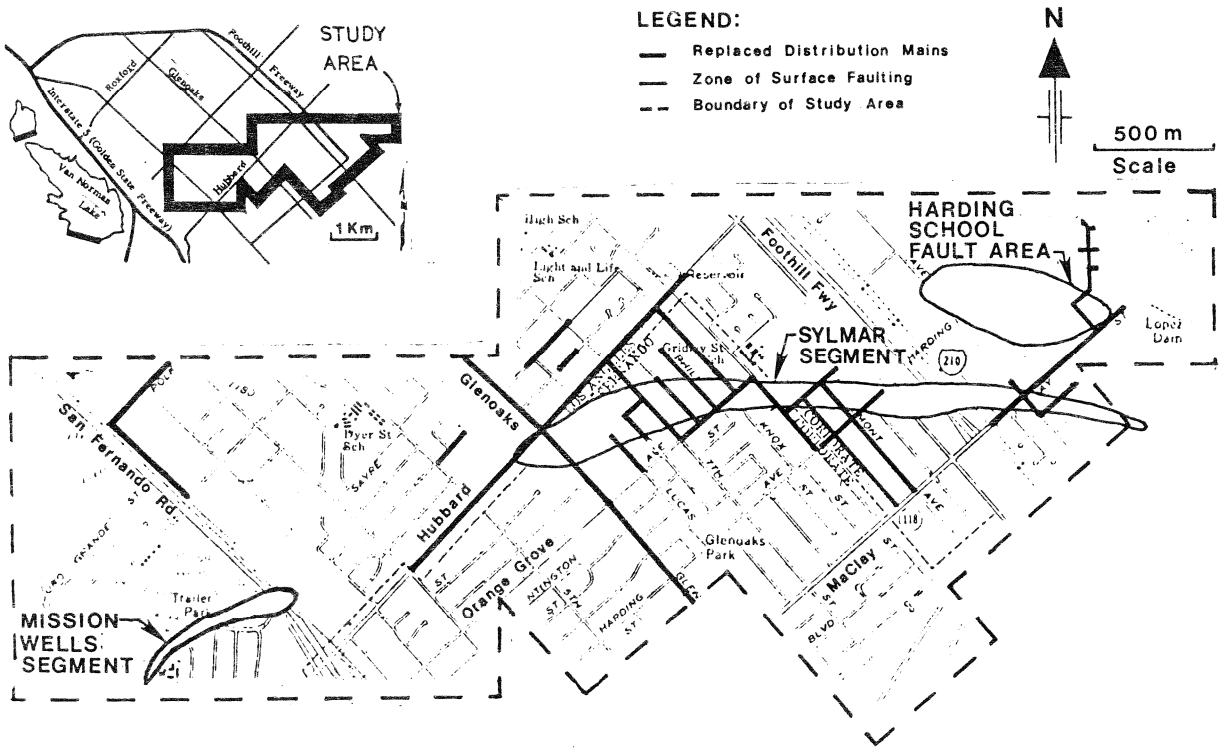

Figure 37. Plan View of Surface Faulting and Replaced Gas Distribution Pipelines (after McCaffrey and O'Rourke, 1983)

area, gas and water distribution pipelines were buried along right-of-ways that followed existing streets. The pipelines were buried at a nominal depth of 0.9 m, measured from the street surface to top of pipe. The soils in the Sylmar segment are mostly silty sands and gravels. A groundwater barrier exists across the Sylmar segment, with the water table measured at depths well below the pipelines of 20 and 40 m on the north and south sides, respectively, of the barrier (Oliver, et al., 1975).

11.1 Gas Distribution Pipelines

Records of gas pipeline repair and replacement in the study area were provided by SCG, and the repair records were checked and supplemented by information reported by SCG (1973). The gas distribution mains principally were composed of 12-m-long segments of 25 to 200-mm internal diameter steel pipe, connected at oxyacetylene welded joints. Gas pressure in the pipelines at the time of the earthquake was approximately 0.24 MPa.

Pipeline segments from 100 m to 2 km in length were replaced within several months after the earthquake. The replaced pipelines are shown in Figure 37. At locations where two or more pipelines were adjacent to each other under the same street, only the replaced pipeline is indicated. Sixteen percent of the total length of all distribution lines in the study area was replaced. There was a high concentration of replacements within and adjacent to the Sylmar segment, with replacements made for 67% of the total length of all lines within the segment. The number of replacements was influenced by the orientation of pipelines relative to the trace of the fault. Sixty-two percent of the total length of northwest-oriented pipelines within the Sylmar segment was replaced, whereas 79% of the total length of northeast-oriented pipelines was replaced.

Figure 38 shows a plan view of the Sylmar segment and Harding School fault area, on which the locations of individual pipeline repairs are plotted. The types of repairs were determined from gas leak repair sheets provided by SCG. The causes of repair typically were noted as breaks in the pipe and damage at welded joints.

Water from broken water distribution lines washed soil and debris into ruptured gas pipelines, so that repairs occasionally were performed to remove blockages at a relatively long distance from the locations of most severe deformation. Three locations associated with repair of gas pipelines clogged with soil and debris are shown in Figure 38. All are located several hundred meters downgrade from areas of concentrated gas pipeline damage.

Gate valves also were damaged by the earthquake, and two locations of valve repair are shown north of the fault zone in Figure 38. Gate valves made of cast iron generally showed a significantly higher incidence of damage than those composed of steel or brass (LePire, 1982).

11.2 Water Distribution Pipelines

Records of water pipeline repair and replacement in the study area were provided by the LADWP and City of San Fernando. Repair records were checked by means of discussions with utility personnel and reference to pipeline damage

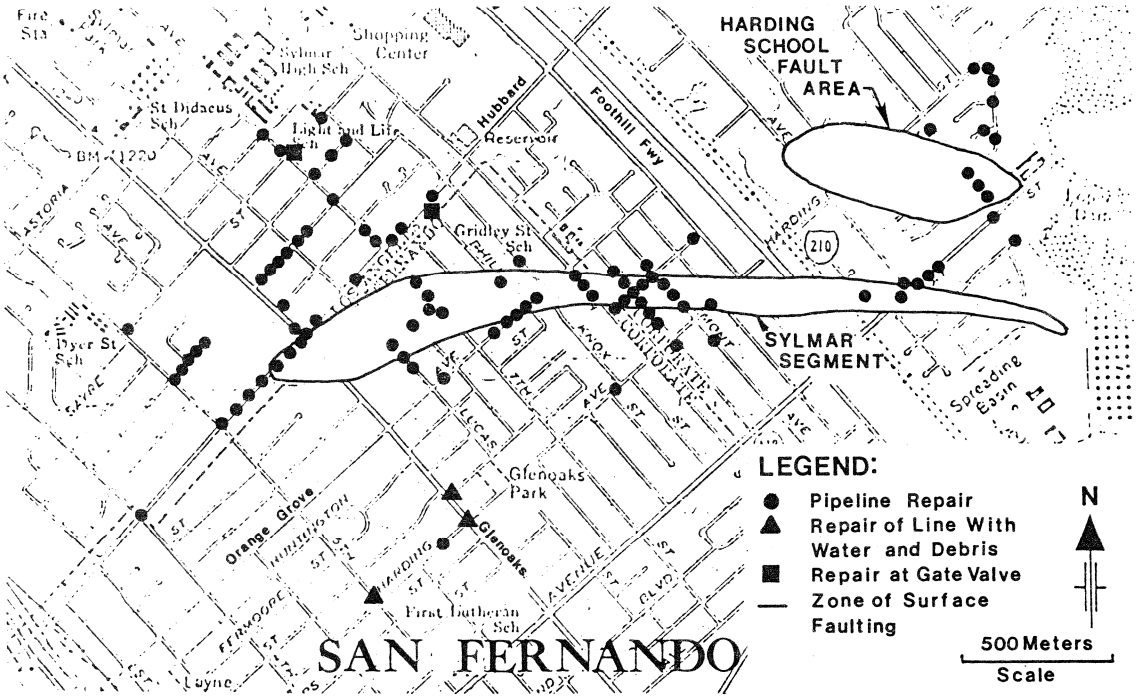

Figure 38. Plan View of Repairs of Gas Distribution Pipelines (after McCaffrey and O'Rourke, 1983)

studies performed by Eguchi (1982). Virtually all of the water mains were metallic pipelines, including steel with welded slip joints and gasket joints, continuous steel, riveted steel, and cast iron with lead-caulked and gasket joints. Water pressure in the pipelines at the time of the earthquake was approximately 0.20 MPa.

As described by Steinbrugge, et al. (1971), the water distribution system of the City of San Fernando was hard hit by the earthquake. Damage from large ground deformations overwhelmed the city's limited work force, and assistance from LADWP, MWD, and the U.S. Army Corps of Engineers was required to make emergency repairs and restore water to the area. The Corps of Engineers, representing the federal government, undertook the reconstruction of the city's damaged distribution network.

Approximately 20 km of pipelines were replaced in the City of San Fernando, with over 14 km replaced as shown in Figure 39. Every water pipeline in the

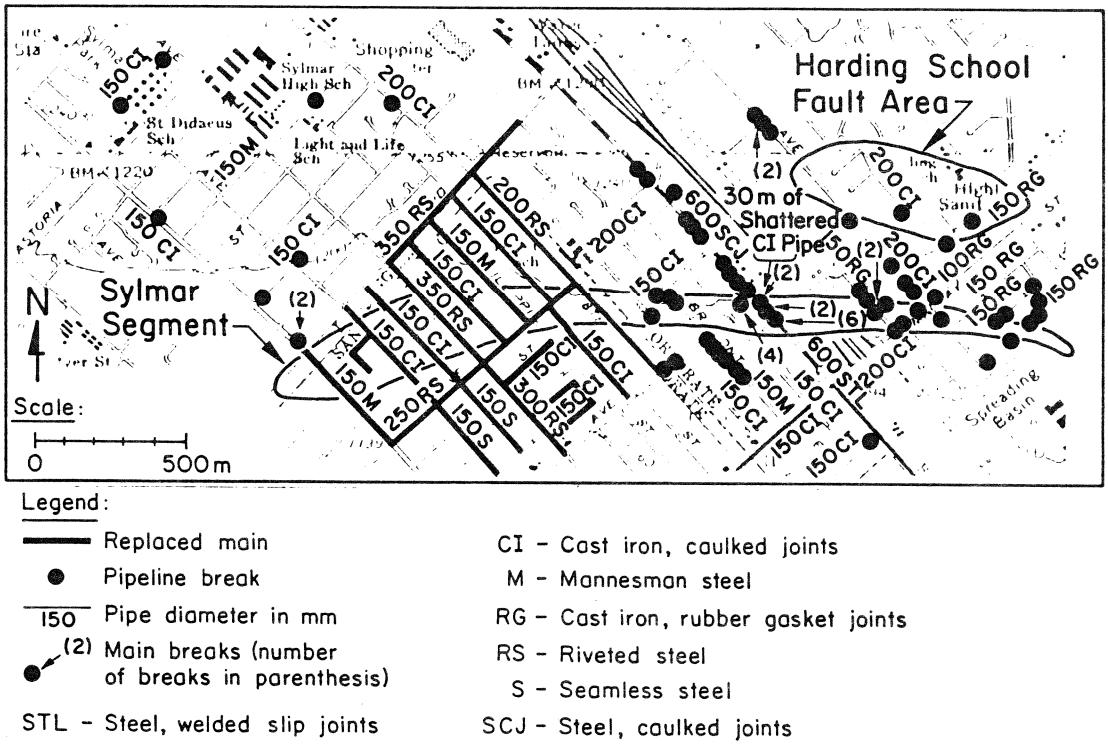

Figure 39. Plan View of Replaced and Repaired Water Distribution Pipelines

city, which crossed or was immediately adjacent to the Sylmar segment of the San Fernando fault, was replaced. The replaced pipelines included mains constructed of riveted steel, continuous steel, and cast iron.

Figure 39 also shows the locations of individual pipeline repairs by the LADWP in relation to the Mission Wells and Sylmar segments of the fault and to the Harding School fault area. It is apparent that there is a high concentration of repairs within the zones of surface faulting. Within and adjacent to the Sylmar segment, there was substantial damage to a 600-mm-diameter steel pipeline. The line was constructed with welded slip joints both within and south of the fault zone, and with cement-caulked joints north of the fault zone. It is likely that the compressive forces generated by thrust within the fault zone were responsible for slip joint failures. The left lateral strike slip motion of the fault would have produced a net tension in this northwest-oriented line north of the fault, thereby causing pullout failure at the cement-caulked joints. Two repairs on a 200-mm-diameter pipeline with welded

slip joints also can be seen where the line crosses the Harding School fault area.

A 150-mm-diameter pipeline composed of Mannesman steel was damaged heavily south of the fault. As pointed out by O'Rourke and Trautmann (1980), this type of steel particularly is vulnerable to corrosion. Corrosion and earthquake-related problems continued with this pipeline; the line was repaired many times after the earthquake until it was replaced in 1975.

12.0 PIPELINE REPAIRS RELATIVE TO THE FAULT ZONE

The pattern of pipeline repair along the Sylmar segment was analyzed as a function of distance from the fault zone centerline. The centerline of the fault was taken at the middle of the zone showing the most severe surface displacements near the southern boundary of the segment. Fifty-one and 32 records of repair for gas and water distribution pipelines, respectively, were used in the analyses.

Figure 40 shows the number of gas main repairs per kilometer of pipeline plotted as a function of distance from the center of predominant fault movement. The repairs were determined for 50-m-wide intervals. The left side of the figure shows the number of repairs on the upthrown and downthrown sides of the fault normalized with respect to the total pipe length in each 50-m-wide interval on the upthrown and downthrown sides, respectively. In a similar manner, the right side part of the figure shows the number of repairs on the northeast and northwest-oriented pipelines normalized with respect to the total pipe length in each 50-m-wide interval for each group of northeast and northwest-oriented pipelines, respectively.

The relatively high number of repairs within 100 m of the fault centerline is related directly to the magnitude and severity of fault movement. At a distance greater than 200 m, there is a significant difference in the level of damage, with the greater number of repairs per kilometer on the upthrown block.

Pipeline orientation relative to the fault also had an effect on damage. Pipelines oriented in the northeast direction were subject to compressive

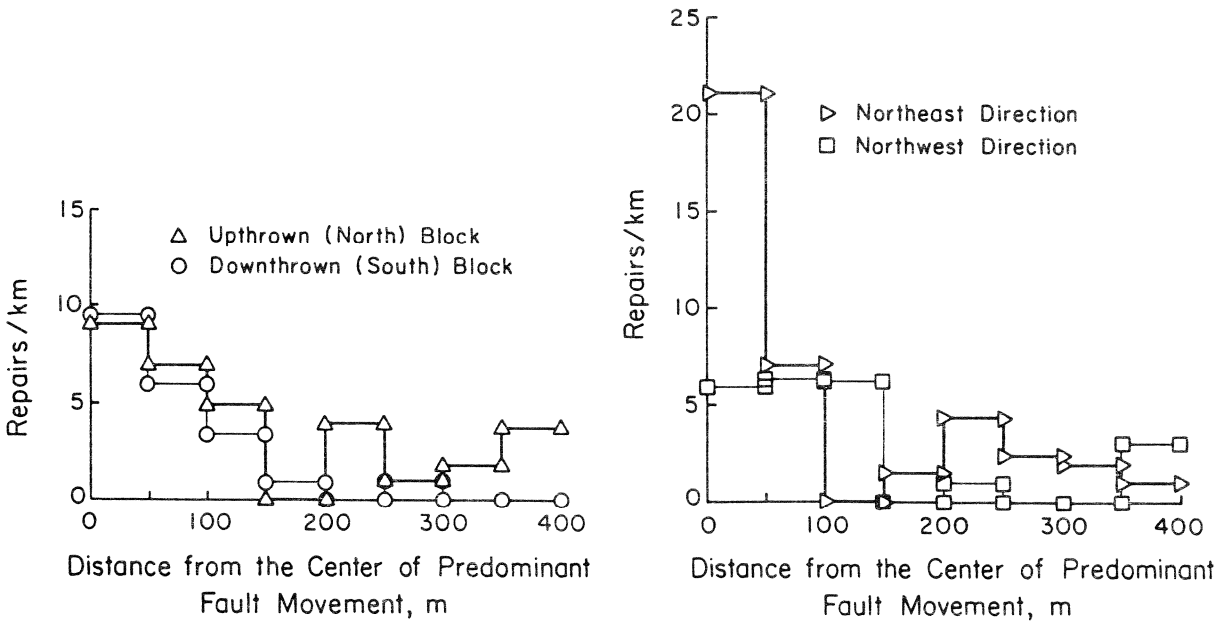

Figure 40. Gas Pipeline Repairs as a Function of Distance from the Fault Zone (after McCaffrey and O'Rourke, 1983)

strains from both the thrust and left lateral strike slip components of fault movement. The number of repairs per kilometer of pipeline at or near the fault centerline was nearly four times higher for the northeast, compared to the northwest-oriented, pipelines.

Figure 41 shows the number of water main repairs per kilometer of pipeline plotted in a similar fashion to Figure 40. The repair rate declines with increasing distance from the fault. Damage on the upthrown side of the fault apparently was more intense than on the downthrown side. Damage also was more severe for northeast-oriented lines near the center of surface faulting, presumably because the additive effects of thrust and left lateral slip resulted in excessive compressive strains. As shown in the figure, roughly 30 m of cast iron main shattered from compressive forces within the zone of faulting along a northeast-oriented street. At distances exceeding 50 to 100 m, the effect of pipeline orientation is less pronounced. Because cast iron pipelines are jointed, they are vulnerable to pullout forces which would have been

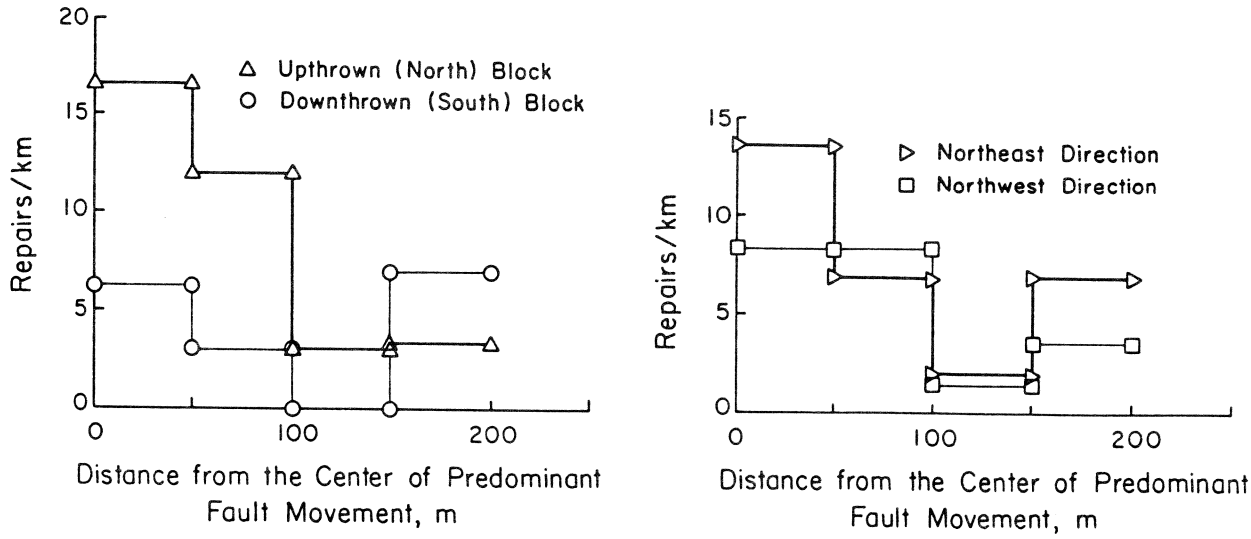

Figure 41. Water Pipeline Repairs as a Function of Distance from the Fault Zone

most severe in response to left lateral slip on northwest-oriented lines.

13.0 PERFORMANCE OF GAS TRANSMISSION PIPELINES

Four natural gas transmission pipelines were located at or near the zones of surface faulting. The lines were composed of welded steel pipe lengths and were buried in silty sand and gravel at depths 1.2 to 1.8 m from the ground surface to the top of pipe. Table 2 lists the internal diameter, type of welds, date of installation, and nominal operating pressure for each pipeline.

Figure 42 shows a plan view of the San Fernando area, on which are superimposed the transmission pipelines and outlines of the Mission Wells and Sylmar segments of the San Fernando fault. The approximate locations of pipeline damage, as well as the locations of explosion craters, are indicated. The explosion craters typically were 3 m to 5 m in diameter, and were formed by the sudden release of high pressure gas.

Table 2. Summary of Information for Gas Transmission Pipelines

Line	Internal Diameter (mm)	Type of Weld	Approximate Date of Installation	Nominal Operating Pressure (MPa)
85	660	Initially oxy-acetylene welded, but rewelded in 1932 with electric arc techniques	1930	2.10
102.9	310	Oxyacetylene	1927	1.04
115	410	Oxyacetylene	1930	1.40
1001	310	Oxyacetylene	1926	1.40

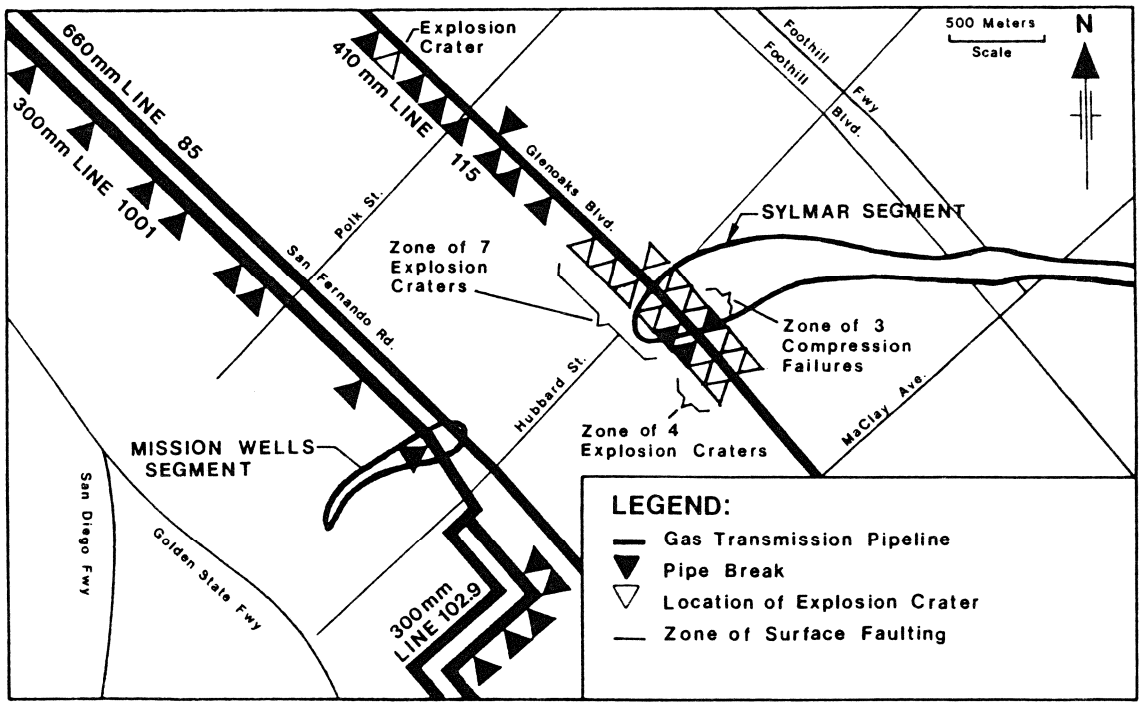

Figure 42. Plan View of Breaks and Explosion Craters for Gas Transmission Pipelines (after O'Rourke and McCaffrey, 1984)

The presence of explosion craters implies that damage to Line 115 occurred rapidly, before escaping gas at a given rupture could diminish pressures at other break locations. Most of the explosion craters were associated with tensile failures at welded joints, and at least one crater was located at a point of severe compressive wrinkling of the pipeline at the southern edge of the fault. Explosion craters at the fault edge and at substantial distances from the zone of faulting suggest that damage north of the fault occurred within a very short time of the damage from permanent ground movements at the fault. There were some fires caused by escaping gas, one of which was reported by Steinbrugge, et al. (1971) at the location of the southernmost crater on Line 115.

There was no damage to Line 85 in the area shown by Figure 42, even though the pipeline crosses the Mission Wells segment. Line 85 originally had been constructed with oxyacetylene welds, but later was repaired and rewelded using electric arc techniques.

Damage to welded steel pipelines has been reported during the 1952 Kern County earthquakes (Lind, 1954; Newby, 1954), when lines with oxyacetylene welds required a greater number of repairs than those with electric arc welds. As discussed by McCaffrey and O'Rourke (1983), the apparently higher incidence of earthquake damage most likely was related to weld quality. Interviews with welders, who repaired damaged gas lines after the earthquake, revealed that welds in damaged areas showed signs of poor root penetration and toe undercutting. These types of imperfections create flaws, which in turn lead to stress concentration and the propagation of fractures.

14.0 OVERVIEW OF PIPELINE PERFORMANCE

The 1971 San Fernando earthquake provides the opportunity to relate large ground deformation, various soil conditions, and the response of buried pipelines of different size, composition, and age. Of particular interest are the areas east and west of the Upper Van Norman Reservoir, where liquefaction-induced soil movements affected high pressure transmission and trunk pipelines carrying water, gas, and oil. On the west side of the Upper Van Norman Reservoir, for example, there were six different pipelines subjected to virtually

the same pattern of ground displacement. Both the construction of the lines and distribution of ground movements are well defined. A reliable record of pipeline performance has been developed in which the locations and specific characteristics of damage are described. Moreover, the record of response involves both failed pipelines and those which were able to sustain large differential movement. The information in this case history is sufficiently detailed to characterize the soil properties, deformation patterns, and pipeline characteristics such that analytical models can be tested against the observations, and the field data used as a basis for verifying or modifying analytical methods.

The pipelines which failed near the Upper Van Norman Reservoir either were constructed with welded slip joints or made of steel with relatively low yield stress. Compressive failures of slip joints in the Granada Trunk Line underscore the vulnerability of these joints to compressive ground strains and bending, which can induce pipe wall wrinkling on the compressive side of the longitudinally flexed pipe. The weakness of welded slip joints under compression also is illustrated by multiple failures in a 600-mm-diameter water main in the zone of surface faulting at the Sylmar segment of the San Fernando fault.

Steels with relatively low yield stress, particularly those manufactured over 20 to 30 years ago, may be characterized by a relatively flat slope when tensile stress is plotted with respect to strain in the post-yield range of axial deformation. O'Rourke, et al. (1988) have shown that the post-yield slope is critically important for the level of maximum strain in the steel when a buried pipeline is subjected to tensile ground movements. In contrast, the steeper post-yield slopes of high stress steels, such as the X-52 steel used for construction of the SCG and Mobil pipelines on the west side of the Upper Van Norman Reservoir, is able to accommodate ground movement with significantly lower levels of local strain.

Pipelines crossing the Mission Wells and Sylmar segments of the San Fernando fault experienced joint failures, which were influenced by defective welds. The records of pipeline response during other U.S. earthquakes (O'Rourke, et al., 1985) corroborate the performance observed in San Fernando. There is a

tendency for steel pipelines constructed before and during the early 1930's to respond poorly to both permanent and traveling ground wave movements. Apparently, pipelines of this vintage did not benefit from the same quality controls during construction which apply today. Pipelines of this age should be considered as potential bad actors and identified as being vulnerable to both transient and permanent ground deformation.

REFERENCES

Association for Development of Earthquake Prediction (ADEP), "Measurement of Permanent Ground Displacements Caused by 1971 San Fernando Earthquake," Research Committee Report No. II-1, Committee on Ground Failures and Damage to Lifeline Facilities, Tokyo, Japan, Aug. 1990.

American Society for Testing and Materials, "Soil and Rock: Building Stones; Geotextiles," Annual Book of ASTM Standards, Vol. 4.08, Section 4, ASTM, Philadelphia, PA, 1989.

Barrows, A. G., J. E. Kayle, R. B. Saul, and F. H. Weber, "Geologic Map of the Fernando Earthquake Area," San Fernando, California Earthquake of 9 February, 1971, Bulletin 196, California Division of Mines and Geology, Sacramento, CA, 1975, Plate 1.

Barrows, A. G., J. E. Kayle, F. H. Weber, and R. B. Saul, "Map of Surface Breaks Resulting From the San Fernando, California, Earthquake of February 9, 1971," San Fernando, California Earthquake of February 9, 1971, Vol. 3, U.S. Department of Commerce, National Oceanographic and Atmospheric Administration, Washington, D.C., 1973, pp. 127-135.

Bennett, M. J., "Liquefaction Analysis of the 1971 Ground Failure at the San Fernando Valley Juvenile Hall, California," Bulletin of the Association of Engineering Geologists, Vol. XXVI, No. 23, 1989, pp. 209-226.

Bolt, B. A. and B. S. Gopalakrishnan, "Magnitude, Aftershocks and Fault Dynamics," San Fernando, California Earthquake of 9 February, 1971, Bulletin 196, California Division of Mines and Geology, Sacramento, CA, 1975, pp. 263-272.

Brown G. A., "Ground Water Geology of the San Fernando Valley," San Fernando, California Earthquake of 9 February, 1971, Bulletin 196, California Division of Mines and Geology, Sacramento, CA, 1975, pp. 31-52

California Division of Highways, "Highway Damage in the San Fernando Earthquake," San Fernando, California Earthquake of 9 February, 1971, Bulletin 196, California Division of Mines and Geology, Sacramento, CA, 1975, pp. 369-380.

Cloud, W. K. and D. E. Hudson, "Strong Motion Data from the San Fernando, California Earthquake of 9 February, 1971," San Fernando, California Earthquake of 9 February, 1971, Bulletin 196, California Division of Mines and Geology, Sacramento, CA, 1975, pp. 273-302.

Coffman, K. L., C. A. Von Hake, and C. W. Stover, Earthquake History of the United States, Publication 541-1, U.S. National Oceanic and Atmospheric Administration, U.S. Geological Survey, Boulder, CO, 1982.

Committee on Safety Criteria for Dams, Safety of Dams: Flood and Earthquake Criteria, National Academy Press, Washington, D.C., 1985.

Converse, Davis, and Associates, "Interim Report: Soil and Geologic Investigation, San Fernando Earthquake, Joseph Jensen Filtration Plant Near Sylmar, California," Unpublished Report Prepared for the Metropolitan Water District of Southern California, Pasadena, CA, April 30, 1971.

Converse Foundation Engineers, "Foundation Investigation, Proposed Sylmar Converter Station, City of Los Angeles," Unpublished Report Prepared for Bechtel Corporation, Pasadena, CA, Oct. 1966.

Cortwright, C., "Effects of the San Fernando Earthquake on the Van Norman Reservoir Complex," San Fernando, California Earthquake of 9 February, 1971, Bulletin 196, California Division of Mines and Geology, Sacramento, CA, 1975, pp. 395-406.

Dixon, S. J and J. W. Burke, "Liquefaction Case History," Journal of the Soil Mechanics and Foundations Division, ASCE, Vol. 99, No. SM11, Nov. 1973, pp. 921-938.

Eguchi, R. T., "Earthquake Performance of Water Supply Components During the 1971 San Fernando Earthquake," Technical Report 82-1396-2a, J. H. Wiggins Company, Redondo Beach, CA, Mar. 1982.

Eguchi, R. T., L. L. Philipson, M. R. Legg, J. H. Wiggins, and J. E. Slosson, "Earthquake Vulnerabilty of Water Supply Systems," The Current State of Knowledge of Lifeline Earthquake Engineering, ASCE, New York, NY, 1981, pp. 277-292.

Fallgren, R. B. and J. L. Smith, "Geologic and Soils Investigation, Sylmar Converter Station, Sylmar, California," Project 71-066-EG, Unpublished Report Prepared for Department of Water and Power, City of Los Angeles, Fugro, Inc., Long Beach, CA, Oct. 1971a.

Fallgren, R. B. and J. L. Smith, "Geologic and Soils Investigation, San Fernando Valley Juvenile Hall, Sylmar, California," Project 71-082-EG, Unpublished Report Prepared for County of Los Angeles, Fugro, Inc., Long Beach, CA, Sept. 1971b.

Fallgren, R. B. and J. L. Smith, "Ground Displacement at San Fernando Valley Juvenile Hall During San Fernando Earthquake," San Fernando, California Earthquake of February 9, 1971, Vol. 3, U.S. Department of Commerce, N.O.A.A., Washington, D.C., 1973, pp. 189-196.

Fallgren, R. B. and J. L. Smith, "Ground Displacement at the San Fernado Valley Juvenile Hall and the Sylmar Converter Station," San Fernando, California Earthquake of 9 February, 1971, Bulletin 196, California Division of Mines and Geology, Sacramento, CA, 1975, pp. 157-164.

Fugro, Inc., "Fault Investigation: San Fernando Valley Juvenile Hall, Sylmar California," Unpublished Report Prepared for County of Los Angeles, Long Beach, CA, Jan. 1975.

GEI Consultants, Inc., "Re-Evaluation of the Lower San Fernando Dam," Project 85669, Report Submitted to U.S. Army Corps of Engineers, Vols. I and II, Winchester, MA, Feb. 1988.

Johns, J. F., "Historical Documentation of the Jensen Plant Earthquake Disaster of February 9, 1971," Unpublished Report Prepared for the Metropolitan Water District of Southern California, Los Angeles, CA, Apr. 1973.

LePire, J. L., Personal Communication, Southern California Gas Company, San Fernando District, 1982.

Lew, H. S., E. V. Leyendecker, and R. D. Dikkers, "Engineering Aspects of the 1971 San Fernando Earthquake," Building Science Series 40, U.S. Department of Commerce, Washington, D.C., Dec. 1971.

Lind, R. J., "What Earthquake Did to 34-in. Line," Gas Age, Vol. 114, No. 3, July 1954, pp. 29-50.

Marachi, D. N., "Dynamic Soil Problems at the Joseph Jensen Filtration Plant," San Fernando, California Earthquake of February 9, 1971, Vol. 1, Part A, U.S. Department of Commerce, N.O.A.A., Washington, D.C., 1973, pp. 815-820.

McCaffrey, M. A. and O'Rourke, T.D., "Buried Pipeline Response to Reverse Faulting During the 1971 San Fernando Earthquake," Earthquake Behavior and Safety of Oil and Gas Storage Facilities, Buried Pipelines, and Equipment, PVP-Vol. 77, ASME, New York, NY, 1983, pp. 151-159.

Metropolitan Water District of Southern California, "Report of Structural Damage to Joseph Jensen Filtration Plant, Earthquake of February 9, 1971," Los Angeles, CA, Mar. 1971.

Metropolitan Water District of Southern California, "Geology, Earthquake Damage, and Water Table Fluctuations - Metropolitan Water District Facilities, Sylmar Area," San Fernando, California Earthquake of 9 February, 1971, Vol. 3, U.S. Department of Commerce, N.O.A.A., Washington, D.C., 1973, pp. 213-222.

Morton, D. M., "Seismically Triggered Landslides in the Area Above the San Fernando Valley," San Fernando, California Earthquake of 9 February, 1971, Bulletin 196, California Division of Mines and Geology, Sacramento, CA, 1975, pp. 145-154.

Morton, D. M. and A. K. Baird, "Tectonic Setting of the San Gabriel Mountains," San Fernando, California Earthquake of 9 February, 1971, Bulletin 196, California Division of Mines and Geology, Sacramento, CA, 1975, pp. 3-6.

Nason, R. D., "Shattered Earth at Wallaby Street, Sylmar," The San Fernando, California Earthquake of February 9, 1971, U.S. Geological Survey, Professional Paper 733, U.S. Department of the Interior and U.S. Department of Commerce, Washington, D.C., 1971, pp. 97-98.

Newby, A. B., "Pipelines Ride the Shock Waves," Proceedings, Pacific Coast Gas Association, Vol. 45, San Francisco, CA, 1954, pp. 105-109.

Oakeshott, G. B., "Geology of the Epicentral Area," San Fernando, California Earthquake of 9 February, 1971, Bulletin 196, California Division of Mines and Geology, Sacramento, CA, 1975, pp. 19-30.

Oliver, H. W., S. L. Robbins, R. B. Grannell, R. W. Alewine, and S. Biehler, "Surface and Subsurface Movements Determined by Remeasuring Gravity," San Fernando, California Earthquake of 9 February, 1971, Bulletin 196, California Division of Mines and Geology, Sacramento, CA, 1975, pp. 195-211.

O'Rourke, T. D., M. D. Grigoriu, and M. M. Khater, "Seismic Response of Buried Pipelines," Pressure Vessel and Piping Technology - A Decade of Progress, C. Sundararjan, Ed., ASME, New York, NY, 1985, pp. 281-323.

O'Rourke, T. D. and P. A. Lane, "Liquefaction Hazards and Their Effects on Buried Pipelines," Technical Report NCEER-89-0007, National Center for Earthquake Engineering Research, Buffalo, NY, Feb. 1989.

O'Rourke, T. D. and M. A. McCaffrey, "Buried Pipeline Response to Permanent Earthquake Ground Movements," Proceedings, 8th World Conference on Earthquake Engineering, Vol. VII, San Francisco, CA, 1984, pp. 215-222.

O'Rourke, T. D., W. D. Meyersohn, M. D. Grigoriu, and M. M. Khater, "Ground Failure Effects on Pipeline System Performance," Proceedings, 9th World Conference on Earthquake Engineering, Vol. VII, Tokyo, Japan, 1988, pp. 79-84.

O'Rourke, T. D. and M. S. Tawfik, "Effects of Lateral Spreading on Buried Pipelines During the 1971 San Fernando Earthquake," Earthquake Behavior and Safety of Oil and Gas Storage Facilities, Buried Pipelines, and Equipment, PVP-Vol. 77, ASME, New York, NY, 1983, pp. 124-132.

O'Rourke, T. D. and C. H. Trautmann, "Analytical Modeling of Buried Pipeline Response to Permanent Earthquake Displacements," Geotechnical Engineering Report 80-4, School of Civil and Environmental Engineering, Cornell University, Ithaca, NY, 1980.

Prysock, T. H. and J. P. Egan, "Roadway Damage During the San Fernando, California Earthquake of February 9, 1971," Report FHWA/CA/T1-80/17, California Department of Transportation, Sacramento, CA, 1981.

Rogers, D. A., "Vertical Deformation, Stress Accumulation, and Secondary Faulting in the Vicinity of the Transverse Ranges of Southern California," California Division of Mines and Geology, Bulletin 203, Sacramento, CA, 1979.

Schoustra, J. and J. K. Yann, "Performance of Foundations at the Sylmar Converter Station," San Fernando, California Earthquake of February 9, 1971, Vol. I, Part B, U.S. Dept of Commerce, N.O.A.A., Washington, D.C., 1973, pp. 821-824.

Scott, J. D., "A Brief Description of the Geologic and Soils Investigation: San Fernando Juvenile Hall, Sylmar, California," Presented for Technical Trip No. 6 - San Fernando Earthquake Zone, National Meeting of the Association of Engineering Geologists, Fugro, Inc., Long Beach, CA, Oct. 23, 1973.

Scott, N. H., "Felt Area and Intensity of the San Fernando Earthquake," San Fernando, California Earthquake of February 9, 1971, Vol. 3, U.S. Department of Commerce, N.O.A.A., Washington, D.C., 1973, pp. 23-48.

Scott, R. F., "The Calculation of Horizontal Accelerations from Seismoscope Records," Bulletin of the Seismological Society of America, Vol. 63, No. 5, Oct. 1973, pp. 1637-1661.

Scott, R. F., "Proposed Jensen Plant Expansion," Unpublished Report Prepared for Metropolitan Water District of Southern California, Los Angeles, CA, Aug. 1987.

Seed, H. B. and P. De Alba, "Use of SPT and CPT Tests for Evaluating the Liquefaction Resistance of Sands," Use of In-Situ Tests in Geotechnical Engineering, ASCE Geotechnical Special Publication No. 6, June 1986, pp. 281-302.

Seed, H. B., I. M. Idriss, and I. Arango, "Evaluation of Liquefaction Potential Using Field Performance Data," Journal of Geotechnical Engineering, ASCE, Vol. 109, No. 3, Mar. 1983, pp. 458-482.

Seed, H. B., K. L. Lee, I. M. Idriss, and F. I. Makdisi, "The Slides in the San Fernando Dams During the Earthquake of February 9, 1971," Journal of the Geotechnical Engineering Division, ASCE, Vol. 101, No. GT7, July 1975, pp. 651-688.

Seed, H. B., K. L. Lee, I. M. Idriss, and F. I. Makdisi, "Analysis of the Slides in the San Fernando Dams During the Earthquake of February 9, 1971," Report EERC 73-2, University of California, Berkeley, CA, June 1973.

Seed, H. B., K. Tokimatsu, L. F. Harder, and R. M. Chung, "Influence of SPT Procedures in Soil Liquefaction Resistance Evaluation," Journal of Geotechnical Engineering, ASCE, Vol. 11, No. 12, Dec. 1985, pp. 1425-1445.

Sharp, R. V., "Displacement on Tectonic Rupture," San Fernando, California Earthquake of 9 February 1971, Bulletin 196, California Division of Mines and Geology, Sacramento, CA, 1975, pp. 157-164.

Smith, S. J., Jr., "Repair of Earthquake Damaged Underground Reservoir," Journal of the Construction Division, ASCE, Vol. 100, No. CO3, Sept. 1974, pp. 449-468.

Southern California Gas Company, "Earthquake Effects on Southern California Gas Company Facilities," San Fernando, California Earthquake of February 9, 1971, Vol. 2, U.S. Department of Commerce, N.O.A.A., Washington, D.C., 1973, pp. 59-66.

Southern California Edison Company, "Earthquake Damage to Southern California Edison Power Facilities," San Fernando, California Earthquake of February 9, 1971, Vol. 2, U.S. Department of Commerce, N.O.A.A., Washington, D.C., 1973, pp. 27-38.

Spellman, H. A., J. R. Stellar, R. J. Shlemon, N. R. Sheahan, and S. H. Mayeda, "Trenching and Soil Dating of Holocene Faulting for a Water Filtration Plant Site, Sylmar, California," Bulletin of the Association of Engineering Geologists, Vol. XXI, No. 1, Feb. 1984, pp. 89-100.

Steinbrugge, K. V., E. E. Schader, H. C. Bigglestone, and C. A. Weers, San Fernando Earthquake, February 9, 1971, Pacific Fire Rating Bureau, 1971.

Subcommittee on Water and Sewerage Systems, "Earthquake Damage to Water and Sewerage Facilities," San Fernando, California Earthquake of February 9, 1971, Vol. 2, U.S. Department of Commerce, N.O.A.A., Washington, D.C., 1973, pp. 75-193.

Tawfik, M. S. and T. D. O'Rourke, "Analysis of Pipelines Under Large Soil Deformations," Cornell Geotechnical Engineering Report 86-1, School of Civil and Environmental Engineering, Cornell University, Ithaca, NY, Mar. 1986.

Thompson, J. E., "San Fernando Valley Juvenile Hall," San Fernando, California Earthquake of February 9, 1971, Vol. 1, Part A, U.S. Department of Commerce, N.O.A.A., Washington, D.C., 1973, pp. 147-162.

U.S. Geological Survey Staff, "Surface Faulting in the San Fernando, California Earthquake of February 9, 1971," The San Fernando, California Earthquake of February 9, 1971, U.S. Geological Survey Professional Paper 733, U.S. Department of the Interior and U.S. Department of Commerce, Washington, D.C., 1971, pp. 55-76.

Weber, F. H., Jr., "Surface Effects and Related Geology of the San Fernando Earthquake in the Sylmar Area," San Fernando, California Earthquake of 9 February, 1971, Bulletin 196, California Division of Mines and Geology, Sacramento, CA, 1975, pp. 71-98.

Wentworth, C.M. and R. F. Yerkes, "Geologic Setting and Activity of Faults in the San Fernando Area of California," The San Fernando, California Earthquake of February 9, 1971, U.S. Geological Survey Professional Paper 733, U.S. Department of the Interior and U.S. Department of Commerce, Washington, D.C., 1971, pp. 6-16.

Wolf, P. R., Elements of Photogrammetry With Air Photo Interpretation and Remote Sensing, 2nd Ed., McGraw-Hill, 1983, pp. 559-602.

Wong, P. J., "Earthquake Effects on Power System Facilities of the City of Los Angeles," San Fernando, California Earthquake of February 9, 1971, Vol. 2, U.S. Department of Commerce, N.O.A.A., Washington, D.C., 1973, pp. 9-25.

Wood, H. O. and F. Neumann, "Modified Mercalli Intensity Scale of 1931," Bulletin of the Seismological Society of America, Vol. 21, No. 4, Dec. 1931, pp. 277-283.

Woodward-Clyde Consultants, "Draft Geotechnical Investigation, Joseph Jensen Filtration Plant, Granada Hills, California," Unpublished Report Prepared for the Metropolitain Water District of Southern California, Vols. 1 - 5, Santa Ana, CA, Oct. 1988.

Woodward-Lundgren and Associates, "Evaluation of the Effects of the February 9, 1971 San Fernando Earthquake on the Balboa Water Treatment Plant," Unpublished Report Prepared for Gibson, Dunn, and Crutcher, Oakland, CA, Dec. 1971.

Wyllie, L. A., F. E. McClure, and H. K. Degenkolb, "Performance of Underground Structures at the Joseph Jensen Filtration Plant," Proceedings, 5th World Conference on Earthquake Engineering, Vol. 1, Rome, Italy, June 1973, pp. 66-75.

Yerkes, R. F., M. G. Bonilla, T. L. Youd, and J. D. Sims, "Geologic Environment of the Van Norman Reservoirs Area," The Van Norman Reservoirs Area, Northern San Fernando Valley, California, Geologic Survey Circular 691-A,B, Washington, D.C., 1974.

Youd, T. L., "Landsliding in the Vicinity of the Van Norman Lakes," The San Fernando, California Earthquake of February 9, 1971, U.S. Geological Survey Professional Paper 733, U.S. Department of the Interior and U.S. Department of Commerce, Washington, D.C., 1971, pp. 105-109.

Youd, T. L., "Ground Movements in Van Norman Lake Vicinity During San Fernando Earthquake," San Fernando, California Earthquake of February 9, 1971, Vol. 3, U.S. Department of Commerce, N.O.A.A., Washington, D.C., 1973, pp. 197-206.

Youd, T. L., "Ground Failure Damage to Buildings During Earthquakes," Foundation Engineering: Current Principles and Practices, Vol. 1, ASCE, New York, NY, 1989, pp. 758-770.

Youd, T. L. and D.M. Perkins, "Mapping Liquefaction-Induced Ground Failure Potential," Journal of the Geotechnical Engineeering Division, ASCE, Vol. 104, No. GT4, Mar. 1978, pp. 433-446.

APPENDIX A

LIST OF GEOTECHNICAL INVESTIGATIONS

Appendix A contains a list of the unpublished geotechnical engineering investigations which were performed at various sites in the Upper Van Norman Reservoir area. The majority of these reports were commissioned by the Metropolitan Water District of Southern California (MWD) for the Joseph Jensen Filtration Plant or by the County of Los Angeles for the San Fernando Valley Juvenile Hall. The list of reports contains the date, the name of the agency, the title of the report, and a brief overview of the field and laboratory tests performed. Many of the soil boring locations are shown in Figures 11 and 24.

A.1 JOSEPH JENSEN FILTRATION PLANT

Report	In-Situ and Laboratory Data
Donald R. Warren Co., "Foundation Investigation," Project No. F63-12617, for McIntire and Aviros, Inc., Jan. 1964, supplements prepared Feb., May, and Aug. 1964	**FIELD:** 37 borings 1.8 to 67 m deep, nonstandard penetration test, groundwater elevation, visual soil classification **LABORATORY:** moisture content, unit weight, direct shear strength, triaxial shear, consolidation-pressure, time-consolidation
Stone Geological Service, Inc., "Major Cuts, Balboa Blvd. Realinement," Project No. 63-166, for Metropolitan Water District (MWD), Dec. 1963, supplements prepared June, Sept. 1965	**FIELD:** 8 borings, geologic reconnaissance
Stone Geological Services, Inc. "Proposed Phase II Cut Slopes," Project No. 66-161, for MWD, Sept. 1966	**FIELD:** geologic reconaissance
Converse Foundation Engineers, "Subsurface Investigation," Project No. 64-677-A, for MWD, Jan. 1965, supplements prepared Feb., July 1965	**FIELD:** 16 borings 6 to 9 m deep, 17 test pits, nonstandard penetration tests, groundwater elevation, visual soil classification. **LABORATORY:** unit weight, moisture content, consolidation, Atterberg limits, X-ray diffraction, differential thermal analyses, direct shear,

Report	In-Situ and Laboratory Data
	swell
Converse, Davis, and Associates, "Foundation Investigation for Proposed Railroad Bridge," Project No. 64-677-A for MWD, June 1966, supplement prepared June 1967	**FIELD:** 7 borings, 10 to 15 m deep, nonstandard penetration tests, groundwater elevation, visual soil classification **LABORATORY:** unit weight, moisture content, direct shear tests, consolidation tests
Converse, Davis, and Associates, "Foundation Investigation, Proposed Balboa Water Treatment Plant," Project No. 66-343-A for MWD, Dec. 1966	**FIELD:** 35 borings 8 to 45 m deep, nonstandard penetration tests, groundwater elevation, visual soil classification **LABORATORY:** unit weight, moisture content, direct shear tests, undrained triaxial tests, Atterberg limits, grain size analyses, consolidation tests
Converse Foundation Engineers, "Subsoil Investigation, Proposed Effluent Conduit from Balboa Treatment Plant to North Portal Balboa Outlet Tunnel," Project No. 67-444-A for MWD, Nov. 1967	**FIELD:** 4 borings 12 to 17 m deep, groundwater elevation, visual soil classification **LABORATORY:** unit weight, moisture content, direct shear, grain size analysis
Converse, Davis, and Associates, "Soil and Geologic Investigation, San Fernando Earthquake," Project No. 71-074-E for MWD, Apr. 1971	**FIELD:** 20 rotary wash borings and 16 bucket auger borings 9 to 37 m deep, standard penetration tests and nonstandard penetration tests, groundwater elevation, visual soil classification, 2021 m of seismic refraction survey, 10 slope indicators installed, 7 test pits at main control building, field density tests, recordings of accelerations during aftershocks, geologic mapping, site inspection **LABORATORY:** unit weight, moisture content, direct shear, peak strength, residual strength, grain size analysis, static triaxial tests, cyclic triaxial tests
Converse, Davis, and Associates, "Results of Dynamic Soil Tests," Project No. 71-074-E for MWD, July 1971	**LABORATORY:** cyclic triaxial tests

Report	In-Situ and Laboratory Data
Woodward, Lundgren, and Associates, "Evaluation of the Effects of the February 9, 1971 San Fernando Earthquake on the Balboa Water Treatment Plant," Project No. G-12345 for Gibson, Dunn, and Crutcher, Dec. 1971	**FIELD:** 14 borings 16 to 31 m deep, standard penetration tests, nonstandard penetration tests, groundwater elevation, visual soil classification, site inspection **LABORATORY:** unit weight, moisture content, grain size analyses, Atterberg limits
Woodward-Clyde Consultants, "Draft Geotechnical Investigation," Project No. 8840172A for MWD, Nov. 1988	**FIELD:** 20 borings 6 to 28 m deep, 62 cone penetration test soundings (7 with piezocone), 9 piezometers installed, cross-hole and down-hole shear and compressional wave velocity measurements, groundwater elevation, visual soil classification **LABORATORY:** unit weight, moisture content, grain size analyses, Atterberg limits, static undrained direct simple shear tests, triaxial tests

A.2 JUVENILE HALL LANDSLIDE

LeRoy Crandall and Associates, "Foundation Investigation for the Proposed San Fernando Valley Juvenile Hall," for County of Los Angeles, Aug. 1961	**FIELD:** 16 borings 2 to 10 m deep, groundwater elevation, visual soil classification **LABORATORY:** unit weight, moisture content
Converse Foundation Engineers, "Foundation Investigation, Proposed Sylmar Converter Station," Project No. 66-459-A for Bechtel Corporation, Oct. 1966	**FIELD:** 21 borings 3 to 9 m deep, groundwater elevation, visual soil classification **LABORATORY:** unit weight, moisture content, direct shear tests, consolidation tests
Fugro, Inc., "Geologic and Soil Investigation, San Fernando Valley Juvenile Hall," Project No. 71-082-EG for County of Los Angeles, Sept. 1971	**FIELD:** 17 borings 9 to 24 m deep, 5 trenches 3 to 5 m deep, 3 seismic refraction surveys 494 m long, groundwater elevation, visual soil classification, geologic mapping **LABORATORY:** unit weight, moisture content, grain size analyses

Report	In-Situ and Laboratory Data
Fugro, Inc., "Geotechnical Investigation for Stabilization and Reconstruction at the San Fernando Valley Juvenile Hall Site," Project No. 71-082-EG for County of Los Angeles, Jan. 1975	**FIELD:** 16 borings 6 to 22 m deep, 5 CPT tests, 3 piezometers installed, nonstandard penetration tests, groundwater elevation, visual soil classification **LABORATORY:** unit weight, moisture content, direct shear tests, permeability tests, compaction tests, grain size analyses, cyclic triaxial tests
Fugro, Inc., "Fault Investigation, San Fernando Valley Juvenile Hall," Project No. 71-082-EG for County of Los Angeles, Jan. 1975	**FIELD:** 2 trenches 244 m long by 12 m deep, and 198 m long by 6 m deep

A.3 MISCELLANEOUS REPORTS

Fugro, Inc., "Geologic Investigations of Earthquake Damage, Van Gough Street School," Project No. 71-061-EG for Los Angeles City Unified School District, Mar. 1971	**FIELD:** trench 20 m long by 4 m deep
Converse Consultants, "Final Report, Foundation, Investigation Proposed Los Angeles Aqueduct Water Filtration Plant at the Yarnell Site," Project No. 80-1257-02 for BC-CDM, a joint venture, Aug. 1982	**FIELD:** 6 borings 5 to 15 m deep, 3 groundwater observation wells, standard penetration tests, groundwater elevation, visual soil classification **LABORATORY:** unit weight, moisture content, direct shear tests, consolidation tests, permeability tests, grain size analyses, compaction test, corrosion test
Converse Consultants, "Final Report, Geotechnical Investigation, Proposed LAAWFP Backwash Water Reclamation Ponds, Yarnell Site," Project No. 80-1257-04 for BC-CDM, a joint venture, Sept. 1982	**FIELD:** 8 borings 3 to 17 m deep, 9 trenches, 17 piezometers installed **LABORATORY:** unit weight, moisture content, direct shear tests, consolidation tests, grain size analyses, compaction test, permeability tests

APPENDIX B

PHOTOGRAMMETRIC ANALYSIS

B.1 METHOD OF MEASUREMENT

Figure B.1 outlines the mapped area where permanent ground displacements were measured photogrammetrically. Pre- and post-earthquake vertical aerial photographs, which were used to prepare the maps, were obtained from the University of California at Santa Barbara. Pre-earthquake photographs were taken on March 19, 1968 at a scale of 1:24000, and post-earthquake photographs were taken on February 10, 1971 at a scale of 1:10000. The flight lines and the approximate centers of the aerial photographs are shown in Figure B.1.

Figure B.1 also shows vertical and horizontal ground control points as squares and triangles, respectively. The control points were used to orient the photographs within the California Zone 7 State Plane coordinate system. The coordinates of the control points were provided by the Los Angeles Bureau of Engineering (LABE). The half-shaded triangles represent control points, such as aerial crosses, which were plainly visible in the aerial photographs. The open squares and triangles represent control points which were located by means of written descriptions and sketches provided by the LABE. The number of control points used for this project was 36 and 44 for pre- and post-earthquake analysis, respectively.

Magnitudes of permanent displacement were determined for objects which were fixed on the ground and visible in both before and after photographs. Manhole covers and the bases of utility poles were selected preferentially for these measurements, although the roofs of undamaged buildings were used in areas where such features could not be found. Nearly 300 measurement points were used in the photogrammetric analysis.

Figure B.2 illustrates the technique for measuring horizontal ground displacements photogrammetrically. The figure shows selected features from the maps compiled by the Japanese research team (ADEP, 1990). Knowing the coordinates

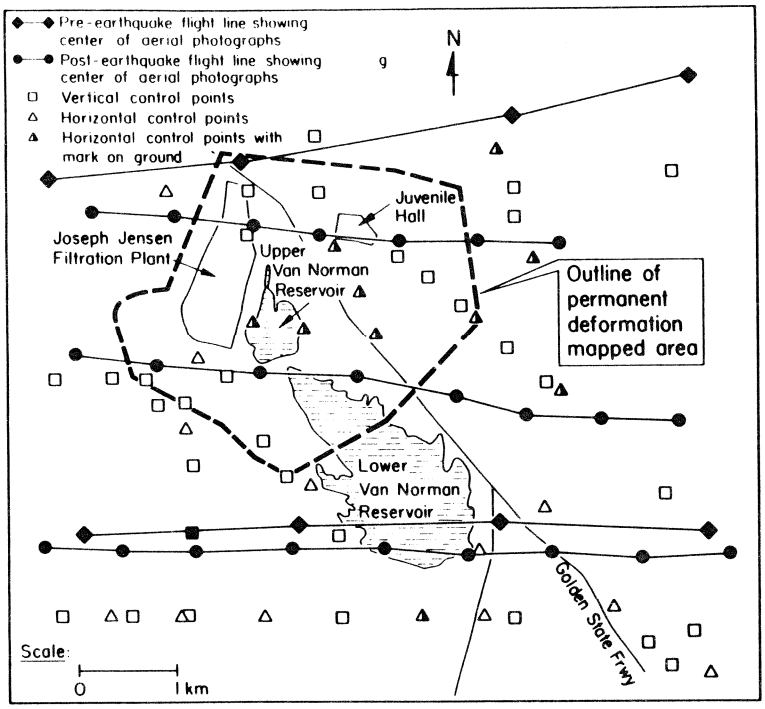

Figure B.1. Map Showing Outline of Mapped Area, Flight Lines, and Control Points Near the Van Norman Reservoir

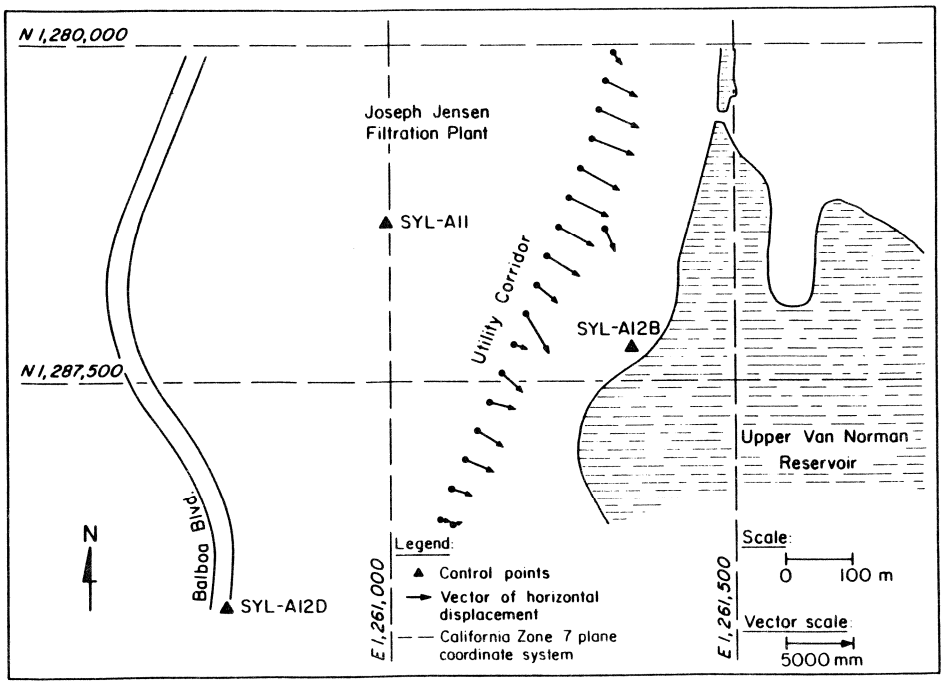

Figure B.2. Map of West Side of Upper Van Norman Reservoir Illustrating the Photogrammetric Technique

of the three control points, shown as filled triangles in the figure, the California Zone 7 coordinate system was oriented and positioned in the pre-earthquake photographs (see Accuracy of Measurements section of this appendix). Then, the coordinates of selected objects, in this case the bases of utility poles along the utility corridor, were determined relative to the coordinate system. The same procedure was repeated using the post-earthquake photographs. The before and after coordinates of the objects then were compared analytically and vectors of displacement were calculated. Examples of the displacement vectors of objects northeast and west of the Upper Van Norman Reservoir are seen in Figures 23 and 10.

B.2 ACCURACY OF MEASUREMENTS

The accuracy of the ground displacement measurements was determined by a 5-step procedure:

Step 1: Ground control points, horizontal control stations, and precise elevation benchmarks were located in the pre-earthquake photographs. Arbitrary coordinates were assigned to the ground control points based upon their relative positions in the photographs.

Step 2: The arbitrary coordinates of the control points were compared with the California Zone 7 coordinates of the control points. The California Zone 7 coordinates were provided by the LABE and were determined by triangulation or traverse. The orientation of the photographs was transformed so that the arbitrary coordinates most closely matched the California Zone 7 coordinates of the control points. This iterative transformation utilized a least squares solution, which minimized the difference between the arbitrary coordinates and the California Zone 7 coordinates of the control points. The equation for the least squares solution is:

$$\sum_{i=1}^{m} (\nu)^2 = \nu_1^2 + \nu_2^2 + \ldots \nu_m^2 = \text{minimum} \qquad \text{(B-1)}$$

in which ν is the difference between the coordinates of the control points

in the California Zone 7 coordinate system and the arbitrary coordinates of the control points.

Step 3: After the least squares solution was applied, the transformed arbitrary coordinates were not the same as the California Zone 7 coordinates of the control points. Accordingly, there was a residual error representing the difference, or lack of compliance, between the two. The accuracy of the pre-earthquake aerial survey is defined as the standard deviation, S, of the differences between the transformed coordinates and the California Zone 7 coordinates:

$$S = \frac{\Sigma \nu^2}{r} \qquad \text{(B-2)}$$

in which r is the number of degrees of freedom and ν is the residual error.

Step 4: Steps 1 through 3 were repeated for the post-earthquake aerial photographs.

Step 5: The accuracy of the permanent ground displacement measurements is defined as the square root of the sum of the squares of the accuracies determined for the pre- and post-earthquake aerial surveys. A more detailed discussion of Random Errors, Least Squares Adjustment, and Coordinate Transformations may be found in Wolf (1983).

Table B.1 presents a summary of the accuracies of the permanent ground displacements. The accuracy of the horizontal displacements was calculated to be $\pm$ 0.47 m, and of the vertical displacements to be $\pm$ 0.42 m.

B.3 TECTONIC MOVEMENTS AND THEIR EFFECTS ON GROUND DISPLACEMENT MEASUREMENTS

Ground displacements represented by vectors and magnitudes of settlement or heave in Figures B.2, 10, and 23 were caused mainly from liquefaction, soil slumping, and landsliding. To a lesser degree, however, the vectors include a displacement component resulting from regional tectonic movements.

Table B.1. Accuracy of Permanent Ground Displacement Measurements

Aerial Survey	Pre-earthquake	Post-earthquake
Number of Control Points	36	44
Accuracy of Aerial Survey	± 0.43m (Hori.) ± 0.35m (Vert.)	± 0.19m(Hori.) ± 0.23m(Vert.)
Accuracy of Measurement of Permanent Ground Displacement	$\sqrt{(0.43)^2+(0.19)^2}=\pm 0.47$m(Hori.) $\sqrt{(0.35)^2+(0.23)^2}=\pm 0.42$m(Vert.)	

In Figure B.3, vectors demonstrate the magnitude and direction of horizontal tectonic movements at selected control points in the Van Norman Reservoirs region. The movement of the control points were calculated by comparing the pre-earthquake coordinates with the post-earthquake coordinates. The pre-earthquake coordinates were surveyed between 1940 and 1970, and the post-earthquake coordinates were surveyed in 1971. The movements are in relation to stations held fixed, which are located 22 km and 30 km from the Van Norman Reservoirs, in the eastern Santa Monica Mountains and Verdugo Mountains, respectively. The measurement of the control point movements is accurate to ± 0.06 m (Yerkes, et al., 1974).

The average magnitude and direction of the control point displacements indicate that the Upper Van Norman Reservoir region experienced westward-trending tectonic movements of about 0.5 m during the earthquake. The exact magnitude of horizontal tectonic movements attributable to the earthquake is unknown, because pre-earthquake creep may have occurred.

The magnitude of tectonic uplift that occurred between the pre- and post-earthquake leveling surveys is represented in Figure B.3 by contours of equal elevation change. The pre-earthquake leveling surveys were conducted between 1968 and 1970, and the post-earthquake leveling surveys were conducted in 1971. The magnitude of tectonic uplift was determined to be about 0.4 m and

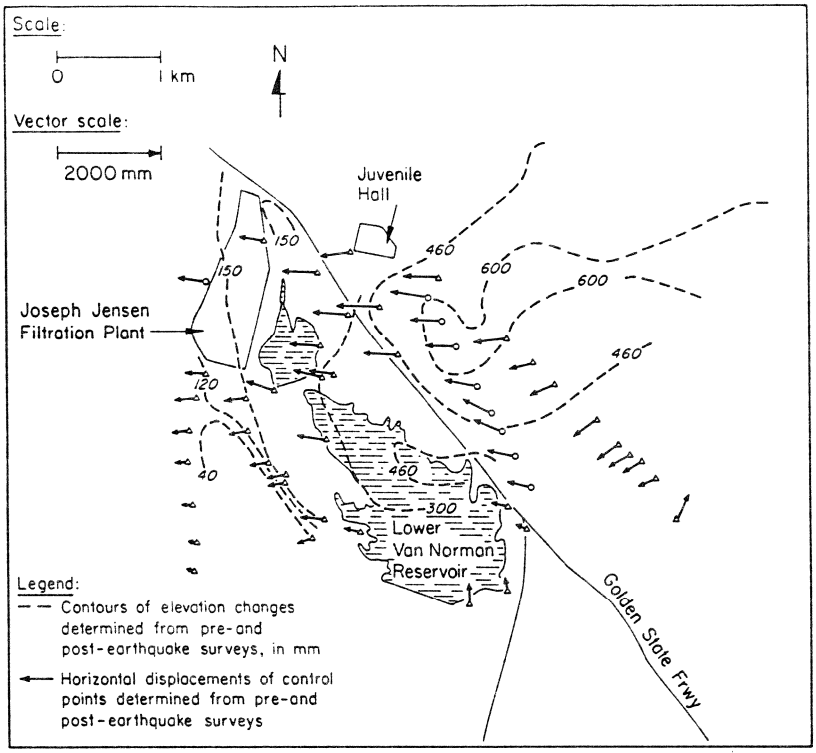

Figure B.3. Regional Tectonic Movements Represented by Horizontal Displacements of Control Points and Contours of Elevation Change

0.15 m on the east and west sides of the Upper Van Norman Reservoir, respectively. The accuracy of the vertical elevation changes was reported to be within 0.015 m (Yerkes, et al., 1974).

The tectonic movements detected in the Upper Van Norman Reservoirs region, as shown in Figure B.3, are consistent with plate tectonics theory of the Transverse Ranges structural province. The theory states that the Upper Van Norman Reservoir region is over a thrust block which has moved westward and has been uplifted several times during the Paleozoic Era. The driving force for these tectonic movements is the great bend in the San Andreas Fault (Figure 1). The bend in the San Andreas Fault causes compressional forces which are relieved by reverse-slip and left-lateral strike slip fault movements along the Sierra Madre Fault Zone. Further discussion regarding the tectonic setting of Southern California may be found in Wentworth and Yerkes (1974), Rogers (1979), and others.

B.4 CONFIRMATION OF ACCURACY OF VECTORS OF DISPLACEMENT

Two methods were employed to verify the accuracy of the vectors of displacement determined by the air photo analysis. The first method compared the vectors of displacement measured by the photogrammetric technique to displacements which were measured by ground level surveys. Ground level surveys were performed along San Fernando Road and along the crest of the Upper Van Norman Reservoir Dam shortly after the earthquake. The second method investigated vectors of displacement at a stable bedrock site located west of the Upper Van Norman Reservoir Dam.

Along San Fernando Road, south of the Juvenile Hall, the displacement of objects was measured by photogrammetric techniques and by the LABE. The LABE measurements were perpendicular offsets from the pre-earthquake straight curbline to points on the post-earthquake position of the curbline (Youd, 1973). Photogrammetric measurements were the pre- and post-earthquake positions of the bases of utility poles on the south side of San Fernando Road. The results from both measurement techniques are presented in Figure B.4. Solid-headed vectors in the figure represent the displacement measurements from LABE, and open-headed vectors represent measurements from the photogrammetric technique.

Favorable agreement was observed between the magnitudes of displacement measured by the photogrammetric technique and by the LABE. A comparison between the two data sets is presented in Table B.2. The first column of Table B.2 presents the horizontal displacement of the utility poles measured by the photogrammetric technique. The second column presents the values from column one, adjusted for regional tectonic movement and expressed as an offset perpendicular to San Fernando Road. Figure B.5 demonstrates the geometric method that was used to calculate the values entered in column two. The adjustment shown in Figure B.5 was intended to duplicate the method by which the offset measurements were performed by the LABE along the curbline of San Fernando Road. The magnitude and direction of regional tectonic movement was 0.69 m west, i.e., the average of the control point movements (see Figure B.3) on the northeast side of the Upper Van Norman Reservoir.

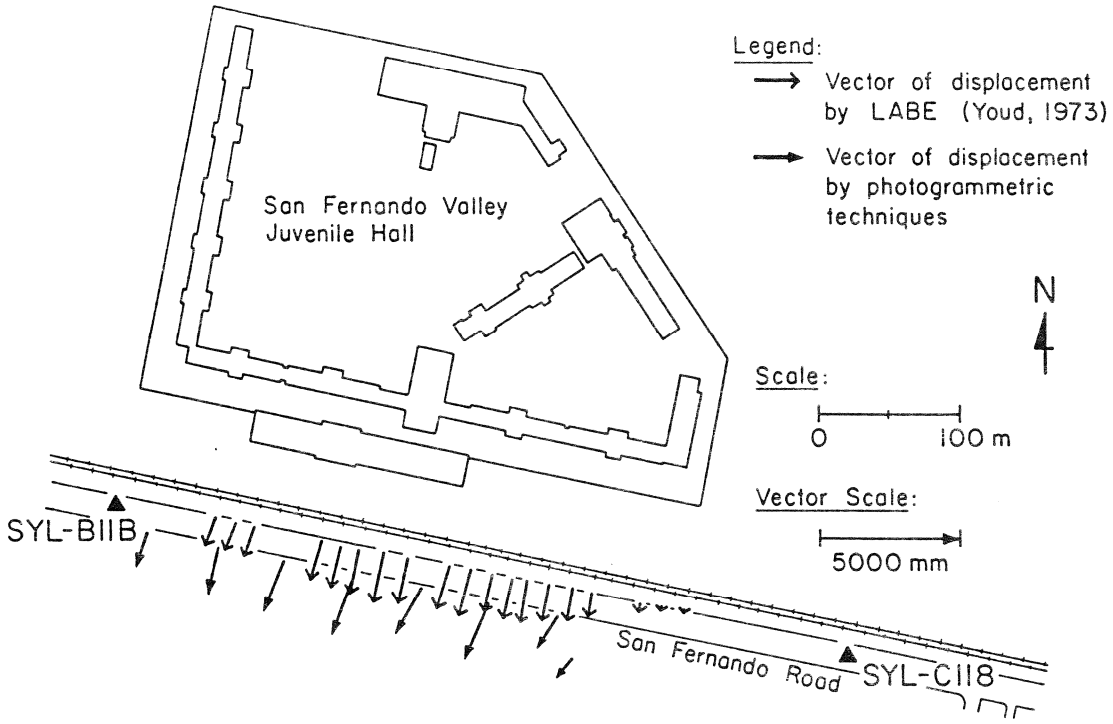

Figure B.4. Vectors of Displacement Along San Fernando Road Determined by Two Measurement Techniques

Table B.2. Comparison of Vectors of Displacement Determined by Two Methods Along San Fernando Road

(1) Photogrammetric Vector Length (m)	(2) Adjusted Photogrammetric Vector Length* (m)	(3) Average LABE Vector Length** (m)	(4) Difference (ABS) (3) - (2) (m)
1.38	1.22	1.20	0.02
1.72	1.59	1.20	0.39
2.03	1.86	1.52	0.34
2.28	2.10	1.71	0.39
1.81	1.57	1.73	0.16
2.15	1.96	1.65	0.31
1.28	1.04	1.33	0.29
0.87	0.63	0.96	0.33

*See Figure B.5
**Average of three LABE vectors

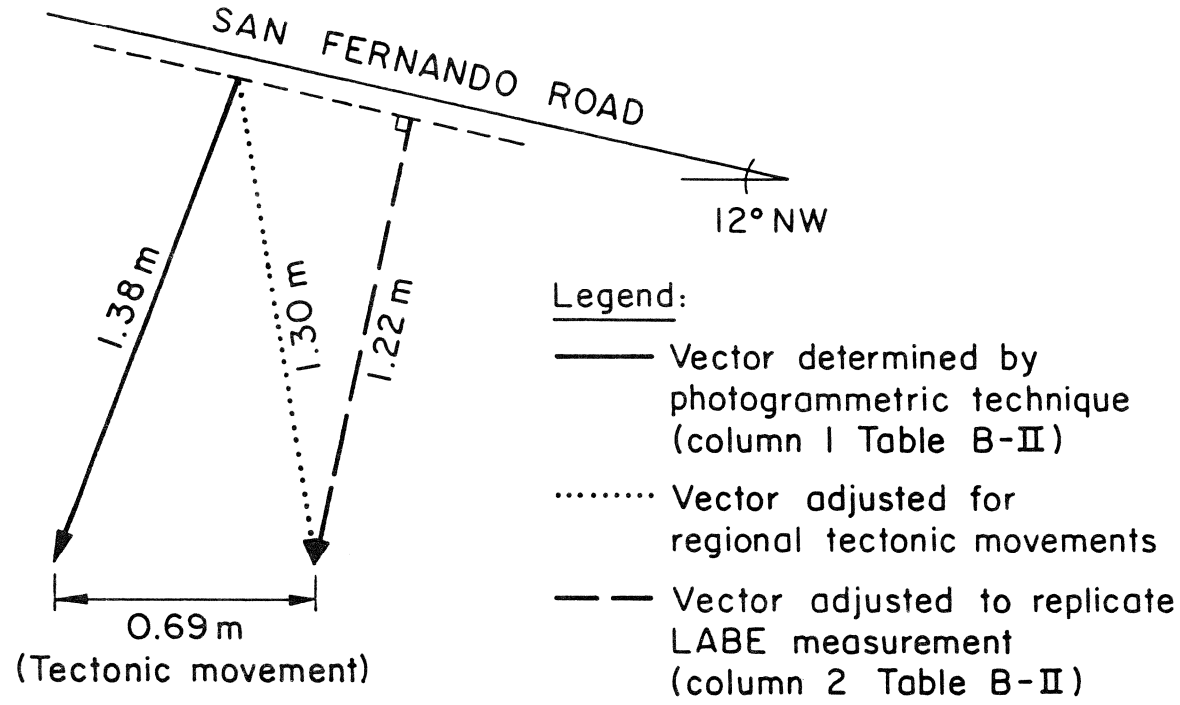

Figure B.5. Method of Adjusting Vectors of Displacement Determined by Photogrammetric Technique

Column three of Table B.2 presents the average of three LABE vectors. The vectors used for this average were the closest vector to the photogrammetric technique vector and the two LABE vectors on either side of the closest vector. The values in column four are the difference between the values in column 3 and the values in column 2. All of the values entered in column 4 are less than the accuracy, 0.47 m, determined for the horizontal photogrammetric measurements.

In addition to the displacement measurements along San Fernando Road, vectors of displacement measured by the photogrammetric technique were compared to displacements determined by ground level survey along the crest of the Upper Van Norman Reservoir Dam. The ground level surveys, as reported by Seed (1973), indicated that the dam experienced 1.5 m of horizontal downstream and 0.9 m of vertical downward movement. The vectors of displacement along the Upper Van Norman Reservoir Dam, as measured by the photogrammetric technique,

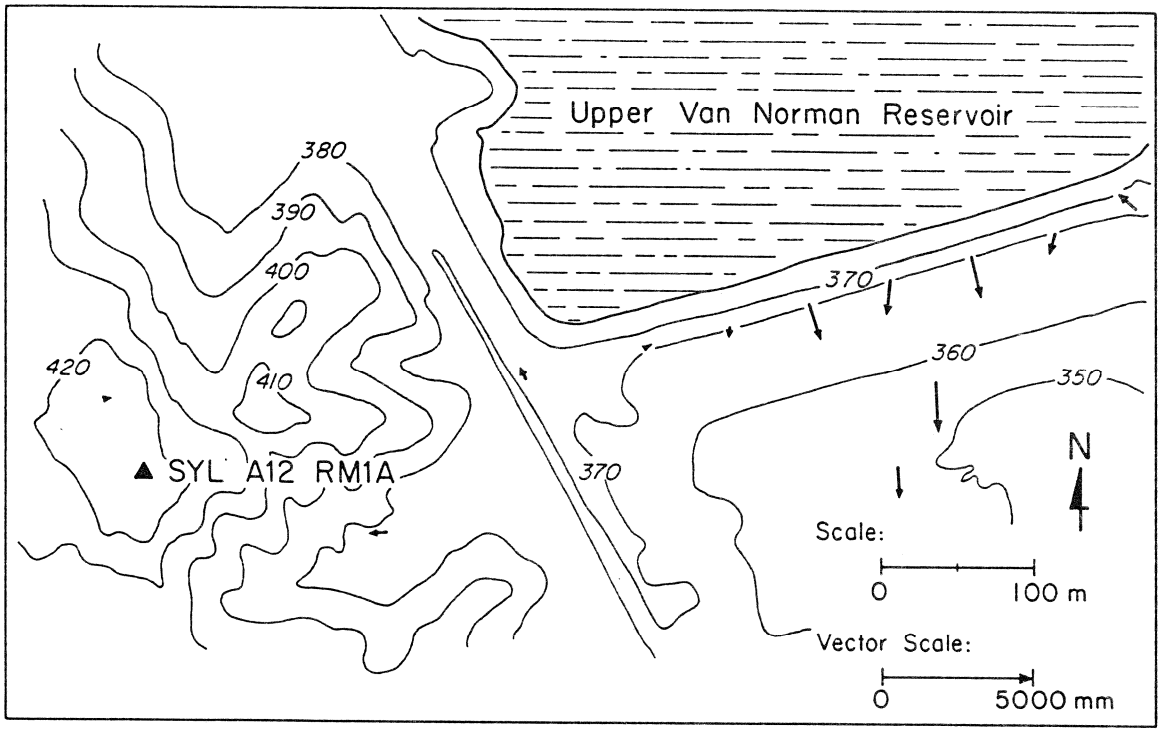

Figure B.6. Vectors of Displacement Determined from Air Photo Analysis Along the Crest and West of the Upper Van Norman Reservoir

are shown in Figure B.6. These measurements show that a maximum of 1.3 m of horizontal downstream movement and 1.4 m of settlement occurred at the utility poles located along the crest of the dam.

In the hills west of the Upper Van Norman Reservoir Dam, movement vectors are plotted at the bases of utility poles embedded in the Saugus Formation. The control point, SYL A12 RM1A, experienced regional tectonic movements of 0.43 m westward (Yerkes, et. al, 1974). Therefore, the nearby vectors of displacement should indicate 0.43 m of westward movement because these sites were unaffected by permanent ground displacement caused by liquefaction or landsliding (Barrows, et al., 1975). The two nearby vectors show 0.53 m of westward movement and 0.17 m of eastward movement. It is not clear on the basis of detailed air photo examination why eastward displacement occurred, although such displacement may be the result of ridge shattering, minor fault displacement, or damage of the utility pole. In contrast, a westward horizontal displacement of 0.53 m is in good agreement with the tectonic movement of the area.

Liquefaction and Ground Failure in the Imperial Valley, Southern California During the 1979, 1981 and 1987 Earthquakes

R. Dobry, Professor
Department of Civil Engineering
Rensselaer Polytechnic Institute
Troy, New York

M.H. Baziar[1]*, Assistant Professor*
University of Tehran
Tehran, Iran

T.D. O'Rourke, Professor
School of Civil and Environmental Engineering
Cornell University
Ithaca, New York

B.L. Roth[2]*, Senior Engineer*
GAI Consultants
Pittsburgh, Pennsylvania

T.L. Youd, Professor
Department of Civil Engineering
Brigham Young University
Provo, Utah

[1] Former Graduate Research Assistant, Department of Civil Engineering, Rensselaer Polytechnic Institute, Troy, New York.
[2] Former Graduate Research Assistant, School of Civil and Environmental Engineering, Cornell University, Ithaca, New York.

ACKNOWLEDGMENTS

The authors wish to extend their appreciation to those who contributed and assisted in the preparation of this chapter.

Steve Bartlett graciously provided us with the updated survey map of Fig. 23 showing the Heber Road site deformations after the 1979 earthquake. Jack McNorgan of the Southern California Gas Company generously provided data and information on pipeline behavior during the same event. We are thankful to Ron Eguchi of Dames and Moore for providing maps and data regarding pipeline, irrigation and drainage repairs, and to Charles Pierce for analyzing data and preparing several figures on damage to irrigation and drainage systems in the 1979 earthquake. We also want to thank Tom Holzer of the US Geological Survey who helped with useful information and discussions on liquefaction and ground failure during the 1987 earthquake. Special thanks are due Ali Avcisoy for preparing some of the figures.

TABLE OF CONTENTS

		Page
Acknowledgments		4–iii
Table of Contents		4–v
List of Tables		4–vii
List of Figures		4–ix
Section		
1.0	INTRODUCTION	4–1
2.0	TECTONIC SETTING, GEOLOGY, AND SEISMIC HISTORY	4–3
3.0	LIQUEFACTION AND GROUND FAILURE IN THE 1979, 1981, AND 1987 EARTHQUAKES	4–6
4.0	THE OCTOBER 15, 1979 EARTHQUAKE	4–11
	4.1 Felt Effect and Intensities	4–11
	4.2 Surface Faulting	4–12
	4.3 Strong Motion Data	4–15
	4.4 Ground Failure	4–19
	4.4.1 Flatlands	4–20
	4.4.2 Earth and Rock Falls and Slides	4–22
	4.4.3 Rivers and Earthworks	4–22
	Rivers	4–23
	Canals (1940, 1979)	4–23
	Irrigation and Drainage Systems	4–25
	Highway Bridges at New River	4–31
	4.5 Damage to Pipelines	4–36
	4.5.1 Natural Gas Pipelines	4–36
	Pipeline Along Highway S–80	4–36
	Pipeline Along Dogwood Road	4–39
	4.5.2 Pipeline Performance in the City of El Centro	4–41

Section			Page
	4.6	The Heber Road Site	4--43
	4.6.1	Location and Surficial Observations of Liquefaction	4--43
	4.6.2	Soil Conditions and Acceleration Records	4--43
	4.6.3	Field Investigations and Laboratory Testing	4--47
	4.6.4	Analysis	4--51
5.0	THE APRIL 26, 1981 WESTMORLAND EARTHQUAKE		4--54
	5.1	Felt Effects, Maximum Intensity, and Surface Faulting	4--54
	5.2	Recorded Accelerations	4--55
	5.3	Ground Failure	4--57
	5.4	Wildlife Soil Profile	4--58
	5.5	Analysis	4--62
6.0	THE NOVEMBER 24, 1987 SUPERSTITION HILLS EARTHQUAKE		4--63
	6.1	Felt Effects and Maximum Intensity	4--63
	6.2	Recorded Accelerations	4--63
	6.3	Liquefaction and Records at Wildlife Site	4--65
	6.4	Analysis	4--67
7.0	SUMMARY		4--74
REFERENCES			4--77

LIST OF TABLES

Table		Page
1	List of Major Earthquakes in the Imperial Valley Since 1900	4--6
2	Surficial Observations of Liquefaction at Different Sites During the 1979, 1981, and 1987 Earthquakes	4--11
3	Peak Accelerations for Several Main Shock Records During the 1979 Earthquake	4--18
4	Characteristics of the Pipelines Influenced by Fault Movements During the 1979 Imperial Valley Earthquake	4--37
5	Water Pipeline Breaks, Lengths, and Break/Length Ratios in the City of El Centro, California (after Eguchi, 1982)	4--42
6	Results of Field Testing for Heber Road Site Reported by Youd and Bennett (1983)	4--47
7	Summary of 1979 Earthquake Records Surrounding the Heber Road Site (Vucetic and Dobry, 1988)	4--48
8	Summary of the Average Field and Laboratory Data Obtained by Four Different Teams for the Heber Road Site (Vucetic and Dobry, 1986)	4--52
9	List of CDMG and Some USGS Strong Motion Accelerograph Stations Which Recorded the April 26, 1981 Westmorland Earthquake	4--57
10	Average Sediment Properties at Wildlife Site and Individual CPT Data	4--61

LIST OF FIGURES

Figure		Page
1	Faults In the Vicinity of Imperial Valley • Denotes Epicenter of 1979 Imperial Valley Earthquake (after Sieh, 1982)	4--2
2	Map of Southern Imperial Valley Showing Pertinent Geographic and Geomorphic Features (Youd and Bennett, 1983)	4--4
3	Horizontal Accelerograms of Two Imperial Valley Earthquakes (Espinosa, 1982) a) Digital Playback of Horizontal Accelerograms of the 1940 Earthquake Record at El Centro Array Station 9 b) Tracing of Horizontal Accelerograms of the 1979 Earthquake Records at El Centro Array Station 9.	4--7
4	Locations of Epicenters and Sites Which Showed Liquefaction for the 1940, 1979, 1981, and 1987 Earthquakes (after Porcella, et al., 1982)	4--8
5	Isoseismal Map of the 1979 Imperial Valley Earthquake (Reagor, et al., 1982)	4--13
6	Preseismic Creep Along the Imperial Fault at Highway S 80 (after Cohn, et al., 1982)	4--14
7	Strong Motion Stations in Imperial Valley, California During the 1979 Earthquake (after Porcella and Matthiesen, 1979)	4--16
8	Locations of Strong Motion Stations in Mexicali Valley, Baja California, Mexico. Stations Underlined are Those From Which Usable Records Were Obtained for the 1979 Imperial Valley Earthquake (Brune, et al., 1982)	4--17
9	Regression Analysis of the Peak Accelerations Recorded During the October 1979 Imperial Valley Earthquake (Seed and Idriss, 1982)	4--19
10	Epicentral Distance Versus Travel Time of Initial S Waves, 1979 Imperial Valley Earthquake (O'Rourke and Dobry, 1982)	4--20
11	Relationship Between Repairs to Irrigation and Drainage Systems and Recent Soils (Soil Distribution after Strahorn, 1924)	4--26

Figure		Page
12	Frequency of Repairs to Irrigation and Drainage Facilities versus Distance to Imperial or Brawley Faults	4--27
13	Number of Repairs/km Versus Distance to Imperial or Brawley Faults	4--28
14	Frequency of Repairs to Irrigation and Drainage Facilities and Peak Vertical and Horizontal Acceleration versus Distance to Imperial or Brawley Faults	4--28
15	Relationships Between Number of Repairs to a) Canals vs. Peak Horizontal Acceleration b) Canals vs. Peak Vertical Acceleration c) Pipelines vs. Peak Horizontal Acceleration d) Pipeline vs. Peak Vertical Acceleration	4--30
16	Frequency of Repairs to Irrigation and Drainage Facilities versus Distance to Epicenter	4--32
17	Location of Bridges 58--05 R/L and Natural Gas Pipelines Intersected by the 1979 Imperial Fault	4--33
18	Profile View of Bridges 58--05 R/L at New River Showing Presumed Subsurface Conditions	4--34
19	Plan View of Bridges 58--05 R/L Showing Ground Surface Topography and Location of Ground Cracks (after Youd and Wieczorek, 1982)	4--34
20	Deformed Shape of 114 mm Natural Gas Pipeline Along Highway S 80 After Excavating 9.8 m Long Trench	4--38
21	Plan View of the City of El Centro Showing Repaired and Replaced Water Lines	4--41
22	Locations of Heber Road, Old Delta, and Buried Stream Channel. Contour Interval, 10 ft (0.305 m) (Youd and Wieczorek, 1982)	4--44
23	Heber Road Site Deformation Due to the 1979 Earthquake (Measurements and Mapping by S. F. Bartlett and T. Y. Youd)	4--45
24	Soil Profile of Heber Road Site (Youd and Bennett, 1983) a) Cross section of sediments b) Logs showing electrical CPT records and SPT N values	4--46

Figure		Page
25	Composite Profile of the Two Studied Sites at Heber Road, Including V_s Measurements (Sykora and Stokoe, 1982)	4--49
26	Grain Size Distribution Curves of the Heber Road Site Sands (Kuo and Stokoe, 1982)	4--50
27	Summary of Average Variation in Low Amplitude Shear Modulus with Confining Pressure for Loading Pressure Sequence (Kuo and Stokoe, 1982)	4--50
28	Liquefaction Susceptibility and Shear Strain Potential Chart Prepared by Seed, 1979 and Seed & Idriss, 1982, with SPT Data from Heber Road and River Park Sites (Youd and Bennett, 1983)	4--53
29	Calculated Displacements for Heber Road Using Newmark's Sliding Block Method (Castro, 1987)	4--54
30	Influence of Shear Wave Velocity on Liquefaction Potential of Sand, from Field and Parametric Studies, Imperial Valley, California, M = 5.5 to 6.5, NRC, 1985, Source: Bierschwale and Stokoe (1984)	4--55
31	Strong Motion Stations in Imperial Valley During the 1981 Earthquake (Maley and Etheredge, 1981)	4--56
32	Aerial Photograph Showing Alamo River Location of Wildlife Array, and Slump in the Bank of Alamo River	4--59
33	Soil Cross Section at Wildlife (Bennett, et al., 1984) a) General Cross Section Across the Flood Plain. The Dashed Line Represents the Approximate Boundary Between Fluvial Deposits and Pre Channel Deposits. Hole #10 is Outside the Flood Plain b) Detailed Cross Section at the Location of the Instrument Station	4--60
34	Shear Wave Velocities Measured at Wildlife Site (Stokoe and Nazarian, 1985) and Used for the Analytical Studies (Dobry, et al., 1989)	4--62
35	Strain Controlled Cyclic Triaxial and Cyclic Direct Simple Shear (DSS) Tests on Intact and Reconstituted Specimens of Wildlife Silty Sand (Dobry, et al., 1989)	4--63

Figure		Page
36	USGS Strong Motion Stations in the Region of the November 24, 1987 Superstition Hills Earthquakes. Trigger Information Refers to the 1315 GMT Event (Porcella, et al., 1987)	4--64
37	Cross Section of Wildlife Site Showing Location of Piezometers (Bennett, et al., 1984)	4--66
38	Instrumental Recordings from the November 24, 1987 Superstition Hills Earthquake (Holzer, et al., 1989a)	4--68
39	Recorded Accelerations (NS Components) and Piezometric Readings at Wildlife Site During the November 24, 1987 Earthquake (Dobry, et al., 1989)	4--69
40	Sand Boils, Lateral Spreading, and Cracks at Wildlife Liquefaction Array (Holzer, et al., 1989b; Youd and Bartlett, 1988)	4--70
41	Soil Profile and Assumed Failure Planes for Newmark Analyses, Wildlife Site, November 24, 1987 Earthquake (Baziar and Dobry, 1991a)	4--72
42	S_u vs $\bar{\sigma}_{1c}$ from Monotonic Undrained Tests on San Fernando Dam Silty Sand (Baziar and Dobry, 1991b)	4--73
43	Measured and Predicted Displacement at Wildlife Site Using Newmark Analysis and Recorded Accelerogram, the November 24, 1987 Earthquake (Baziar and Dobry, 1991b)	4--73
44	Effect of Sliding Block Angle of the Wildlife Site on Predicted Displacement (Baziar and Dobry, 1991b)	4--74

LIQUEFACTION AND GROUND FAILURE IN THE IMPERIAL VALLEY, SOUTHERN CALIFORNIA DURING THE 1979, 1981, AND 1987 EARTHQUAKES

1.0 INTRODUCTION

The Imperial Valley is a sparsely populated, mostly agricultural, flat area located in Southern California near the Mexican border (Fig. 1). The strong motion accelerogram obtained during the 1940 earthquake (M_w = 7.1) at the City of El Centro, contained the largest peak horizontal ground acceleration ever recorded (a_p = 0.33g), and was extensively used by earthquake engineers for several decades. In the last 20 years or so, our strong motion database has multiplied several times, and many ground accelerations larger than 0.33g have been recorded in California and elsewhere. On the other hand, the occurrence in the Imperial Valley of three strong earthquakes of magnitude M_w = 5.9 to 6.5 between 1979 and 1987, together with the number and quality of the records obtained during these ground shakings, have converted the area into an important field laboratory for seismological and geotechnical earthquake engineering studies.

Both the 1940 and the three more recent earthquakes induced liquefaction and ground failure, with the 1979 event also causing damage to buried pipelines due to surface faulting and travelling wave effects. In the three recent earthquakes, and especially in the 1979 event, ground failure affected irrigation and drainage systems, roads, canals, river earthworks, and bridges. Sand boiling, ground cracking, and lateral spreading were observed in all three earthquakes.

At the time of the 1979 event, a strong motion accelerograph array consisting of 13 stations had been installed by the U.S. Geological Survey (USGS) in a straight line perpendicular to the Imperial Fault. The array gave precious information on the attenuation of ground motions with distance for this M_w = 6.5 earthquake, and together with other instruments installed by the USGS and the California Division of Mines and Geology (CDMG), provided a clear picture of the shaking experienced by the Valley. A number of acceleration records were also obtained in the 1981 (M_w = 5.6) and 1987 (M_w = 6.5) earthquakes. These ground

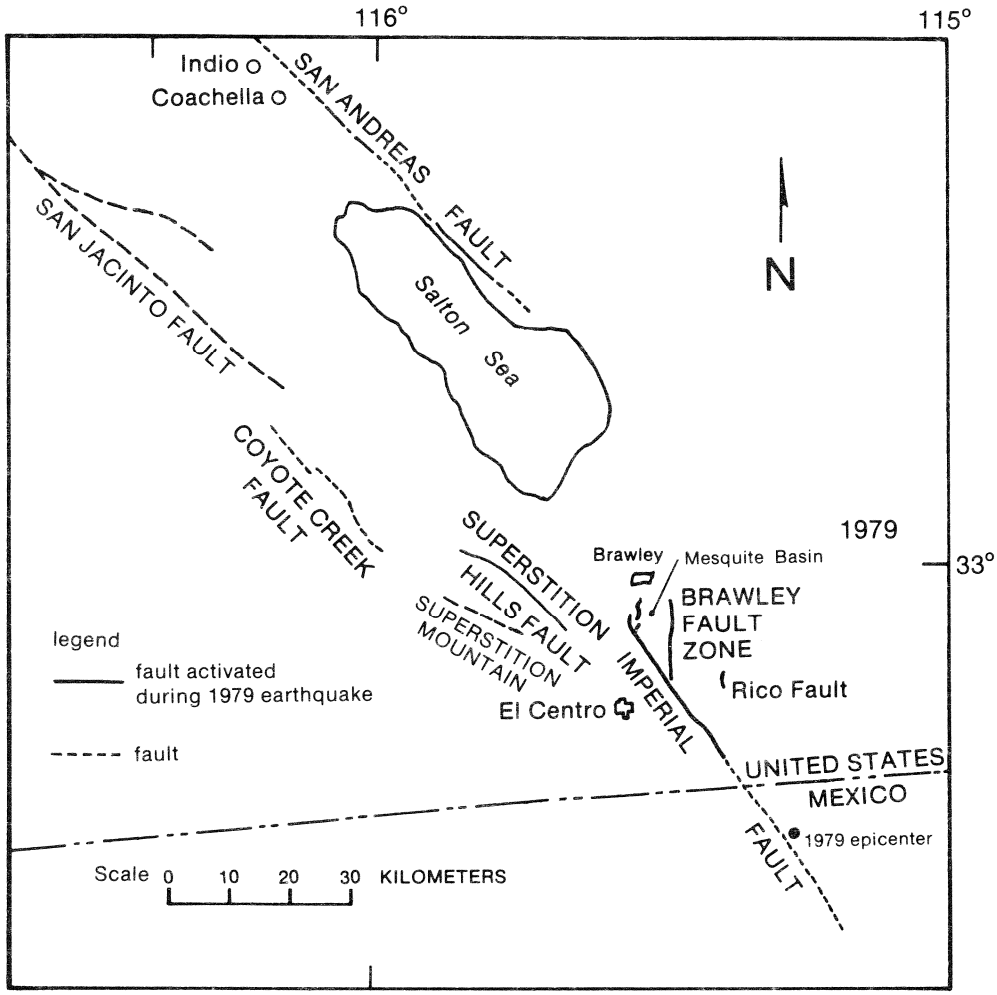

Figure 1. Faults in the Vicinity of Imperial Valley
• Denotes Epicenter of 1979 Imperial Valley Earthquake
(after Sieh, 1982)

motion data have proven useful for the evaluation and analysis of the observed cases of liquefaction and ground failure.

During the 1987 event, a unique set of acceleration and piezometric records was obtained by a special array of instruments installed by the USGS at the Wildlife site, which experienced liquefaction and lateral spreading. This is the first case in which excess pore water pressures up to 100% of the initial effective overburden pressure have been measured during an earthquake.

This chapter documents and reviews systematically the evidence of liquefaction and ground failure and associated effects on constructed facilities -- as well as damage to buried pipelines due to surface faulting and travelling waves -- during the 1979, 1981, and 1987 earthquakes. Although much of the evidence presented is necessarily descriptive, quantitative and statistical information is provided as much as possible. In particular, correlations are presented for the 1979 event between ground motions and damage to irrigation and drainage systems, and between fault slip and pipeline damage. Also, two cases of lateral spreading of great importance due to their unique characteristics (Heber Road site, 1979; and Wildlife site, 1987) are reviewed and described in some detail, including relevant geotechnical information and analyses of the failures.

2.0 TECTONIC SETTING, GEOLOGY, AND SEISMIC HISTORY

The Imperial Valley in southeastern California, is the birthplace of the San Andreas fault system (Fig. 1). The Imperial fault, located at the southern end of the San Andreas fault, appears to be transferred northward into two major fault branches of the San Andreas system the San Jacinto and San Andreas faults (Fuis, et al., 1982). These faults are demonstrably linked in creep and strain behavior to the Imperial fault (Allen, et al., 1972; Thatcher, 1979).

The Imperial Valley lies in the southern part of the Salton Basin. This basin, 130 km wide by 200 km long, is underlain by Tertiary and Quaternary marine, continental, and lacustrine sediments to 6,000 m depth. The lowest part of the valley corresponds to the Salton Sea and is 70 m below sea level. During recent geologic time, the Colorado River, east of the Valley, has flooded the Imperial Valley and transported to it large quantities of sediment. As recently as 300 to 400 years ago the valley was covered by a large lake called Lake Cahuilla (Sharp, 1981).

During the high stand of Lake Cahuilla, fluvial stream deposits and a delta were formed on the south shore (Fig. 2). The delta, delineated by a lobe of higher ground (Bennett, et al., 1981), is generally underlain by sandy soil, whereas the surrounding lake-bottom soils are clay rich (Strahorn, et al., 1924).

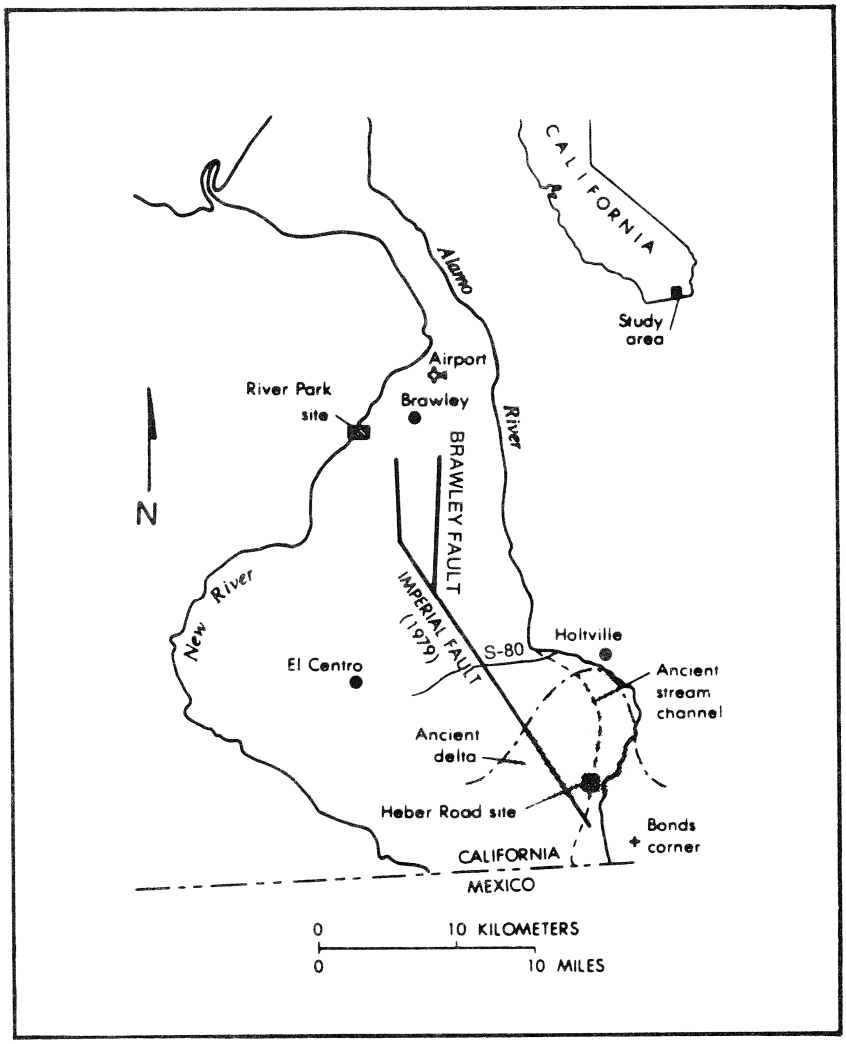

Figure 2. Map of Southern Imperial Valley Showing Pertinent Geographic and Geomorphic Features (Youd & Bennett, 1983)

During the 1979 earthquake, numerous liquefaction and ground failure effects, including those at the Heber Road site, developed on this delta. The Alamo and New Rivers collect excess irrigation water from the valley, runoff from the surrounding foothills, and occasional flood water from the Colorado River, in a northward flow to the Salton Sea. Typical fluvial sedimentary features including channel, point-bar, levee, and overbank deposits are present around these two rivers. During the 1979 earthquake, ground cracks and sand boils developed on many fluvial deposits along these rivers, including those at the River Park site (Youd and Wieczorek, 1982). The geology of the Imperial Valley

has been summarized by Dibblee (1954), Kovach, et al. (1962), Biehler, et al. (1964), Elders, et al. (1972), Sharp (1982), Youd and Bennett (1983), and Bennett, et al. (1984).

Throughout the twentieth century it has been observed that earthquake activity in the Imperial Valley typically occurs as swarm sequences along the Brawley fault zone, (Figs. 1–2) interspersed with events of magnitude 5 to 7 in main–shock/after–shock sequences along the Imperial Valley fault. Although the historical record before 1940 is incomplete, it can be concluded that changes in the spatiotemporal seismicity pattern evolve at a rate measured in tens of years (Johnson and Hill, 1982).

The Imperial Valley has undergone several similar size earthquakes in the recent past, including the well known event of moment magnitude 7.1 near the City of El Centro on May 18, 1940 (Table 1). The table reveals that the main shocks in the valley commonly occur in pairs of similar size separated by a few hours. However, in both 1940 and 1979 the second earthquake was an aftershock about one unit of magnitude smaller than the main shock. The seismic moment for the 1940 event was about 56×10^{18} N–m (Kanamori and Anderson, 1975). It is significant that the seismic moment magnitude reported for the 1979 event is about one–tenth that of the 1940 event. This suggests that the overall fault displacement during the 1979 earthquake was only a small perturbation compared with that of the 1940 event.

Figure 3 shows the horizontal acceleration records at El Centro Array station 9 for the 1940 and 1979 earthquakes (Porcella and Matthiesen, 1979; Espinosa, 1982). During the May 18, 1940 event the accelerograph at this station ran out of scale and the accelerogram had to be extrapolated beyond the limits of the original record (Neumann, 1942). This record was used worldwide for many years in earthquake engineering studies as representative of strong ground motion close to the earthquake source. The comparison of the recorded accelerations for these two events at El Centro shows that, although both events originated approximately from the same source, the shaking of the 1940 event had higher

Table 1. List of Major Earthquakes in the Imperial Valley Since 1900

NO.	Date-local	Time (GMT)	M_L	M_W	Liquefaction Occurence	Length of Fault-km	Maxi slip-m	References
1	April 19, 1906	0030	6.0	–	–	–	–	Townley & Allen (1939) Toppozada , et al. (1978)
2	June 23, 1915	0359	6.3	–	–	–	–	Beal (1915)
3	June 23, 1915	0456	6.3	–	–	–	–	
4	May 28, 1917	0606	5.5	–	–	–	–	Townley & Allen (1939) Toppozada, et al. (1978)
5	January 1, 1927	0816	5.8	–	–	–	–	Townley & Allen (1939) Toppozada, et al. (1978)
6	January 1, 1927	0913	5.5	–	–	–	–	
7	May 18, 1940	0436	6.3-6.5	7.1	✓	65	5.9	Kanamori & Anderson (1975) Kanamori & Jennings (1978) Neumann (1942) Richter (1958) Johnson , et al. (1982) USGS (1982) Reager , et al. (1982) Sharp, et al. (1982)
8	May 18, 1940	0635	5.5	–	–	–	–	
9	October 15, 1979	2316	6.6	6.5	✓	31	0.78	Johnson , et al. (1982) USGS (1982) Reager , et al. (1982) Sharp, et al. (1982)
10	October 15, 1979	0658	5.8	–	–	–	–	
11	April 26, 1981	0509 [1]	5.6	5.9	✓	20 [2]	0.014 [3]	McJunkin & Kaliakin (1981)
12	November 23, 1987	0154	6.2 [4]	–	–	–	–	Porcella, et al. (1987) Bradey , et al. (1989)
13	November 24, 1987	1315	6.6 [4]	6.5	✓	–	–	

M_L = local magnitude
M_W = moment magnitude

1 = Pacific Day Time
2 = right-lateral offset
3 = surface rupture
4 = surface wave magnitude

frequency content and a significantly longer duration (see also Trifunac and Brune, 1970). Both the 1940 and 1979 earthquakes were complex events, possibly involving multiple ruptures (Porcella, et al., 1982; Espinosa, 1982).

3.0 LIQUEFACTION AND GROUND FAILURE IN THE 1979, 1981, and 1987 EARTHQUAKES

In the last decade, the Imperial Valley has been struck by a number of earthquakes, most notably those of 1979, 1981, and 1987. The epicenters of these three events (Fig. 4) were located within 40 km of the intersection of

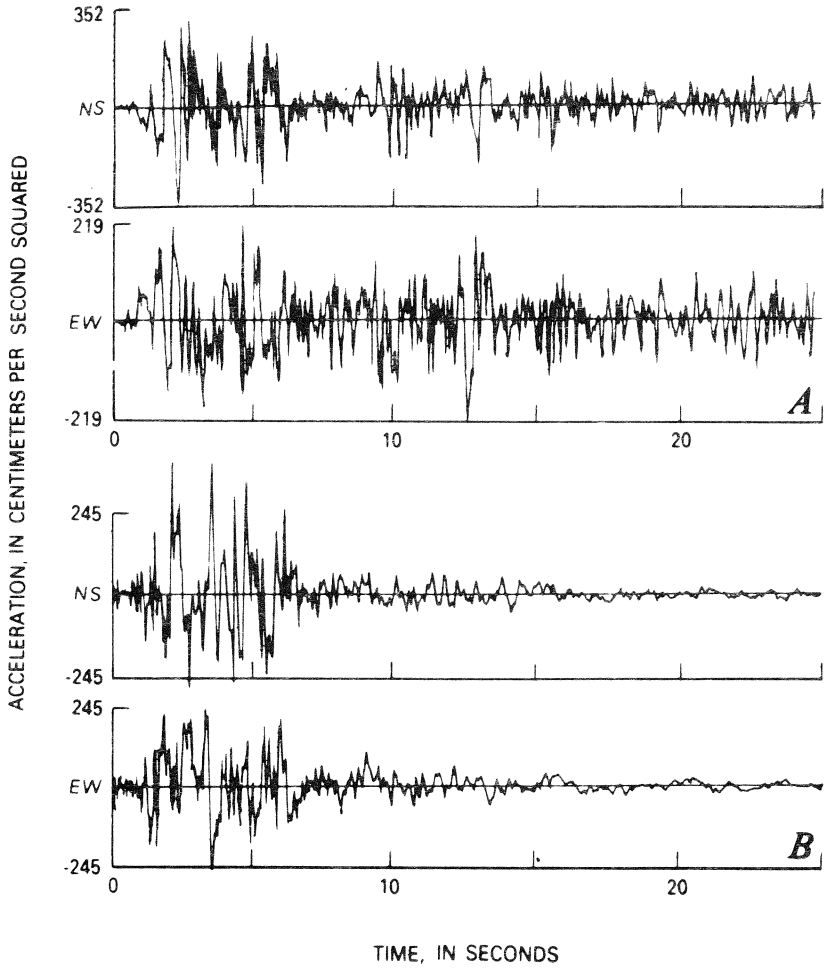

Figure 3. Horizontal Accelerograms of Two Imperial Valley Earthquakes (Espinosa, 1982)
a) Digital Playback of Horizontal Accelerograms of the 1940 Earthquake Record at El Centro Array Station 9
b) Tracing of Horizontal Accelerograms of the 1979 Earthquake Records at El Centro Array Station 9

Highways 8 and 86. Liquefaction and secondary ground failure occurred in all three earthquakes. Ground failure causing damage to canals was also reported for the 1940 earthquake, as discussed later in Section 4.4.3.

After the October 15, 1979 Imperial Valley earthquake, there were many observations of surficial effects of liquefaction, including numerous sand boils, ground cracks, slumpings, ground settlements, and lateral spreadings.

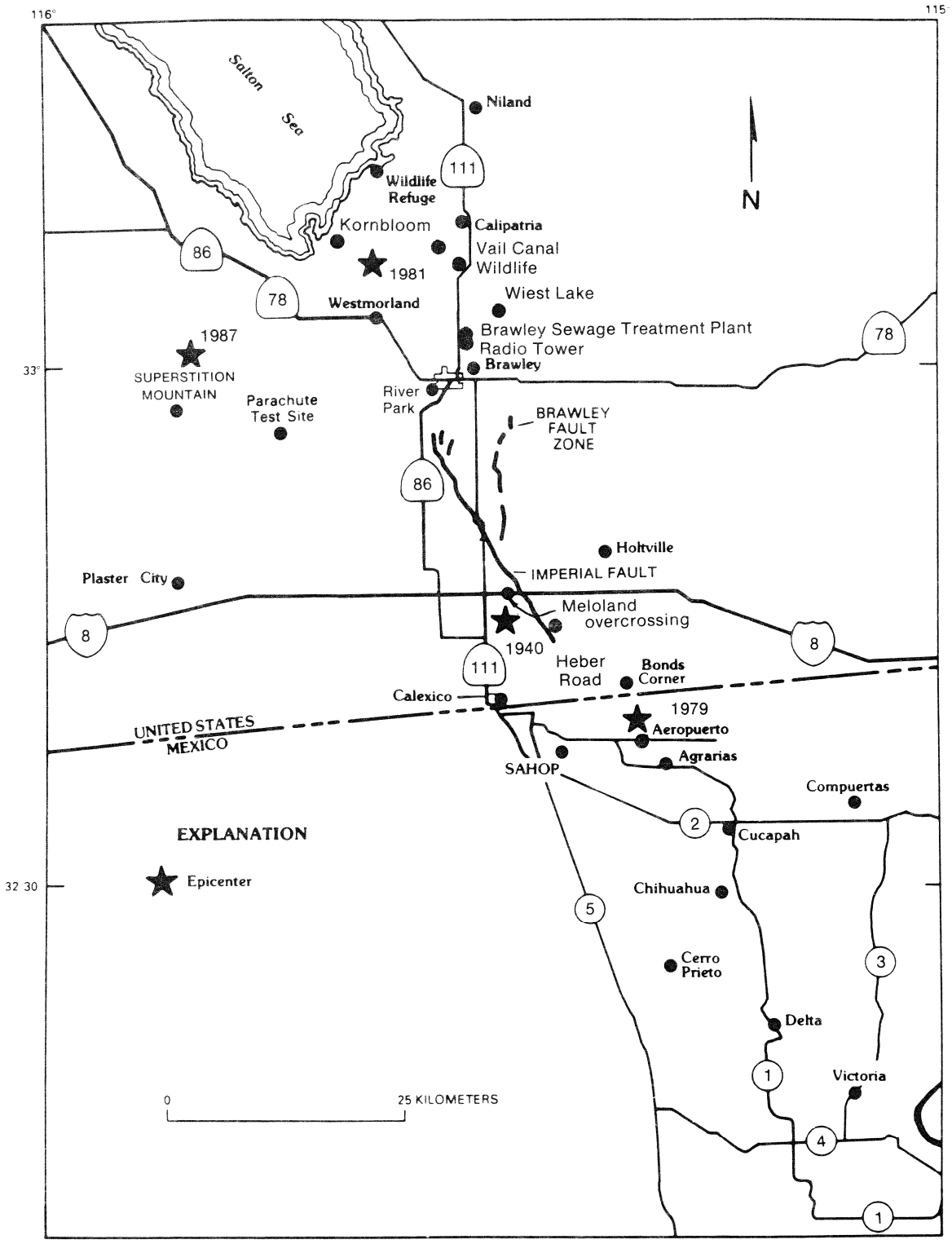

Figure 4. Locations of Epicenters and Sites which Showed Liquefaction for the 1940, 1979, 1981, and 1987 Earthquakes (after Porcella, et al., 1982)

These sites (Youd and Wieczorek, 1982) include (see Fig. 4 for locations):

i) the Heber Road site, 13.5 km from the epicenter,
ii) Wiest Lake, about 50 km from the epicenter,
iii) River Park, 45 km from the epicenter, and
iv) Radio Tower, 47 km from the epicenter.

In Heber Road, a maximum of 4.2 m lateral spreading is reported; this site will be discussed in more detail in Section 4.6. In Wiest Lake, sand boils erupted at three different times: during the main shock, during an after-shock about ten hours after the main shock, and during an after-shock on the afternoon of October 17, 1979. Ground cracks and incipient lateral spreading were also present at this site. In a large graded area called River Park, along the east side of New River at the southwestern edge of Brawley, hundreds of sand boils and numerous small (less than 5 cm width) ground cracks were formed. At this site, water continued to seep from some of the sand boils for two weeks after the earthquake. A buried concrete drainpipe, 400 mm in diameter, was ruptured in one place beneath the liquefied layer in the River Park area. In Radio Tower, several sand boils expelled considerable volumes of water and sand creating a small pond in the New River flood plain, 100 m east of the KROP radio tower.

Among all sites which liquefied during the 1979 event, only Radio Tower showed surficial manifestations of liquefaction during the April 26, 1981 Westmorland earthquake. At this site, located 14.2 km from the 1981 epicenter, small amounts of water and sediment spurted from several 1979-event sand boils, spotting the top of the old sand boil deposits with new sediments (Youd and Wieczorek, 1984). The slight rejuvenation of these sand boils suggests that the shaking intensity at the site in 1981 was near the threshold needed to generate liquefaction in the underlying sediment. This hypothesis is supported by the fact that Radio Tower is the most distant site with exhibited sand boils in the 1981 event. Small ground fissures were also observed at sites as far as 14.2 km from the epicenter (Radio Tower) and a large fissure with a 150 mm-wide opening was also reported at a distance 11 km east of the epicenter. Surface observation of liquefaction was reported at several sites after the 1981 earthquake, including several sand boils and a series of cracks 25 m north of Vail Canal to

the west of Alamo River; numerous sand boils, fissures, and slumped banks in the Imperial Wildlife Management Area, here referred to as Wildlife site; and hundreds of sand boils and fissures on Kornbloom Road. The Wildlife site was instrumented in 1982 to monitor liquefaction occurrence during future earthquakes. A complete description of localities which showed surficial observation of liquefaction in 1981 is given by Youd and Wieczorek (1984).

The Wildlife site (Fig. 4) also liquefied during the November 24, 1987 Superstition earthquake. Numerous sand boils, fissures as large as 126 mm in width, a slump at the bank river, and lateral spreading causing up to 232 mm lateral displacement were reported for the 1987 event. This site is the subject of more detailed discussion in Sections 5 and 6. After the 1987 earthquake, Holzer (1990) examined the same sites for which Youd and Wieczorek (1984) had reported liquefaction in the 1981 event, and found no evidence of liquefaction at any of them except for Wildlife.

Table 2 summarizes the epicentral distances for eight sites, including those previously described. These are only a few of the sites which experienced liquefaction during the 1979 and 1981 events. Due to the long fault rupture in the 1979 earthquake, the corresponding distances from the fault rupture are also included for this event. As seen in Table 2, during the 1979 earthquake the site farthest from the source which showed any surficial manifestation of liquefaction was Wiest Lake, 13 km from the fault rupture and 47 km from the epicenter.

The most distant sites showing surficial effects of liquefaction are at 47 km, 14 km, and 30.5 km away from the epicenters for the 1979, 1981, and 1987 earthquakes, respectively. This trend is generally consistent with the moment magnitudes of these earthquakes which were, respectively, 6.5, 5.9, and 6.5 (Table 2).

Table 2. Surficial Observations of Liquefaction at Different Sites During the 1979, 1981, and 1987 Earthquakes

		1979 $M_L = 6.6$ $M_W = 6.5$					1981 $M_L = 5.6$ $M_W = 5.9$				1987 $M_S = 6.6$ $M_W = 6.5$			
		Sand Boils	Cracks	Lateral Spread	Distance* km	Epicentral Distance km	Sand Boils	Cracks	Lateral Spread	Epicentral Distance km	Sand Boils	Cracks	Lateral Spread	Epicentral Distance km
1	Wildlife	-	-	-	19	53.8	✓	✓	✓	9.8	✓	✓	✓	30.5
2	Heber Road	✓	✓	✓	1.6	11.5	-	-	-	47.1	-	-	-	53
3	Radio Tower	✓	✓	-	9.8	45.2	✓	-	-	14.2	-	-	-	30
4	Vail Canal	-	-	-	23	56.2	✓	✓	-	7.7	-	-	-	29
5	Korn Bloom	-	-	-	27.3	61.5	✓	✓	-	3.8	-	-	-	21
6	River Road	✓	✓	✓	6.1	42.8	-	-	-	16	-	-	-	26
7	Wiest Lake	✓	✓	-	12.9	47.1	-	-	-	14.8	-	-	-	34
8	Brawley Sewage Treatment	✓	✓	-	6.8	46.2	-	-	-	14	-	-	-	30

M_L = local magnitude

M_W = moment magnitude

M_S = surface wave magnitude

* nearest distance from fault rupture (approximate)

4.0 THE OCTOBER 15, 1979 EARTHQUAKE

4.1 Felt Effects and Intensities

The 1979 Imperial Valley earthquake occurred on October 15 at 23:16:54 GMT. It was felt over an area of 128,000 km^2, as far as Los Angeles, California, Las Vegas, Nevada, Phoenix, Arizona, and the northern part of Mexico, and it injured 73 people (Reagor, et al., 1982). The property damage was estimated at about 30 million dollars. There were relatively few injuries, as the main area affected by the earthquake was sparsely populated and contained relatively small structures.

The epicenter was located 3 km south of the United States Mexico border, approximately 10 km east of Mexicali, Mexico, at 32°38.61' N latitude and 115°18.53' W longitude. Although the epicenter was in Mexico, no surface rupture was observed south of the United States--Mexico border. The focal depth

(Chavez, et al., 1982) was about 9.7 km, which is slightly more than the average depth for earthquakes in the Imperial Valley earthquake (6 to 8 km), as reported by Johnson (1979).

The 1979 earthquake, with a local magnitude $M_L = 6.6$ (Chavez, et al., 1982) was the largest earthquake occurring in California after the 1971 San Fernando event. A maximum Modified Mercalli Intensity (MMI) of VII was assigned to this earthquake, although an MMI of IX was observed at the Imperial County Service Building in El Centro (Rojahn and Ragsdale, 1980). The corresponding MMI isoseismals shown in Fig. 5 suggests an MMI of VI to VII for the Imperial Valley. A seismic moment of 6×10^{18} N-m and $M_w = 6.5$ (Johnson, et al., 1982) was obtained for this event from long period Love and Raleigh waves.

4.2 Surface Faulting

During the 1979 earthquake, surface faulting occurred along the Imperial fault, the Brawley fault zone, and the Rico fault (Fig. 1). The Rico fault near Holtville showed a 200 mm vertical offset but no horizontal slip. The Brawley fault ruptured discontinuously along multiple strands over a length of 13.1 km with a predominantly vertical displacement. The largest right-lateral component of slip was about 70 mm at Keystone and Harris Road (Sharp, et al., 1982). The Mesquite basin block (Fig. 1) dropped as much as 410 mm relative to the Imperial fault and 150 mm relative to the Brawley fault zone.

The Imperial fault showed surface rupture along a segment of 30.5 km (Sharp, et al., 1982). Sharp, et al. also reported that this activated segment in 1979 corresponds approximately to the northern half of the known length of the fault, taken to be the extent of the 1940 surface rupture. This 30.5 km segment of Imperial fault, along with 3 km of the fault trace north of the northernmost recorded 1940 breaks, are marked by well-defined Holocene scarps (Sharp, 1977). The maximum right lateral cumulative horizontal slip after 160 days was about 780 mm at a point about 5.6 km from the south end of the rupture along the Imperial fault.

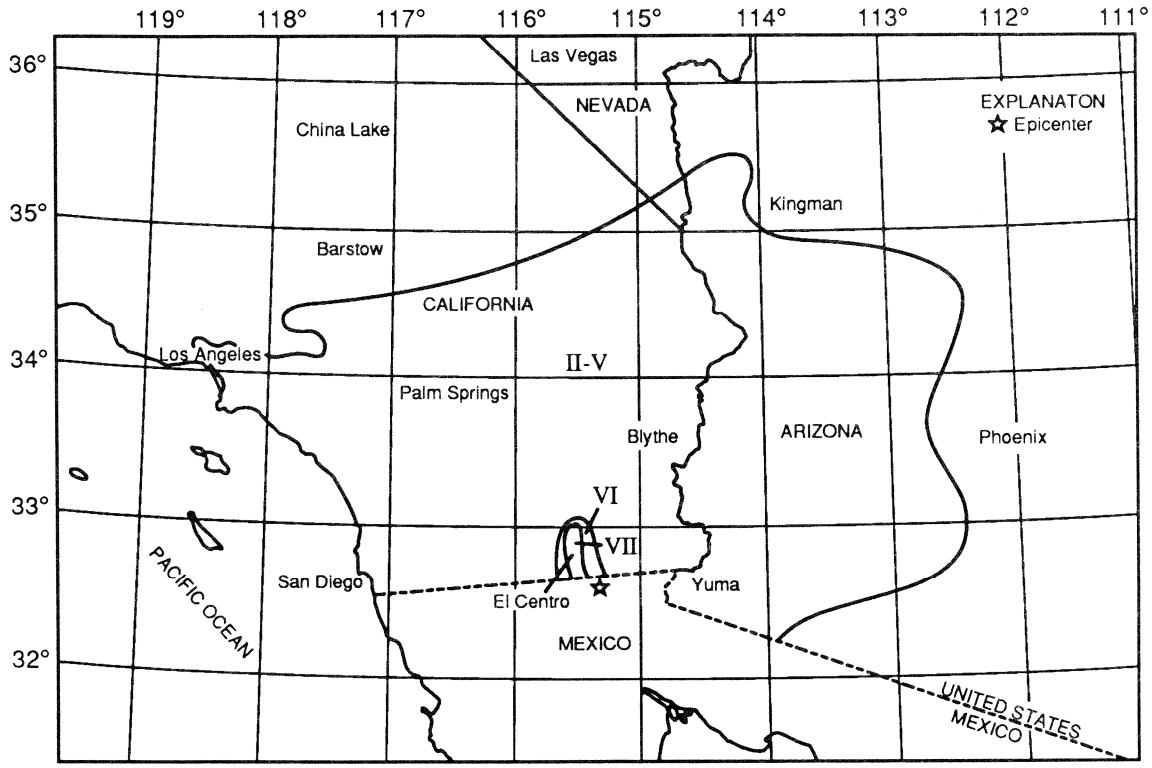

Figure 5. Isoseismal Map of the 1979 Imperial Valley Earthquake (Reagor, et al., 1982)

Sieh (1982) reported that short cracks of less than 1 m in length, parallel to the main fault trace and being dextral movements of as much as 10 mm, were observed along the trace of the San Andreas fault. Fuis (1982) found right lateral horizontal displacements, ranging from 1 to 22 mm along the Superstition Hill fault for a distance of 22.5 km.

Preseismic creep along the Imperial fault was monitored by six theodolite alignment arrays installed in 1967, four continuously recording taut-wire creepmeters installed in 1975, and two nail files installed in 1977. A nail file consists of a line of seven steel studs; three studs on either side of the fault, initially in a straight line. A discussion of the installation and operation of these instruments is given by Goulty, et al. (1978) and by Cohn, et al. (1982). One of the alignment arrays was installed across the fault at County Highway S-80 joining Holtville and El Centro (see Fig. 2 for locations). The measurements from this alignment array are presented graphically in Figure 6.

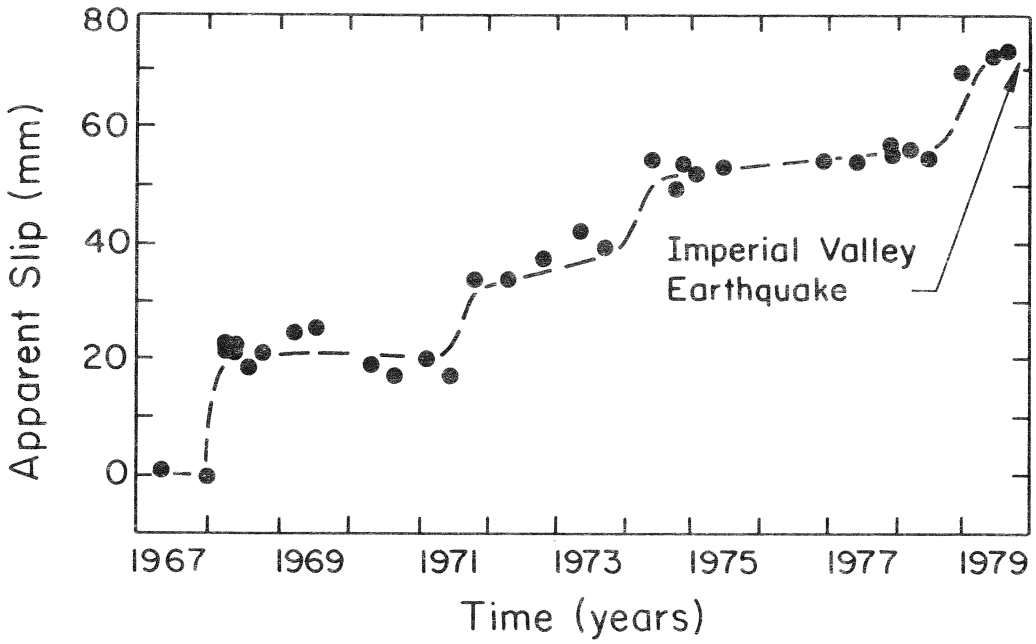

Figure 6. Preseismic Creep Along the Imperial Fault at Highway S--80 (after Cohn, et al., 1982)

The figure shows four well--defined pulses of motion at time intervals of about 2 years. The sum of these four pulses divided by the 12 year monitoring period is equal to the average creep rate of 6.2 mm/yr. By extrapolating this average creep rate back to 1948, it is estimated that 192 mm of right--lateral creep may have occurred at this location before the 1979 earthquake.

Offsets of the Highway S--80 pavement caused by slip during the 1979 earthquake (coseismic slip) were measured by Hart (1981) and by Sharp, et al. (1982). Two days after the main shock Hart measured 250 mm of right--lateral slip and a vertical slip component of 30--40 mm, west side up. He estimated that 50 mm of afterslip had already occurred by the time of his measurement. The magnitude of slip measured by Sharp, et al. (1982) four days after the earthquake was 275 mm.

Afterslip at a rate greater than the background creep rate continued for several years after the main shock. Sharp, et al. (1982) and Cohn, et al. (1982) determined that the afterslip rate decreased logarithmically with increasing time after the earthquake. The equation proposed by Sharp for determining the

total fault displacement resulting from coseismic slip and afterslip is:

$$D = a + b \log(t) \qquad (1)$$

in which D is the fault displacement calculated in mm, t is the time in days, and a and b are best fit constants obtained from linear regression analysis of the measured slips of the roadway pavement. For the Highway S 80 site, the values of a and b are 207 and 129.3, respectively.

4.3 Strong Motion Data

The first accelerograph in Imperial Valley was installed at the site of the Imperial Irrigation District (formerly the Southern Sierra Power Co.) substation on Commercial Avenue in the Town of El Centro in July 1932 (Array Station No. 9 in Fig. 7). As a result of a joint effort by the U.S. Geological Survey (USGS), California Division of Mines and Geology (CDMG), and California Institute of Technology (CIT), the number of accelerograph stations in the Imperial Valley were substantially increased in 1973 (Hill, et al., 1975). The USGS also deployed specialized ground motion arrays to study the source mechanism, attenuation of ground motion, and differential ground motions. At the time of the 1979 earthquake there were four arrays in operation in addition to other individual stations (Fig. 7). These arrays were:

1. The USGS El Centro array, aligned transverse to the Imperial fault and made up of 13 stations spaced 3 to 5 km and extended to 45 km. This array, designated as #1 in Fig. 7, was designed to provide information on attenuation of the ground motion with distance from the causative fault, and also to provide information on near field motions for interpretation of the motions and source mechanism. The accelerographs in this array were located in small fiberglass housings (representing free field) as well as in buildings (Rojahn, et al., 1982; Porcella, et al., 1982).

2. The USGS differential array, installed in 1979 in cooperation with the Federal Highway Administration, which consisted of a 305 m-long array of six triaxial accelerometers at unequal spacings, designed to obtain differential ground displacement data for use in studies of bridges,

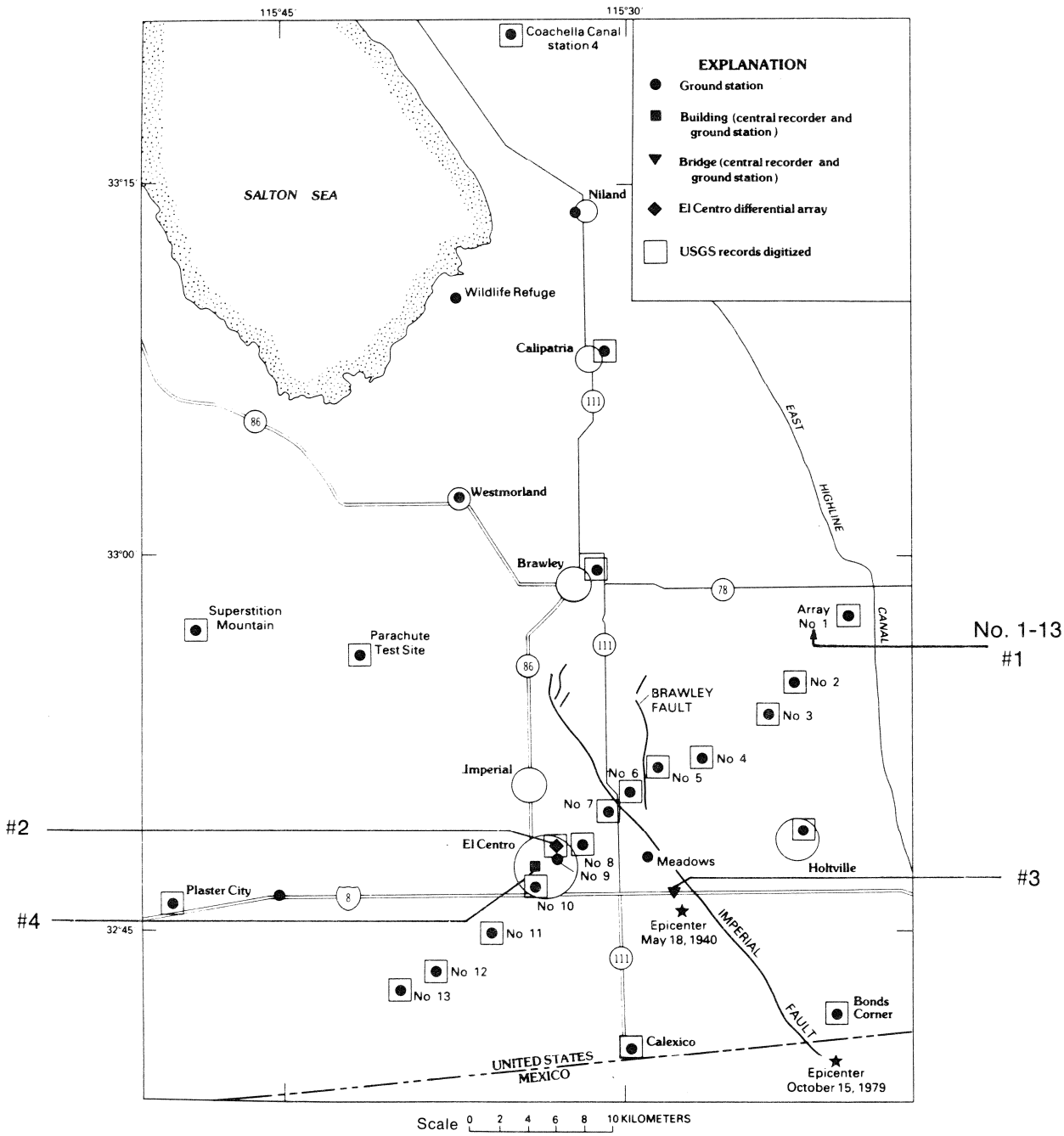

Figure 7. Strong-Motion Stations in Imperial Valley, California During the 1979 Earthquake (after Porcella and Matthiesen, 1979)

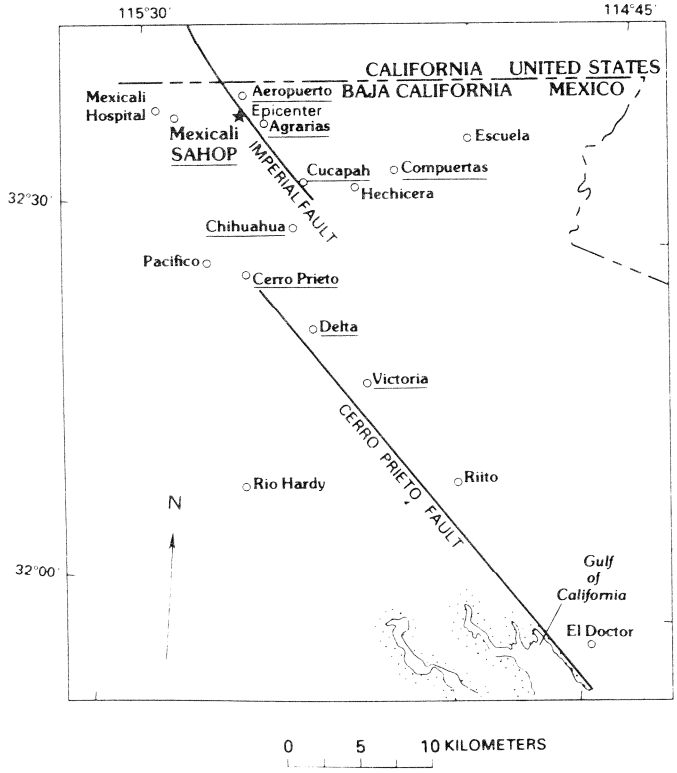

Figure 8. Locations of Strong-Motion Stations in Mexicali Valley, Baja California, Mexico. Stations Underlined are those from which Usable Records were Obtained for the 1979 Imperial Valley Earthquake (Brune, et al., 1982)

dams, pipelines and other extended structures. These stations are marked as #2 in Fig. 7.

3. The CDMG instrumentation on the Meloland Road--Interstate Highway 8 over crossing, marked as #3 in Fig. 7, with a 26--channel accelerograph system, including 3 channels at a nearby ground site representing the free field (Rojahn, et al., 1982).

4. The CDMG instrumentation on the Imperial County Services Building, shown as #4 in Fig. 7, with a 13 channel system, as well as a nearby free field triaxial accelerograph at ground level (Rojahn and Mork, 1982).

During the main shock, many strong motion stations inside the United States were triggered within an epicentral distance of 150 km. Besides these stations, a network of 13 strong motion accelerographs in Baja California, Mexico (Fig. 8)

Table 3. Peak Accelerations for Several Main-Shock Records During the 1979 Earthquake

Station	Component	Peak Acceleration (g)
El Centro Array Station 7	230° up	0.52 0.65
El Centro Array Station 6	230° up	0.45 1.74
Bonds Corner	230° up	0.81 0.47
El Centro Array Station 8	230° up	0.50 0.55

were operated by the Centro de Investigacion Cientifica y Educacion Superior de Ensenada, Universidad Nacional Autonoma de Mexico, and the University of California, San Diego (Brune, et al., 1982). Some of these stations provided usable records for this earthquake.

For the 1979 earthquake the maximum recorded vertical and horizontal accelerations were 1.74 g at El Centro array Station 6, and 0.81 g at Bonds Corner Station, respectively (Table 3). The attenuation of peak horizontal acceleration with distance from the fault rupture for this earthquake, plotted by Seed and Idriss (1982) from the records, is reproduced in Fig. 9. By plotting the time of initial S wave arrival versus epicentral distance, O'Rourke and Dobry (1982) found an apparent horizontal propagation velocity of strong motion of 3.68 km/sec (Fig. 10). This velocity is useful for determining ground strains and possible distortions of buried pipelines.

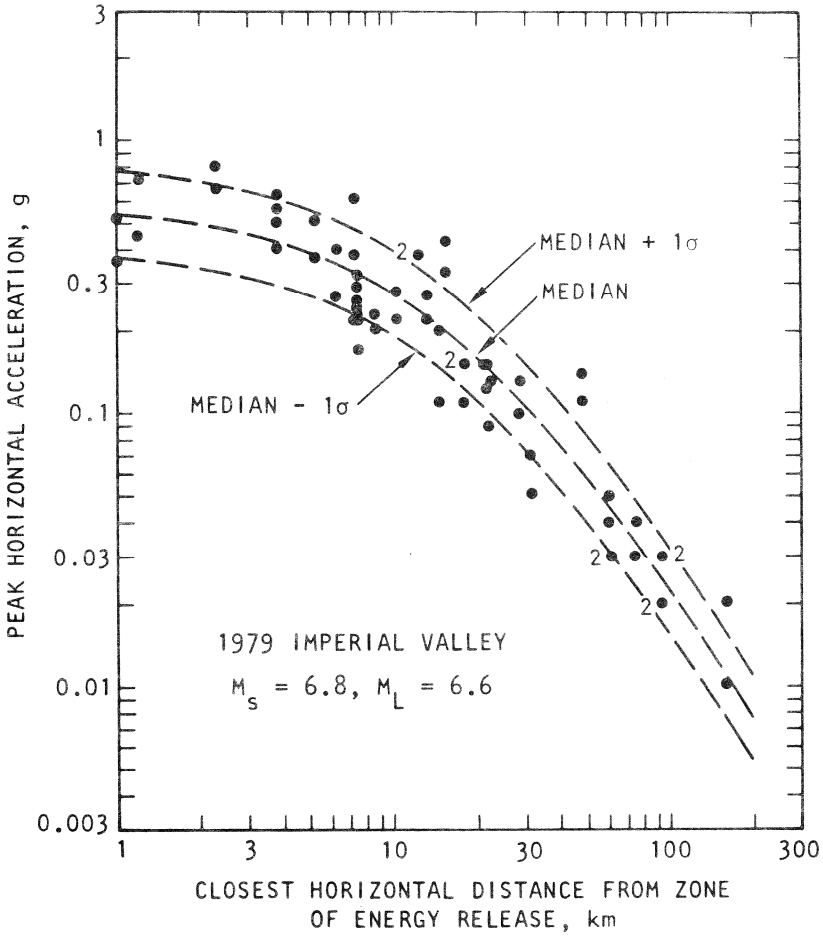

Figure 9. Regression Analysis of the Peak Accelerations Recorded during the October 1979 Imperial Valley Earthquake (Seed and Idriss, 1982)

4.4 Ground Failure

During the 1979 Imperial Valley earthquake and its aftershocks, large ground failure and secondary ground effects attributed to liquefaction were reported in the Imperial Valley region. Surficial effects of liquefaction such as earth slumps, lateral spreads, ground settlement, earth falls, rock falls, sand boils, and ground and pavement cracks were observed at 38 different sites in the Valley (Youd and Wieczorek, 1982). Three categories of ground failures can be identified in the 1979 earthquake as follows:

- Flatlands: primarily liquefaction and compaction of soil, sand boiling, and ground cracking.

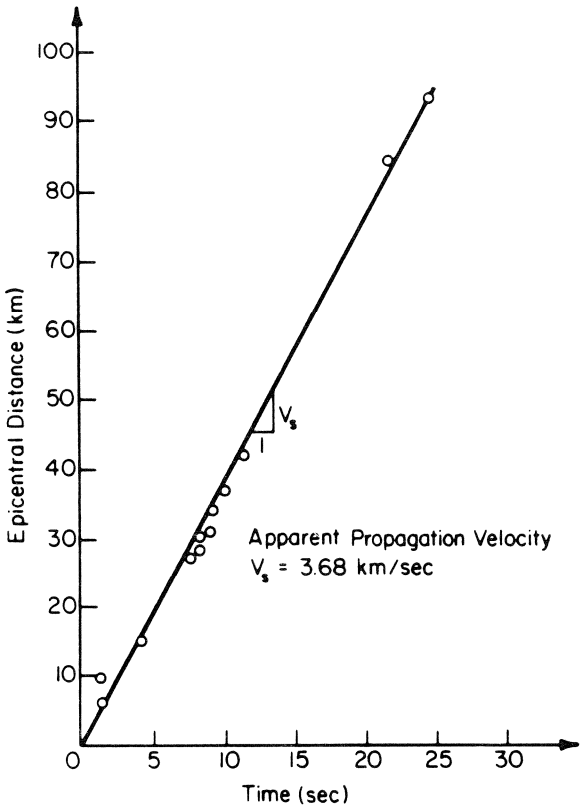

Figure 10. Epicentral Distance Versus Travel Time of Initial S Waves, 1979 Imperial Valley Earthquake (O'Rourke and Dobry, 1982)

- Steep river bluffs and hillsides: earth and rock falls and slides.
- River, canals and highway embankments: slumps and lateral spreads.

These three categories are separately discussed in the next few pages.

4.4.1 **Flatlands**

Ground failures in the flatlands included lateral spreads, ground settlement, sand boils, slumps and fissures in roadways and small canals, and broken irrigation and drainage pipes. Sand boils, with diameters ranging from 0.3 to 1.0 m erupted along straight or curved lines. They were observed either in groups (up to hundreds) or single ones, with no definite pattern and with or without connection to cracks.

Youd and Wieczorek (1982) reported that flatlands liquefaction occurred primarily in two geological settings:

a) channel, flood plain, and artificial-fill deposits along the New and Alamo Rivers, and

b) cultivated areas containing sandy subsoil such as in the area west of the Alamo River between Holtville and the United States-Mexican border, where contours of the land surface and soil surveys show a lobe of higher ground composed of sand dunes and sandy soil (Fig. 2).

Ground cracks were common in many areas of ground failure and in areas containing sand boils. The maximum crack displacements were reported as 50 and 100 mm in the horizontal and vertical directions, respectively. For detailed description of sand boil and ground crack locations refer to Youd and Wieczorek (1982). Only a brief description of some sites which experienced lateral spreading is presented here.

1. At a site 1.5 km south of the border and 0.5 km southwest of the Imperial fault, the head of a small lateral spread intersected a concrete-lined canal, ruptured the canal lining, and displaced the floor of the canal about 200 mm laterally to form a gentle curve.

2. On State Highway 98, an east-facing scarp, about 100 mm high, fractured the pavement and continued into a field to the south, where crop rows were shifted as much as 110 mm laterally.

3. A lateral spread severely disrupted the pavement on Heber Road, 1 km east of Mets Road. The spread shifted the road and parallel unlined canal about 1.2 m southward toward a 2-m deep depression in Heber Dunes County Park south of the canal. This site is the subject of detailed discussion in Section 4.6.

4. The cracks adjacent to Heber Road and 0.6 km east of the bridge over the Alamo River were arcuate and apparently formed the head of an incipient lateral spread that shifted slightly northward toward the river.

5. In the southern part of the fissures zone, 2.4 km northeast of Heber Road, a small amount of left-lateral displacement associated with lateral spreading was observed.

6. Several ground cracks disrupted a parking lot and an adjacent unpaved picnic area on the east shore of Wiest Lake. The arcuate pattern of some of the cracks indicates incipient lateral spreading toward the lake.

4.4.2 Earth and Rock Falls and Slides

Most earth falls along the bluffs of the New and Alamo Rivers were reported to be within 12 km of the fault surface rupture, although a few were as distant as San Felipe Creek, 35 km from the rupture (Youd and Wieczorek, 1982). These silty bluffs stand in near vertical slopes under static conditions, and the low tensile strength of the silt makes these bluffs susceptible to failure during earthquake shaking.

The largest earth fall generated by the 1979 earthquake was the bluff of the New River, north of Brawley, California, which collapsed over a length of 400 m, blocking Fredricks Road with 4000 m^3 of sandy-silt debris.

A half dozen rock slides and falls, generally less than 10 m^3, were reported from aerial and ground reconnaissance of Cargo Muchacho, Fish Greek, Coyote, and Jacumba Mountains. Two small (less than 1 m^3 volume) rock slides occurred in a cut slope of fresh jointed gneiss along Interstate Highway 8 at Devils Canyon, in the Jacumba Mountains. However, in the same area no rock slides or falls were observed in the natural slope, which was as high and steep as the cut.

4.4.3 Rivers and Earthworks

Failures of canals and river and highway embankments took the form of settlements, slumps, incipient slumps, and incipient lateral spreads. The last three were most probably caused by inertial forces larger than the existing soil shear strength, or by loss of strength due to liquefaction, or by a combination of both (Youd and Wieczorek, 1982). In particular, they damaged

concrete lined irrigation canals and occasionally disrupted the flow of water. Settlements resulted from compaction of subsurface material, primarily artificial fill. Slump displacements as high as 1.0 m were observed in the river banks. In a few cases, the slump displacement combined with the settlement in the approach fill structurally damaged some bridges. Youd and Wieczorek (1982) reported that the traffic across several bridges was halted due to settlements of 150 mm in the bridge approach fill.

Slumping affected river, canals, and highways embankments. Slumps, including those in canal banks, were concentrated within 10 km of the surface rupture. The farthest known slump was 15 km away.

Rivers. Incipient slump cracks in river banks were observed for a distance of 34 km, along the New River between Seelay and Rutherford Roads north of Brawley, and for a distance of 40 km along the Alamo River between State Highway 98 and Wiest Lake. The reported cracks were generally 10 to 100 mm wide and roughly parallel to the nearby bank. In some places the crack openings were several tenths of a meter.

Slumps and incipient earth slumps were reported in the southwest part of Brawley and in a picnic area of River Park along the New River southwest of Brawley. Fissures having up to 50 mm vertical separation crossed County Highway S--80, about 125 m west of the New River, and also along both the New and Alamo Rivers (Castle and Youd, 1972).

Canals (1979 and 1940). The most extensively damaged canal was the All American Canal constructed in the late 1930's. The total damage to the canal was estimated to be about $982,000 (Youd and Wieczorek, 1982). Settlements, slumps, incipient slumps, and incipient lateral spreads occurred along a 13 km long section between Drop No.5 near the Ash Canal and the East Highline Canal. The damage was concentrated on a 1.5 km-long section of the All American Canal, near the Alamo River. The rapid repair of damage prevented any detailed mapping of the embankment deformations. Rotational earth slumps that threatened to breach the canal, incipient slumps, lateral spreads, and many undifferentiated fissures caused extensive cracks on the embankment and also in the compacted

fill around the structures. Along the All American Canal, the damage was distributed as far as 10 km east and 3 km west of the Imperial fault. Youd and Wieczorek (1982) reported that there was no evidence of large scale liquefaction around the canal, but localized liquefaction may have contributed to failure in some places.

Slumping and incipient slumping which extended approximately 500 m along the east side of the East Highline Canal, east of Holtville, was another example of canal damage during the 1979 earthquake. A third canal that suffered damage was the South Alamo Canal. In one place and for a length of 100 m, both sides of this canal were badly cracked, with a crack zone width of 15 m and vertical crack offsets of 50 to 100 mm.

Also, the east bank of the South Alamo Canal showed fissures in a 0.5 km length, located from 1.0 km north of State Highway 98 to the right angle turn south of the sand dunes. These fissures were caused by incipient slumping or lateral spreading toward the canal. The cracks reported at this site showed as much as 100 mm of opening and vertical offset.

Other sites which also suffered from slumps during the 1979 earthquake include: the Barbara Worth Drain, 4 km west of Holtville, and the banks and part of the shoulder of Worthington Road which slumped into a drainage ditch parallel to the road.

Clark (1940), Ulrich (1941), and Sylvester (1979) reported that during the 1940 earthquake the damage to the canals extended from Holtville in the north to the Solfatara Canal in the south, including Holtville Main Drain, All American, East Highline, Central Main, Alamo and Solfatara Canals for a total length of 119.7 km. This canal damage in 1940 was much more extensive than in 1979. This is consistent with the comparison of lengths of fault rupture for the two earthquakes, discussed earlier. Although many of the same sites were damaged during both the 1979 and 1940 events, in several of them the damage was more severe in the 1940 earthquake. Canal damage caused by slumping of banks in 1940 extended from Holtville, California, to the Solfatara Canal in northern Mexico, but in 1979 it extended only from Holtville to the United States--Mexican border

(Youd and Wieczorek, 1982). Although the damage was not clearly associated with the occurrence of liquefaction in the 1940 earthquake, the soil in the affected areas generally contains sand layers, whereas that in unaffected areas does not (Strahorn, et al., 1924).

Irrigation and Drainage Systems. In the Imperial Valley, water for domestic, industrial, and agricultural use originates at the Colorado River and is transported to a network of canals by the All American Canal. Tile drains from agricultural fields are connected to a network of drainage canals which empty into the Salton Sea. The canals and drains are either unlined or lined with unreinforced concrete. During the 1979 Imperial Valley earthquake, the irrigation and drainage network was temporarily disrupted. Damage consisted of cracked canal linings, soil slumps, pipe breaks, and nonoperating gates. A detailed discussion of specific damage sites is presented in Youd and Wiezorek (1982). The distribution of damage to irrigation and drainage systems was recorded in some detail by the Imperial Irrigation District (1980a, b, and c) and was analyzed for this case history investigation.

Figure 11 shows a plan view of the Southern half of the Imperial Valley on which are superimposed circles and triangles representing repairs to the drainage and irrigation network as reported by the Imperial Irrigation District (1980a, b, c). The triangles represent damage to pipelines, inlets, and outlets and the circles represent repairs to cracked canals or where slumps occurred. Also shown in the figure are the outlines of the sandy soils as reported on the US Department of Agriculture (USDA) soil survey map of 1924 (Strahorn, et. al., 1924). These sandy soils are described as gravelly, fine, loamy, or coarse sands, riverwash, and dune sand. The areas not identified as sandy soils are clay and silty clay deposits.

The drainage and irrigation network forms a grid over the area affected by the 1979 earthquake. Thus, a correlation may be drawn between rates of repair and soil type. Other than repairs to canals which crossed the fault, about half of the repairs were in or on the margins of sandy soils, and half were in clayey soils. Since the sandy soils comprise only about 20% of the total land area, it is estimated that four out of five repairs would occur in canals in sandy soils

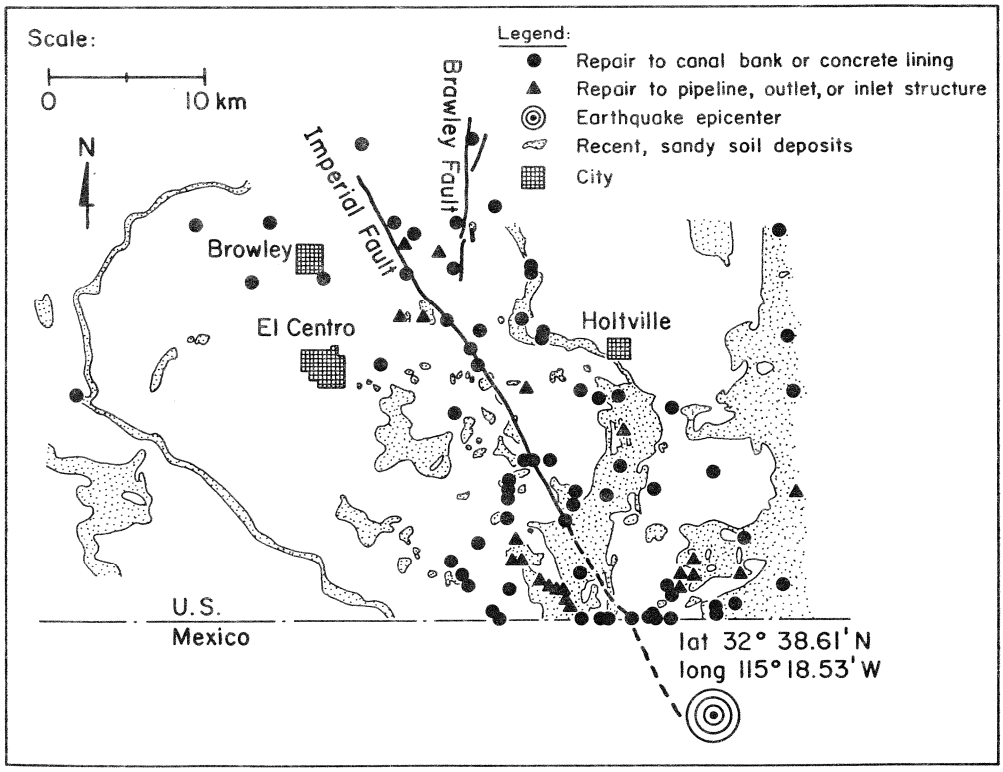

Figure 11. Relationship Between Repairs to Irrigation and Drainage Systems and Recent Soils (Soil Distribution after Strahorn, 1924)

if the sandy and clayey soils were distributed equally. Accordingly, the USDA soils map appears to be a useful tool for predicting the broad distribution of damage to pipelines or canals in this seismically active region.

Figure 12 presents the frequency of repairs as a function of the shortest distance to the Imperial or Brawley faults. At each repair location the shortest distance to either the Imperial or Brawley fault was measured. Each bar on the histogram represents the fraction of total repairs within a 1 km wide band parallel to, and on both sides of, the corresponding fault. The total number of repairs was 89. A clear trend of decreasing damage as the distance to the fault increases can be seen in this plot. Because the spatial distribution of irrigation and drainage systems was more or less uniform over the whole area, Fig. 12 reflects mainly the effect on damage of attenuation of ground shaking intensity with distance. Approximately 50% of the repairs occurred within

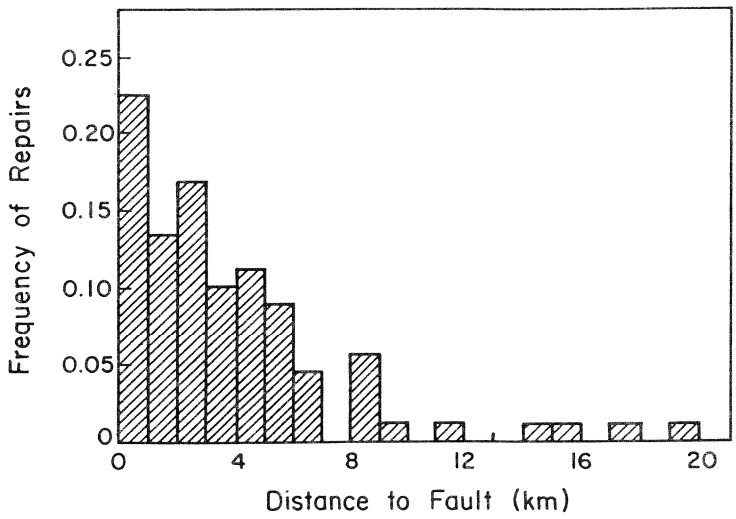

Figure 12. Frequency of Repairs to Irrigation and Drainage Facilities versus Distance to Imperial or Brawley Faults

3 km of either fault and about 95% of the repairs occurred within 10 km of either fault. The frequency of repairs was evenly distributed east and west of the faults.

The rate of repair, expressed as repairs/km, is shown in Fig. 13 as a function of distance from either fault as defined above. The length of canal and pipeline within 1--km--wide bands either side of the causative faults was estimated by measuring the length of canals in each square mile section of the U.S. Geological Survey Quadrangle maps. The mean length of the canals in any section was found to be 4.8 km/square mile, which equals 1.82 km/km^2. The similarity in shape of the histograms in Figs. 12 and 13 relates to the fact that the density of irrigation conduits is relatively constant within the area of study.

Peak horizontal and vertical accelerations recorded by the El Centro strong motion accelerometer array (see Figs. 7 and 9) are superimposed on the histogram of frequency of repairs in Figure 14. As shown in Fig. 7, the six stations east of the Imperial fault were closer to the Brawley fault, while the seven stations west of the Imperial fault were closer to the Imperial fault; the corresponding shortest distances to the corresponding fault are used in Fig. 14. When two array stations are at the same distance from the faults, the average peak acceleration of the two is plotted. For example, at Array Station 6, which is

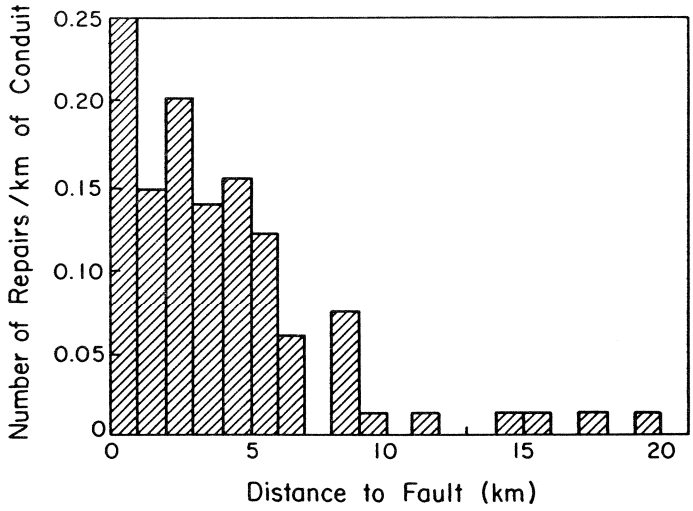

Figure 13. Number of Repairs/km versus Distance to Imperial or Brawley Faults

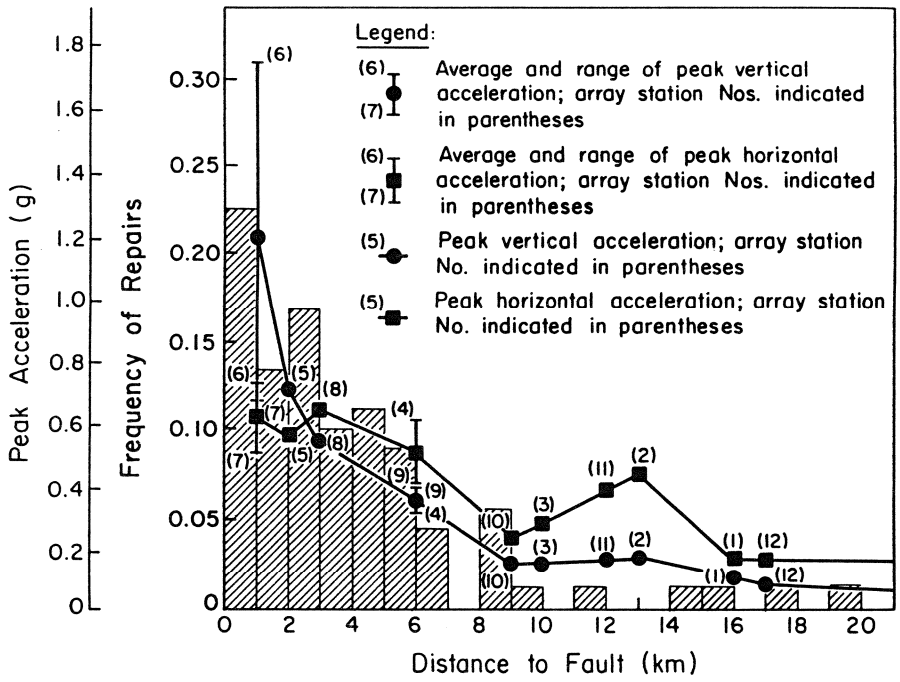

Figure 14. Frequency of Repairs to Irrigation and Drainage Facilities and Peak Vertical Acceleration versus Distance to Imperial or Brawley Faults

1 km from the Brawley fault, the peak horizontal acceleration was 0.72 g and at Array Station 7, which is 1 km from the Imperial fault, the peak horizontal acceleration was 0.52 g. The average peak horizontal acceleration, 0.62 g, is plotted as a square, and the peak horizontal acceleration range, 0.52 to 0.72 g, is represented by a vertical bar in the figure. The average peak vertical accelerations at Array Stations 6 and 7 are also plotted in the figure in a similar manner.

The attenuation curve for the peak vertical acceleration in Fig. 14 closely follows the trend of the frequency of repairs as a function of distance to the corresponding fault. The peak horizontal acceleration also shows a trend generally consistent with repair frequency, although the trend is not as well matched with repairs as that of the vertical accelerations. For distances to the fault up to about 9 km, both acceleration and repair frequency decrease rapidly with distance. Beyond 9 km, the frequency of repairs is low and more or less independent of distance; a similar trend is present in the acceleration curves, with the horizontal acceleration increasing somewhat between 9 and 13 km.

Clearly the need for repairs increased as the accelerations became more severe. Such a trend can be represented by an exponential function which is relatively simple in form and easy to evaluate.

To establish an upper bound relationship between number of repairs and peak acceleration, exponential regressions were developed as shown in Figs. 15a to 15d. These regressions represent conservative estimates of damage because their exponential form, by definition, requires that points of zero repair are discounted from the relationships. The number of repairs is related to the number of repairs per kilometer by dividing number of repairs by the approximate length of canals within a 1-km wide band.

There appears to be a well defined trend between the number of canal repairs and both peak horizontal and vertical acceleration. As shown in Figs. 15a and 15b, the coefficients of determination, r^2, are 0.72 and 0.68 for exponential

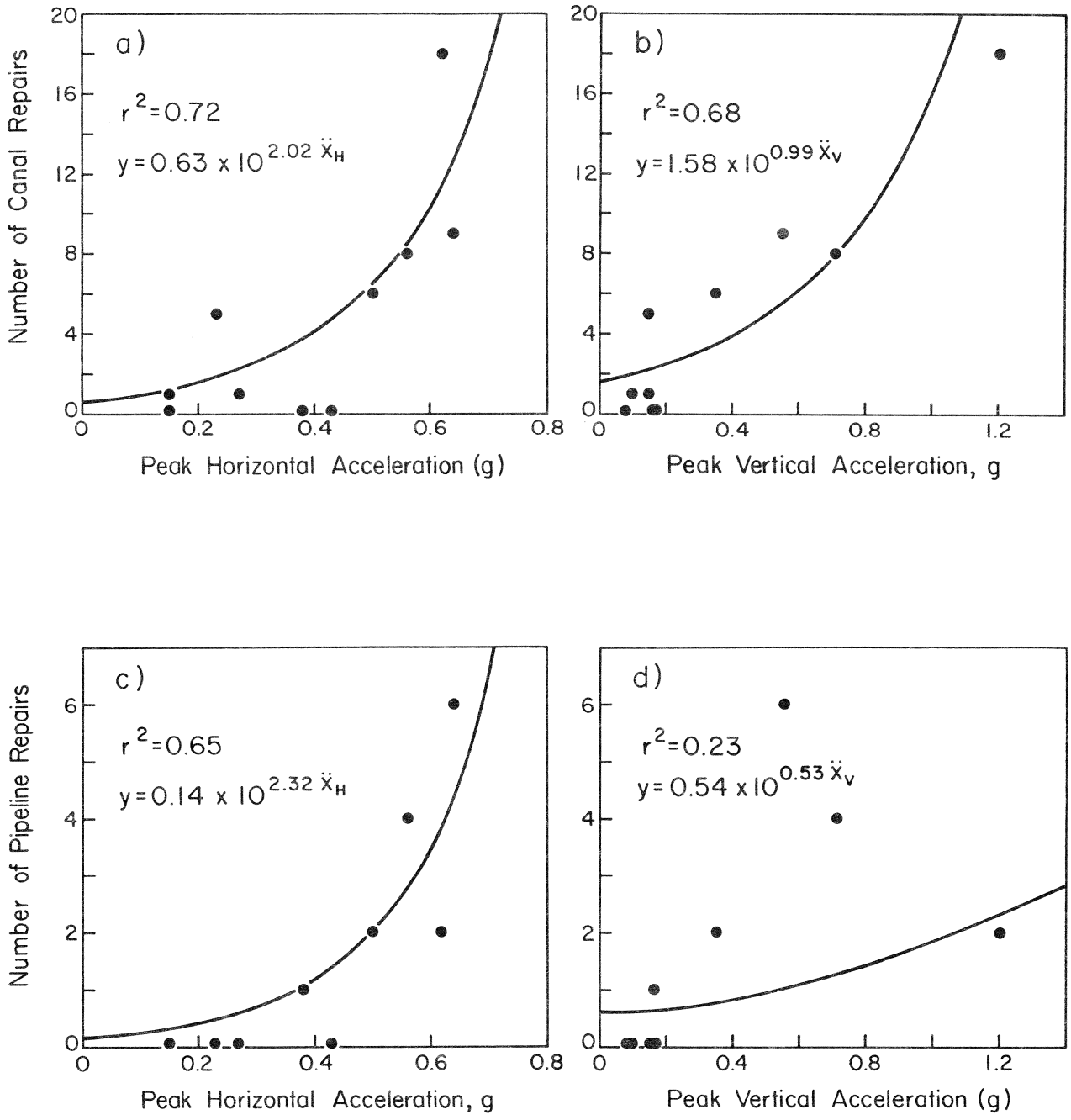

Figure 15. Relationships Between Number of Repairs to
a) Canals vs. Peak Horizontal Acceleration
b) Canals vs. Peak Vertical Acceleration
c) Pipelines vs. Peak Horizontal Acceleration
d) Pipeline vs. Peak Vertical Acceleration

regressions relating non-zero repairs and peak vertical and horizontal accelerations, respectively.

Figures 15c and 15d show the number of pipeline repairs in the irrigation and drainage system as a function of peak horizontal and peak vertical accelerations. Figure 15c shows that the non-zero number of repairs correlates reasonably well with peak horizontal acceleration. In contrast, Figure 15d does not show a clear relationship between number of pipeline repairs and peak vertical acceleration. The lack of a correlation between pipeline damage and vertical acceleration is consistent with theoretical models. Vertically oriented ground motion causes mainly bending deformation in horizontal pipes and the associated pipeline strains are from one to two orders of magnitude less than the longitudinal strains caused by horizontally oriented components of ground motion (O'Rourke, et al., 1985).

The frequency of repairs was also investigated with respect to distance from the earthquake epicenter. Circular arcs centered at the epicenter were drawn at radial increments of 5 km. The number of repairs within each band was then counted. The results of the analysis are presented as the histogram of Fig. 16. The number of repairs decreases as the epicentral distance increases. Moreover, 60% of the repairs are within 5 to 20 km of the epicenter. Data were not available for the closest 5 km, which were located in Mexico. An anomalously large group of 7 repairs was observed at a distance of 45 to 50 km from the epicenter. These data can be attributed to the aftershock which occurred near Brawley around midnight on the 15th of October. This aftershock was reported by the residents of Brawley to have been stronger than the main shock: MMI VIII versus MMI VII, respectively, Nason (1982).

Highway Bridges at New River. Although several highway bridges were damaged by the 1979 Imperial Valley earthquake, the most severe damage occurred at Bridges 58-05 R/L, which is the New River crossing of Highway 86. The two parallel bridges, constructed in 1953, are located about 3 km west of the City of Brawley and 41 km north west of the earthquake epicenter as shown in Fig. 17. Each bridge is a 60 m long span of reinforced concrete slabs supported on nine sets of six piles. The piles are Raymond step-tapered shells below groundline with

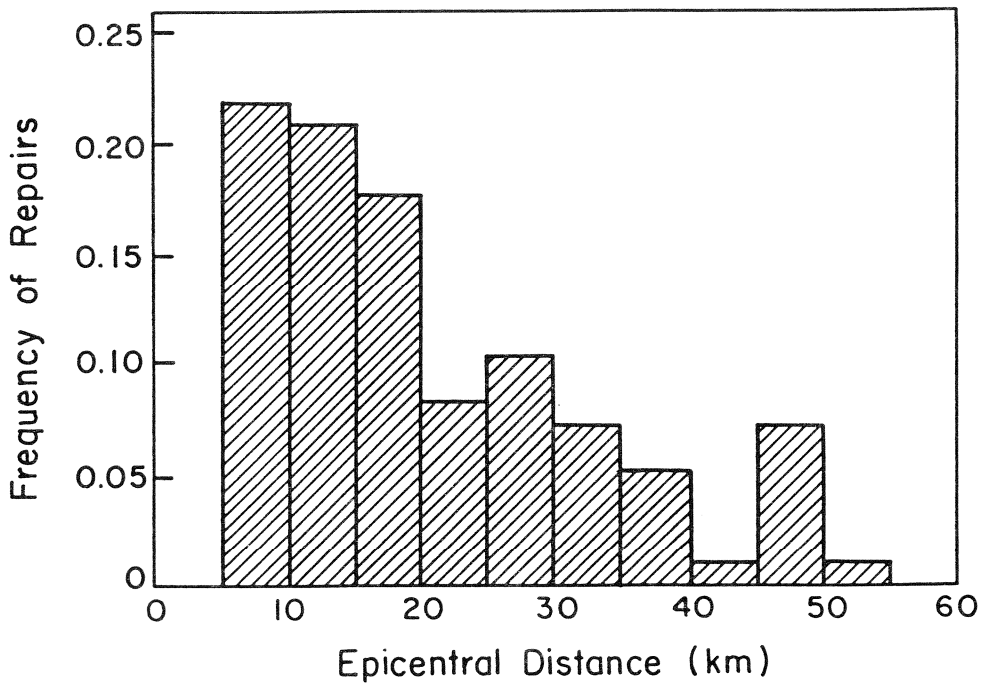

Figure 16. Frequency of Repairs to Irrigation and Drainage Facilities versus distance to Epicenter

octagonal cast--in--place PCC extensions to the caps. The minimum depth of embedment of the piles was about 9 m.

A longitudinal view of the bridges is shown in Fig. 18. The subsurface conditions are presented qualitatively in the figure on the basis of borings prepared by the California Division of Transportation in 1951. The soils were described in the boring logs as fine to very fine loose sand with laminations of clay, silt, and silty sand to depths of 7--12 m below the ground surface. Underlying the loose, fine sand is dense, fine, clean sand. At the time of the exploration borings, the water table was located as shown in the figure. No in--situ penetration or laboratory tests were performed.

Before the 1979 earthquake, settlement and downslope movement of the embankment soils had been observed and epoxy had been applied to cracks in the concrete at the tops of piles. The maximum pre--earthquake soil movements were estimated to

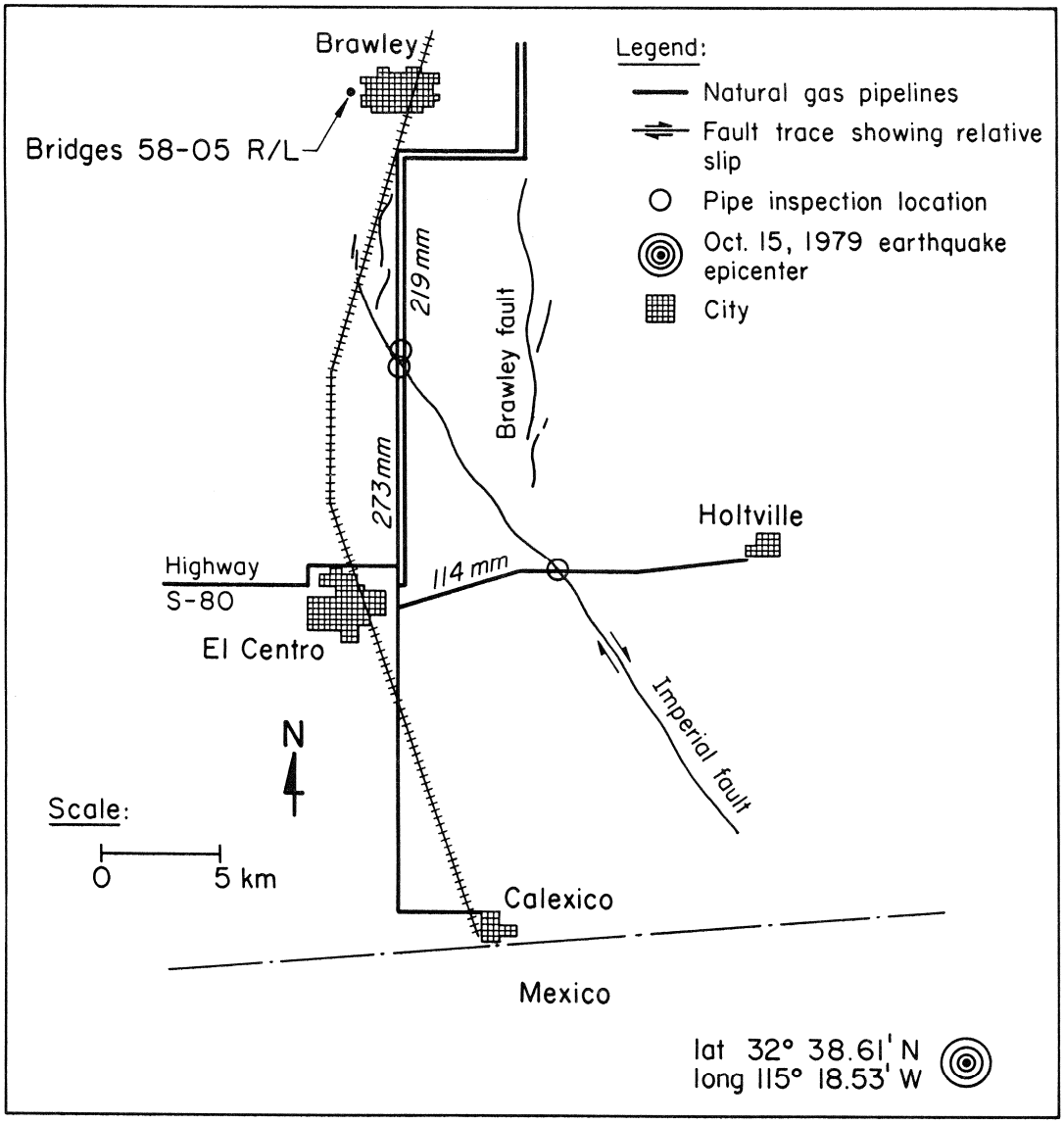

Figure 17. Location of Bridges 58-05 R/L and Natural Gas Pipelines Intersected by the 1979 Imperial Fault

be 175 mm; equivalent to the estimated maximum movement that resulted from the earthquake (Degenkolb and Jurach, 1980).

A plan view showing the location of earthquake-induced ground cracks and the relative movements of the bridges is shown in Fig. 19. Ground cracks and soil slumping were observed on both the east and west river banks. Soil slumped

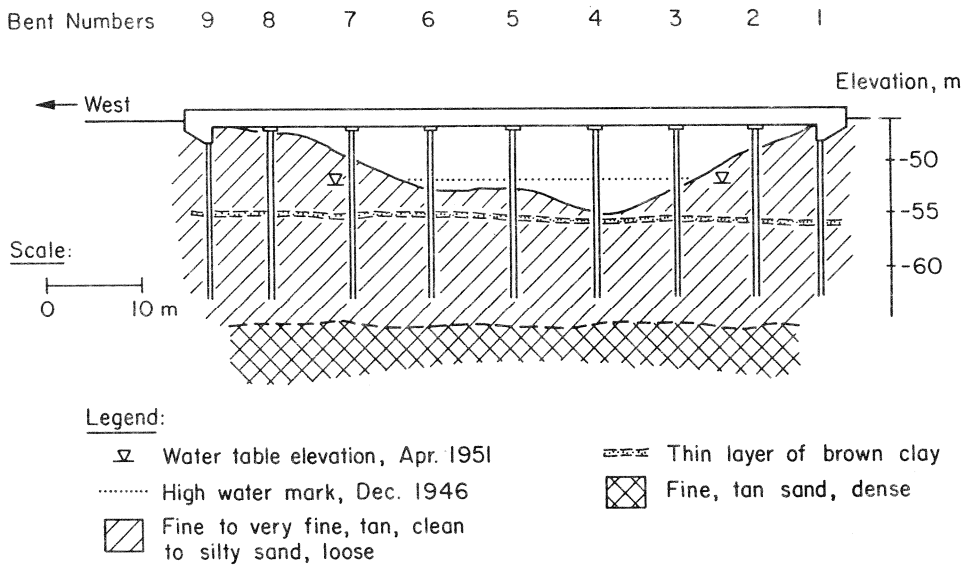

Figure 18. Profile View of Bridges 58--05 R/L at New River Showing Presumed Subsurface Conditions

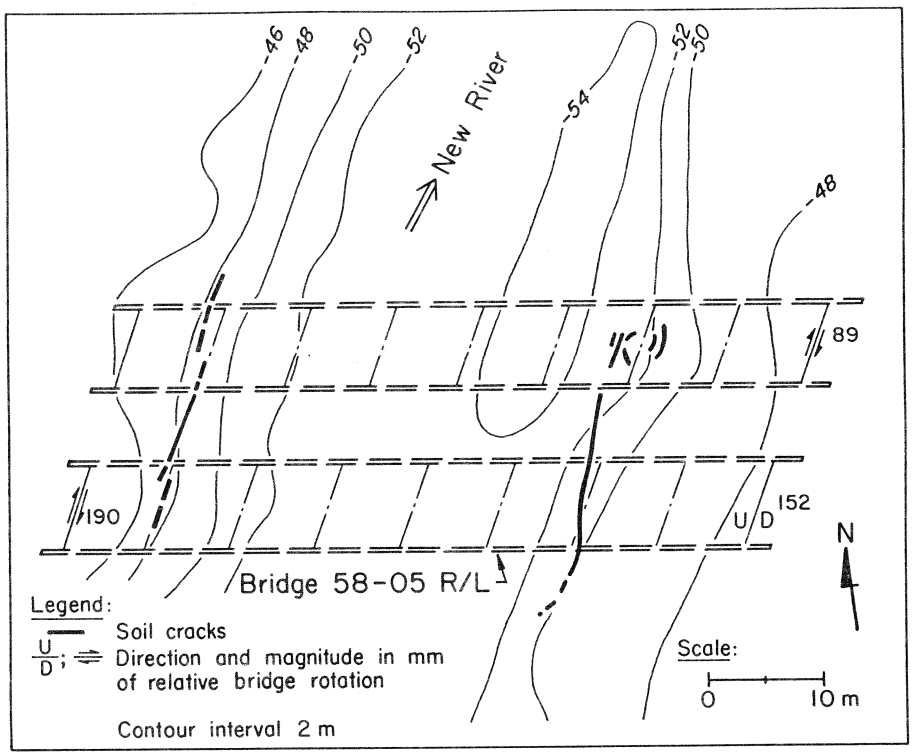

Figure 19. Plan View of Bridges 58--05 R/L Showing Ground Surface Topography and Location of Ground Cracks (after Youd and Wieczorek, 1982)

toward the river at least 100 mm (Youd and Wiezorek, 1982). Conical depressions had formed on the downslope side of the base of the piles, and soil was compressed around the upslope faces. Settlement around the piles was measured as 40 mm. No sand boils were seen beneath the bridges.

Accounts of damage to the bridges were presented by Youd and Wieczorek (1982), Degenkolb and Jurach (1980), and Wosser, et al. (1982). Damage was relatively slight. Counterclockwise rotation of the superstructure in a horizontal plane cracked and tilted the support piles and the wingwalls. The tops of piles at Bent 2 (see Fig. 18) had open horizontal cracks on their northern faces and spalls on their southern. Similarly, the top of the piles at Bent 8 had open horizontal cracks on their southern faces and spalls on their northern faces. The piles at Bents 2 and 8 were tilted 3.2° in the direction of bridge rotation (Youd and Wiezorek, 1982). The relative rotation of the bridges and the pattern of concrete damage at the tops of the piles was most likely caused by southwestern movement of the foundation soils on the east bank of the river and northeastward movement of the foundation soils on the west bank of the river.

An 89-mm-diameter natural gas line, which was attached to the outside of the northern edge of the north bridge, was influenced by the bridge rotation. The gas line was buried along the north shoulder of Highway 86 and then was attached to the bridge with binding U bolts as it crossed the New River. Upon removal of the support bracket at the east wing wall, the pipeline was observed to deform northerly 13 mm. With successive aftershocks, the line continued to deflect northerly until it was offset about 150 mm (Degenkolb and Jurach, 1980). The line was pinched closed by Southern California Gas Company as a safety precaution until the aftershock activity subsided. The pinched section was then replaced with new piping without incident (McNorgan, 1990).

Evidence such as ground cracks, soil slumping, and the presence of loose saturated sands suggests that liquefaction of the bridge foundation soils may have occurred. At New River Park, located about 1 km south of the bridges, hundreds of sand boils, a slump, and numerous ground cracks were observed (Youd and Bennett, 1983). Youd and Bennett performed soil borings and a liquefaction potential analysis for the New River Park site. They concluded that

liquefaction occurred in two distinct soil layers; a loose silty flood plain deposit and the top of a thick point-bar deposit that was overlain by a clay layer. Because of the similarity in depositional environments, it is possible that soils at the New River bridge crossing were likewise prone to liquefaction.

4.5 Damage to Pipelines

Earthquake effects on lifeline systems, including electrical power, transportation, and water and sewage facilities, has been described in several sources (e.g., Leeds, 1980, and U.S. Geological Survey, 1982). Of particular interest here is the damage sustained by natural gas and water pipelines. Difficulties with gas pipelines were caused primarily by surface faulting along the Imperial fault, whereas damage in water distribution and trunk systems was due primarily to traveling ground wave effects. Damage to pipelines in the irrigation and drainage network, as well as damage to a gas pipeline near a bridge over the New River, have been discussed in Section 4.4.3.

4.5.1 Natural Gas Pipelines

Three natural gas pipelines operated by the Southern California Gas Company (SCG) were affected by ground deformation along the Imperial fault. The locations of the pipelines relative to the Imperial fault are shown in Fig. 17. Two high pressure lines are located along Dogwood Road, and the third crosses the fault about 6.4 km east of the City of El Centro along County Highway S-80. Information about the pipelines, including installation date, composition, coating, joint type, depth of soil cover, and operating pressure, is presented in Table 4. Although pipeline breaks did not occur, SCG decided to excavate the lines so that visual inspections could be performed.

Pipeline Along Highway S-80. Along Highway S-80, about 60 m north of the westbound lane, a 114-mm-diameter natural gas pipeline was intersected by the Imperial fault. To evaluate the magnitude of fault displacement imposed on the pipeline since its 1948 installation, it is important to recognize that fault deformation at this site was actually the sum of three components: preseismic creep, coseismic slip, and afterslip. As mentioned before in Section 4.2 and

Table 4. Characteristics of the Pipelines Influenced by Fault Movements During the 1979 Imperial Valley Earthquake

Characteristics	Pipeline Location		
	North Side State Rt. S-80	EastSide Dogwood Rd. Line No. 6000	West Side Dogwood Rd. Line No. 6001
Installation Date	1948	1948	1966
Dimensions	114 mm O.D. 5 mm wall	219 mm O.D. 7 mm wall	273 mm O.. 5 mm wall
Composition	A - 25 Steel	API Grade B Steel	Grade X - 42 Steel
Weld Type	Acetylene	Electric Arc	Electric Arc
Coating	No. 56 [a]	Somastic [b]	No. 56 [a]
Depth of Cover	900 mm sandy backfill dumped and rolled	900 mm sandy backfill dumped and rolled	900 mm sandy backfill dumped and rolled
Operating Pressure	2.8 MPa	2.8 MPa	5.0 MPa
Yield Stress	170 MPa	240 MPa	290 MPa

[a] No. 56 coating consists of successive layers of: 1) red oxide primer, 2) filled asphalt, 3) two spiral wraps of cellulose acetate, 4) filled asphalt, and 5) paper wrapper

[b] Somastic coating composed of asphalt, aggregate, and fiber mixture

shown in Fig. 6, these three types of slips had been monitored at County Highway S--80.

Using Eq. 1 with a = 207 and 129.3 (see discussion in Section 4.2), 408 mm of slip was calculated for the coseismic slip of the October 15 earthquake plus the afterslip accumulated until November 20, 1979, the time of the pipeline inspection. Therefore, between the time of installation and inspection, it is possible that 600 mm of cumulative fault displacement had occurred at the

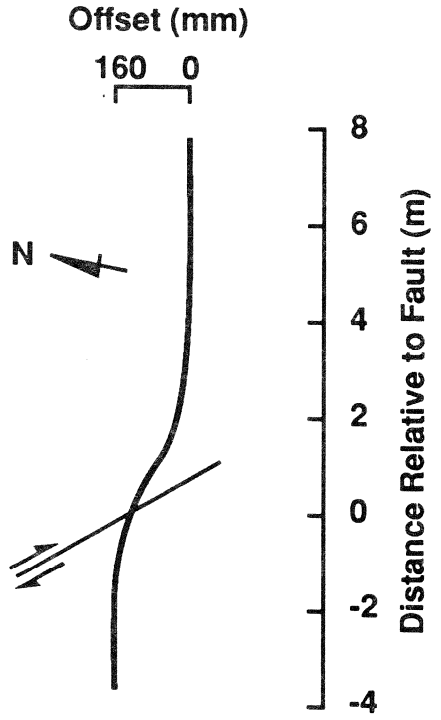

Distance from Fault (m)	Offset from Linear Length (mm)
6.1	6
5.5	6
4.9	3
4.3	0
3.7	0
3.0	13
2.4	19
1.8	32
1.2	57
0.6	89
0	117
0.6	133
1.2	140
1.8	146
2.4	146
3.0	143
3.7	140

Figure 20. Deformed Shape of 114 mm Natural Gas Pipeline Along Highway S--80 after Excavating 9.8 m Long Trench

pipeline by preseismic creep, coseismic slip, and afterslip. Another estimate of the cumulative fault displacements is given by Hart (1981), who observed 1000 mm of offset in the old pavement of Highway S--80 since the 1940 earthquake.

A detailed description of the pipeline inspection along Highway S--80 is provided by McNorgan (1989). The inspection of the pipeline by SCG began with a 9.8 m--long excavation centered at the fault. Upon removal of the backfill it was noted that the pipeline was deformed in an S--shape. The displacements perpendicular to the pipeline, relative to its position at the western edge of the trench, were measured by SCG personnel (McNorgan, 1989). A sketch of the pipeline--fault intersection, the deformed shape of the pipeline, and the results of these initial measurements are presented in Fig. 20. The measurements disclose a maximum offset of approximately 146 mm within a 9.6 m wide zone astride the fault centerline.

Due to the orientation of the pipeline with respect to the fault movement, net tensile stresses within the pipline were induced by the right-lateral fault displacement. Stresses in the pipeline were relieved by excavating the backfill. Since no pipeline damage was observed, the excavation was backfilled without further remediation.

Pipelines Along Dogwood Road. Two high pressure pipelines, 219 mm and 273 mm in diameter, crossed the Imperial fault at two places along Dogwood Road, approximately 9.5 km north of the City of El Centro. The locations of the fault-pipeline intersections are shown by circles in Fig. 17. The main fault intersected the pipelines at about 60° and a splay of the fault intersected the pipelines about 170 m north of the main fault at an angle of 17°.

The pipelines along Dogwood Road were also subjected to preseismic fault creep, coseismic slip and afterslip. The closest preseismic creep observation station was at the intersection of the Imperial fault with Worthington Road, 4 km southeast of the Dogwood Road site. A nail file had been installed there in 1977, about two years before the October 15, 1979 earthquake. The creep rate determined by this nail file during the two year monitoring period was about 8 mm/yr. Thus, the magnitudes of preseismic creep imposed on Pipeline Nos. 6000 and 6001 may have been as high as 248 mm and 104 mm, respectively. These are believed to represent upper bound values of the preseismic creep because the preseismic creep rates measured at Worthington Road were influenced by an abnormally high displacement of 15 mm in 1978. Cohn, et al. (1982) have suggested that a more accurate estimate of the preseismic creep rate would be 5 mm/yr.

Displacements caused by coseismic slip and afterslip on the main fault were calculated using Eq. 1. The values of the constants a and b were 94 and 59, respectively, Sharp, et al. (1982). Thus, 186 mm of combined coseismic slip and afterslip were calculated for the day the pipeline was inspected on November 21, 1979, and about 250 mm of combined slip were calculated for the day the pipeline was cut in February 1981. Between the time of installation and cutting, it is possible that 400 mm of cumulative fault displacement had been imposed on the 219-mm-diameter pipeline, and 315 mm of displacement on the

273-mm-diameter pipeline. Vertical displacements were also imposed on the pipeline. Twelve days after the earthquake, 50 mm of vertical displacement, southwest side up, were measured by Hart (1981).

At the fault splay which intersected Dogwood Road, 170 m north of the main fault, vertical displacements resulting from coseismic slip and afterslip were estimated on the basis of a predictive equation developed by Sharp, et al. (1982). On the day the pipelines were cut in February 1981, it is estimated that 284 mm of vertical displacement had been imposed on the pipelines.

A detailed description of the inspection of pipeline No. 6001 is given by McNorgan (1989). The 273-mm-diameter pipeline was inspected in a short excavation located at the fault crossing and the section of the pipe south of the fault was found to be displaced westward 70 mm. The excavation was increased to 11 m and additional lateral displacements were observed. Approximately 16 m of the pipeline were exposed and inspected 6 m north of the original excavation. During excavation the pipe was observed to deflect eastward 250 mm. Similarly, 6 m south of the original excavation the pipeline was exposed for a length of 18 m and the pipeline was observed to deflect eastward 180 mm. The two excavations were then backfilled and the 6 m of backfill immediately north and south of the original excavation was removed. Pipeline deflections did not occur in either of these two 6 m long excavations.

Due to the orientation of the pipeline with respect to the fault movement, compressive stresses were known to exist in the pipelines. Because of this potentially hazardous condition, SCG elected to relieve the stresses in the pipeline using a carefully planned procedure. Details of the stress removal operation carried out in February 1981 are presented in McNorgan (1989). To relieve the compressive stresses, a 3 m long section of pipe was removed. After removing the pipe section and excavating 61 m of the line, approximately 120 mm of expansion were observed.

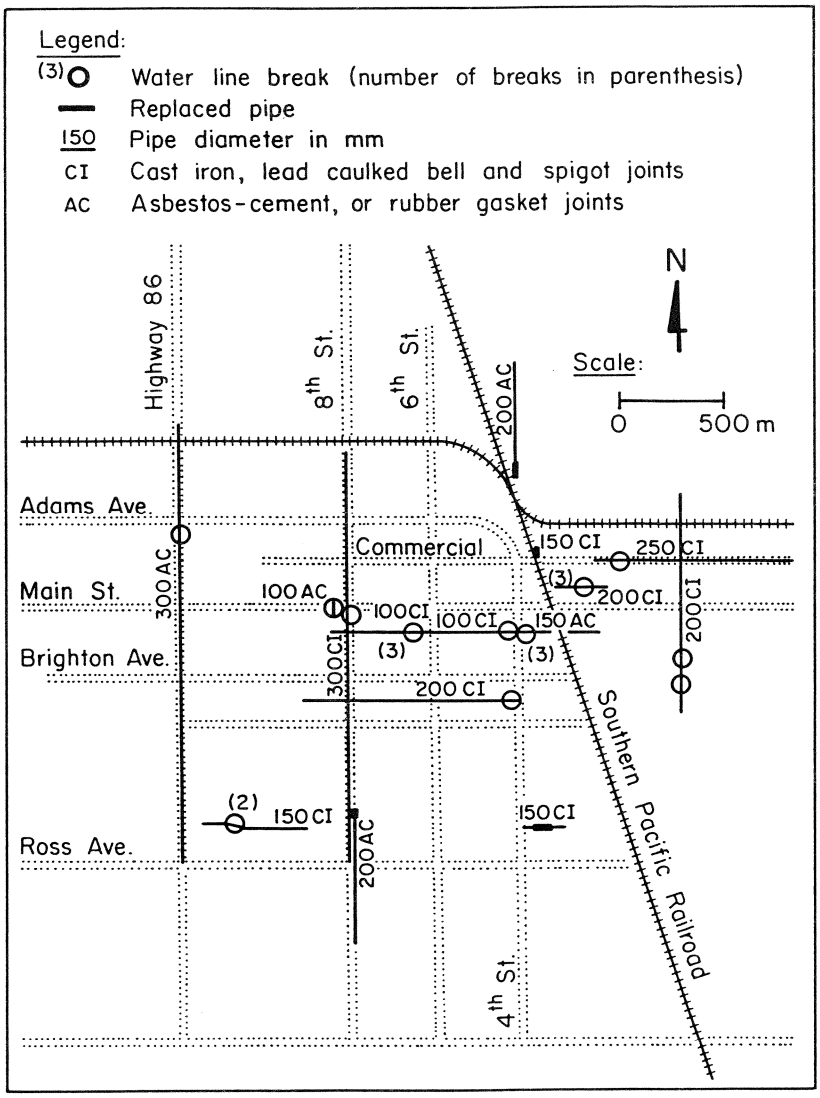

Figure 21. Plan View of the City of El Centro Showing Repaired and Replaced Water Lines

4.5.2 Pipeline Performance in the City of El Centro

The City of El Centro is located 30 km north of the earthquake epicenter and 10 km west of the nearest fault break. A MMI of VII was estimated for El Centro (Nason, 1982). After the earthquake, 25 pipeline breaks were found in the water supply network (Eguchi, 1982). Water line repair and replacement locations compiled by the City of El Centro are shown in Fig. 21. The repair

Table 5. Water Pipeline Breaks, Lengths, and Break/Length Ratios in the City of El Centro, California (after Eguchi, 1982)

Pipe Materials	Parameters	Pipe Diameter Range (mm)				Total
		<150	200 - 280	300 - 400	450 - 890	
Asbestos-Cement	Breaks	4	1	1	0	6
	Length (km)	51.83	30.41	13.79	3.73	99.76
	Ratio (breaks/km)	0.077	0.033	0.074	--	0.06
Cast Iron	Breaks	10	8	1	--	19
	Length (km)	6.86	6.33	5.34	--	18.53
	Ratio (breaks/km)	1.45	1.26	0.19	--	0.03
Steel	Breaks	--	--	--	0	0
	Length (km)	--	--	--	4.6	4.6
	Ratio (breaks/km)	--	--	--	--	--

records were checked with studies performed by Eguchi (1982). Three types of pipelines were in service at the time of the earthquake: cast iron pipes, asbestos cement pipes, and steel mains. The pipeline diameter in millimeters for each damaged line is shown in the figure. The locations of pipeline breaks are shown as open circles with a number adjacent to the circle indicating the number of breaks. Replaced line segments are indicated by heavy solid lines.

Table 5 shows the distribution of breaks and the break to-length ratio as a function of pipeline diameter and material type. Six breaks occurred in asbestos cement pipes and 19 breaks occurred in cast iron pipes. The highest break-to-length ratio occurred in the 150 mm and 200 mm cast iron pipelines with lead-caulked bell and spigot joints. These pipes were installed about 40 years ago in the older parts of the City. Most were installed without cement lining which would have protected them against internal corrosion (Eguchi, 1982). All breaks, in both the asbestos cement and the cast iron pipes, were longitudinal splits which occurred away from the joints (Eguchi, 1982; Waller and Ramanathan, 1980).

Subsurface conditions in the City of El Centro generally consist of 3.5 m of stiff clay overlying lenses of silty sand. The lenses of silty sand are below the water table which is artificially recharged by irrigated farmlands (Shroeder, 1990). No ground failures (Youd and Wiezorek, 1982) or surface fault breaks were reported in this area (Sharp, et al., 1982). The observed pipeline damage was most likely the result of travelling ground wave effects.

4.6 The Heber Road Site

4.6.1 Location and Surficial Observations of Liquefaction

The Heber Road site is located 1.6 km northeast of the beginning of the Imperial fault surface rupture (Figs. 2, and 4). At this site a significant lateral spread caused damage to Heber Road. The spread, 160 m wide and about 100 m long, shifted the road and a parallel canal toward a 2 m deep depression in Heber Dunes County Park. This depression is a remnant of the old stream channel that previously passed through the area (Fig. 22). Arcuate ground cracks and scarps formed around the margins and head of spread. Sand boils erupted at several places on the spread (Youd and Wieczorek, 1982; Youd and Bennett, 1983).

In December 1988, Youd and Bartlett surveyed the site to determine the exact amounts and locations of ground deformations for Heber Road. They assumed that the road and canal were straight before the earthquake between the sections surveyed. The outcome of this effort, reproduced in Fig. 23, shows a maximum of 4.24 m (13.9 ft) lateral spread observed on the southern edge of the unlined canal adjacent to the road. The northern edge of the canal, closer to the road, moved laterally up to 2.29m (7.5 ft).

4.6.2 Soil Conditions and Acceleration Records

Youd and Bennett (1983) described the soil conditions at Heber Road site (Fig. 24) as:

> A 0.9 m to 1.5 m thick layer of sandy fill caps the Heber Road site. Beneath the fill, the cross-section contains a 3.4 m to 4 m thick layer composed of silt and fine sand with three distinct subunits. A dense fine sand of point-bar origin (Unit A_1) lies beneath the fill in the western

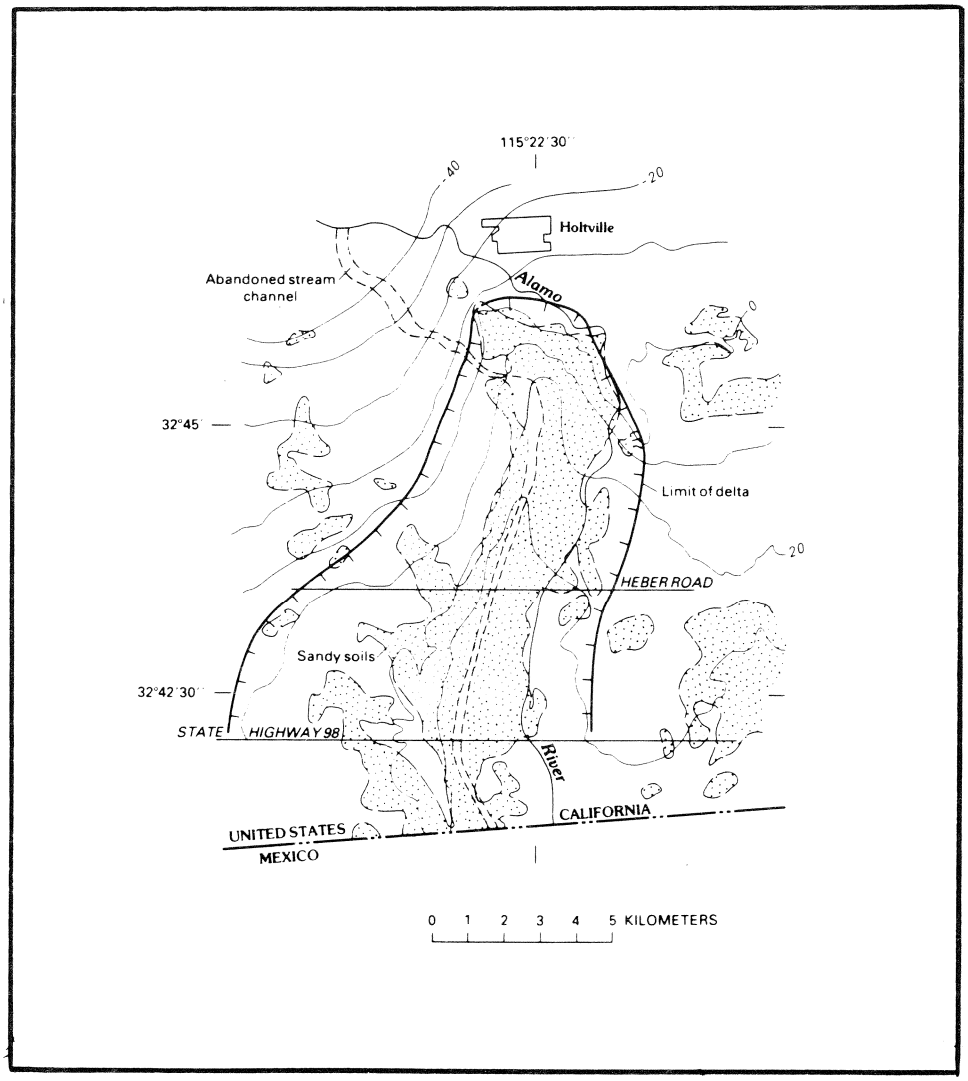

Figure 22. Locations of Heber Road, Old Delta, and Buried Stream Channel. Contour Interval, 10 ft (0.305 m) (Youd and Wieczorek, 1982)

part of the section. This sand is characterized by static cone point resistances of 110 kg/cm^2 to 180 kg/cm^2 (mechanical) or 120 kg/cm^2 to 260 kg/cm^2 (electrical) and SPT--values of 29 to 36 blows/ft (safety hammer) or 32 to 35 blows/ft (donut hammer). The central part of the section contains loose, very fine sand and silty sand that is a natural channel fill deposited by the ancient stream (Unit A_2). This sand is characterized by static cone point resistances of 10 kg/cm^2 to 40 kg/cm^2 (mechanical) or 10 kg/cm^2 to 50 kg/cm^2 (electrical) and SPT--values of 1 to 7 blows/ft (safety hammer) or 2 to 4 blows/ft (donut hammer). The eastern part of the section contains moderately--dense sand and silty--sand overbank deposits (Unit A_3 characterized by static cone point resistances of 25 kg/cm^2 to 75 kg/cm^2 (mechanical) or 20 kg/cm^2 to 125 kg/cm^2 (electrical) and SPT--values of 9 to 13 blows/ft (safety hammer) and 17

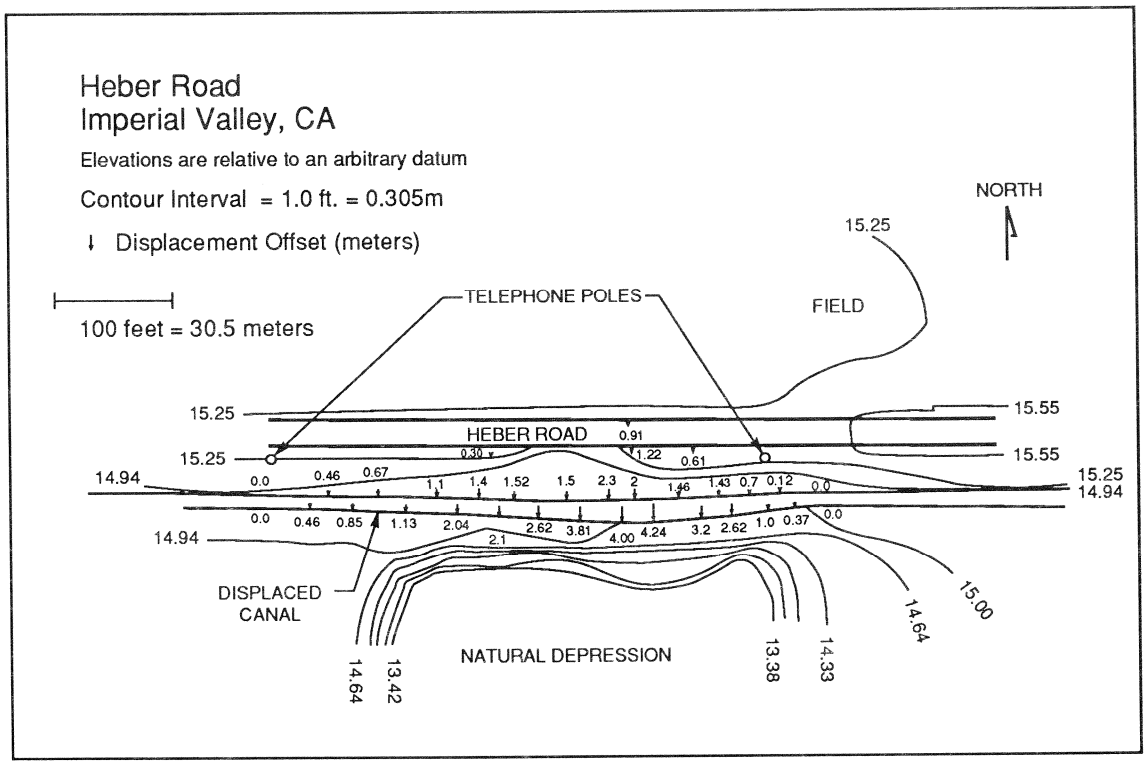

Figure 23. Heber Road Site Deformation Due to the 1979 Earthquake (Measurements and Mapping by S. F. Bartlett and T. Y. Youd)

to 19 blows/ft (donut hammer). The water table depth was at about 1.8 m during the tests in December 1979 and January 1981, and at about 2.6 m during the tests in May 1982. Below the fluvial sand units lie alternating, continuous layers of medium-stiff lacustrine clays and dense channel or deltaic sands. The electrical point cone resistance (CPT) values given above are consistent with results from similar tests at the Heber Road site reported by Douglas and Martin (1982).

Surficial effects of liquefaction were concentrated over Unit A_2 (Channel Fill, CF), the old channel, the loosest saturated sand in the section. Clearly, this is the unit that liquefied during the 1979 earthquake. Pore water pressures may have risen in the other sand units including Units A_1 (Point Bar, PB) and A_3 (Levee, L), but other than the linear array of sand boils over a drain line east of the channel, no surficial liquefaction effects occurred beyond the channel.

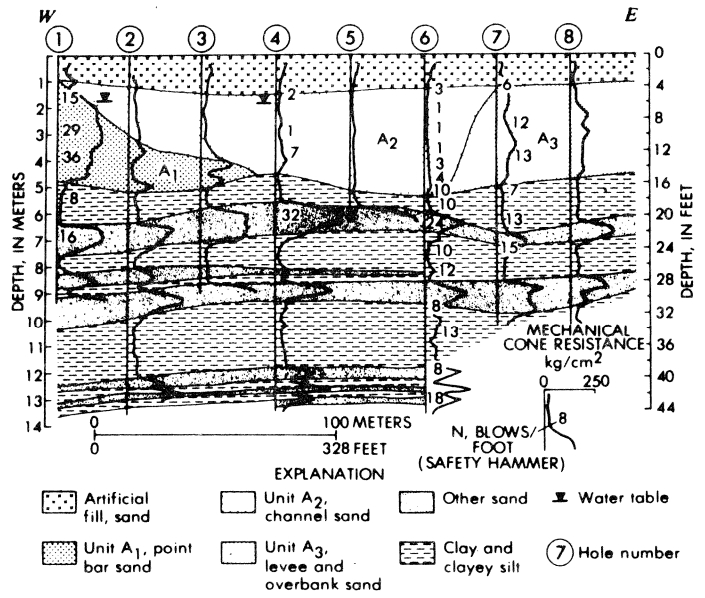

(a)

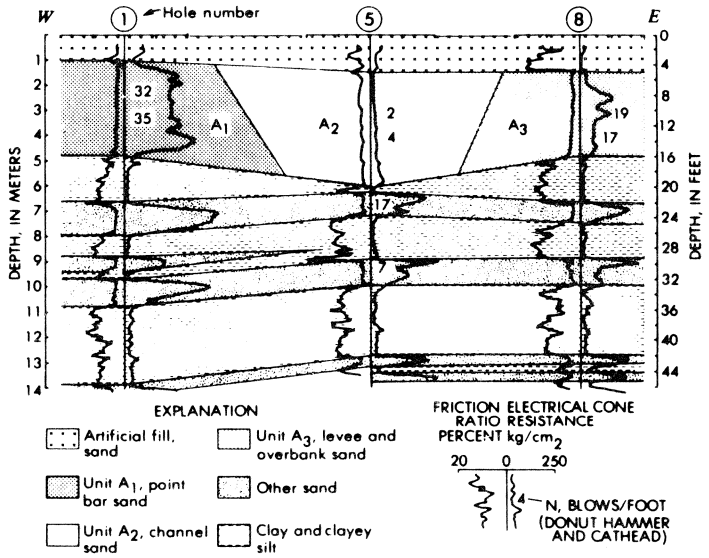

(b)

Figure 24. Soil Profile of Heber Road Site (Youd and Bennett, 1983)
a) Cross-section of sediments
b) Logs showing electrical CPT records and SPT N-values

Table 6. Results of Field Testing for Heber Road Site Reported by Youd and Bennett (1983)

Field Testing		Unit A_1 Point Bar	Unit A_2 Channel Fill	Unit A_3 Levee	Coefficient of Energy%
SPT blows/ft	Safety Hammer	29 - 36	1 - 7	9 - 13	68
	Donut Hammer	32 - 35	2 - 4	17 - 19	72
CPT kg/cm^2	Mechanical	110 - 180	10 - 40	25 - 75	
	Electrical	120 - 260	10 - 50	20 - 125	

1 kg/cm^2 = 98.07 KPa

Table 6 presents a summary of the information described above, as well as the coefficient of energy for the safety and donut SPT hammers used by Youd and Bennett (1983).

Four acceleration records were obtained at the stations closely surrounding the Heber Road site: Meloland, Holtville, Calexico, and Bonds Corner. A summary of recorded ground motion parameters during the 1979 earthquake is given in Table 7.

4.6.3 Field Investigations and Laboratory Testing

Extensive field investigations and laboratory testing programs were performed to determinate the soil properties at the Heber Road Site (HRS). Youd and Bennett (1983) performed CPT and SPT tests. Similar tests at the same site and at River Park site were performed by Douglas and Martin (1982). Sykora and Stokoe (1982) from the University of Texas conducted field seismic testing at the three sand deposits of the HRS to determine the variation of low amplitude shear wave velocity with depth (Fig. 25). These field seismic test results evidently reflect the different densities of the three HRS deposits. The grain size distribution in Fig. 26 shows that the three sands are similar, differing

Table 7. Summary of 1979 Earthquake Records Surrounding the Heber Road Site (Vucetic and Dobry, 1986)

Abbreviated Name	Name and Description	Site Geology	Epicentral Distance (km)	Distance From Fault (km)	Acceleration			
					Direction (azimuth)	Maximum		Duration (sec)
						Traced From Film (g)	From Tape After Processing (g)	
Meloland	El Centro, Meloland Road-Interstate Highway 8 Overcrossing, Ground	Alluvium	18	1	360° (N) up 270° (W)	0.32 - -	0.32 0.23 0.30	6 4 7
Holtville	Holtville Post Office, 1-story building	Alluvium	20	8	315° up 225°	0.22 0.31 0.26	0.22 0.23 0.25	7.5 7.0 6.2
Calexico	Calexico Fire Station, Fifth and Mery 1-story building	Alluvium	15	(9)	315° up 225°	0.22 0.21 0.28	0.20 0.18 0.27	9.5 8.8 10.8
Bonds Corner	Bonds Corner, Highways 98 and 115, 1-story building	Alluvium	6	(3,4)	230° up 140°	0.81 0.47 0.66	0.79 0.35 0.59	13.2 12.0 13.3

( ) = The values in brackets are perpendicular distances from an imaginary extension of the fault surface rupture.

only in their fines content, which is larger in the CF and smaller in the L and PB sands.

Laboratory tests were performed by three different groups: Kuo and Stokoe (1982) from the University of Texas (UT); Ladd(1982) from Woodward-Clyde Consultants (WCC), and Vucetic and Dobry (1988) from Rensselaer Polytechnic Institute (RPI). Kuo and Stokoe performed index properties tests, four static isotropically consolidated undrained triaxial tests ($\overline{CIU}$), and resonant column tests with application of small and large cyclic shear strains (low and high amplitude tests) at different isotropic confining pressures. The results of the low amplitude resonant column tests for each sand were reduced by Kuo and Stokoe to the single final relationship between effective confining pressure and low amplitude shear moduli, G_{max} shown in Fig. 27. At the WCC laboratory, the following tests were performed on PB and CF sands: index property tests; one $\overline{CIU}$ static and one $\overline{CIU}$ dynamic (fast loading) tests for each sand, twelve triaxial cyclic stress-controlled tests on undisturbed and composite reconstituted

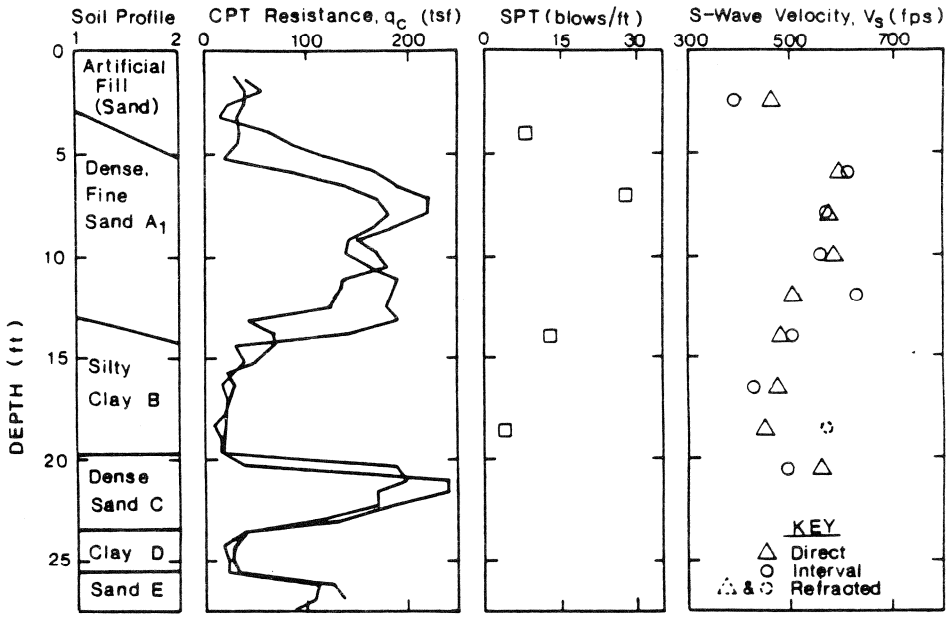

(a) POINT BAR SITE

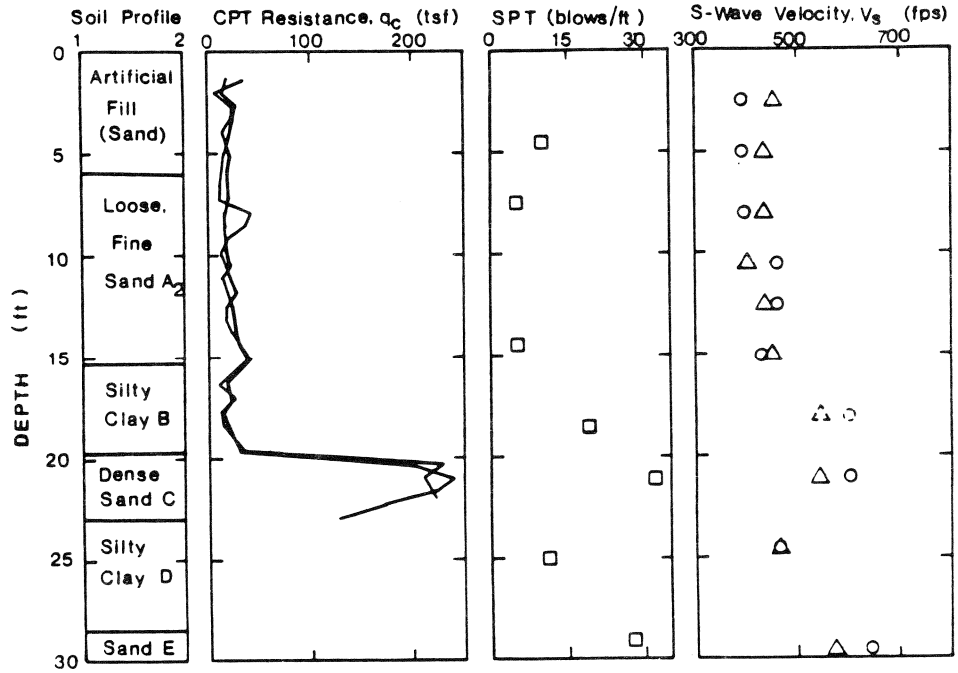

(b) CHANNEL FILL SITE

Figure 25. Composite Profile of the Two Studied Sites at Heber Road, Including V_s Measurements (Sykora and Stokoe, 1982)

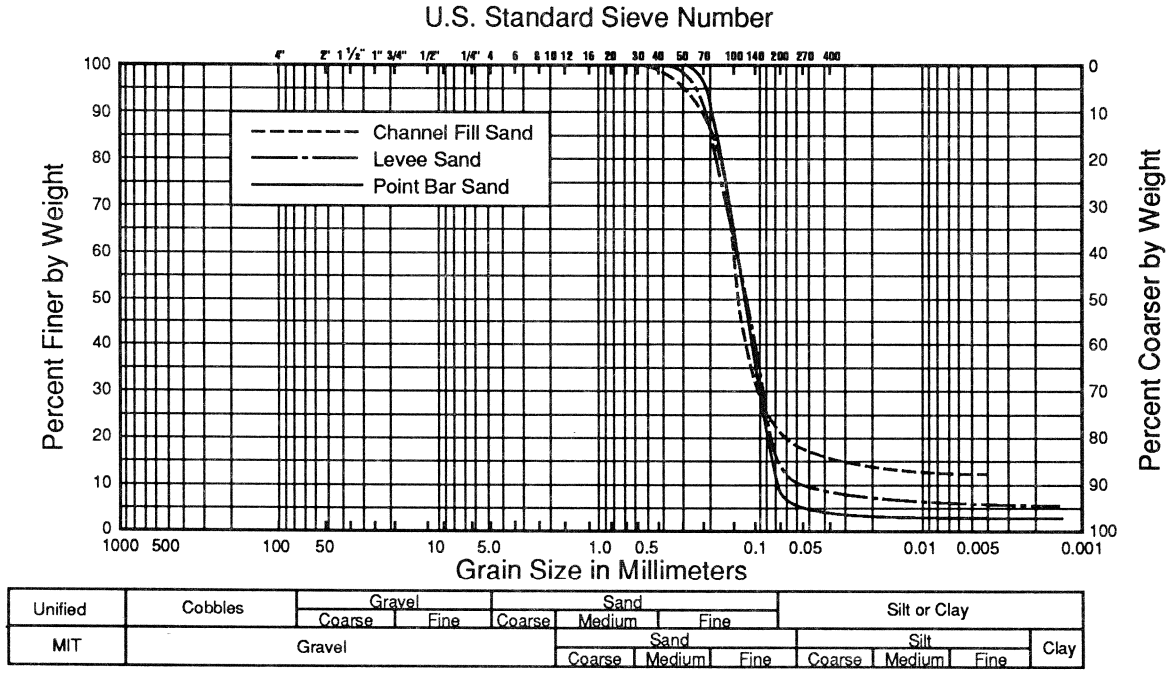

Figure 26. Grain Size Distribution Curves of the Heber Road Site Sands (Kuo and Stokoe, 1982)

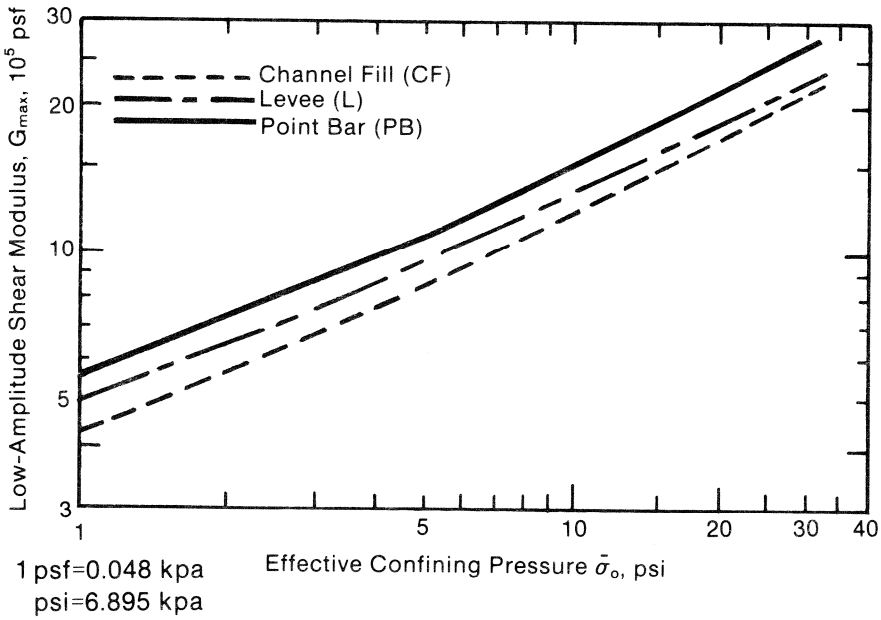

Figure 27. Summary of Average Variation in Low-Amplitude Shear Modulus with Confining Pressure for Loading Pressure Sequence (Kuo and Stokoe, 1982)

specimens with isotropic effective consolidation stresses 1.0, 1.5, and 2.0 ksf, and a series of nine cyclic strain-controlled tests on each sand including triaxial as well as NGI direct simple shear tests on both undisturbed and composite reconstituted specimens. At the RPI laboratory, eight triaxial cyclic strain-controlled tests were conducted on CF sand reconstituted at different densities.

Table 8 summarizes the results of the field and laboratory testing by USGS, UT, and WCC. The values of G_{max} in Table 8 are clearly associated with the three different relative densities of the three sands deposits as shown by the cone and standard penetration tests: CF is loose, L is medium dense, and PB is a dense sand. The higher values of G_{max} obtained in the lab compared to the measured G_{max} in the field could be due to disturbance during transportation of the tube samples to the lab, as discussed by Kuo and Stokoe (1982) and Vucetic and Dobry (1988).

4.6.4 Analysis

Youd and Bennett (1983) used the standard penetration charts developed by Seed (1979) and Seed, et al. (1983) to analyze the liquefaction at the Heber Road site. They assumed that the entire 3.7-m thickness of Unit A_1 liquefied and deformed during the earthquake. Thus a surface displacement of 2.1 m (7 ft), as occurred at the southern edge of the road during the 1979 earthquake over Unit A_1 near Hole 6, yields an average shear deformation of 58% for the layer. In this method, the maximum acceleration of 0.80 g recorded at Bonds Corner was used. From the analysis (Fig. 28), they found that for an earthquake of magnitude 6.6, the Channel Fill (Unit A_2) is highly susceptible to liquefaction and has large shear-strain (or deformation) potential, which is in good agreement with the observed field behavior. Figure 28 shows that Unit A_3 is also susceptible to liquefaction but with more limited shear-strain potential than Unit A_2. Figure 28 also shows that the Point Bar deposit (Unit A_3) is resistant to liquefaction, which is consistent with the fact that no surface evidence of liquefaction or shear deformation was found for that unit in the field.

Table 8. Summary of the Average Field and Laboratory Data Obtained by Four Different Teams for the Heber Road Site (Vucetic and Dobry, 1986)

Properties	FIELD RESULTS			LABORATORY RESULTS					
	Youd & Bennett (1983)-USGS Sykora & Stokoe (1982)-UT			Kuo & Stokoe (1982)-UT			Ladd (1982)-WCC		
	PB	L	CF	PB	L	CF	PB	L	CF
Soil Description or Classification Symbol	Dense fine sand	Loose very fine sand and silty sand	Moderately dense sand and silty sand	SP-SM	SM	SM	–	–	–
Unit Gravity, γ_s (pcf)	–	–	–	167.3	164.8	164.2	167.6	–	167.7
Mean Grain Size, D_{50} (mm)	0.112	0.081	0.107	0.12	0.12	0.13	0.14	–	0.13
Percentage of fines (%)	–	–	–	10	15	22	14.2	–	22.6
Average Standard Penetration Test - SPT, N (blows/foot)	32.5	12.5	2.6	–	–	–	–	–	–
Cone Penetration Test - CPT, Resistance (kg/cm^2)	203	71	18	–	–	–	–	–	–
Dry Unit Weight, γ_{dr} (pcf)	–	–	–	100.4	95.7	101.6	99.7	–	100.3
Void Ratio, e_o	–	–	–	0.67	0.72	0.62	0.69	–	0.67
Maximum Shear Modulus, G_{max} (ksf)	1283	786	734	970*	930*	820*	653*	–	856*
Permeability (cm/sec)	–	–	–	–	–	–	4.2×10^{-3}	–	1.2×10^{-3}

* G_{max} values measured in the two laboratories are corrected to account for the in-situ effective stresses

1 pcf = 16.02 kg/m^3 = 0.157 kN/m^3

1 kg/cm^2 = 98.07 KPa

1 ksf = 47.88 KPa

Castro (1987) used the same Bonds Corner record, a_{max} = 0.8 g, and the G_{max} field data obtained by Sykora and Stokoe (1982) to analyze the Heber Road site. In his method he used the Newmark type analysis to evaluate the lateral displacement (Fig. 29). He concluded that only the yield acceleration of Unit A_2 was less than the average acceleration computed for the sliding block during the earthquake,thus suggesting that only this unit would experience large deformations. This is in agreement with the field observations. He backfigured from the 1.68 m measured average displacement of the road, a value of 4.79 Kpa yield strength from Fig. 29. This is consistent with the very loose condition of the soil as indicated by the low measured blow counts (SPT) of 0 to 1 blow/ft and cone penetration resistance (CPT) of about 490 to 1471 Kpa.

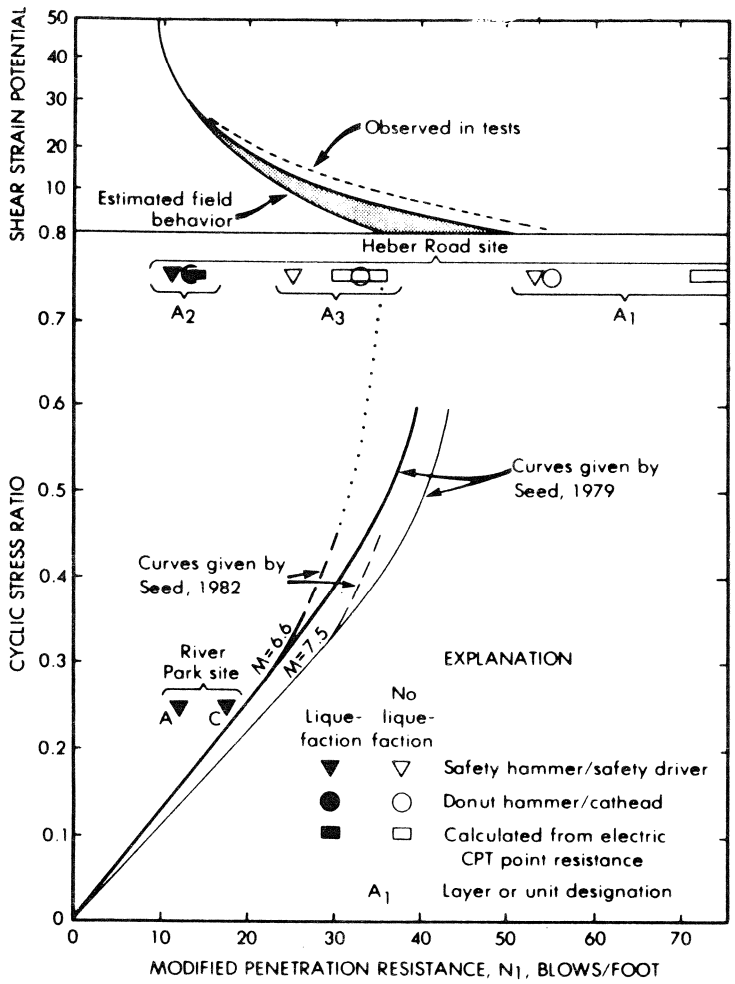

Figure 28. Liquefaction Susceptibility and Shear Strain Potential Chart Prepared by Seed, 1979 and Seed & Idriss, 1982, with SPT Data from Heber Road and River Park Sites (Youd and Bennett, 1983)

It must be noted that both Youd and Bennett (1983) and Castro (1987) utilized the maximum and average observed displacements reported at the time (2.1 and 1.7 m, respectively). These numbers are consistent with displacements measured north of the canal in the subsequent survey shown in Fig. 23, but they are smaller than those measured at the southern edge of that canal (4.2 m maximum displacement).

Bierschwale and Stokoe (1984) used the values of shear wave velocities measured at Heber Road site and other saturated sandy sites affected by the 1979 and 1981 earthquakes, in conjunction with estimated peak ground accelerations for the same sites to produce the site liquefaction evaluation chart of Fig. 30.

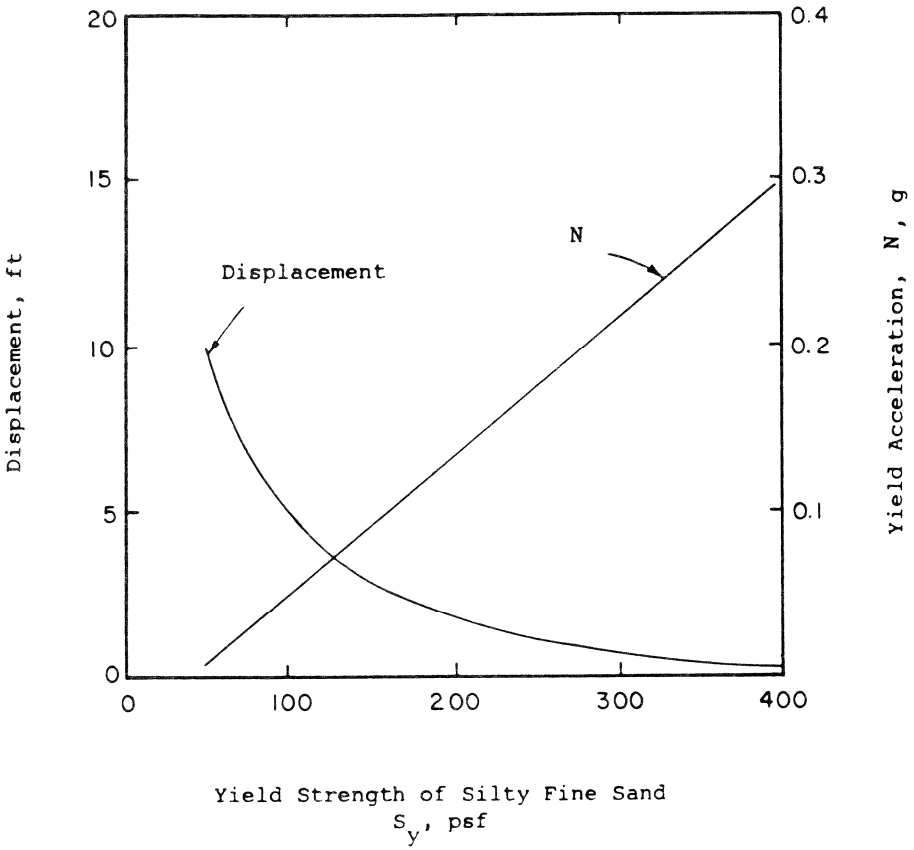

1 psf = 0.048 kpa

Figure 29. Calculated Displacements for Heber Road Using Newmark's Sliding Block Method (Castro, 1987)

5.0 THE APRIL 26, 1981 WESTMORLAND EARTHQUAKE

5.1 Felt Effect, Maximum Intensity, and Surface Faulting

On April 26, 1981 a moderate-magnitude earthquake (M_L = 5.6, McJunkin and Kaliakin, 1981; M_W = 5.9, Youd and Wieczorek, 1984) occurred at 0509 PDT. The epicenter was located about 8 km N-NW of Westmorland, Imperial County, California (Fig. 31) at approximate 33.102° N latitude and 115.637° W longitude (McJunkin and Kaliakin, 1981). Westmorland, the community closest to the epicenter, suffered more damage than other areas. Many buildings in Westmorland sustained some nonstructural damage from the main event. McJunkin and Kaliakin (1981) reported that in this area a number of unreinforced adobe buildings partially collapsed and many mobile homes were jolted from their supports. Some

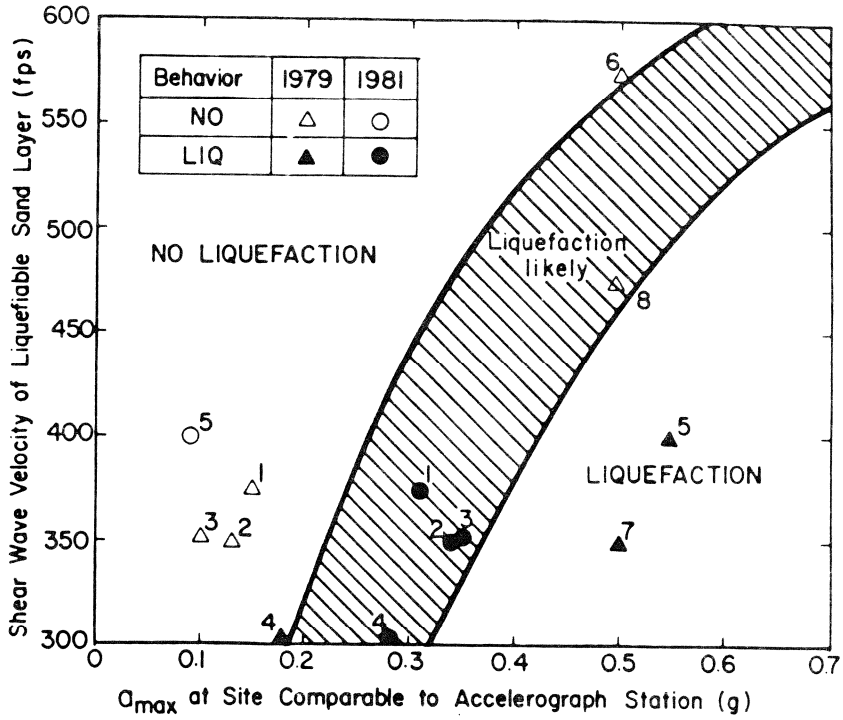

Figure 30. Influence of Shear Wave Velocity on Liquefaction Potential of Sand, from Field and Parametric Studies, Imperial Valley, California, M = 5.5 to 6.5, NRC, 1985, Source: Bierschwale and Stokoe (1984)

damage to irrigation canals and levees were also reported from seismic shaking. The total damage estimate exceeded 1.5 million dollars. No surface faulting was reported for this event in the epicentral region either by CDMG or USGS. However, the investigators from CDMG and USGS did observed surface rupture along segments of the Superstition Hills and Imperial faults (see Figs. 1 and 4 for locations of faults and epicenters). A maximum of 14 mm right-lateral offset along approximately two-thirds of the mapped trace of Superstition Hills fault was reported by McJunkin and Kaliakin (1981).

5.2 Recorded Accelerations

Three CDMG stations and 22 out of 29 USGS stations within 28 km of the epicenter recorded the earthquake (Fig. 31). Of these, six stations with epicentral distances ranging between 7 and 24 km recorded peak horizontal accelerations larger than 0.10 g (Table 9). All of these stations were on the deep alluvial soil deposits representative of the area, except for the Superstition Mountain

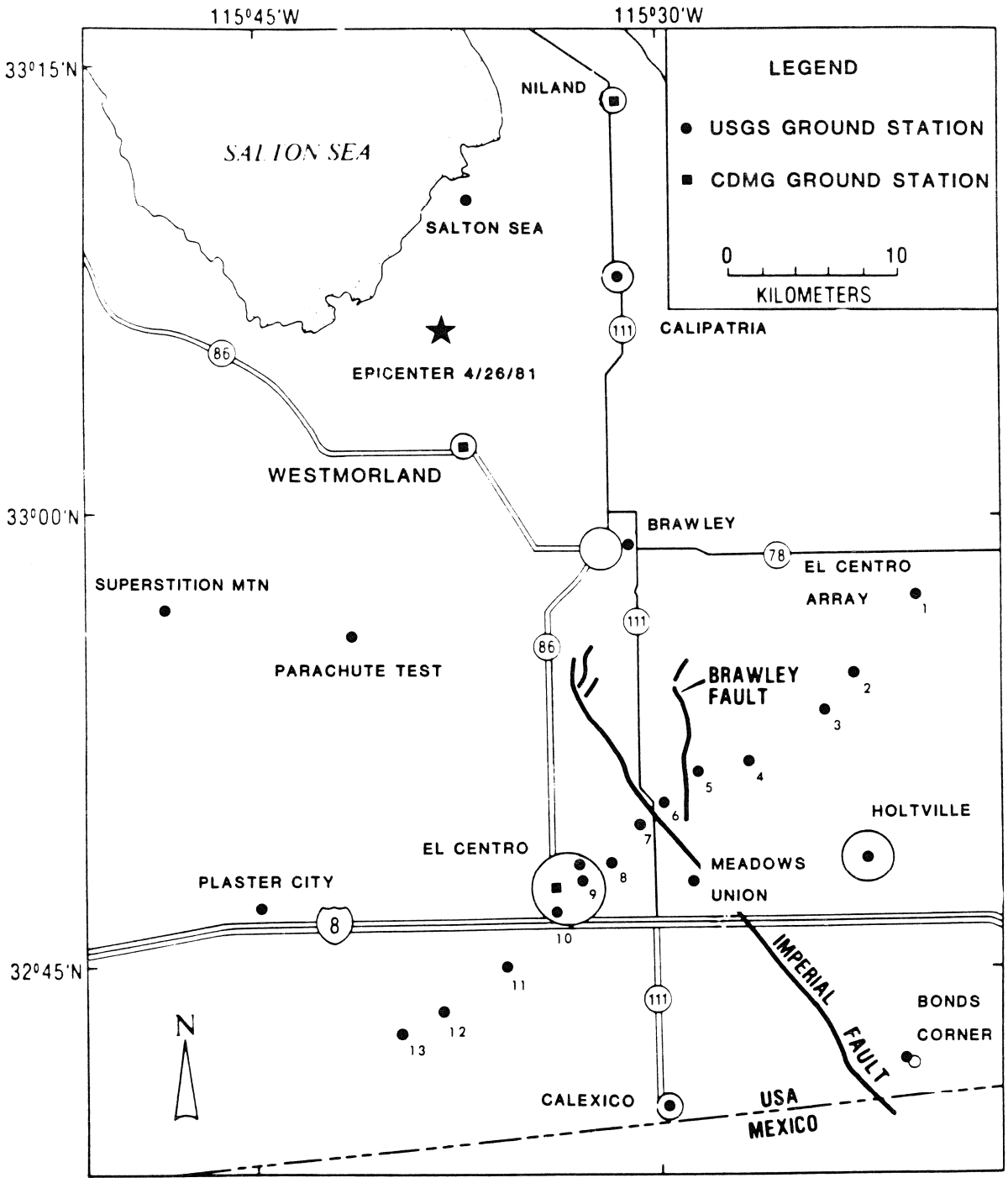

Figure 31. Strong-Motion Stations in Imperial Valley during the 1981 Earthquake (Maley and Etheredge, 1981)

Table 9. List of CDMG and Some USGS Strong-Motion Accelerograph Stations Which Recorded the April 26, 1981 Westmorland Earthquake

	Station	Site Geology	Epicentral Distance km	Acceleration Components: g			Operated By
				Vertical	Horizontal	Horizontal	
1	Westmorland	deep alluvial	7	0.8	0.49	0.39	CDMG
2	Salton See	deep alluvial	9		0.22		USGS
3	Brawley	"	17		0.18		"
4	Miland	"	19	0.13	0.19	0.11	CDMG
5	Parachute Test Facility	"	20		0.23		USGS
6	Superstition Mountain	granite	24		0.11		"
7	El Centro	"	35	<0.05	<0.05	<0.05	CDMG

station, which is on granite (Maley and Etheredge, 1981). The largest recorded acceleration was 0.49 g, at a 7 km epicentral distance.

5.3 Ground Failure

Youd and Wieczorek (1984) visited many localities north of Westmorland, covering a 150 km^2 area, after the 1981 earthquake. They observed surface liquefaction effects including sand boils, fissures, slumping, lateral spreading, and ground settlement in many places. All these locations lie in the northwestern part of the Imperial Valley between Westmorland and the Salton Sea. All except one of the 1981 liquefaction sites visited by Youd and Wieczorek were within an epicentral distance of 14 km. The most distant site showing surficial effects of liquefaction was in the New River flood plain about 100 m east of the KROP radio tower, 14.2 km away from the epicenter. As evidenced by eruption of very small amounts of water through the 1979 sand boils at this site after the 1981 earthquake, Youd and Wieczorek suggested that this site was probably shaken with an intensity near the threshold for generating liquefaction in the underlying sediment during the 1981 event.

Small fissures were observed as far as 14.2 km from the epicenter. The largest fissure was 300 mm wide, with a scarp as high as 200 mm. It appeared in connection with slumping toward a river and was reported at an epicentral distance of 11 km. Sand boils were observed both in groups and individually, with diameters ranging from 0.15 m to as much as 20 m. Lateral spreading, resulting in a few tenths of a meter displacement caused by soil weakening due to liquefaction, was reported 2.7 km northwest of Westmorland. At that site no other secondary effects of liquefaction, such as sand boils, were observed. North of the Alamo River, about 4.5 km south of Calipatria, the shape of fissures indicated development of a minor lateral spread toward the Alamo River. Also, at several places along the Alamo River within the Imperial Wildlife Management area, segments of the bank as wide as 5 m collapsed into the river. At one place, a 2 to 3 m of river bank slumped into the river cutting a small road (Fig. 32). Later, this slump seems to have controlled the direction of lateral spreading of the ground toward the river in the 1987 earthquake (Section 6.3). At this site, in 1981, numerous sand boils and fissures were also reported concentrated near the channel. Some, however, were located as far as 100 m from the river.

5.4 Wildlife Soil Profile

As mentioned above and also earlier in Section 3.0, the Wildlife site liquefied during the 1981 Westmorland earthquake. Since then this site has been under extensive investigation. A team from USGS (Bennett et al., 1984) performed a thorough field exploration including cone penetration (CPT) and standard penetration (SPT) tests.

The soil profile at this site (Fig. 33) is described by Bennett, et al. (1984) as follows:

> The deposit between a depth of 0 and 2.5 m (Unit A) consists of very loose and very soft interbedded micaeous sandy silt, silt, and clayey silt.
>
> The deposit between a depth of 2.5 m and 6.8 m (unit B) contains two subunits, B_1 (2.5 m –3.5 m) and B_2 (3.5 m –6.8 m). Subunit B_1 consists of very loose to loose, dark grayish–brown, moderately sorted sandy silt. Small–scale cross bedding is common. The contact between subunits B_1 and B_2 is gradational. Subunit B_2 consists of loose to medium dense, dark

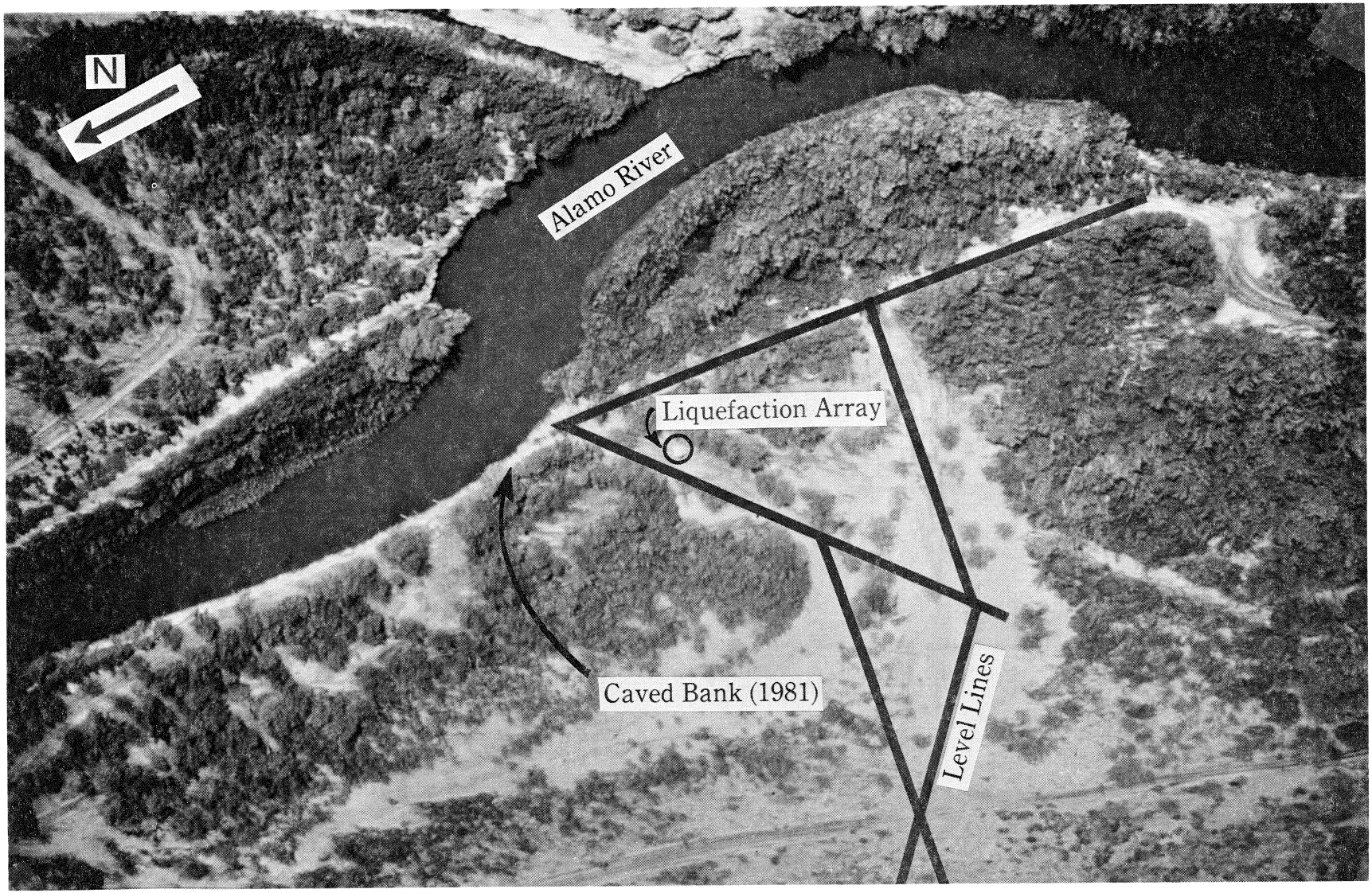

Figure 32. Aerial Photograph Showing Alamo River Location of Wildlife Array, and Slump in the Bank of Alamo River

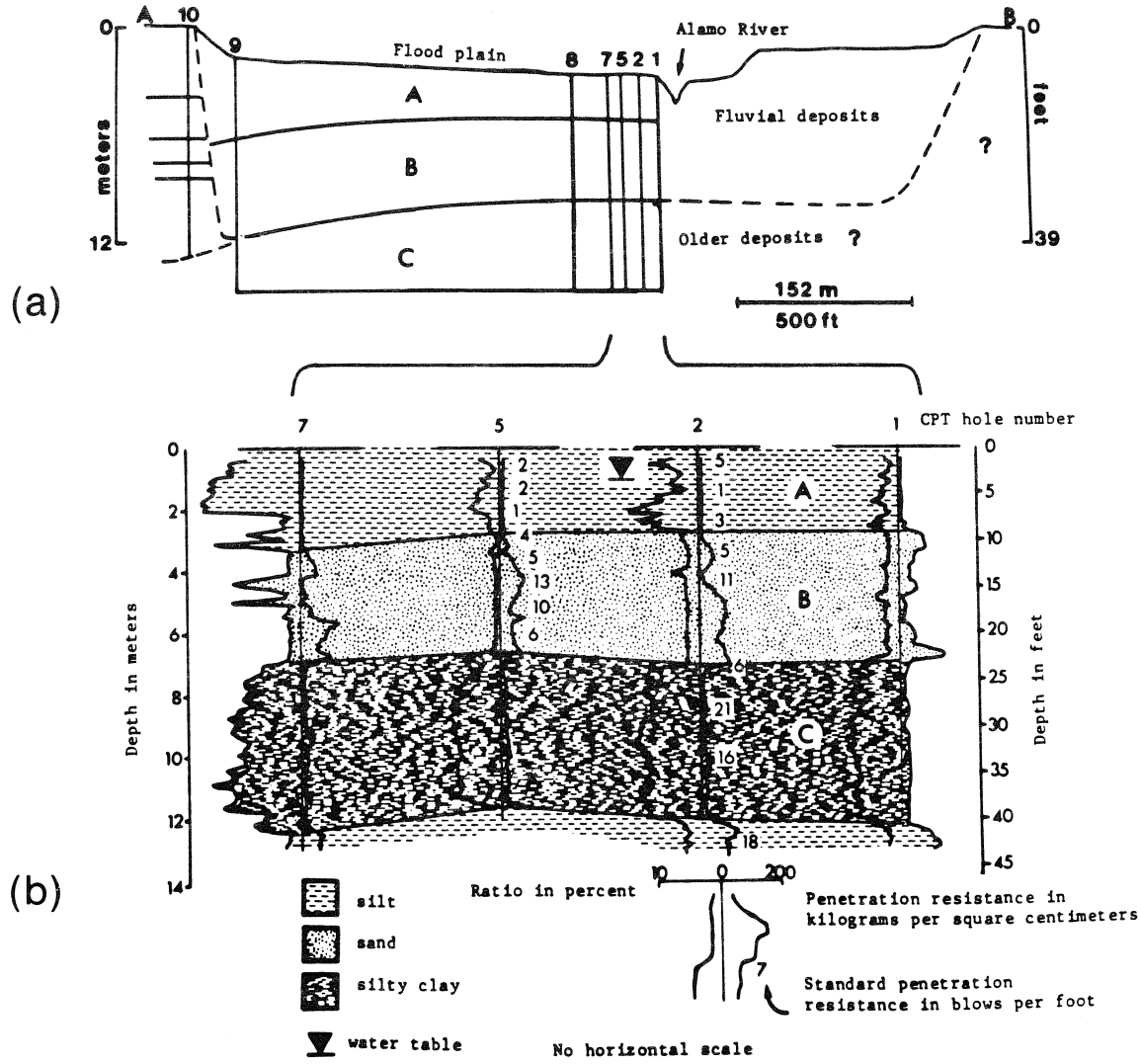

Figure 33. Soil Cross--Section at Wildlife (Bennett, et al., 1984)
a) General Cross--Section Across the Flood Plain. The Dashed Line represents the Approximate Boundary Between Fluvial Deposits and Pre--Channel Deposits. Hole #10 is Outside the Flood Plain
b) Detailed Cross--Section at the Location of the Instrument Station

grayish--brown to dark brown, well--sorted silty sand to very fine sand. The coarsest sediment occurs at the base of the unit, with a sharp break to finer sediment that coarsens upward to about 4 m. The sediment then fines upward through B_2 into B_1.

The deposit between a depth of 6.8 m and 12 m (Unit C) contains two subunits, C_1 (6.8 m --7.5 m), and C_2 (7.5 m --12 m). Subunit C_1 consists of medium to stiff, dark grayish--brown, clayey silt. The contact with

Table 10. Average Sediment Properties at Wildlife Site and Individual CPT Data

Unit	m depth	CPT kg/cm ^{2}qc/Rf%	SPT N blows/ft	GRAIN SIZE CHARACTERISTICS		WATER PROPERTIES	description
				sd/st/cl	Cu/d50	wn/wl/Pl	
A	2.5	6/3.02	2.3	10/71/19	12/.027	34/30/7	silt with sand and clay, L I = 1.6
B_1	3.5	21/0.99	3	37/55/8	11/.055	-	sandy silt, mod. sorted
B_2	6.8	57/1.24	8.4	73/25/2	3/.089	-	silty sand to sand well sorted
C_1	7.5	14/4.52	10.3	4/69/27	-/.013	30/36/16	clayey silt, L I = 0.6
C_2	12	20/7.53	18.5	2/31/67	-/.002	26/64/32	silty clay, L I = - 0.2
D	17.5		18	10/74/16	17+/.030	28/28/4	silty with clayey and sandy beds moderately to poorly sorted
E	21.5			38/41/21	19+/.051	26/ /	silty sand alternates with clayey silt, well to very poorly sorted
F	24.3			19/60/21	17+/.031	29/33/12	clayey silt, very poorly sorted
G	26.5			5/51/44	-/.011	30/51/27	silty clay and clayey silt

1 kg/cm ^{2} = 98.07 KPa

underlying subunit C_2 is gradational over a short distance. Subunit C_2 consists of medium to very stiff, dark reddish-gray, silty clay. The sediment in this subunit is very fine grained and uniform throughout the site.

The deposit between a depth of 12 m and 17.5 m (Unit D) consists of medium dense, olive gray to dark grayish-brown, moderate to very poorly sorted silt. The very dense upper part of the unit is a cemented silt. Interbeds of silt, clayey silt, and sandy silt are less than 0.7 m thick. The coarsest sediment occurs at the bottom of the unit. The nature of the contact of this unit with the underlying unit is uncertain.

The deposits below a 17.5-m depth are reported as moderately sorted sand and clayey silt and silty clay between 17.5 m and 21.5 m, well-sorted silty sand and poorly sorted sandy silt and clayey silt between 21.5 m and 26.5 m, and very stiff clayey silt and silty clay between 24.3 m and 26.5 m.

Table 10 summarizes the average sediment properties at this site.

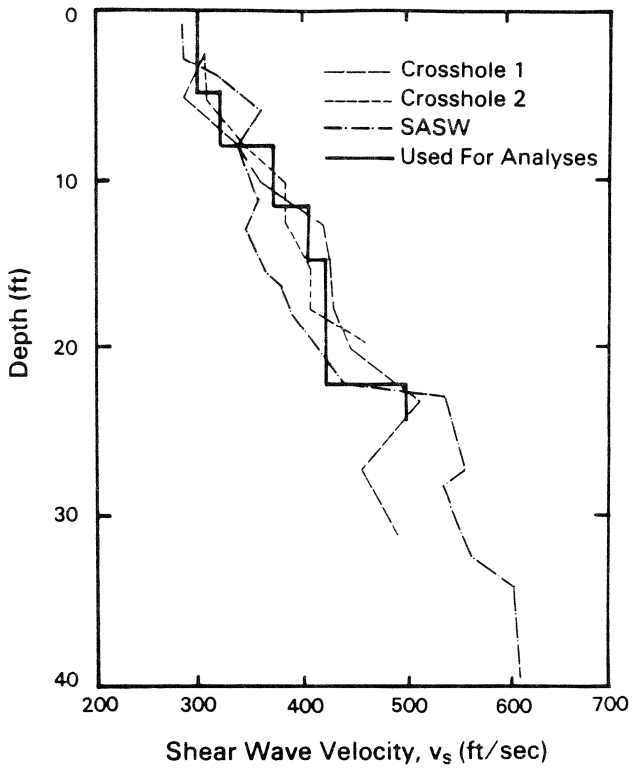

Figure 34. Shear Wave Velocities Measured at Wildlife Site (Stokoe & Nazarian, 1985) and Used for the Analytical Studies (Dobry, et al., 1989)

5.5 **Analysis**

Vucetic and Dobry (1988) performed one dimensional analytical studies to evaluate the behavior of the above soil profile during the 1981 earthquake. The recorded acceleration at Parachute Test site, scaled to a_{max} = 0.5 g, was used as input excitation to nonlinear computer program DESRAMOD, which is a modified version of DESRA originally developed by Lee and Finn (1978).

Field seismic testing, including shear wave velocity measurements to a depth of 12.20 m, was conducted by a team from the University of Texas, and the results are summarized in Fig. 34 (Haag, et al., 1985; Stokoe and Nazarian, 1985). Static and cyclic laboratory tests on intact and reconstituted soil specimen from the site were performed at the University of Texas, Woodward Clyde Consultants, and Rensselaer Polytechnic Institute (Haag and Stokoe, 1985; Ladd, 1984; Vucetic and Dobry, 1988; Dobry, et al., 1989). Figure 35 presents results

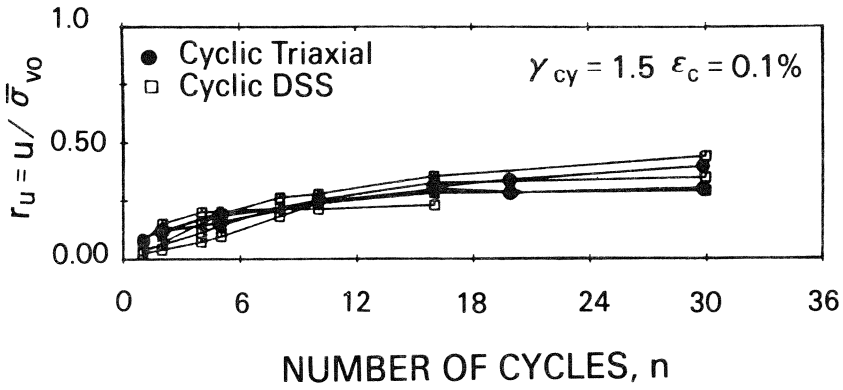

Figure 35. Strain-Controlled Cyclic Triaxial and Cyclic Direct Simple Shear (DSS) Tests on Intact and Reconstituted Specimens of Wildlife Silty Sand (Dobry, et al., 1989)

of pore pressure buildup obtained from strain controlled cyclic triaxial and direct simple shear tests by Vucetic and Dobry (1988).

6.0 THE NOVEMBER 24, 1987 SUPERSTITION HILLS EARTHQUAKE

6.1 Felt Effects and Intensity

On November 23, 1987 at 17:54 PST (0154 GMT) an earthquake with magnitude $M_S = 6.2$ (Brady et al, 1989), $M_W = 5.9$ (Youd and Bartlett, 1988), occurred in the Imperial Valley, California, near the southern margin of the Salton Sea. Within 12 hours, on November 24, at 0515 PST (1315 GMT) another earthquake with $M_S = 6.6$, $M_W = 6.5$, with epicentral coordinates of 33.01° N and 115.84° W shook an area extending to San Diego and Los Angeles, California, Tempe, Arizona, and Las Vegas, Nevada. The epicenters for both earthquakes are shown in Fig. 36 (Porcella et al., 1987). These earthquakes caused 2 deaths and four million dollars in property damage in the Imperial Valley.

6.2 Recorded Accelerations

During the first shock, the recorded peak horizontal ground accelerations exceeded 0.10 g at six stations, with a maximum recorded ground acceleration of 0.22 g at Calipatria, 26 km from the epicenter (Porcella et al., 1987). During

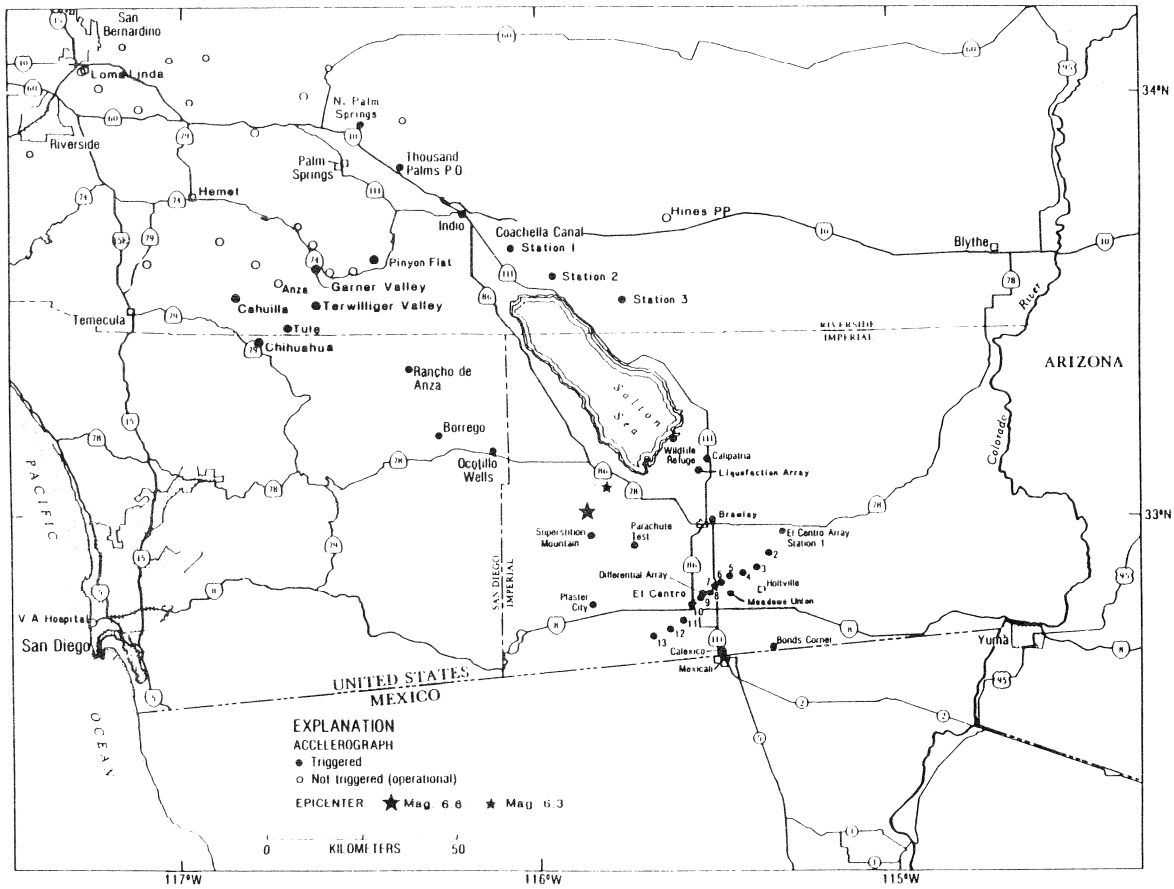

Figure 36. USGS Strong--Motion Stations in the Region of the November 24, 1987 Superstition Hills Earthquakes. Trigger Information Refers to the 1315 GMT Event (Porcella, et al., 1987).

the main event, $M_S = 6.6$, 25 of the 39 devices included in the National Strong Motion Instruments Network (NSMIN) triggered and recorded maximum horizontal ground accelerations larger than 0.10 g (Fig. 36). The Superstition Mountain station, the closest NSMIN instrument (7 km) to the epicenter, recorded horizontal acceleration of 0.90 g and 0.70 g and a vertical acceleration of 0.60 g. The Superstition Mountain is a linear granitic block that protrudes approximately 180 m above the valley floor.

Porcella, et al. (1987) compared the records of Superstition Mountain and of nearby Parachute Test site for this event, with the records from the Imperial Valley earthquakes of 1979 and 1981, and concluded that amplification due to topographic effects may not be significant in this area. They also reported

that two later earthquakes produced generally equal or greater peak accelerations and considerably longer durations of strong shaking (3 to 4 times longer) at the Parachute Test site than at the Superstition Mountain site.

The Parachute Test site station, the second closest NSMIN accelerograph to the epicenter, is located approximately 55 m southwest of the 1987 Superstition Hill fault surface displacement. Peak accelerations of 0.45 g and 0.53 g were recorded in the horizontal and vertical directions, respectively, with the duration of strong shaking ranging from 11.3 to 14.5 seconds (Porcella et al., 1987). The near surface shear wave velocity for this site, 443 m/s between depths of 10 to 30 m, is the highest among the 22 Imperial Valley sites investigated during the 1981 survey (Porcella, 1984).

6.3 Liquefaction and Records at Wildlife Site

A unique set of records of the M_S = 6.6 earthquake was obtained on the Alamo River flood plain at the Imperial Wildlife Liquefaction Array, 32 km from the epicenter. Alamo River, a perennial stream, occupies a 3.7 m deep channel, 23 m east of the center of the array and controls the water table elevation located at about 1.2 m depth (Holzer et al., 1989a). The soil profile at this site, already discussed in Section 5.4, is shown again in Fig. 37. This site had been instrumented in 1982 to monitor future earthquakes (Bennett, et al., 1984). The selection of the Wildlife site was based on the widespread observation of liquefaction effects during the 1930, 1950, 1957, and 1981 earthquakes and the existence of loose silt and silty sand at the site. The instrumentation included: two Strong Motion (SM) accelerographs installed at the surface and at 7.5 m deep below a potentially liquefiable zone; and five electric pore pressure transducers distributed within the silty sand layer which liquefied during 1981 event, as well as a sixth transducer in another silty layer at 12 m depth (Figs. 33 and 37). A series of points around the instrument array were selected as survey control points to monitor possible lateral ground deformations of the site. In addition, an inclinometer casing to detect permanent lateral subsurface deformation, extended to a depth of 8.8 m, was installed near the instrument array (Holzer, et al., 1989a). Since then,

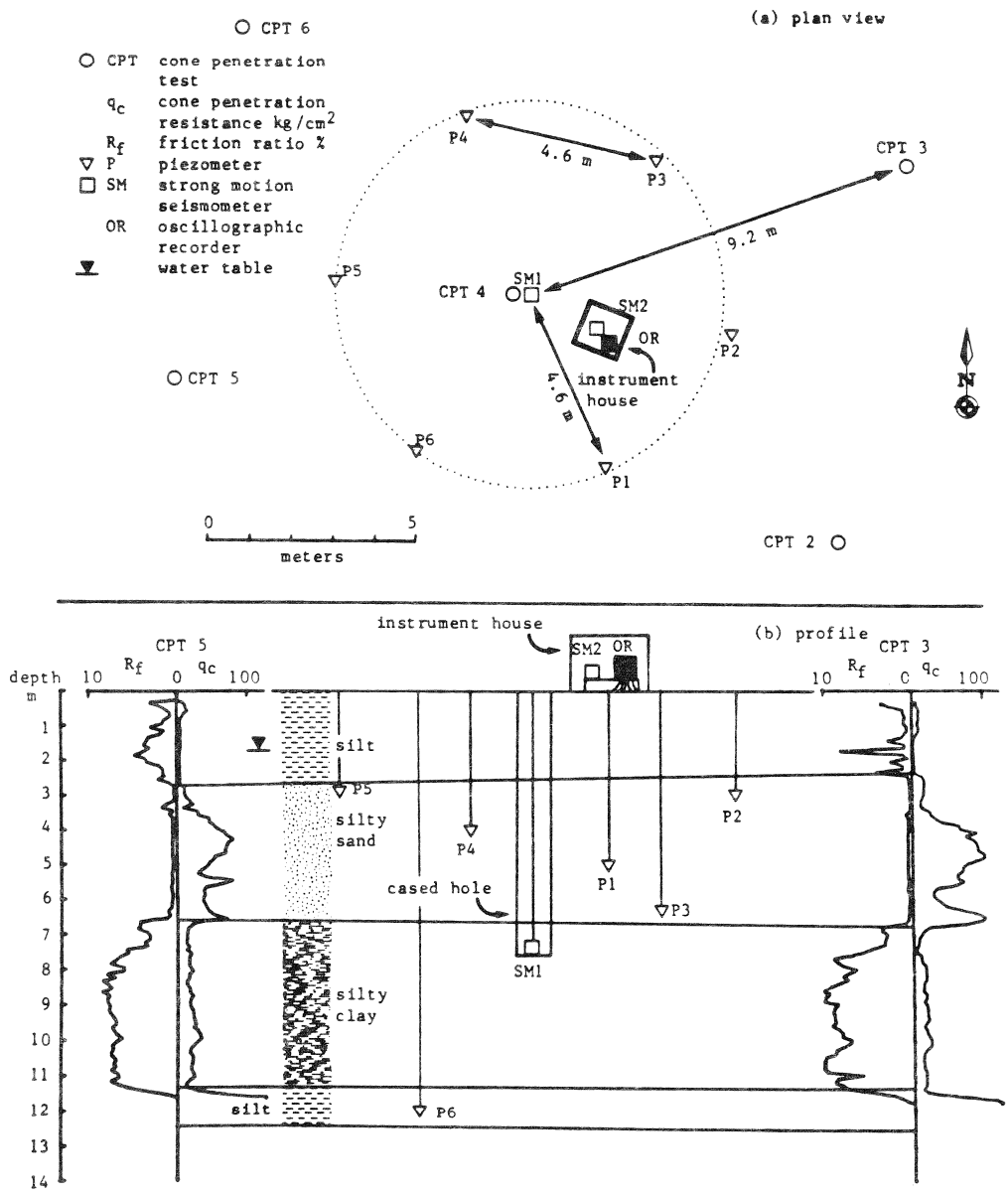

Figure 37. Cross-Section of Wildlife Site Showing Location of Piezometers (Bennett, et al., 1984)

several investigators have conducted field and laboratory studies to measure the soil properties at the site.

The earthquake records obtained from the Wildlife site (Brady et al., 1989) reveal that the November 23 event did not generate permanent excess pore pressures in the sand layer. The November 24 event, on the other hand, caused

excess pore pressures which built up to 100 percent of the initial effective overburden pressure. This is the first time a record has been obtained providing engineers and scientists with information about the effect of a natural earthquake on pore pressures, in a case in which initial liquefaction (100% pore pressure ratio) and associated lateral spreading occurred. The accelerations recorded at the surface and at 7.5m depth, and the recorded pore pressure rises, are shown in Figs. 38 and 39.

Figure 40 shows the locations of sand boils and fissures (lateral displacement cracks) observed in the Wildlife site after the earthquake. A maximum of 232 mm lateral ground deformation was recorded from the movement of the survey control points. This movement was generally in the direction of the Alamo River, and especially in a N15E direction, toward the slump at the river bank which had cut the small road in the 1981 earthquake, see Fig. 32. Thus, it can be hypothesized that the existence of this pre existing slump controlled the movement of the ground toward the river in the 1987 event, and caused the 180 mm lateral spread measured in the N15E direction. Holzer, et al. (1989a) reported that the cracks on the surface were 126 mm in width, with the top of the inclinometer casing having been deflected approximately 180 mm in the N15°E direction relative to its base beneath the liquefied layer, indicating that the upper layer slid obliquely into the north trending Alamo River. They estimated that the subsurface horizontal shear strain, estimated from the curvature of the casing, had been greatest (approximately 4 %) in the upper part of the silty sand.

6.4 Analysis

Figure 38 shows that there was a time delay in the pore pressure increases with respect to the strong part of the shaking. The pore pressures continued to rise after the strong ground shaking had essentially ceased, with about half of the total increase occurring during the latter period. As reported by Youd and Bartlett (1988), possible reasons for this continued rise include:

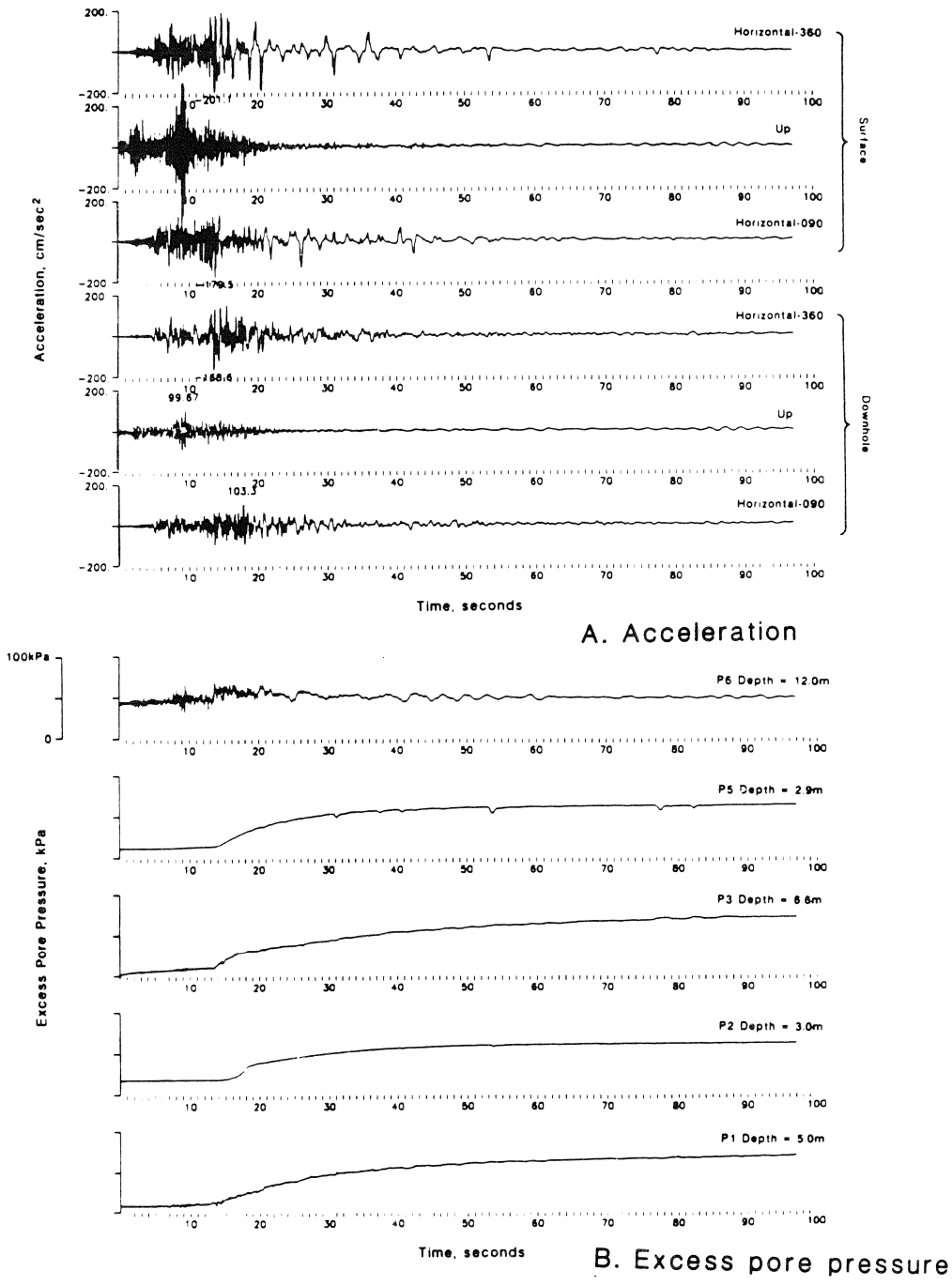

Figure 38. Instrumental recordings from the November 24, 1987 Superstition Hills Earthquake (Holzer, et al., 1989a)

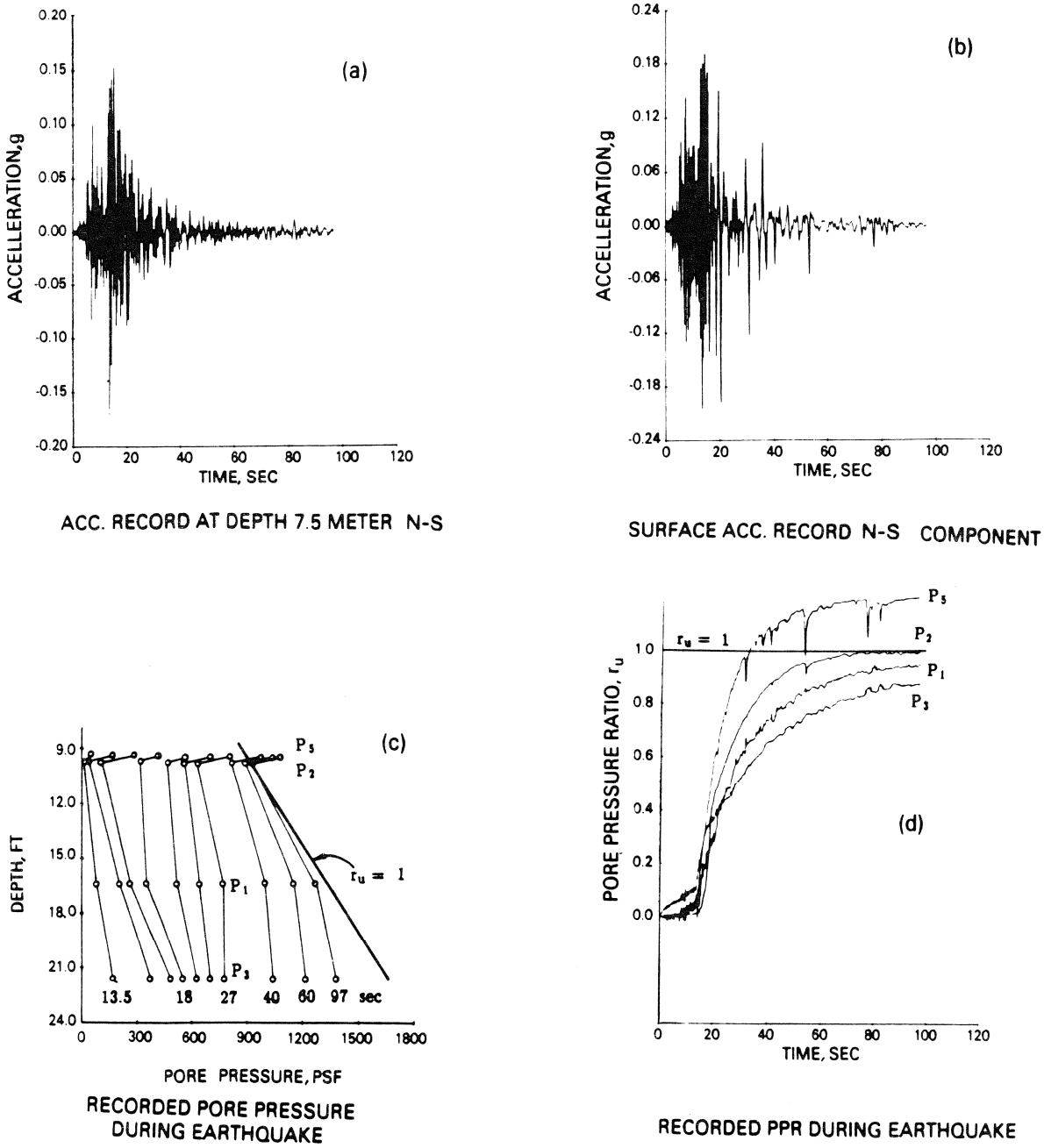

Figure 39. Recorded Accelerations (NS Components) and Piezometric Readings at Wildlife Site During the November 24, 1987 Earthquake (Dobry, et al., 1989)

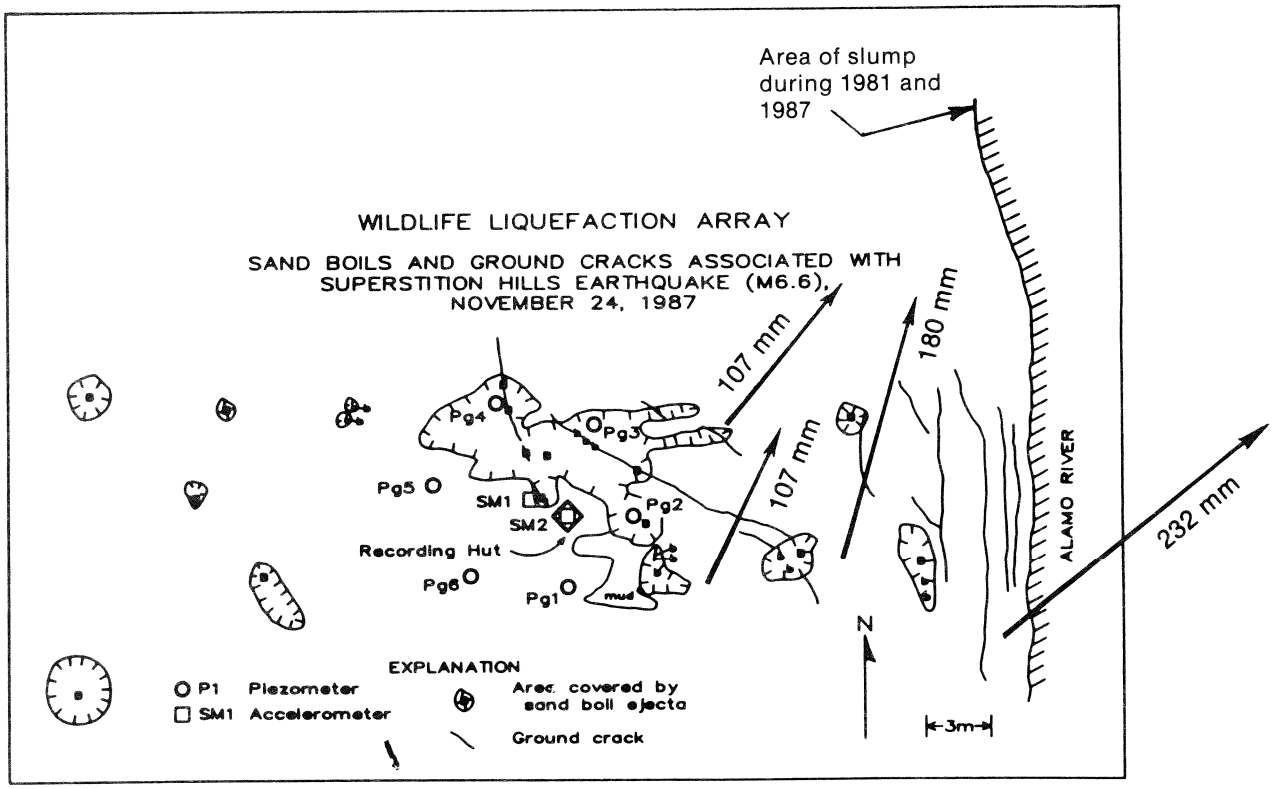

Figure 40. Sand boils, Lateral Spreading, and Cracks at Wildlife Liquefaction Array (Holzer, et al., 1989b; Youd & Bartlett, 1988)

1) The increase of pore pressures during strong shaking may have sufficiently softened the soil so that late arriving smaller motions generated a large enough shear strains to continue the pore pressure generation process.

2) Due to nonuniformities in the silty sand layer, a more rapid increase of pore pressures may have occurred in loose pockets of sediment some distance from the piezometers. In that case, the time required for pore pressure equilibrium to occur within the layer could have led to a delayed pressure response at the piezometer.

3) Soil disturbance during instrument placement could have created dense pockets of soil around each piezometer. Thus, time would be required to transmit the pore pressure increases through the densified zone to the pore pressure transducers.

Hushmand, et al. (1991) recently conducted a field investigation of the quality of the piezometers, and they concluded that only piezometer P_5 at a depth of

2.9 m, was functioning properly, while P_1, P_2 and P_3 responded either erratically or with a long delay. As the behavior of P_5 in Fig. 38 is not qualitatively different from the others, this observation by Hushmand, et al. (1991) does not change substantially the conclusions and discussion above. Youd and Bartlett (1988) also concluded that the observed doubling of the shear-wave travel time between downhole and surface accelerometers, from 0.06 to 0.12 seconds, determined from observations at 13.6 and 16 seconds, respectively, marks the softening of the silty sand layer and consequent possible development of high shear strains even though the strong shaking may have ceased.

This pore pressure response of the Wildlife Site during the 1987 earthquake has been analyzed by Keane and Prevost (1989) and Dobry, et al. (1989), using nonlinear one dimensional programs. Keane and Prevost used finite element program DYNA 1, while Dobry, et al. used program DESRAMOD. In both cases, reasonable agreement was found between predicted and measured pore pressures. In their paper, Dobry, et al. concluded that the rapid pore pressure increase corresponding to the strong shaking part between 13.6 and 21 seconds, was probably due to the seismic shear stresses reaching or exceeding the residual strengths of the very loose to loose sandy silt and silt layers existing in the site at shallow depths.

It is interesting to note that the ground surface accelerogram of Figs. 38 and 39 exhibits a dozen or so high frequency spikes as high as 0.12 g, predominantly negative, with their timing corresponding precisely to simultaneous fast transient pore pressure drops in the shallow piezometers, P2 and P5. These accelerations/pore pressure spikes are probably associated with the dynamics of the lateral spreading (Holzer, et al., 1989a; Dobry, et al., 1989).

Baziar and Dobry (1991a, b) evaluated the 180 mm lateral spreading in the N15°E direction shown in Fig. 40, using Newmark's sliding block method of analysis. Figure 41 presents the two sliding blocks analyzed, under the assumption that the failure occurred in the top loose to very loose sandy silt and silt layers. In Fig. 41, it was assumed that the vertical crack which opened 17.7 m from the river (see Fig. 40), marked the end of the sliding block. In the analysis, it was assumed that the block could only slide toward the free face along the river,

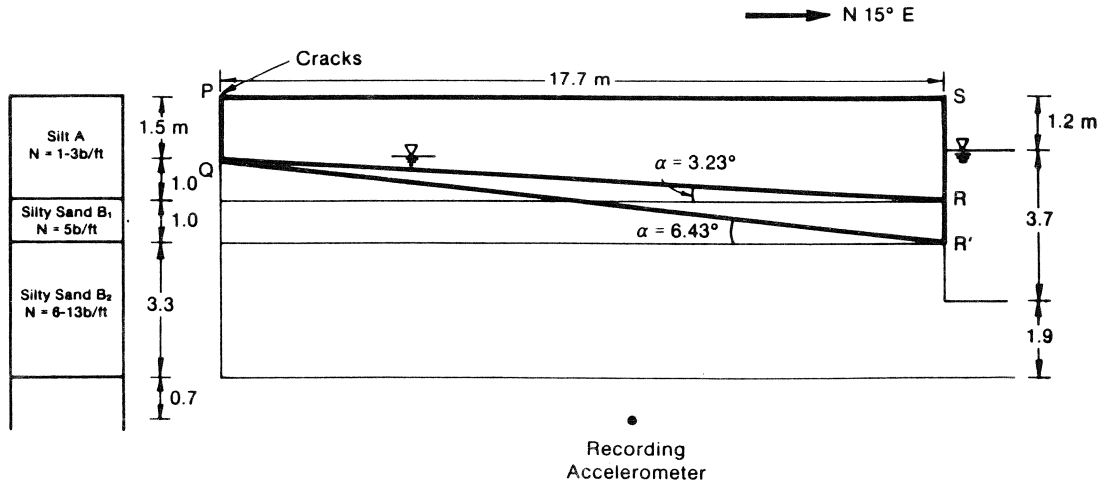

Figure 41. Soil Profile and Assumed Failure Planes for Newmark Analyses, Wildlife Site, November 24, 1987 Earthquake (Baziar & Dobry, 1991a)

with any sliding back away from the river prevented by soil debris filling up the cracks.

Figure 42 presents the results of laboratory tests on loose reconstituted layered silty sand deposited in water used to determine the residual shear strength of the soil, S_u, used in the analysis. These tests provided an estimated in-situ $S_u = 0.145\ \bar{\sigma}_v$, where $\bar{\sigma}_v$ = vertical effective overburden pressure, which was in turn used to obtain the yield accelerations at which either of the two blocks in Fig. 41 started sliding toward the river. Figure 43 shows the comparison between predicted (19 and 317 mm) and measured (180 mm) lateral ground displacements (see Baziar and Dobry, 1991b for more details). The two predicted displacements bound the measured value, and this provides a degree of confidence about the residual shear strength and failure mechanisms assumed in the analyses. On the other hand, the sensitivity of the calculated displacement, which varies by a factor of 17 when either of the two failure mechanisms of Fig. 41 is assumed, illustrates the uncertainties involved in the analytical prediction of permanent ground displacements due to lateral spreading. Figure 44 shows how the predicted displacement in this case increases as the slope angle α in Fig. 41 goes from $\alpha = 0°$ to $\alpha = 7.0°$.

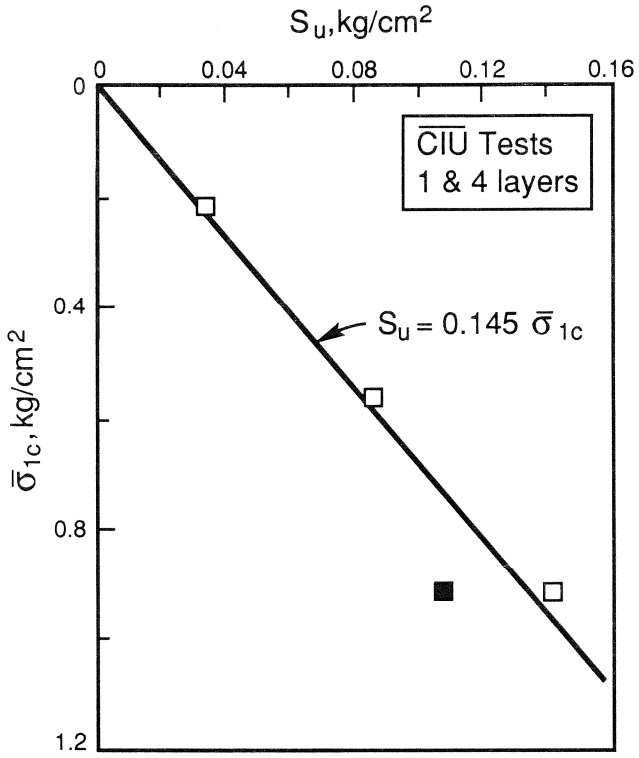

Figure 42. S_u vs. $\bar{\sigma}_{1c}$ from Monotonic Undrained Tests on San Fernando Dam Silty Sand (Baziar & Dobry, 1991b)

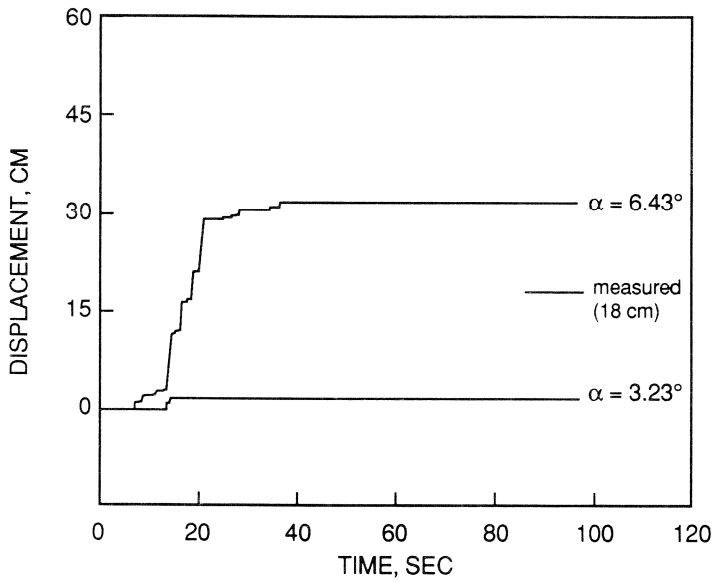

Figure 43. Measured and Predicted Displacement at Wildlife Site Using Newmark Analysis and Recorded Accelerogram, the November 24, 1987 Earthquake (Baziar & Dobry, 1991b)

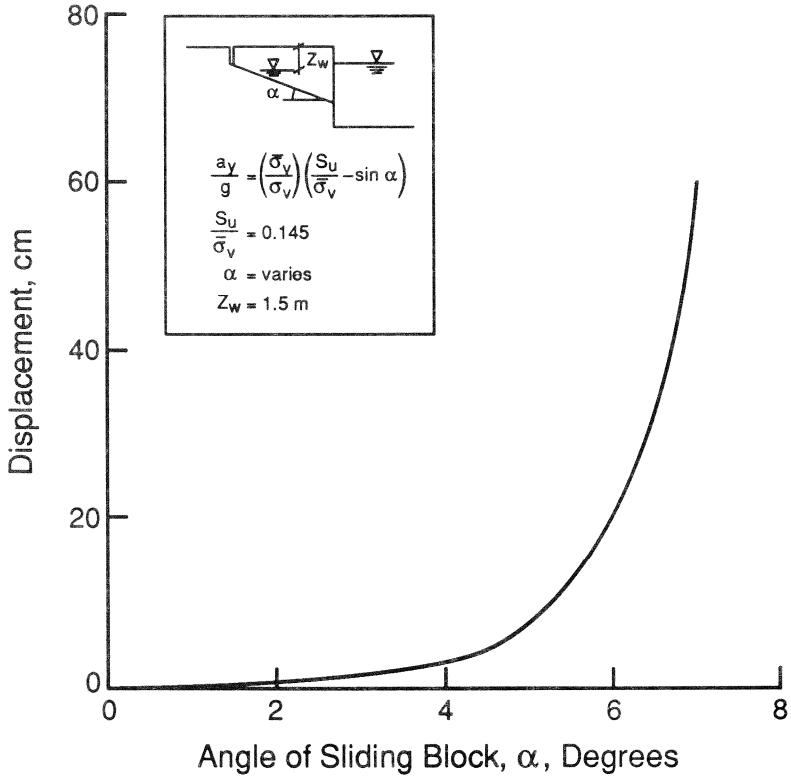

Figure 44. Effect of Sliding Block Angle of the Wildlife Site on Predicted Displacement (Baziar & Dobry, 1991b)

7.0 SUMMARY

The Imperial fault and other seismic sources in the Imperial Valley have been responsible for a number of significant earthquakes throughout the 20th Century (Table 1), with liquefaction and ground failure observed in the 1940, 1979, 1981, and 1987 events. For the more recent three earthquakes, good records of the ground shaking are available, and the cases of liquefaction and ground failure have been amply documented and studied. These cases are systematically reviewed throughout the chapter, including reported effects of the ground failure on constructed facilities. Repeated liquefaction was observed at some sites between the different events. Damage to buried pipelines due to surface faulting and travelling waves in the 1979 earthquake is also discussed.

The October 15, 1979 Imperial Valley earthquake, with a magnitude $M_w = 6.5$, occurred primarily on the Imperial fault at both sides of the United States Mexico border (Fig. 1), with surface rupture observed along a 30.5 km segment on the United States side. A number of strong ground motion records were obtained in both Mexico and the United States, most notably from a USGS free field array perpendicular to the fault (Fig. 7), and with a maximum recorded horizontal ground acceleration of 0.81 g. Numerous effects of liquefaction were observed as far as 47 km from the epicenter (13 km from the fault rupture), including sand boils, ground cracks, slumpings, ground settlement, and lateral spreads. The ground failure affected irrigation and drainage systems, roads, canals, river earthworks, and bridges. Of special interest is the lateral spread observed at Heber Road site, located less than 2 km from the fault, with a maximum 4.2 m lateral displacement. The field investigations, laboratory testing, analyses and evaluations available for this site are reviewed and discussed. Correlations are presented between rate of repairs to irrigation and drainage systems in this agricultural area, versus both distance to the fault and recorded ground acceleration. The damage sustained by water and natural gas buried pipelines due to travelling waves and fault rupture is also discussed; the effect of fault rupture on pipelines crossing the Imperial fault is evaluated with the help of measurements and estimates of the fault slip before, during, and after the 1979 earthquake.

The smaller April 26, 1981 Westmorland earthquake, with a magnitude $M_w = 5.9$, had its epicenter north of the 1979 fault rupture (Fig. 4). No surface faulting was reported. Twenty five strong ground motion records were obtained, with a maximum horizontal acceleration of 0.49 g at an epicentral distance of 7 km. Surface liquefaction effects were observed as far as 14 km from the epicenter, with these effects including sand boils, fissures, slumping, lateral spreading, and settlement throughout the northwestern part of the Imperial Valley. One of the sites that liquefied and developed a slump toward the Alamo river in 1981 was the Wildlife site, which was subsequently instrumented and liquefied again during the 1987 earthquake.

The November 24, 1987 Superstition Hills earthquake, with a magnitude $M_w = 6.5$, had its epicenter to the southwest of the 1981 event (Fig. 4). Twenty five strong ground motion records were obtained, with a maximum horizontal acceleration of 0.91 g at an epicentral distance of 7 km. Liquefaction and lateral spreading, with a maximum lateral ground displacement of 232 mm, occurred again at the Wildlife site, 30.5 km from the epicenter. This was the only site for which liquefaction was reported. The measured ground surface peak acceleration at the site was 0.21 g. Most of the lateral spreading (180 mm) was in the same general direction as the 1981 slump, indicating a possible relation between the two incidents. Inclinometer readings suggested that the maximum ground straining occurred in the upper 3.5 m of the soil profile, containing very loose to loose silt and sandy silt (the groundwater table was at 1.5 m depth). The site had been thoroughly studied and instrumented with accelerometers and piezometers since 1981, and for the first time excess pore water pressures up to 100% of the initial effective overburden pressure were measured during an earthquake. The characteristics of the site, based on field exploration and field and laboratory testing results, are reviewed in detail. The acceleration and pore pressure records, as well as the measured lateral displacement, are discussed and evaluated with the help of available analytical results including Newmark's sliding block calculations.

REFERENCES

Allen, C. R., Wyss, M., Brune, J. N., Grantz, A., and Wallace, R.E. (1972) "Displacements on the Imperial, Superstition Hills, and San Andreas Faults Triggered by the Borrego Mountain Earthquake, in the Borrego Mountain Earthquake of April 9, 1968," U.S. Geological Survey Professional Paper 787, pp. 87--104.

Baziar, M.H., and Dobry, R. (1991a) "Liquefaction Ground Deformation Predicted from Laboratory Tests," Proceedings, Second International Conference on Recent Advances in Geotechnical Earthquake Engineering and Soil Dynamics, St. Louis, MO, USA, March.

Baziar, M. H., and Dobry, R. (1991b) "Engineering Evaluation of Permanent Ground Deformations Due to Seismically--Induced Liquefaction," Research Report for NCEER, Civil Engineering Dept., Rensselaer Polytechnic Institute, Troy, NY.

Beal, C.H. (1915) "The Earthquake in the Imperial Valley, California, June 22, 1915," Seismological Society of America Bulletin, Vol. 5, pp. 130--149.

Bennett, M.J., Youd, T.L., Harp, E.L., and Wieczorek, G.F. (1981) "Subsurface Investigation of Liquefaction, Imperial Valley Earthquake, California, Oct. 15, 1979," Open--File Report 81--502, U.S. Geological Survey.

Bennett, M.J., Mc Laughlin, P.V., Sarmiento, J.S., and Youd, T.L. (1984) "Geotechnical Investigation of Liquefaction Sites, Imperial Valley, California," Open--File Report 84--252, U.S. Geological Survey, Menlo Park, California.

Biehler, S., Kovach, R.L., and Allen, C.R. (1964) "Geophysical Framework of Northern End of Gulf of California Structural Province," in Van Andel, T.H., and Shor, G.G. Jr, eds., Marine Geology of the Gulf of California, American Association of Petroleum, Geologist Memoir 3, pp. 126--143.

Bierschwale, J. G., and Stokoe II, K. H. (1984) "Analytical Evaluation fo Liquefaction Potential of Sands Subjected to the 1981 Westmorland Earthquake," Geotechnical Eng. Rept. GR--84--15, Civil Eng. Dept., University of Texas, Austin, TX.

Brady, A.G., Perez, V., and Mork, P.N. (1982) "Digitization and Processing of Main--Shock Ground--Motion Data from the U.S. Geological Survey Accelerograph Network," The Imperial Valley California Earthquake Oct. 15, 1979, U.S. Geological Survey, Professional Paper 1254, pp. 385 406.

Brady, A.G., Mork, P.N., Seekins, L.C., and Switzer. J.C. (1989) "Processed Strong--Motion Records from the Imperial Wildlife Liquefaction Array, Imperial County, California, Recorded During the Superstition Hills Earthquake, Nov. 24, 1987," Open--File Report 89--87, U.S. Geological Survey, Menlo Park, California.

Brune, J.N., Vernon III, F.L., Simons, R., Prince, J., and Mena, E. (1982) "Strong-Motion Data Recorded in Mexico During the Main Shock," The Imperial Valley California Earthquake Oct. 15, 1979, U.S. Geological Survey, Professional Paper 1254, pp. 319 249.

Castle, R.O., and Youd, T.L. (1972) "Engineering Geology in the Borrego Mountain Earthquake of April 9, 1968," U.S. Geological Survey, Professional Paper 787, pp. 158-174.

Castro, G. (1987) "On the Behavior of Soils During Earthquakes-Liquefaction," In: A. S. Cakmak (ed.), Developments in Geotechnical Engineering 42, Soil Dynamics and Liquefaction, Department of Civil Engineering, Princeton University, Princeton, NJ 08544.

Chavez, D., Gonzales, J., Reyes, A., Medina, M., Duarte, C., Brune, J.N., Vernon III, F.L., Simons, R., Hutton, L.K., German, P.T., and Johnson, C.E. (1982) "Main-Shock Location and Magnitude Determination Using Combined U.S. and Mexican Data," The Imperial Valley California Earthquake October 15, 1979, U.S. Geological Survey, Professional Paper 1254, pp. 51 54.

Clark, T.A. (1940) "Report of Earthquake Damage in Imperial Valley, May 18, 1940," U.S. Bureau of Reclamation, All-American Canal Project Report, 40 p.

Cohn, S.N., Allen, C.R., Gillman, R., and Goulty, N.R. (1982) "Preearthquake and Postearthquake Creep on the Imperial Valley Fault and the Brawley Fault Zone," The Imperial Valley California Earthquake October 15, 1979, U.S. Geological Survey, Professional Paper 1254, pp. 161 182.

Degenkolb, O.H., and Jurach, P. (1980) "Highway and Bridge Damage Imperial Valley Earthquake of October 15, 1979," Reconnaissance Report Imperial County, California Earthquake, October 15, 1979, Earthquake Engineering Research Institute, Berkeley, pp 85-96.

Dibblee, T.W. Jr. (1954) "Geology of the Imperial Valley Region, California, in Geology of the Natural Provinces," Chap. 2 of Jahns, R.H., ed., Geology of Southern California, California Division of Mines Bulletin 170, V. 1, pp. 21-28.

Dobry, R., Elgamal, A.W., Baziar, M.H., and Vucetic, M. (1989) "Pore Pressure and Acceleration Response of Wildlife Site During the 1987 Earthquake," Proceedings, Second U.S.-Japan Workshop on Liquefaction, Large Deformation and Effects on Buried Pipelines, Niagara Falls, New York, pp. 145 160.

Douglas, B.J., and Martin, G.R. (1982) "In Situ Testing in Regions Liquefied During the 1979 Imperial Valley Earthquake," Grant No. PFR-8007419, National Science Foundation, Washington D.C.

Eguchi, R.L. (1982) "Water System Facility Performance During 24 World Wide Earthquake, Earthquake Performance of Water and Natural Gas Supply Systems," Technical Report 82-1396, J.H. Wiggins Company, Redondo Beach, California.

Elders, W.A., Rex, R.W., Meidav, Tsvi, Robinson, P.T., and Biehler, S. (1972) "Crustal Spreading in Southern California", Science, Vol. 178, No. 4056, pp. 15--24.

Espinosa, A.F. (1982) "M1 and M0 Determination from Strong--Motion Accelerograms, and Expected--Intensity Distribution," The Imperial Valley California Earthquake Oct. 15, 1979, U.S. Geological Survey, Professional Paper 1254, pp. 433 438.

Fuis, G.S. (1982) "Displacement on the Superstition Hills Fault Triggered by the Earthquake," The Imperial Valley California Earthquake Oct. 15, 1979, U.S. Geological Survey, Professional Paper 1254, pp.145 154.

Fuis, G.S., Mooney, W.D., Healey, J.H., McMechan, G.A., and Lutter, W.J. (1982) "Crustal Structure of the Imperial Valley Region," The Imperial Valley California Earthquake Oct. 15, 1979, U.S. Geological Survey, Professional Paper 1254, pp. 25 49.

Goulty, N.R., Burford, R.D., Allen, C.R., Gilman, R., Johnson, C.E., and Keller, R.P. (1978) "Large Creep Events on the Imperial Fault, California," Seismological Society of America Bulletin, Vol. 68, No. 2, pp. 517--521.

Haag, E.D., and Stokoe II, K.H. (1985) "Laboratory Investigation of Static and Dynamic Properties of Sandy Soils Subjected to the 1981 Westmorland Earthquake," Research Report, Geotechnical Engineering Center, University of Texas at Austin.

Haag, E.D., Nazarian, S., and Stokoe II, K.H. (1985) "Seismic Investigation of Five Sites in the Imperial Valley, California, After the 1981 Westmorland Earthquake," Research Report, Geotechnical Engineering Center, University of Texas at Austin.

Hart, E.W. (1981) "Preliminary Map of October 1979 Fault Rupture, Imperial and Brawley Faults, Imperial County, California," California Division of Mines and Geology, 7.5 minute Quadrangle, Scale 1:24,000.

Hill, D.P., Mowinckel, P., and Peake, L.G. (1975) "Earthquake, Active Faults, and Geothermal Areas in the Imperial Valley, California", Science, V. 188, No. 4195, p. 1306--1308.

Holzer, T.L., Youd, T.L., and Hanks, T.C. (1989a) "Dynamics of Liquefaction During the 1987 Superstition Hills, California Earthquake," Science, Vol. 244, pp. 56--59.

Holzer, T.L., Youd, T.L., and Bennett, M.J. (1989b) "In Situ Measurement of Pore Pressure Build Up During Liquefaction," Proceedings of the 20th Joint Meeting of the U.S.-Japan Cooperative Program in the Natural Resources, Panal on Wind and Seismic Effects, U.S. Department of Commerce.

Holzer, T.L. (1990) Personal Communication.

Hushmand, B., Crouse, C. B., and Kavazanjian, Jr., E. (1991) "Accuracy of the Pore-Water Pressures Recorded at Wildlife Site During Magnitude 6.6 Imperial Valley Earthquake of 24 November 1987," Research Report, The Earth Technology Corporation, Long Beach, CA.

Imperial Irrigation District (1980a) "Drainage System," Drawing # 8201.

Imperial Irrigation District (1980b) "Fault Lines of the October 15, 1979 Earthquake," Drawing # 8426.

Imperial Irrigation District (1980c) "Report on Damage to Water Control Facilities of the Imperial Irrigation District," pp 1-16.

Johnson, C.E. (1979) "CEDAR- An Approach to the Computer Automation of Short-Period Local Seismic Networks, Seismotectonics of the Imperial Valley of Southern California," Ph.D. Thesis, California Institute of Technology.

Johnson, C.E., Rojahn, C., and Sharp, R. (1982) "The Imperial Valley, California, Earthquake of Oct. 15, 1979, Introduction," The Imperial Valley California Earthquake Oct. 15, 1979, U.S. Geological Survey, Professional Paper 1254, pp. 1 3.

Johnson, C.E., and Hill, D.P. (1982) "Seismicity of the Imperial Valley," The Imperial Valley California Earthquake Oct. 15, 1979, U.S. Geological Survey, Professional Paper 1254, pp. 15 24.

Kanamori, H., and Anderson, D.L. (1975) "Theoretical Basis of Some Empirical Relations in Seismology," Bulletin of the Seismological Society of America, Vol. 65, No. 5, pp. 1073-1095.

Kanamori, H., and Jennings, P.C. (1978) "Determination of Local Magnitude from Strong-Motion Accelerograms," Bulletin of the Seismological Society of America, Vol. 68, No. 2, pp. 471-485.

Keane, C.M., and Prevost, J.H. (1989) "An Analysis of Earthquake Data Observed at the Wildlife Liquefaction Array Site, Imperial Valley County, California," Proceedings, Second U.S.-Japan Workshop on Liquefaction, Large Ground Deformation, and their Effects on Lifeline Facilities, Niagara Falls, New York, pp. 176 192.

Kovach, R.L., Allen, C.R., and Press, F. (1962) "Geophysical Investigations in the Colorado Delta Region", Journal of Geophysical Research, Vol .67, No. 7, pp. 2845-2871.

Kuo, J.H.C., and Stokoe II, K.H. (1982) "Laboratory Investigation of Static and Dynamic Soil Properties of Three Heber Road Sands after Oct. 15, 1979 Imperial Valley Earthquake," Research Report GR82-25, Geotechnical Engineering Center, Civil Eng. Dept., University of Texas, Austin, pp. 171.

Ladd, R.S. (1982) "Geotechnical Laboratory Testing Program for Study and Evaluation of Liquefaction Ground Failure Using Stress and Strain Approaches, Heber Road Site, Oct. 15, 1979 Imperial Valley Earthquake," Volumes I to III, Woodward Clyde Consultants, Eastern Region, Clifton, New Jersey.

Ladd, R.S. (1984) "Laboratory Investigation of Sands from Wildlife Site," unpublished data.

Lee, M.K.W., and Finn, W.D.L. (1978) "DESRA-2: Dynamic Effective Stress Response Analysis of Soil Deposits with Energy Transmitting Boundary Including Assessment of Liquefaction Potential," Soil Mechanics Series, No. 38, Department of Civil Engineering, University of British Columbia, Vancouver, B.C., Canada

Leeds, D.J., Editor, Brandow, G.E., Coordinator (1980) "Reconnainssance Report Imperial County, California Earthquake, October 15, 1979," Earthquake Engineering Research Institute, Berkeley, pp. 85-96.

Maley, R.P., and Etheredge, E.C. (1981) "Strong-Motion Data from Westmorland, California Earthquake of April 26, 1981," Open-File Report No. 81-1149, U.S. Department of Interior, Geology Survey, Menlo Park, California.

McJunkin, R.D., and Kaliakin, N.A. (1981) "Strong-Motion Records Recovered from the Westmorland California Earthquake of 26 April, 1981," California Division of Mines and Geology, Sacramento, California 95816.

McNorgan, J.D. (1989) "Relieving Seismic Stresses Locked in Gas Pipeline," Proceedings, Second U.S.-Japan Workshop on Liquefaction, Large Ground Deformation and Their Effects on Lifelines, National Center for Earthquake Engineering Research, Technical Report NCEER-89-0032, Buffalo, NY, September, pp. 363-369.

McNorgan, J.D. (1990) Personal Communication, Southern California Gas Company.

Nason, R. (1982) "Seismic Intensity Studies in the Imperial Valley," The Imperial Valley California Earthquake October 15, 1979, U.S. Geological Survey, Professional Paper 1254, pp. 259 264.

Neumann, F. (1942) "United States Earthquakes-1940," U.S. Department of Commerce, Coast and Geodetic Survey, Serial 647, 74 pp.

NRC (1985) Liquefaction of Soils During Earthquakes, National Research Council, National Academy of Science, Washington, DC.

O'Rourke, M., and Dobry, R. (1982) "Apparent Horizontal Propagation Velocity for the 1979 Imperial Valley Earthquake," Bulletin of the Seismological Society of America, Vol. 72, No. 6, pp. 2377-2380.

O'Rouke. T., Grigoriu, M.D., and Khater, M.M. (1985) "Seismic Response of Buried Pipelines," Pressure Vessel and Piping Technology -- A Decade of Progress, C. Sundararjan, Ed., ASME, New York, NY, pp 281--3.

Porcella, R.L., and Matthiesen, R.B. (1979) "Preliminary Summary of the U.S. Geological Survey Strong--Motion Records From the Oct. 15, 1979 Imperial Valley Earthquake," U.S. Geological Survey, Open--File Report 79--1654, 41 pp.

Porcella, R.L., Matthiesen, R.B., and Maley, R.P. (1982) "Strong--Motion Data Recorded in the United States," The Imperial Valley California Earthquake Oct. 15, 1979, U.S. Geological Survey, Professional Paper 1254, pp. 289 318.

Porcella, R.L. (1984) "Geotechnical Investigations at Strong--Motion Stations in the Imperial Valley, California," U.S. Geological Survey, Open--File Report 84--562.

Porcella, R.L., Etheredge, E., Maley, R., and Switzer, J. (1987) "Strong Motion Data from the Superstition Hills Earthquakes 0154 and 1315 (GMT), Nov. 24 1987," Open--File Report 87--672, U.S. Geological Survey, Menlo Park, California.

Reagor, B.G., Stover, C.W., Algermissen, S.T., Steinbrugge, K.V., Hubiak, P., Hopper, M.G., and Barnhard, L.M. (1982) "Preliminary Evaluation of the Distribution of Seismic Intensities," The Imperial Valley California Earthquake Oct. 15, 1979, U.S. Geological Survey, Professional Paper 1254, pp. 251 258.

Richter, C.F. (1958) Elementary Seismology, San Francisco, W.H. Freeman, 768 pp.

Rojahn, C., and Ragsdale, J.T. (1980) "Strong Motion Records from the Imperial County Service Building, El Centro," In: Leeds, D.J. (ed.), Imperial County, California, Earthquake Oct. 15, 1979, Berkeley, Calif., Earthquake Engineering Research Institute, Reconnaissance Report, pp. 173--184.

Rojahn, C., and Mork, P.N. (1982) "An Analysis of Strong--Motion Data from a Severely Damaged Structure -- The Imperial County Services Building, El Centro, California," The Imperial Valley California Earthquake Oct. 15, 1979, U.S. Geological Survey, Professional Paper 1254, pp. 357 375.

Rojahn, C., Ragsdale, J.T., Raggett, J.D., and Gates, J.H. (1982) "Main--Shock Strong--Motion Records from the Meloland Road--Interstate Highway 8 Overcrossing," The Imperial Valley California Earthquake Oct. 15, 1979, U.S. Geological Survey, Professional Paper 1254, pp. 377 383.

Schroeder, J. (1990) Personal Communication, J.D. Hess Testing Corporation, El Centro, California.

Seed, H.B. (1979) "Soil Liquefaction and Cyclic Mobility Evaluation for Level Ground During Earthquakes," Journal of the Geotechnical Engineering Division, ASCE, Vol. 105, No. GT2, pp. 201–255.

Seed, H.B., and Idriss, I.M. (1982) "Ground Motions and Soil Liquefaction During Earthquakes," Engineering Monograph on Earthquake Criteria, Structural Designs and Strong Motion Research, Earthquake Engineering Research Institute, Berkeley, CA.

Seed, H.B., Idriss, I.M., and Arango, I. (1983) "Evaluation of Liquefaction Potential Using Field Performance Data," Journal of Geotechnical Engineering Division, ASCE, Vol. 109, No. 3, pp. 458–482.

Sharp, R.V. (1977) "Holocene Traces of the Imperial Fault in South–Central Imperial County, california," U.S. Geological Survey, Open–File Report 77–815.

Sharp, R.V. (1981) "Variable Rates of the Late Quaternary Strike–Slip on San Jacinto Fault Zone, Southern California", Journal of Geophysical Research, Vol. 86, No. B3, pp. 1754–1762.

Sharp, R.V. (1982) "Tectonic Setting of the Imperial Valley Region, in the Imperial Valley, California, Earthquake of Oct. 15, 1979," The Imperial Valley California Earthquake Oct. 15, 1979, U.S. Geological Survey, Professional Paper 1254, pp. 5 14.

Sharp, R.V., Leinkaemper, J.J., Bonilla, M.G., Burke, D.B., Fox, B.F., Herd, D.G., Miller, D.M., Morton, D.M., Ponti, D.J., Rymer, M.J., Tinsley, J.C., Yount, J.C., Kahle, J.E., Hart, E.W., and Sieh, K.E. (1982) "Surface Faulting in the Central Imperial Valley," The Imperial Valley California Earthquake Oct. 15, 1979, U.S. Geological Survey, Professional Paper 1254, pp. 119 143.

Sieh, K.E. (1982) "Slip Along the San Andreas Fault Associated with the Earthquake'" The Imperial Valley California Earthquake Oct. 15, 1979, U.S. Geological Survey, Professional Paper 1254, pp. 155 159.

Strahorn, A.T., Watson, E.B., Kocher, A.D., and Eckmann, E.C. (1924) "Soil Survey of the El Centro Area, California, in Field Operations of the Bureau of Soils," Washington, U.S. Government Printing Office, pp. 1633–1688.

Stokoe II, K.H., and Nazarian, S. (1985) "Use of Raleigh Waves in Liquefaction Studies," Proceedings, Measurement and Use of Shear Wave Velocity for Evaluating Dynamic Soil Properties, GED, ASCE, Denver Colorado.

Sykora, D.W., and Stokoe II, K.H. (1982) "Seismic Investigation of Three Heber Road Sites After the Oct. 15, 1979 Imperial Valley Earthquake," Geotechnical Engineering Report GR82–24, University of Texas at Austin.

Sylvester, A.G. (1979) "Earthquake Damage in Imperial Valley, California, May 18, 1940 as Reported by T.A. Clark," Bulletin of the Seismological Society of America, Vol. 69, No. 2, pp. 547--568.

Thatcher, W. (1979) "Horizontal Crustal Deformation from Historic Geodetic Measurements in Southern California," Journal of Geophysical Research, Vol. 84, No. B5, pp. 2351--2370.

Townley, S.D., and Allen, M.W. (1939) "Descriptive Catalog of Earthquakes of the Pacific Coast of the United States, 1769 to 1928," Bulletin of the Seismological Society of America, Vol. 29, No. 1, pp. 1--297.

Toppozada, T.R., Parke, D.L., and Higgins, C.T. (1978) "Seismicity of California 1900--1931," California Division of Mines and Geology, Special Report 135.

Trifunac, M. D., and Brune, J. N. (1970) "Complexity of Energy Release During the Imperial Valley, California Earthquake of 1940," Bulletin of the Seismological Society of America, Vol. 60, No. 1, pp. 137 160.

Ulrich, F.P. (1941) "The Imperial Valley Earthquakes of 1940," Bulletin of the Seismological Society of America, Vol. 31, No. 1, pp. 13--32.

U.S. Geological Survey (1977) "Western Hemisphere Strong--Motion Accelerograph Station List--1976," Open--File Report 77--374, U.S. Geological Survey, Menlo Park, California.

U.S. Geological Survey (1982) " The Imperial Valley California, Earthquake of Oct. 15, 1979," Professional Paper 1254, U.S. Geological Survey, Menlo Park, California.

Vucetic, M., and Dobry, R. (1986) "Study and Evaluation of a Liquefaction Ground Failure Using Stress and Strain Approaches: Heber Road Site, October 15, 1979 Imperial Valley Earthquake," Research Report, Dept. of Civil Engineering, Rensselaer Polytechnic Institute, Troy, New York.

Vucetic, M., and Dobry, R. (1988) "Pore Pressure Build Up and Liquefaction at Level Sandy Sites During Earthquakes," Research Report, Department of Civil Engineering, Rensselaer Polytechnic Institute, Troy, New York.

Waller, R., and Ramanathan, M. (1980) "Site Visit Report on Earthquake Damage to Water and Sewerage Facilities El Centro California, November 15, 1979," Reconnaissance Report Imperial County California Earthquake, October 15, 1979, Earthquake Engineering Research Institute, pp. 97--106.

Wosser, T.D., Campi, S.D., Fovinci, G.K., and Smith, W.H. (1982) "Damage to Engineering Structures in California," The Imperial Valley California Earthquake October 15, 1979, U.S. Geological Survey, Professional Paper 1254.

Youd, T.L., and Bennett, M.J. (1981) "Liquefaction Site Studies Following 1979 Imperial Valley Earthquake," Preprint 81--584, ASCE National Convention, St. Louis, Mo, October.

Youd, T.L., and Wieczorek, G.F. (1982) "Liquefaction and Secondary Ground Failure in the Imperial Valley, California, Earthquake of Oct. 15, 1979," The Imperial Valley California Earthquake Oct. 15, 1979, U.S. Geological Survey, Professional Paper 1254, pp. 223--246.

Youd, T.L., and Bennett, M.J. (1983) "Liquefaction Sites, Imperial Valley, California", Journal of Geotechnical Engineering Division, ASCE, Vol. 109, No. 3, pp. 440--457.

Youd, T.L., and Wieczorek, G.F. (1984) "Liquefaction During 1981 and Previous Earthquakes Near Westmorland, California," Open--File Report 84--680, U.S. Geological Survey, Menlo Park, California.

Youd, T.L., and Bartlett, S.F. (1988) "U.S. Case Histories of Liquefaction--Induced Ground Failure," Proceedings, First Japan--U.S. Workshop on Liquefaction, Large Ground Deformation, and Their Effects on Lifeline Facilities, Tokyo, Japan, pp. 22 31.

Large Ground Deformations and Their Effects on Lifeline Facilities: 1989 Loma Prieta Earthquake

T.D. O'Rourke, Professor
School of Civil and Environmental Engineering
Cornell University
Ithaca, New York

J.W. Pease, Graduate Research Assistant
School of Civil and Environmental Engineering
Cornell University
Ithaca, New York

ACKNOWLEDGMENTS

The research presented in this case history was sponsored by the National Center for Earthquake Engineering Research, Buffalo, NY and the National Science Foundation under Grant No. BCS-90 11458. Special thanks are extended to T. Dickerman of the San Francisco Water Department, F. Blackburn of PWSS, Ltd., A. Nielsen of the San Francisco Fire Department, J. Clark of Pacific Gas and Electric Co., and P.T. Law and S. Yu of the Clean Water Program, all for their help in gathering lifeline data. Special thanks also are extended to T. Holzer and M. Bennett of USGS, R. Darragh and D. Koutsoftas of Dames and Moore, H. Taylor and H. Yap of Harding Lawson Associates, M. Power of Geomatrix, R.B. Nowinski of Applied Geotechnical Engineering, and R. Chew of Robert Y. Chew Geotechnical for their help in gathering geotechnical data. The assistance of Ted Gowdy, who helped prepare data bases and performed three-dimensional computer analyses, is deeply appreciated. The support given by Harry Stewart of Cornell University in technical review, data collection, and intellectual comradery is gratefully acknowledged. D. Meyersohn helped to organize and prepare cross-sectional profiles of soils in the South of Market area. Bruce Roth, currently of GAI Consultants, Inc., is thanked for his excellent assistance in collecting information during earthquake reconnaissance. A. Avcisoy and K.J. Stewart, who prepared the drawings and manuscript, respectively, are duly recognized for their skills and contributions.

TABLE OF CONTENTS

	Page
Acknowledgments	5-iii
Table of Contents	5-v
List of Tables	5-vii
List of Figures	5-ix

Section		Page
1.0	INTRODUCTION	5-1
2.0	TECTONIC SETTING, INTENSITY, AND FELT EFFECTS	5-4
3.0	STRONG MOTION RECORDS	5-8
4.0	OBSERVATIONS OF LIQUEFACTION EFFECTS	5-13
	4.1 Mission Creek	5-16
	4.2 South of Market	5-18
	4.3 Foot of Market	5-20
	4.4 Marina	5-21
5.0	EARTHQUAKE EFFECTS ON SAN FRANCISCO WATER SUPPLY	5-26
	5.1 San Francisco Water Distribution System	5-26
	5.2 Performance of MWSS	5-29
	5.3 Performance of AWSS	5-29
	5.4 AWSS Simulation Studies	5-31
6.0	LIFELINE SYSTEM PERFORMANCE IN THE MARINA	5-35
	6.1 Historic Development	5-35
	6.2 Water Supply Lifeline Damage	5-38
	6.3 Gas Distribution Lifeline Damage	5-43
	6.4 Wastewater Conveyance Lifeline Damage	5-43
	6.5 Ground Deformation and Pipeline Repair	5-46
7.0	WATER SUPPLY DAMAGE IN SOUTH OF MARKET AREA	5-47
8.0	GLOBAL PATTERNS OF PIPELINE DAMAGE	5-51
9.0	SUBSURFACE CONDITIONS IN THE MARINA	5-54
	9.1 Evaluation of Soil Conditions from SPT Measurements	5-62
	9.2 Evaluation of Soil Conditions from CPT Measurements	5-64
10.0	SUBSURFACE CONDITIONS IN THE SOUTH OF MARKET AREA	5-68

Section		Page
11.0	SUBSURFACE CONDITIONS IN THE MISSION CREEK AREA	5-73
12.0	CONCLUDING REMARKS	5-76
REFERENCES		5-80

LIST OF TABLES

Table		Page
1	Summary of Damage to Auxiliary Water Supply System	5-30
2	Summary of MWSS Pipeline Damage in the Marina	5-42
3	Repair/Replacement Statistics for Collector Sewer Pipe in the Marina	5-45
4	Summary of MWSS Pipeline Repairs for Various Sites in San Francisco	5-53

LIST OF FIGURES

Figure		Page
1.	Map of Area Most Severely Affected by the Loma Prieta Earthquake	5-5
2.	Areal Distribution of Aftershocks Along the San Andreas Fault	5-5
3.	Isoseismal Map for the San Francisco Bay Region for the Loma Prieta Earthquake	5-7
4.	Map of Modified Mercalli Intensities in San Francisco	5-8
5.	Map of San Francisco and Oakland Area Showing Peak Horizontal Accelerations at Various Sites	5-10
6.	Time Records of Horizonal Acceleration at Three Rock Sites in San Francisco	5-11
7.	Time Records of Horizontal Acceleration at Yerba Buena and Treasure Islands	5-12
8.	Plan View of San Francisco Showing Zones of 1906 Soil Liquefaction and Inspection After the 1989 Earthquake	5-15
9.	Map and Photographs of Liquefaction-Induced Ground Deformation in the Mission Creek Area	5-17
10.	Map and Photographs of Liquefaction-Induced Ground Deformation in the South of Market Area	5-19
11.	Map and Photographs of Liquefaction-Induced Ground Deformation in the Foot of Market Area	5-22
12.	Map and Photographs of Liquefaction-Induced Ground Deformation in the Marina District	5-23
13.	Sunset Reservoir System of the MWSS	5-27
14.	Typical Portion of the Distribution System of the MWSS	5-27
15.	San Francisco AWSS	5-28
16.	Conditions Used in Computer Simulation of AWSS Performance During the Loma Prieta Earthquake	5-32
17.	Results of AWSS Simulation with Negligible Water Loss from Leaking Joints	5-34

Figure		Page
18.	Results of AWSS Simulation with Leaking Joints Modeled	5-34
19.	Map of the Marina Showing the 1857 Shoreline	5-36
20.	Map of the Marina Showing the 1906 Waterfront and Effects of the 1906 Earthquake	5-37
21.	Map of the Marina Showing Locations of Pipeline Repairs to the MWSS	5-39
22.	Map of the Marina Showing AWSS Pipelines Replaced as a Result of the 1989 Earthquake	5-40
23.	Map of the Marina Showing the Locations of Damage to the AWSS and High Pressure Gas Distribution System	5-40
24.	Linear Regression of Repair Rate of MWSS vs. Nominal Pipe Diameter	5-42
25.	Map of the Marina Showing Locations of Replaced and Repaired Wastewater Conveyance Pipelines	5-45
26.	Map of the Marina Showing Contours of Settlement Caused by Post-Liquefaction Consolidation	5-48
27.	Map of the Marina Showing Contours of Repair Rates for the MWSS	5-48
28.	MWSS Pipeline Repairs in South of Market Area	5-50
29.	AWSS Pipeline and Hydrant Repairs in South of Market Area	5-50
30.	Water Supply Pipeline Breaks and Zones of Soil Liquefaction Caused by 1906 San Francisco Earthquake	5-52
31.	Water Supply Pipeline Breaks and Zones of Soil Liquefaction Caused by 1989 Loma Prieta Earthquake	5-52
32.	Repair Rate of Cast Iron Pipeline Systems versus Modified Mercalli Intensity	5-54
33.	Plan View of Soil Borings and Soundings in the Marina	5-55
34.	Soil Profile Along Cross-Section A-A′ in the Marina	5-56
35.	Soil Profile Along Cross-Section B-B′ in the Marina	5-57
36.	Map of the Marina Showing Contours of Bedrock	5-58
37.	Contours of Equal Elevation for Bottom of Holocene Bay Mud in the Marina	5-58

Figure		Page
38.	Erosional Surface Beneath Holocene Bay Mud in Relation to San Francisco Topography	5-59
39.	Contours of Equal Elevation for Top of Holocene Bay Mud in the Marina	5-59
40.	Three-Dimensional View of the Subsurface Rock and Soil Features at the Marina	5-61
41.	Cyclic Stress Ratio Plots of Three Soil Types in the Marina	5-63
42.	Soil Profiles with Corrected SPT Values Plotted as a Function of Depth	5-65
43.	Soil Profiles with CPT Values Plotted as a Function of Depth	5-67
44.	Map of South of Market Showing Borings and Cross-Sections	5-69
45.	Soil Profile Along Cross-Section A-A' in the South of Market Area	5-69
46.	Soil Profile Along Cross-Section B-B' in the South of Market Area	5-70
47.	Soil Profile Along Cross-Section C-C' in the South of Market Area	5-71
48.	Cyclic Stress Ratio Plot for Fills and Sands in the South of Market Area	5-73
49.	Map of Mission Creek Area Showing Borings and Cross-Sections	5-74
50.	Soil Profile Along Cross-Section A-A' in the Mission Creek Area	5-75
51.	Soil Profile Along Cross-Section B-B' in the Mission Creek Area	5-75
52.	Cyclic Stress Ratio Plot for Fill at a Site of Liquefaction in the Mission Creek Area	5-77

1.0 INTRODUCTION

The 1989 Loma Prieta earthquake was one of the most important earthquakes to occur in the coterminous United States since the 1906 San Francisco earthquake. The event was responsible for the deaths of 63 people, injuries sustained by 3,757 people, and more than 12,000 homeless (Governor's Board of Inquiry, 1990; McNutt and Sydnor, 1990). Over 1300 buildings were destroyed, with 20,000 damaged. Approximately 3500 businesses were seriously disrupted, with 400 lost (Governor's Board of Inquiry, 1990). The earthquake received unprecedented media coverage, striking during prime time broadcasting of the third game of the World Series. As a result, millions of viewers were able to see immediately the effects of the earthquake and to monitor by television post-earthquake events, such as the fire in the Marina District of San Francisco and the search and rescue operations at the collapsed Cypress Viaduct of Route I-880. (Please refer to Figures 1 and 4 for the locations of cities, districts, and transportation arteries mentioned in the Introduction.)

The Loma Prieta earthquake was important for at least three major reasons. To start, the earthquake generated an exceptionally large data base of strong motion records, illustrating the importance of site response. Analyses of strong motion data have shown substantially higher peak accelerations at sites underlain by Holocene bay mud and loose fills than those measured at comparable distances from the epicenter at both rock and alluvial sites (e.g., Campbell, 1991). Furthermore, the Holocene mud accelerations are significantly larger than those predicted by virtually all commonly used attenuation relationships for California earthquakes (Plafker and Galloway, 1989; Earthquake Engineering Research Institute, 1990; Reichle, et al., 1990; Campbell, 1991). At some locations, such as Yerba Buena and Treasure Islands, the strong motion data provide for a direct comparison between the seismic response of rock and soil deposits involving Holocene bay mud and loose saturated fill. These comparisons permit a direct empirical evaluation of site amplification (e.g., Darragh and Shakal, 1991), as well as verification of numerical methods, incorporating equivalent linear procedures (e.g., Idriss, 1989; Hyrciw, et al., 1990).

A second major factor contributing to the importance of the Loma Prieta

earthquake is liquefaction. Soil liquefaction and associated ground deformations were documented at numerous locations in San Francisco (O'Rourke, et al., 1990; 1991b; Chameau, et al., 1991; Harding Lawson Associates, et al., 1991; 1992); areas adjacent to San Francisco Bay (Seed, et al., 1990; Earthquake Engineering Research Association, 1990); and the Santa Cruz and Monterey Bay areas (Plafker and Galloway, 1989; Earthquake Engineering Research Institute, 1990). Investigations of soil liquefaction in San Francisco have shown a clear and consistent relationship between ground deformations caused by soil liquefaction and damage to underground pipeline systems (O'Rourke, et al., 1990; 1991b). Moreover, detailed soil investigations in areas of liquefaction have helped to clarify existing procedures for predicting post-liquefaction consolidation and have pointed out the most effective in-situ measurements for assessing the degree of post-liquefaction consolidation (O'Rourke, et al., 1991a; 1992).

The third significant aspect of the Loma Prieta earthquake was damage to lifelines. Perhaps the most enduring images of the Loma Prieta earthquake, enhanced by live television coverage, were the multi-span collapse of the Cypress Structure of Route I-880, the collapse of a single span of the San Francisco-Oakland Bay Bridge, and the fire in the Marina District of San Francisco. These three occurrences are representative of the damage related both directly and indirectly to earthquake effects on lifeline networks. In the case of the Marina fire, ruptures caused by liquefaction in the pipelines of two independent water supply systems severely hampered fire fighting activities, with the result that a catastrophic fire was narrowly averted.

In addition to damage at the Cypress Structure and the San Francisco-Oakland Bay Bridge, a bridge collapsed at its crossing of the Struve Slough along Highway 1 near Watsonville. Ten bridges were closed due to structural damage, including the Embarcadero Freeway and a portion of the viaduct for Route I-280, both in San Francisco (McNutt, 1990). A significant portion of the Embarcadero Freeway eventually was torn down, and damaged portions of I-280 still were closed two years after the earthquake. Bridge and viaduct closures in the San Francisco Bay area resulted in disruption of local transportation. Closures of the San Francisco-Oakland Bay Bridge, Cypress Structure, and

Embarcadero Freeway in combination required the rerouting of travelers carried by 480,000 vehicles per day (McNutt, 1990). As a result of the bridge and viaduct failures, a special Board of Inquiry was convened by the Governor of California (Governor's Board of Inquiry, 1990), and substantial changes in design, retrofit procedures, and research were initiated in both California and throughout the United States.

Approximately 1.4 million customers were without electrical service after the earthquake, and approximately 150,000 customers suffered interruption of normal gas service, of which roughly 90% was customer initiated (McNutt, 1990). Damage to water supplies was widespread and, in several cases, severe. In San Francisco, there were approximately 160 breaks in water main and service lines, with a temporary loss of the fire department's water system in the lower elevations of the central business and neighboring districts. There were over 200 water main breaks in areas adjoining the eastern shore of San Francisco Bay, more than 300 in the Monterey and Santa Cruz areas, and 155 in San Jose (McNutt, 1990; Earthquake Engineering Research Institute, 1990). Ground failure, particularly soil liquefaction, played a large role in causing damage to water mains (McNutt, 1990). There was extensive damage to wastewater conveyance systems, including a break in a 1.7-m-diameter force main in San Francisco, which was used to carry as much as 40% of the city sewage. Structural and non-structural damage at the San Francisco International Airport caused its closure for 12 hours. Liquefaction caused settlement and extensive cracking of approximately 900 m of the main runway of the Oakland International Airport. Port facilities in San Francisco and Oakland were damaged by soil liquefaction. Liquefaction-induced settlement and lateral displacement at the Port of Oakland caused severe damage to wharf facilities supported by batter piles (Earthquake Engineering Research Institute, 1990), and resulted in the loss of three large bridge cranes and about 30% of the terminal area (McNutt, 1990).

A full treatment of the geotechnical and lifeline aspects of the Loma Prieta earthquake is well beyond the scope of this study. Instead, this work concentrates on the liquefaction and large ground deformations which occurred in the City of San Francisco and their effects on lifeline networks, particularly the water supply systems. This approach is similar to that adopted for the case

study of the 1906 San Francisco earthquake in this volume, and provides for a comparison of the effects of two severe earthquakes of different magnitude and epicenter in the same city. Soil liquefaction, major pipeline damage, and fires occurred at virtually the same locations in both events.

Portions of this work embody the results of previous investigations supported partially or in full by the National Center for Earthquake Engineering Research (NCEER). In particular, excerpts from other studies (O'Rourke, et al., 1990; 1991a; b; 1992) are incorporated directly at appropriate locations throughout the text.

2.0 TECTONIC SETTING, INTENSITY, AND FELT EFFECTS

The earthquake occurred on October 17, 1989 at 5:04 p.m. Pacific Standard Time. The main shock hypocenter was located near Loma Prieta Mountain in the Santa Cruz Mountains at 37° 02′ N. latitude and 121° 53′ W. longitude. The main shock depth was 17.6 km. A substantial body of information has been published on the seismological aspects of the earthquake, and for additional details, reference should be made to other sources of information (e.g., Plafker and Galloway, 1989; Earthquake Engineering Research Institute, 1990; McNutt and Sydnor, 1990; and special issues of both the Geophysical Research Letters, 1990 and Bulletin of the Seismological Society of America, 1991).

Figure 1 shows the earthquake epicenter and areas of most intense seismic shaking. The epicenter was approximately 16 km east northeast of Santa Cruz and 97 km southeast of San Francisco. The earthquake was generated by rupture of the San Andreas fault. The rupture propagated bilaterally to cover a total distance of about 40 km in about 7 to 10 seconds (Earthquake Engineering Research Institute, 1990). Had the rupture propagated unilaterally, the duration of shaking would have been approximately twice as long, thereby increasing substantially the potential for damage.

The areal distribution of aftershocks approximately 21 days after the main shock is shown in Figure 2. The length of fault conforming to the trace of the aftershocks is similar to the total distance of bilateral rupture. The aftershocks clearly define a 70°-dipping (to the southwest) fault plane below 5 km,

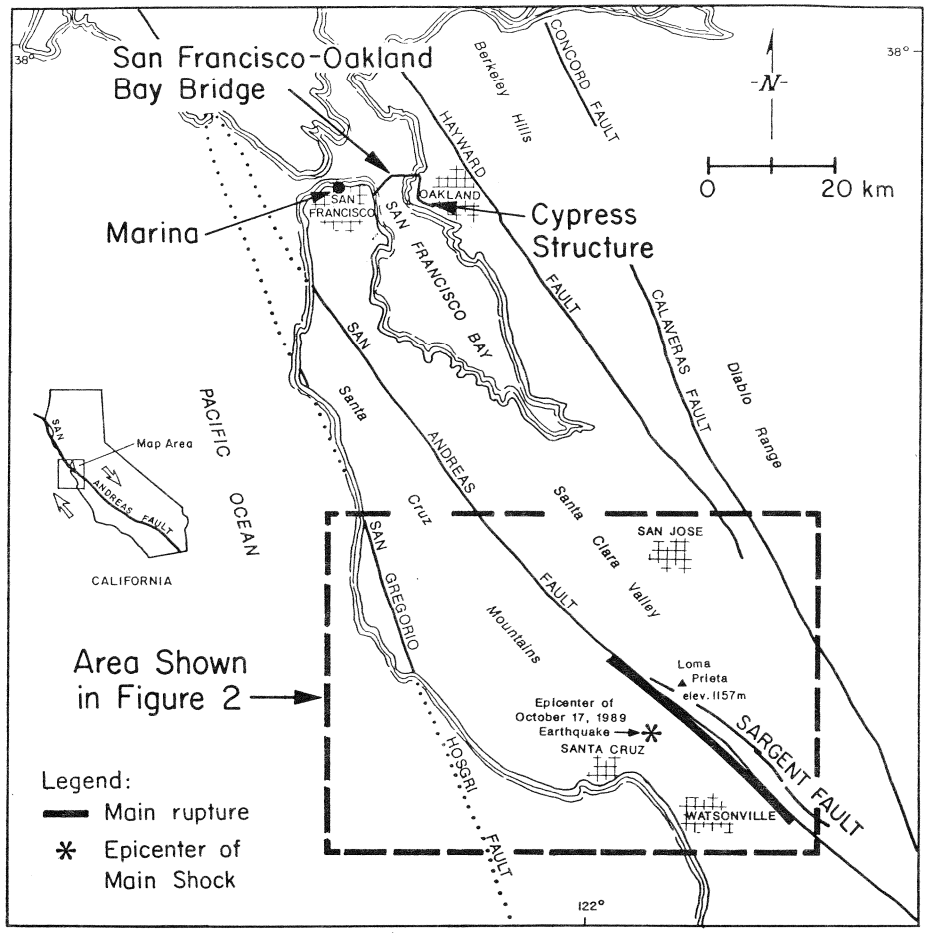

Figure 1. Map of Area Most Severely Affected by the Loma Prieta Earthquake

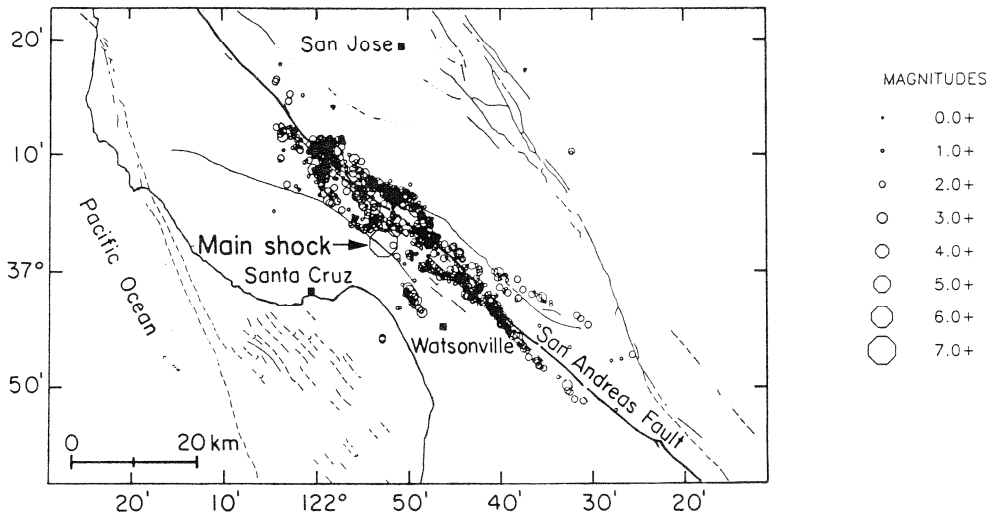

Figure 2. Areal Distribution of Aftershocks Along the San Andreas Fault (after Plafker and Galloway, 1989)

the assumed top of the rupture surface (Plafker and Galloway, 1989; Campbell, 1991). The trend in aftershocks becomes increasingly more diffuse at depths less than 5 km, a characteristic which is consistent with the lack of a through-going right lateral surface rupture. Numerous extensional fissures were apparent along various ridges in the Santa Cruz Mountains, but these deformational features have been linked to shaking-induced gravitational spreading and downslope movement, and are not an expression of surface faulting (Ponti and Wells, 1991). Geodetic measurements taken the day after the main shock show an average 1.9 m of right lateral strike slip and 1.3 m of reverse slip.

Various measures of earthquake magnitude have been summarized by Hanks and Krawinkler (1991) and Campbell (1991). The body wave, surface wave, and local magnitudes were M_b = 6.5, M_s = 7.1, and M_L = 7.0, respectively. Preliminary estimates of the seismic moment indicate 2.2 - 3.8 x 10^{26} dyne-cm, which corresponds to a moment magnitude of M_w = 6.9.

The earthquake was felt over an area of roughly 1,000,000 km^2, from Los Angeles on the south to the Oregon-California border on the north, and to western Nevada on the east (Plafker and Galloway, 1989). Figure 3 shows the distribution of Modified Mercalli Intensities (MMI) in the areas most severely shaken by the earthquake. McNutt and Toppozada (1990) report that the land area shaken by MM VII or greater, which can cause significant damage to structures, was 4300 km^2. By comparison, the land area affected by similar intensities during the 1906 San Francisco earthquake was 48,000 km^2 (Toppozada and Parke, 1982).

The intensity in the epicentral area adjoining Santa Cruz was MM VIII. Isolated instances of MM IX were assigned to the locations of the collapsed Cypress Structure, collapsed San Francisco-Oakland Bay Bridge, damaged Embarcadero Freeway, and Marina District of San Francisco. The MMI values mapped in the City of San Francisco are shown in Figure 4. The MMI values shown in the figure are identical to those reported in previous publications (Plafker and Galloway, 1989; Earthquake Engineering Research Institute, 1990), with the exception that MM VIII has been assigned to a part of the South of Market area

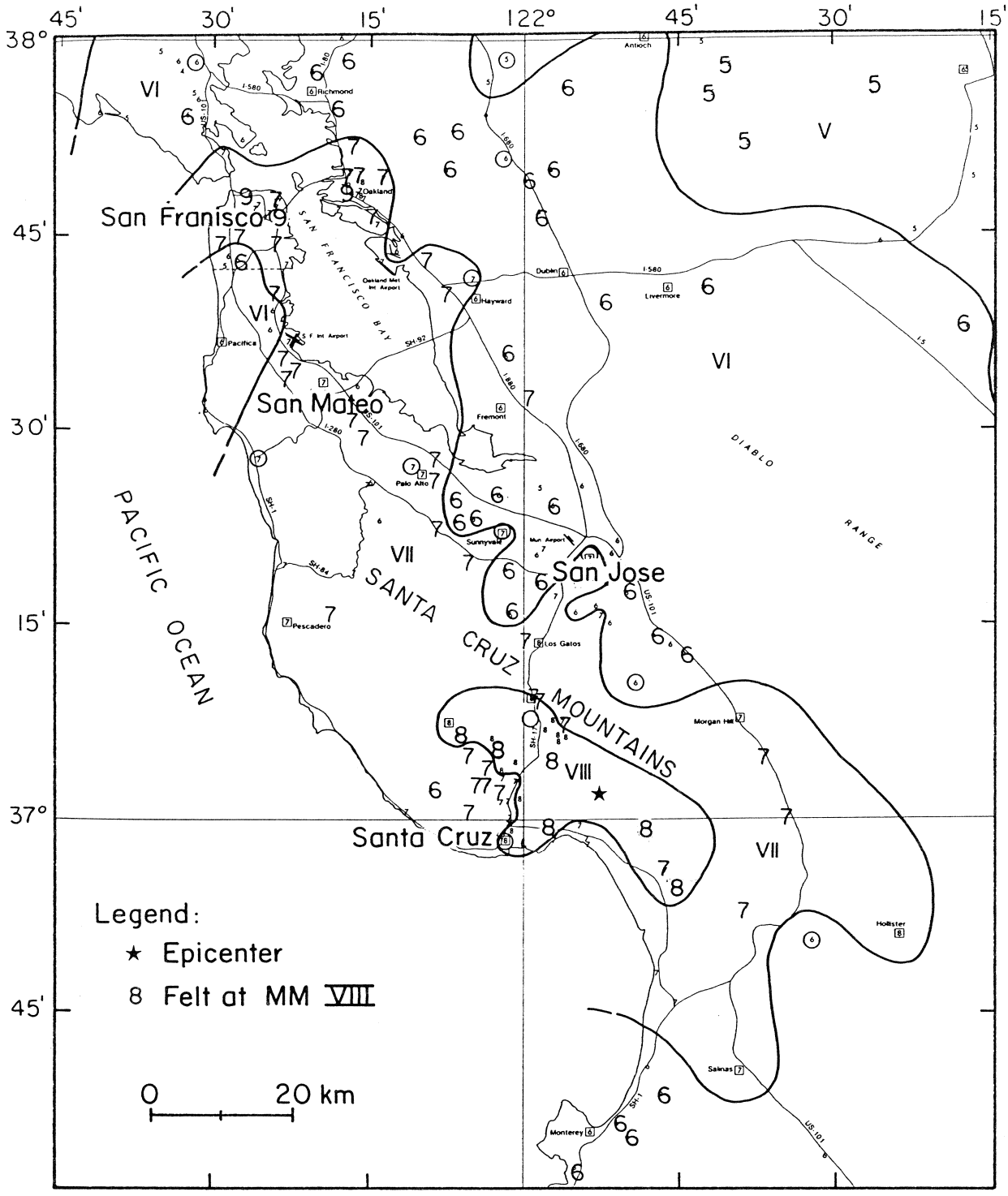

Figure 3. Isoseismal Map for the San Francisco Bay Region for the Loma Prieta Earthquake (after McNutt and Toppazada, 1990)

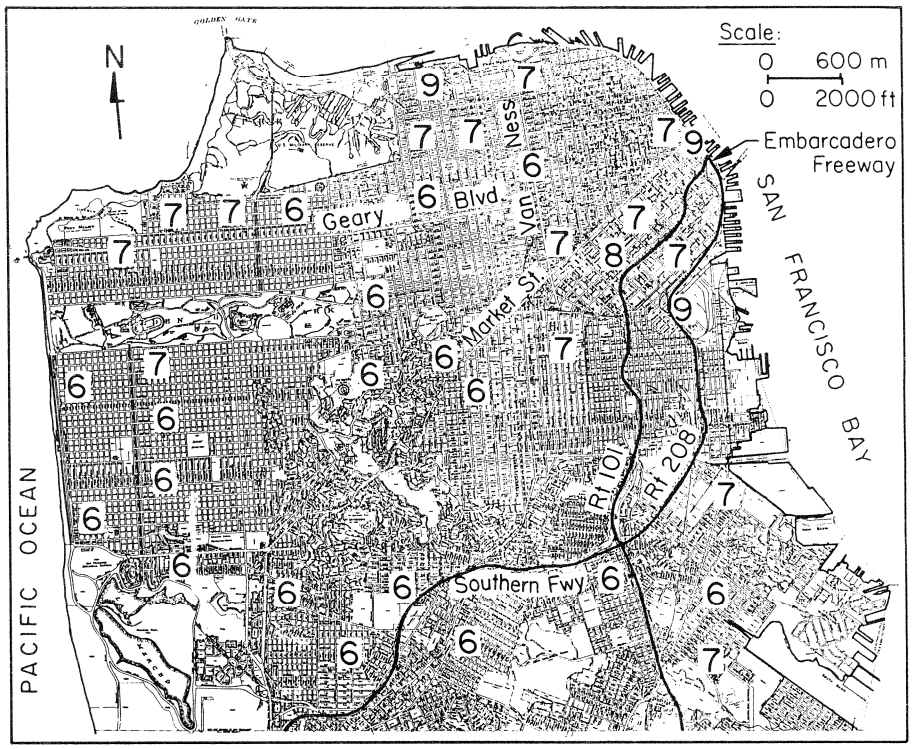

Figure 4. Map of Modified Mercalli Intensities in San Francisco (adapted from Plafker and Galloway, 1989)

in the vicinity of 5th and 7th Sts. on the basis of damage to timber and unreinforced masonry buildings. The pattern shown in the figure indicates that intensities in San Francisco varied from MM VI in areas underlain by rock, to MM IX in areas adjacent to the bay underlain by soft Holocene bay mud and loose sands.

3.0 STRONG MOTION RECORDS

The earthquake produced strong motion data at 131 sites. Stations in the epicentral area showed peak horizontal accelerations as high as 0.64 g. The most distant station in Santa Rosa, at 175 km from the epicenter, recorded about 0.05 g. A digest of the strong motion recordings published by the Earthquake Engineering Research Institute (1990) indicates that peak accelerations at free-field sites underlain by Holocene bay mud were as much as 3.7 times larger than those observed at rock sites at comparable distances. Average free-field peak accelerations on rock, alluvium, and Holocene bay mud were, respectively,

1.6, 1.8, and 4.5 times larger than those predicted by the average values of the most commonly used attenuation relationships for California (Joyner and Boore, 1988). Analyses of strong motion data by Campbell (1991) reveal a strong dependence of peak acceleration on direction, with 68% higher accelerations in San Francisco and Oakland than those at more northerly azimuths. In general, the directional bias in peak horizontal acceleration follows the geologic "grain" of the region, parallel to the San Andreas fault, and conforms to the distribution of MMI in the Bay area.

Figure 5 presents a map of the area of San Francisco and Oakland on which the peak horizontal accelerations are plotted at selected sites. The accelerations were recorded at free-field instruments (ground) and in the basements or ground floors of buildings, most of which have two stories or less (structure). The lowest values, mostly from 0.06 to 0.09 g, were recorded at stations on rock in San Francisco, Yerba Buena Island, and Berkeley. Peak horizontal accelerations as large as 0.2 to 0.25 g were recorded on alluvial and Holocene bay mud sites. The largest acceleration of 0.41 g was measured in a hangar at a bay mud site at Alameda Naval Base. Horizontal ground accelerations at sites underlain by loose fill and Holocene bay mud, relative to those at comparable distances on rock, generally indicate increased peak amplitude and duration of shaking at periods near 1 Hz (Earthquake Engineering Research Institute, 1990).

Time records of horizontal acceleration in the east-west direction (direction of strongest shaking) at three rock sites in San Francisco (locations indicated in Figure 5) are presented in Figure 6. With the exception of a high spike of 0.21 g for the Presidio, there is a strong similarity among the records. Strong motion begins at about 8 seconds after triggering and continues for approximately 12 to 13 seconds.

Of special interest are the recordings from a pair of seismometers deployed at Yerba Buena and Treasure Islands, the locations for which are shown in Figure 5. Figure 7 presents the time records of horizontal acceleration in the east-west direction for each site. The recording on rock at Yerba Buena has very similar characteristics to those shown in Figure 6. The recording on soil at Treasure Island shows a pronounced amplification of acceleration relative to

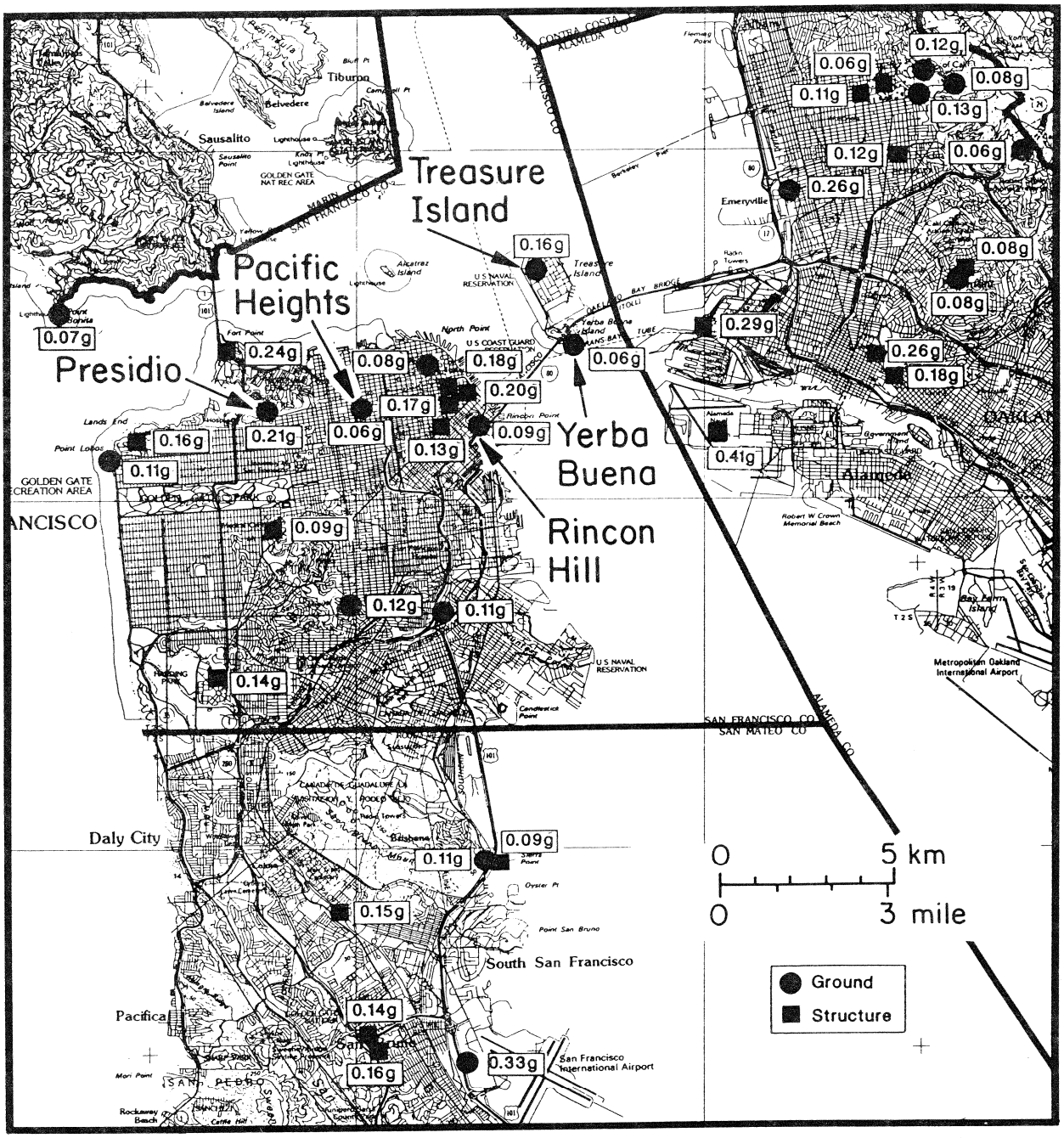

Figure 5. Map of San Francisco and Oakland Area Showing Peak Horizontal Accelerations at Various Sites

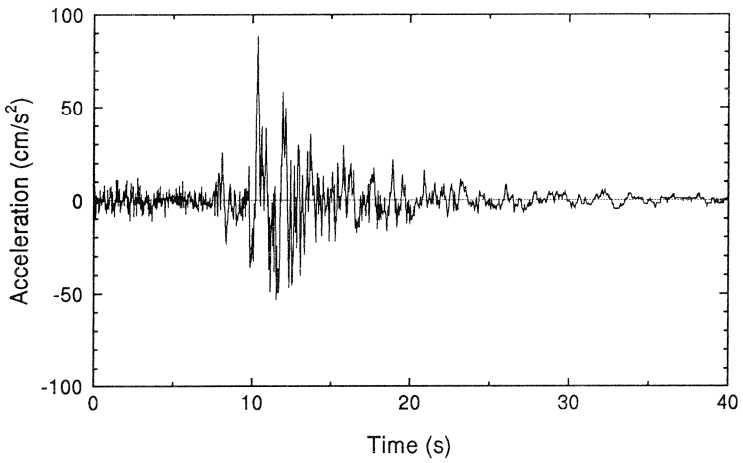

a) Rincon Hill East-West Direction

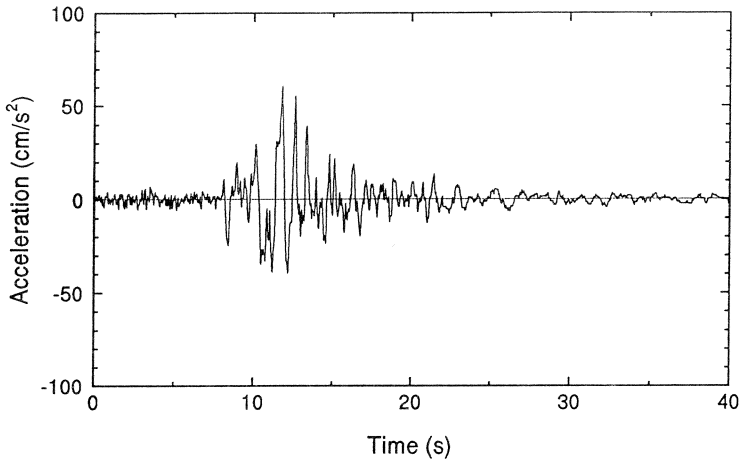

b) Pacific Heights East-West Direction

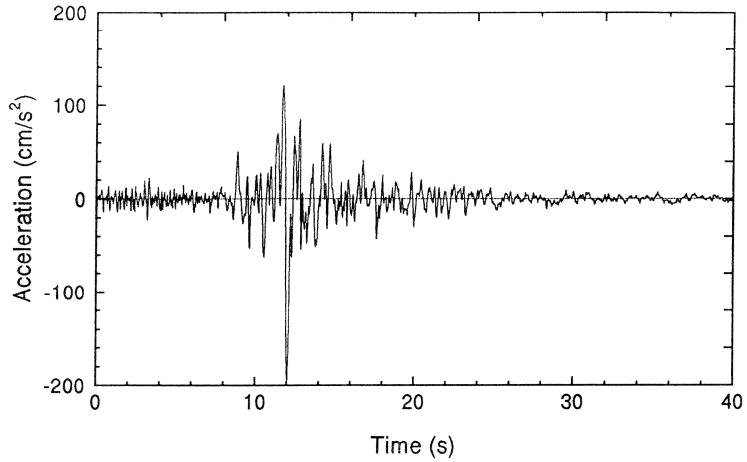

c) Presidio East-West Direction

Figure 6. Time Records of Horizontal Acceleration at Three Rock Sites in San Francisco

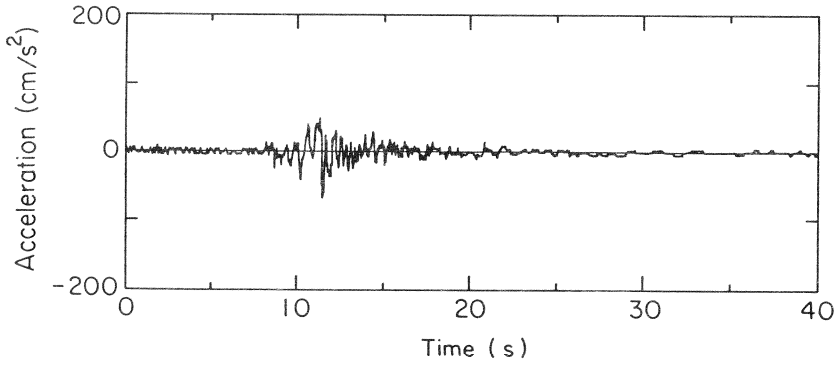

a) Yerba Buena, East-West Direction

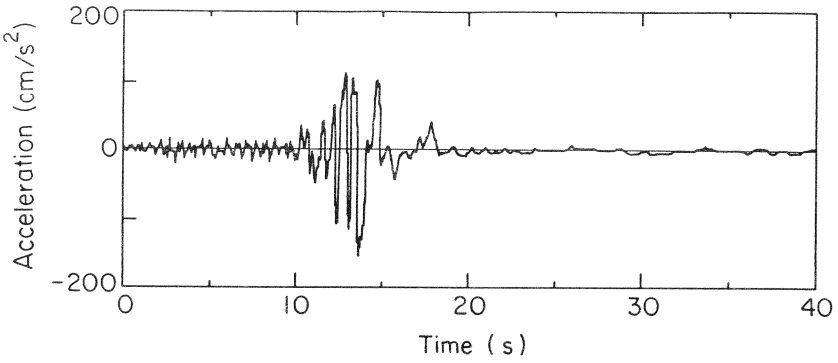

b) Treasure Island, East-West Direction

Figure 7. Time Records of Horizontal Acceleration at Yerba Buena and Treasure Islands

the Yerba Buena site.

The soil conditions at Treasure Island have been described in detail elsewhere (e.g., Idriss, 1990; Hyrciw, et al., 1991). They consist of approximately 10 m of loose hydraulic fill underlain by approximately 15 m of soft Holocene bay mud, with substantially stiffer and stronger deposits of old bay sediments to a depth of 90 m, where bedrock is encountered. Sand boils and ground deformations were observed and mapped near the station on Treasure Island (Egan and Wang, 1990), thereby showing that liquefaction occurred at this location. It should be recognized that the recording at Treasure Island has a sudden drop at about 15 seconds, and thereafter displays characteristics which various investigators attribute to the onset and effects of liquefaction (Idriss, 1990;

Hanks and Brady, 1991).

The Treasure Island-Yerba Buena recordings provide empirical evidence of site amplification, with a 2.7 magnification of peak acceleration from rock to soil site during the main shock. Idriss (1990) and Hyrciw, et al. (1991) have used these records to validate analytical models, using equivalent linear procedures, and to explore the factors contributing to site amplification under conditions of one-dimensional wave propagation. Hanks and Brady (1991) suggest that the Treasure Island accelerogram is the most likely strong motion surrogate for the filled areas of the Marina District, for which no main shock records are available.

Darragh and Shakal (1991) have analyzed the smoothed Fourier amplitude spectra of Treasure Island records relative to Yerba Buena for the main shock and four aftershocks. Compared to the rock site, the strong motion at the soft-soil site was amplified by a factor of approximately three over a frequency range of 0.5 to 2.0 Hz. Moreover, the amplifications they have evaluated are much higher for weak motion. For example, near 1 Hz, they show an increasing amplification as earthquake magnitude decreases. For events with M_L = 7.0, 4.3, 4.1, 3.5, and 3.3, the maximum soil-rock amplifications are 4, 12, 17, 19, and 25, respectively. Such observations are consistent with the studies of Chin and Aki (1991), who show that the strong difference in amplification factor between rock and soft-soil sites observed for weak motion tend to disappear at acceleration levels higher than 0.10 to 0.30 g. These findings provide strong evidence of nonlinear site response where loose fills and Holocene bay mud are present, and indicate that site amplification depends on the amplitude of incoming waves at the locations of such soils.

4.0 OBSERVATIONS OF LIQUEFACTION EFFECTS

There has been a substantial body of post-earthquake observations published on liquefaction and ground deformations generated by the Loma Prieta earthquake in San Francisco (e.g., O'Rourke, et al., 1990; 1991b; Earthquake Engineering Research Institute, 1990; Seed, et al., 1990; Harding Lawson Associates, et al., 1991; 1992). In this case history, emphasis is placed on the four areas

illustrated in Figure 8. For each of these locations, there is significant evidence of soil liquefaction and large ground deformations during the 1906 San Francisco earthquake. Accordingly, a treatment of these areas allows for direct and detailed comparison between the effects of two major earthquakes at the same locations.

It should be recognized that soil liquefaction effects were observed at locations in San Francisco other than those highlighted in Figure 8. Descriptions of liquefaction effects along the Embarcadero are provided by Seed, et al. (1990) and Chameau, et al. (1991), and liquefaction at Hunter's Point is discussed by Chameau, et al. (1991). In general, the influence of liquefaction outside the areas shown in Figure 8 was minor, with the exceptions of Pier 45 and Hunter's Point.

Seed, et al. (1990) report that liquefaction-induced damage to Pier 45 and its warehouse structures caused full or partial closure of several warehouses and temporary relocation of some seafood processing operations. Large longitudinal cracks were observed along the length of the pier. Harding Lawson Associates, et al. (1992) report that Pier 45 was constructed by building a rock seawall along the perimeter of the pier, and then filling the enclosed area with sandy sediments dredged from the bay near the pier. It was this loose hydraulic fill which liquefied, resulting in sand boils, settlement, and lateral deformation.

Hunter's Point is located in the southeastern part of San Francisco, as shown in the inset diagram of Figure 8. Liquefaction effects were observed in a fill area of the naval base at this location. Chameau, et al. (1991) report that three cellular cofferdams at the naval base were subjected to extensive lateral displacements and settlements, and that one of the cells collapsed. Chameau, et al. also present cone penetration test data pertaining to soil conditions at Hunter's Point and select locations along the Embarcadero, both before and after the earthquake.

The areas of prominent soil liquefaction in 1989 and 1906, shown in Figure 8, include the Mission Creek, South of Market, Foot of Market, and Marina districts. Each of these areas was investigated after the 1989 earthquake within

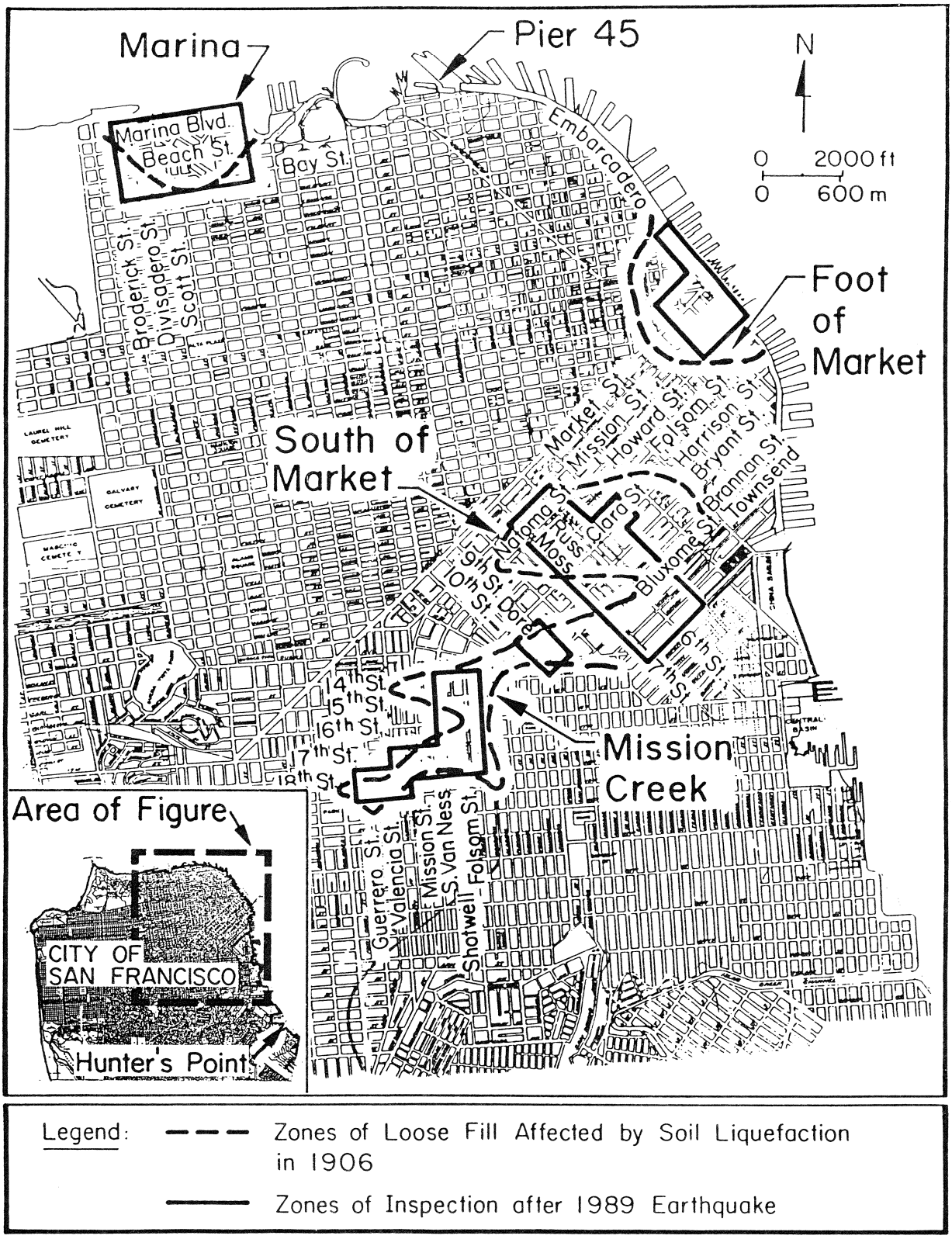

Figure 8. Plan View of San Francisco Showing Zones of 1906 Soil Liquefaction and Inspection After the 1989 Earthquake

the approximate boundaries shown by the solid lines. A description, with maps and photos, is given of the observed ground deformations under each of the following headings.

4.1 Mission Creek

After the 1989 earthquake, significant liquefaction effects were observed at two locations in the Mission Creek area, as depicted in Figure 9. The map in the upper left of Figure 9 shows the locations of and directions in which photographs of liquefaction-induced ground deformation were taken in 1906 and 1989. The map shows the original water course and adjacent marshland of Mission Creek in the vicinity of Dore and Bryant Sts. This map and the adjoining map, showing the area bounded by 17th, Folsom, 20th, and Capp Sts., are similar to the maps of Mission Creek presented in the case history of the 1906 San Francisco earthquake by O'Rourke, et al. (this volume).

About 300 mm of subsidence were observed in a parking lot off Dore St. approximately 30 m north of its intersection with Bryant St. This was a location of substantial settlement and lateral spreading in 1906. There was about 100 mm of settlement of the sidewalk adjacent to the building on the northeast corner of Dore and Bryant Sts. and differential settlement of the structure. The sidewalk along Bryant St. adjacent to the building was buckled and a water service had been ruptured. Photo a shows differential settlement of 1.5 m on Dore St. in 1906 compared with approximately 300 mm of differential settlement on Dore St. in 1989, as shown in Photo b.

The most prominent damage caused by soil liquefaction in the Mission Creek area occurred as differential settlement, racking, and tilting of Victorian two to four-story timber frame buildings on South Van Ness (formerly Howard St.), Shotwell, and Folsom Sts. between 17th and 18th Sts. Sand boils were observed at all these locations. The most severe damage was observed at the middle west side of Shotwell St., where maximum building settlements on the order of 200 to 400 mm occurred. Photo c shows differential settlement and tilting of timber structures in 1906 on the east side of South Van Ness between 17th and 18th Sts. Photo d shows differential settlement and tilting of similar

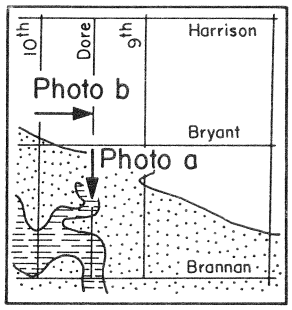

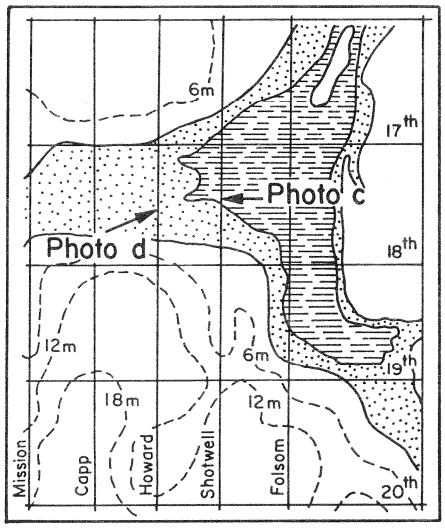

Legend:
- Original water course
- Marsh
- --- Contour lines

Contour interval 6m

Scale: 0 200 m

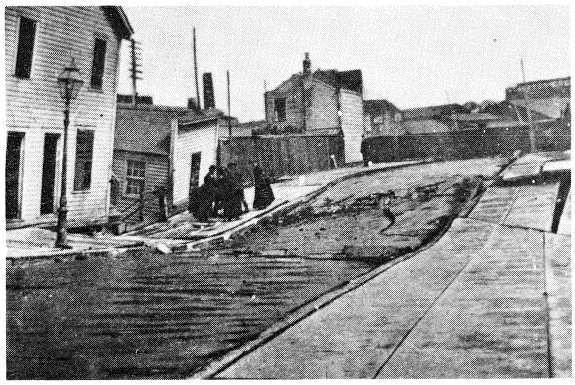

Photo a. Large Differential Settlement on Dore St. Between Bryant and Brannon Sts. in 1906 [after Lawson, et al., 1908]



Photo b. Differential Settlement Along Dore St. Just North of Bryant St. in 1989 (photograph by T.D. O'Rourke)



Photo c. Racking and Settlement of Houses on South Van Ness Between 17th and 18th Sts. in 1906 [after Lawson, et al., 1908]



Photo d. Racking and Settlement of Houses on Shotwell St. Between 17th and 18th Sts. in 1989. These Houses are Directly Behind the Location of Houses in Photo c (photograph by T.D. O'Rourke)

Figure 9. Map and Photographs of Liquefaction-Induced Ground Deformation in the Mission Creek Area

structures in 1989 on the west side of Shotwell St. between 17th and 18th Sts. In contrast to this damage, the area west of Mission St. apparently was unaffected by soil liquefaction, even though lateral spreading and subsidence of 1.5 to 2.0 m were observed at Valencia and Guerrero Sts. in 1906.

Elsewhere in the Mission Creek area, differential settlement and prominent street cracks were observed along 14th St. between Folsom and Harrison. Differential settlements at two to four-story Victorian timber frame buildings were observed on the north side of 15th St. about 30 m west of Folsom in an area where sand boils were apparent along the curb line. The occupants of these structures claimed that settlement had continued for as long as four days after the earthquake.

4.2 South of Market

Figure 10 presents photographs of liquefaction-induced ground movement in the South of Market area. A street map, illustrating the location of the old Sullivan Marsh is provided, on which the locations and camera directions of the photographs are indicated. The map is similar to maps of the South of Market area presented in the 1906 San Francisco earthquake case history (this volume).

Sand boils were observed along curb and building lines at various locations on 7th, 6th, Natoma, Russ, Moss, Clara, Bluxome, and Townsend Sts. From Mission to Folsom St., 10 to 30-mm-wide cracks were observed down the centerline of 7th St., with differential settlement to the east and west of the cracks. As shown in Photo a, differential movement of roughly 300 mm was observed at the southeast corner of Natoma and 7th Sts., with severe deformation of the two and three-story timber frame buildings at this location. The differential movement was caused by both settlement along the sidewalk and uplift of the building. The building was founded on a continuous concrete mat with contiguous basement walls. This water-tight foundation was subjected to buoyancy forces. When the building was demolished, uplift deformation of the foundation mat could be seen clearly in the remains of the mat and basement walls exposed by removal of the superstructure. This building and adjacent ground deformations were close to the location where a 300-mm-diameter water main ruptured, which will be

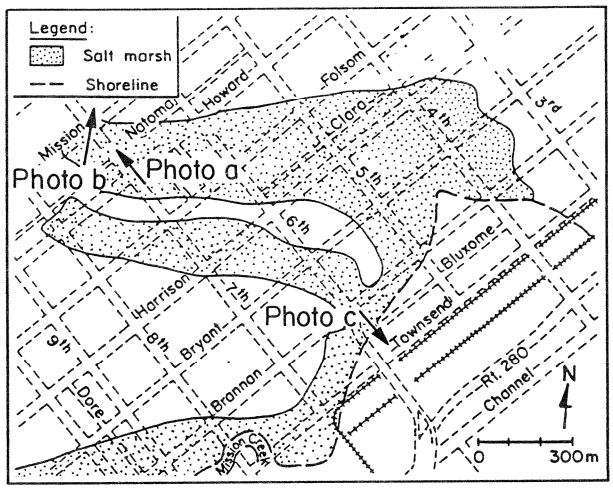



Photo a. Differential Movement of 100 to 300 mm Adjacent to Building at Corner of 7th St. and Natoma St. (photograph by T.D. O'Rourke)



Photo c. Differential Settlement at Corner of 6th St. and Townsend St. (photograph by T.D. O'Rourke)

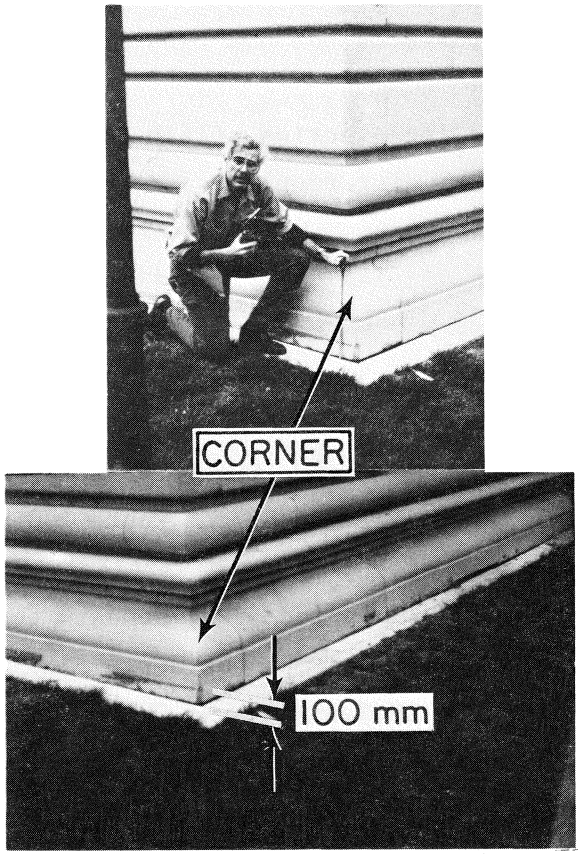

Photo b. Settlement of 100 mm at U.S. Post Office, Corner of 7th and Mission Sts. (photograph by J. Isenberg)

Figure 10. Map and Photographs of Liquefaction-Induced Ground Deformation in the South of Market Area

discussed later in this case history.

Sand flowed into the basement of a building at the corner of Howard and 7th Sts., filling it with approximately 600 mm of material. Differential settlements and cracks were apparent on 6th St. between Folsom and Harrison Sts. Approximately 300 mm of differential settlement and sand boils were observed beneath the Route 280 elevated highway near the intersection of 6th, Bluxome, and Townsend Sts. Compression ridges in the form of buckled street pavements and sidewalks were observed along Russ St., approximately 30 to 60 m north of Folsom St. Ground movement was observed as far north as the corner of the U.S. Post Office on 7th and Mission Sts. Photo b shows differential settlement of 100 mm, which is evident in the photo from the vertical distance between remnant mortar lines and block ornamentation once joined to the building.

At the intersection of 6th St. with Bluxome and Townsend Sts., there was substantial differential settlement. Beneath the western curb line of 6th St. at this location, there is a 2-m-diameter concrete sewer supported on piles. The ground settled sharply adjacent to each side of the sewer, with settlements of roughly 400 to 500 mm at the northeast corner of 6th and Townsend Sts. relative to the sewer centerline. Photo c shows local differential settlement of roughly 150 mm adjacent to the building at the northeast corner of 6th and Townsend Sts. Differential settlements of 150 to 250 mm were observed adjacent to pile-supported columns of the Route 280 highway ramp at this location. Abrupt settlement with a maximum vertical offset of 200 mm was measured to the west of the pile-supported sewer beneath the Route 280 ramp. Differential settlements were apparent along the north side of Townsend St. for a distance of about one block to the east and west of its intersection with 6th St. Sand boils were observed beneath the Route 280 highway ramp. No sand boils or differential settlements were observed in the vicinity of the rail yard immediately south of Townsend St.

4.3 Foot of Market

Differential settlements and lateral displacements were observed along the Embarcadero from Howard St. to just north of the Ferry Building. Subsidence

of approximately 300 mm was observed immediately north of the intersection of Market St. and the Embarcadero. Sand boils were observed along the Embarcadero between the Ferry Building and Pier 1. A map of the Foot of Market area with locations and camera directions of photographs is presented in Figure 11.

Photo a shows a prominent crack, with as much as 100 mm of vertical offset, which occurred in 1989 immediately north of the intersection of Market St. and Embarcadero. The crack extended roughly 60 m in a northeasterly direction from the intersection. In comparison, Photo b shows fissures after the 1906 earthquake in the pavement along East St. (now the Embarcadero) about two to three blocks south of Market St. These fissures are evidence of vertical and lateral movements of approximately 600 to 900 mm toward the bay.

Photo c shows a prominent 25-mm-wide crack which opened beneath the Embarcadero Freeway, running parallel to the seawall for the full distance between Howard and Mission Sts. The crack indicates lateral movement toward the bay at a distance of about 20 m behind the seawall. Differential settlements of 25 to 100 mm were observed adjacent to the pile-supported columns of the Embarcadero Freeway, as shown in Photo d.

4.4 Marina

The Marina was the site of some of the most devastating and well publicized damage caused by the earthquake. The damage occurred in two to four-story timber frame structures with concrete and masonry bearing wall foundations. The worst damage was concentrated at apartment buildings with multiple garages at ground level. These structures lacked sufficient strength and stiffness to resist shear distortion caused by seismic shaking. Where buildings with soft bottom stories were located at street corners or adjacent to open spaces, the absence of support from neighboring structures resulted in severe racking and, occasionally, structural collapse.

A map of the Marina District with locations and camera directions is presented in Figure 12. Superimposed on the map are the 1857 shoreline and 1906 waterfront. The Marina was developed by reclaiming land adjacent to the bay by

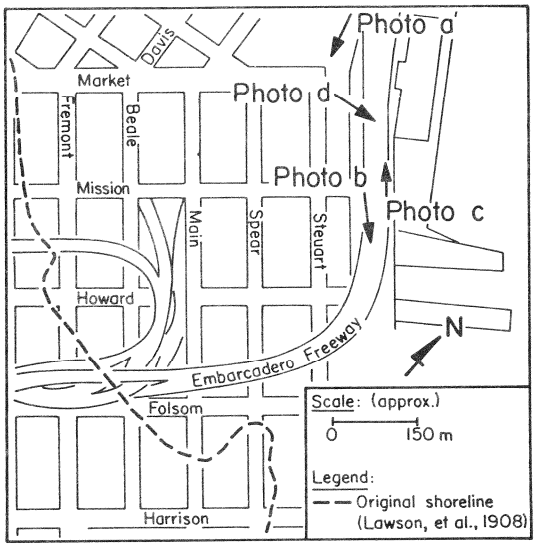



Photo a. Differential Settlement on the Embarcadero Near the Intersection of Market St. in 1989 (photograph by T.D. O'Rourke)



Photo b. Large Differential Ground Movements and Fissures on East St. (Embarcadero) in 1906 [after Himmelwright, 1906]

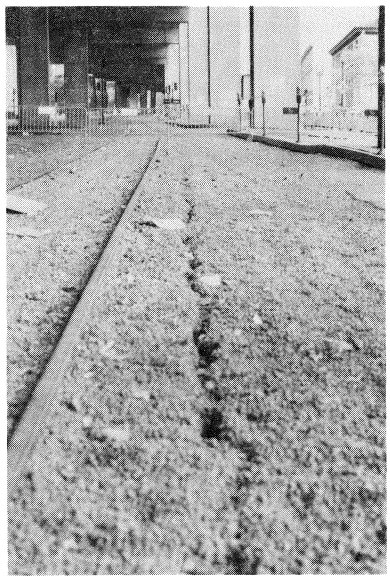

Photo c. Open 25-mm Crack Beneath the Embarcadero Freeway Between Howard and Mission Sts. Showing Movement Toward the Bay (photography by T.D. O'Rourke)



Photo d. Differential Settlement Adjacent to Pile-Supported Column of Embarcadero Freeway Near Mission St. (photograph by T.D. O'Rourke)

Figure 11. Map and Photographs of Liquefaction-Induced Ground Deformation in the Foot of Market Area

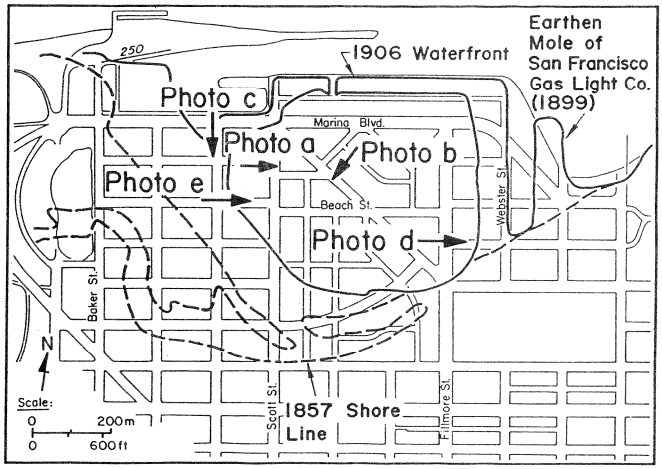

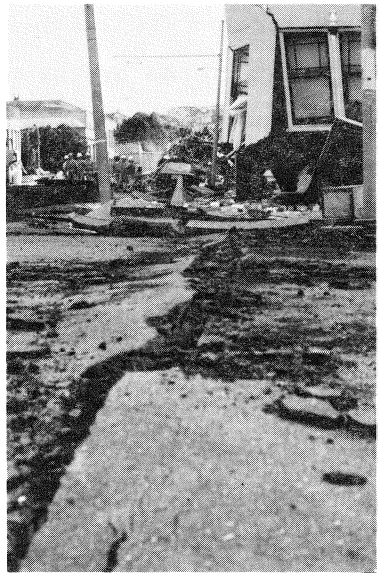

Photo c. Buckled Pavements and Ground Deformations at Corner of Divisardero St. and Jefferson St. (photograph by T.D. O'Rourke)

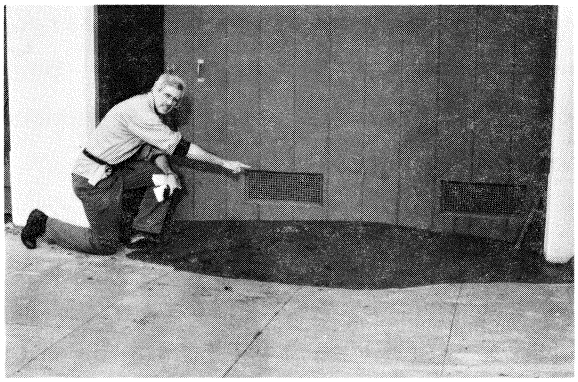

Photo a. Sand Ejected from Garage of Building on Scott St. (photograph by H.E. Stewart)



Photo d. Ruptured Pavement and 75 to 125 mm of Settlement, N. Point St. (photograph by T.D. O'Rourke)

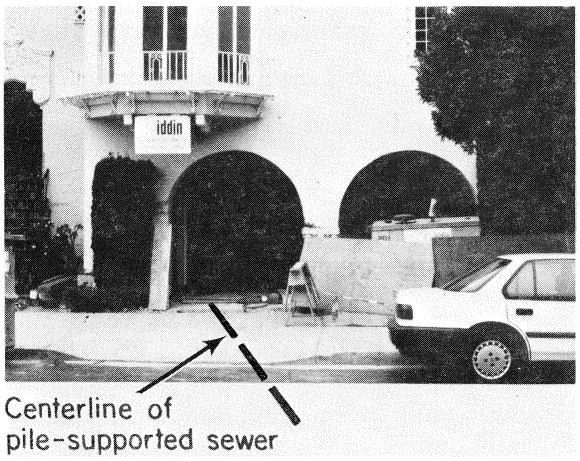

Photo b. Building Damaged by 300 mm of Differential Settlement Over Pile-Supported Sewer (photograph by T.D. O'Rourke)

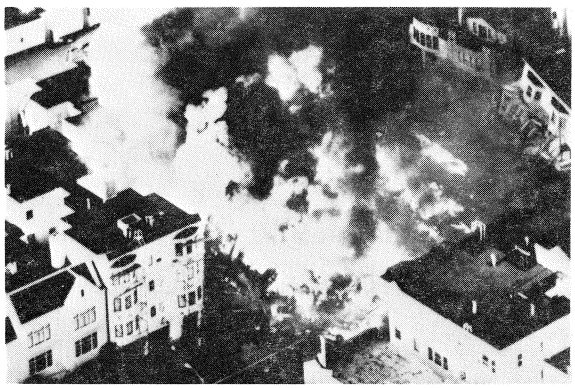

Photo e. Aerial View of Burning and Collapsed Buildings at Divisadero and Beach Sts. (photograph courtesy of EQE, Inc.)

Figure 12. Map and Photographs of Liquefaction-Induced Ground Deformation in the Marina District

means of loose fill, either end-dumped or hydraulically placed in two major stages, as depicted by the previous shoreline and waterfront. A more detailed discussion of the development of the Marina is given in a forthcoming section of this work.

Throughout the Marina, there was direct evidence of soil liquefaction in the form of sand boils. Sand boils were observed on virtually every street where there was damage to buildings. Sand boils were observed along curb lines, sidewalks, and foundation bearing walls. In many instances, sand erupted into garages, forming deposits 300 to 600 mm thick. Sand boils also were observed in the front gardens and back yards of houses and at several locations on Marina Green. Photo a shows sand which had been ejected in the garage of a building on Scott St. and had flowed into the driveway in front of the structure. Although ground shaking was the principal cause of building damage, permanent ground movements also contributed to structural distortion. Permanent ground deformation was evident on virtually all streets.

Photo b shows severe distortion of a building on Cervantes Blvd. that had been constructed over a pile-supported 2.3-m outfall sewer. The building was subjected to 300 mm of differential movement when a bearing wall on liquefied soil settled relative to a bearing wall over the sewer. Buckled and fractured sidewalks and street pavements were apparent throughout the Marina District. Most buckled streets had compressive ridges oriented in a north-south direction, which appears to be perpendicular to the direction of strongest seismic shaking. Photo c shows the intersection of Divisadero and Jefferson Sts. Differential settlement and the buckled pavements of roadways and sidewalks are evident in the photo.

The pattern of cracking and surface ruptures in the streets did not show a coherent sense of displacement or lateral movement in a preferred direction. Conspicuous permanent settlements and lateral displacements were confined to relatively small areas. For example, local differential settlements and lateral movements of 50 to 100 mm were observed at the northwest corner of Beach and Divisadero, southwestern corner of Divisadero and Jefferson, and on North Point St. approximately 60 m west of Webster. Photo d shows ruptured street

pavements and curbside settlement of 75 to 125 mm on North Point St. between Fillmore and Webster Sts. Lateral displacement of 175 mm northward over 30 m was measured in the Winfield Scott School playground, roughly 40 m east of the intersection of Beach and Divisadero.

At the intersection of Divisadero and Beach Sts., several four-story timber frame buildings collapsed or were severely racked by strong ground shaking. A fire broke out in the collapsed structure on the northwest corner of the intersection. Photo e provides an aerial view of the fire which erupted at this location and of the collapsed building across Divisadero.

Along the northern boundary of Marina Green, a prominent 50-mm-wide crack was observed roughly 12 m behind and parallel to the seawall. Sand had been ejected along this fissure. Differential settlements as large as 200 mm were observed adjacent to portions of the seawall, although no lateral deformation or settlement of the seawall was apparent. Cracks and fissures approximately 25 mm wide were observed in the road entering Marina Green, directly north of the intersection of Scott St. and Marina Blvd. Differential settlements of approximately 50 to 100 mm were observed in Marina Green adjacent to a pile-supported 2.3-m-diameter concrete sewer and surrounding a circular underground sewage pump station

Of special interest are ground movements and structural response at the St. Francis Yacht Club, located adjacent to the bay in the northwestern corner of the Marina Green area. The northwestern portion of the two-story clubhouse is supported on 400-mm-square prestressed concrete piles driven to depths of approximately 18 m. Differential settlement as large as 200 mm was observed between this part of the structure and the southern wing of the building, which was supported on spread footings. There was severe structural distortion in the southern wing of the building, whereas the pile-supported section of the building was functional, with little visible damage.

Prominent ground fissures were observed parallel to the retaining wall immediately north of the yacht club at distances of 12 to 50 m from the wall. The cumulative crack widths suggest that northward lateral displacements exceeding

600 mm occurred in this area. Along the north side of the clubhouse is a deck supported on timber piles. Lateral spreading resulted in approximately 600 mm of horizontal movement toward the bay, which displaced the deck and timber piles away from the main clubhouse. Some deformation could be seen in the 400-mm concrete piles supporting the main building. There was a distinct inclination of each pile beneath the northern building line, indicating that underlying sections of the piles had rotated outward relative to the pile caps.

5.0 EARTHQUAKE EFFECTS ON SAN FRANCISCO WATER SUPPLY

5.1 San Francisco Water Distribution System

The City of San Francisco receives its water from two systems of reservoirs and pipelines: the Municipal Water Supply System (MWSS) and the Auxiliary Water Supply System (AWSS). The MWSS supplies potable water for domestic and commercial uses, as well as for fire fighting via hydrant and sprinkler systems. The AWSS supplies water exclusively for fire fighting purposes.

The MWSS provides water from 18 different reservoirs and a number of smaller storage tanks. The water is stored at different levels creating zones, or districts, where water is distributed within a certain range of pressure. There are 23 different pressure districts, of which the Sunset and University Mound Reservoir Systems are the largest. Figure 13 shows a plan view of the Sunset Reservoir System in which the trunk, or feeder, mains are indicated. The pipelines in this portion of the feeder main network range in diameter from 250 to 1500 mm, and vary in composition from riveted and welded steel to cast iron. There are approximately 483 km of feeder pipelines in the MWSS.

Figure 14 shows a plan view of part of the distribution system which is typical of the makeup and configuration of this type of piping throughout the city. Distribution pipelines are principally 100, 150, and 200 mm in diameter. They receive water from the feeder main network for delivery to hydrants and buildings. There are approximately 1350 km of distribution piping in the AWSS.

After the earthquake and fire of 1906, the AWSS was constructed to provide emergency fire protection (Manson, 1908). This system, shown in Figure 15, was

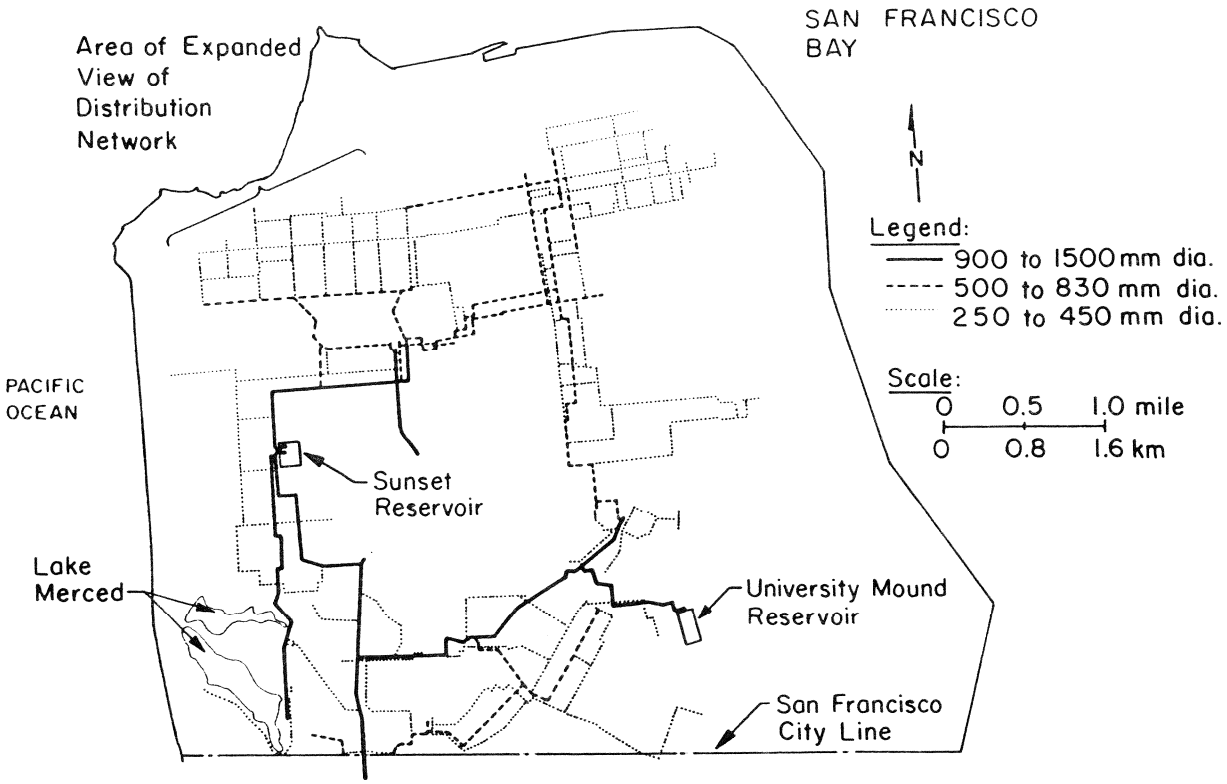

Figure 13. Sunset Reservoir System of the MWSS

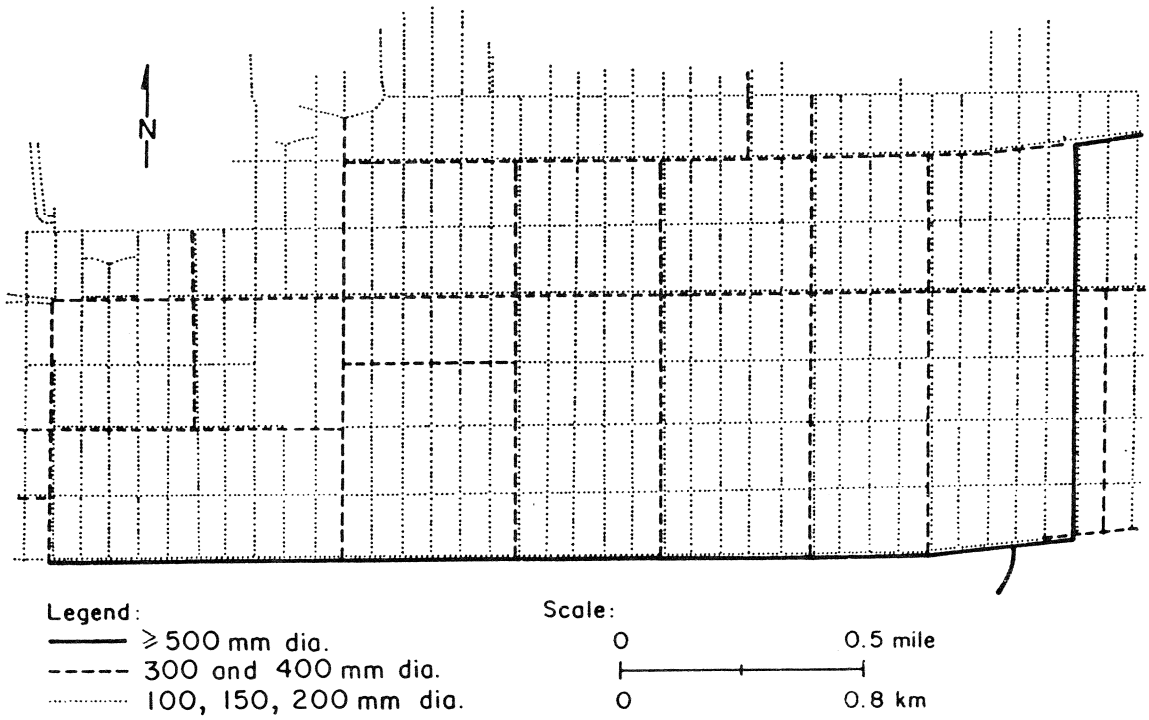

Figure 14. Typical Portion of the Distribution System of the MWSS

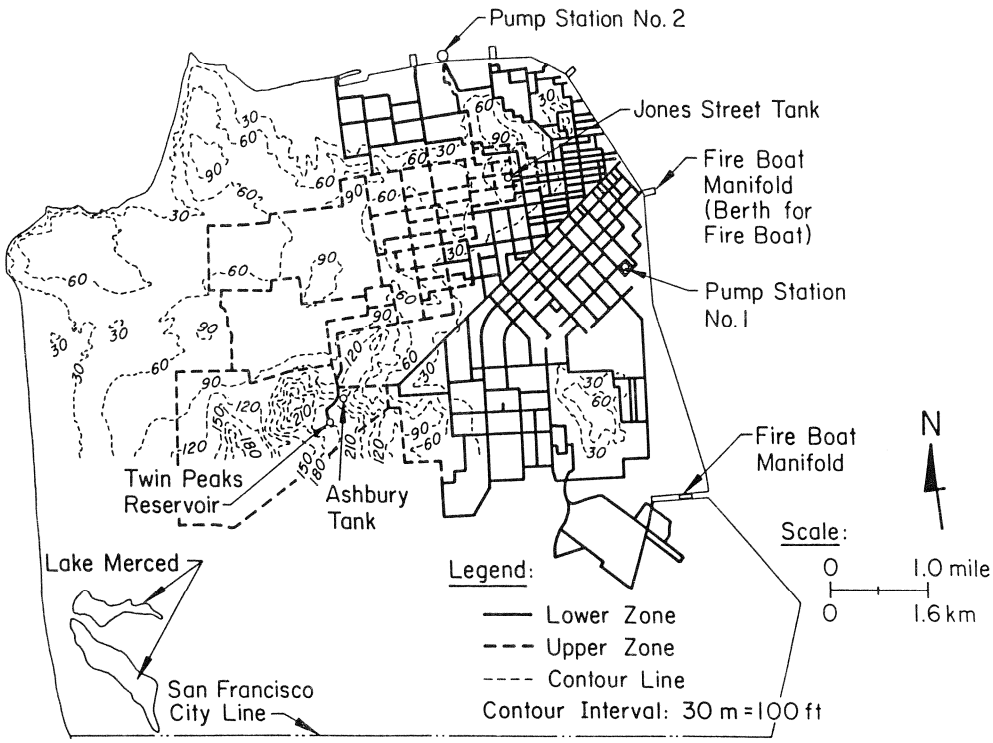

Figure 15. San Francisco AWSS

intended to augment the city's existing fire fighting capacity by providing a supplementary network that would work independently of, but in parallel with, the MWSS. It is separated into an upper and lower zone. Each zone operates nominally at a pressure of about 1 MPa, which is approximately 2.5 times the pressure in the domestic municipal system. The system is supplied by the Twin Peaks Reservoir, the Ashbury Tank, and the Jones St. Tank, which hold 38, 1.9, and 2.8 million liters, respectively. Two pump stations can pump salt water from San Francisco Bay into the system to augment the water supply. The stations have four diesel pumps, each of which can pump 9500 liters/min. at 2 MPa into the lower zone. The city's fireboat, "Phoenix," can be connected to each of five manifolds to inject an additional 38,000 liters/min. at 1 MPa into the lower zone. Additional water for fire fighting is stored in a series of underground cisterns, each of which holds an average of about 284,000 liters.

The AWSS is the only high pressure system of its type in the U.S. It comprises approximately 200 km of buried pipe, with nominal diameters ranging from 250

to 500 mm. At the time of the earthquake, nearly 160 km of the system were cast iron, to which about 40 km of ductile iron pipe had been added during the past several decades. The AWSS has no building connections or service lines; only fire hydrants can draw from the system.

5.2 Performance of MWSS

Damage was relatively low throughout the MWSS, with the exception of the Marina, where there were 123 repairs in the system. In the Foot of Market and South of Market areas (see Figure 8), there were 21 repairs. About five pipeline repairs were performed in the area around Islais Creek, and nine repairs were undertaken in other portions of the system. Damage was manifested in the piping network as broken service connections, round cracks in mains, and leaking joints. The majority of the damage was concentrated in the distribution pipelines of 100 to 200-mm diameter. Reservoirs, pumps, and valves generally performed in a satisfactory manner.

5.3 Performance of AWSS

Table 1 summarizes the damage in the AWSS with respect to approximate street location and characteristics of the damage. The damaged pipelines were composed of cast iron. Hydrants were the most vulnerable parts of the system, with damage being concentrated at elbows. Typical construction involves a 200-mm-diameter cast iron elbow affixed to a concrete thrust pad beneath the street surface hydrant. Damage at hydrant elbows occurred as 45° fractures centered on the elbows. Even though substantial damage was sustained by the MWSS in the Marina, there was only one instance of AWSS repair in this area. This occurred at a leaking joint at Scott and Beach Sts.

The most serious damage was the break of a 300-mm-diameter cast iron main on 7th St. between Mission and Howard Sts. Water flow through this break, supplemented by losses at broken hydrants, emptied the Jones St. Tank (see Figure 15) of its entire storage of 2.8 million liters in approximately 30 to 40 minutes. Loss of this reservoir supply led to the loss of water and pressure throughout the lower zone of the AWSS. This resulted in an especially sensitive condition in the Marina, where damage in the MWSS had cut off alternative sources of

Table 1. Summary of Damage to Auxiliary Water Supply System

Location	Description
Mission and Fremont Sts.	Hydrant elbow break
5th St. between Harrison and Bryant Sts.	Hydrant elbow break
6th St. between Howard and Folsom Sts.	Pipe to hydrant broken at 45° elbow where it passes over sewer
6th and Bluxome Sts.	Broken hydrant; hit by falling brick work
7th St. between Howard and Mission Sts.	300-mm-diameter main broken where it passes beneath a sewer
Folsom and 18th Sts.	Joint leak[1] at a hydrant tee on hydrant side of tee
Scott and Beach Sts.	Joint leak[1] at a 300-mm-diameter pipeline tee

[1]Leaks were relatively small

pipeline water.

When fire broke out at the corner of Divisadero and Beach Sts., water to fight the fire was drafted and relayed from the lagoon in front of the Palace of Fine Arts, approximately three blocks away. The fireboat, "Phoenix," and special hose tenders were dispatched to the site. Approximately two hours after the main shock, water was being pumped from the fireboat and conveyed by means of 125-mm-diameter hosing, which had been brought to site by the hose tenders. Eventually, the supply of water to the fire was about 23,000 liters/ min. The fire was brought under control within about three to four hours after the earthquake.

The special hose tenders and large-diameter hoses belong to the Fire Department's Potable Water Supply System (PWSS), which can move throughout the city

and connect with the fireboat, underground cisterns, the underground pipeline network, and other sources of water to provide an additional measure of flexibility under emergency circumstances. The system had been implemented only two years before the earthquake.

The Twin Peaks Reservoir can be opened remotely by an electrically-controlled valve. However, because of electricity loss after the earthquake, this valve only could be operated manually. About three hours after the earthquake, the Twin Peaks Reservoir was opened into the upper zone, which in the meantime had received its pressure from the Ashbury Tank. It was decided to keep the valves connecting the upper and lower zones closed so that a substantial supply of water and sufficient pressure would be available in the higher elevations.

As described earlier, the AWSS is designed to receive water from two pump stations. Because the Jones St. Tank had emptied and part of the system had gone dry, significant time was required to pump water from the stations back into the lower zone. Approximately three to four hours of careful pumping and venting were needed to avoid water hammer effects.

5.4 AWSS Simulation Studies

To understand better the performance of the AWSS, computer simulations of the network were performed with the program GISALLE (Graphical Interactive Serviceability Analysis for LifeLine Engineering). This program was developed to represent the AWSS as part of a special demonstration project to develop advanced techniques of computer graphics for lifeline systems, and to prove the feasibility of applying these techniques to a real system (Khater, et al., 1989; Grigoriu and O'Rourke, 1989). GISALLE has been checked successfully against special fire flow tests run by the San Francisco Fire Department. The computer model is built around a hydraulic-pipeline-network program that has been modified so as to allow the simulation of post-earthquake damage states. A special code has been developed for GISALLE to model accurately the hydraulic performance of damaged systems with many pipeline breaks.

Figure 16 shows a plan view of the system that was simulated to reproduce the

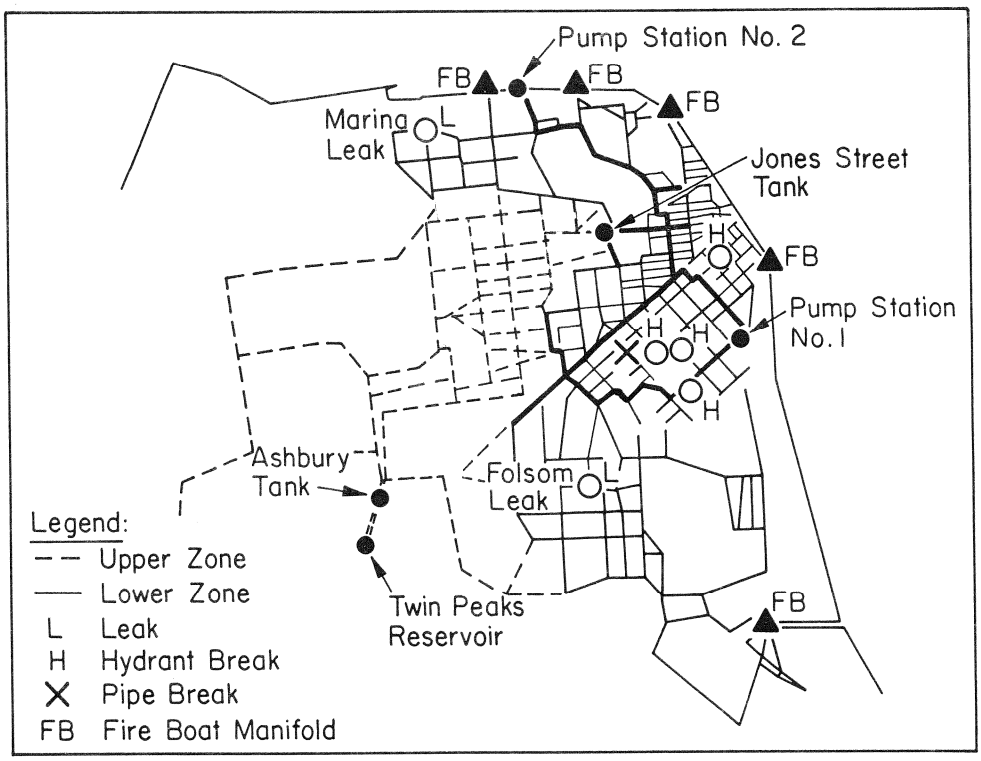

Figure 16. Conditions Used In Computer Simulation of AWSS Performance During the Loma Prieta Earthquake

conditions on the night of the earthquake. Water in the lower zone was supplied by the Jones St. Tank. The lower and upper zones were isolated from one another with closed gate valves. Pump Stations 1 and 2 were not included in the simulation to replicate the system conditions immediately following the earthquake.

Damage of the AWSS occurred as a broken 300-mm-diameter main on 7th St., four broken hydrants, and two leaking joints. The approximate locations of these damage components are illustrated in the figure.

Two models of the system were analyzed by a) neglecting water losses from leaking joints, and b) treating the leaking joints as open hydrants. By analyzing both situations, pressures and flows consistent with the system performance were bounded.

Figures 17 and 18 show the results of the analyses in graphical format. In each figure, open arrows denote water egress either from the Jones St. Tank or damaged components. The solid arrows denote internal flow. Zones of potential soil liquefaction in the South of Market and Foot of Market areas also are shown.

The South of Market area had been recognized as a zone of potentially unstable ground, called an infirm area, and had been isolated from adjoining portions of the network by closed gate valves. Only one open gate valve was provided for this zone at the intersection of Market and 6th Sts., as illustrated in the figures. This gate valve was designed to be operated remotely with utility-supplied electric power. Because of electric power loss at the time of the earthquake, the valve could not be closed remotely. Consequently, water flow through this gate valve in each figure equals the sum of water losses from the broken main and two broken hydrants in this particular infirm area of the system.

In Figures 17 and 18, the total flow rates from the Jones St. Tank are 65,000 and 78,000 liters/min., respectively. The increase in flow rate for the second case represents the additional draw on the system from modeling leaks as equivalent to open hydrants. Given that the normal operating capacity of the Jones St. Tank is approximately 2.72 million liters of a maximum 2.84 million liters, the time required to empty the Jones St. tank would have been between 42 and 35 minutes, pertaining to the conditions in Figures 17 and 18, respectively.

This estimated time to loss of tank agrees with observations during the earthquake. Scawthorn and Blackburn (1990) report that, when the first engine arrived at the Marina fire approximately 45 minutes after the earthquake, it could not draw water from the AWSS hydrants. This time for engine arrival exceeds that analyzed for loss of the Jones St. Tank. Moreover, it was estimated that loss of water from a height of 10.6 to 5.8 m in the Jones St. tank took approximately 15 to 20 minutes. This decrease in water level involves a loss of approximately 1.2 million liters, resulting in an outflow of 60,000 to 80,000 liters/min. over the estimated time span, which is consistent with the analytical results.

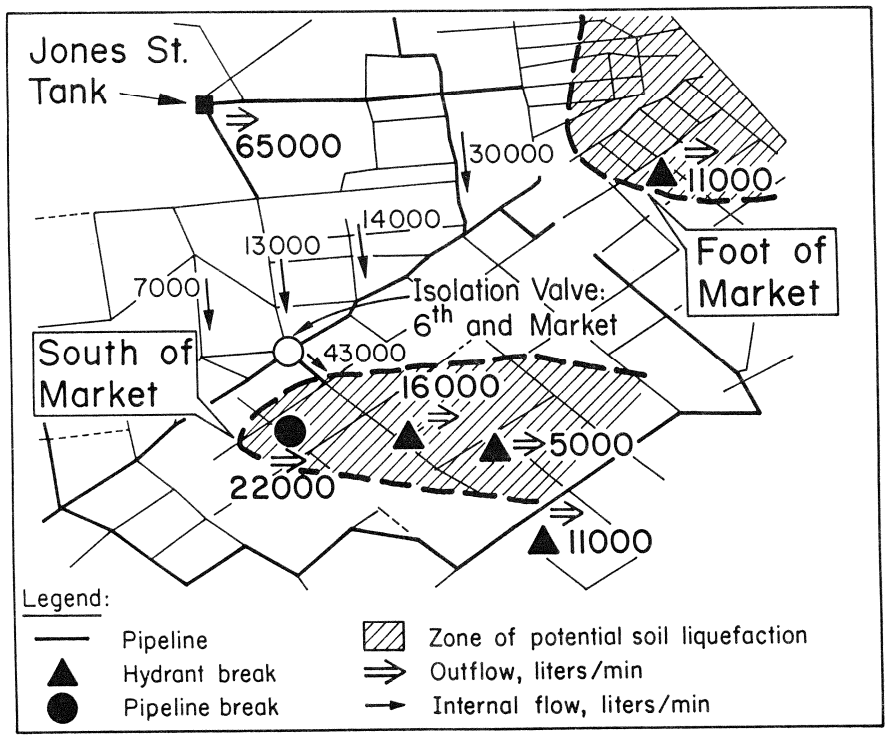

Figure 17. Results of AWSS Simulation with Negligible Water Loss from Leaking Joints

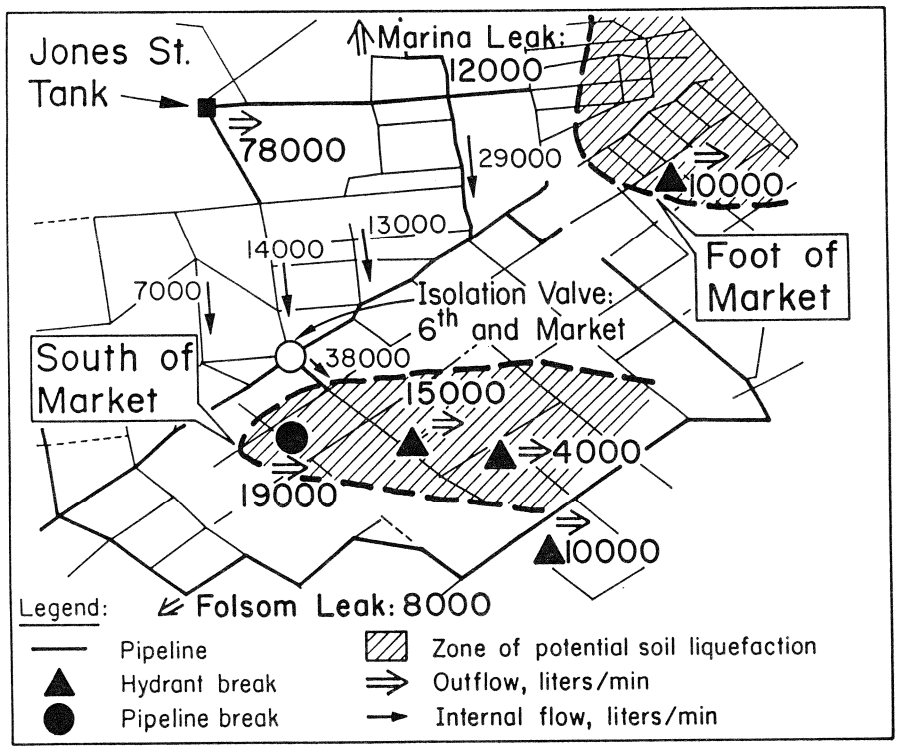

Figure 18. Results of AWSS Simulation with Leaking Joints Modeled

The AWSS performance and computer simulations emphasize how rapidly water can be lost and how important automatic control of isolation gate valves can be. The simulations also underscore the importance of hydrant breaks. In both Figures 17 and 18, the combined flow from two broken hydrants in the South of Market infirm area equals the flow from the ruptured 300-mm main.

6.0 LIFELINE SYSTEM PERFORMANCE IN THE MARINA

The Marina was the most heavily damaged neighborhood of San Francisco, and is a particularly interesting subject for case study analysis. Various reports and papers have been written about the Marina (e.g., U.S. Geological Survey, 1990; Mitchell, et al., 1990; O'Rourke, et al., 1991a; b; Bardet, et al., 1991; Bonilla, 1991; Harding Lawson Associates, et al., 1991), and reference to these works can be made for additional information.

In this study, the Marina is identified as being bounded by San Francisco Bay on the north, the Presidio property line on the west, and Lombard St. and Laguna St. on the south and east, respectively. As shown later in this work, the area west of Laguna St. overlies the deepest part of an underlying bedrock basin and includes the location of loose fills. Furthermore, the area covers virtually all locations of lifeline damage and pipeline replacements as a result of the Loma Prieta earthquake.

6.1 Historic Development

Like several other sites in the San Francisco Bay area, the Marina has been developed by placing sandy fills on soft clays and silts. Figure 19 shows a plan view of the Marina on which is superimposed the 1857 shoreline, as mapped by the U.S. Coast Survey (1857). Along its western boundary, there was a prominent sand spit known as Strawberry Island, with adjacent salt water marshes. Sand dunes, 6 to 12 m high, were located south of the shoreline, and are especially prominent in the southeast portion of the figure.

To aid industrial development, a seawall was built in the 1890s (Olmsted, et al., 1977). The seawall was constructed by dumping rock, which had been ferried in rail cars to the site on barges, and backfilling in places behind

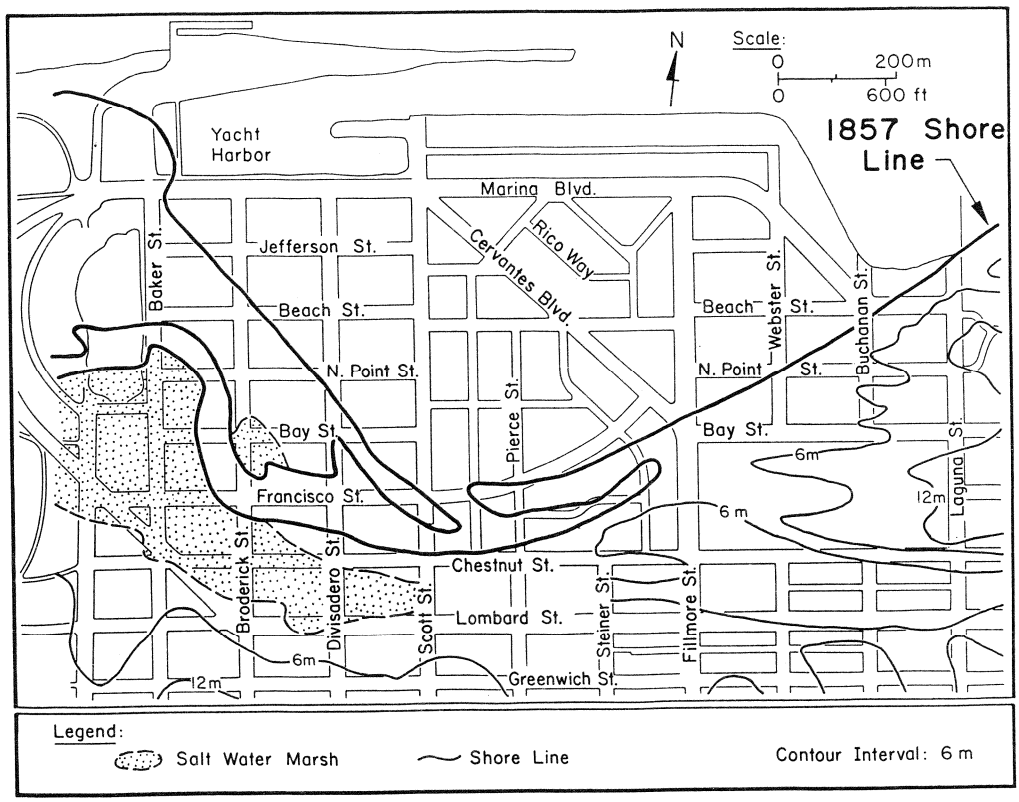

Figure 19. Map of the Marina Showing the 1857 Shoreline

the rock embankment with sand taken primarily from the dunes. Similar construction was performed by the San Francisco Gas and Light Company to establish an earthen mole. Figure 20 shows the seawall and earthen mole (Sanborn Ferris Map Co., 1905) which represents the waterfront and extent of filling at the time of the 1906 earthquake. This configuration of seawall, embankment, and artificial fill remained essentially unchanged until 1912, when construction on site was started for the 1915 Panama Pacific International Exposition.

Although the Marina was not developed extensively in 1906, there are nevertheless several historic accounts of damage in this area (Jones, 1906; Gilbert, et al., 1907; Lawson, et al., 1908), some of which are summarized in Figure 20. Lawson, et al. (1908), for example, drew attention to evidence of severe ground shaking in the hatchured zone of Figure 20, extending from North Point St. between Lyon and Broderick to the shore. In this area, timber structures were thrown out of vertical, reminiscent of the shear deformation sustained by four-story timber buildings during the 1989 earthquake. Moreover, the Baker St.

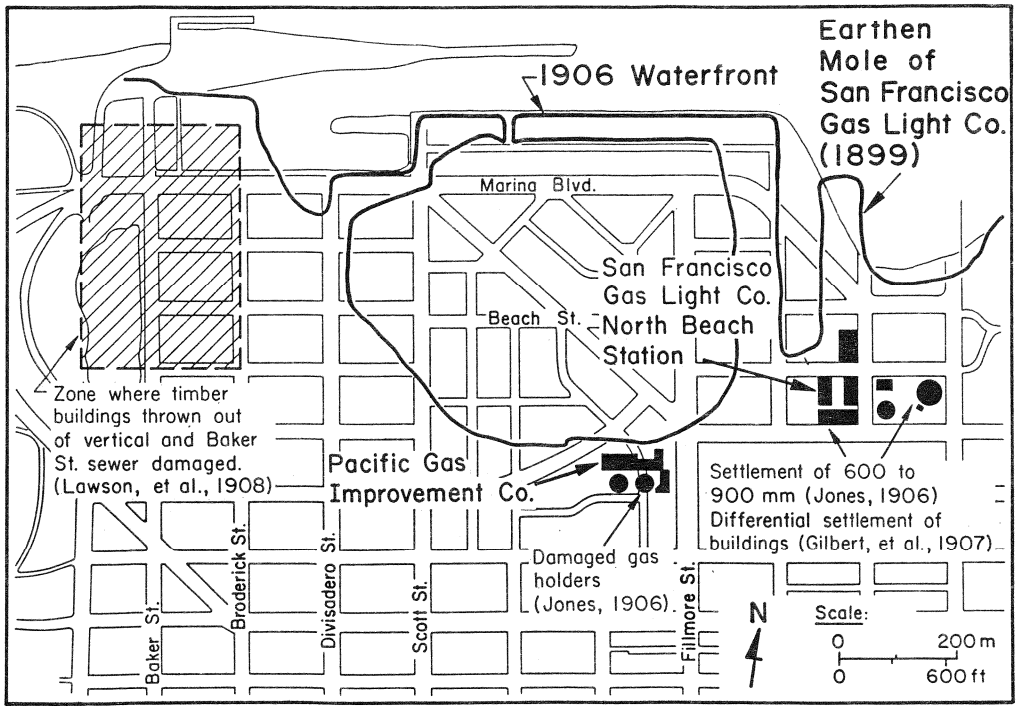

Figure 20. Map of the Marina Showing the 1906 Waterfront and Effects of the 1906 Earthquake

sewer was damaged, which implies that permanent ground deformation occurred in this area.

The most comprehensive observations of damage are associated with the coal gasification plants, which were located in the southeastern part of the Marina in 1906. Gilbert, et al. (1907) reported that all buildings at the San Francisco Gas and Electric (renamed from the original San Francisco Gas Light Co.) plant sustained damage, and that the ground settled "very considerably" at this location. Jones (1906) reported from 600 to 900 mm of settlement adjacent to the principal gas holder at the North Beach Station. The settlement ruptured the 600-mm-diameter outlet connections of the holder, causing all the stored gas to escape.

In 1912, the lagoon enclosed by the seawall was filled with dredged soil pumped from bay deposits located approximately 90 m offshore. Relatively strict

control of the fill material was exercised. The opening along the northern line of the seawall was used to sluice out fine-grained and organic materials during hydraulic filling. It was estimated that 70% of the fill placed in this way was sand (Olmsted, et al., 1977).

In summary, the placement of fill in the Marina may be simplified as having occurred in two prominent stages. The first stage was associated with the placement of land-tipped, or end-dumped, fills. Most of these soils were placed until about 1900 adjacent to both the original shoreline and the old Strawberry Island, and as part of the seawall. The second major stage of filling occurred in 1912, when sandy sediments were dredged and pumped into the lagoon bounded by the old seawall. On the basis of historic development, it is possible to discriminate three general types of soils in the Marina: 1) natural soils associated with the original beach and sand spit deposits, 2) fill tipped from shore or during seawall construction, and 3) hydraulic fill. Areas underlain by each of these soils types behaved differently during the 1989 earthquake, and are analyzed later in this work.

6.2 Water Supply Lifeline Damage

Within the Marina, in an area bounded by the 1857 shoreline on the south (U.S. Coast Survey, 1857) and the current shoreline on the north, there are approximately 11.3 km of pipelines belonging to the MWSS and 2.3 km of pipelines belonging to the AWSS. The MWSS water mains are 100, 150, 200, and 300 mm in diameter, whereas the AWSS water mains are predominantly 250 and 300 mm in diameter. The pipelines in both systems are composed of pit cast iron, and many were installed in the Marina between late 1924 and 1925. The MWSS pipelines were built predominantly with cement caulked, bell-and-spigot couplings, whereas the AWSS pipelines were built with special couplings, as described in the discussion of pipeline damage which follows. All pipelines were buried at nominal depths to top of pipe between 0.9 and 1.2 m.

Figure 21 shows a plan view of the MWSS pipelines and repairs relative to the current street system, 1906 waterfront, and 1857 shoreline. Repairs were made at locations of sheared or disengaged service connections with mains, flexural

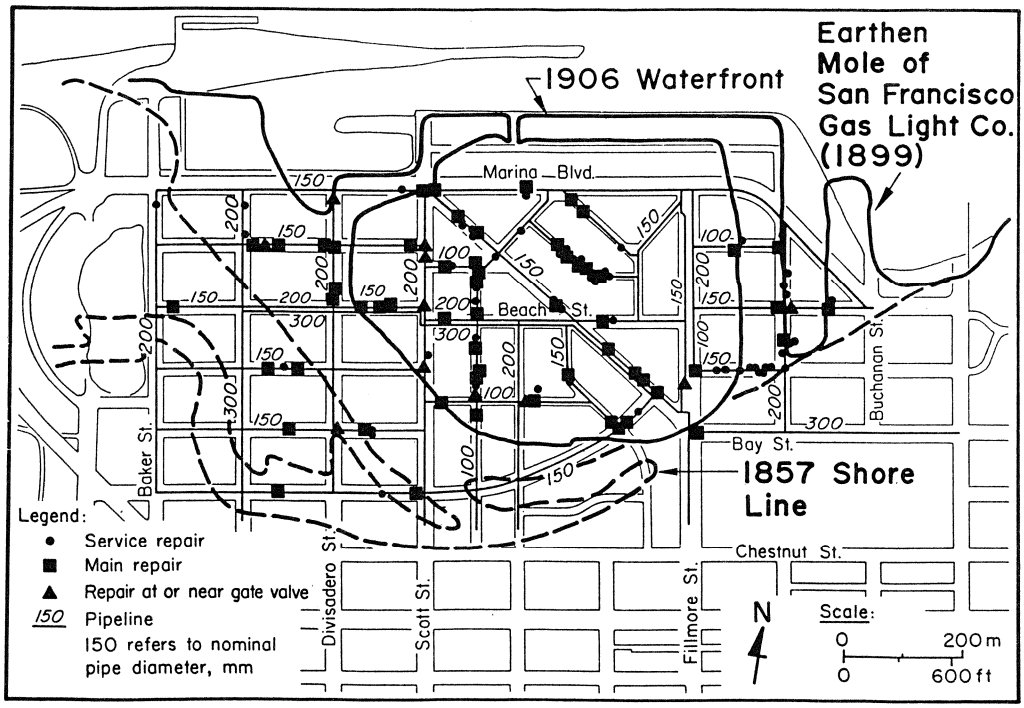

Figure 21. Map of the Marina Showing Locations of Pipeline Repairs to the MWSS

round cracks in mains, and longitudinally split sections of main. In some cases, damage was concentrated at or near gate valves. These devices tend to anchor the pipelines, and therefore may contribute to locally pronounced deformation and stresses. The figure shows the locations of repairs to: a) services, b) mains, and c) sections at or near gate valves.

Figure 22 shows a plan view of the MWSS water mains which were replaced after initial repair. These mains were most heavily damaged in areas of largest surface settlement, and therefore most likely to be subject to continuing rupture and maintenance difficulties in the future. Approximately 2.7 km of mains were replaced, primarily in or immediately adjacent to areas underlain by hydraulic fill.

Even though substantial damage was sustained by the MWSS in the Marina, there was only one instance of AWSS repair in this area. The repair occurred at a leaking joint at Scott and Beach Sts., as shown in Figure 23. It should be

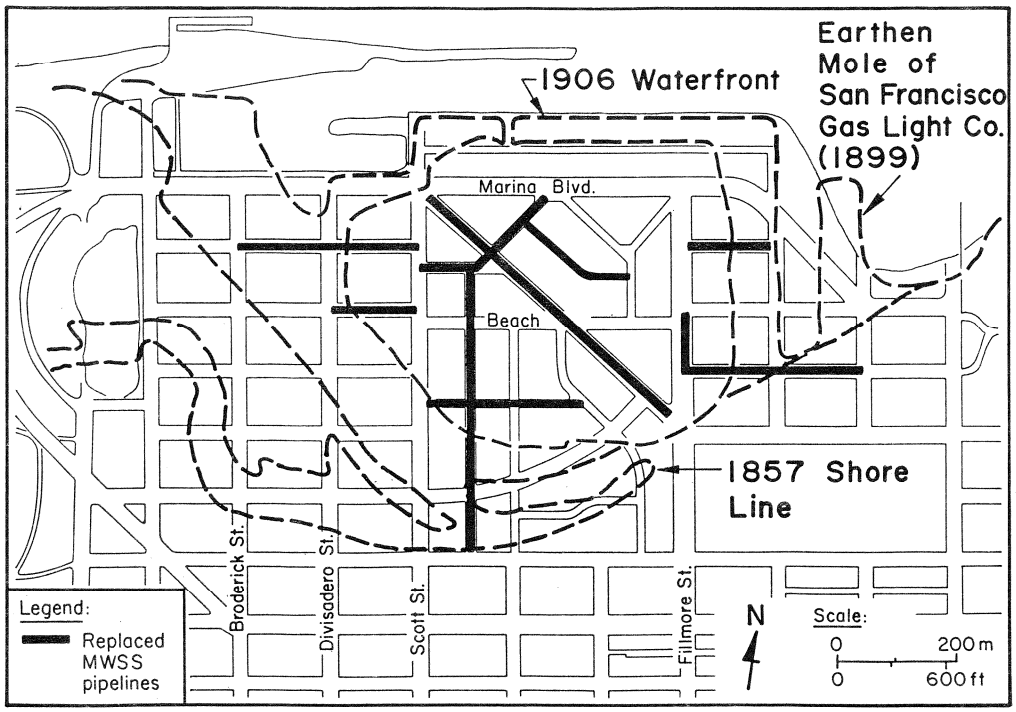

Figure 22. Map of the Marina Showing AWSS Pipelines Replaced as a Result of the 1989 Earthquake

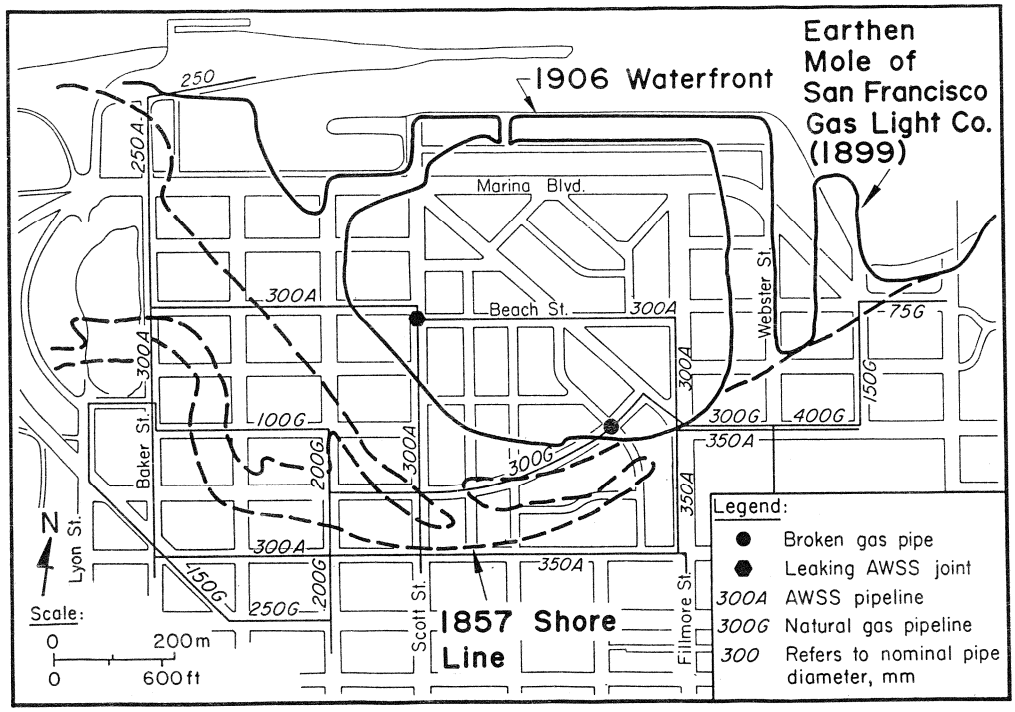

Figure 23. Map of the Marina Showing the Locations of Damage to the AWSS and High Pressure Gas Distribution System

recognized that Figure 23 shows both the AWSS and high pressure gas distribution network in the Marina. The AWSS and natural gas mains are labeled "A" and "G," respectively. The term "high pressure" is intended to distinguish pipelines conveying gas at approximately 200 kPa from low pressure distribution lines at approximately 2 kPa.

Table 2 summarizes the MWSS pipeline damage reported by the San Francisco Water Department as of 1 November, 1989. Repair statistics are tabulated according to nominal pipe diameter, number of repairs, length of pipe of each diameter, and repair rate. The repair rate is the number of repairs in mains, including those at or near gate valves, divided by the total length of pipeline of a particular diameter. Service connections typically are made with pipe substantially smaller than the main, and in many cases, the performance of service connections cannot be linked directly with the diameter of the main. Thus, the service repairs listed in Table 2 are not included in the repair rate/km based on pipe diameter, but are included in the total repair rate, since they contribute to an overall assessment of system damage. The repair statistics pertain to the area of MWSS pipeline damage bounded by Baker St., Marina Blvd., and Buchanan St. on the west, north, and east, respectively; and by Bay and Chestnut Sts. on the south.

There were 123 repairs to the MWSS mains and services, more than three times the number of repairs in the entire MWSS outside the Marina. There were 69 repairs to mains, including those at or near gate valves, with over 80% of these attributed to flexural round cracks. In contrast, there was only one leaking joint in a 300-mm-diameter AWSS pipeline out of 2290 m of 300 and 250-mm-diameter pipelines within the area of MWSS damage described above. This results in a repair rate of 0.43 repairs/km.

In Figure 24, the repair rates for MWSS and AWSS pipelines are plotted as a function of nominal pipe diameter. The slope of the linear regression is approximately -3, which implies that pipeline repair was inversely proportional to the cube of the pipe diameter. Since the moment of inertia of a given pipe is a function of diameter cubed, the regression analysis indicates that damage was influenced strongly by the longitudinal bending resistance of the

Table 2. Summary of MWSS Pipeline Damage in the Marina

Pipeline Diameter mm	Main Repairs	Repairs at or Near Gate Valves	Service Line Repairs	Length of Pipe m	Repair Rate Repairs/km
100	16	2		1250	14.40
150	33	8		5600	7.32
200	7	2		3300	2.73
300	1	-		1200	0.83
TOTALS	57	12	54	11350	10.84[a]

[a]Total repair rate including mains and service lines

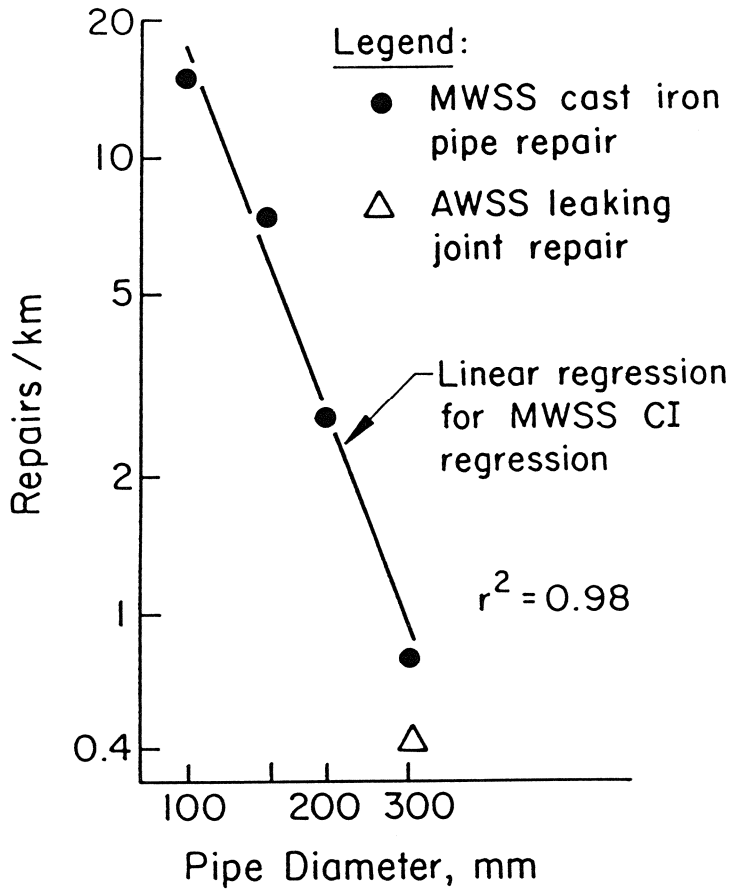

Figure 24. Linear Regression of Repair Rate of MWSS vs. Nominal Pipe Diameter

pipelines. Hence, it appears that bending stress caused by differential settlement of the underlying soil was the main cause of pipe failure, and that resistance of such stress, resulting from flexible AWSS joints and increasing pipe diameter, was responsible for the lowest repair rates.

6.3 Gas Distribution Lifeline Damage

Only one location of damage was reported for the high pressure gas distribution lines at a miter joint near the boundary of hydraulic fill and the 1857 shoreline. The high pressure mains were constructed mostly of Grade B steel with electric arc girth welds.

In contrast to the high pressure system, there was substantial damage to the low pressure gas distribution mains. Approximately 13.6 km of steel and cast iron mains, ranging from 100 to 300 mm in diameter, were replaced within the area bounded by Laguna, Lombard, and Lyon Sts., and the bay (Phillips and Virostek, 1990). A little over half of this number was replaced with medium density polyethylene (MDPE) piping inserted within existing steel and cast iron pipes. The remainder was replaced by direct burial of MDPE piping. The nominal diameters of replacement pipes were 50 to 150 mm, with about 90% of the piping having a 50 mm diameter.

6.4 Wastewater Conveyance Lifeline Damage

In San Francisco, wastewater is collected, transported, and treated under the Clean Water Program. The wastewater system consists of 1159 km of collector sewers, ranging in diameter from 200 mm to 600 mm, 241 km of transport sewers, ranging in diameter from 900 mm to 2.3 m, and a series of storage culverts to hold water during heavy runoff for later transport and treatment. Approximately 77% of the collection and transport sewers are over 50 years old.

Three types of sewage conduit are located in the Marina and were affected by the earthquake: 1) collector sewers, ranging in diameter from 200 to 600 mm, 2) outfall sewers, ranging in diameter from 1.5 to 2.3 m, and 3) a 3 to 5-m-wide reinforced concrete box culvert along Marina Blvd. The collector sewers were composed mainly of vitrified clay pipe in lengths nominally 1.5 to 1.8 m

long with mortared joints. This type of pipe is relatively weak and brittle. Since about 1960, the Clean Water Program has been installing vitrified clay pipe, which is significantly stronger and equipped with polyethylene gaskets at the joints to promote flexibility.

Figure 25 shows damage to the wastewater conveyance system. Damage at the outfall sewers occurred primarily because of broken connections between the pile-supported outfalls and collector sewers, which settled differentially relative to the outfalls. The outfall sewer along Pierce St. at the center of the figure was a circular reinforced concrete structure, ranging in diameter from 1.8 to 2.3 m, supported on timber piles, with an invert depth about 3 m below ground surface. It was heavily damaged north of the seawall on Marina Green. The 1.5-m-diameter Baker St. outfall, which was of similar construction, was cracked and fractured at a turning point (location of triangle in Figure 25), where a joint connects it to an overflow weir. Minor cracking was observed along the invert of the Marina Blvd. box culvert.

Within the area bounded by Baker St., Marina Blvd., Buchanan St., and Chestnut St., there were 9.8 km of vitrified clay pipe collector sewers, of which approximately 2 km were replaced or repaired as a result of the earthquake. The lengths of pipelines in which repairs and replacements were made are shown in Figure 25 on the basis of records provided by the Clean Water Program. Much of the damage was in the form of cracked and crushed joints. Approximately 1.4 km of vitrified clay pipe was replaced with stronger clay pipe, utilizing gasketed joints. Nearly 73% of the replaced or repaired pipes were located in or immediately adjacent to (within half a block) areas of hydraulic fill.

Table 3 summarizes the repair and replacement statistics for collector pipes by listing nominal diameter, length at the time of earthquake, length repaired or replaced, and percentage repaired or replaced. In contrast to the MWSS damage, the collector main damage does not correlate with nominal pipe diameter. With the exception of the 250-mm and 600-mm-diameter pipes, the percentage of repaired or replaced mains varies from 15 to 28%. The overall percentage of repaired or replaced collector mains within the area of damage was 20%.

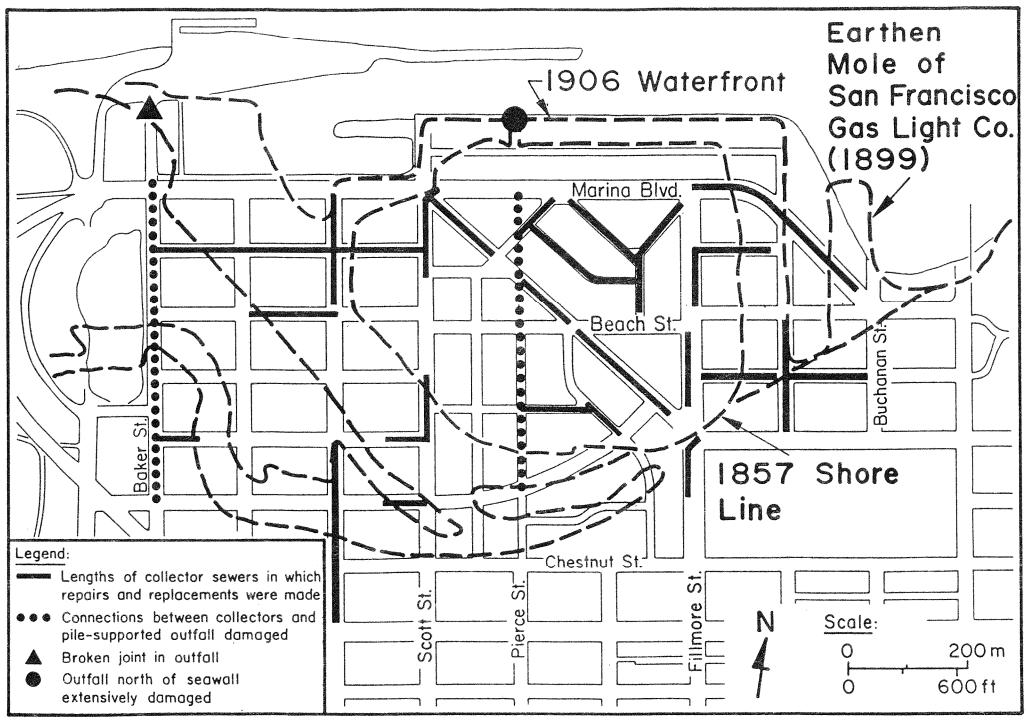

Figure 25. Map of the Marina Showing Locations of Replaced and Repaired Wastewater Conveyance Pipelines

Table 3. Repair/Replacement Statistics for Collector Sewer Pipe in the Marina

Diameter mm	Length m	Length Replaced or Repaired, m	% Replaced or Repaired
200	5345	1127	21
250	300	143	48
300	875	152	17
375	950	175	18
450	580	87	15
525	930	258	28
600	805	0	0
TOTALS	9785	1942	20

6.5 Ground Deformation and Pipeline Repair

Settlements caused by the Loma Prieta earthquake were evaluated on the basis of survey data collected in 1961, 1974, and 1989 and published by Bennett (1990), as well as a detailed evaluation of subsurface conditions in the Marina by O'Rourke, et al. (1991a). Settlement data were confined to street intersections.

It was assumed that the settlement from 1961 to 1974 principally was caused by secondary compression of Holocene bay mud. From the survey data base, the incremental secondary compression, ΔS, was regressed relative to the thickness of Holocene bay mud, H, to obtain the best linear fit of the data with slope $\Delta S/H = 0.0011$. This slope is related to soil properties in the form:

$$\frac{\Delta S}{H} = C_{\alpha\epsilon} \log(t_2/t_1) \qquad (1)$$

in which $C_{\alpha\epsilon}$ is the coefficient of secondary compression, defined as the ratio of the change in one-dimensional vertical strain to the change in log time after the end of primary consolidation, and t_2 and t_1 are times since the placement of hydraulic fill in 1912 to 1961 and 1974, respectively.

A value of $C_{\alpha\epsilon} = 0.011$ was calculated with Eqn. 1, which compares very favorably with $C_{\alpha\epsilon}$ determined for Holocene bay mud on the basis of one-dimensional consolidation tests (Dames and Moore, 1989). On the basis of 42 test results with stress increments to levels of 1.2 to 2.5 times the preconsolidation pressure, the mean value for $C_{\alpha\epsilon}$ was 0.011, with a standard deviation of 0.004.

The value of $C_{\alpha\epsilon} = 0.011$ was used to calculate the incremental secondary compression for each survey point between 1974 and 1989. These values were subtracted from the difference in actual survey measurements to yield "corrected" settlements that would represent best the amount of vertical movement caused by liquefaction-associated consolidation of the fills underlying the Marina. Settlement contours were developed from these corrected measurements with the computer program "Surfer" (Golden Software, Inc., 1985), using a procedure referred to as kriging, in which contours are developed with minimal estimation

variance from a statistical evaluation of the input data (Ripley, 1981).

The resulting settlement contours are shown in Figure 26. The maximum settlements occurred in the hydraulic fill, with decreasing amounts of vertical deformation in the land and barge-tipped fills and areas underlain by natural beach and sand bar deposits.

To represent the distribution of MWSS damage, the Marina was divided into a grid of approximately 40 cells, and the number of repairs per length of pipeline in each cell was counted. Each repair rate then was normalized with respect to a reference length of 300 m to provide a consistent basis for evaluation. Contours of equal repairs per 300 m of pipeline were drawn and superimposed on the street system and previous shorelines, as illustrated in Figure 27. The contours of pipeline repair rates are related closely to the settlement contours, hydraulic fill, and 1857 shoreline. Inspection of Figures 26 and 27 shows that the locations of closely spaced settlement contours, indicating the largest local settlement slopes, correspond to the locations of relatively high pipeline repair rates. High concentrations of pipeline repair fall within the area of hydraulic fill. The heaviest repair concentration occurs at the junction of the hydraulic fill, seawall, and 1857 shoreline, except for an isolated area on Rico Way, where unusual stresses were generated as a result of pipeline construction along the curved street.

The spatial patterns of damage in Figures 25 and 27 and their close relationship with the pattern of settlement in Figure 26 show a strong link between pipeline damage and differential movement. Differential movement is most heavily concentrated at the boundaries among the fill, natural soils, and old seawalls. It is important to note that damage to the relatively large 300-mm MWSS main (see Figure 21) and 300-mm gas pipeline (see Figure 23) both occurred very close to the boundary between hydraulic fill and the 1857 shoreline, where differential settlements were concentrated.

7.0 WATER SUPPLY DAMAGE IN SOUTH OF MARKET AREA

As in the Marina, pipeline damage in the South of Market area occurred in

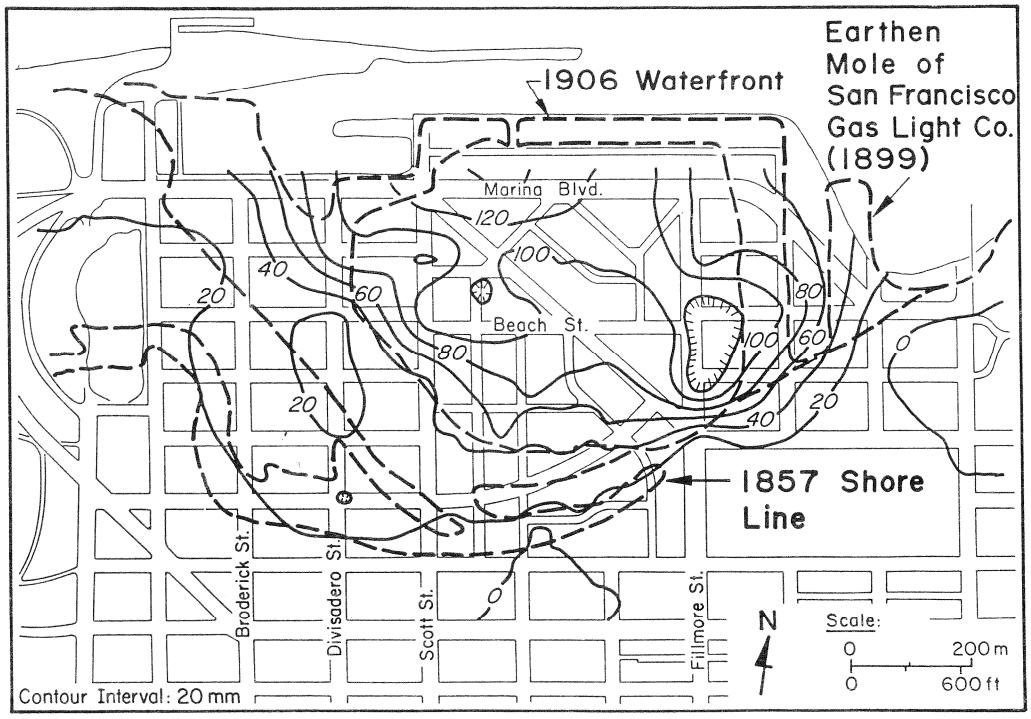

Figure 26. Map of the Marina Showing Contours of Settlement Caused by Post-Liquefaction Consolidation

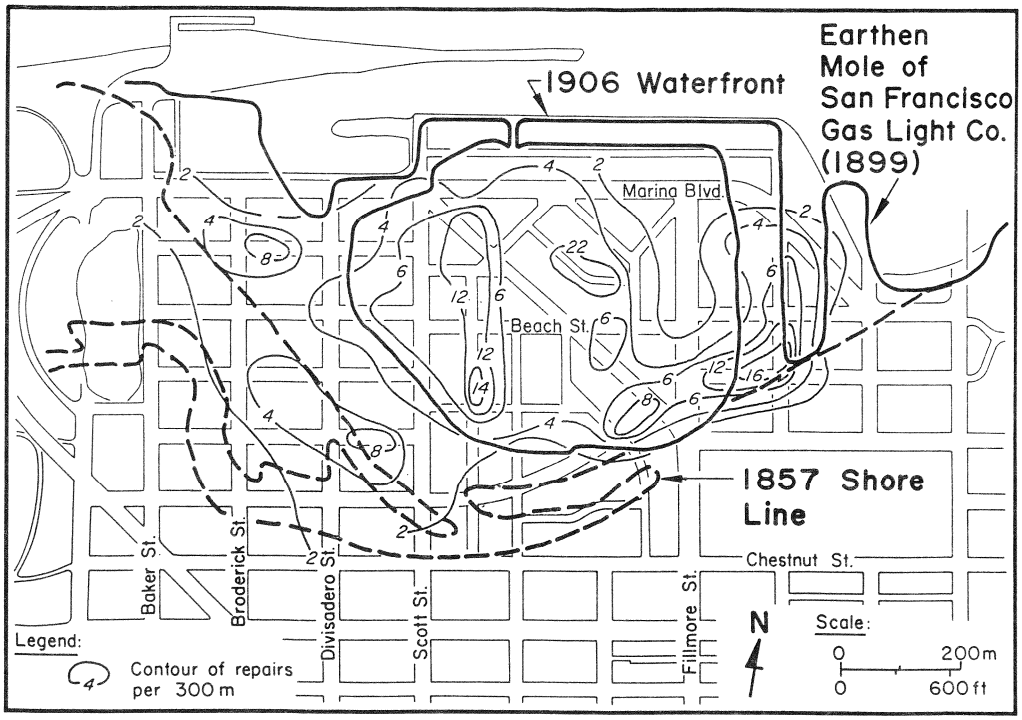

Figure 27. Map of the Marina Showing Contours of Repair Rates for the MWSS

locations where loose sandy fills had been placed over deposits of soft to medium clay. Figures 28 and 29 show pipeline repairs in the South of Market area for the MWSS and AWSS, respectively. The pipeline repairs, pipeline network, and current street system are shown relative to salt marshes and the shoreline of Mission Bay, which once were located at this site. The marshes and shoreline were established by reference to topographical maps prepared by the U.S. Coast Survey (1853; 1857). The area was filled during the years between 1850 and 1865, primarily with material excavated from nearby sand dunes (Dow, 1973; Roth and Kavazanjian, 1984).

The highest concentration of pipeline repairs was in the area bounded by 8th, Mission, 5th, and Harrison Sts. As described in Section 4.2, differential settlements and fractured pavements (indicating lateral movement) were observed throughout this area. Although the level of damage was much more severe in 1906, it is interesting to note that some of the pipeline damage in 1989 occurred in the same general area as in 1906. For example, Reynolds (1906), in reporting on the condition of buried electrical conduits, stated: "Along 7th St. from Mission to Howard, the earth was displaced from 5 to 8 ft (1.5 to 2.4 m) in a direction lengthwise to conduit. This caused some of the manholes to crush... The conduit was pulled apart at other places, and cables were wrenched and torn apart from their boxes..." Numerous additional descriptions of buried lifeline damage in the South of Market and other locations of 1906 San Francisco have been compiled, and the reader is referred to these sources for additional information (e.g., Youd and Hoose, 1978; O'Rourke and Lane, 1989).

It should be recognized that time-dependent settlement has occurred in the South of Market area because of consolidation of underlying clay in response to the weight of fill and buildings. During field investigations along parts of Clara St., for example, it was apparent that some buildings had experienced differential settlement well before the earthquake. Such differential settlement tends to reduce the capacity of buried pipelines to resist transient and permanent ground displacements, and may have contributed to the earthquake damage in this general area.

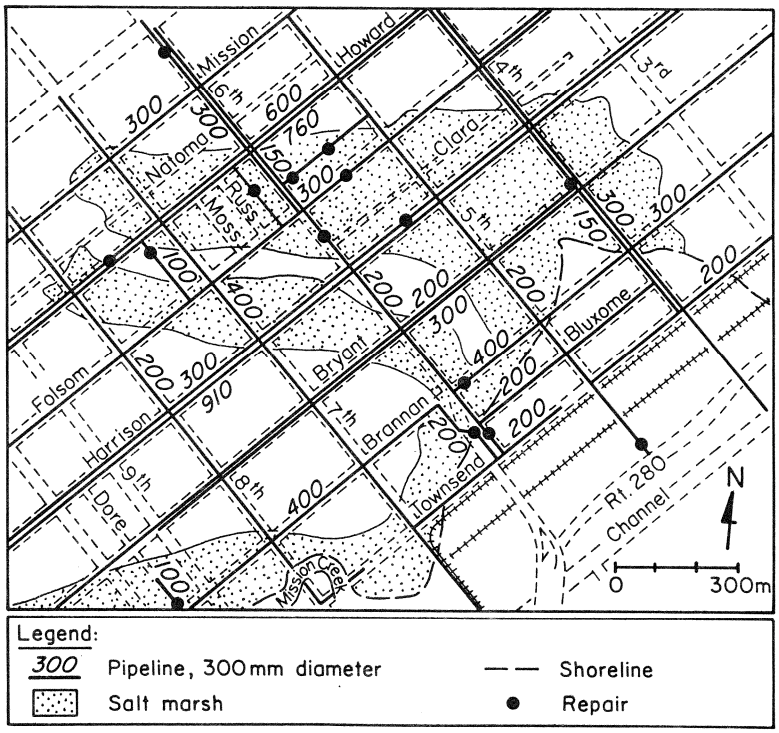

Figure 28. MWSS Pipeline Repairs in South of Market Area

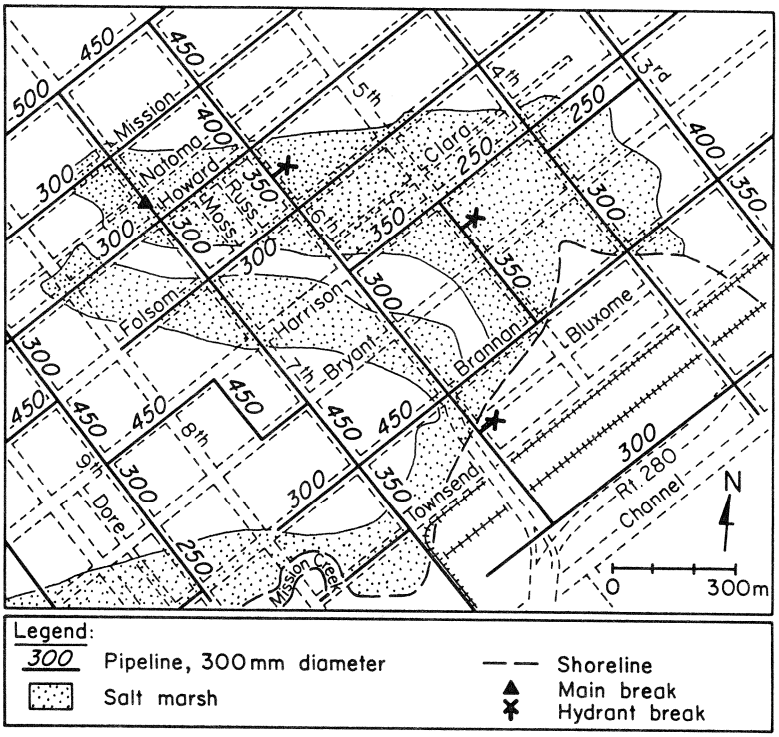

Figure 29. AWSS Pipeline and Hydrant Repairs in South of Market Area

8.0 GLOBAL PATTERNS OF PIPELINE DAMAGE

Figure 30 shows a plan view of the location of breaks in the water distribution system of San Francisco after the 1906 earthquake (O'Rourke, et al., 1985). This plot of pipeline breaks was developed on the basis of maps by Schussler (1906) and Manson (1908), which show the locations of principal water main ruptures. Superimposed on the plot are the boundaries in which lateral spreading from soil liquefaction was observed during the 1906 earthquake. The boundaries of lateral spreading are plotted on the basis of zones delineated by Youd and Hoose (1975) and Hovland and Darragh (1981). The agreement among the zone boundaries from the different studies is good. Although the zones of lateral spreading account for only 5% of the built-up area of 1906 affected by strong ground shaking, approximately 52% of all pipeline breaks occurred inside or within one city block of these zones.

Figure 31 shows the locations of water pipeline system repairs after the 1989 Loma Prieta earthquake. Zones of potential soil liquefaction, based on maps by Youd and Hoose (1975) and Hovland and Darragh (1981), also are shown. Repairs to both the MWSS and AWSS are indicated by the appropriate symbols. The site of the Marina is shown, but because of the extensive MWSS damage at this location, repair plots are not indicated.

By comparing Figures 30 and 31, it is clear that pipeline breaks in 1989 and 1906 were clustered at similar locations in liquefaction-prone areas. The consistency in damage patterns, combined with the facts that: 1) pipelines tend to deform as the ground deforms, and 2) a pipeline network covers a broad area, provides an opportunity to use the pipeline system as an observational tool which reflects local earthquake severity. At the same time, the damage observations establish an empirical framework from which to estimate the potential levels of pipeline repairs relative to local geologic and geotechnical site characteristics.

Table 4 summarizes the number of water main repairs, total linear distance of main, and repairs per distance for several areas of San Francisco. Also included in the table are the Modified Mercalli Intensities (MMI) associated

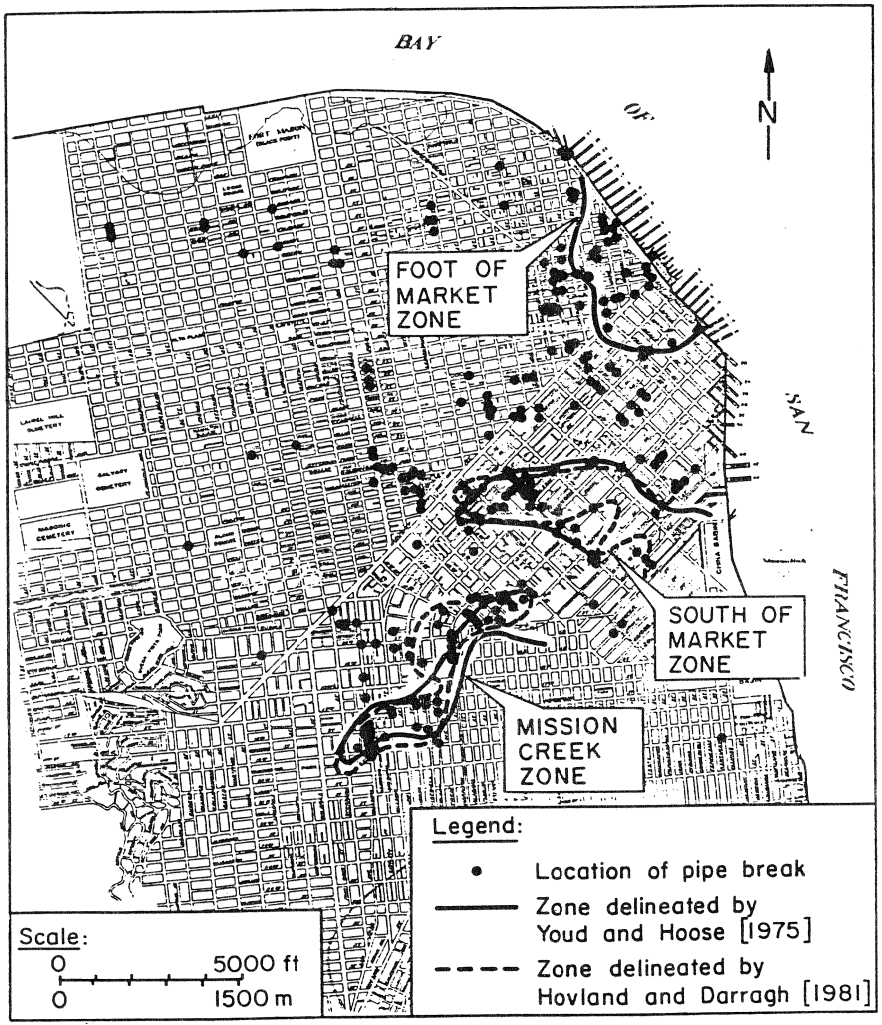

Figure 30. Water Supply Pipeline Breaks and Zones of Soil Liquefaction Caused by 1906 San Francisco Earthquake (after O'Rourke, et al., 1985)

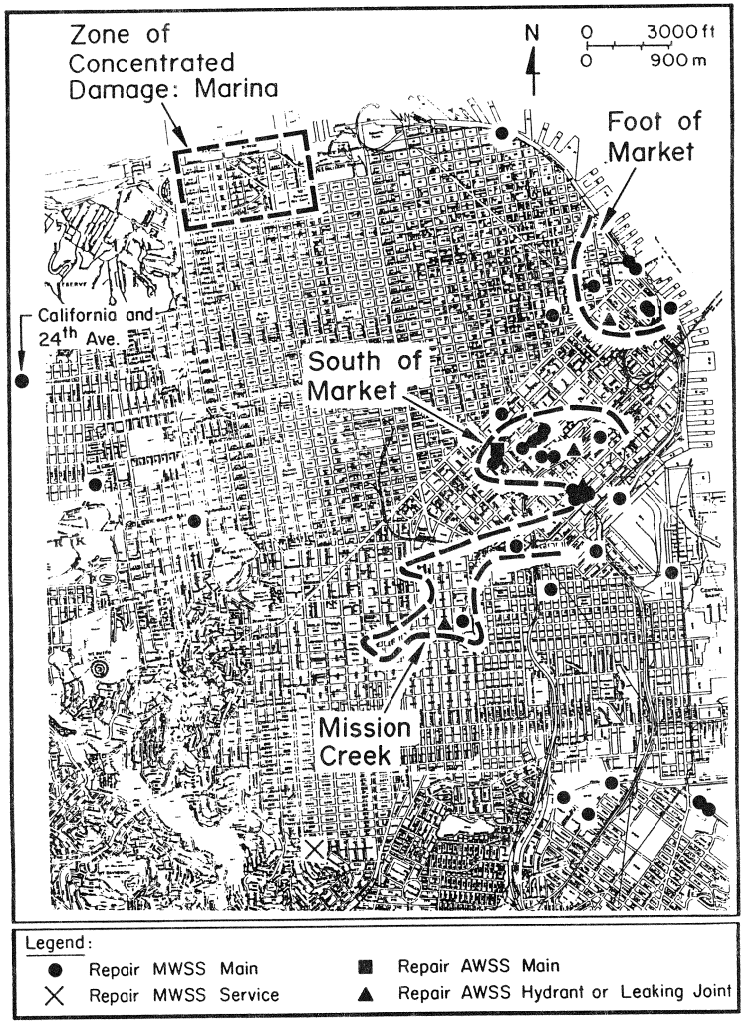

Figure 31. Water Supply Pipeline Breaks and Zones of Soil Liquefaction Caused by 1989 Loma Prieta Earthquake

Table 4. Summary of MWSS Pipeline Repairs for Various Sites in San Francisco[a]

Site	Repairs	Length of Pipeline, km	Repairs per km	Modified Mercalli Intensity, MMI
Marina	69	11.3	6.11	IX
South of Market	13	17.1	0.76	VIII
Foot of Market	6	13.8	0.43	VII
Mission Creek	2	15.1	0.13	VII
Remainder of System	15	1740	0.01	VI

[a]Repairs to services not included

with each area, as reported previously in this work.

Table 4 shows substantial differences in pipeline repair rates for different sectors of the city. In effect, the repair rate is an index of seismic intensity. In Figure 32, the repair statistics for Loma Prieta are combined with repair statistics for other earthquakes to explore further the relationship between pipeline damage and MMI. All data in the plot represent systems composed entirely or predominantly of cast iron lines.

As illustrated in the figure, there is a linear trend of repairs/km with MMI. Moreover, the trend in the Loma Prieta data is consistent with that of the other western U.S. earthquakes. It should be recognized that the data in Figure 32 have been plotted without distinguishing damage related to traveling ground waves in comparison to damage caused by permanent ground movements. For MM VIII or larger, damage will be affected principally by permanent ground movements in areas vulnerable to soil liquefaction. Such empirical evidence implies that cast iron pipeline damage varies exponentially with MMI. Repair

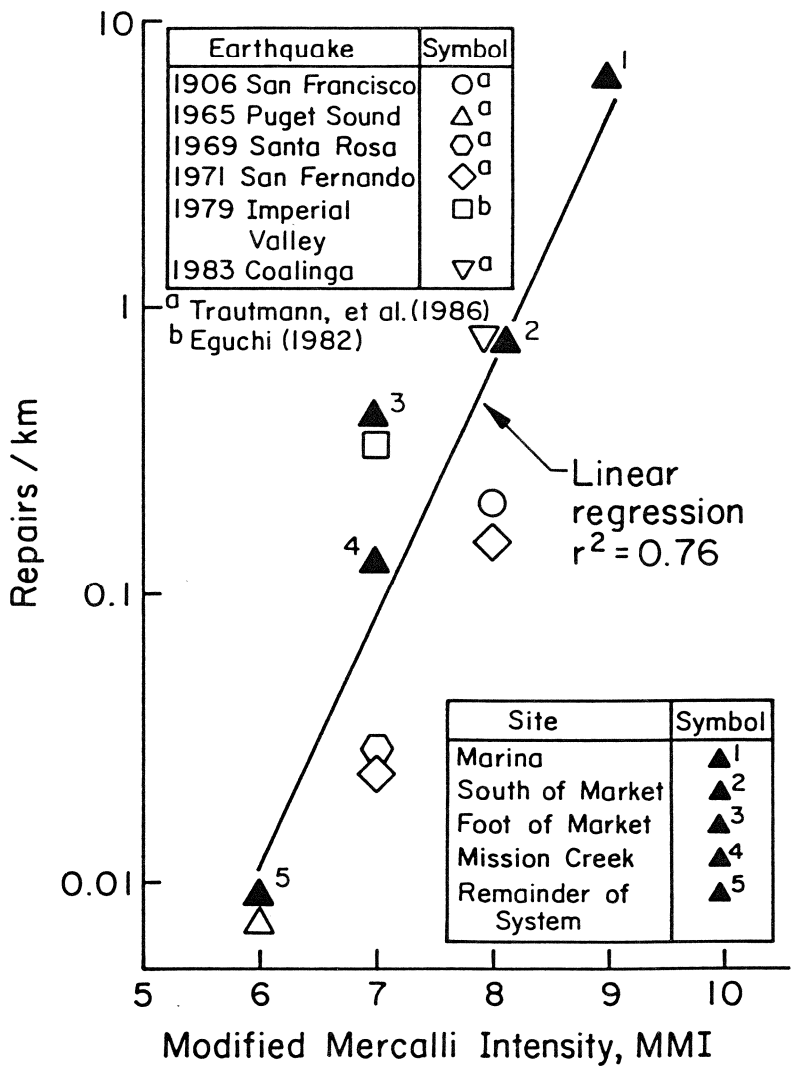

Figure 32. Repair Rate of Cast Iron Pipeline Systems versus Modified Mercalli Intensity

rates increase by roughly an order of magnitude for each single digit advance in the MMI scale.

9.0 SUBSURFACE CONDITIONS IN THE MARINA

Figure 33 shows a plan view of borings and soundings for which records were collected to evaluate subsurface conditions in the Marina. The borings were performed for engineering projects which both preceded and followed the Loma Prieta earthquake, although the majority were performed to clarify foundation

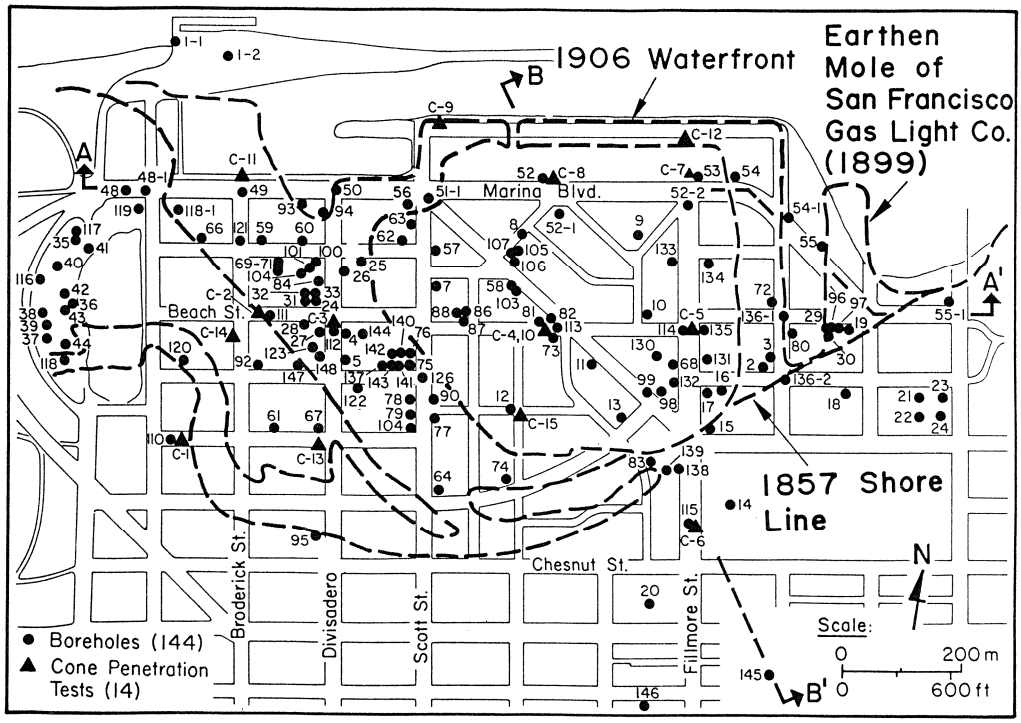

Figure 33. Plan View of Soil Borings and Soundings in the Marina

conditions beneath buildings during repair and reconstruction after the earthquake. In total, 144 conventional borings and 14 cone penetration test (CPT) soundings are shown in the figure, and were used in the assessment of subsurface conditions.

On the basis of the boring and sounding information, two cross-sections are shown in Figures 34 and 35. The cross-sections provide information about the types of soils, water levels, fines contents, plasticity, and approximate undrained shear strengths of soft to medium clays. Standard penetration tests (SPT) were performed in conjunction with many of the conventional borings, and selected uncorrected SPT values are given.

Figure 34 (cross-section A-A') shows loose fill extending along Marina Blvd. from approximately Baker to Buchanan Sts., with a maximum depth of about 9 m. This distance correlates well with the distance between locations of the 1857

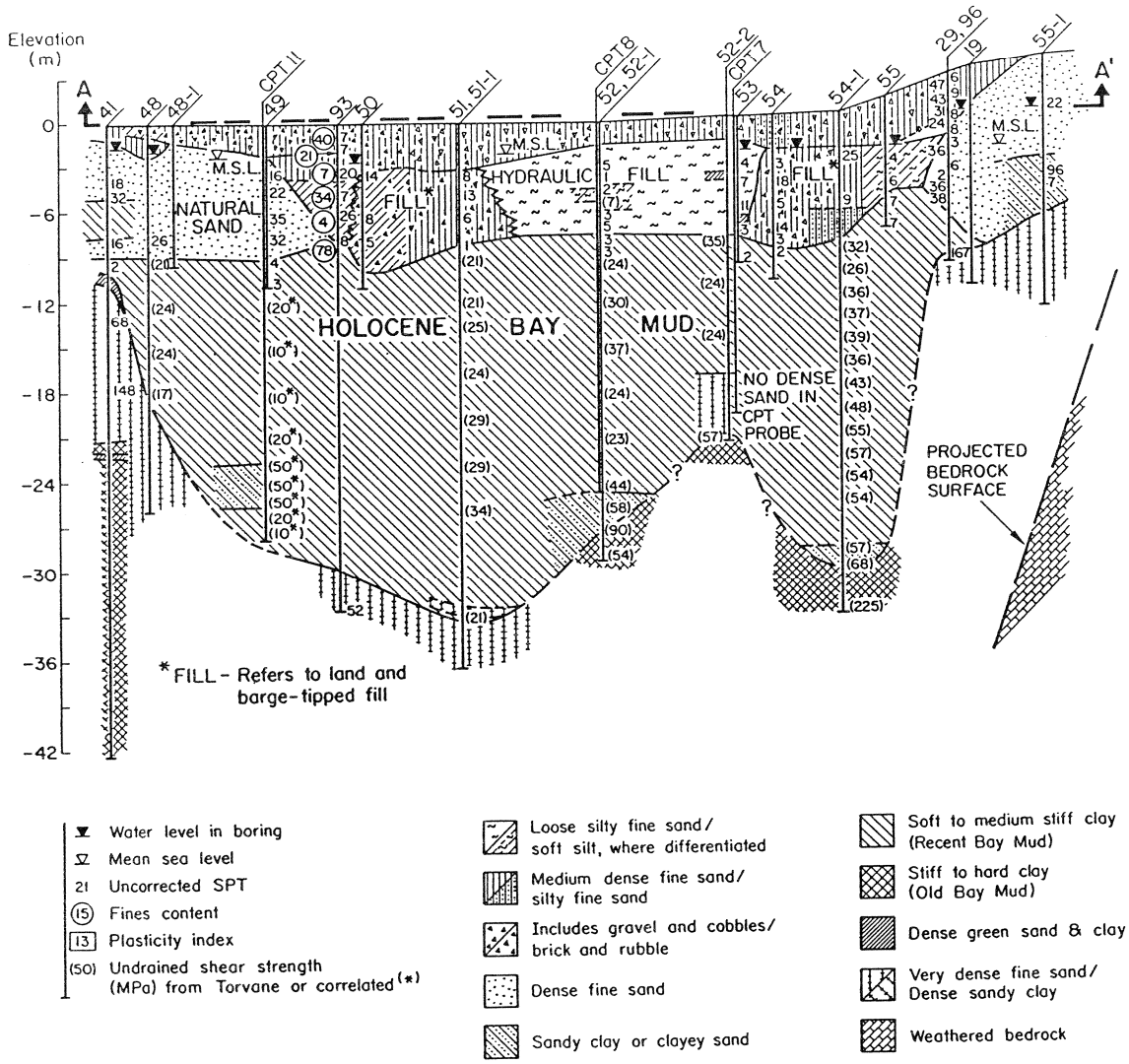

Figure 34. Soil Profile Along Cross-Section A-A' in the Marina

shoreline shown in Figures 19 and 33. The depth to water table is approximately 2.5 m. Underlying the loose fills and natural sand deposits is Holocene bay mud, which varies in thickness along Marina Blvd. from 9 to 32 m. Underlying the Holocene bay mud are dense sands and stiff to hard clays.

Figure 35 (cross-section B-B') shows a subsurface profile oriented in a northwest direction through the hydraulic fill. The hydraulic fill is characterized by low SPT values. Holocene bay mud increases rapidly in thickness towards the bay from a location about two blocks from the Marina waterfront.

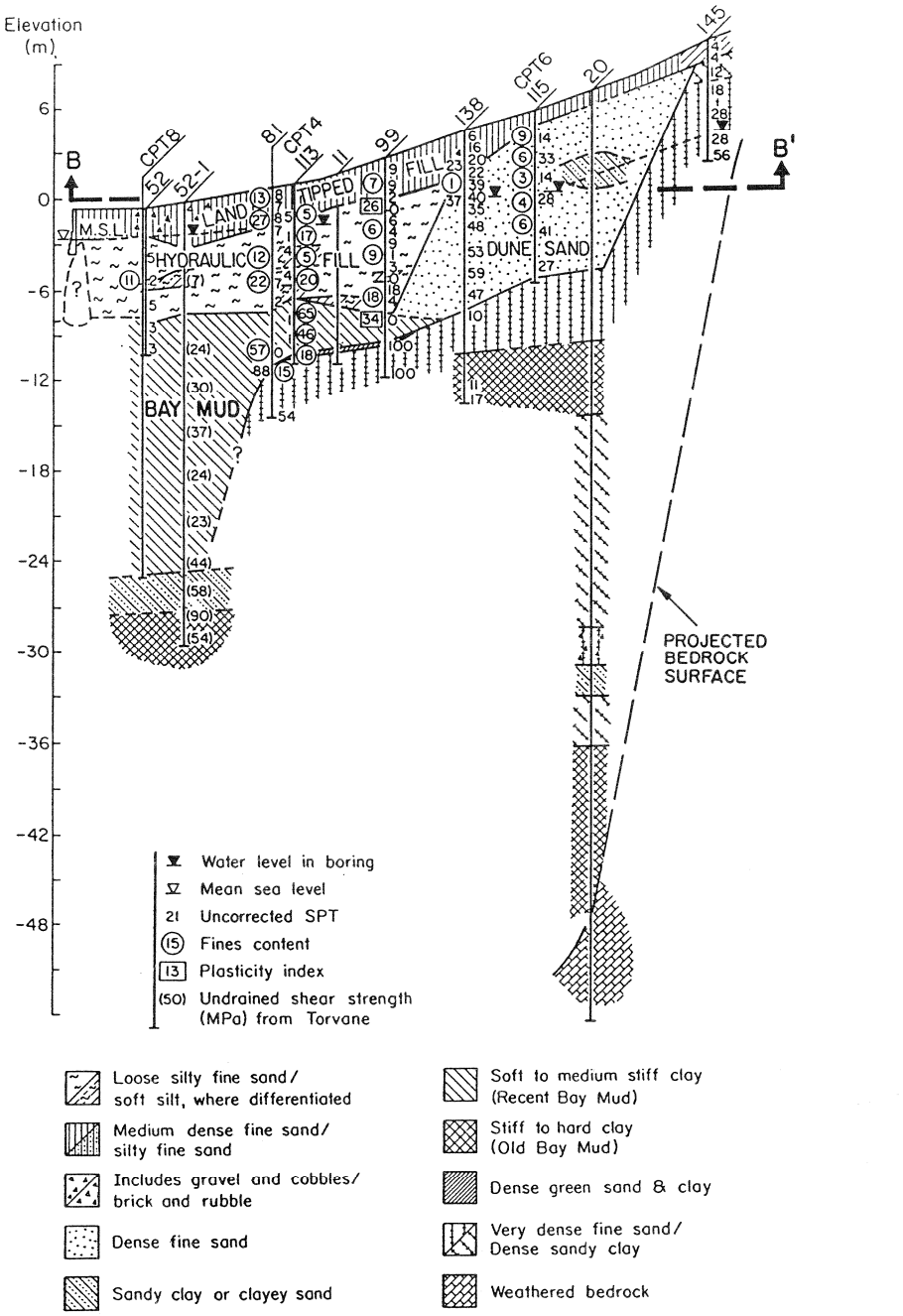

Figure 35. Soil Profile Along Cross-Section B-B' in the Marina

Borehole and outcrop information were analyzed with a geostatistics procedure embodied in the computer program "Surfer" (Golden Software, Inc., 1985). This method of analysis is the same as that employed for generating the contours of surface settlement in Figure 26. Figures 36, 37, 38, and 39 show contours for the bedrock and the bottom and top of the Holocene bay mud underlying the Marina. Similar subsurface contour plots have been discussed elsewhere (O'Rourke,

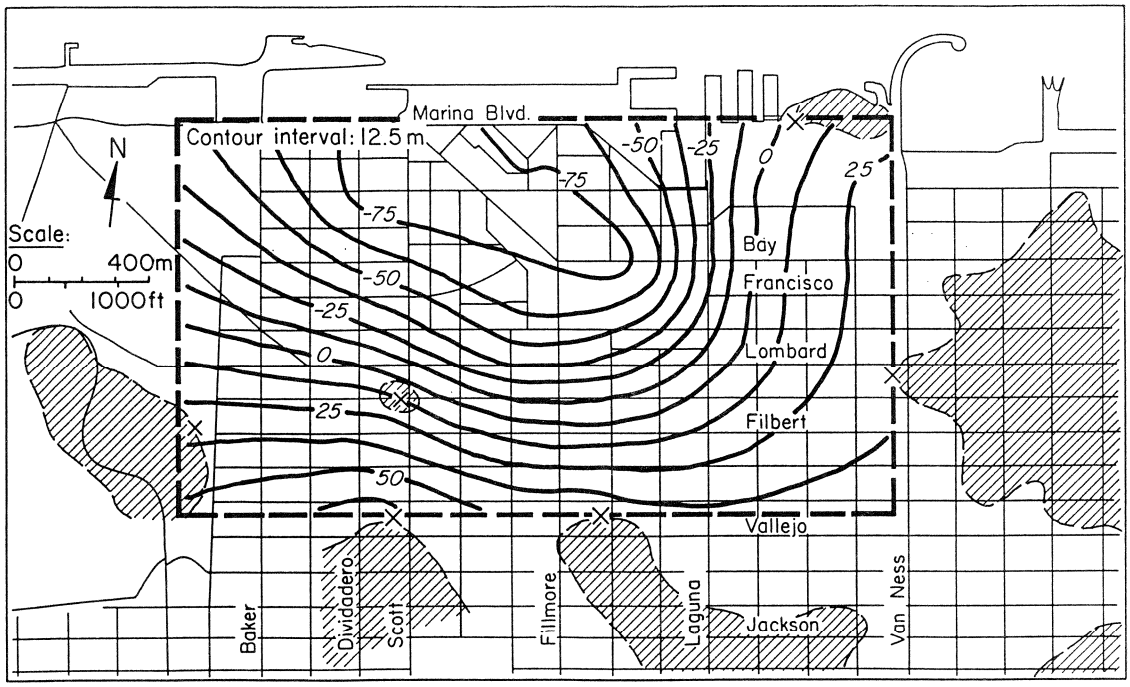

Figure 36. Map of the Marina Showing Contours of Bedrock

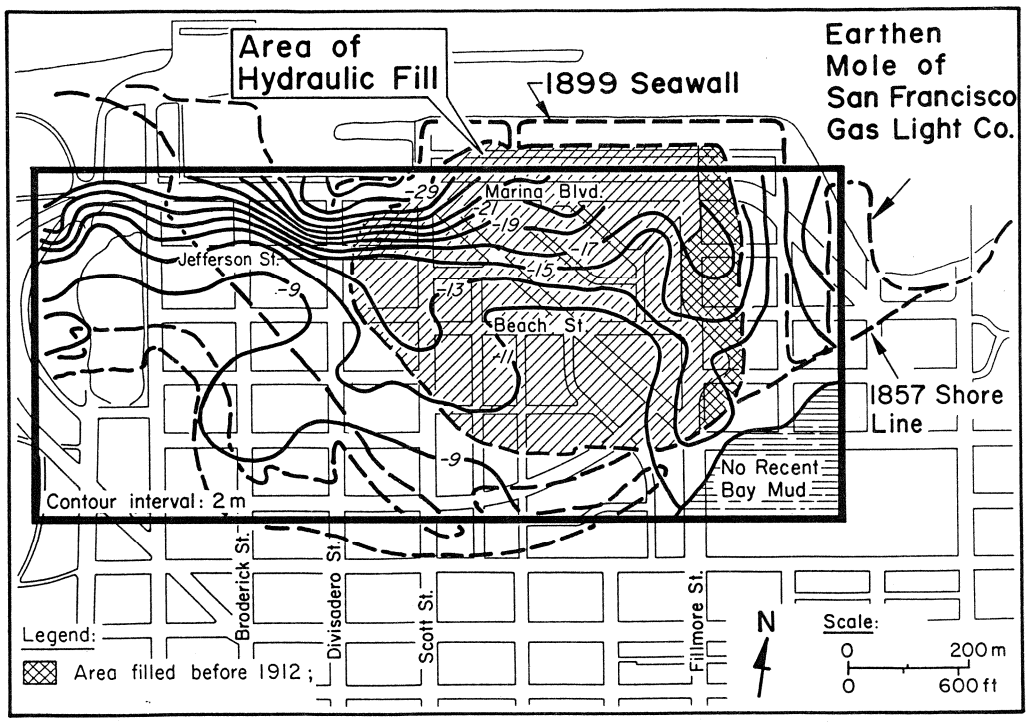

Figure 37. Contours of Equal Elevation for Bottom of Holocene Bay Mud in the Marina

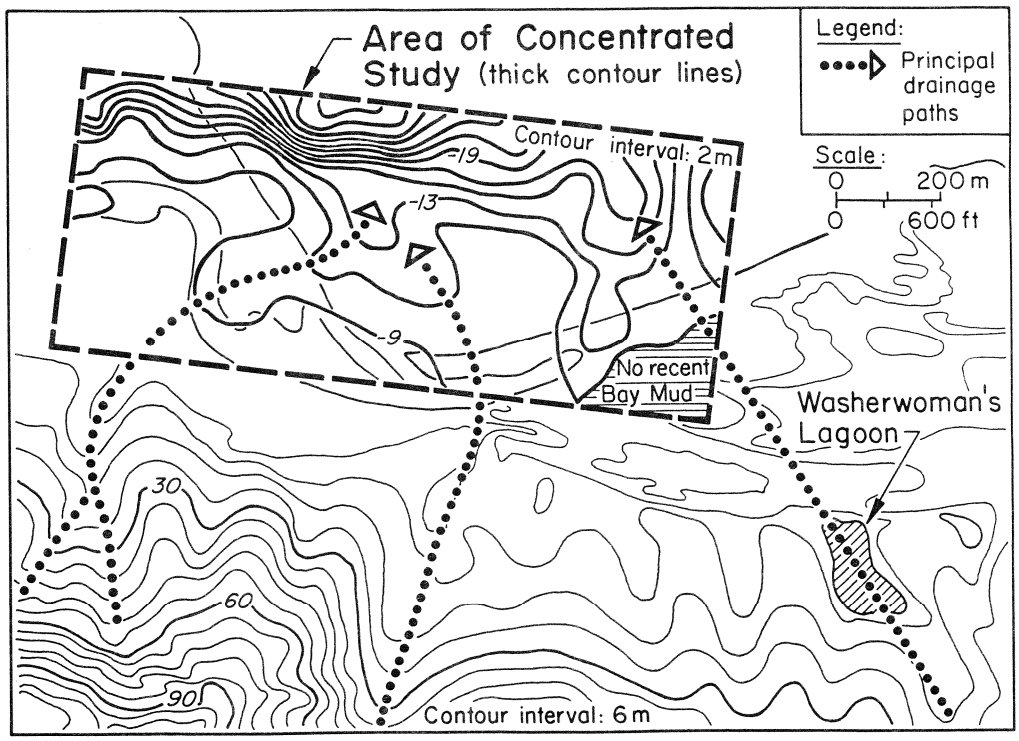

Figure 38. Erosional Surface Beneath Holocene Bay Mud in Relation to San Francisco Topography

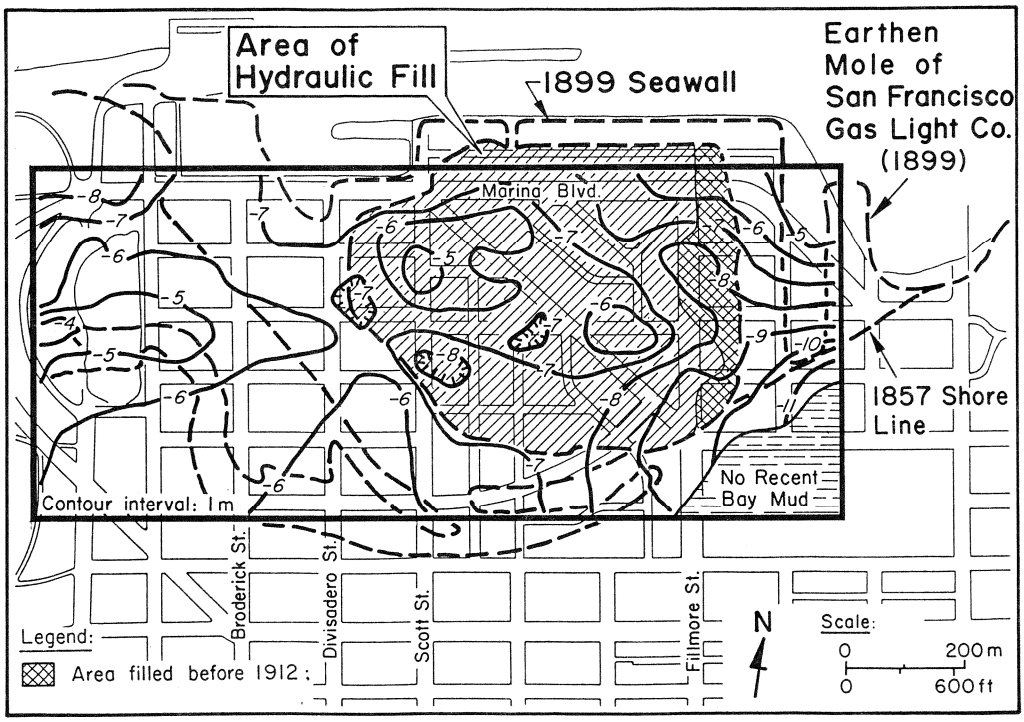

Figure 39. Contours of Equal Elevation for Top of Holocene Bay Mud in the Marina

et al., 1991b), and only a brief description is given here. All contours are expressed in terms of elevation relative to the San Francisco datum.

Figure 36 indicates that the Marina is underlain by an oblong bedrock basin, with its long axis oriented west by northwest. The basin is over 75 m deep below Marina Blvd.

Figure 37 shows that the Holocene bay mud thickens rapidly towards the bay, with its steepest bottom surface from Broderick to Scott Sts. between Marina Blvd. and Jefferson. Slopes of the bottom surface in this region are locally as steep as 10°.

Figure 38 shows the contours of the bottom of Holocene bay mud superimposed to scale on a contour map of northern San Francisco. The San Francisco contours are based on one of the original coastal surveys of this area (U.S. Coast Survey, 1857). The basal contours of the mud are consistent with drainage features converging on the Marina from higher elevations to the south. A prominent drainage line crosses the old Washerwoman's Lagoon and intersects the eastern sector of the erosional surface beneath the mud. Similar to the long axis of the bedrock basin, this drainage line is oriented in a northwest direction, subparallel to major structural features which have been mapped in San Francisco (Schlocker, 1974).

Figure 38 shows that the top surface of the mud is irregular. This irregularity is especially noticeable beneath the hydraulic fill, and takes the form of a hummocky surface with mounds and depressions. Such an irregular surface is consistent with the method of filling whereby sands were pumped into various portions of the lagoon, causing local bearing failures, with associated mounding of displaced fine-grained sediments. Across the rest of the site, the top surface of the Holocene bay mud is in contact with natural sands and does not show disturbed features.

Figure 40 shows a three-dimensional view in which the street surface of the Marina, fill and natural sand deposits, and Holocene bay mud are superimposed on the bedrock basin underlying the Marina. The three-dimensional view has

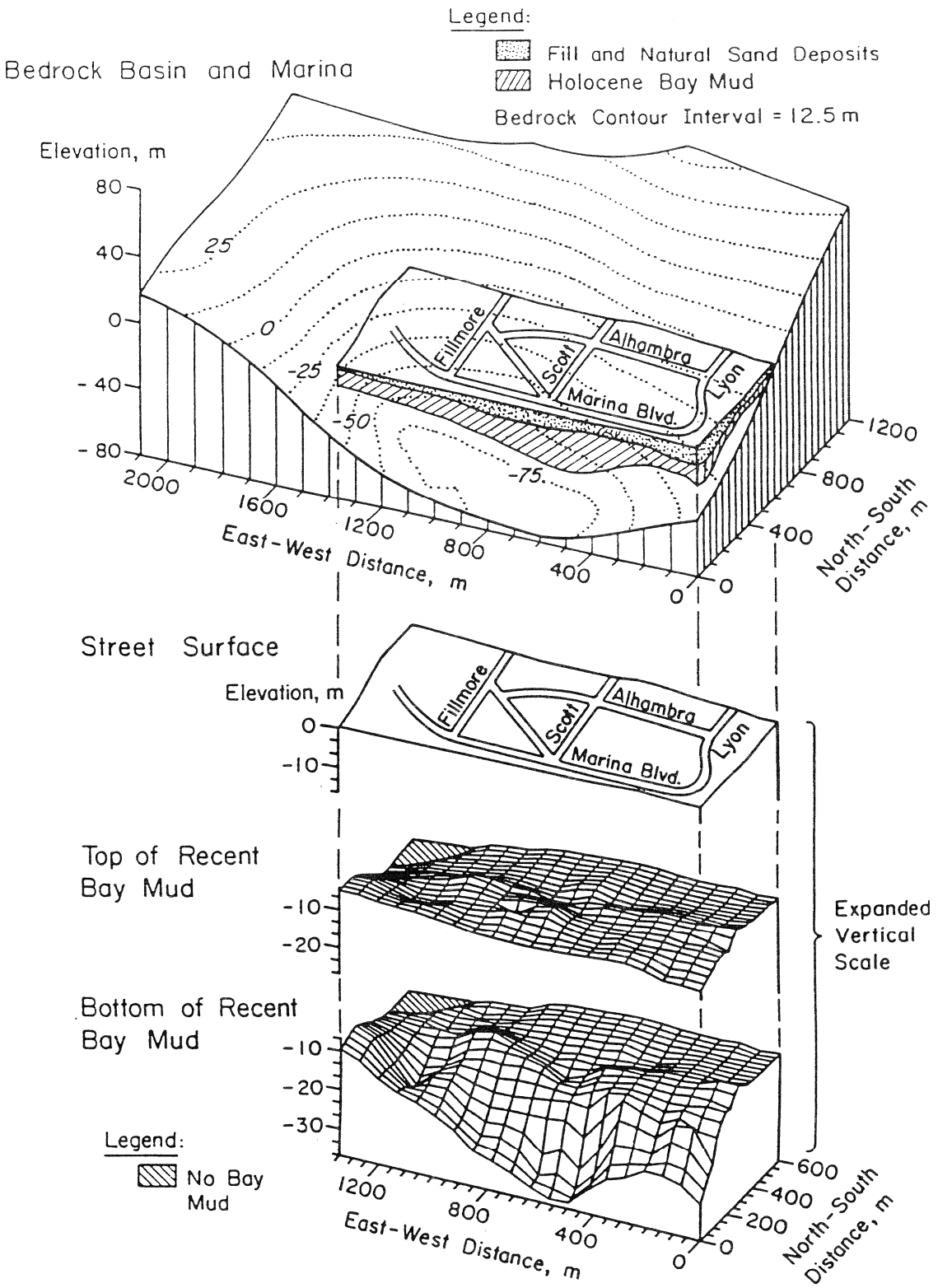

Figure 40. Three-Dimensional View of the Subsurface Rock and Soil Features at the Marina

been developed from the perspective of an observer looking towards the southeast from an elevated position northwest of the Marina. Beneath the view of the bedrock basin are the street surface and top and bottom of Holocene bay mud, shown at an expanded vertical scale to emphasize the topographical features of each level.

9.1 Evaluation of Soil Conditions from SPT Measurements

The Marina provides an excellent opportunity to examine the characteristics and liquefaction response of three different soil types: 1) hydraulic fill, 2) land-tipped fills, and 3) natural sand deposits. The locations of these deposits can be delineated with reasonable accuracy on the basis of historic records and the many soil borings and soundings performed in the Marina.

Liquefaction potential analyses were performed for each soil type using the empirical relationship between cyclic stress ratio and corrected SPT values developed by Seed, et al. (1983; 1985). The SPT values were obtained from 75 different borings in which tests were performed in accordance with ASTM specifications (ASTM, 1991a). The SPT values were corrected for factors such as in-situ confining stress and energy losses, following the recommendations of Seed, et al. (1983; 1985). The cyclic stress ratios for various depths were calculated assuming a peak acceleration of 0.2 g, which is consistent with the peak horizontal component of acceleration recorded at the nearby Presidio (Earthquake Engineering Research Institute, 1990).

Figure 41 shows the cyclic stress ratio plots for the three soil types. In each figure, the empirical dividing lines for various fines contents between liquefiable (left side) and non-liquefiable (right side) soils are plotted for a magnitude 7.1 earthquake. The fines content refers to percentage weight of the soil which is silt-sized or smaller (0.075 mm). In each figure, a histogram showing the frequency distribution of corrected SPT values, $(N_1)_{60}$, is given. In-situ density of the soil is related to $(N_1)_{60}$ so that each histogram provides a measure of the variation in soil density as inferred from SPT measurements. Normal and gamma probability density functions are fitted to the data. The mean, $\bar{x}$, standard deviation, s, and number of data in each sample are listed. The mean and standard deviation pertain to a normal distribution.

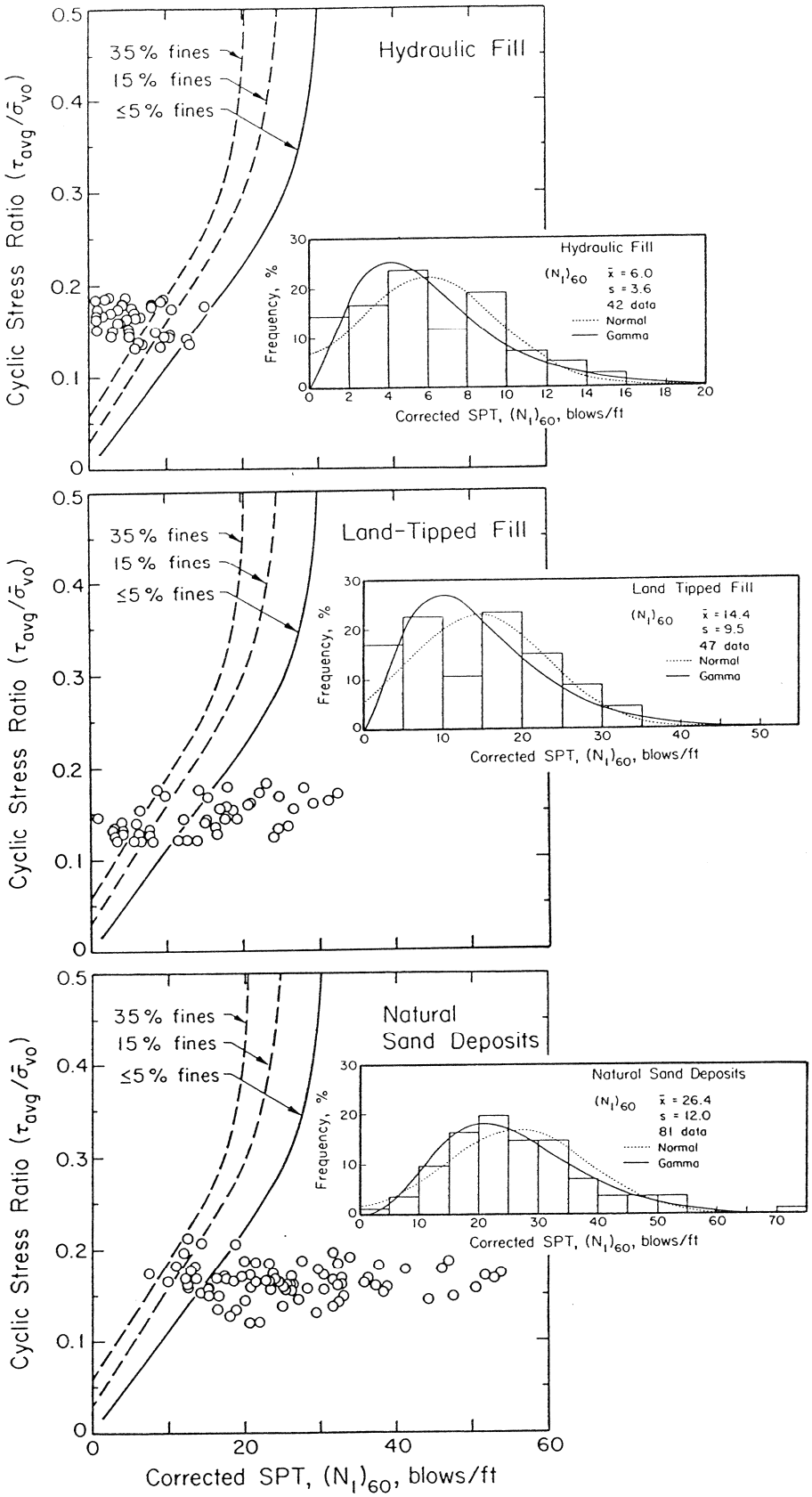

Figure 41. Cyclic Stress Ratio Plots of Three Soil Types in the Marina

The most striking feature of the plots is the relatively high susceptibility to liquefaction displayed by the hydraulic fill. The corrected SPT values for at least half of the measurements in the sample are less than 6. This implies that the hydraulic fill would have a very low undrained residual shear strength, perhaps lower than 5 kPa, based on empirical relationships suggested by Seed (1987).

Both the land-tipped fill and natural soils show increasing resistance to liquefaction. These soils also show a successively larger range of in-situ densities, reflected by the SPT values. Roughly half the land-tipped fill data plot to the left of the 5% fines curve, whereas only about 15% of the natural sand data plot in the same zone. The land-tipped fill shows the highest variability with respect to corrected SPT values, with a coefficient of variation of 0.65 for $(N_1)_{60}$.

Figure 42 shows profile views of the hydraulic fill, land-tipped fill, and natural sand deposits with corrected SPT values plotted as a function of depth. Superimposed on the plots are liquefaction potential lines for various fines contents, developed according to the recommendations of Seed, et al. (1983; 1985). Although these plots provide only a general picture of the subsurface conditions because they lump all data into a single cross-section, they nevertheless show some interesting trends. A relatively uniform distribution of low in-situ density with depth is indicated for the hydraulic fill, whereas there is a marked tendency for increasing density with depth for areas underlain by land-tipped fill. The natural sand deposits show a wide variation of in-situ density with depth, with most densities outside the range susceptible to liquefaction during the Loma Prieta earthquake.

9.2 Evaluation of Soil Conditions from CPT Measurements

As illustrated in Figure 33, 14 CPT soundings were used in this study of the Marina. The majority of these have been reported by Bennett (1990) and Bardet and Kapuskar (1991). The CPT measurements were performed in accordance with ASTM specifications (ASTM, 1991b). The CPT soundings can resolve subsurface conditions in considerably more detail than SPT measurements, and therefore

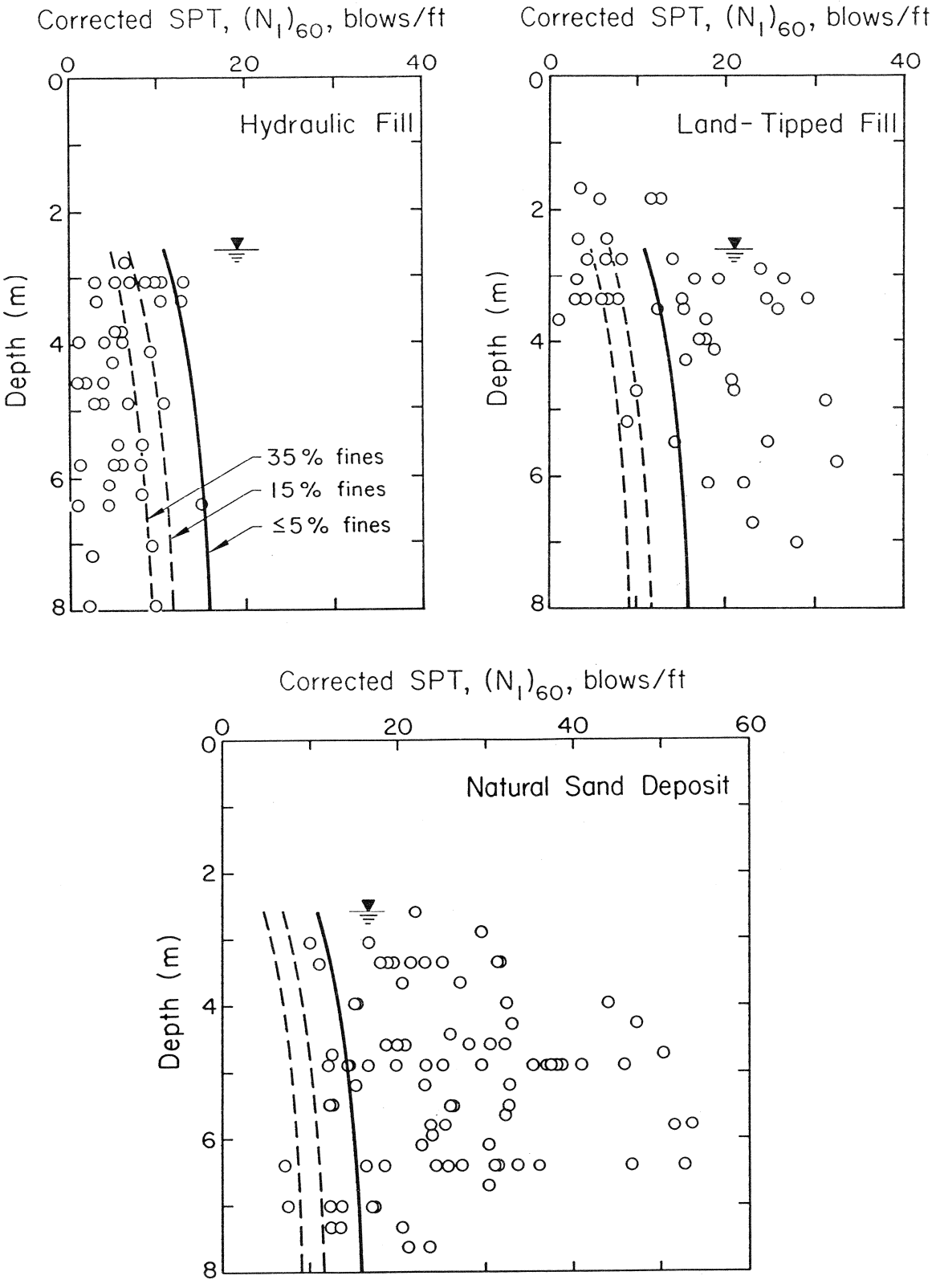

Figure 42. Soil Profiles with Corrected SPT Values Plotted as a Function of Depth

provide a more accurate picture of variations of in-situ density and soil type.

Liquefaction potential analyses were performed for all CPT soundings in hydraulic fill areas using the empirical correlations between cyclic stress ratio and modified cone tip resistance, q_{c1}, proposed by Seed and DeAlba (1986). The modified cone tip resistance involves normalizing the measured tip resistance with respect to an effective overburden stress of roughly 100 kPa, according to the recommendations of Seed and DeAlba (1986). The cyclic stress ratios for various depths were calculated in a similar manner to those for the SPT evaluations by assuming a peak acceleration of 0.2 g.

As an illustration of the process, consider the normalized CPT profiles shown in Figure 43. Liquefaction potential lines were plotted as a function of depth for three combinations of fines content and mean grain size, as shown in the key diagram. The combinations of fines content and mean grain size were chosen to be consistent with the composition of the fills and natural sands in the Marina.

The CPT data for each sounding first was analyzed to identify the soil type at each depth according to the recommendations of Robertson and Campanella (1983) and Olsen and Farr (1986). Based on the soil identification, the appropriate liquefaction potential line was used to evaluate whether the soil type at a given depth was susceptible to liquefaction during the Loma Prieta earthquake. The appropriate liquefaction lines at various depths are shown as thick dark lines.

Figure 43 presents the CPT profiles for three soundings in the hydraulic fill, which from north to south are designated as C8, C4, and C15 (see Figure 11). The q_{c1} values are shown at 0.3-m (1-ft) intervals. For example, C8 indicates the presence of liquefiable sands and silty sands between the depths of 3 and 4.5 m, and again at 5.5 to 6.5 m. Between 4.5 and 5.5 m, the cone penetrated silt and silty clay, which can be interpreted as not susceptible to liquefaction. Accordingly, no darkened line is indicated for this depth interval. The measurements at C4 show the presence of liquefiable sands and silty sands, generally from 2.6 to 7 m, with thin intervening layers of clayey silt, which can

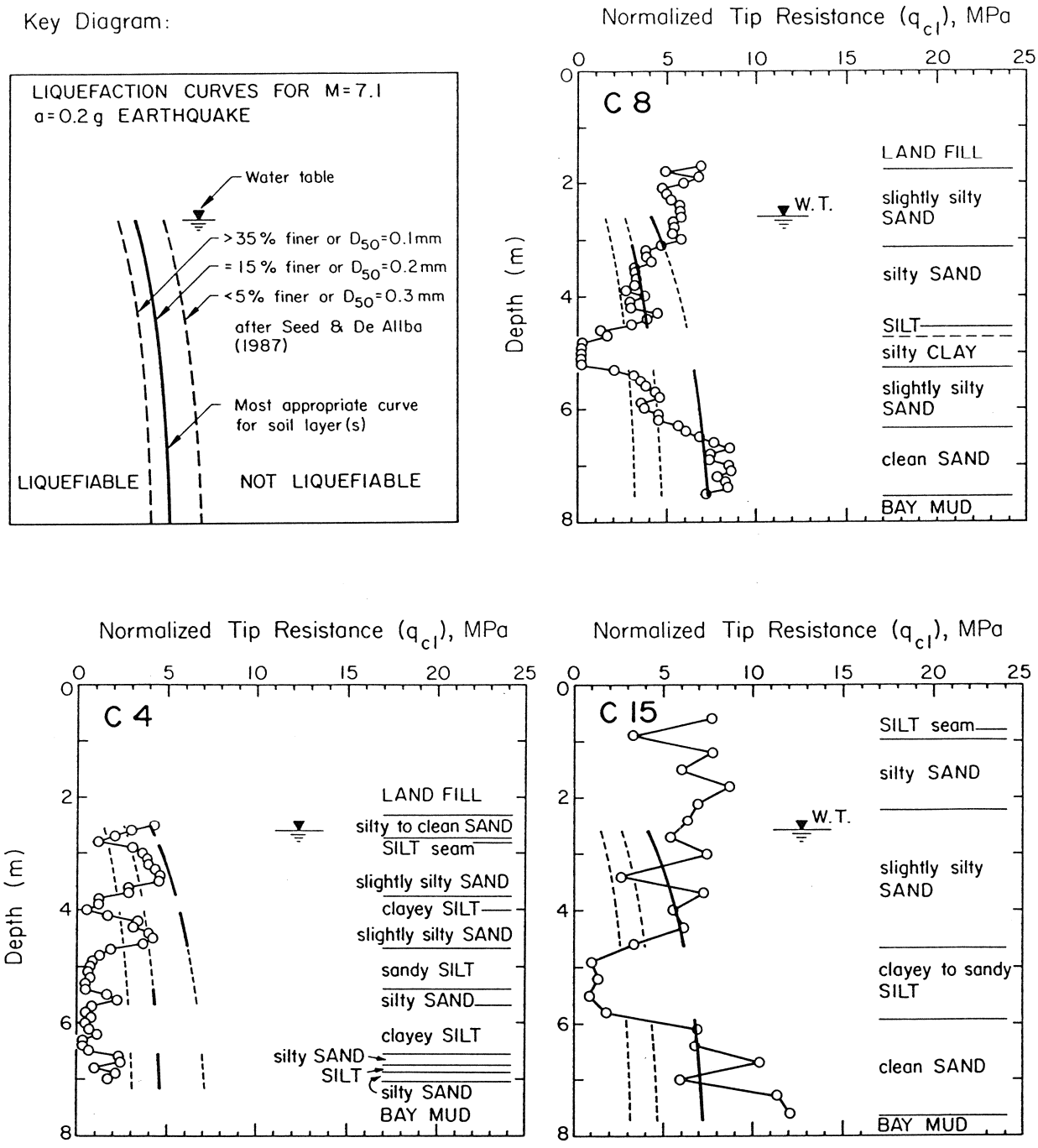

Figure 43. Soil Profiles with CPT Values Plotted as a Function of Depth

be interpreted as not susceptible to liquefaction. The measurements at C15 show only occasional thin seams of sand and silty sand, which clearly are susceptible to liquefaction.

In general, the liquefaction potential deduced from CPT measurements corroborates the average trends shown by the SPT measurements for hydraulic fill, land-tipped fill, and natural sand deposits. The advantage of the CPT soundings is the precision to which potentially liquefiable and non-liquefiable layers can be delineated. This precision permits an additional level of detail in evaluating the post-liquefaction consolidation at various locations.

10.0 SUBSURFACE CONDITIONS IN THE SOUTH OF MARKET AREA

Figure 44 shows a map of the South of Market area on which various boreholes and cross-sectional lines are superimposed. The map is similar to the ones presented in Figures 28 and 29. The outlines of the old shoreline of Mission Bay and the marsh that once occupied this site are illustrated relative to the current street system.

Figures 45, 46, and 47 present soil profiles along cross-sections A-A', B-B', and C-C', respectively. The profiles have been developed primarily from borehole data acquired from site investigations for building construction before the Loma Prieta earthquake. Much of the borehole data used for cross-sections A-A' and B-B' have been used by Harding Lawson Associates, et al. (1991) to delineate subsurface conditions in the South of Market area. New data have been introduced by means of boring C-1, near the intersection of 6th and Howard Sts. The borings used to construct the soil profile along cross-section C-C' also were performed for site investigations before the Loma Prieta earthquake, although the majority of these have not been presented in any other report or publication.

Although blow counts were obtained at virtually all the borings, most of these values were not acquired by means of standard testing procedures. Only STP measurements performed according to ASTM standards (ASTM, 1991a) are indicated in the profiles. The uncorrected SPT values are listed as the uncircled numbers adjacent to the borings. The circled numbers indicate the percentage by

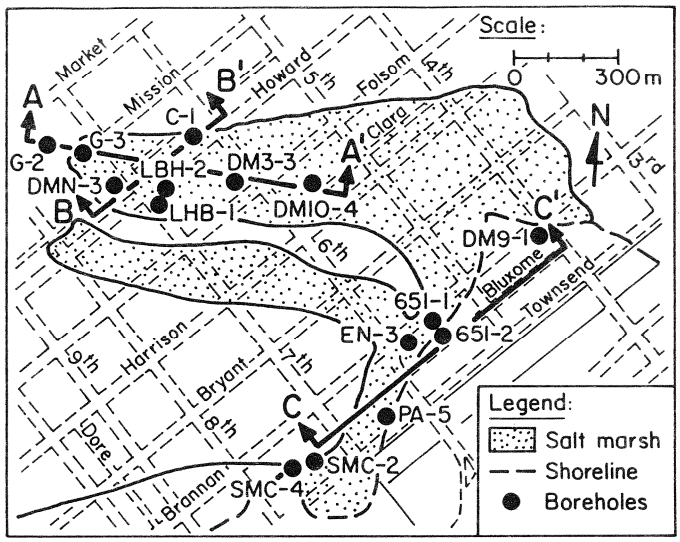

Figure 44. Map of South of Market Showing Borings and Cross-Sections

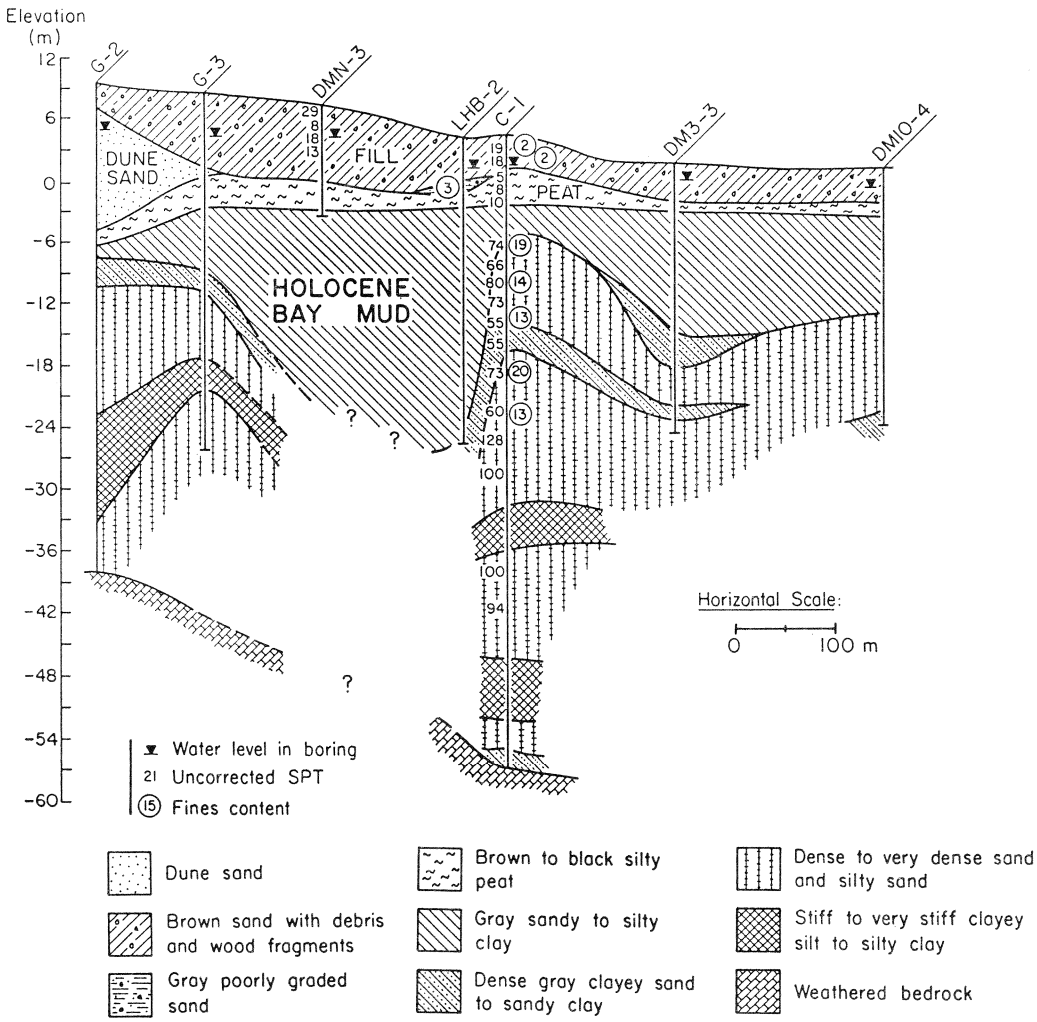

Figure 45. Soil Profile Along Cross-Section A-A' in the South of Market Area

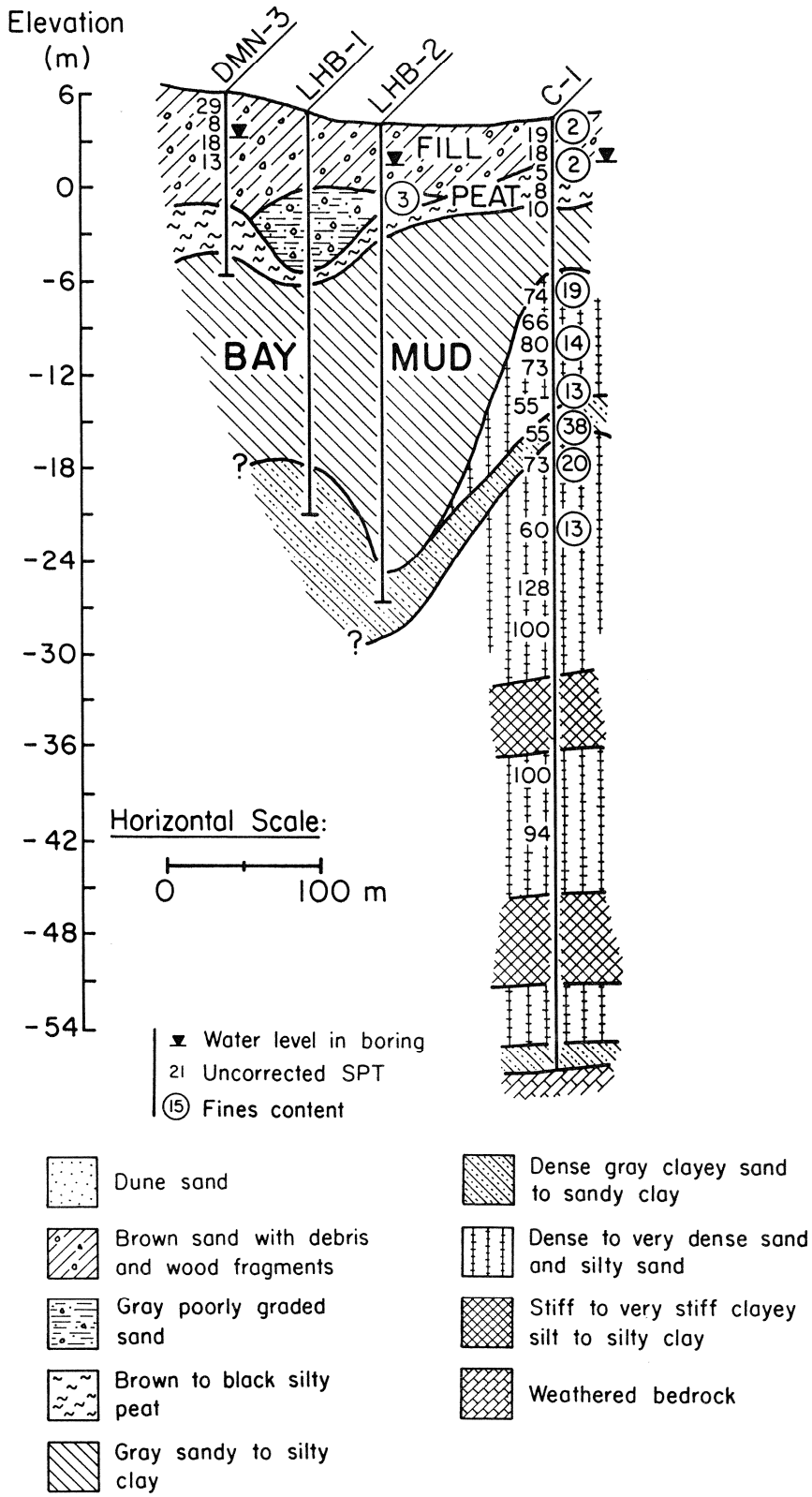

Figure 46. Soil Profile Along Cross-Section B-B' in the South of Market Area

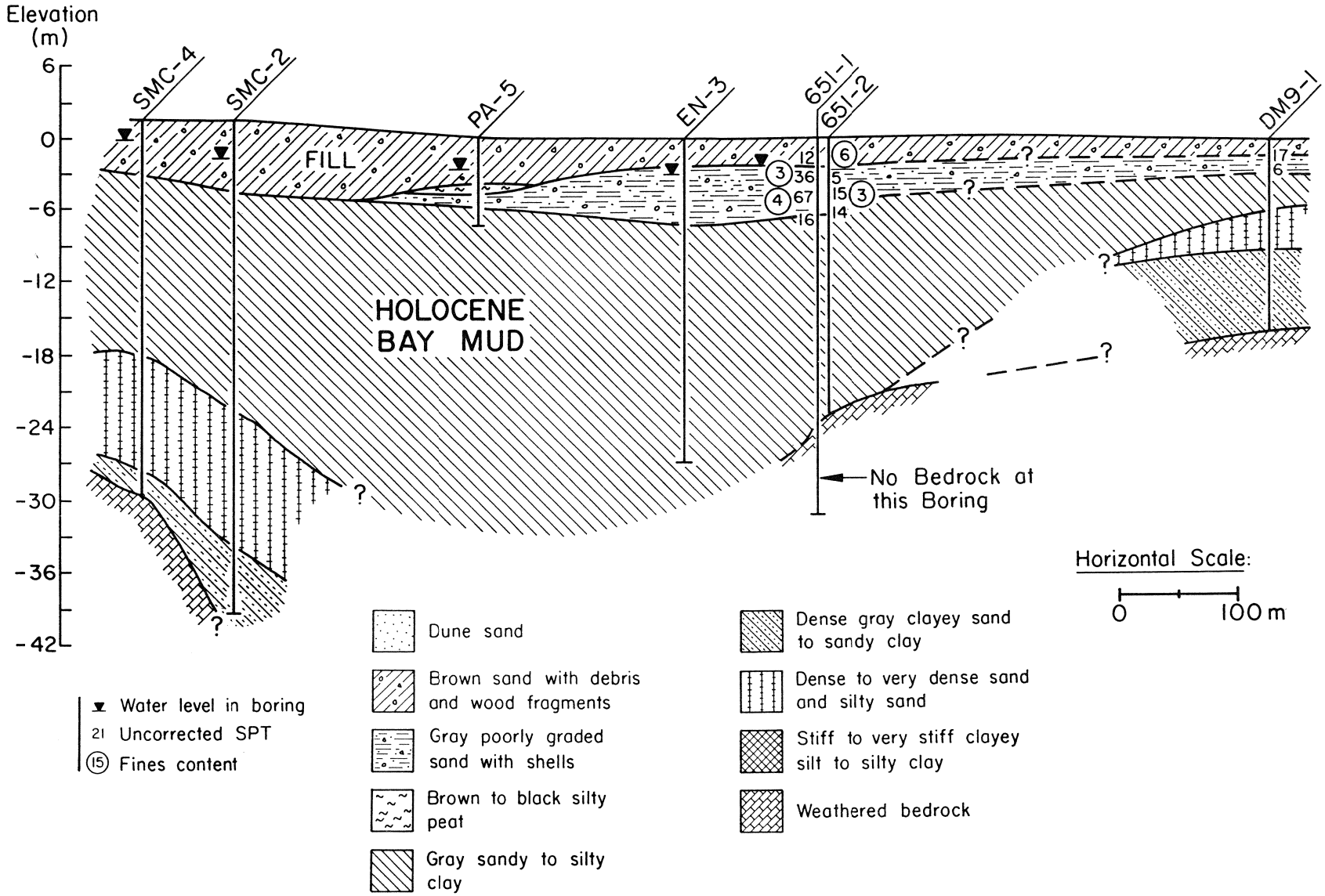

Figure 47. Soil Profile Along Cross-Section C-C' in the South of Market Area

weight of fines determined from split spoon samples retrieved from the elevations shown in the figure.

Figure 45 shows the soil profile along the approximate longitudinal axis of Sullivan's Marsh, which once was present in the South of Market area. Near the northwestern boundary of the old marsh, the water table is from 3 to 4 m below ground surface. The water table is from 1.5 to 2 m deep near the southeastern end of the cross-section. Loose to medium dense sandy fills are present at depths ranging from 6 to 9 m. The fill is underlain by a peat deposit, approximately 1 to 2 m thick. The Holocene bay mud along this cross-section is quite variable in thickness, ranging from only 3 m near the intersection of 6th and Howard Sts., to approximately 21 m just south of 7th and Howard Sts., and 12 m near 6th and Folsom Sts. Weathered serpentine bedrock was encountered at a depth from ground surface of approximately 60 m in boring C-1.

Figure 46 shows the soil profile along Howard St. between 6th and 7th Sts. In this area, prominent liquefaction-induced ground deformation was observed after the 1906 and 1989 earthquakes. The water table is from 3 to 4 m below ground surface. The fill is approximately 6 m thick, and is underlain by 1 to 1.5 m of peat and by Holocene bay mud of variable thickness.

Figure 47 shows the soil profile along cross-section C-C', which is approximately parallel to the old shoreline. The water table is approximately 2 to 3 m below ground surface. There are from 3 to 7 m of loose to medium brown fill and gray sands in the upper portion of the profile. The gray sands contain shell fragments and organics, and are present in those parts of the cross-section which are outboard of the old shoreline. The maximum depth of Holocene bay mud is at least 20 m, with thickness diminishing to the northeast.

Liquefaction potential analyses were performed for the fill and upper gray sands using the empirical relationship between cyclic stress ratio and corrected STP values developed by Seed, et al. (1983; 1985), in accordance with the procedures described in Section 9.1. The cyclic stress ratios for various depths were calculated assuming a peak acceleration of 0.2 g. Figure 48 shows the cyclic stress ratio plots for the sandy fill along cross-sections A-A' and

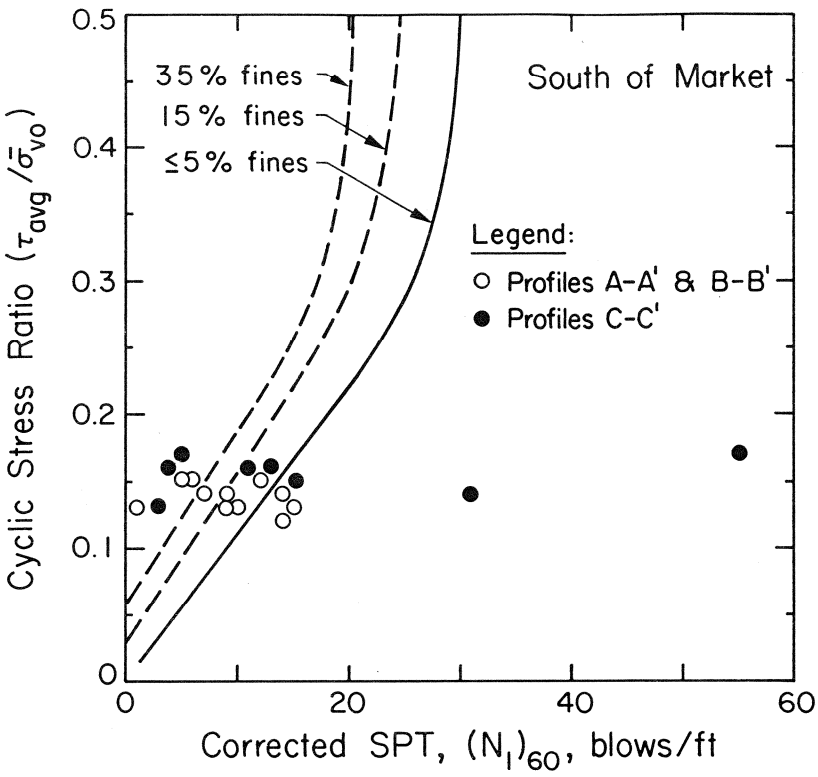

Figure 48. Cyclic Stress Ratio Plot for Fills and Sands in the South of Market Area

B-B' and for the upper brown fill and gray sands along cross-section C-C'. Only the corrected SPT values for soil below the water table were used. In the figure, the empirical dividing lines for various fines contents between liquefiable (left side) and non-liquefiable (right side) soils are plotted for a magnitude 7.1 earthquake. The borehole data indicate that the fills and sands are relatively clean, with many samples having less than 5 to 10% by weight of fines. With the exception of two anomalously high values, the $(N_1)_{60}$ data indicate that the fill in the South of Market area is highly susceptible to soil liquefaction for an event comparable in magnitude and intensity to those experienced during the Loma Prieta earthquake.

11.0 SUBSURFACE CONDITIONS IN THE MISSION CREEK AREA

Figure 49 shows an inset map of the Mission Creek area similar to that shown in the upper right corner of Figure 9. The area of most severe liquefaction-induced damage in the Mission Creek area in 1989 is identified on this map and

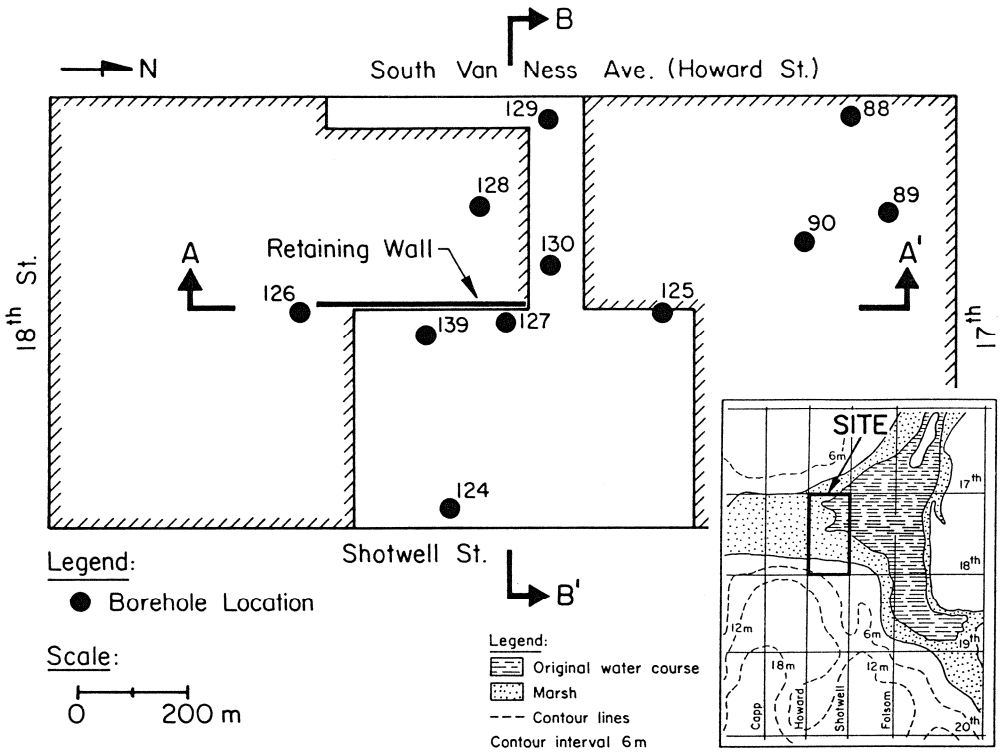

Figure 49. Map of Mission Creek Area Showing Borings and Cross-Sections

corresponds to the block bounded by South Van Ness Ave. and 17th, Shotwell, and 18th Sts. It should be recognized that the old Howard St. on the inset map corresponds to the current South Van Ness Ave.

Figures 50 and 51 present soil profiles along cross-sections A-A' and B-B', respectively. The cross-sections and corresponding boreholes are shown in Figure 49. Borehole data were acquired from site investigations performed after the Loma Prieta earthquake, as part of a reconstruction effort for the two to four-story timber-frame buildings damaged by liquefaction-induced differential settlement at this site.

Figures 50 and 51 show the soil profiles, with a water table approximately 1 to 3 m below ground surface on the eastern half of the site. A higher level of fill (approximately 2.5 m higher) exists on the western half of the site. A retaining wall and embankment slope separate the eastern and western portions of the block. Uncorrected SPT values are listed adjacent to each boring in the

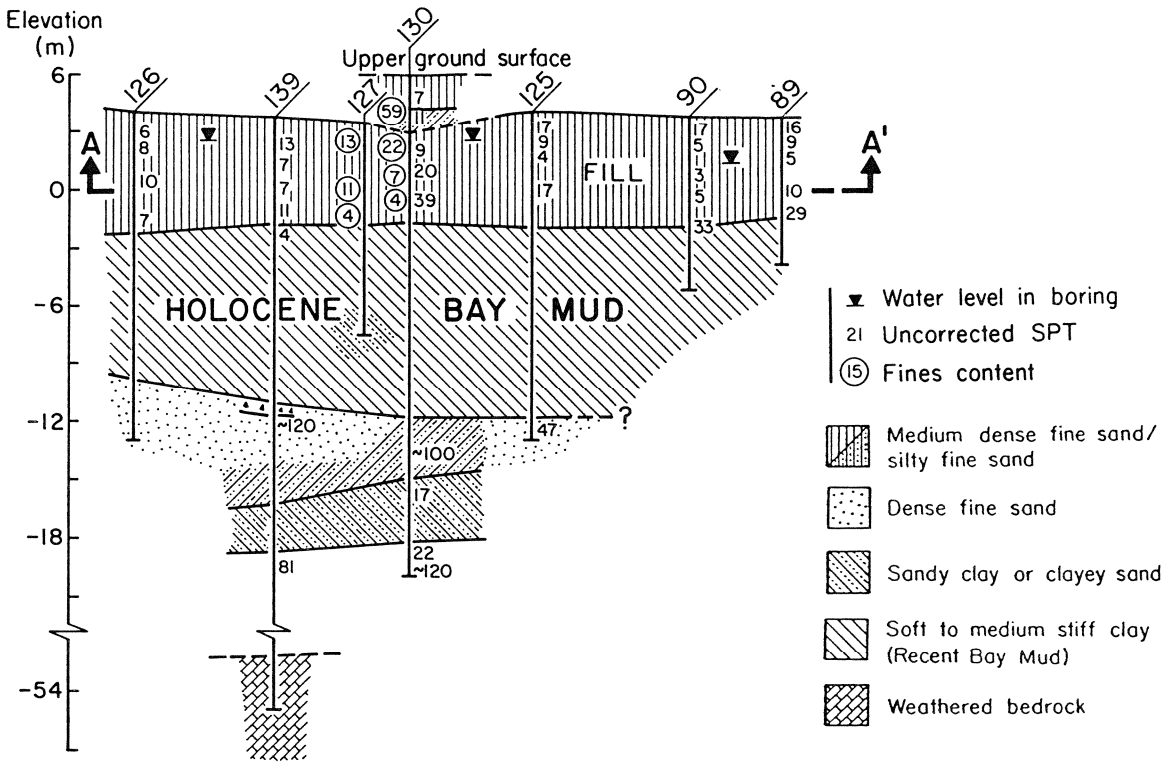

Figure 50. Soil Profile Along Cross-Section A-A' in the Mission Creek Area

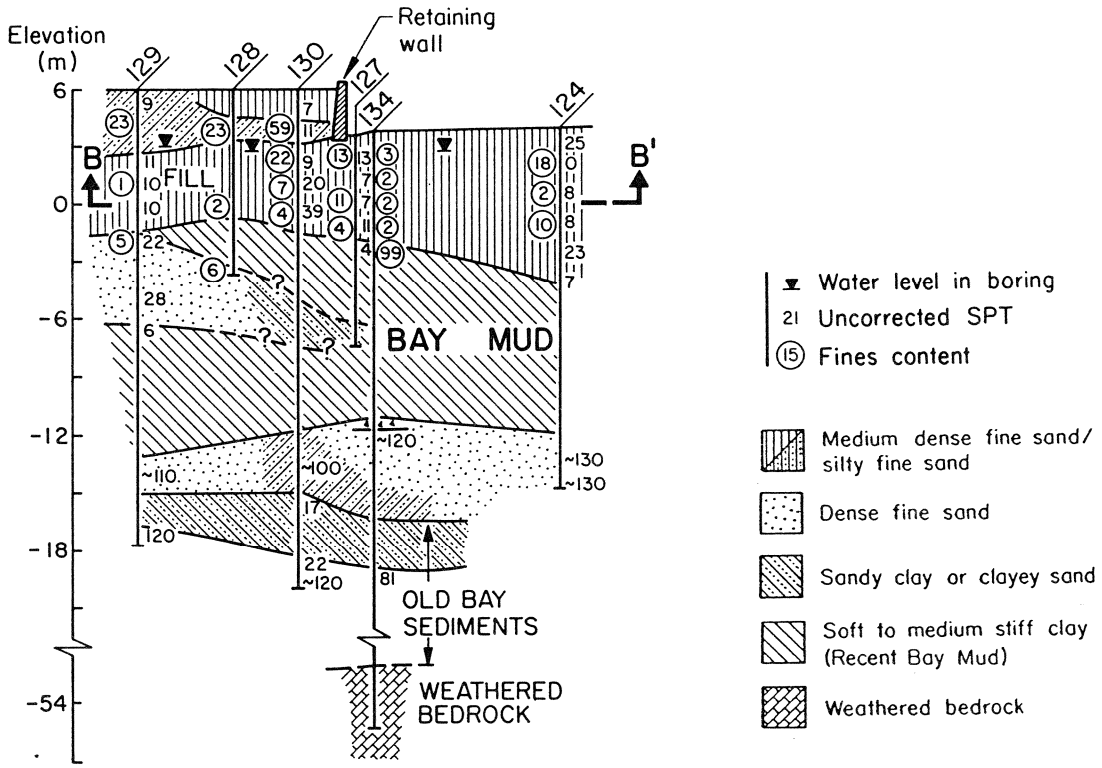

Figure 51. Soil Profile Along Cross-Section B-B' in the Mission Creek Area

profiles as uncircled numbers. The circled numbers indicate the percentage by weight of fines from split spoon samples retrieved from the elevations shown in the figure.

Below the retaining wall and embankment, there are approximately 4 to 6 m of loose to medium dense fill. As indicated by several relatively low SPT values, the fill is very loose in some locations. Overall, the fill is a relatively clean, uniform, fine-grained sand. The fill is underlain by about 9 m of Holocene bay mud, with approximately 40 m of dune sands and stiff clays, to weathered serpentine bedrock at a depth of roughly 60 m from the ground surface.

Liquefaction-potential analyses were performed for the fill using the empirical relationship between cyclic stress ratio and corrected STP values developed by Seed, et al. (1983; 1985), in accordance with the procedures described in Section 9.1. The cyclic stress ratios for various depths were calculated assuming a peak acceleration of 0.2 g. In a manner similar to Figure 48, Figure 52 shows the cyclic stress ratio plots for the sandy fill along cross-sections A-A′ and B-B′. Only the corrected SPT values for soil below the water table were used. In the figure, the empirical dividing lines for various fines contents between liquefiable (left side) and non-liquefiable (right side) soils are plotted for a magnitude 7.1 earthquake. The fill is relatively clean, with many samples having less than 5 to 10% by weight of fines. The $(N_1)_{60}$ data indicate that the fill at the South Van Ness and Howard St. site is highly susceptible to soil liquefaction for an event comparable in magnitude and intensity to those experienced during the Loma Prieta earthquake.

12.0 CONCLUDING REMARKS

Soil liquefaction in San Francisco caused by the 1989 Loma Prieta earthquake occurred at the same locations that liquefaction was observed after the 1906 earthquake. The four main areas of San Francisco affected by soil liquefaction in 1989 and 1906 are the Marina, Foot of Market, South of Market, and Mission Creek areas. Liquefaction effects involved subsidence, lateral movements, and loss of bearing of shallow foundations, with differential settlement, racking, and tilting of two to four-story timber structures.

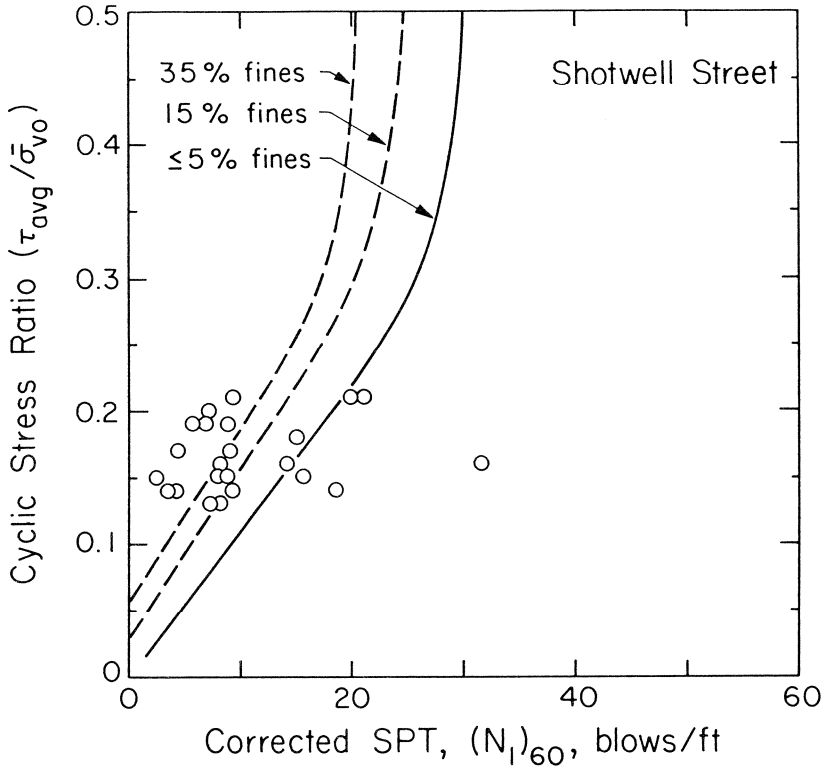

Figure 52. Cyclic Stress Ratio Plot for Fill at a Site of Liquefaction in the Mission Creek Area

One of the most distinctive features of the earthquake was the concentration of permanent ground movements, sand boils, and pipeline and structural damage at specific locations of the city underlain by Holocene bay mud. Amplification of bedrock motions through the deposits of soft clay and silt contributed to strong shaking and damage at the surface. Such amplification also was responsible for triggering soil liquefaction by contributing to accelerations and corresponding levels of cyclic stress which would not have been attained without the presence of soft bay sediments. In the Marina, Foot of Market, South of Market, and Mission Creek areas, there are prominent deposits of Holocene bay mud, with maximum thicknesses of 20 to 40 m. Each site has been filled with loose granular material, typically 6 to 9 m thick, with the water table at depths of 1 to 4 m below ground surface.

Because the history of development in the Marina is well understood, it is possible to identify the different types of granular deposits in this district

with reasonable accuracy. At least three different types of granular soil can be identified: 1) hydraulic fill, 2) fill tipped from shore or during seawall construction, and 3) natural beach, dune, and sand spit deposits. Data assembled in this case history help quantify the relative susceptibility to liquefaction of these materials. Moreover, data obtained from cone penetration tests (CPT) are shown to provide a more refined and accurate means of identifying liquefiable soils in comparison to the information from standard penetration tests (SPT), especially for stratified soils such as hydraulic fill that contain relatively thin silt and clay layers.

In the Marina, there were 123 repairs to pipelines of the Municipal Water Supply System (MWSS) of San Francisco, more than three times the number of repairs in this system throughout the rest of the city. The consequent loss of water severely hampered fire fighting efforts in the district. Approximately 13.6 km of gas distribution piping were replaced, and over 20% of the wastewater collector lines were repaired or replaced. In the Marina, damage to the MWSS and wastewater conveyance system was caused primarily by soil deformation arising from post-liquefaction consolidation. The remarkable correlation between pipeline damage and surface settlement at this site, both with respect to magnitude and spatial distribution, is perhaps the clearest demonstration in any earthquake of pipeline network vulnerability to liquefaction-induced ground deformation.

Damage patterns for water supply pipelines are remarkably similar for both the 1906 and 1989 earthquakes. Pipeline repair following earthquakes is an index of seismic severity, and repair records help to quantify the vulnerability of various parts of the city. There is a direct correlation between pipeline repairs per km and MMI, as developed on the basis of damage statistics and observations associated with the Loma Prieta and other western U.S. earthquakes.

Computer simulations of the Auxiliary Water Supply System (AWSS) performance during the earthquake are consistent with observations in the field. The computer simulations indicate that water was lost from the lower zone reservoir of the system in about 35 to 40 minutes. Moreover, the computer simulations

emphasize the importance of an independent power supply for isolation valves, and the substantial effect that hydrant breaks have on water lost from the system. Computer analyses have shown that two hydrant breaks can result in water leakage equivalent to the break of a 300-mm main at locations such as the South of Market area.

The events of the earthquake show that flexibility provided by the Portable Water Supply System (PWSS) was of critical importance in controlling and suppressing the fire that erupted in the Marina. The ability to operate with portable hosing and draft from a variety of water sources, including underground cisterns and fireboats, provides a valuable extra dimension in the city's emergency response.

REFERENCES

American Society for Testing and Materials, "Standard Test Method for Penetration Test and Split-Barrel Sampling of Soils," Annual Book of Standards (D-1586-84), Vol. 4.08, ASTM, Philadelphia, PA, 1991a, pp. 232-239.

American Society for Testing and Materials, "Standard Test Method for Deep, Quasi-Static, Cone and Friction-Cone Penetration Tests of Soil," Annual Book of Standards (D-3441-86), Vol. 4.08, ASTM, Philadelphia, PA, 1991b, pp. 439-444.

Bardet, J.P. and M. Kapuskar, "Site Investigation of the Marina District of San Francisco in September 1990," Report to the National Science Foundation, Civil Engineering Department, University of Southern California, Los Angeles, CA, Feb. 1991.

Bardet, J.P., M. Kapuskar, and G.R. Martin, "Dynamic Response of the Marina District of San Francisco During the 1989 Loma Prieta Earthquake," Proceedings, 3rd Japan-U.S. Workshop on Earthquake-Resistant Design of Lifeline Facilities and Countermeasures for Soil Liquefaction, NCEER-91-0001, National Center for Earthquake Engineering Research, Buffalo, NY, Feb. 1991, pp. 109-128.

Bennett, M.J., "Ground Deformation and Liquefaction of Soil in the Marina District," Open File Report 90-253, USGS, Menlo Park, CA, Effects of the Loma Prieta Earthquake on the Marina District, San Francisco, CA, Apr. 1990, pp. D-1 - D-36.

Bonilla, M.G., "The Marina District, San Francisco, California: Geology, History, and Earthquake Effects," Bulletin of the Seismological Society of America, Vol. 81, No. 5, Oct. 1991, pp. 1958-1979.

Bulletin of the Seismological Society of America, "The 1989 Loma Prieta, California Earthquake and Its Effects," Special Issue, Vol. 81, No. 5, Oct. 1991.

Campbell, K.W., "An Empirical Analysis of Peak Horizontal Acceleration for the Loma Prieta, California Earthquake of 18 October 1989," Bulletin of the Seismological Society of America, Vol. 81, No. 5, Oct. 1991, pp. 1838-1858.

Chameau, J.L., G.W. Clough, F. Reyna, and J.D. Frost, "Liquefaction Response of San Francisco Bayshore Fills," Bulletin of the Seismological Society of America, Vol. 81, No. 5, Oct. 1991, pp. 1998-2018.

Chin, B.-H. and K. Aki, "Simultaneous Study of the Source, Path, and Site Effects on Strong Ground Motion During the 1989 Loma Prieta Earthquake: A Preliminary Result on Pervasive Nonlinear Site Effects," Bulletin of the Seismological Society of America, Vol. 81, No. 5, Oct. 1991, pp. 1859-1884.

Dames and Moore, "Factual Report, Site Investigation for Completion of Preliminary Design - Phase I Muni Metro Turnaround Facility," Report for Bechtel National, Inc., Dames & Moore, San Francisco, CA, Job No. 185-215-03, Vols. I, II, and III, Nov. 1989.

Darragh, R.D. and A.F. Shakal, "The Site Response of Two Rock and Soil Station Pairs to Strong and Weak Ground Motion," Bulletin of the Seismological Society of America, Vol. 81, No. 5, Oct. 1991, pp. 1885-1899.

Dow, G.R., "Bay Fill in San Francisco: A History of Change," M.A. Thesis, California State University, San Francisco, July 1973.

Earthquake Engineering Research Institute, "Loma Prieta Earthquake Reconnaissance Report," L. Benuska, Tech. Ed., Earthquake Spectra, Supplement to Vol. 6, May 1990.

Egan, J.A. and Z.-L. Wang, "Liquefaction-Related Ground Deformation and Its Effects on Facilities at Treasure Island, San Francisco, During the October 17, 1989 Loma Prieta Earthquake," Proceedings, 3rd Japan-U.S. Workshop on Earthquake-Resistant Design of Lifeline Facilities and Countermeasures for Soil Liquefaction, NCEER-91-0001, National Center for Earthquake Engineering Research, Buffalo, NY, Feb. 1991, pp. 57-76.

Eguchi, R., "Water System Facility Performance During 24 World-Wide Earthquakes," Technical Report 82-1396-2b, J.H. Wiggins Co., Redondo Beach, CA, Mar. 1982.

Geophysical Research Letters, Vol. 17, No. 9, Aug. 1990.

Gilbert, G.K., R.L. Humphrey, J.S. Sewell, and F. Soule, "The San Francisco Earthquake and Fire of April 18, 1906 and Their Effects on Structures and Structural Materials," Bulletin 324, U.S. Geological Survey, U.S. Government Printing Office, Washington, D.C., 1907.

Golden Software, Inc., "Surfer," Golden, CO, 1985.

Governor's Board of Inquiry, "Competing Against Time," Report to Governor George Deukmejian, C.C. Thiel, Jr., Ed., May 1990.

Grigoriu, M.D. and T.D. O'Rourke, "Serviceability of the San Francisco Auxiliary Water Supply System, Proceedings, International Conference on Structural Safety and Reliability, San Francisco, CA, Aug. 1989.

Hanks, T.C. and A.G. Brady, "The Loma Prieta Earthquake, Ground Motion, and Damage in Oakland, Treasure Island, and San Francisco, Bulletin of the Seismological Society of America, Vol. 81, No. 5, Oct. 1991, pp. 2019-2047.

Hanks, T.C. and H. Krawinkler, "The 1989 Loma Prieta, California Earthquake and Its Effects: Introduction to the Special Issue," Bulletin of the Seismological Society of America, Vol. 81, No. 5, Oct. 1991, pp. 1415-1423.

Harding Lawson Associates, Dames & Moore, Kennedy/Jenks/Chilton, and EQE Engineering, "Liquefaction Study: Marina District and Sullivan Marsh Area, San Francisco, California," Final Report prepared for the City and County of San Francisco, Department of Public Works, Aug. 1991.

Harding Lawson Associates, Dames & Moore, Kennedy/Jenks/Chilton, and EQE Engineering, "Liquefaction Study: North Beach, Embarcadero Waterfront, South Beach, and Upper Mission Creek Area, San Francisco, California," Final Report prepared for the City and County of San Francisco, Department of Public Works, Jan. 1992.

Hovland, H.J. and R.D. Darragh, "Earthquake-Induced Ground Movements in the Mission Bay Area of San Francisco in 1906," Proceedings, 2nd Specialty Conference of the Technical Council on Lifeline Earthquake Engineering, Oakland, CA, Aug. 1981, pp. 293-309.

Hryciw, R.D., K.M. Rollins, M. Homolka, S.E. Shewbridge, and M. McHood, "Soil Amplification at Treasure Island During the Loma Prieta Earthquake," Proceedings, 2nd International Conference on Recent Advances in Geotechnical Earthquake Engineering and Soil Dynamics, St. Louis, MO, Mar. 1991, Vol. II, pp. 1679-1685.

Idriss, I.M., "Response of Soft Soil Sites During Earthquakes," Proceedings, H. Bolton Seed Memorial Symposium, Berkeley, CA, May 1990, pp. 273-290.

Jones, E.C., "The Story of the Restoration of the Gas Supply in San Francisco After the Fire," Proceedings, 14th Annual Meeting of the Pacific Gas Association, San Francisco, CA, Sept. 1906, pp. 350-364.

Joyner, W.B. and D.M. Boore, "Measurement, Characterization and Prediction of Strong Motion," Proceedings, Conference on Earthquake Engineering and Soil Dynamics - Recent Advances in Ground Motion Evaluation, J.L. Von Thon, Ed., ASCE Geotechnical Special Publication No. 20, 1988, pp. 43-102.

Khater, M.M., M.D. Grigoriu, and T.D. O'Rourke, "Serviceability Measures and Sensitivity Factors for Estimating Seismic Performance of Water Supply Systems," Proceedings, 9th World Conference on Earthquake Engineering, Tokyo, Japan, Vol. VII, 1989, pp. 123-128.

Lawson, A.C., et al., The California Earthquake of April 18, 1906: Report of the California State Earthquake Investigation Commission, Pub. No. 87, Carnegie Institute, Washington, D.C., 1908, Two Volumes and Atlas.

Manson, M., "Report on Auxiliary Water Supply System for Fire Protection for San Francisco, California," Report of the Board of Public Works, San Francisco, CA, 1908.

McNutt, S.R. and R.H. Sydnor, Editors, "The Loma Prieta (Santa Cruz Mountains), California Earthquake of 17 October, 1989," Special Publication 104, California Division of Mines and Geology, Sacramento, CA, 1990.

McNutt, S.R., "Summary of Damage and Losses Caused by the Loma Prieta Earthquake," Special Publication 104, California Division of Mines and Geology, 1990, pp. 131-138.

McNutt, S.R. and T.R. Toppozada, "Seismological Aspects of the 17 October, 1989 Earthquake," Special Publication 104, California Division of Mines and Geology, 1990, pp. 11-27.

Mitchell, J.K., M. Tahir, R.E. Kayen, and R.B. Seed, "Soil Conditions and Earthquake Hazard Mitigation in the Marina District of San Francisco," Report to the Mayor of San Francisco, CA, May 1990.

Olmsted, R., N. Olmsted, and A. Pastron, "San Francisco Waterfront: Report on Historical Cultural Resources for the North Shore and Channel Outfalls Consolidation Projects," San Francisco Wastewater Management Program, City of San Francisco, CA, Dec. 1977.

Olsen, R.S. and J.V. Farr, "Site Characterization Using the Cone Penetrometer Test," Use of In-Situ Tests in Geotechnical Engineering, S.P. Clemence, Ed., Geotechnical Specialty Publication No. 6, ASCE, New York, NY, 1986, pp. 854-868.

O'Rourke, T.D. and P.A. Lane, "Liquefaction Hazards and Their Effects on Buried Pipelines," Technical Report NCEER-89-0007, National Center for Earthquake Engineering Research, Buffalo, NY, 1989.

O'Rourke, T.D., M.D. Grigoriu, and M.M. Khater, "Seismic Response of Buried Pipes," Pressure Vessel and Piping Technology - A Decade of Progress, C. Sundararajan, Ed., ASME, New York, NY, 1985, pp. 281-323.

O'Rourke, T.D., H.E. Stewart, F.T. Blackburn, and T.S. Dickerman, "Geotechnical and Lifeline Aspects of the October 17, 1989 Loma Prieta Earthquake in San Francisco," Technical Report NCEER-90-0001, National Center for Earthquake Engineering Research, Buffalo, NY, Jan. 1990.

O'Rourke, T.D., J.W. Pease, and H.E. Stewart, "Lifeline Performance, Soil Conditions, and Ground Deformation in the Marina Associated with the 1989 Loma Prieta Earthquake," Marina Chapter, Vol. II, National Earthquake Hazards Reduction Program Report to Congress, U.S. Geological Survey, 1992 (in press).

O'Rourke, T.D., T.E. Gowdy, H.E. Stewart, and J.W. Pease, "Lifeline Performance and Ground Deformation in the Marina During 1989 Loma Prieta Earthquake," Proceedings, 3rd Japan-U.S. Workshop on Earthquake-Resistant Design of Lifeline Facilities and Countermeasures for Soil Liquefaction, NCEER-91-0001, National Center for Earthquake Engineering Research, Buffalo, NY, Feb. 1991a, pp. 129-146.

O'Rourke, T.D., T.E. Gowdy, H.E. Stewart, and J.W. Pease, "Lifeline and Geotechnical Aspects of the 1989 Loma Prieta Earthquake," Proceedings, 2nd International Conference on Recent Advances in Geotechnical Earthquake Engineering and Soil Dynamics, St. Louis, MO, Mar. 1991b, Vol. II, pp. 1601-1612.

Phillips, S.H. and J.K. Virostek, "Natural Gas Disaster Planning and Recovery: the Loma Prieta Earthquake," Pacific Gas and Electric Company, San Francisco, CA, Apr. 1990.

Plafker, G. and J.P. Galloway, Eds., "Lessons Learned from the Loma Prieta, California Earthquake of October 17, 1989," U.S. Geological Survey Circular 1045, U.S. Geological Survey, Denver, CO, 1989.

Ponti, D.J. and R.E. Wells, "Off-Fault Ground Ruptures in the Santa Cruz Mountains, California: Ridge-Top Spreading versus Tectonic Extension During the 1989 Loma Prieta Earthquake," Bulletin of the Seismological Society of America, Vol. 81, No. 5, Oct. 1991, pp. 1480-1510.

Reichle, M.S., R.D. Darragh, M.-J. Huang, T. Cao, U.R. Vetter, and A.F. Shakal, "Preliminary Analysis of Processed Strong Motion Data from the Loma Prieta Earthquake," Special Publication 104, California Division of Mines and Geology, 1990, pp. 47-58.

Reynolds, L.E., "How Electricity Was Served to Consumers and Street Car Lines by the San Francisco Gas and Electric Company After the Fire," Proceedings, 14th Annual Meeting of the Pacific Coast Gas Association, San Francisco, CA, Sept. 1906, pp. 365-373.

Ripley, B.D., Spatial Statistics, John Wiley and Sons, New York, NY, 1981.

Robertson, P.K. and R.G. Campanella, "Interpretation of Cone Penetration Tests. Part I: Sand," Canadian Geotechnical Journal, Vol. 20, No. 4, Nov. 1983, pp. 718-733.

Roth, R.A. and E. Kavazanjian, Jr., "Liquefaction Susceptibility Mapping for San Francisco, California," Bulletin of the Association of Engineering Geologists, Vol. 21, No. 4, Nov. 1984, pp. 459-478.

Sanborn Ferris Map Company, "Insurance Maps, San Francisco, California," Vol. 4, New York, NY, 1899 updated to 1905.

Scawthorn, C. and F.T. Blackburn, "Performance of the San Francisco Auxiliary and Portable Water Supply Systems in the 17 October, 1989 Loma Prieta Earthquake," Proceedings, 4th U.S. Conference on Earthquake Engineering, Palm Springs, CA, Vol. 1, 1990, pp. 171-180.

Schlocker, J., "Geology of the San Francisco North Quadrangle, California," Geologic Survey Professional Paper 782, U.S. Government Printing Office, Washington, D.C., 1974.

Schussler, H., The Water Supply of San Francisco, California, Martin B. Brown Press, New York, NY, 1906.

Seed, H.B., "Design Problems in Soil Liquefaction," Journal of the Geotechnical Engineering Division, ASCE, New York, NY, Vol. 113, No. 8, Aug. 1987, pp. 827-845.

Seed, H.B. and P. DeAlba, "Use of SPT and CPT Tests for Evaluating the Liquefaction Resistance of Sands," Use of In-Situ Tests in Geotechnical Engineering, S.P. Clemence, Ed., Geotechnical Special Publication No. 6, ASCE, New York, NY, 1986, pp. 281-302.

Seed, H.B., I.M. Idriss, and I. Arango, "Evaluation of Liquefaction Potential Using Field Performance Data," Journal of Geotechnical Engineering, ASCE, New York, NY, Vol. 109, No. 3, Mar. 1983, pp. 458-482.

Seed, H.B., K. Tokimatsu, L.F. Harder, and R.M. Chung, "Influence of SPT Procedures in Soil Liquefaction Resistance Evaluations," Journal of Geotechnical Engineering, ASCE, New York, NY, Vol. 111, No. 12, Dec. 1985, pp. 1425-1445.

Seed, R.B., et al., "Preliminary Report on Principal Geotechnical Aspects of the October 17, 1989 Loma Prieta Earthquake," Report UCB/EERC-90/05, University of California, Berkeley, CA, Apr. 1990.

Toppozada, T.R. and D.L. Parke, "Areas Damaged by California Earthquakes: 1900-1949," Open File Report 82-17 SAC, California Division of Mines and Geology, 1982.

Trautmann, C.H., T.D. O'Rourke, M.D. Grigoriu, and M.M. Khater, "Systems Model for Water Supply Following Earthquakes," Lifeline Seismic Risk Analysis - Case Studies, R. Eguchi, Ed., ASCE, New York, NY, 1986, pp. 30-50.

U.S. Coast Survey, Topographic Map of "City of San Francisco and Its Vicinity, California," surveyed by R.D. Cutts, 1853.

U.S. Coast Survey, Topographic Map of "City of San Francisco and Its Vicinity, California," surveyed by A.F. Rodgers, 1857.

U.S. Geological Survey, "Effects of the Loma Prieta Earthquake on the Marina District, San Francisco, California," Open File Report 90-253, Menlo Park, CA, Apr. 1990.

Youd, T.L. and S.N. Hoose, "Historic Ground Failures in Northern California Triggered by Earthquakes," Geologic Survey Professional Paper 993, U.S. Government Printing Office, Washington, D.C., 1978.

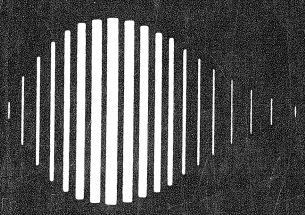

National Center for Earthquake Engineering Research
State University of New York at Buffalo